TRILATERAL SEMINAR AND

SEVENTH EUROPEAN SUMMER SCHOOL ON SUPRAMOLECULAR, INTERMOLECULAR, INTERAGGREGATE INTERACTIONS AND SEPARATION CHEMISTRY

JULY 20-23, 2012

PROCEEDINGS AND SELECTED LECTURES

A.N. FRUMKIN INSTITUTE OF PHYSICAL CHEMISTRY AND ELECTROCHEMISTRY

RUSSIAN ACADEMY OF SCIENCES
(IPCE RAS)

MOSCOW - RUSSIA

7TH EUROPEAN SUMMER SCHOOL ON SUPRAMOLECULAR, INTERMOLECULAR,
INTERAGGREGATE INTERACTIONS AND SEPARATION CHEMISTRY –
RUSSIAN – FRENCH – GERMAN TRILATERAL SEMINAR –
PROCEEDINGS AND SELECTED LECTURES. JULY 20-23, 2012, MOSCOW, RUSSIA
(Eds. K.E.GERMAN, L.B.BOINOVICH, A.YU. TSIVADZE)

Publishers ID GRANICA, 2012

UDK 546.718 : 539.16 : 547.8

ISBN 978-5-9933-0090-0

PREFACE

The Seminar has called leading scientist from Russia, France and Germany in the fields of supramolecular chemistry, colloid systems stability, formation, structure and interparticle interactions, with a particular emphasis on the applications to the separation chemistry. Special attention was given to these topics in relevance to nuclear waste management and geological disposal of these wastes. The participants addressed directly the critical gaps in the understanding of processes crucial for safe nuclear waste disposal, decontamination/remediation technologies, separations in nuclear waste cycle etc.

The special objective of the seminar was to promote international collaboration and strengthen discussion in the field of supramolecular, intermolecular, interaggregate interactions and separation chemistry to fill the conceptual gaps in knowledge of formation and stability of radionuclide containing nanoparticles, both in model and in real systems, as well as the role and behavior of nanoparticles in application processes such as separation, remediation or vitrification technologies.

The Seminar has covered important topics that were related to international research efforts and covered by several EC FP-7 projects and various bilateral programs (e.g. RFBR-Helmholtz joint program). This Seminar enabled to stimulate the effective scientific discussion on the institutional level and to enhance the joint application to unique pooled facilities like synchrotrons, accelerator centers, etc.

The agreement and work plan for joint studies between Russian, German and French institutes related to supramolecular chemistry, colloid chemistry and separation sciences was the main institutional result of the Seminar. Special attention was paid to the young researches in these fields to support their research mobility to other institutes.

The Seminar has approved the Johannes Gutenberg University Mainz, Institute of Nuclear Chemistry with Prof. Tobias Reich as the principle organizer for the 8th European Summer school in 2013.

Chair of the seminar
Director of IPCE RAS, academician Aslan Yu. Tsivadze

French co-chair, Dr. Stéphane Pellet-Rostaing
Institut de Chimie Séparative de Marcoule
UMR 5257 (CEA,CNRS, ENSCM & UM2)

German co-. chair Prof. Dr. Horst Geckeis
Karlsruhe Institute of Technology (KIT),
Institute for Nuclear Waste Disposal

Funding agencies:
Russian Foundation for Basic Research (RFBR)
National Center for Scientific Research (CNRS)
German Research Foundation (DFG)

French delegation arrived at the hotel Ibis Paveletskaya, 20 July, 2010

O. Pecheur, V.Fisher, B.Koenig, B.Beele at the Poster session of the 7th European Summer School 22 July, 2012.

PROGRAM OF THE 7TH EUROPEAN SUMMER SCHOOL ON SUPRAMOLECULAR, INTERMOLECULAR, INTERAGGREGATE INTERACTIONS AND SEPARATION CHEMISTRY – RUSSIAN – FRENCH – GERMAN TRILATERAL SEMINAR

Friday, July 20 2012 Arrival of the participants.

Arrivals at Domodedovo Airport
Arrivals at Sheremetyevo Airport
17-00-20-00 Info-reception at IBIS Hotel Paveletskaya

Saturday, July 21 2012
First Session
(IPCE, Principle Building Conference Hall)
Session chair : Prof. L.B. Boinovich

9h 30 **Openning ceremony**.
Welcome address by **Prof. Aslan Tsivadze, Prof. Burkhard Koenig , Dr. Stephane Pellet-Rostaing**.

9h 55 **Aslan.Yu.Tsivadze** (Russia) - “Innovative development on the basis of supramolecular systems”.
10h 40 **Burkhard Koenig** (Regensburg, Germany) - "Organic Chemistry with Visible Light: Luminescent Chemosensors and Chemical Photocatalysts".
11h 40 **Wais Hosseini** (Strasbourg, France) - "Molecular tectonics: control of porosity and molecular crystals".

12h 25 **Student presentation session.**

1. **Stephan Balk.** Dynamic analyte recognition by artificial synthetic vesicles.
2. **Susanne Dengler.** Investigation of Ion specifities via NMR.

12h 45 Discussions in frame of SENA collaboration and Poster session.

Session chair: Prof. Burkhard Koenig

14 h 00 **Boris F. Myasoedov** (Russia) - “Separation methods in solving

the problems of radiochemistry”.

14h 45 **Jean Weiss** (Strasbourg, France) - "Selective recognition of imidazoles: an assembling tool for highly linear molecular wires".

15h 45 **Ivan G. Tananaev** (Russia) - "Nanoindustry in radiochemistry and radioecology".

16h 30 **Students presentation session**

1. **Anna Sinelshchikova -** Phosphoryl-porphyrinates - new receptors for supramolecular chemistry **.**
2. **Pawel JEWULA.** Calix[4]arene-Based Tetrapodal Ligand Incorporating Cyclic Hydroxamic Acids as Chelating Units.
3. **Olivia Pecheur (CEA, France).**

17h00 Discussions and Poster Session.

Sunday, July 22, 2012
Second Session
(IPCE, Principle Building Conference Hall)

Session chair: Prof. Wais Hosseini.

9h 55 **Ludmila Boinovich** (Moscow, Russia) "Surface forces as the basis for the analysis of interaggregate interactions".

10h 40 **Stephane Pellet-Rostaing** (Marcoule, France) - “Control in selective ion separation in molecular systems via supramolecular and colloidal interactions”.

11h 40 **Tobias Reich** (Johannes Gutenberg-Universität Mainz, Germany) - "Sorption and diffusion of actinides in clays”.

12h 25 **Student presentation session.**

1. **Nils Stöbener**. “Developing resonance ionization mass spectrometry (RIMS) for the ultratrace analysis of neptunium” .
2. **Ugras Kaplan**. Plutonium speciation.
3. **Alesya Maruk.** Bifunctional radiopharmaceutical

12h 45 Discussions and Poster session.

Session chair: Dr. Pellet-Rostaing.

14 h 00 **Alexandre Varnek** (Strasbourg, France) - “Chemoinformatics: time to predict”.

14h 45 **Horst Geckeis** (Karlsruhe, Germany) - “Actinide environmental behavior – role of nanoparticle formation”.

15h 45 **Werner Kunz** (Regensburg, Germany) – “Specific ion effects in solutions, at interfaces, and in colloidal systems”.

16h 15 **Students presentation session.**

1. **Yana Obruchnikova.** Speciation and separation chemistry of Tc for SNF reprocessing.
2. **Veronika Fisher.** Deep Eutectic Solvents
3. **Michael Klossek.** Nanostructured Liquids, Colloids and Environmentally Acceptable Liquid Media
4. **Alexander Martynov.** Synthesis and conformational behaviour of phthalocyanines, bearing lateral coordinating macrocyclic substituents.

17 h 00 **Moscow Round-trip.**

Monday, July 23 2012
Third Session
(IPCE, Principle Building Conference Hall + ScientificTV)

Session Chair : Prof. Tobias Reich.

9h45 **Stepan Kalmykov** – “Environmental Chemistry of actinides in microparticles from different nuclear sites”.

10h25 **Björn B. Beele**, Udo Müllich, Andreas Geist, Petra J. Panak - “Partitioning and Transmutation – BTP-type N-Donor ligands in the SANEX Process “.

10h45 Konstantin German**, Grigory Kolesnikov.** “Macro-receptors for Tc and Re : Structural predictions, supramolecular-based template synthesis and new properties”.

Session chairs: Prof. Horst Geckeis and acad. A.Yu. Tsivadze.

12h 00 **Daniel Meyer -** "Colloidal and supra-molecular aspects of 5f elements in solution".

12h 30 **Andrei Shirjaev -** “Speciation in radioactive Pu-waste-glassforms.”

13h 00 **Student presentation session**:

1. **Bayrita Egorova –** “Pertechnetate-ion binding by organic ligands in aqueous solutions”.
2. **Alesya Maruk –** “Bifunctional radiophrmaceuticals for nuclear medicine”.
3. **Yulia Buchatskaya**. “Sorption preconcentration of radionuclides using detonation nanodiamonds”.

13h 30 Concluding remarks. Award ceremony. Approval of the 8-th Summer school planning. Closing ceremony.

7th European Summer School - IPCE RAS 2012

Innovative developments on the basis of supramolecular systems

Aslan Yu. Tsivadze

A.N. Frumkin Institute of Physical Chemistry and Electrochemistry, Russian Academy of Sciences

http://www.phyche.ac.ru

What is INNOVATION?

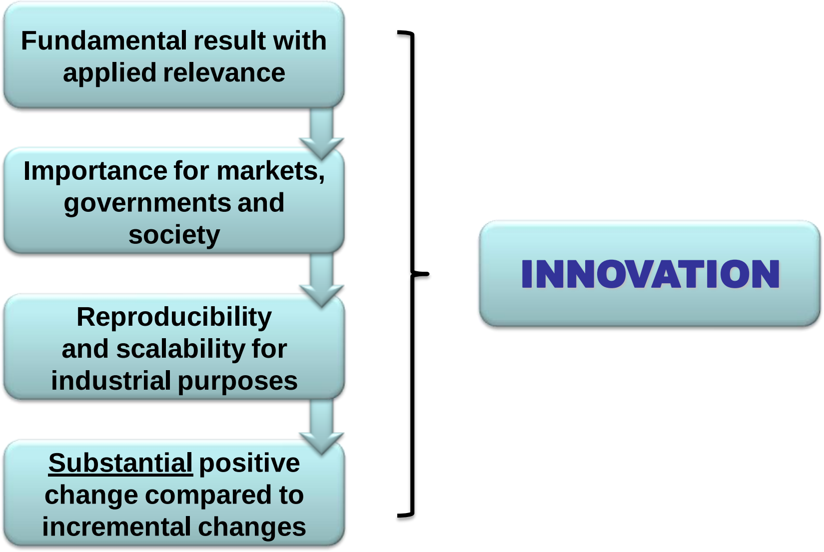

Fundamental result with applied relevance

Importance for markets, governments and society

Reproducibility and scalability for industrial purposes

<u>Substantial</u> positive change compared to incremental changes

INNOVATION

Crown-ethers in separation processes

- High selectivity of complex formation with metal ion having similar chemical properties
- High chemical stability
- Can be easily regenerated

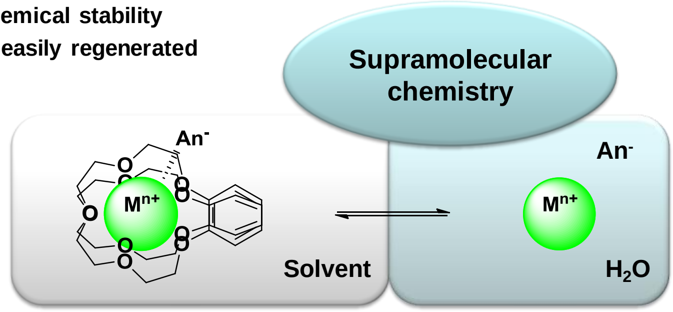

- Structure of crown-ethers, providing optimal lypophylic-hydrophylic balance
- The effect of solvent
- The effect of anion
- Conformation of crown-ether
- Substituents in crown-ether

Separation of isotopes by crown-ethers

Crown-ether	M	Separation coefficient	Extraction system	Ref.
DCH18C6	Ca	1.001	$CaCl_2$ $H_2O-CHCl_3$	B.E. Jepson, R. De Witt, 1976
[2.2.1]	Li	1.041	$LiCF_3COO$ $H_2O-CHCl_3$	B.E. Jepson, G.A.Cairns, 1979
B15C5	Li	1.045	12M LiCl $H_2O-CHCl_3$	K.Nishizawa, T.Takano, 1988
B15C5	Li	1.030 T=293K) 1.080 (T=213K)	LiSCN $H_2O-CHCl_3$	A.Yu.Tsivadze et al., 1984, 1990
Amalgam process	Li	1.05		
DCH18C6	K	1.0007	KI $H_2O-CHCl_3$	A.Yu.Tsivadze et al., 1991
B15C5	Mg	1.0017	$Mg(CCl_3COO)_2$ $H_2O-CHCl_3$	A.Yu.Tsivadze et al., 1990

Separation of isotopes by crown-ethers

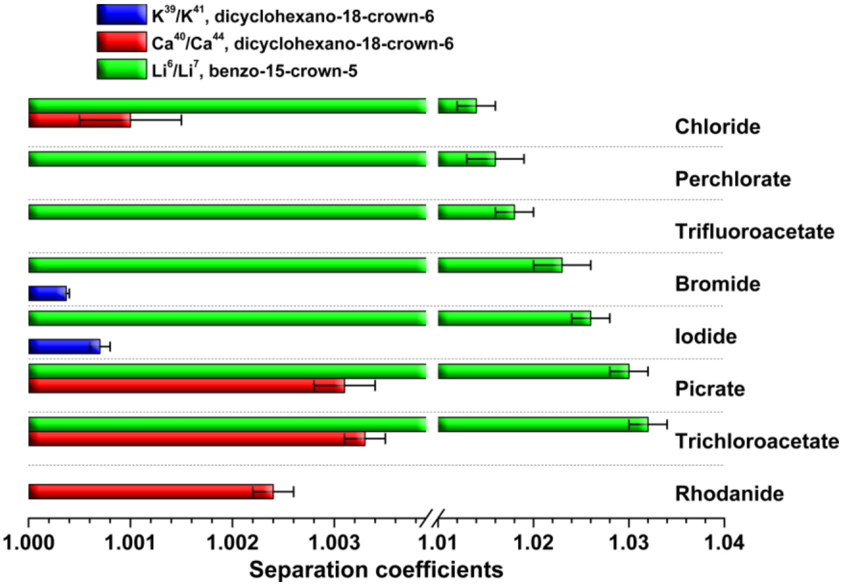

Tsivadze A.Yu., Zhilov V.I., Demin S.V., Russ. J. Coord. Chem., 996, t.22, #4

Separation of LITHIUM isotopes by crown-ethers

№	Crown-ether	Anion	Solvent	Separation coefficient
1	Benzo-15-crown-5	Cl_3CCOO^-	$CHCl_3$	1,030 1,030*
2	Benzo-15-crown-5	ClO_4^-	$CHCl_3$	1,016
3	Benzo-15-crown-5	ClO_4^-	$PhNO_2$	1,027*
4	Benzo-15-crown-5	SCN^-	$PhNO_2$	1,029 1,029*
5	15-crown-5	Cl_3CCOO^-	$CHCl_3$	1,029
6	Dicyclohexano-18-crown-6	ClO_4^-	$CHCl_3$	1,007

* Determined by multistep exhausting

Principal scheme of multi-step lithium isotope separation

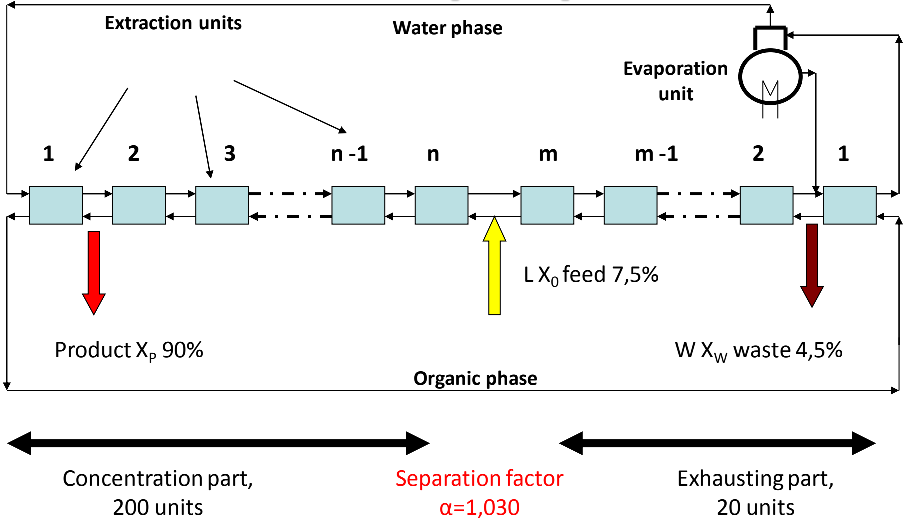

PUREX – Plutonium-Uranium EXtraction

- ✚ **Complete separation of U and Pu from fission products ~10^9; U/Pu separation factor > $7 \cdot 10^5$.**
- ▬ **accumulation of a great volume of radioactive liquid waste** - ***Russia now accumulated about 1.5×10^9 Ci***

Moreover, the current extraction scheme includes:

(1)intercycle evaporation;
(2)nitric acid regeneration;
(3)thermal decomposition of U and Pu nitrates;
(4)pre-concentration of liquid radioactive wastes.

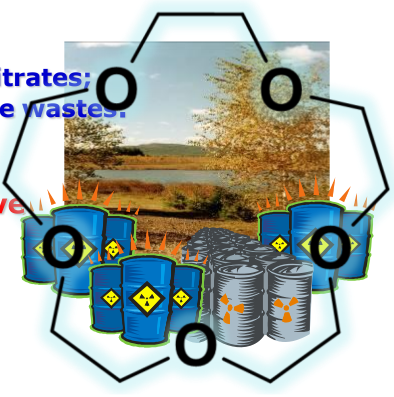

These operations leads to the exothermic heat explosions that, have already happened several times:

Savannah River 1953, 1975
Oak Ridge 1959
Tomsk 1993.

Application of crown-ethers in recovery of nuclear waste

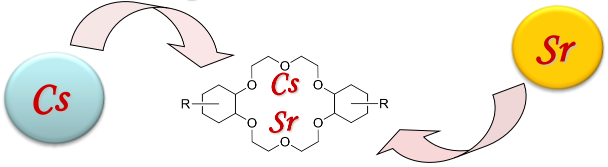

- The efficient extraction scheme of Sr and Cs recovery by crown-ether was developed and successfully tested in Russia, productive association “MAYAK” – mixture of 80% 18C6 and 20% 21C7 in fluorinated alcohols was used to process >90 m^3 of highly active waste and 10^6 Ci of Sr (98%) and Cs (90%) was isolated

- Similar approach is used in USA (Oak Ridge National Laboratory, Argonne National Laboratory) DB15-crown-5 and DBDCH-18-crown-6 were used for extraction of Sr from radioactive waste)

Crown-ethers can be applied for efficient selective extraction and separation of elements with similar chemical properties (lanthanides and actinides)

Extraction of REE by crown-ethers

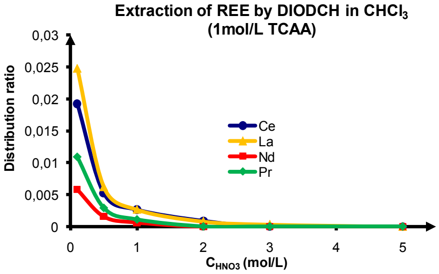
Extraction of REE by DIODCH in $CHCl_3$ (1mol/L TCAA)

The concentrations of REE in the organic phase increases with the decrease content of nitric acid in the aqueous phase.

The elements of the cerium group are extracted better than elements of the yttrium group.

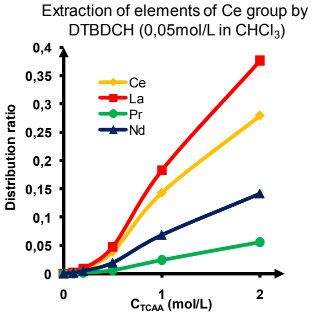
Extraction of elements of Ce group by DTBDCH (0,05mol/L in $CHCl_3$)

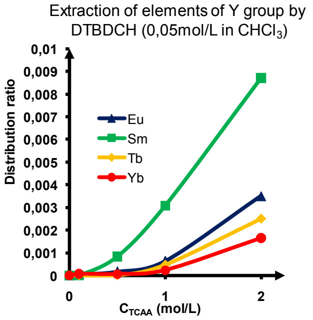
Extraction of elements of Y group by DTBDCH (0,05mol/L in $CHCl_3$)

Separation factors of REE during extraction (chloroform – H_2O) from HNO_3 in the presence of 1M TCAA*

*TCAA = CCl_3COOH

Crown-ether	[HNO_3] M	Separation Factors									
		La/Ce	La/Pr	La/Nd	La/Yb	Ce/Pr	Ce/Nd	Ce/Yb	Pr/Nd	Pr/Yb	Nd/Yb
DCH	0,1	0,88	1,38	2,76	300	1,57	3,14	341	2,00	217	109
	0,5	0,92	1,39	2,37	153	1,52	2,59	167	1,71	110	64,5
DIODCH	0,1	1,29	2,27	4,26	8,39	1,77	3,30	6,50	1,87	3,68	1,98
	0,5	1,19	2,15	3,88	18,7	1,80	3,25	15,6	1,81	8,69	4,81
DTBDCH	0,1	1,28	2,69	7,49	777	2,10	5,86	608	2,79	289	104

Even for lanthanide separation the separation factors are high and reach the value up to 777 for La/Yb and other element separation.

It was shown that bis(butyloxyhydroxophosphoryl)-dibenzo-21C7 can selectively extract Am(III) and Eu(III). The D_M values in chloroform-nitric acid system and separation factor ($f_{Am/Eu}$) are extremely high.

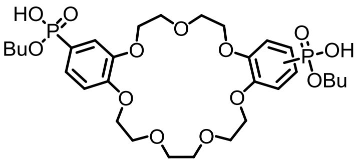

[HNO_3],M	D_{Am}	D_{Eu}	$f_{Am/Eu}$
0,01	814	8,8	92,5
0,1	5,7	2,8	2,0
0,5	0,1	0,1	1,0
1,0	0,01	0,01	1,0
3,0	<0,01	<0,01	-

Values of distribution coefficients of Am(III) and Eu(III), extracted by 0,05M solutions of CP-211 in chloroform (chelate group - (BuO)(OH)P(O)-; n = 21) in dependence on HNO_3 concentration

Extraction of metals by open-cycle analogs (podands)

- Synthetically obtained open-cycle polyethers (podands) show unique complexation properties towards metals. They are perspective for separation and pre-concentration of metal ions (^{40}K, ^{87}Rb, ^{89}Sr, ^{137}Cs) due to high selectivity of extraction.
- The preparation of open-cycle analogs are more simple and economically reasonable if compared with crown-ethers.

we studied the extraction characteristics (distribution coefficients, extraction constants, stoichiometry and stability constants of complexes) of different chemical systems with varying anion, extractant, solvent and temperature.

Advantages of phosphorylopodands:

- Synthetic availability (yields 70-95%, simplicity of synthesis and isolation).
- High stability constants of comlexes with metals (similar or even <u>higher</u> with the ones of crown-ether)
- Low toxicity, LD_{50} over 800-1000 mg/kg (mouse). For dicyclohexyl-18-crown-6 LD_{50}=250-300 mg/kg.

Applicability:

- Active components for efficient extraction, separation and concentration of s-, p-, d- and f-elements
- Efficient ionophores for various cations (Li^+, Ca^{2+}, Cu^{2+}, Pb^{2+}, etc.) and also some biogenic amines through membranes of ionoselective electrodes.
- Selective sorption materials for analysis and purification of various solutions, both environmental and technological

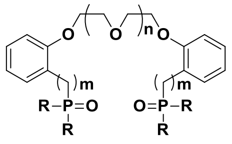

m=0,1 n=0,1...4
R=Ph, Alk, OAlk, OH

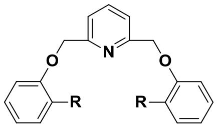

R = $P(O)Ph_2$, $CH_2P(O)Ph)_2$

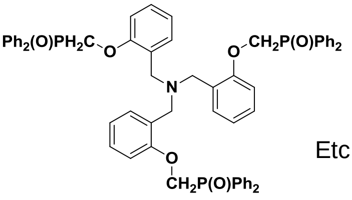

Etc.

Extraction of REE by phosphorylpodand

The concentrations of REE in the organic phase increases with the increase content of nitric acid in the aqueous phase.

The elements of the yttrium group are extracted better than elements of the cerium group.

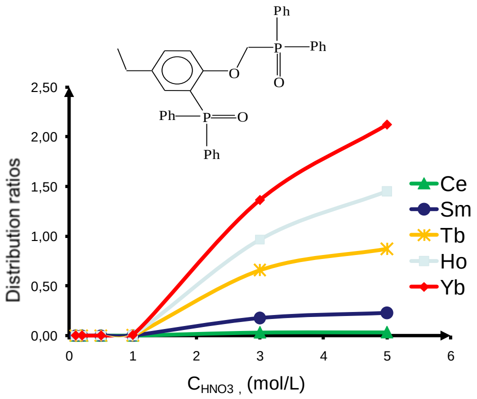

Separation factors									
Ce/La	Pr/La	Nd/La	Yb/La	Pr/Ce	Nd/Ce	Yb/Ce	Nd/Pr	Yb/Pr	Yb/Nd
1,8	2,0	1,7	79	1,1	0,9	44	0,9	40	47

Structure of Yb complex

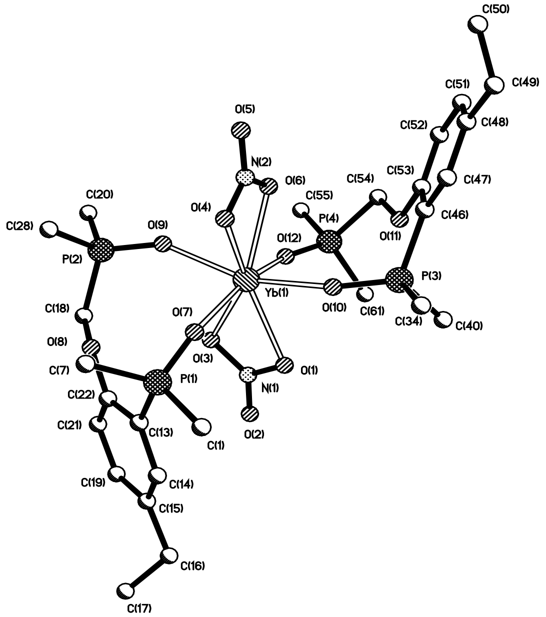

Acyclic analogues of crown-ethers (podands) for the preparation of cation-selective sorbents

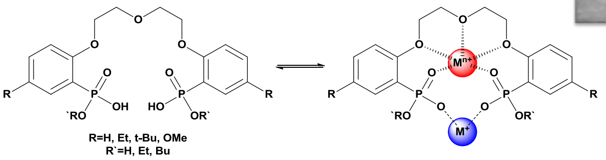

The series of efficient and selective sorbents was made in IPCE RAS, based on phosphorylated acyclic podands

The main advantages of these sorbents are their high selectivity towards lanthanides and actinides, as well as their reusability. Their extraction characteristics exceed the ones of previously developed analogues (for example, manufactured by Eichrom Technologies)

Acyclic analogues of crown-ethers (podands) for the preparation of cation-selective sorbents

Sorbent preparation

- The beads, made of copolymer of divinylbenzene and styrene are used (40-70mkm, 150-250mkm) .
- The carrier in volatile solvent (chloroform, acetone) is mixed with the podand and the solvent is evaporated

Sorbent characteristics

•Active component:	15,5 %/1 g of a carrier
•Beads size:	40-70 mkm or 150-250 mkm
•Surface area:	700-800 m^2/g
•Porosity volume	2 ml/g

Application of phosphorylpodands-based sorbents in nuclear chemistry

Due to the difference in dynamic distribution coefficients of actinides upon the variation of nitric acid concentration, there was developed the approach to separation of thorium, uranium, neptunium and plutonium by dynamic chromatography

Dynamic distribution coefficients			
U(IV)	**Th(IV)**	**Np(IV)**	**Pu(IV)**
150	**300**	**500**	**620**

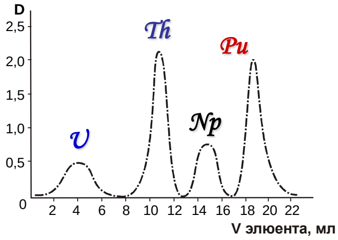

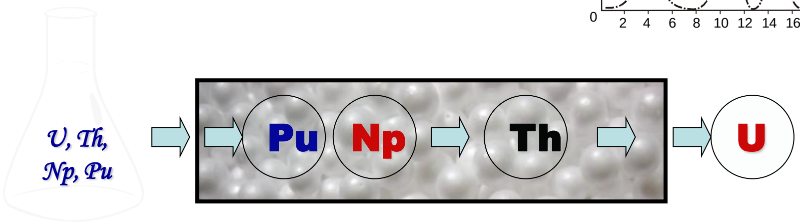

Industrial group “MAYAK” (Russia) uses this approach for the analysis of Th in ^{238}Pu, used for isotope batteries

Sorbents, based on neutral phosphorylpodands are used in analytical and industrial separation and purification of ^{99}Mo from neutron-exposed uranium targets. ^{99}Mo is used to prepare ^{99m}Tc, applied in diagnostic radio- pharmaceutical.

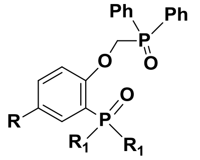

R=H, Et, OMe

R1=OEt, Bu, Ph, p-Tol

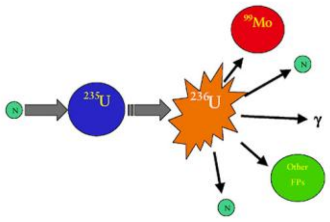

Yield of Mo-99 ~ 6%

The task: separation Mo-99 from concomitant impurities (Zr-95, Nb-95, Tc-99 и U-235) and delivery of residual U-235 to additional neutron exposure

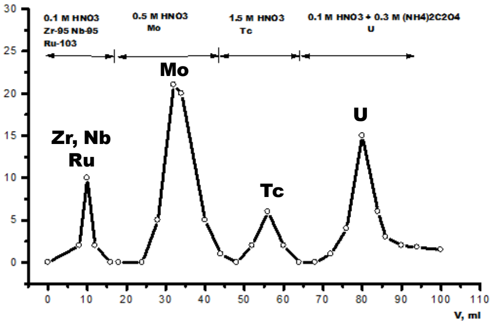

Chromatogram of separation of radionuclides, containing in neutron-exposed uranium targets

Ion-selective sensors, based on crown-substituted tetrapyrrol compounds

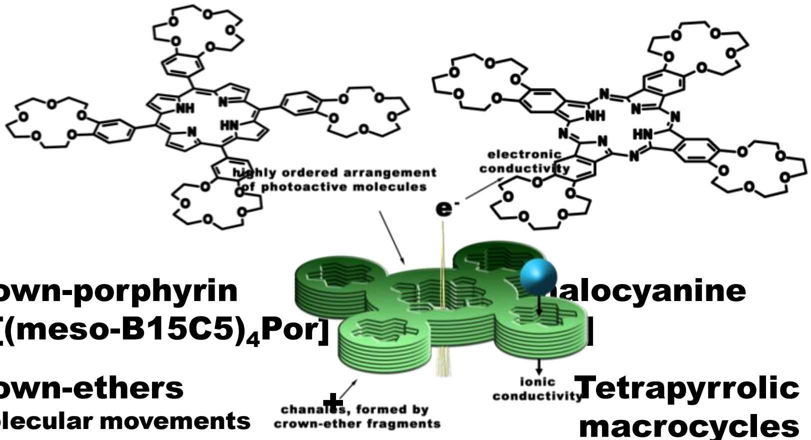

Crown-porphyrin
H$_2$[(meso-B15C5)$_4$Por]

alocyanine
]

Crown-ethers
- **Molecular movements**
- **Selective binding of ions and small molecules**

Tetrapyrrolic macrocycles
- **Electron transfer**
- **π-π interaction**

⇒Crown-porphyrins, crown-phthalocyanines

- **Cation-induced formation of conducting supramolecular assemblies**

Na$^+$/K$^+$ optical selectivity: determination of Na$^+$ and K$^+$ in biological liquids

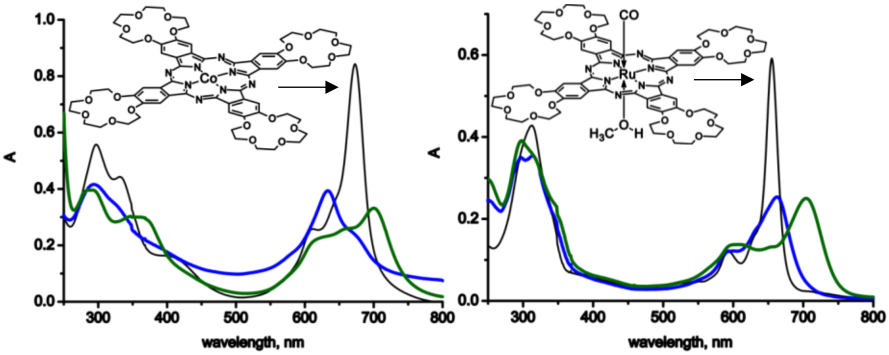

— **Co(R$_4$Pc)** **λ_{max}=670 nm**

— **Co(R$_4$Pc) + NaSCN** **λ_{max}=630 nm**

— **Co(R$_4$Pc) + KSCN** **λ_{max}=737 nm**

— **(R$_4$Pc)Ru(CO)(MeOH)** **λ_{max}=655 nm**

— **(R$_4$Pc)Ru(CO)(MeOH) + NaSCN** **λ_{max}=704 nm**

— **(R$_4$Pc)Ru(CO)(MeOH) + KSCN** **λ_{max}=662 nm**

Na^+/K^+ optical selectivity: Assemblies, formed by cobalt and ruthenium complexes

- **$Co[(15C5)_4Pc]$ + KSCN**
  Cofacial dimer

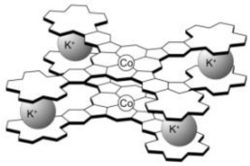

- **$(R_4Pc)Ru(CO)(MeOH)$ + KSCN**
  Brick-wall like J-aggregates

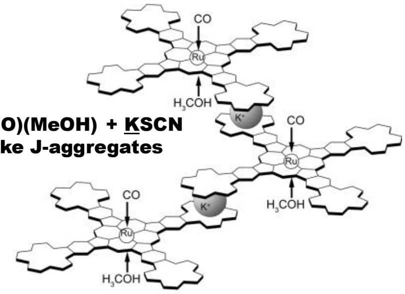

- **$Co[(15C5)_4Pc]$ + NaSCN**
  Brick-wall like assembly
  with bridging SCN^-

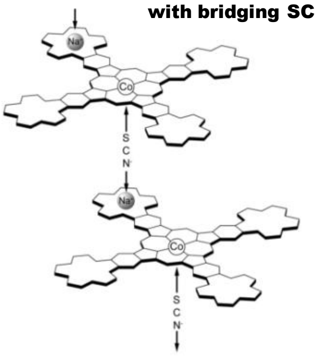

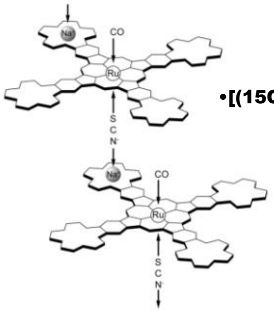

- **$[(15C5)_4Pc]Ru(CO)(MeOH)$ + NaSCN**
  Brick-wall like assembly
  with bridging SCN^-

Drawbacks of common ionoselective membranes

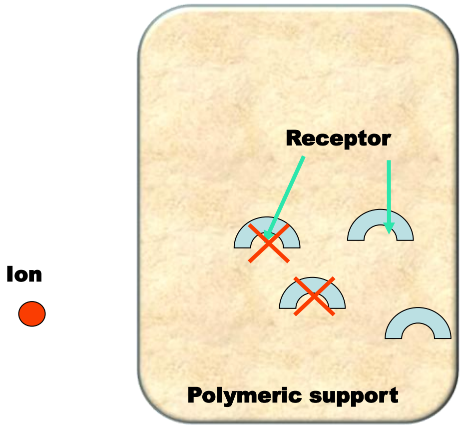

1. Low quantity of ionophore in polymeric matrix
2. Only part of receptor takes part in binding
3. Slow diffusion over large distances

Crowned porphyrins as receptors to potassium cations in solution

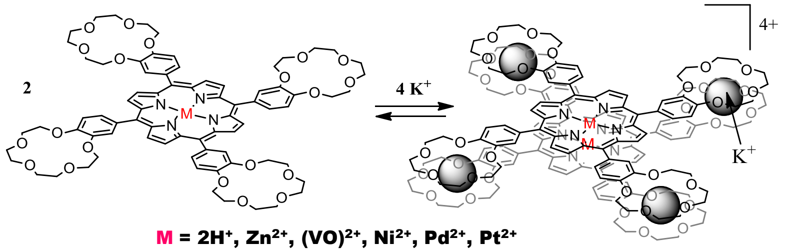

M = $2H^+$, Zn^{2+}, $(VO)^{2+}$, Ni^{2+}, Pd^{2+}, Pt^{2+}

Drawbacks of these compounds as receptors for K+ cations :

- H_2TCP is insoluble in alcohols and in water,

- Porphyrinates of transition metals manifest weak fluorescence (ZnTCP, (VO)TCP) or do not possess fluorescence (NiTCP, CuTCP)

V. Thanabal, V. Krishnan. *Inorg. Chem.*,1982, **21**, 3606.

V. Thanabal, V. Krishnan. *J. Amer. Chem. Soc.*, 1982, **104**, 3643.

R. Chitta, L. M. Rogers. *Inorg. Chem.*, 2004, **43**, 6969.

Aluminum crowned porphyrin as fluorescent sensor to potassium cations in water

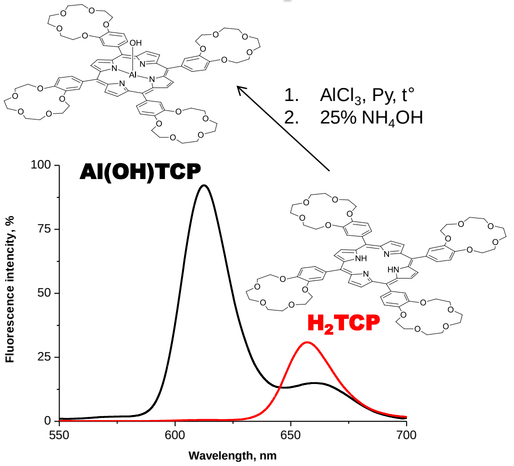

Fluorescence spectra of Al(OH)TCP and free base porphyrin H_2TCP in DMF at equal absorbance of irradiating light with λ = 430 nm

Advantages of Al(OH)TCP in comparison with free base porphyrin H_2TCP:

- Strong fluorescence as compared to free base porphyrin H_2TCP shifted to blue region

- Solubility in water!

- Stability of aluminum(III) porphyrinate in a wide range of pH

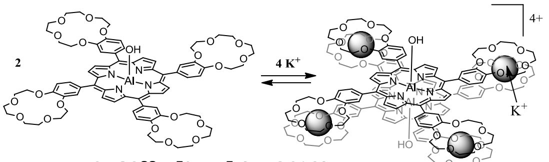

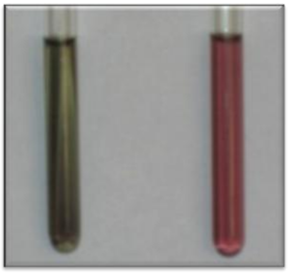

K **~ 6x10^{22} L^{5}/Mol^{5} (at 20°C)**

UV-Vis spectral changes following the reaction of 1.4 X 10^{-6} M Al(OH)TCP in water with K^{+}

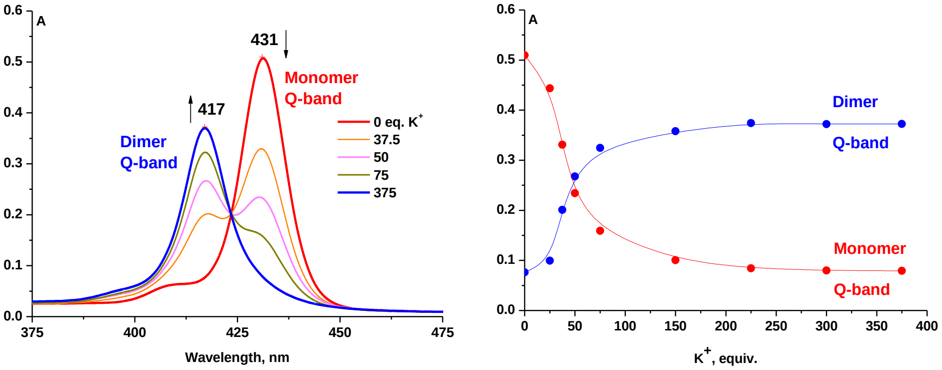

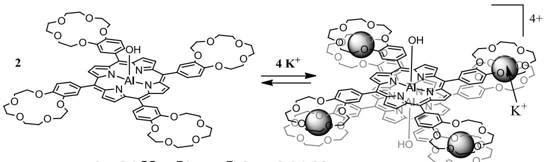

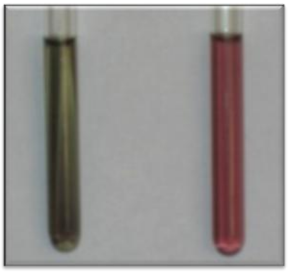

K **~ 6x10^{22} L^{5}/Mol^{5} (at 20°C)**

Luminescence spectral changes following the reaction of 0.7 X 10^{-7} M Al(OH)TCP in water with K^{+}

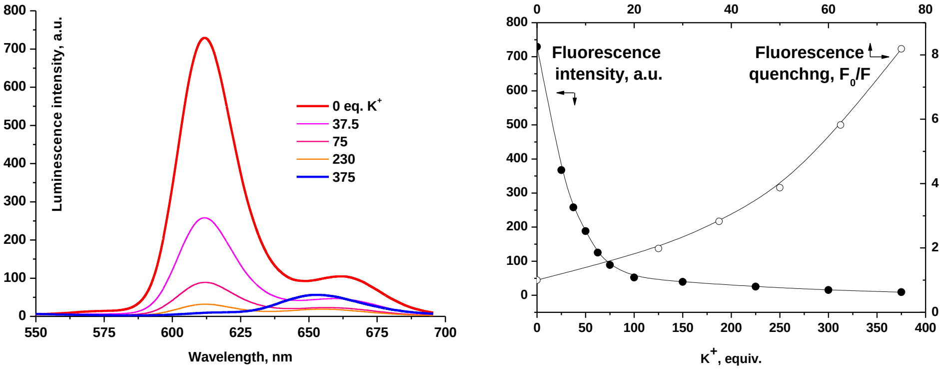

Temperature-dependent self-assembly of (TCP)AlCl in toluene

T=20°   T=110°C

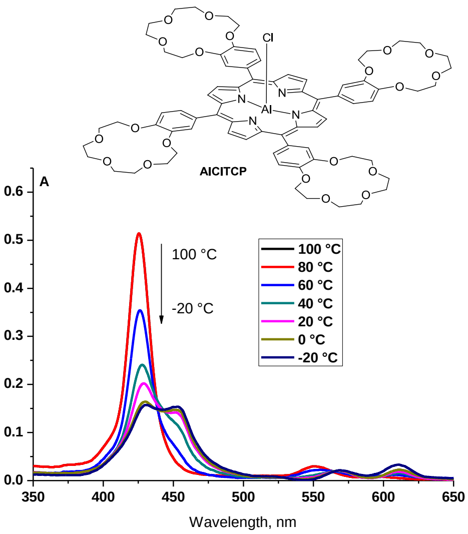

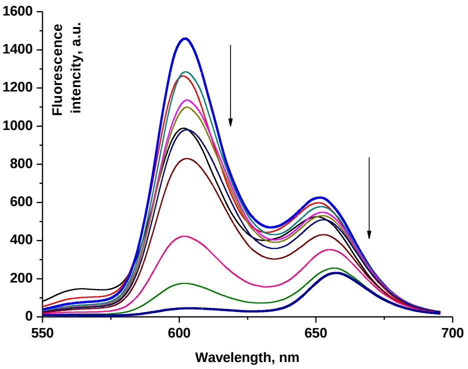

Changes of UV-Vis spectrum of AlCl(TCP) in toluene upon heating and cooling (C~ 1x10^{-6} M)

Changes of luminescence spectrum of AlCl(TCP) in toluene upon heating and cooling (C~ 1x10-6 M)

Temperature-dependent self-assembly of (TCP)AlCl in toluene

T=20°   T=110°C

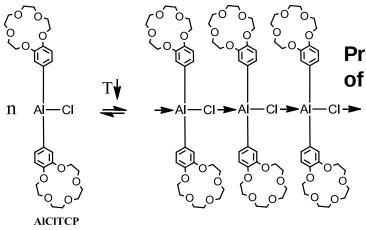

Proposed mechanism of aggregation

Molecular size~ 2.5 nm

Dynamic light scattering measurements

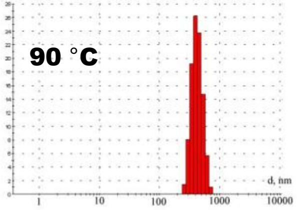

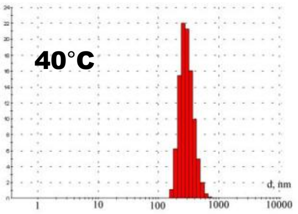

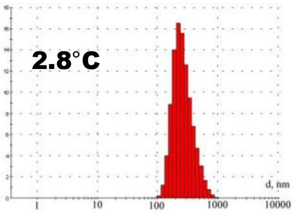

Solution of AlCl(TCP) in toluene can be used as a reversible termochromic indicator due to high color contrast even at 1x10^{-6} M
(only ~ 1.5 мг AlClTCP in 1 liter of a solution !!!)

Tetra-15-crown-5-phthalocyaninato-aluminum $[(15C5)_4Pc]Al(OSO_3H)$

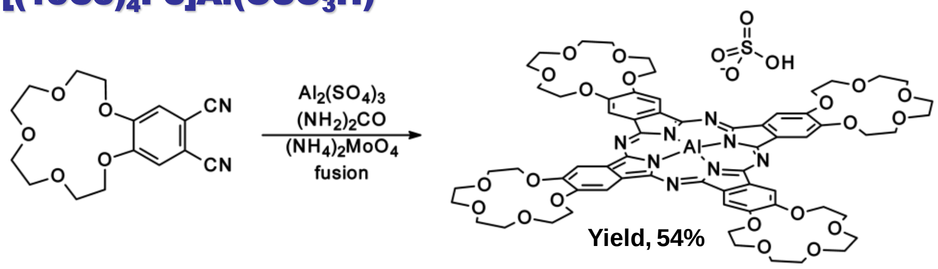

Yield, 54%

✚ Single isomer, amphiphylic and readily available. Performs high affinity to lungs, liver and spleen tumors

− Non-toxic upon light irradiation because of strong tendency to aggregations in aqueous media, which quenches luminescence and PDT effect

A.Yu. Tsivadze et al. Patent of Russia, №2079499, 1994, November 22

E.O. Tolkacheva et al. Rus. J. of Inorg. Chem. 1995, v.40, №3, p. 449-453.

Synthesis of aluminum Crownphthalocyaninate

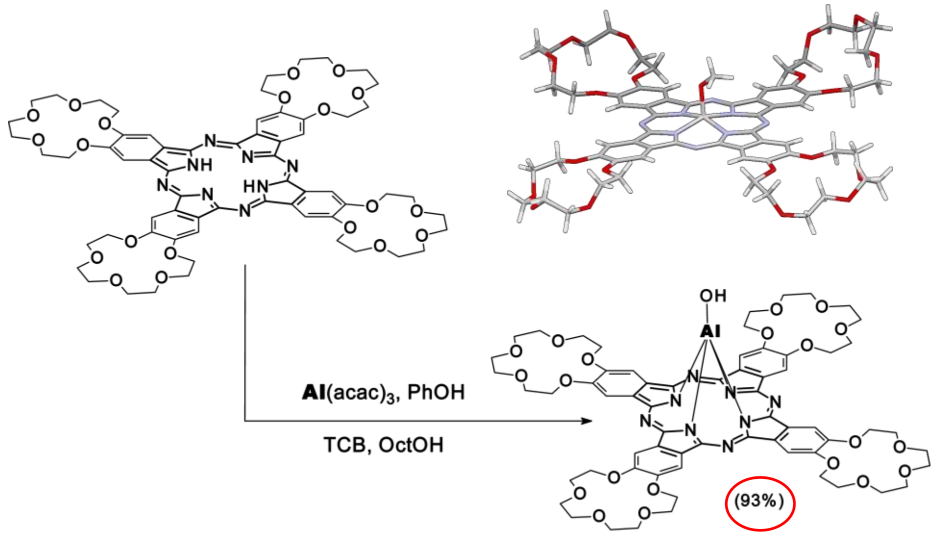

(93%)

Luminescent properties of [(15C5)$_4$Pc]Al(OH)

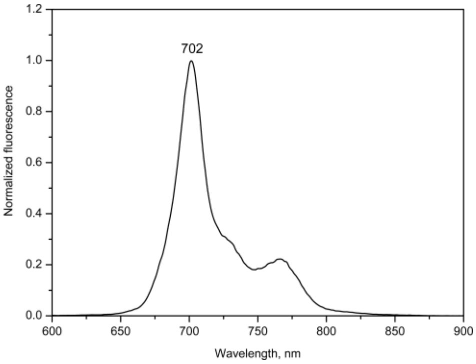

The emissive ability of **1** in MeOH (λ_{em} = 688 nm) is of the same order that in CHCl$_3$ solutions.

The fluorescence of **1** in DMSO (λ_{em} = 702 nm) is almost twice as large, probably due to possible coordination of DMSO molecules as axial ligands to aluminum leading to [(15C5)$_4$Pc]Al(DMSO)$_2$(OH).

The process of solvent coordination prevents aggregation of complex.

Interaction of [(15C5)$_4$Pc]Al(OH) with NaF in CHCl$_3$ (UV-vis)

CHCl$_3$

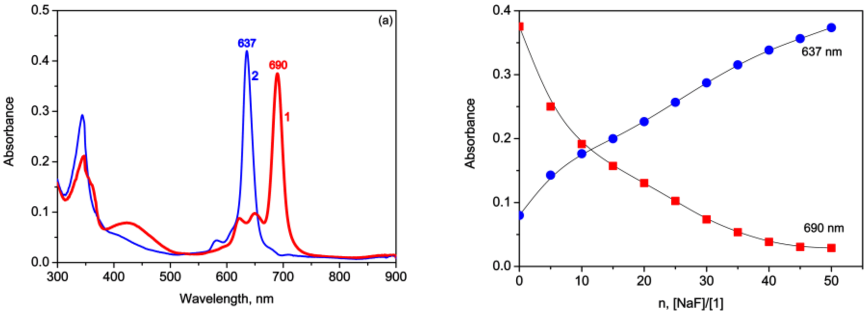

(a) Absorption spectra of [(15C5)$_4$Pc]Al(OH) in CHCl$_3$ (1), after adding NaF (2);

(b) dependence of absorbance of the Q (0,0) band maximum **1** in CHCl$_3$ and at 637 nm on n = [NaF]/[(15C5)$_4$Pc]Al(OH).

Interaction of $[(15C5)_4Pc]Al(OH)$ with NaF in $CHCl_3$ (fluorescence)

$CHCl_3$

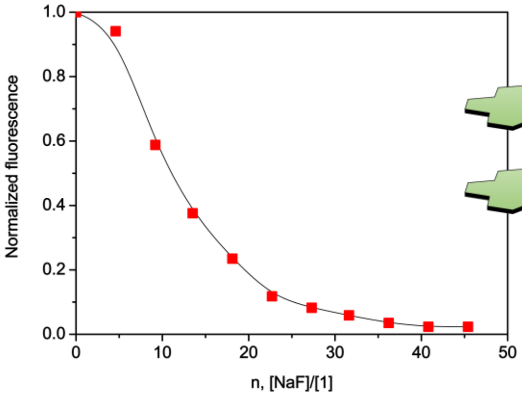

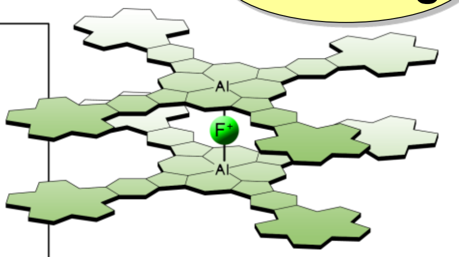

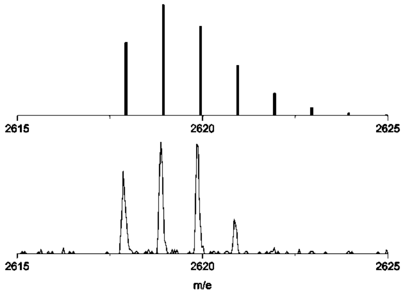

Normalized fluorescence for titration of solution of $[(15C5)_4Pc]Al(OH)$ in $CHCl_3$ with NaF.

Interaction of $[(15C5)_4Pc]Al(OH)$ with NaF or NaOH in DMSO (UV-vis)

DMSO

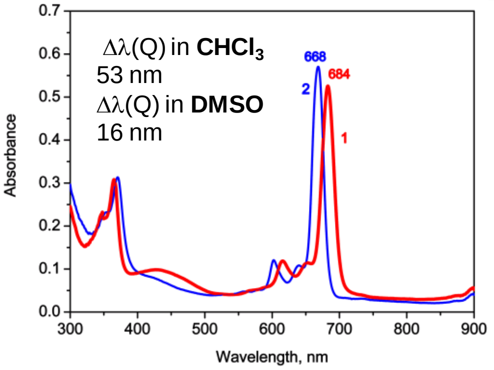

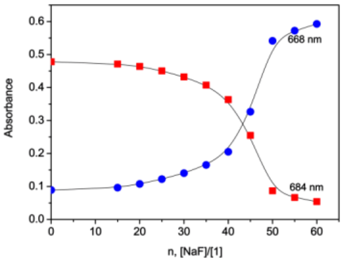

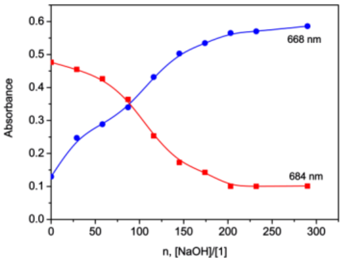

(a) Absorption spectra of $[(15C5)_4Pc]Al(OH)$ in DMSO (1), after adding NaF (NaOH) (2);
(b) dependence of absorbance of the Q(0,0) band maximum of $[(15C5)_4Pc]Al(OH)$ in DMSO and at 668 nm on n = [NaF]/ $[(15C5)_4Pc]Al(OH)$;
(c) dependence of absorbance of the Q(0,0) band maximum of $[(15C5)_4Pc]Al(OH)$ in DMSO and 668 nm on n = [NaOH]/ $[(15C5)_4Pc]Al(OH)$.

Interaction of $[(15C5)_4Pc]Al(OH)$ with NaF in DMSO (fluorescence)

DMSO

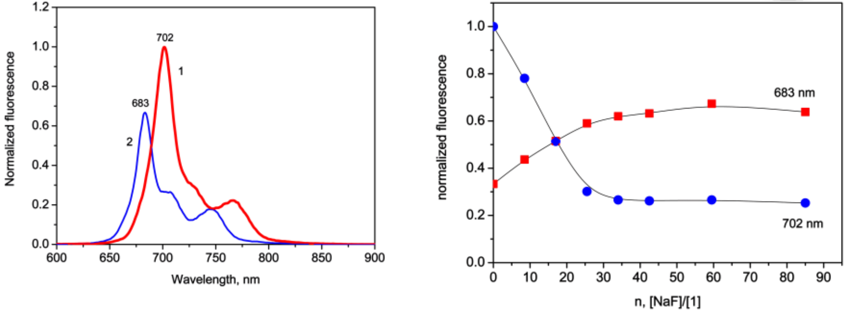

(a) Fluorescent spectra of $[(15C5)_4Pc]Al(OH)$ in DMSO (1), after adding NaF (2) ;
(b) normalized fluorescence for the titration of solution of $[(15C5)_4Pc]Al(OH)$ in DMSO with NaF.

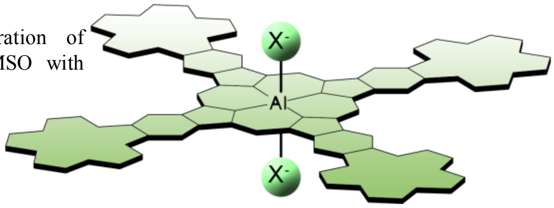

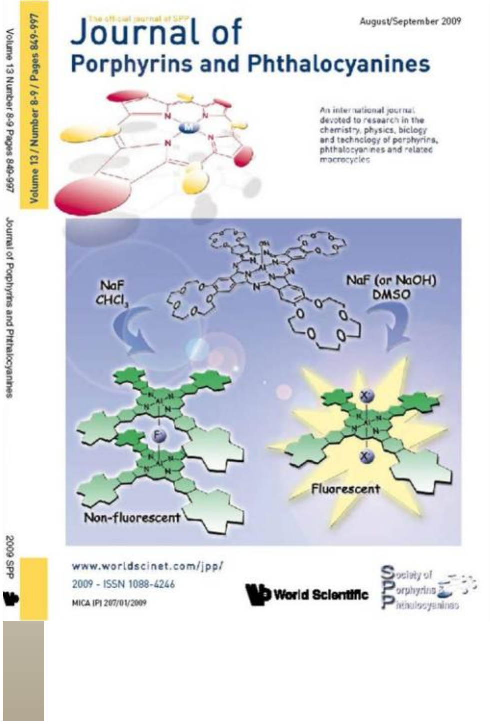

Volume 13 Number 8-9 Pages 849-997

Volume 13 / Number 8-9 / Pages 849-997

The official journal of SPP

Journal of Porphyrins and Phthalocyanines

August/September 2009

An international journal devoted to research in the chemistry, physics, biology and technology of porphyrins, phthalocyanines and related macrocycles

Journal of Porphyrins and Phthalocyanines

www.worldscinet.com/jpp/
2009 - ISSN 1088-4246
MICA (P) 207/01/2009

World Scientific

Society of Porphyrins & Phthalocyanines

2009 SPP

Selective sensor for the recognition of F^- and OH^- anions in organic media

L. Lapkina, A.Tsivadze,
Yu.Gorbunova.
J. Porphyrins Phthalocyanines,
2009, v.13

What to do?

I	II
Institutes of RAS are the founders of start-up companies.	Institutes of RAS are partners of start-up companies.
+ No	+ Good inroads to Skolkovo project
– Only intellectual properties (patents) are possible contributed stock	– No

Thank you for your kind attention!

Heterogeneised crown-ethers type ligands for isotope fractionation

The main purpose of the project is to identify factors affecting the coefficient of separation of isotopes by chemical exchange.
This will be carried out processes of isotope separation of Zn, Gd and Ca in systems with crown ethers of different structure.
- Choosing of the most effective extraction systems and study their characteristics. (2012)
- Selection of the method of extraction chromatography multiplying of the isotope effect. (2012)
- Determination of the coefficient of isotope separation and the influence on it various factors. (2013)
- Immobilization of crown ethers (oxa, oxa-aza, aza) on adsorbents. The main emphasis of the work will be to determine the adsorption behaviour of organic chelating agents on Amberlite XAD resins and to apply chelating agent impregnated XAD resins to the isotope separation. (2012)
- Synthesis of reactive crown ethers and preparation of chelating materials bearing crown ethers (oxa, oxa-aza, aza). Organic or hybrid organic/inorganic supports will be considered taking into account the control of the properties of the chelating materials and their characterisation. (2012/2013)

Prof. W. Kunz giving invited lecture at the 7th European Summer School 22 July 2012

Prof. S.N. Kolmykov, academician B.F. Myasoedov, Prof. T. Reich, Dr. Kolomiez, Prof. V.E. Baulin, academician A.Yu.Tsivadze, Prof. W. Kunz during the coffe-break in IPCE RAS 21 July, 2012

"Organic Chemistry with Visible Light: Luminescent Chemosensors and Chemical Photocatalysts".

Burkhard Koenig (Regensburg, Germany)

Invited lecture

Trilateral seminar on supramolecular, intermolecular, interaggregate interactions and separation chemistry, IPCE RAS, Moscow, Russian Federation

20.-23.07.2012

Organic Chemistry with Visible Light: Luminescent Chemosensors and Chemical Photocatalysts

Burkhard König

Universität Regensburg

Universität Regensburg

Burkhard König
Department of Chemistry and Pharmacy

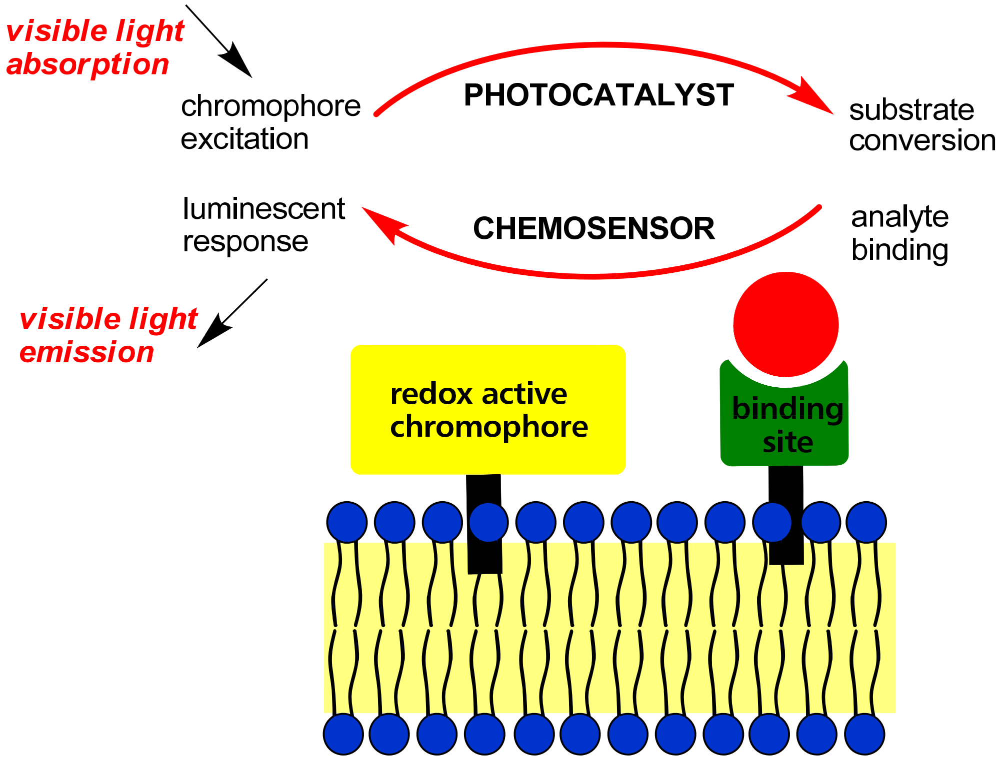

visible light absorption

chromophore excitation

PHOTOCATALYST

substrate conversion

luminescent response

CHEMOSENSOR

analyte binding

visible light emission

Molecular binding site + dye = chemosensor !

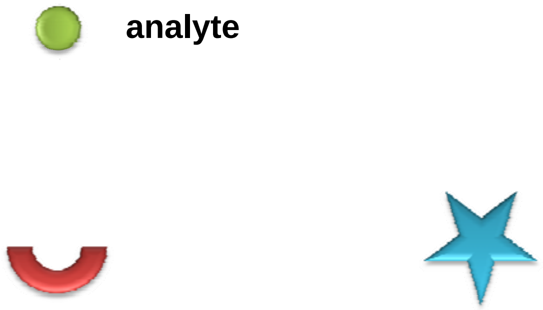

analyte

Selectivity ?
Affinity ?

binding site

reporter dye

Molecular binding site + dye = chemosensor !

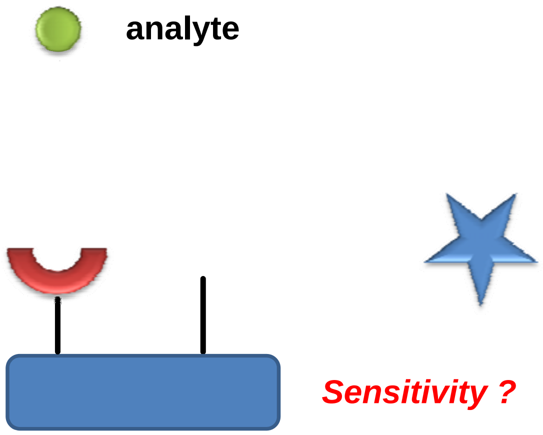

analyte

binding site

reporter dye

Sensitivity ?

Reversible coordinative bonds

HSAB-guided selectivity

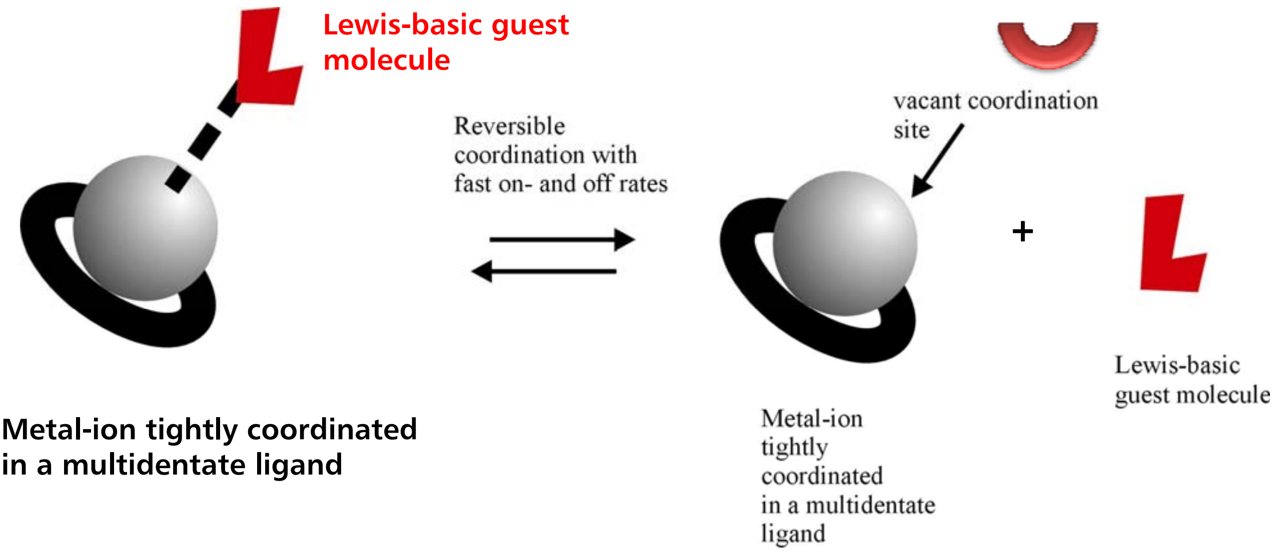

Metal-ion tightly coordinated in a multidentate ligand

Use of reversible coordinative bonds in molecular recognition:
M. Kruppa, BK, *Chem. Rev*. **2006**, *106*, 3520

Reversible coordinative bonds

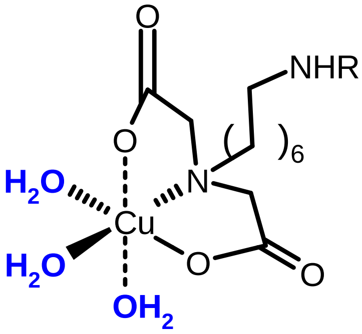

Copper imido diacetato (IDA) complex
binds histidine and pyrophosphate

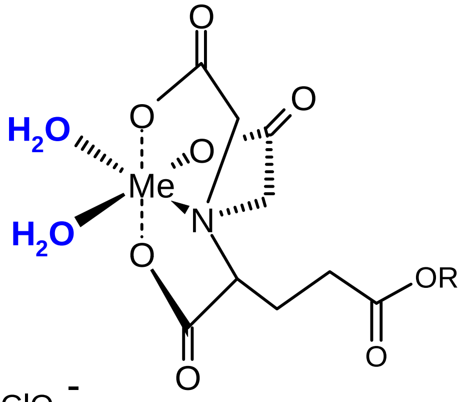

Nitrilo triacetato (NTA) metal complex
binds histidine

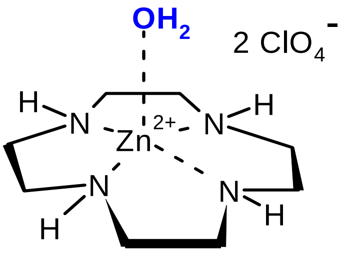

Zinc-cyclen complex
binds phosphates and imides

Dipeptide Chemosensors

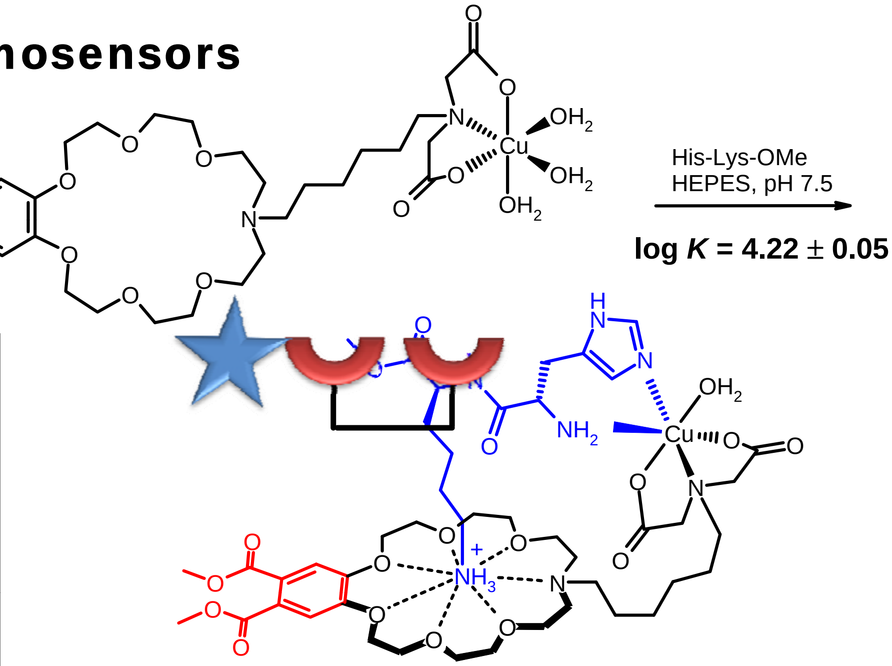

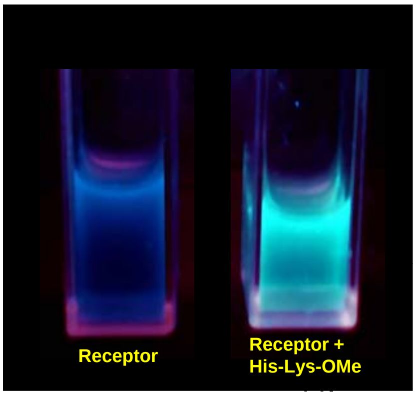

Kruppa, C. Mandl, S. Miltschitzky, BK *J. Am. Chem. Soc.* **2005**, *127*, 3362;
A. Riechers, S. Stadlbauer, A. Späth, BK, *Chem. Eur. J.* **2008**, *14*, 2536;
A. Grauer, A. Riechers, S. Ritter, BK, *Chem. Eur. J.* **2008**, *14*, 8922.

SDS PAGE Phosphoprotein staining

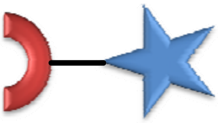

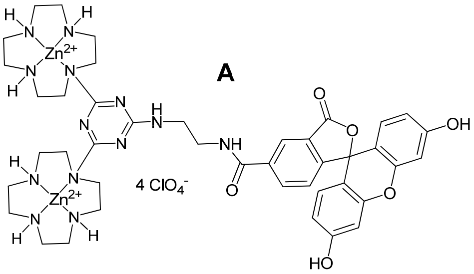

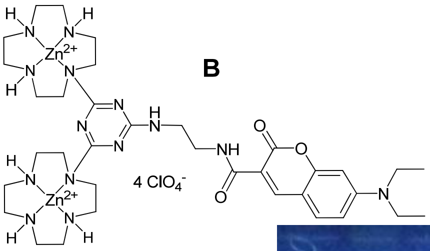

Marie-Curie ITN
www.chebana.eu

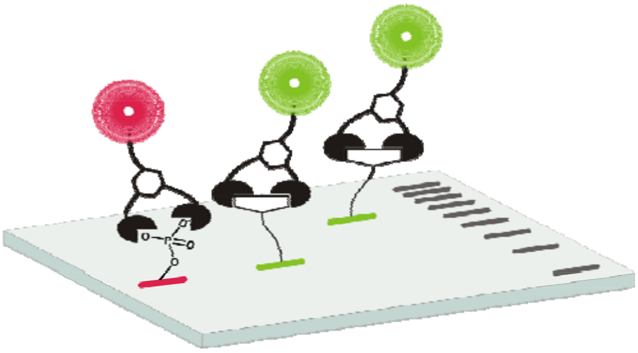

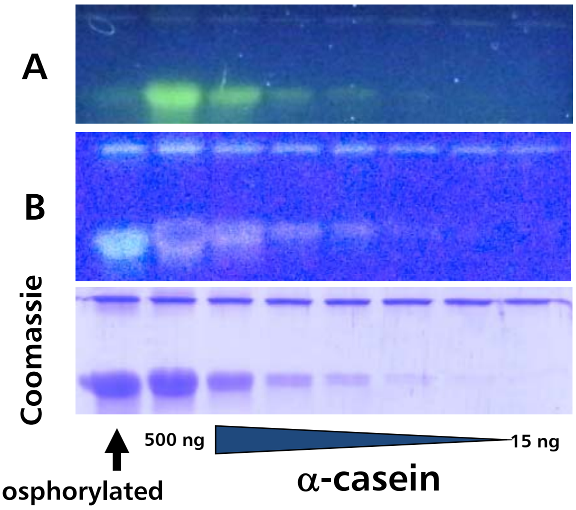

A. Riechers, F. Schmidt, S. Stadlbauer, BK,
Bioconj. Chem. **2009**, *20*, 804–807;
patent pending.

Photochromic enzyme inhibitor

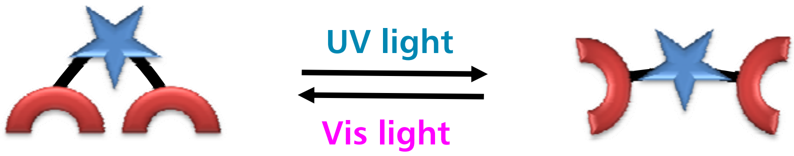
UV light

Vis light

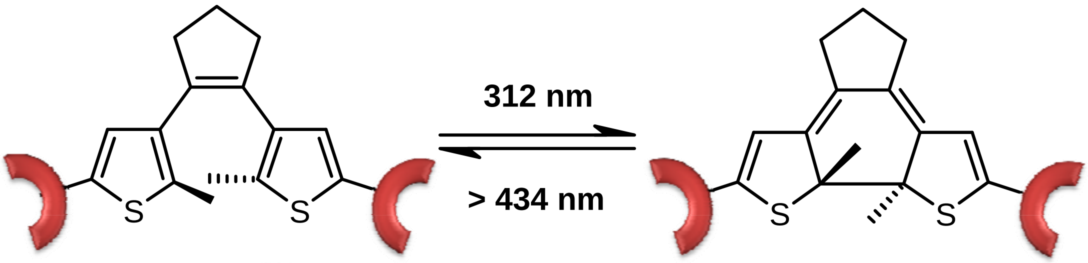
312 nm

> 434 nm

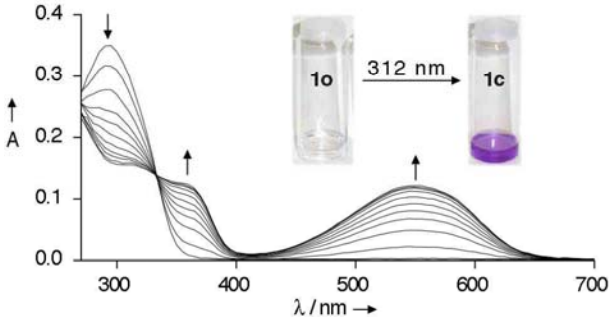

Photochromic enzyme inhibitor

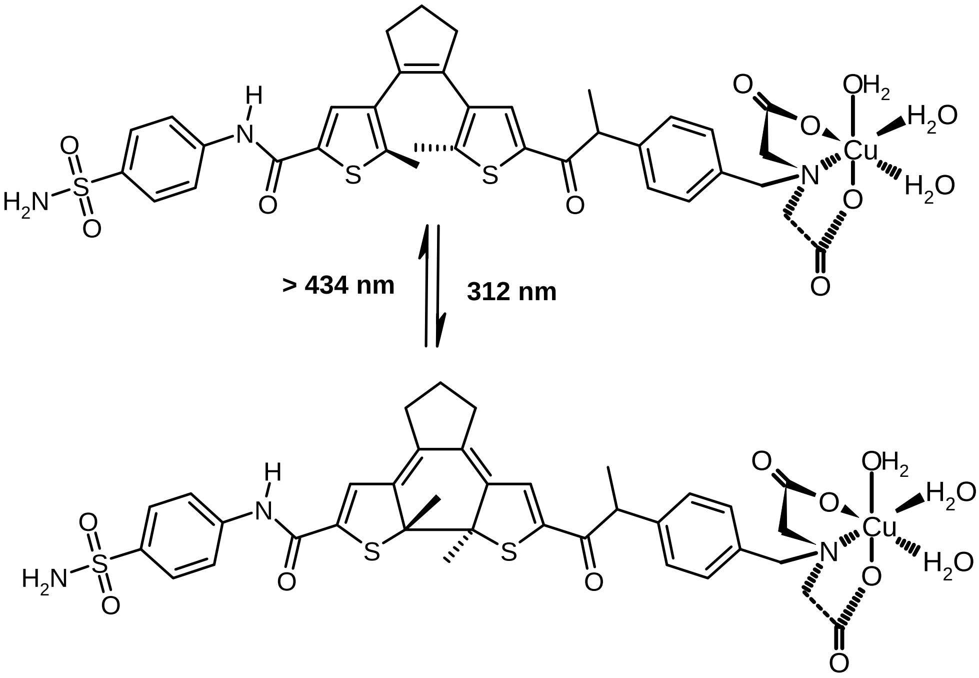
> 434 nm

312 nm

D. Vomasta, C. Högner, N. R. Branda, BK, *Angew. Chem. Int. Ed.* **2008**, 47, 7644;
D. Vomasta, A. Innocenti, BK, C. T. Supuran, *Bioorg. Med. Chem. Lett.* **2009**, *19*, 1283.

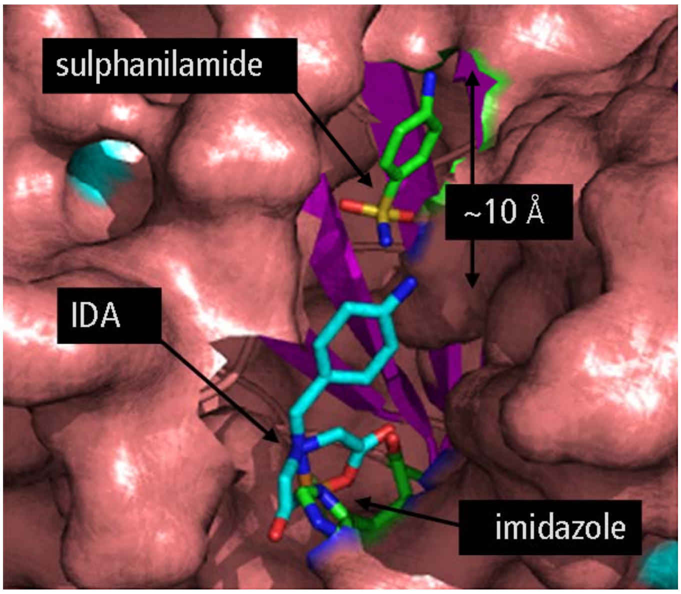

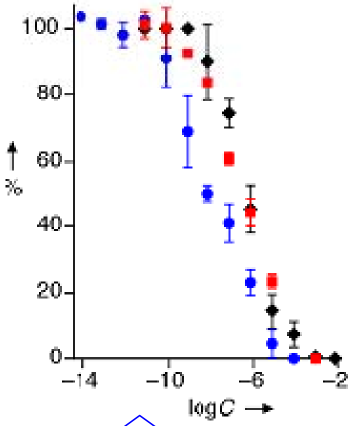

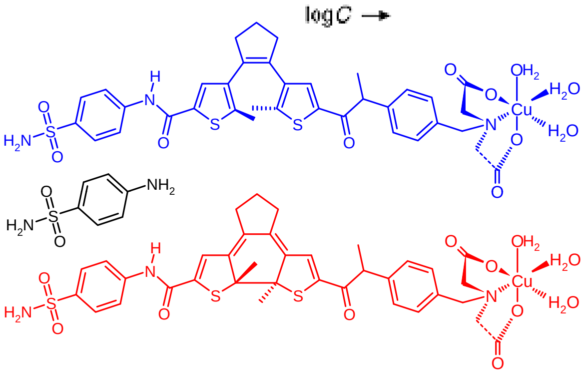

Human Carbonic Anhydrase I

$$CO_2 + H_2O \rightleftharpoons H_2CO_3$$

D. Vomasta, C. Högner, N. R. Branda, BK, *Angew. Chem. Int. Ed.* **2008**, 47, 7644.

Assembly of binding sites in membranes

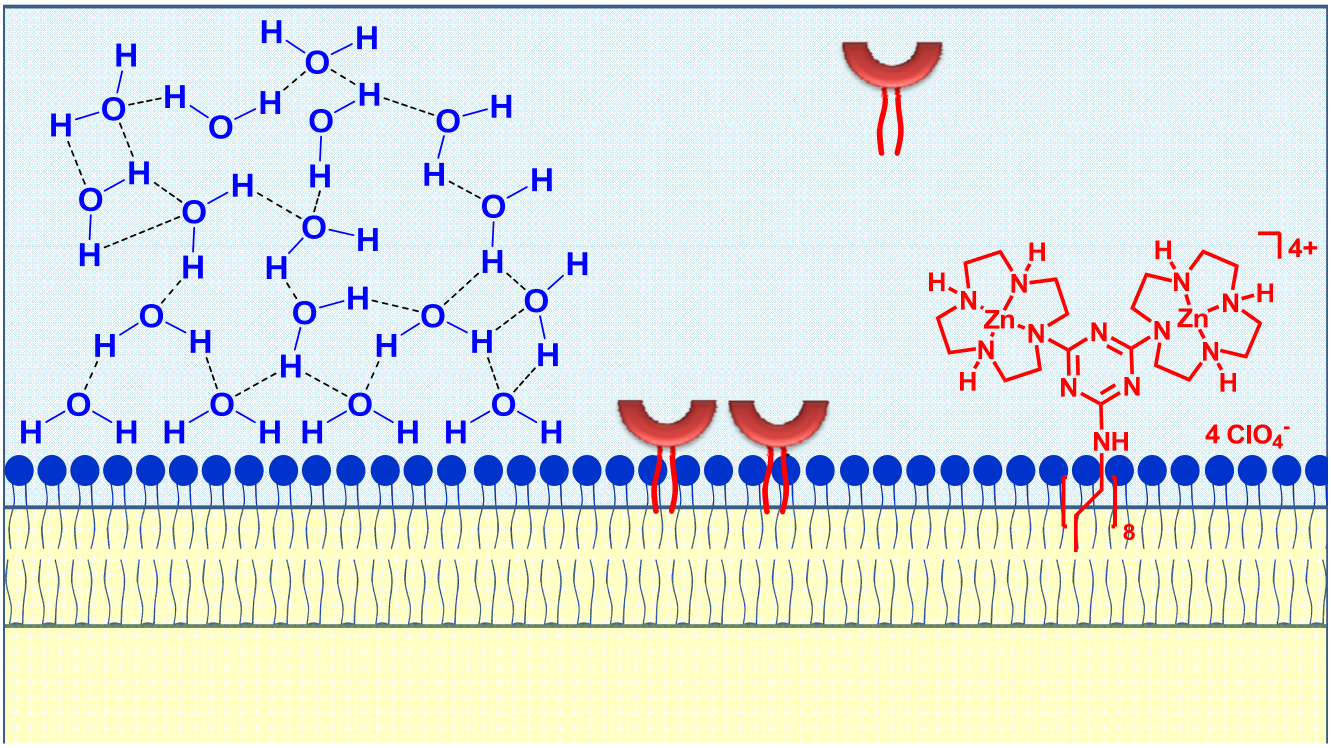

Co-embedding of binding site and dye . . .

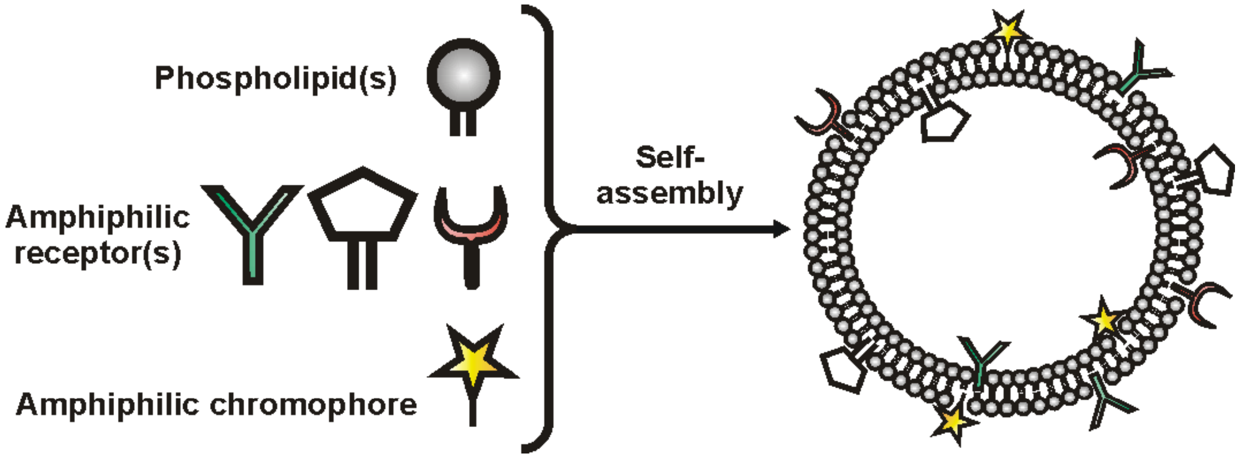

B. Gruber, S. Stadlbauer, A. Späth, S. Weiss, M. Kalinina, BK, *Angew. Chem*. **2010**, *49*, 7125.

.... facilitates quick optimization of properties

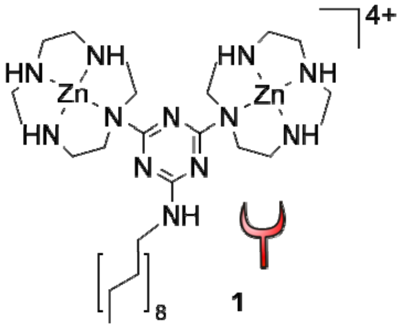
1

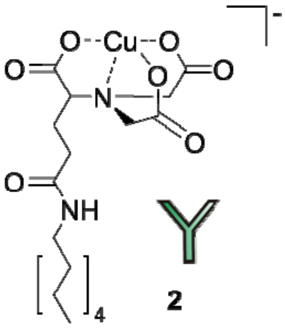
2

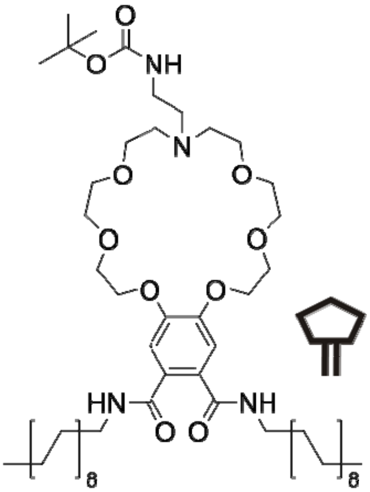
3

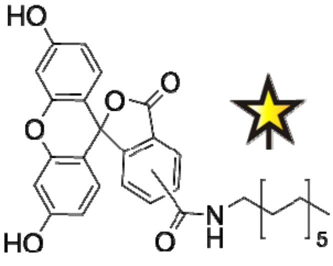
4

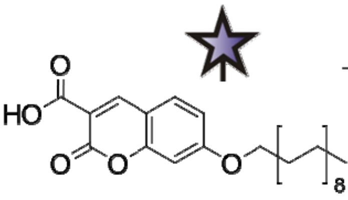
5

B. Gruber, S. Stadlbauer, A. Späth, S. Weiss, M. Kalinina, BK, *Angew. Chem*. **2010**, *49*, 7125.

Sensory mechanism

Mixed domains of receptors and dyes formed during assembly

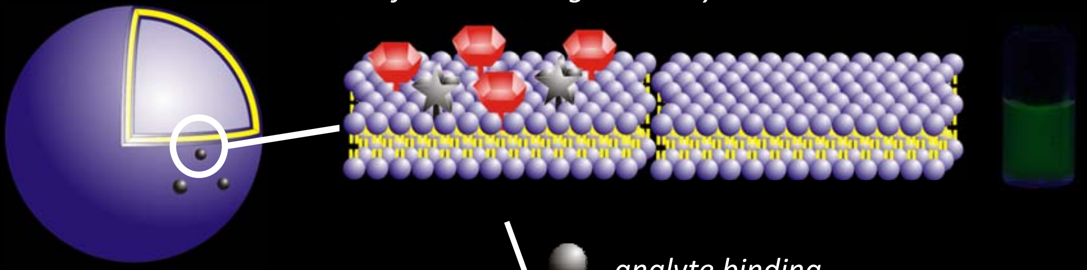

analyte binding

emission “on”

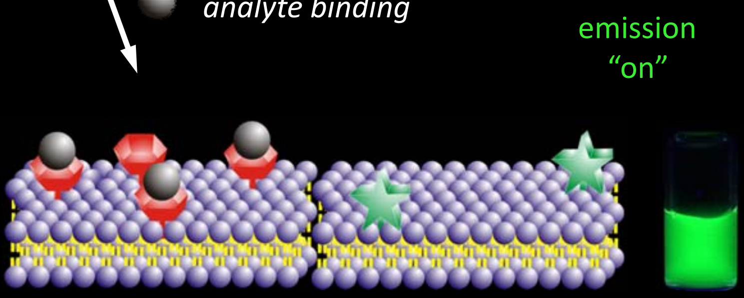

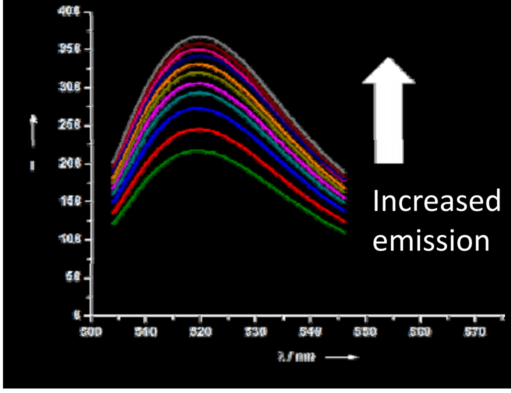

Increased emission

reporter dye is extruded out of the membrane domains

Sensory mechanism

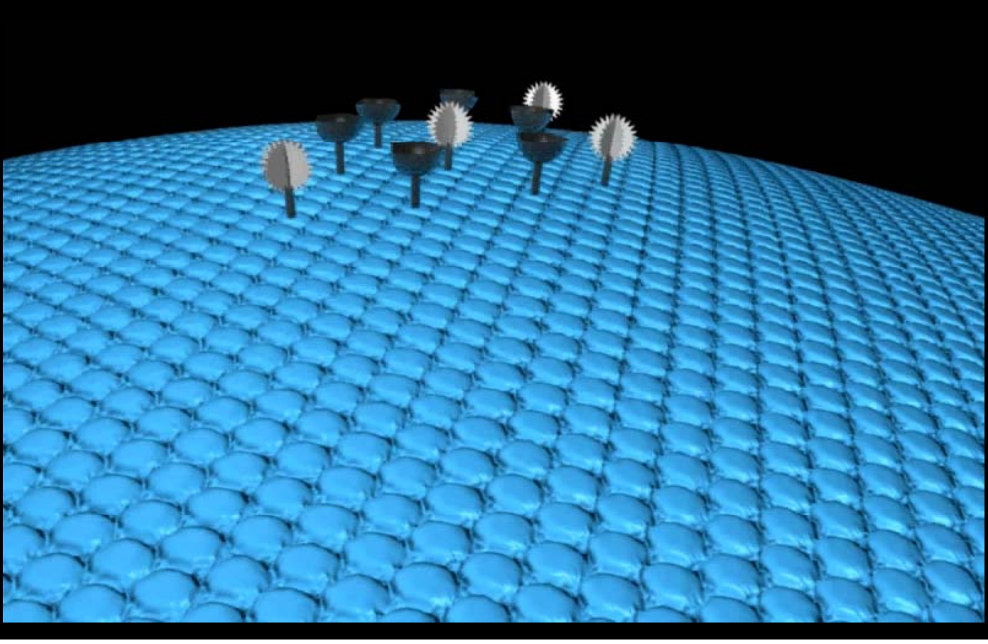

Analyte induced arrangement of receptors

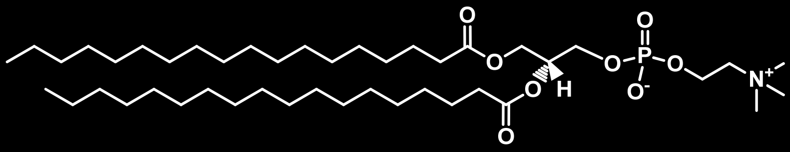

Vesicle membrane:

DSPC

T_M = 54 °C

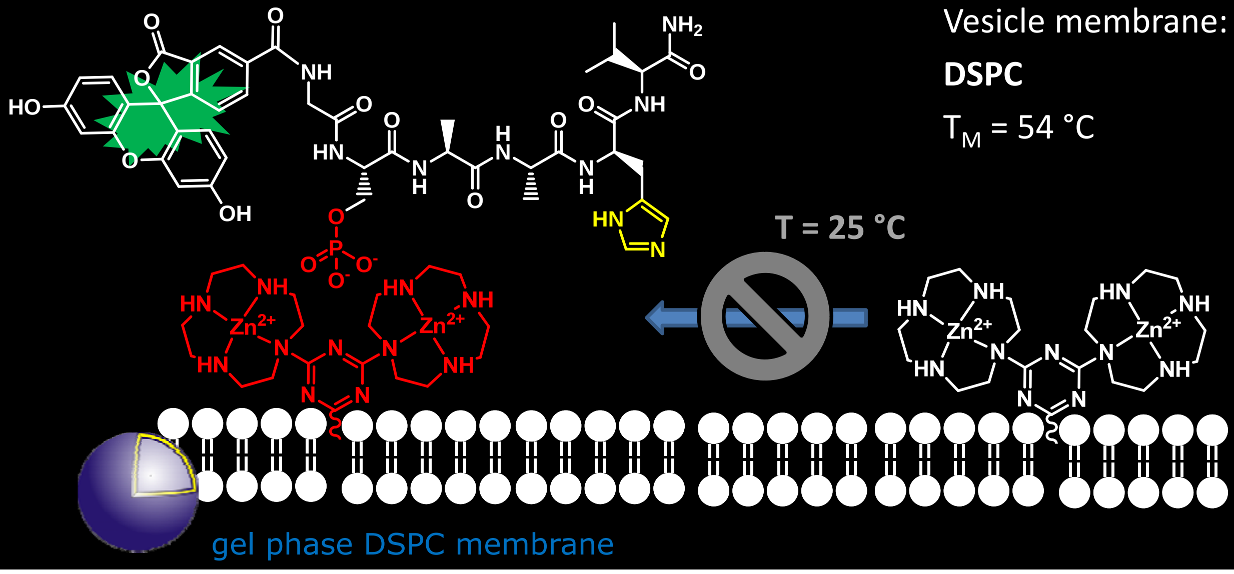

T = 25 °C

gel phase DSPC membrane

Analyte induced arrangement of receptors

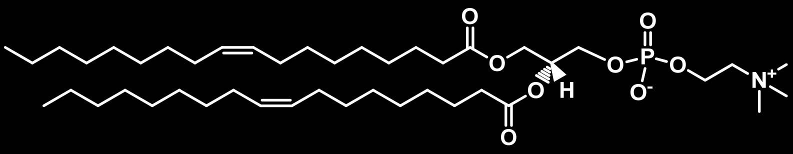

Vesicle membrane:

DOPC

T_M = -20 °C

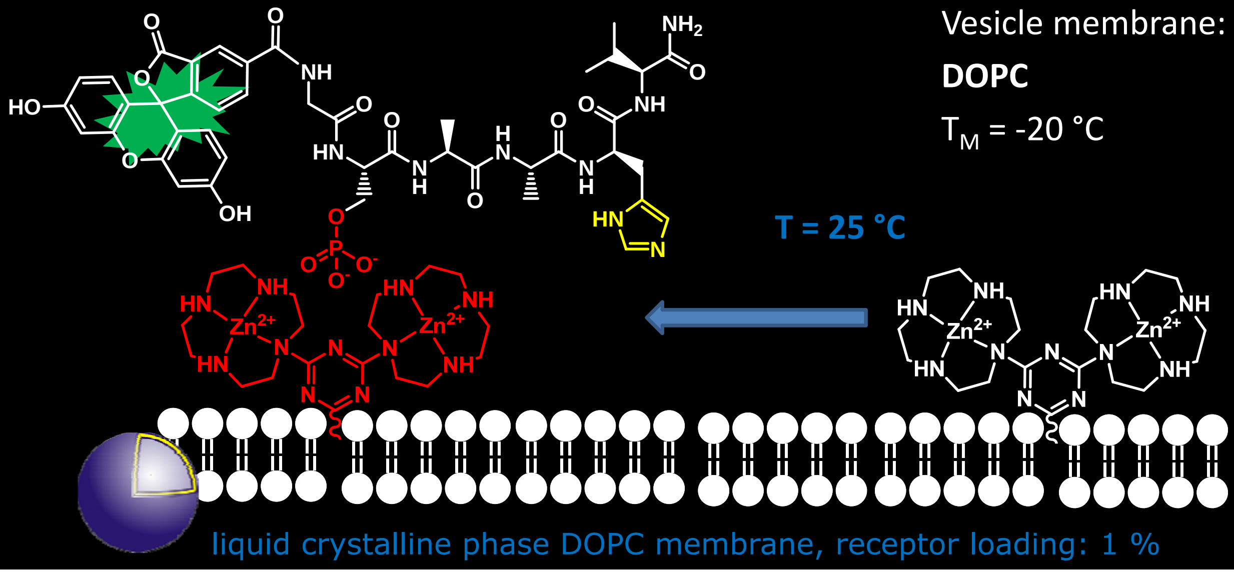

T = 25 °C

liquid crystalline phase DOPC membrane, receptor loading: 1 %

Analyte induced arrangement of receptors

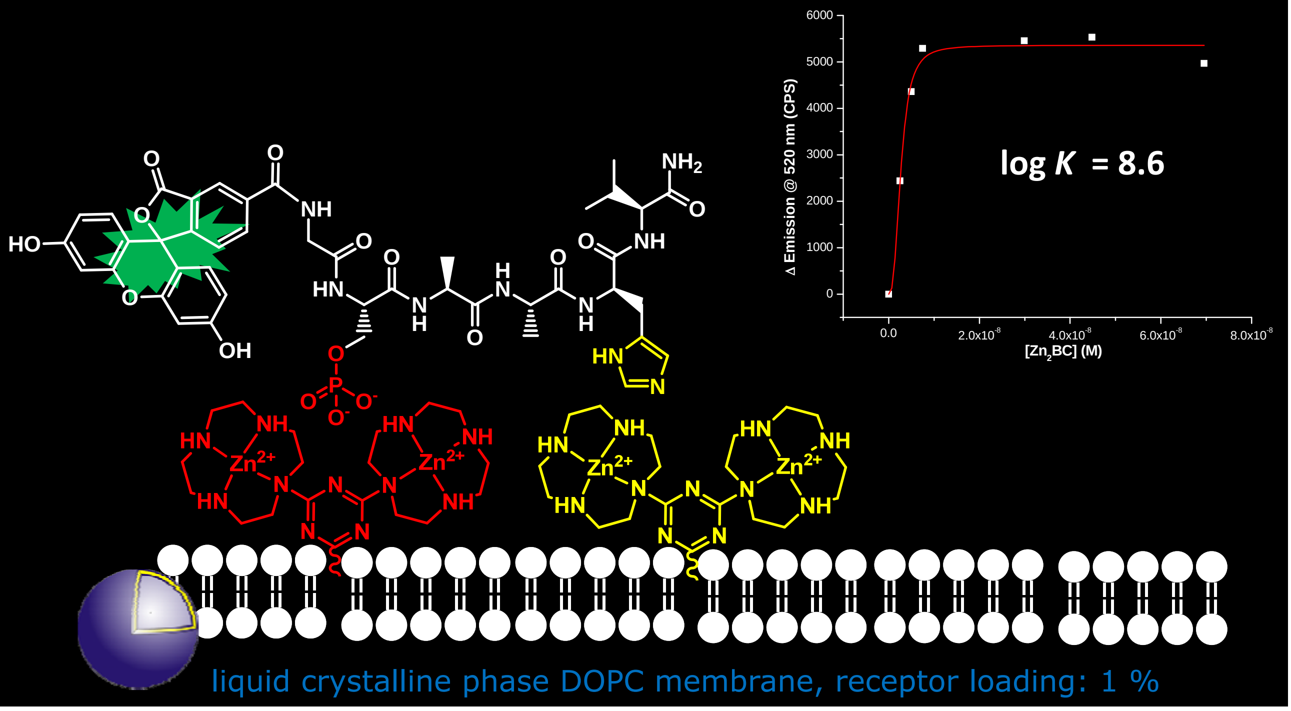

liquid crystalline phase DOPC membrane, receptor loading: 1 %

Burkhard König
Department of Chemistry and Pharmacy

Protein surfaces as templates – towards artificial antibodies

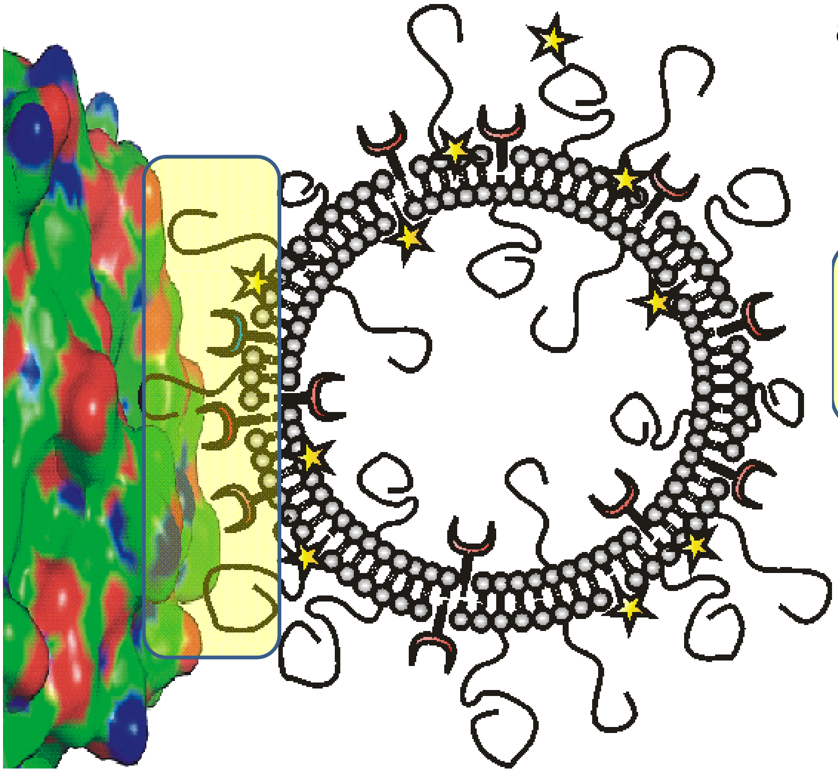

ordered interface
for
specific interaction

Catalysis at the interface

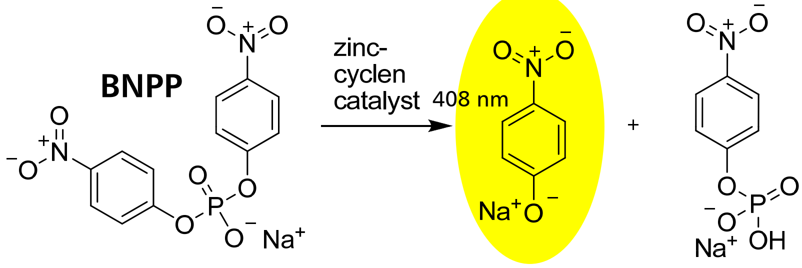

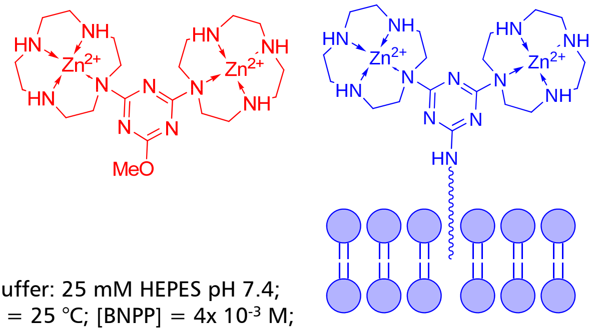

Buffer: 25 mM HEPES pH 7.4;
T = 25 °C; [BNPP] = 4x 10^{-3} M;
[Zn2+] = 5.5x10^{-6} M

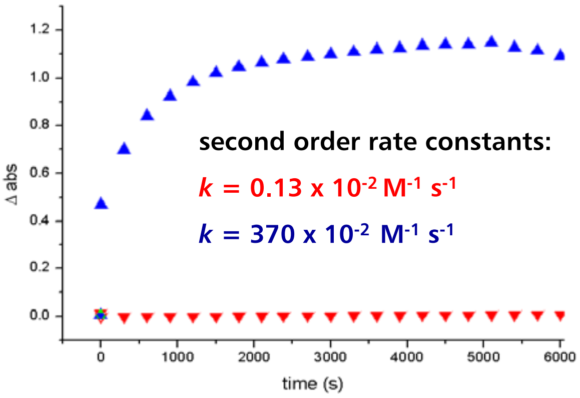

second order rate constants:

$k = 0.13 \times 10^{-2}\ M^{-1}\ s^{-1}$

$k = 370 \times 10^{-2}\ M^{-1}\ s^{-1}$

BK, M. Subat, K. Woinaroschy et al. *Inorg. Chem.* **2007**, *46*, 4336; M. Subat, K. Woinaroschy, C. Gerstl, B. Sarkar, W. Kaim, BK, *Inorg. Chem*. **2008**, *47*, 4661.

Catalysis at the interface

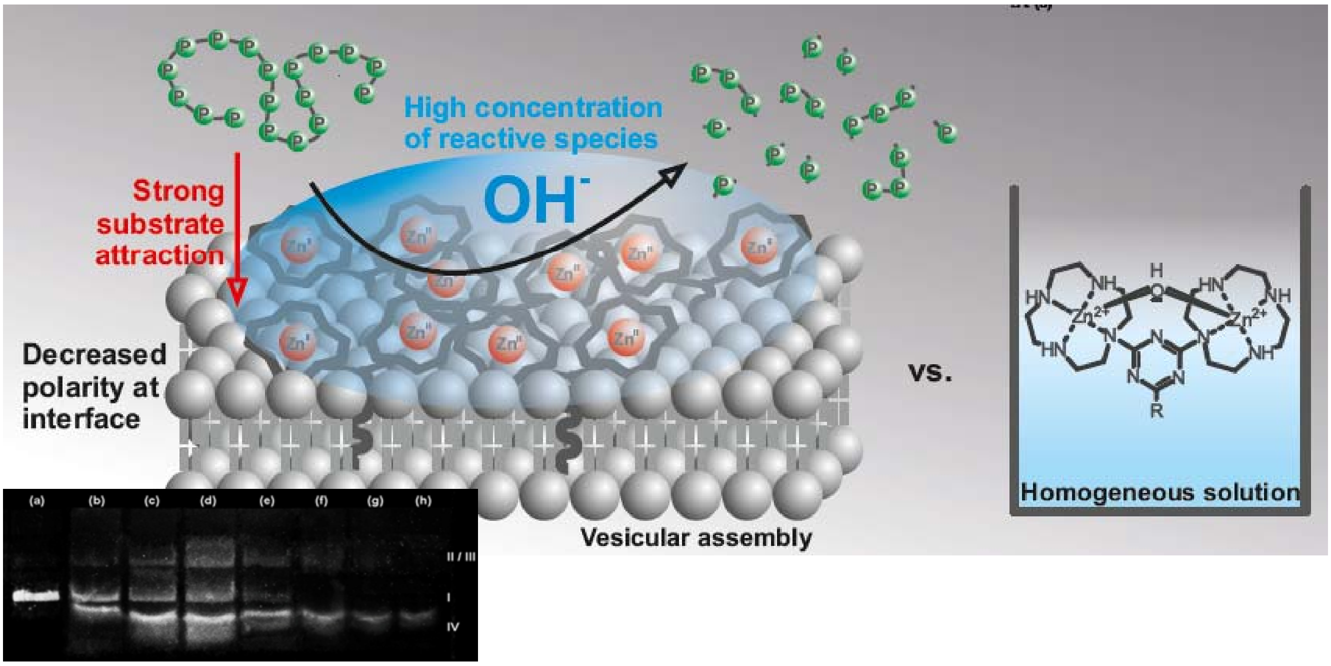

B. Gruber, S. Stadlbauer, E. Kataev, J. Aschenbrenner, BK, *J. Am. Chem. Soc*. **2011**, *133*, 20704.

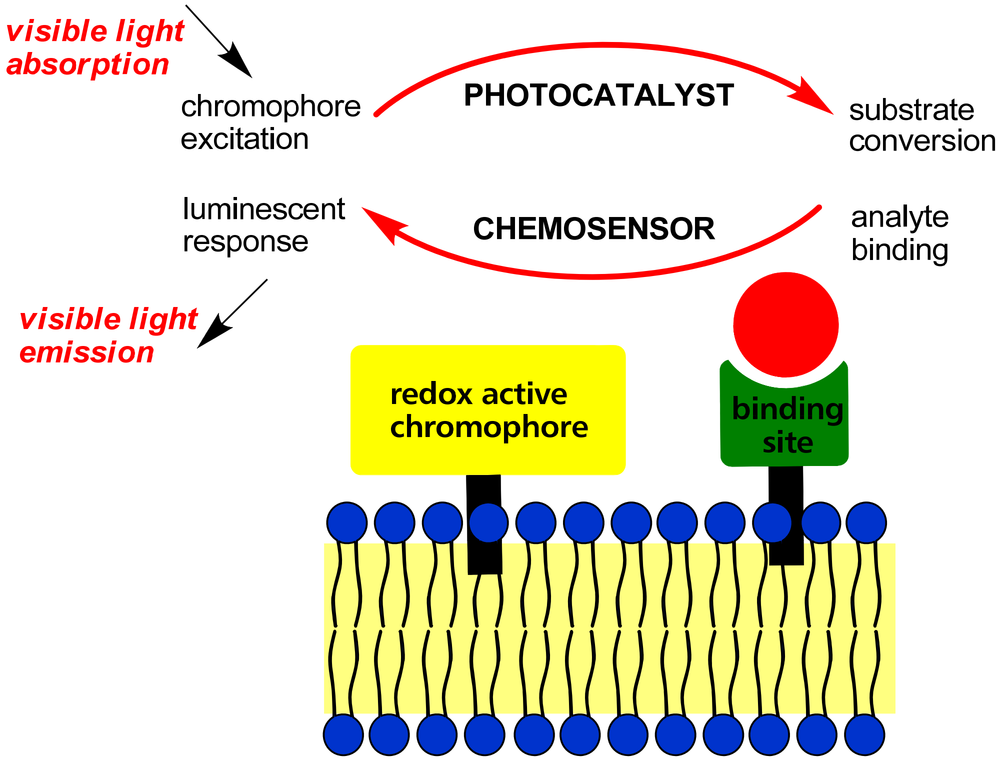

Visible light and chemistry

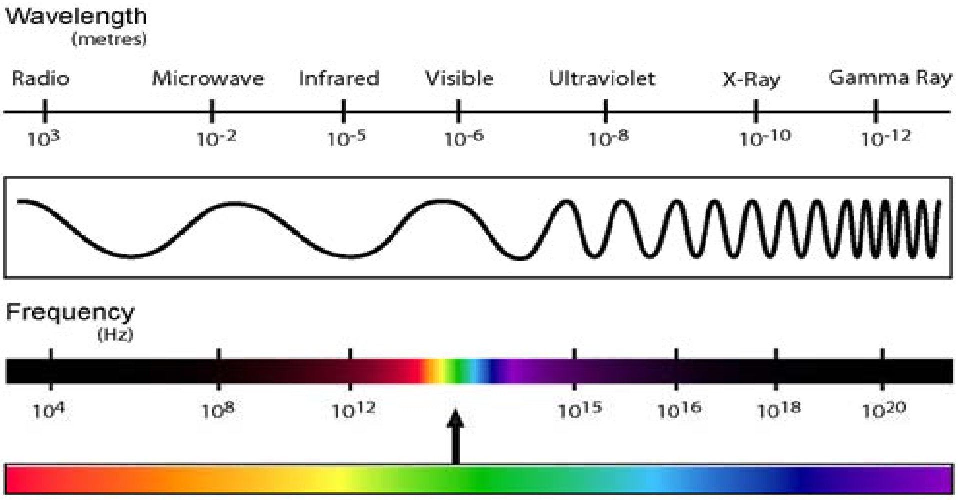

10^{-29}	10^{-24}	10^{-20}	10^{-16}	J
0.0000006	0.06	600	6.000.000	KJ/mol

C-C: 415 KJ/mol

C-O: 360 KJ/mol

Molecular binding site + dye = photocatalyst !

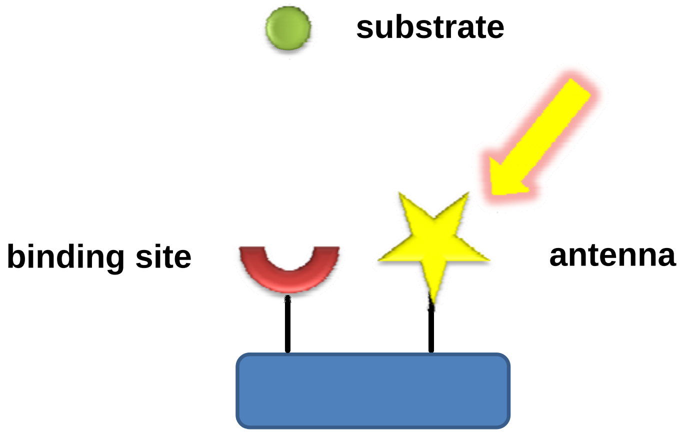

- Visible light for excitation of chromophore
- Close proximity of antenna chromophore and substrate binding site
- Control of reaction selectivity by catalyst binding site

Molecular binding site + dye = photocatalyst !

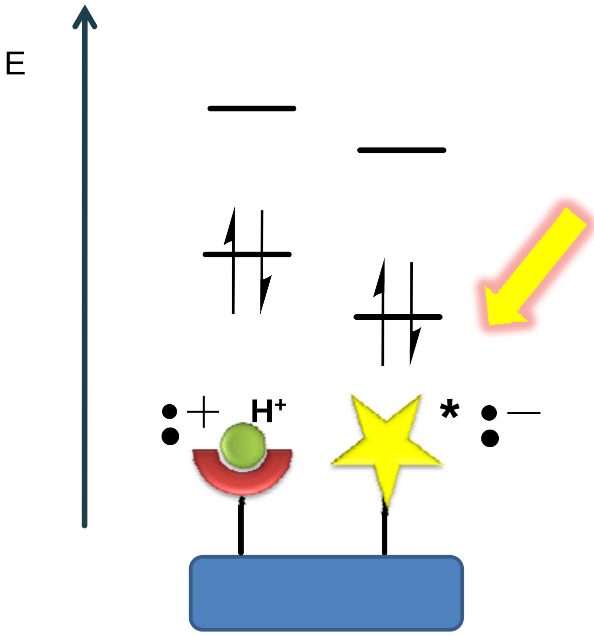

Reaction in photomicroreactor

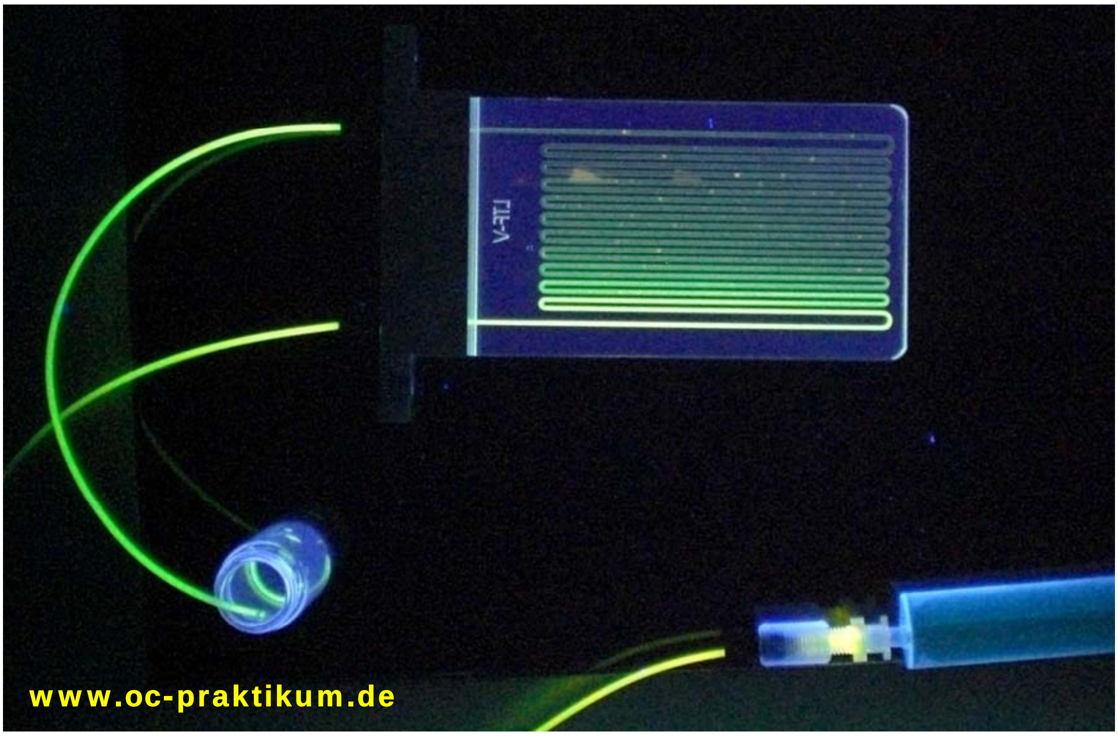

www.oc-praktikum.de

LED / solar cell-based quantum yield determination

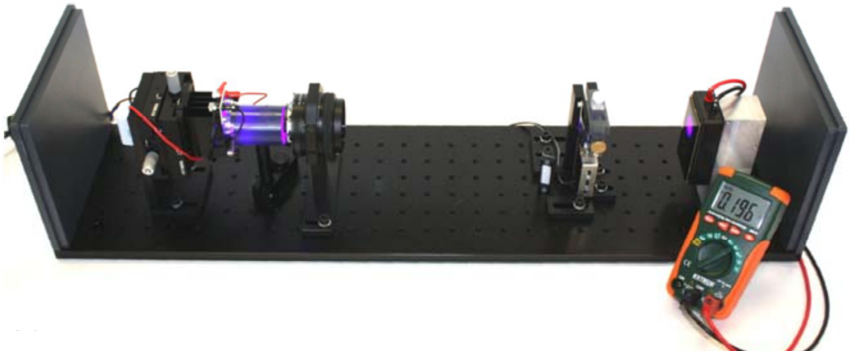

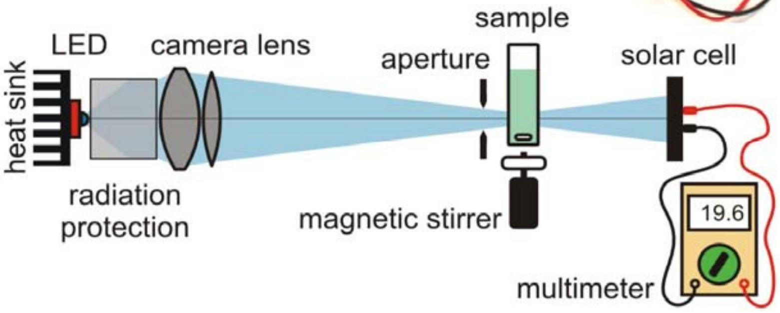

U. Megerle, R. Lechner, B. König, E. Riedle, *Photochem.Photobiol.Sci*. **2010**, *9*, 1400.

Photocatalytic reaction mechanisms

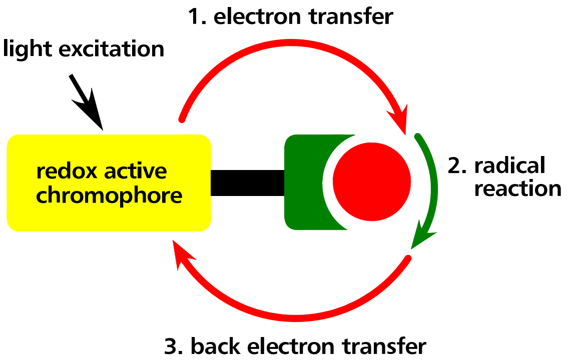

light excitation

1. electron transfer

redox active chromophore

2. radical reaction

3. back electron transfer

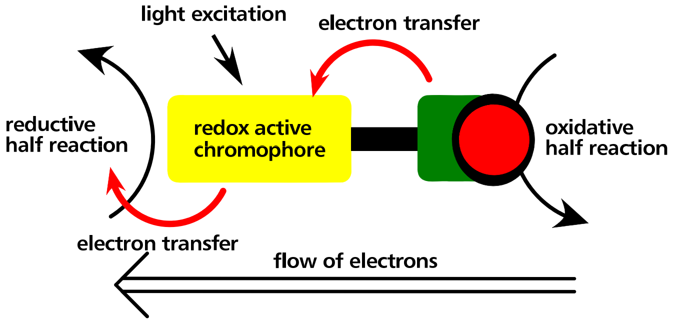

light excitation

electron transfer

reductive half reaction

redox active chromophore

oxidative half reaction

electron transfer

flow of electrons

Catalysis of chemical reactions by electrons

Coupling of two redox processes

Flavin photocatalysis

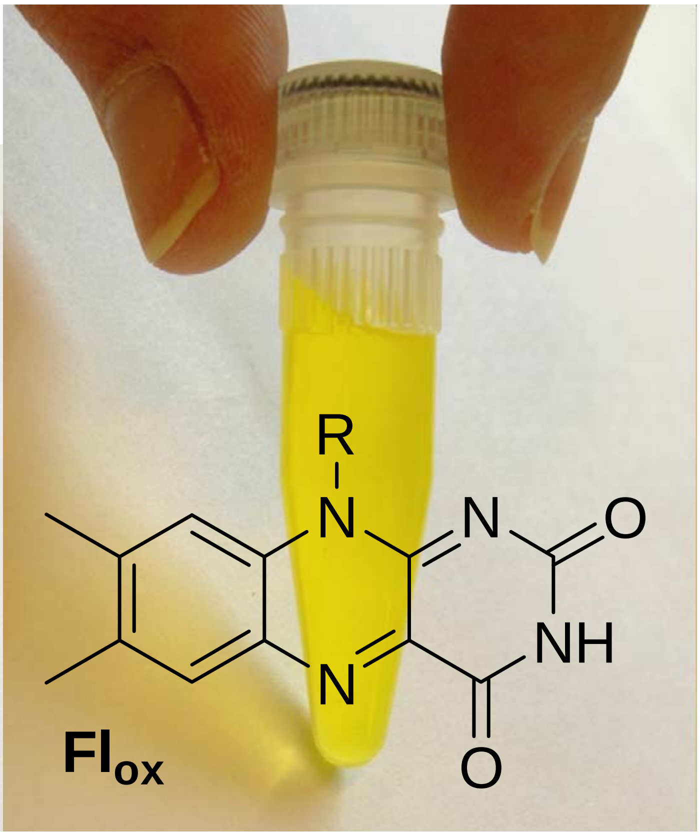

Fl_{ox}

Flavin redox states

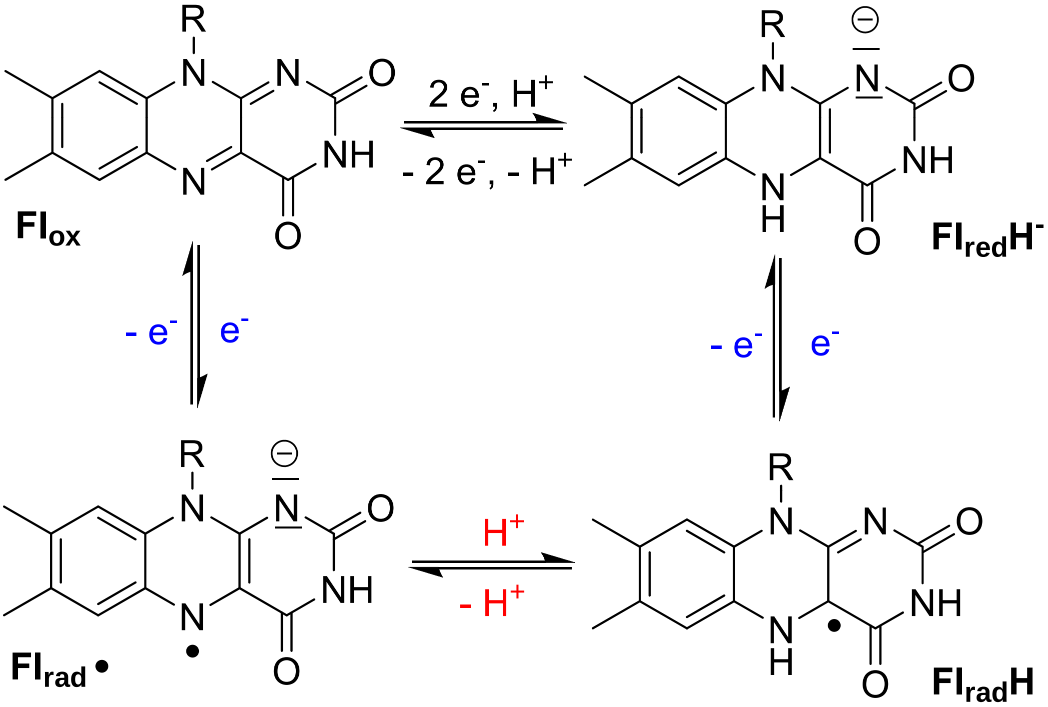

Blue light excitation

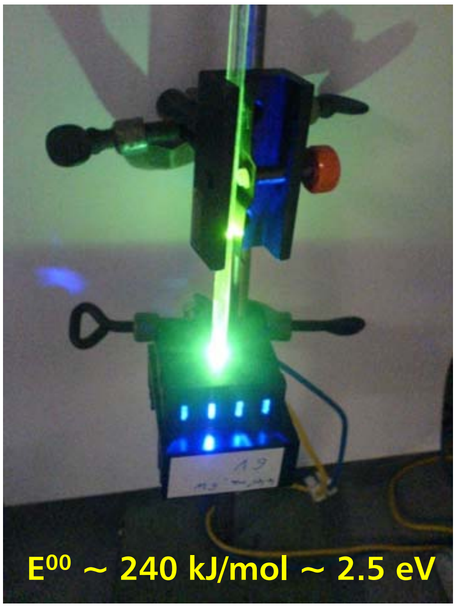

E^{00} ~ 240 kJ/mol ~ 2.5 eV

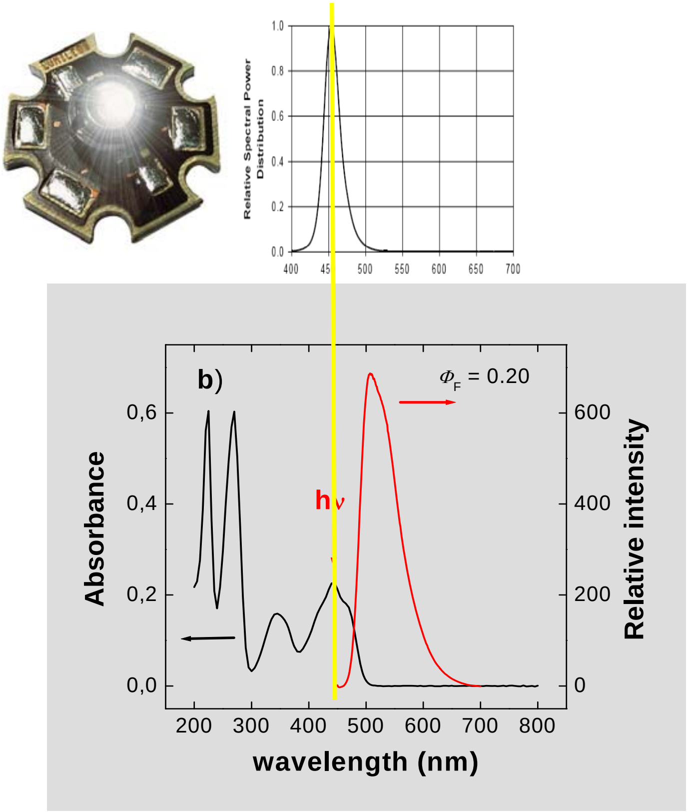

Immobilized flavins as photocatalysts

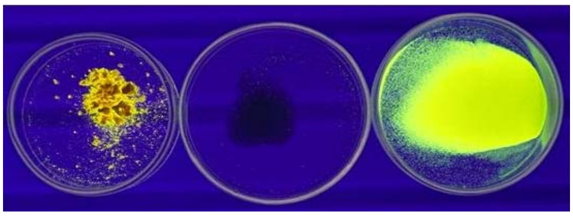

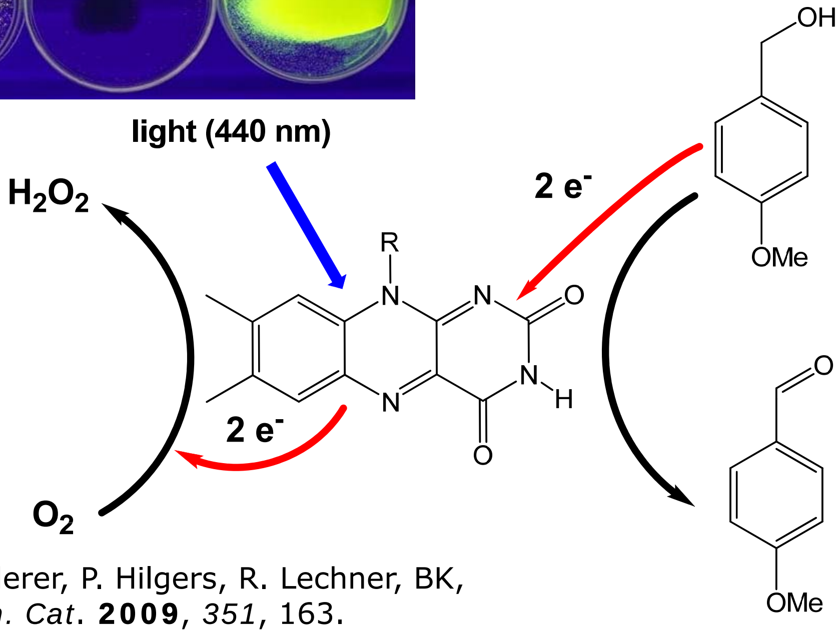

TOF > 800 h^{-1}

in water

2 mM aAlkohol,
10 mol% RFT,
Reaction time:
3 min

H. Schmaderer, P. Hilgers, R. Lechner, BK,
Adv. Synth. Cat. **2009**, *351*, 163.

Reaction mechanism

Only triplet chemistry
leads to products

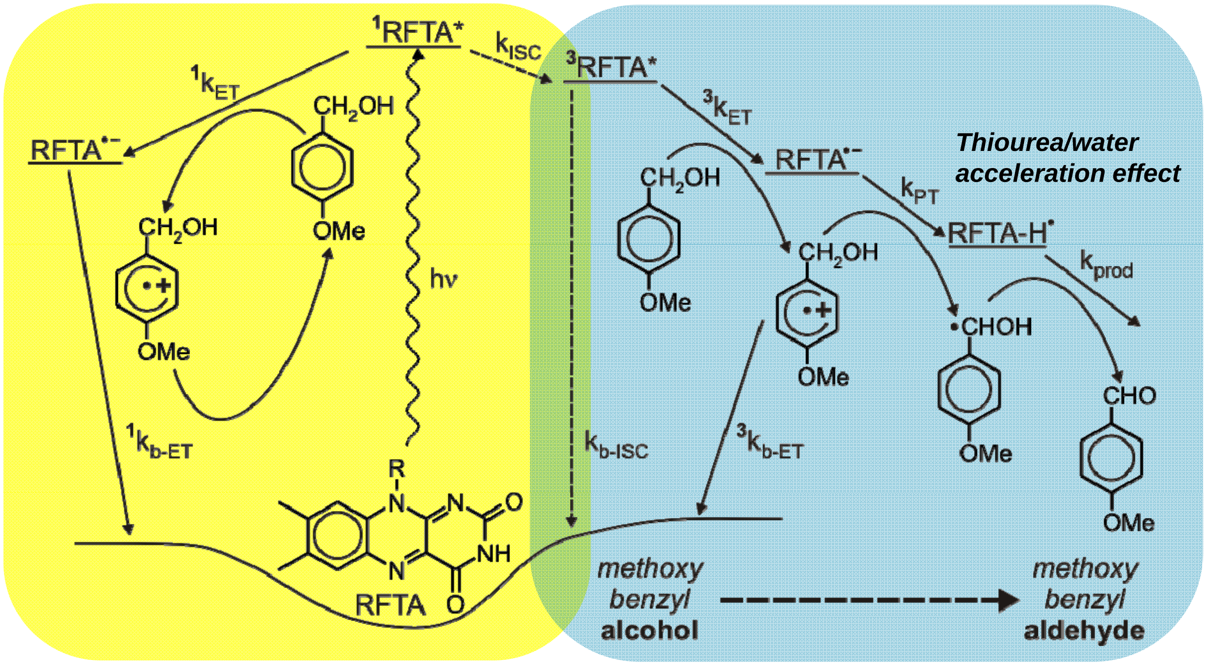

U. Megerle, M. Wenninger, R.-J. Kutta, R. Lechner, B. König, B. Dick, E. Riedle
Phys. Chem. Chem. Phys., **2011**, *13*, 8869.

Other flavin-mediated photooxidations

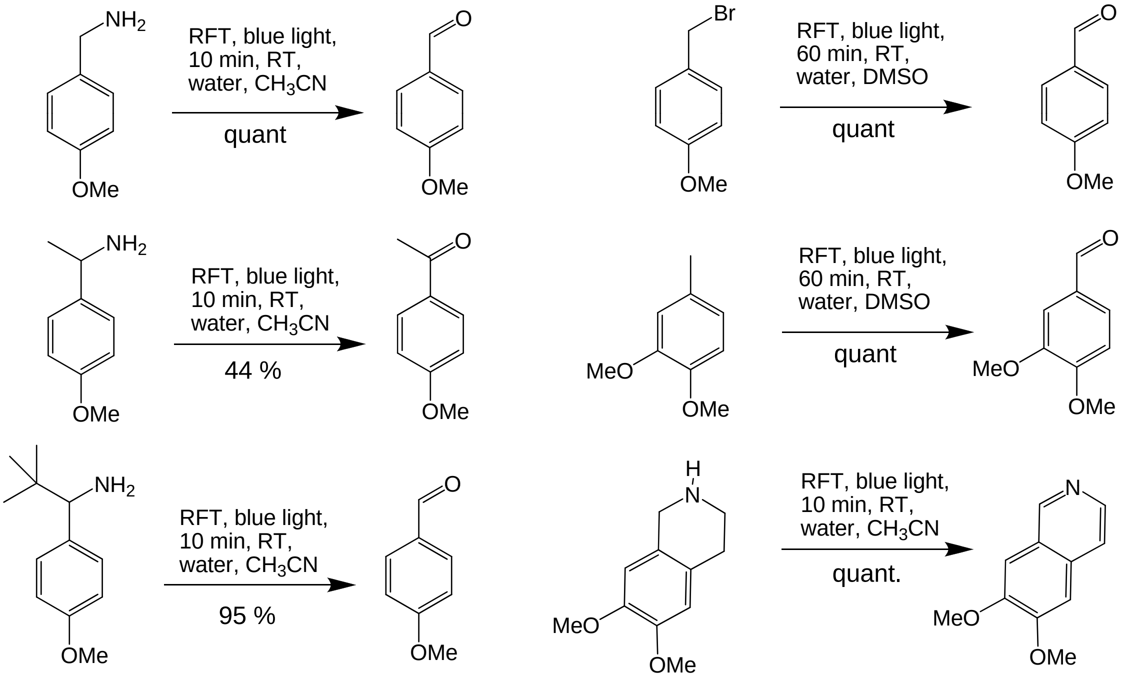

R. Lechner, BK, *Synthesis*, **2010**, 1712 - 1718.

Other flavin-mediated photooxidations

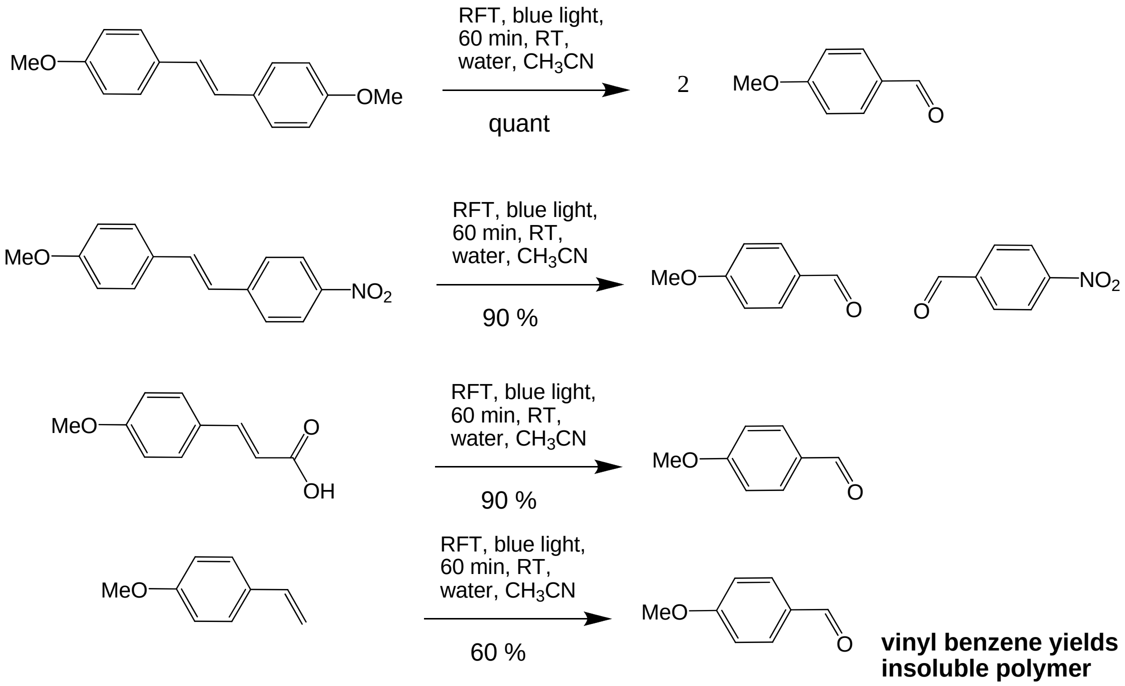

vinyl benzene yields insoluble polymer

R. Lechner, S. Kümmel, BK, *Photochem. Photobiol. Sci.*, **2010** *9*, 1367.

The dawn of old stars

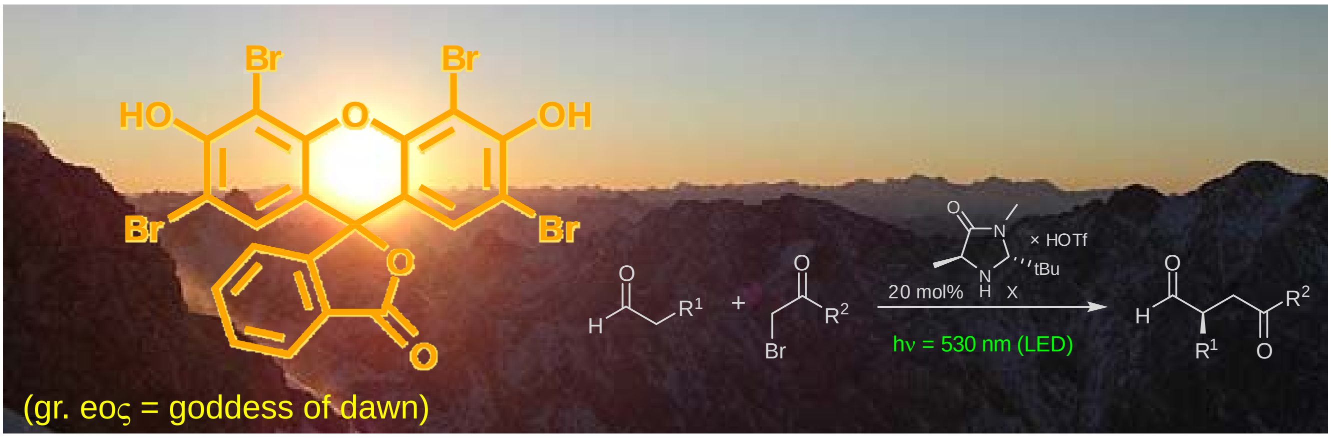

(gr. eoς = goddess of dawn)

M. Neumann, S. Füldner, BK, K. Zeitler *Angew. Chem.* **2011**, *123*, 981.

Organophotoredox catalysis - potentials

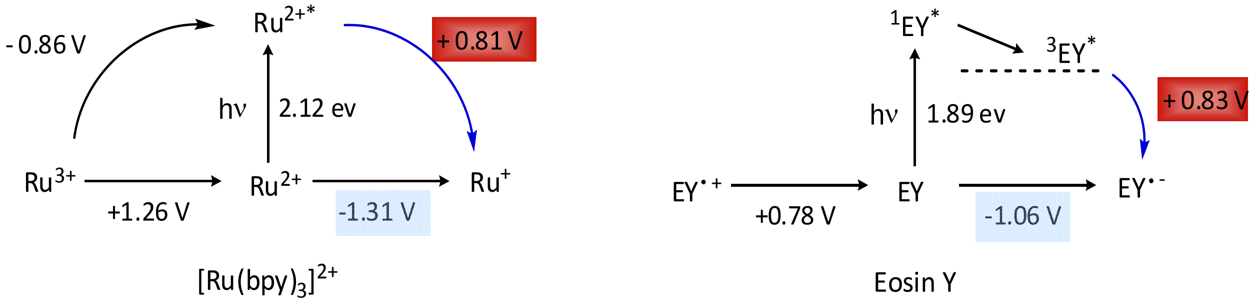
Ru^{2+*}
- 0.86 V
+ 0.81 V
hν
2.12 ev
Ru^{3+}
Ru^{2+}
Ru^{+}
+1.26 V
-1.31 V
[Ru(bpy)$_3$]$^{2+}$

^{1}EY*
^{3}EY*
+ 0.83 V
hν
1.89 ev
EY$^{\bullet +}$
EY
EY$^{\bullet -}$
+0.78 V
-1.06 V
Eosin Y

M. Neumann, S. Füldner, BK, K. Zeitler *Angew. Chem.* **2011**, *123*, 981

Organophotoredox catalysis – mechanism

proposed mechanism – probably wrong

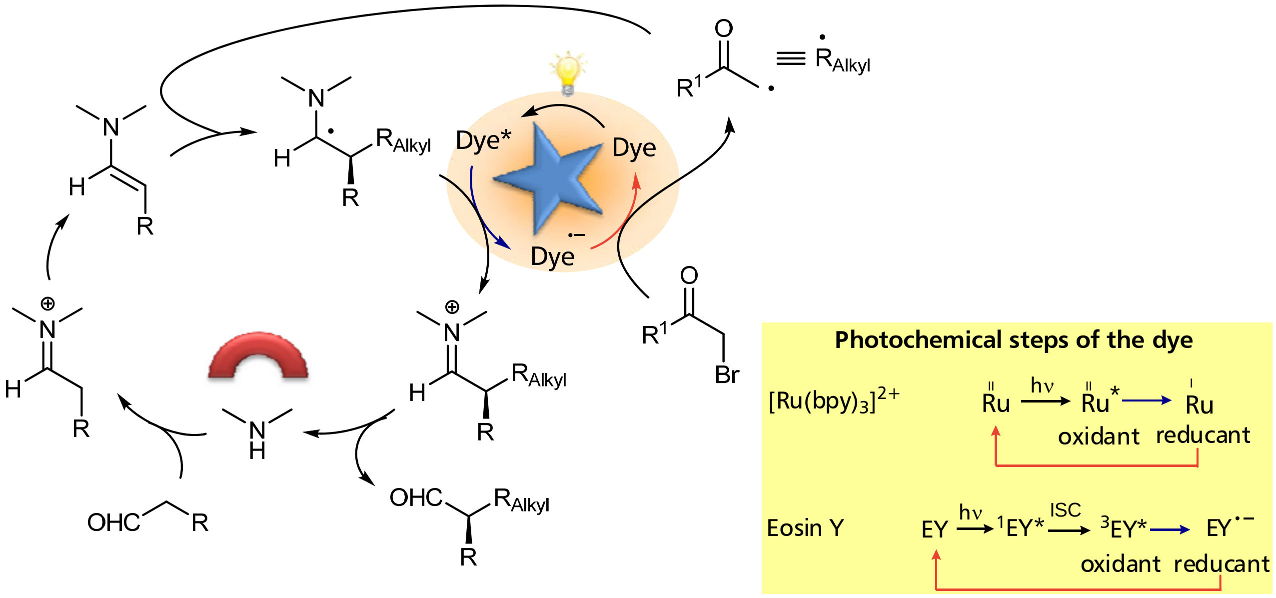

Photochemical steps of the dye

$[Ru(bpy)_3]^{2+}$ $\overset{II}{Ru} \xrightarrow{h\nu} \overset{II}{Ru}^{*} \rightarrow \overset{I}{Ru}$
oxidant reducant

Eosin Y EY $\xrightarrow{h\nu}$ $^{1}EY^{*} \xrightarrow{ISC}$ $^{3}EY^{*} \rightarrow EY^{\bullet -}$
oxidant reducant

M. Neumann, S. Füldner, BK, K. Zeitler *Angew. Chem.* **2011**, *123*, 981

Asymmetric organophotoredox catalysis

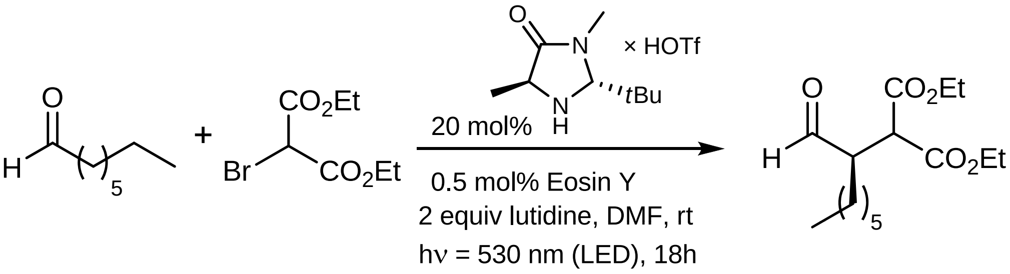

0.5 mol% Eosin Y
2 equiv lutidine, DMF, rt
hν = 530 nm (LED), 18h

conditions	Yield [%]	ee [%]
MacMillan: white light, $[Ru(bpy)_3]Cl_2$	63	77
LED, Eosin Y, 0 °C	70	81
LED, Eosin Y, – 5 °C	85	88
Sunlight, Eosin Y, ≈ 30 °C	77	76

M. Neumann, S. Füldner, BK, K. Zeitler *Angew. Chem.* **2011**, *123*, 981

Enantioselective heterogeneous photocatalysis

Selection of the right semiconductor

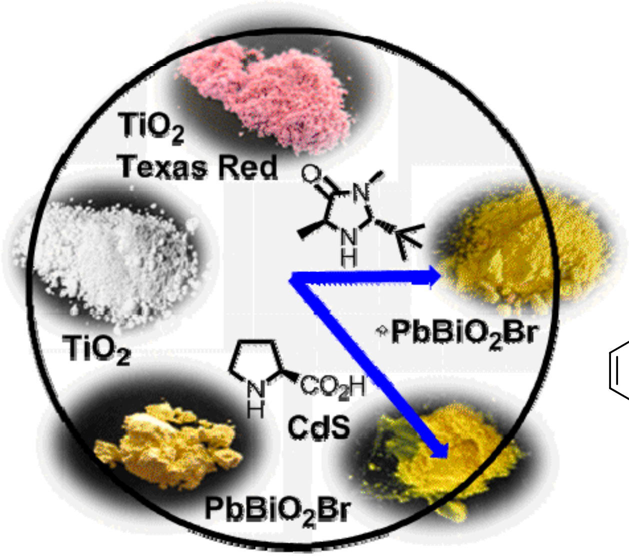

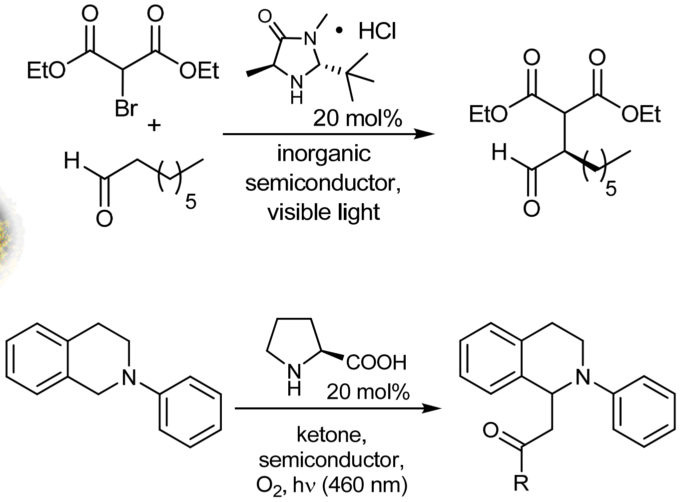

M. Cherevatskaya, S. Füldner, C. Harlander, M. Neumann, S. Kümmel, S. Dankesreiter, A. Pfitzner, K. Zeitler, BK, *Angew. Chem. Int. Ed.* **2012**, *51*, 4062

Enantioselective heterogeneous photocatalysis

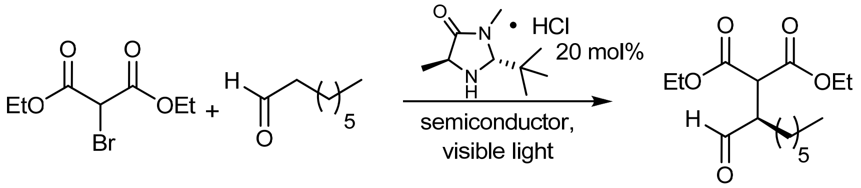

TiO$_2$ -Texas Red

PbBiO$_2$Br

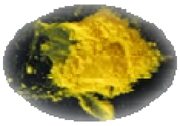

Wave-length [nm]	Reaction time [h]	Reaction temp. [°C]	Yield [%]	*ee* [%]
440	3	20	76	74
440	20	-10	40	83
530	20	20	55	72
530	20	-10	65	81
440	20	20	84	72
440	20	-10	49	83
455	3	20	41	71
455	10	-10	69	80

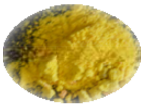

CdS
No reaction

M. Cherevatskaya, S. Füldner, C. Harlander, M. Neumann, S. Kümmel, S. Dankesreiter, A. Pfitzner, K. Zeitler, BK, *Angew. Chem. Int. Ed.* **2012**, *51*, 4062.

Enantioselective heterogeneous photocatalysis

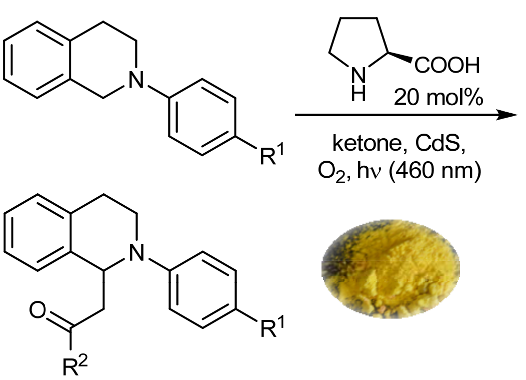

R^1	Ketone	Product	Reaction time [h]	Yield [%]
H	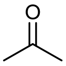	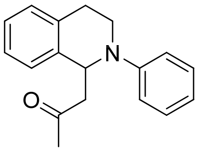	24	87 – quant.
OMe			18	89
H	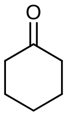	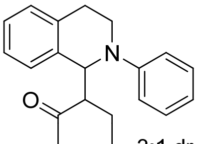 3:1 dr.	24	79
H	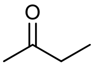	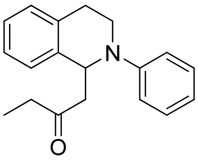	15	76

Enantioselective heterogeneous photocatalysis

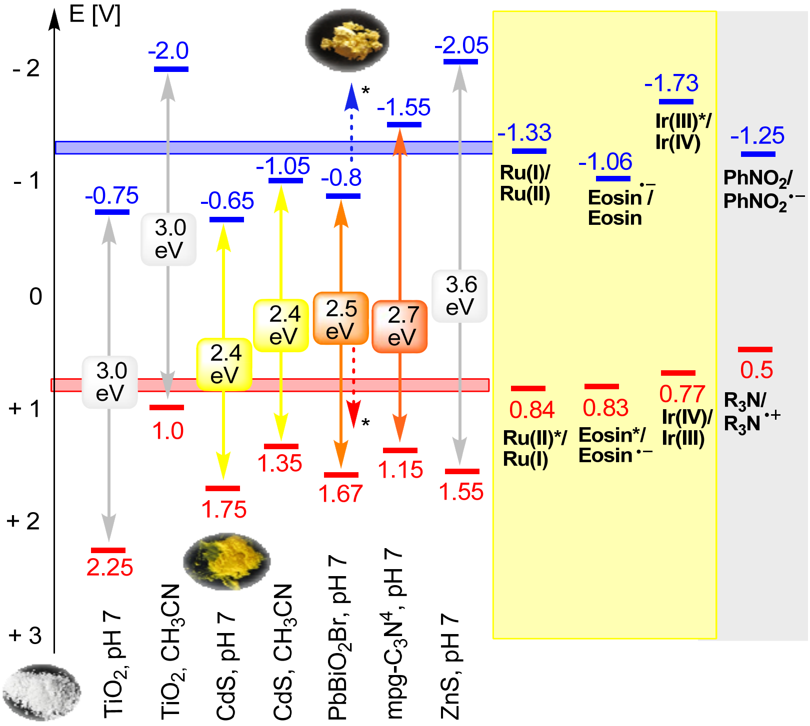

Visible Light Direct C-H Arylation

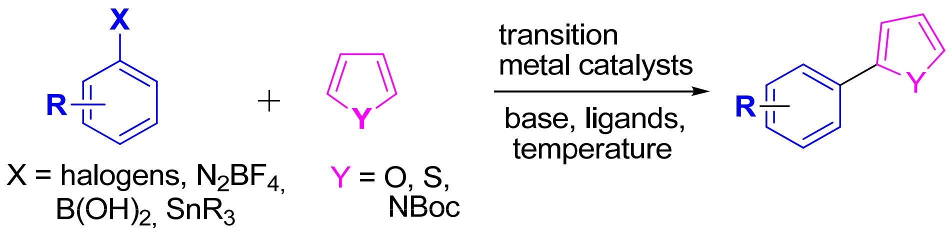

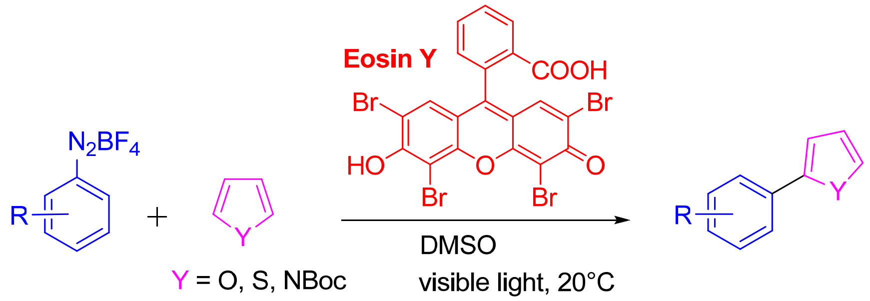

D. Prasad Hari, P. Schroll, BK, *J. Am. Chem. Soc.* **2012,** *134*, 2958.

Visible Light Direct C-H Arylation

proposed mechanism – probably wrong

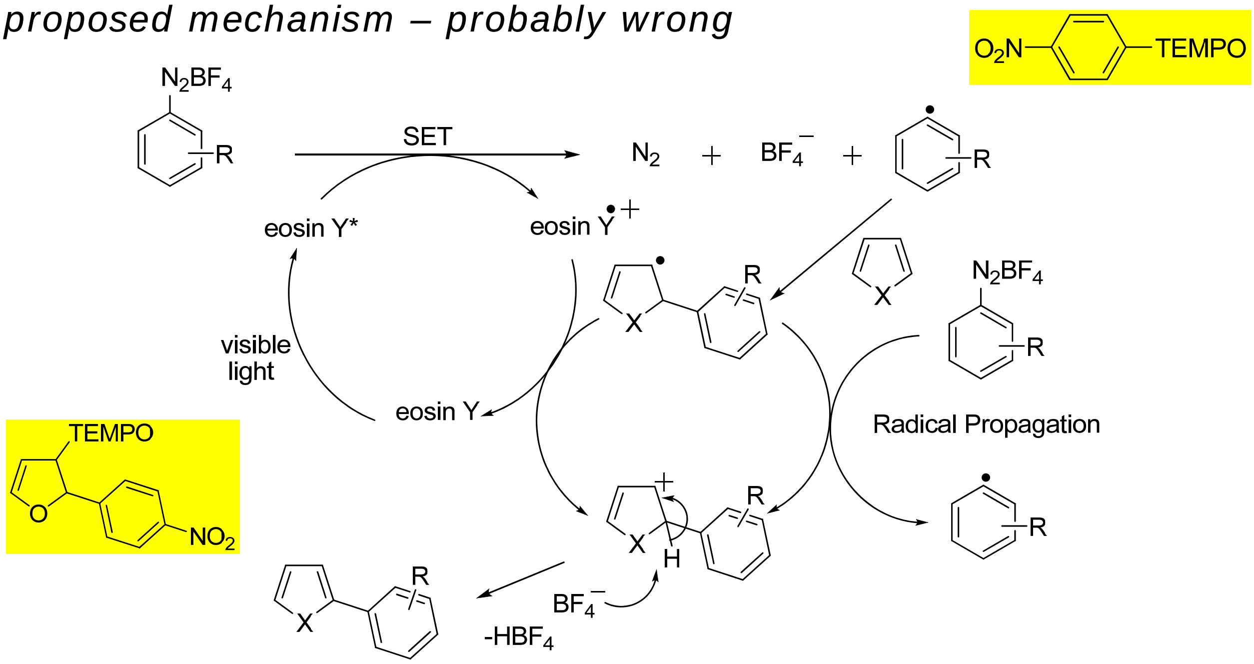

D. Prasad Hari, P. Schroll, BK, *J. Am. Chem. Soc.* **2012,** *134*, 2958.

Visible Light Direct C-H Arylation

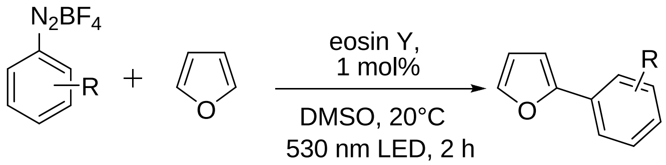

Selected examples

substrate	product	Yield [%]
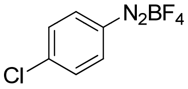	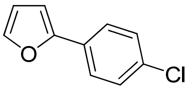	74
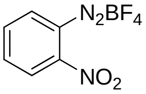	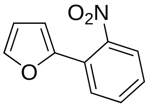	86
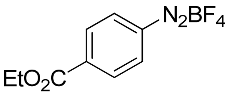	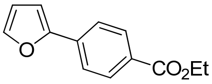	78
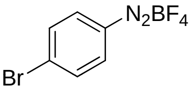	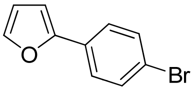	84
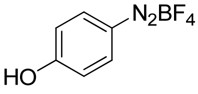	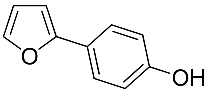	40

D. Prasad Hari, P. Schroll, BK, *J. Am. Chem. Soc.* **2012,** *134*, 2958.

Visible Light Direct C-H Arylation

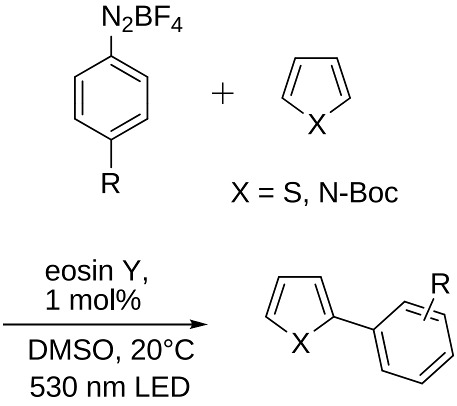

Selected examples

R	substrate	product	Yield [%]
NO_2	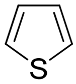	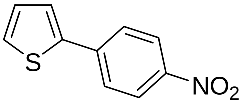	70
NO_2	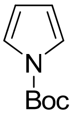	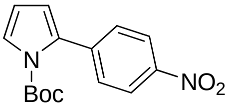	61
CO_2 Et	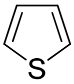	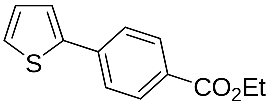	60
NO_2	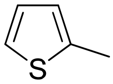	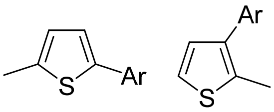 (5:1) Ar = 4-NO_2-C_6H_4	53
NO_2	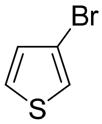	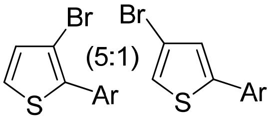 Ar = 4-NO_2-C_6H_4	60

Photo-Meerwein arylation of alkenes, alkynes and enones

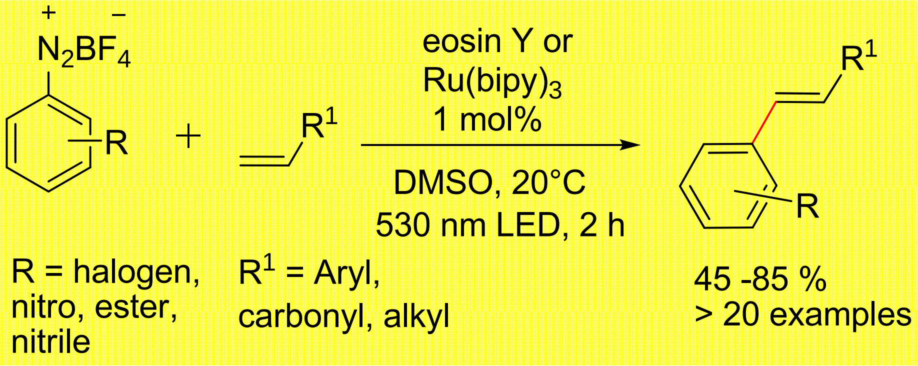

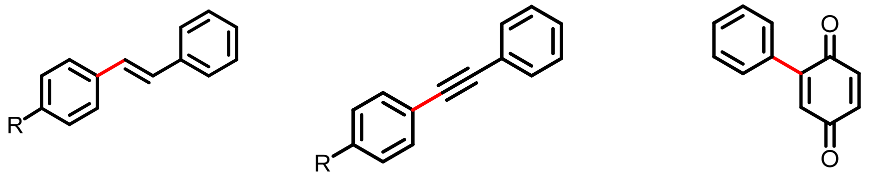

D.Prasad Hari, P. Schroll, BK, *Chemistry Open* **2012**, DOI: 10.1002/open.201200011

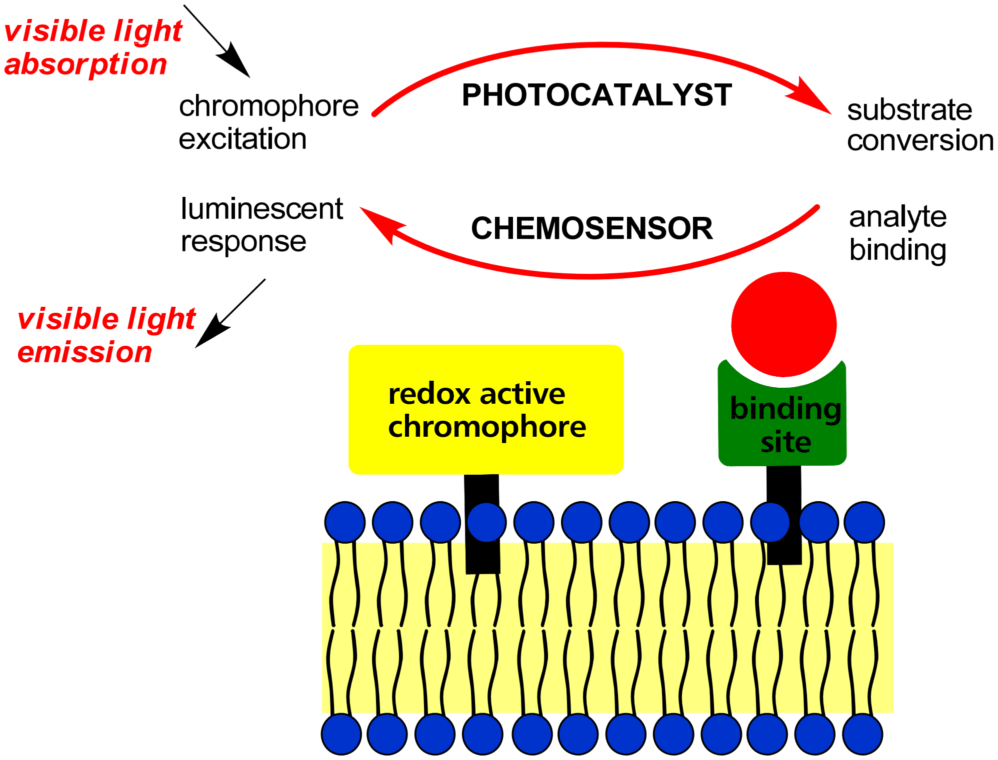

visible light absorption

chromophore excitation

PHOTOCATALYST

substrate conversion

luminescent response

CHEMOSENSOR

analyte binding

visible light emission

redox active chromophore

binding site

Thank you !

***Alumni club*:**

Dr. Harald Zieg, Dr. Mario Pelka, Dr. Martin Rödel, Mirjam Sax, Dr. Clemens Horn, Dr. Stefanie Leue, Thorsten Graf, Bernhard Lerche, Daniela Fischer, Andreas Fuchs, Dr. Tom Fricke, Dr. Wolfgang Pitsch, Natascha Naarmann, Dr. Hans-Christoph Gallmeier, Dr. Roland Reichenbach-Klinke
Dr. Mike Kercher, Miriam Kemter, Dr. Radek Cibulka, Dr. Katerina Cernovska, Dr. Valery Kozhevnikov, Dr. Maria Hechavarria Fonseca, Dr. Michael Klein, Martin Eiblmeier, Dr. Christoph Bonauer; Dr. Christian Mandl; Björn Bartel; Dr. Thomas Walenzyk; Dr. Stefan Miltschitzky; Dr. Thomas Suhs; Dr. Michael Kruppa; Dr. Veronika Michlova; Dr. Xiaoqiang Li, Dr. Xuqin Li; Dr. Georg Dirschl; Dr. Jiri Svoboda; Dr. Kristina Woinaroschy; Dr. Stefan Ritter; Dr. Giovanni Imperato; Barbara Freund
Daniel Gölderniz, Dr. Maity Prantik, Dr. Daniel Vomasta, Dr. Andreas Grauer, Dr. Michael Egger, Dr. Jens Geduhn, Dr. Harald Schmaderer, Dr. Florian Ilgen, Dr. Stefan Stadlbauer, Dr. Amilan Jose, Dr. Muruganantham Rajendran (Anand), Ina Ehlers, Markus Daerr, Florian Kinzl, Dr. Dr. Robert Lechner, Dr. Andreas Späth, Dr. Alexander Riechers, Dr. Anna Berlicka, Matthias Wrobel, Veronika Flügel, Stefan Füldner, Sandip Bhowmik, Dr. Carolin Fischer, Dr. Stefan Weiß, Dr. Evgeny Katayev, Dr. Tatiana Mitkina, Christoph Harlander, Olga Kulikova, Dr. Cristian Puentes

The group 2012:

Carolin Russ, Andreas Hohenleutner, Benjamin Gruber, Susanna Schmidtbauer, Peter Raster, Josef Herrmann, Mouchumi Bhuyan, Michael Dobmeier, Karin Lehner, Peter Schroll, Stefan Balk, Tobias Lang, Natasha Kuzmanovic, Andreas Müller, Durga Prasa, Thea Hering, Christoph Stanglmeier, Malte Hansen, Stefan Troppmann, Qui Sun

Support:

DFG, Deutsche Bundesstiftung Umwelt, DAAD, Alexander von Humboldt Stiftung, Evonik Stiftung, Fachagentur Nachwachsende Rohstoffe, bayrische Forschungsstiftung, Volkswagen Stiftung.

Collaborations:

Prof. Maria Kalinina, Moskau
Prof. Hans R. Kalbitzer, Regensburg
Profs Paul Hanson, Jeff Aubé, Kansas
Prof. Uday Maitra, Bangalore

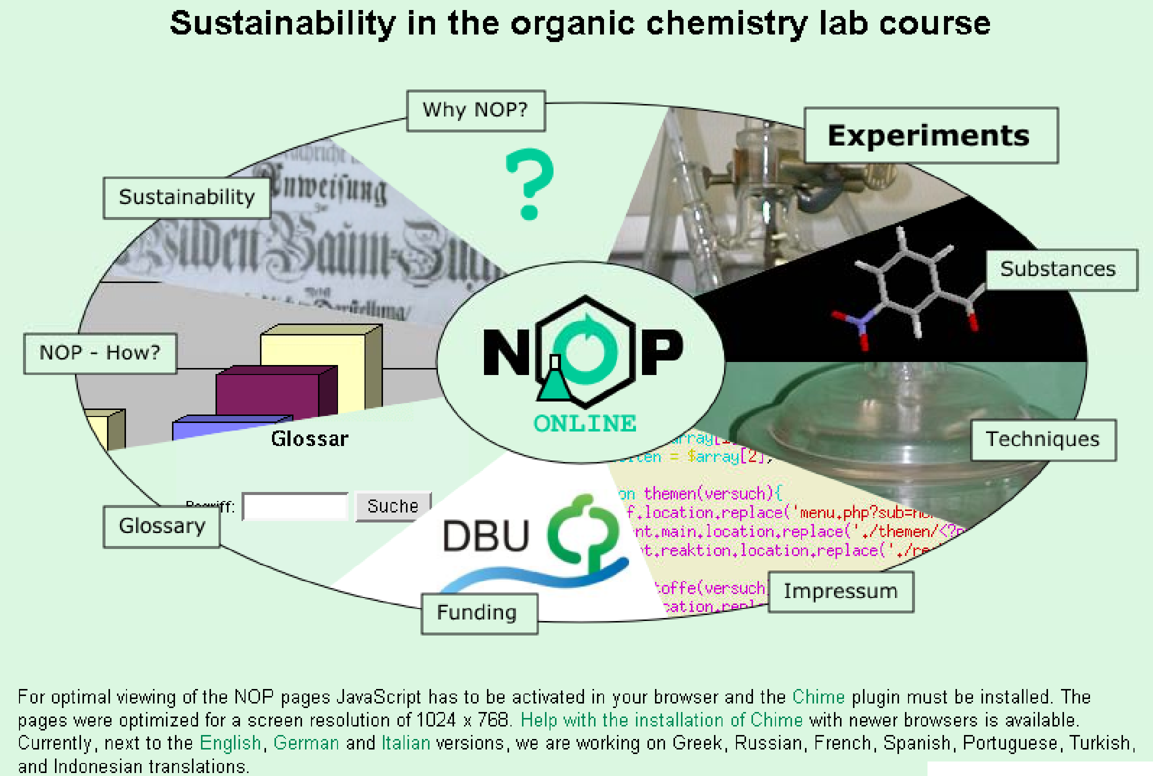

For optimal viewing of the NOP pages JavaScript has to be activated in your browser and the Chime plugin must be installed. The pages were optimized for a screen resolution of 1024 x 768. Help with the installation of Chime with newer browsers is available. Currently, next to the English, German and Italian versions, we are working on Greek, Russian, French, Spanish, Portuguese, Turkish, and Indonesian translations.

http://www.oc-praktikum.de

DBU
Deutsche Bundesstiftung Umwelt

"Molecular tectonics: control and molecular crystals"

Wais Hosseini (Strasbourg, France)

Invited lecture

Trilateral seminar on supramolecular, intermolecular, interaggregate interactions and separation chemistry, IPCE RAS, Moscow, Russian Federation

20.-23.07.2012

"Molecular tectonics: from molecules to complex systems"

Mir Wais Hosseini

University of Strasbourg

e-mail: hosseini@unistra.fr

The design and construction of periodic architectures in the crystalline phase or at surfaces are attracting considerable interest over the last two decades. For both design and analysis of molecular crystals, we have developed a strategy called molecular tectonics which is based on the formation of molecular networks through the design of complementary tectons or molecular construction units. The generation of molecular networks and subsequently of crystals is achieved by self-assembly processes based on repetitive molecular recognition events. This approach, combining supramolecular synthesis and self-assembly processes in the solid state, is operational and versatile and allows the design and construction of a variety of complex purely organic or hybrid architectures. The approach will be presented and illustrated by a variety of tectons and networks.

Molecular Tectonics : from atoms to molecules, from molecules to networks, from networks to crystals, from crystals to crystals of crystals

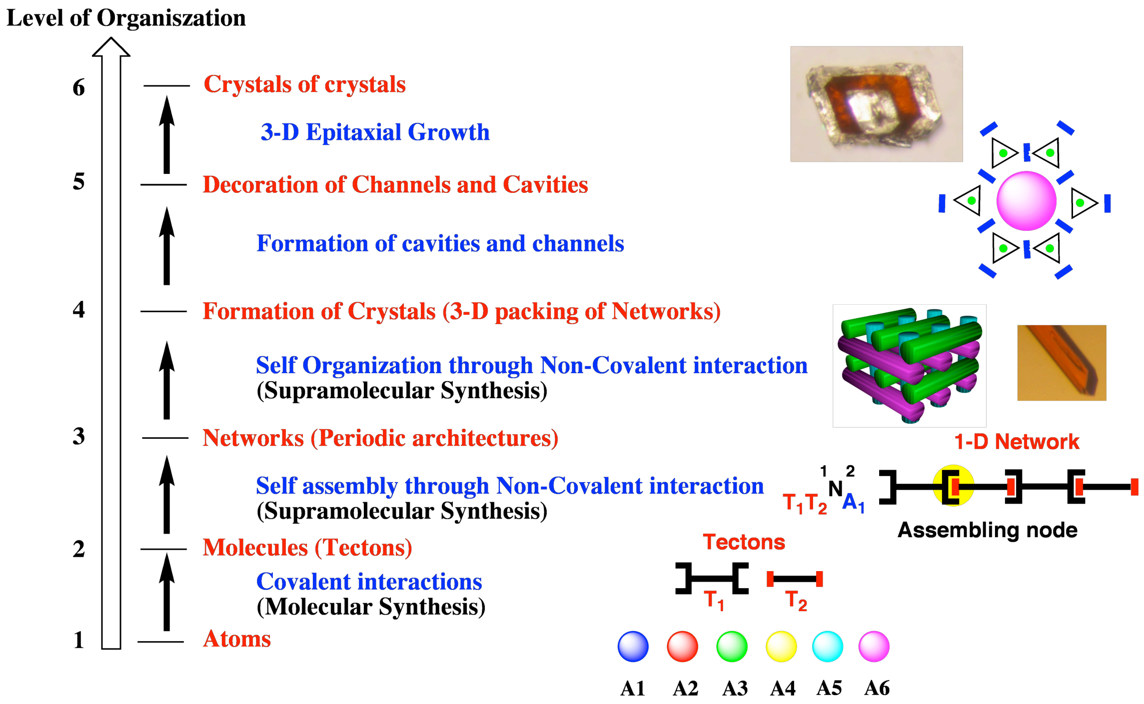

[1] Hosseini, M. W. *Acc. Chem. Res.*, **2005**, *38*, 313.
[2] Hosseini, M. W. *Chem. Commun.*, Focus Article, **2005** ,582.
[3] Hosseini, M. W. *Cryts.Eng.Comm.*, **2004**, *6*, 318
[4] Hosseini, M. W. *Actualité Chimique.*, **2005**, *290-291*, 59.
[5] Hosseini, M. W. "LES AVANCEES DE LA CHIMIE", *Actualité Chimique*, **2011**, *348-349*, 36.

DYNAMIC ANALYTE RECOGNITION BY ARTIFICIAL SYNTHETIC VESICLES

S. Balk, B. König

Universität Regensburg, Universitätsstr. 31, 93040 Regensburg

Mimicking recognition processes at natural cell membranes we recently reported synthetic vesicles with multi-receptor surfaces as chemo sensors for small biomolecules.[1] Functional phospholipid-based membranes are used for optical sensing by fluorescent labelling of embedded molecules.[2] To understand the physical interactions of vesicular anchored receptors we developed a simple model system for the dynamic recognition: bivalent target molecules spatially rearrange multiple membrane-embedded receptors equipped with FRET labels. These liposomal tethered amphiphiles are assumed to form patches and approximate with the addition of a binding partner to give a typical FRET response.

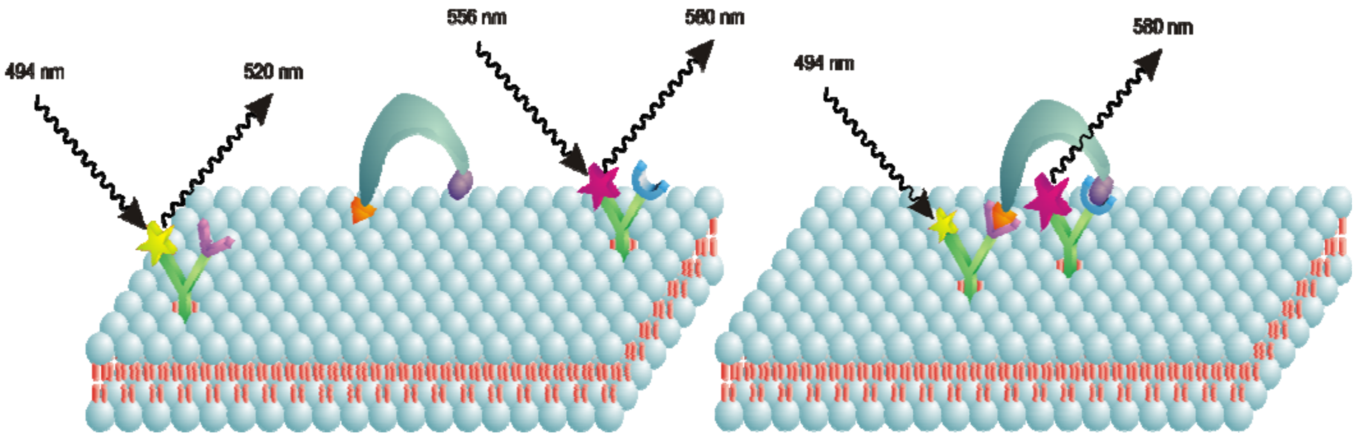

Figure 1. Spatial rearrangement of FRET labeled receptor molecules by analyte binding

The influence of analyte binding towards the FRET signal was investigated by emission titrations. The investigation of these dynamic interactions is part of an approach towards imprinted vesicles as soft nanoparticles with ordered surfaces that perfectly match a templating target molecule.

[1] B. Gruber, S. Stadlbauer, K. Woinaroschy, B. König, Org. Biomol. Chem., **2010**, 8, 3704-3714.

[2] B. Gruber, S. Stadlbauer, A. Späth, S. Weiss, M. Kalinina, B. König, *Ang. Chem. Int. Ed.* **2010**, 49, 7125.

Dynamic Analyte Recognition by Artificial Synthetic Vesicles

M. Sc. Stefan Balk
Institute of Organic Chemistry
Prof. Dr. Burkhard Koenig

Universität Regensburg

Universität Regensburg

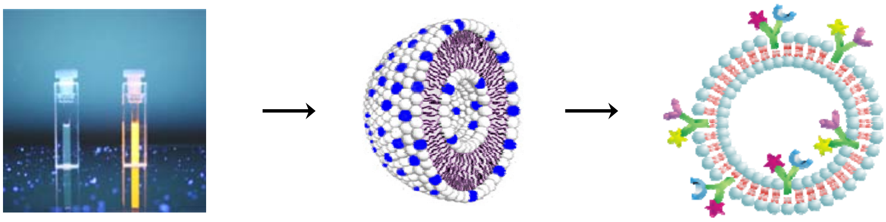

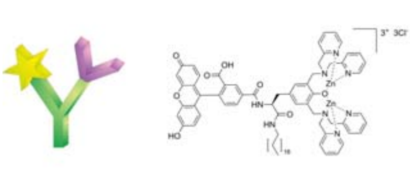

Zn-Dpa

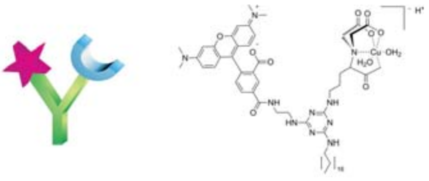

Cu-NTA

B. Gruber, S. Stadlbauer, K. Woinaroschy, B. König, Org. Biomol. Chem., **2010**, 8, 3704-3714.
B. Gruber, S. Stadlbauer, A. Späth, S. Weiss, M. Kalinina, B. König, *Ang. Chem. Int. Ed.* **2010**, 49, 7125.

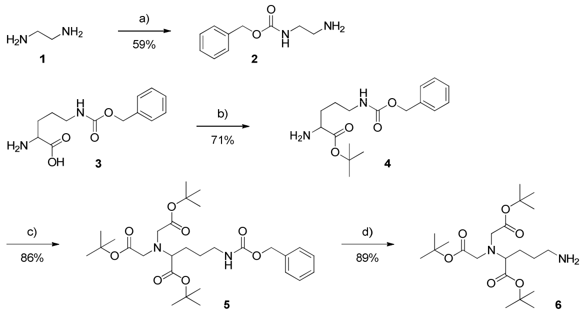

Synthesis of an amphiphilic, fluorescent copper complex: (a) Cbz chloride, DCM, 0°C, 3 h; (b) tert butyl acetate, $HClO_4$, RT, 72 h; (c) bromo tert butyl acetate, DMF, 55°C, 20 h; (d) Pd/C.H_2, EtOH, RT, 72 h.

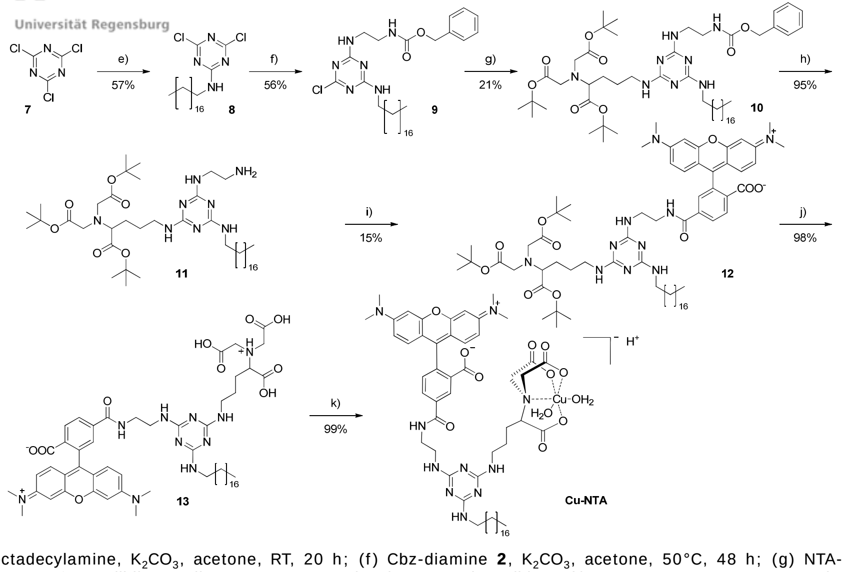

(e) octadecylamine, K_2CO_3, acetone, RT, 20 h; (f) Cbz-diamine **2**, K_2CO_3, acetone, 50°C, 48 h; (g) NTA-precursor **6**, collidine, dioxane, 140°C (MW), 1.5 h; (h) Pd/C, H_2, EtOH, RT, 48 h; (i) carboxytetramethylrhodamine, TBTU, HOBt, DIPEA, DMF, 0°C, 1 h / 40°C, 24 h; (j) TFA, RT, 24 h; (k) $Cu_2(OH)_2CO_3$, MeOH, 60°C, 4 h.

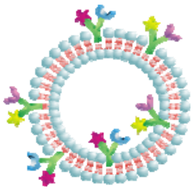

Bivalent analyte binding

Rearrangement of receptors inside a fluid membrane

Spatial proximity provides FRET signaling

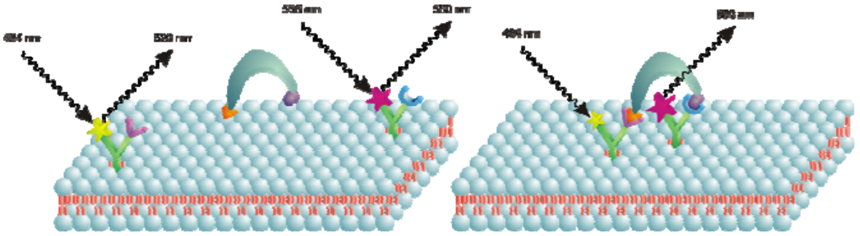

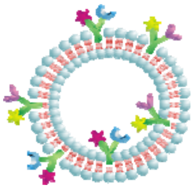

Vesicle built up from **DOPC** and functionalized with Fluorescein labeled Zn-Dpa-receptors (ex. 494 nm, em. 520 nm) and Rhodamine labeled Cu-NTA-receptors (ex. 556 nm, em. 580 nm).

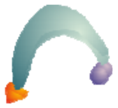

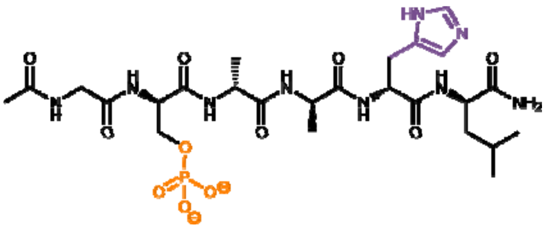

Peptide **P$_2$** (Ac-Gly-phos.Ser-Ala-Ala-His-Leu-NH$_2$) is binding to a vesicle functionalized with 0.5 mol% of each receptor.

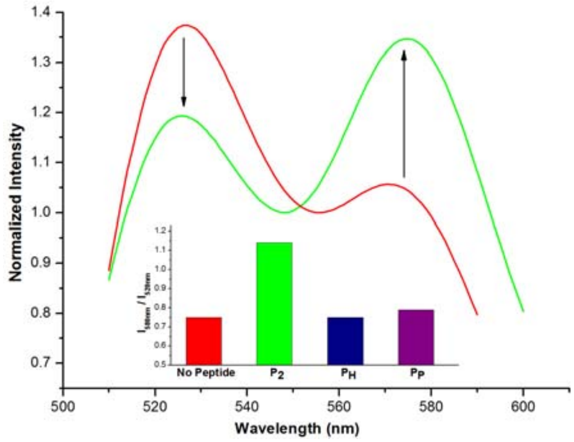

Fluorescence spectra of DOPC vesicles containing labelled receptors **Zn-Dpa** and **Cu-NTA** (0.5 mol% each) in the absence (red) and presence (green) of peptide $\mathbf{P_2}$.

B. Gruber, S. Balk, S. Stadlbauer and B. König, **2012**, in prepapration.

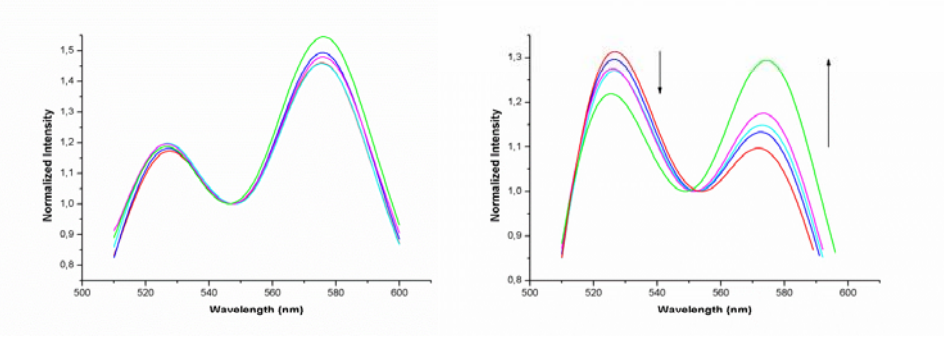

Emission spectra of DSPC vesicles (left) and DOPC vesicles (right) functionalized with 0.5 mol% **Cu-NTA** and **Zn-Dpa** each in the presence of increasing amounts of peptide $\mathbf{P_2}$.

Universität Regensburg

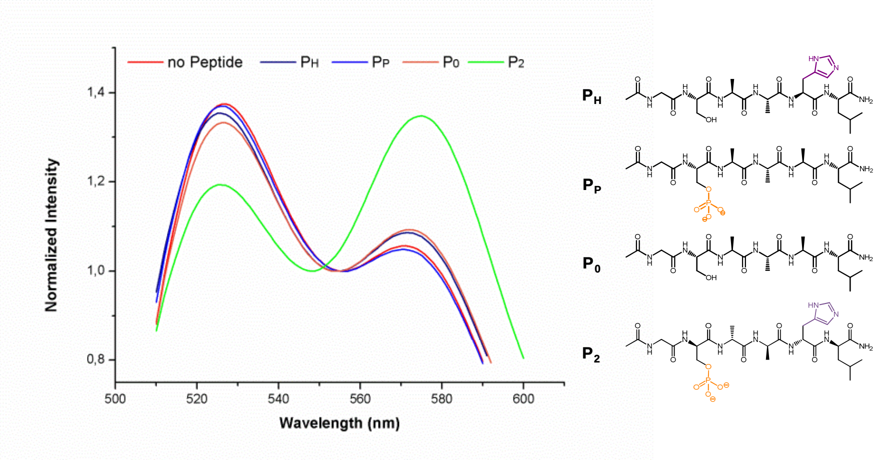

Emission spectra of DOPC vesicles (0.5 mol% **Cu-NTA** and **Zn-Dpa**) in the presence of equivalent amounts of the control peptides $\mathbf{P_H}$, $\mathbf{P_P}$ and $\mathbf{P_0}$ compared to the binding peptide $\mathbf{P_2}$.

Universität Regensburg

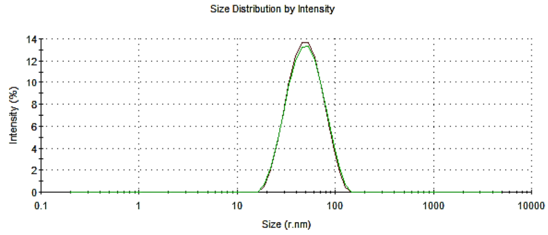

Observed particle size distribution for mixtures of DOPC/**Cu-NTA**-vesicles (0.1 mol%) and DOPC/**Zn-Dpa**-vesicles (0.1mol%) before (black) and after (green) treatment with **P2** showing no apparent crosslinking and increase in vesicle size.

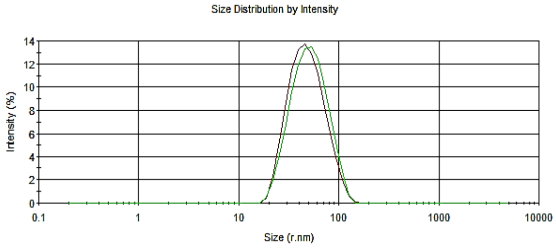

Observed particle size distribution for DOPC vesicles functionalized with **Cu3** and $\mathbf{Zn_21}$ (0.1 mol% each) before (black) and after (green) treatment with **P2** showing no apparent crosslinking and increase in vesicle size.

Summary

Artificial vesicles for bivalent analyte binding with fluorescent labeled receptors

Receptor movement inside fluid membranes to improve binding events

Rearrangement of vesicular embedded receptor molecules cause significant FRET signaling

Outlook

Temperature influence on binding events in gel-phase membranes

Imprinting of vesicles to improve ordered surfaces

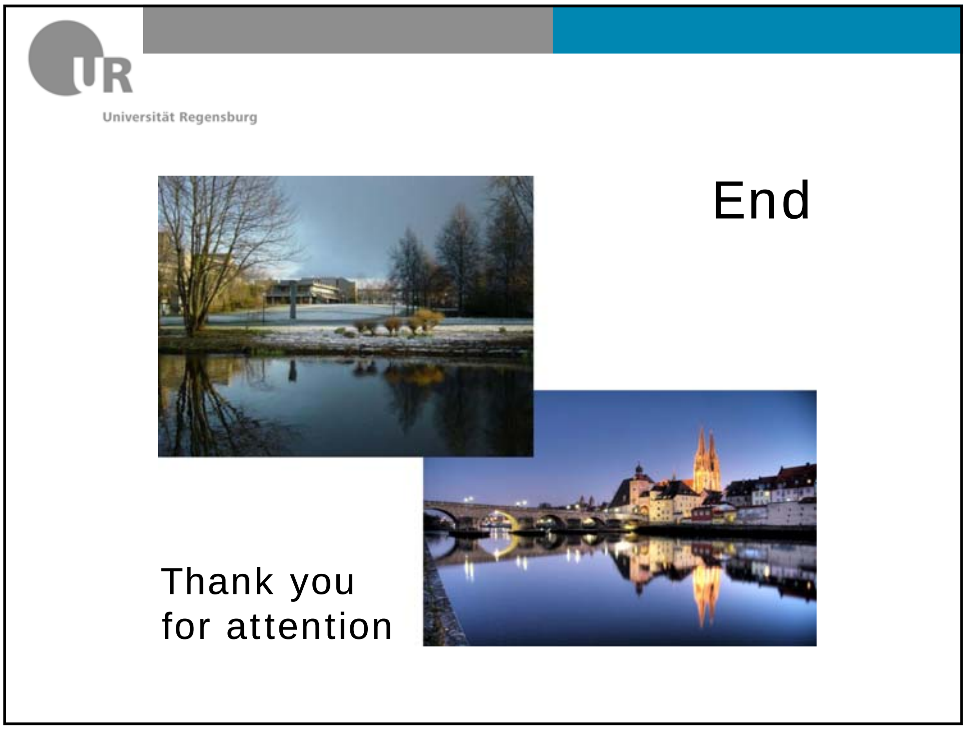

End

Thank you
for attention

Investigation of Ion specifities via NMR

Susanne Dengler M.Sc.
Institute of Physical and Theoretical Chemistry
FAKULTÄT FÜR CHEMIE UND PHARMAZIE

7th European Summer School
Moscow, 20-23 July 2012

Universität Regensburg

Universität Regensburg

Susanne Dengler M.Sc.
Institute of Physical and Theoretical Chemistry
FAKULTÄT FÜR CHEMIE UND PHARMAZIE

How specific are Ion specifities

- According to Collin`s concept more chaotropic ions interact more strongly with more chaotropic (oppositely charged) headgroups and more cosmotropic ions more strongly with more cosmotropic headgroups.
- For example lithium ions should interact more strongly with alkylcarboxylates (cosmotropic) than sodium ions. For alkylsulphates (chaotropic) the conversed behaviour is suspected[1].
- The aim of our work was to investigate whether the specifities are comparable strong.

➔ We derterminded the quadrople splitting of sodium (Δ_{Na}) and lithium (Δ_{Li})in lamellar liquid crystalls.

Theoretical Background

- Quadrupole splitting Δ occurs only for nuclei with a spin I >1/2.
- It results from the interaction of electric nuclear quadrupole moment and the electric field gradient at the nucleus.
- The magnitude of splitting depends beside the temperature and other factors also on the extend of anisotropy.
- In an isotropic environment the orientation dependent quadrupol splitting averages to zero.
- Δ can be positive or negative. Changes in the relative values can be taken to indicate changes in ion binding[2, 3].

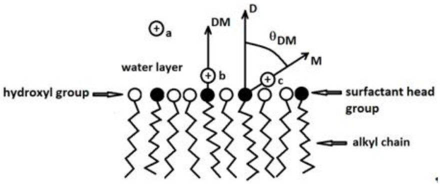

Theoretical Background

- Sodium ions in contact with head groups (“bound”, fraction p_b) have a finite Δ value (Δ_b) while those more than ca. 3-4 Å from the surface have Δ values of zero, (“free” fraction p_f) ($p_f + p_b = 1$).
- The problem was that it was difficult to obtain absolute values of the quadrupole splitting.
- But it is ideal for the monitoring of competitive ion binding.
- In a mixture of two ions, A & B, you will observe, that if B displaces A then the Δ values of A will decrease on addition of B. Those of B will also decrease because the highest fraction of bound B ions occurs with small additions of B. Fortunately there are several cations that possess nuclear quadrupole moments.
- We have selected ^{23}Na and ^{7}Li for study because they have high sensitivity and can easily be measured with conventional multi-frequency high resolution spectrometers. Also, they are reported to have different specific binding capabilities with different anions.

Susanne Dengler M.Sc.
Institute of Physical and Theoretical Chemistry
FAKULTÄT FÜR CHEMIE UND PHARMAZIE

Investigated Samples

- We have chosen two surfactant systems for study, dodecyl sulphate/octanol and dodecyl carboxylate/octanol.

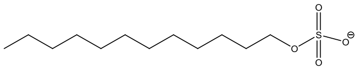

Dodecyl sulphate

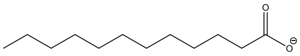

Dodecyl carboxylate

- These are thought to have very different specifities for Li or Na[1].
- Octanol is employed as a cosurfactant because it is necessary for the formation of a lamellar phase.

Susanne Dengler M.Sc.
Institute of Physical and Theoretical Chemistry
FAKULTÄT FÜR CHEMIE UND PHARMAZIE

Investigated Samples

- Each sample contains D_2O, octanol and surfactant. The surfactants are either carboxylate surfactants (SDC and LiDC) or sulphate surfactants (SDS and LiDS).
- The molar ratio of the sodium surfactant to lithium surfactant varies from 0 to 100 % sodium surfactant in 20 % steps.
- In each sample the molar ratio of SDS + LiDS to octanol was 1:1, and due to the lower solubility of carboxylates in water, the molar ratio of SDC + LiDC to octanol was reduced to 1:3.
- The concentrations of SDS+LiDS+octanol and SDC+LiDC+octanol in D_2O were 35 wt % to 75 wt % in 10 wt % steps.
- The carboxylate samples were measured at 300 K and 310 K.

Results

Typical Na- and Li-NMR

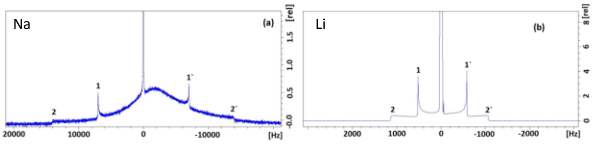

^{23}Na-NMR spectrum of a 35 wt % sample with a composition of SDC/LiDC = 2/3 at 300 K. The relative intensity of the signals is plotted against the frequency in [Hz]. (b) ^{7}Li-NMR spectrum of a 35 wt % sample with a composition of SDS/LiDS = 2/3 at 300 K. The relative intensity of the signals is plotted against the frequency in [Hz].

- The quadrupole splitting (Δ) is equal to one half the distance between the signals 1 and 1`and one quarter the distance between 2 and 2`.
- These distinct features can be seen for nearly all mixtures.
- In the sulphate as well as in the carboxylate systems the ^{23}Na splitting is much larger than the ^{7}Li splitting, the values of both being in good agreement with those in the literature[4-6].

Results

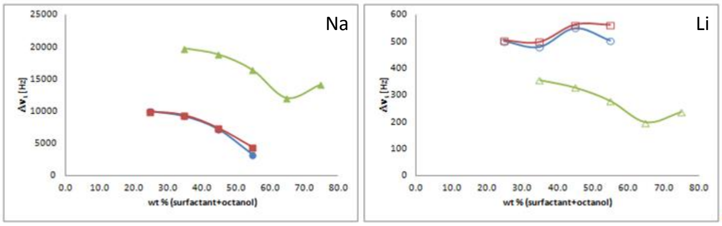

Sodium splitting with increasing concentration of surfactant and octanol (left) and lithium splitting with increasing concentration of surfactant and octanol (right). ● SDC/LiDC = 1:0 at 300 K, ■ SDC/LiDC = 1:0 at 310 K, ▲ SDS/LiDS = 1:0 at 300 K, ○ SDC/LiDC = 0:1 at 300 K, ☐ SDC/LiDC = 0:1 at 310 K, △ SDS/LiDS = 0:1 at 300 K.

- The lithium splittings are roughly constant for the carboxylate samples and decreases in the sulphate samples.
- The sodium splitting decreases with concentration in both the carboxylate and the sulphate samples.
- The decrease of sodium splitting for both surfactants seems to be unlikely but it is due to the different binding sites bs (on the surface of the head group; positive Δ value) and bb (between the head groups; negative Δ value)

Results

Ion specifity of carboxylate

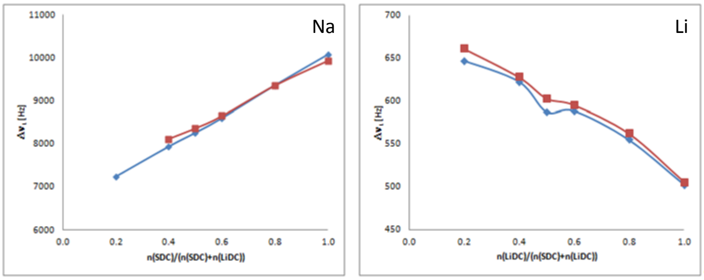

Sodium splitting with increasing amount of sodium (left) and lithium splitting with increasing amount of lithium (right) at 300 K and 310 K for 25 wt % SDC/LiDC/octanol in D_2O. ● 300 K, ■ 310 K.

The Na splitting increasing with increasing concentration whereas Li splitting decreases.
→changes in Δ values reflect changes in ion binding
→Li binding to carboxylate is stronger than Na

Results

Ion specifity of carboxylate

- The addition of Li ions displaces Na ions from the surface, decreasing the Na Δ values.
- For the Li ions, the largest fraction of bound ions occurs at the lowest Li concentration, and this decreases with added Li ions because a larger fraction must replace the free Na ions.

Results

Ion specifity of sulphate

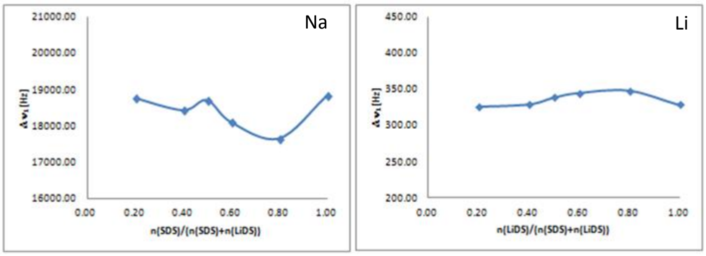

Sodium splitting with increasing amount of sodium (left) and lithium splitting with increasing amount of lithium (right) at 300 K for 45 wt % sample.

- The Δ values show only small changes with varying amounts of sodium and lithium.
- The marginally change of the splittings is a hint only of a slight preference of the sulphate head group to sodium.
- The non-monotonic behaviour points to a slight preferential location of Na ions in the bb site.

Conclusion

- The quadrupole splitting clearly reflects differences in the local environment of lithium and sodium in liquid crystalline phases.
- The ion specificity of the sulphate head group towards sodium and lithium is much less pronounced than the ion specificity of the carboxylate head group.
- Lithium has a higher propensity towards carboxylate compared to sodium.
- The specificity is more pronounced at smaller absolute surfactant/co-surfactant concentration.
- At higher temperatures the ions have a higher tendency to bind at the bs site rather than at the bb site.

→ NMR quadrupole splitting measurements are suitable for the study of specific ion effects in colloidal systems.

Thank you for your Attention

References

1. Collins, K.D., *Ions from the Hofmeister series and osmolytes: effects on proteins in solution and in the crystallization process.* Methods, 2004. **34**: p. 300.
2. Jungwirth, P. and D.J. Tobias, *Specific Ion Effects at the Air/Water Interface.* Chemical Reviews, 2006. **106**: p. 1259.
3. Schwierz, N., D. Horinek, and R.R. Netz, *Reveresed Anionic Hofmeister Series: The Interplay of Surface Charge an Surface Polarity.* Langmuir, 2010. **26**: p. 7370.
4. Lindblom, G., *Ion binding in liquid crystals studied by NMR: III. Sodium-23 quadrupolar effects in a model membrane system.* Acta Chemica Scandinavica, 1971. **25**(7): p. 2767.
5. Soderman, O., Arvidson, G., Lindblom, G. and K. Fontell, *The Interactions between Monovalent Ions and Phosphatidyl Cholines in Aqueous Bilayers* European Journal of Chemistry, 1983. **134**: p. 309.
6. Everiss, E., G.J.T. Tiddy, and B.A. Wheeler, *Phase Diagram and NMR Study of the Lyotropic Liquid Crystalline Phases Formed by Lithium Perfluoro-Octanoate and Water.* Journal of Chemical Society: Faraday Transaction I, 1976. **72**: p. 1747.

Prof. S.N. Kolmykov giving lecture on the environmental behavior of actinide nanoparticles, 23 July 2012

Dr. B. Beele, Ms. V. Tregubova, Dr. G. Kolesnilov - 7th European Summer School. 22 July, 2012


GEORGE HEVESY
1885–1966


JOURNAL OF RADIOANALYTICAL CHEMISTRY
DR. B.F. MYASOEDOV 2012
1968


Kona
Sugar Shack
No Vacancy

George Hevesy Medal Award

George Hevesy Medal Award 2012 is presented to:

Academician Professor

Dr. Boris F. MYASOEDOV

Russian Academy of Sciences,

Moscow, Russia


MARC IX

Hevesy medal award lecture

RADIOCHEMISTRY: PAST, PRESENT AND PROSPECTS

Professor Boris F. MYASOEDOV

Russian Academy of Sciences

History of the Russian Academy of Sciences

Peter the Great founded the Russian Academy of Sciences in **1724**

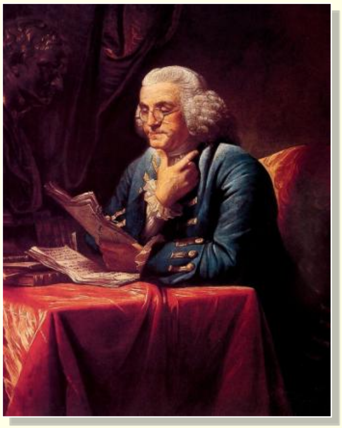

Benjamin Franklin was the first American who was elected as a Foreign Member of the Russian Academy of Sciences (1789)

The Russian Academy of Sciences 18th century, Saint Petersburg

Kunstkamera building, the first headquarters of the Russian Academy of Sciences

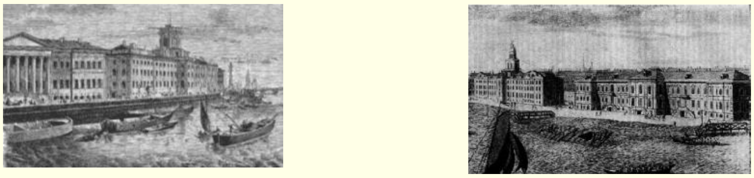

The Russian Academy of Sciences Today

➢ Members of RAS	1 209
➢ Professors	9 785
➢ Ph.D.	26 230

Total – 113 129, – 55 490 researchers

➢ Research Institutes	422
➢ Scientific journals	150
➢ Scientific Councils	48

Organizational Structure of Russian Academy of Sciences

Department	Institutions
➢ Mathematical Sciences	8
➢ Energy, Mechanical Engineering, Mechanics and Control Processes	17
➢ Earth Sciences	22
➢ Physical Sciences	23
➢ Chemistry and Material Science	21
➢ Social Sciences	23
➢ Nanotechnologies and Information Technologies	15
➢ Biological Sciences	37
➢ History and Philological Sciences	16

Regional branches (the number of Institutions):

Siberian	Urals	Far East
(77)	(40)	(33)

Regional Scientific Centers 15; Institutions 51

Marie Curie – the Founder of Radiochemistry

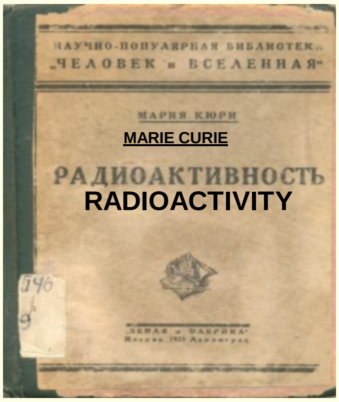

MARIE SKLODOWSKA CURIE was French-Polish physicist and chemist famous for her pioneering research on radioactivity. She is best known as the discoverer of the radioactive elements Po and Ra and as the first person honored with two Nobel prizes

V. I. Vernadsky – the famous Russian Scientist, Geochemist, Philosopher

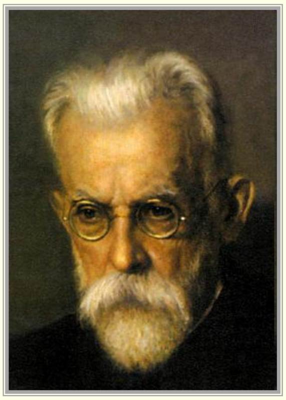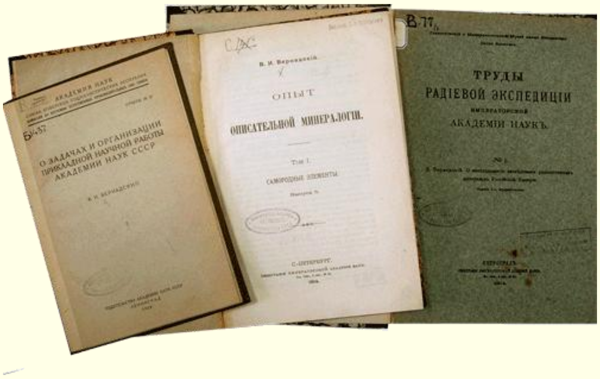

V. Vernadsky was the first who appreciated the importance of radioactivity in development of the human society

V.I. Vernadsky. "Modern problems in the field of radium." 1910

Main Directions of Our Research

- Synthesis of Md, No, Lr, Rf (1954 – 1960)
- Chemistry of protactinium (1960 – 1969)
- Actinium: preparation, chemistry (1972 – 1982)
- Chemistry of transuranium elements (1969 - …)
- Radioanalytical chemistry for nuclear fuel cycle (1970 - ...)
- Radioactive waste management (1975 -...)
- Environmental radioanalytical ;;chemistry (1984 -…)

Synthesis of New Elements

(from Past to Present)

^{101}Md	^{102}No	^{103}Lr	104
$5f^{13}$	$5f^{14}$	$5f^{14}6d^1$	$5f^{14}6d^27s^2$
258.0984	259.1011	262.1098	261
Seaborg	Seaborg	Ghiorso	
1955	1956	1961	

- **Synthesis of the new elements in the reactions of interaction of C, N, O ions accelerated in a cyclotron with U and Pu nuclei**
- **The latest achievements in the synthesis of the new elements**

Experiments on Synthesis of Nobelium (1959)

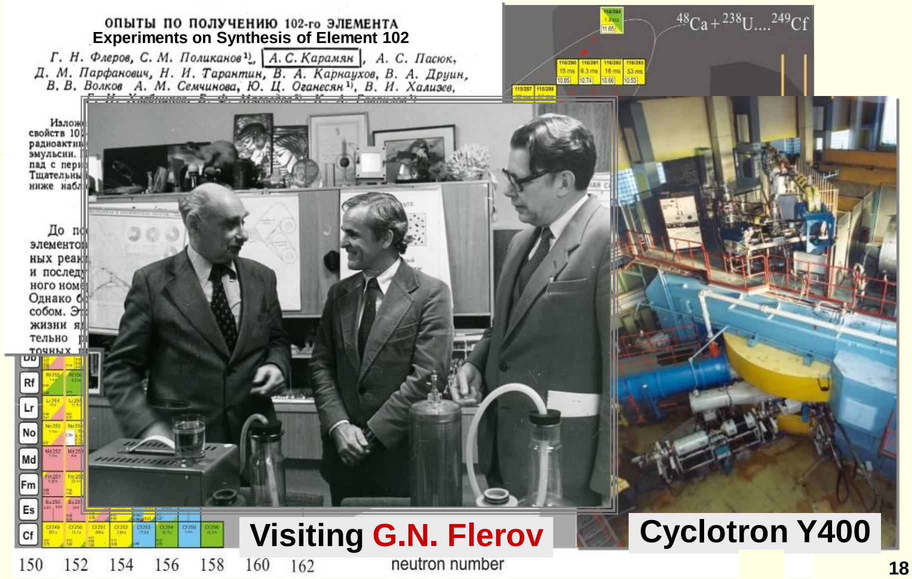

ОПЫТЫ ПО ПОЛУЧЕНИЮ 102-го ЭЛЕМЕНТА

Experiments on Synthesis of Element 102

Г. Н. Флеров, С. М. Поликанов[1], *А. С. Карамян*, *А. С. Пасюк*, *Д. М. Парфанович*, *Н. И. Тарантин*, *В. А. Карнаухов*, *В. А. Друин*, *В. В. Волков А. М. Семчинова*, *Ю. Ц. Оганесян*[1], *В. И. Хализев*,

Visiting **G.N. Flerov**

Cyclotron Y400

Discussion on the Names of Elements 103 – 106

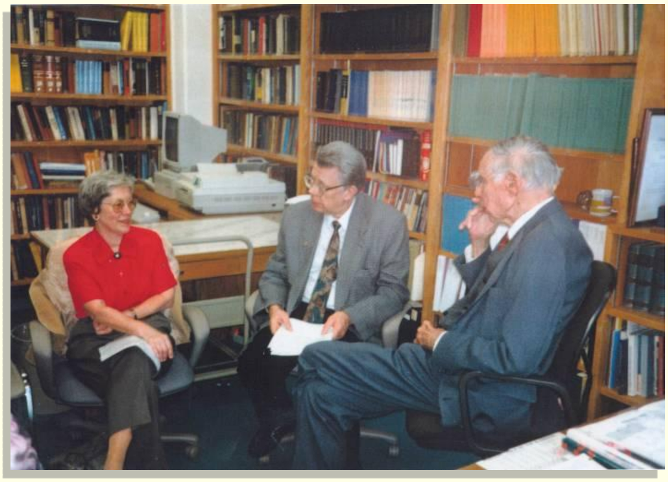

G. Seaborg and D. Hoffman

New Synthesized Elements

Names of the Elements Approved by IUPAC

Element	Name		Symbol
101	Менделевий	Mendelevium	Md
102	Нобелий	Nobelium	No
103	Лоуренсий	Lawrencium	Lr
104	Резерфордий	Rutherfordium	Rf
105	Дубний	Dubnium	Db
106	Сиборгий	Seaborgium	Sg
107	Борий	Bohrium	Bh
108	Хассий	Hassium	Hs
109	Мейтнерий	Meitnerium	Mt
110	Дармштадтий	Darmstadtium	Ds
111	Рентгений	Roentgenium	Rg
112	Коперниций	Copernicium	Cn

*114, 116 under approving by IUPAC

Glenn T. Seaborg, the Noble Prize Laureate

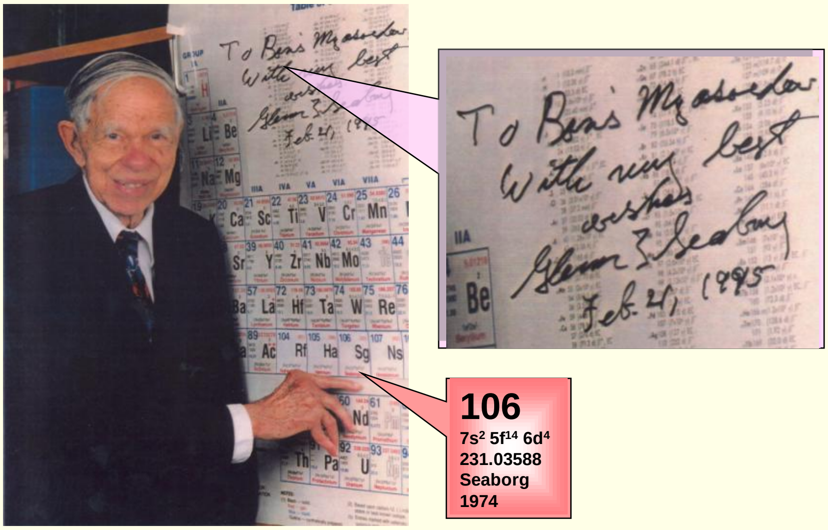

106
$7s^2\ 5f^{14}\ 6d^4$
231.03588
Seaborg
1974

Discovery of the elements with atomic numbers greater than or equal to 113

(IUPAC Technical Report)

Pure Appl. Chem., Vol. 83, No. 7, pp. 1485–1498, 2011

The IUPAC/IUPAP Joint Working Party (JWP) on the priority of claims to the discovery of new elements 113–116 and 118 has reviewed the relevant literature pertaining to several claims.

It was determined that the **Dubna-Livermore** collaborations share in the fulfillment of those criteria both for elements Z = 114 and 116

Provisional Recommendation – Names and Symbols of the Elements with Atomic Numbers 114 and 116

08 December 2011

A joint IUPAC/IUPAP Working Party (JWP) has confirmed the discovery of the elements with atomic numbers 114 and 116. In accord with IUPAC procedures, the discoverers proposed names as follows:

FLEROVIUM with the symbol, Fl, for the element 114

LIVERMORIUM with the symbol Lv for the element 116.

The Inorganic Chemistry Division recommended these proposals for acceptance.

IUPAC seeks your comments.

^{91}Pa
5f^{2}6d^1
231.03588
O. Hahn
1918

Chemistry of Protactinium

(1960 – 1969)

Thorium homogenious reactor

$$^{232}\mathrm{Th}\ (n,\gamma)\ ^{233}\mathrm{Th} \xrightarrow{\beta^-} {}^{233}\mathrm{Pa} \xrightarrow{\beta^-} {}^{233}\mathrm{U}$$


Laboratory of Prof. M.Haissinsky
(Institute of Radium, Paris, France, 1960)

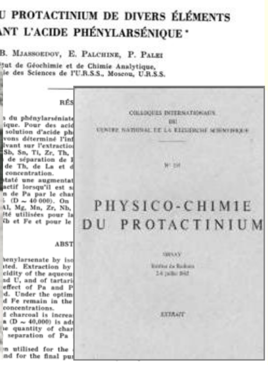

SÉPARATION DU PROTACTINIUM DE DIVERS ÉLÉMENTS UTILISANT L'ACIDE PHÉNYLARSÉNIQUE *

par B. Mjasoedov, E. Palchine, P. Palei

Institut de Géochimie et de Chimie Analytique, Académie des Sciences de l'U.R.S.S., Moscou, U.R.S.S.

PHYSICO-CHIMIE DU PROTACTINIUM

EXTRAIT

The first publication

Recovery of Protactinium-231

(1969)

About **200 mg of Pa** were recovered from ~30 tons of U_3O_8 by co-precipitation with $Zr_3(PO_4)_4$ and preconcentration on MnO_2 at the uranium plant in Glazov city

Moscow

Glazov

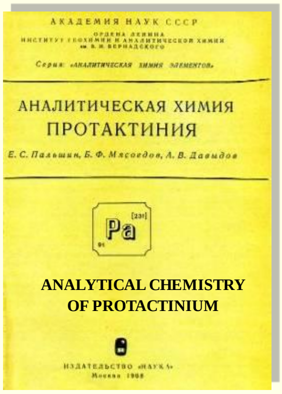
АКАДЕМИЯ НАУК СССР
ОРДЕНА ЛЕНИНА
ИНСТИТУТ ГЕОХИМИИ И АНАЛИТИЧЕСКОЙ ХИМИИ
им. В. И. ВЕРНАДСКОГО
Серия: «Аналитическая химия элементов»

АНАЛИТИЧЕСКАЯ ХИМИЯ
ПРОТАКТИНИЯ
Е. С. Пальшин, Б. Ф. Мясоедов, А. В. Давыдов

Pa [231] 91

ANALYTICAL CHEMISTRY
OF PROTACTINIUM

ИЗДАТЕЛЬСТВО «НАУКА»
Москва 1968

---

^{89}Ac
$6d^17s^2$
227,0278
Debierne
1899

Actinium

Recovery of weight quantities of ^{227}Ac from ~100 g ^{226}Ra irradiated by neutrons

- The photometric method of actinium determination was first developed
- Extraction of ^{227}Ac with Arsenazo III, PMBP, TOPO, D2EHPA from acidic solutions and with amines and quaternary ammonium salts from alkaline solutions
- Effective methods of separation of Ac from Ra, U, Th, TUE and REE were developed


АНАЛИТИЧЕСКАЯ ХИМИЯ ЭЛЕМЕНТОВ
З.К.КАРАЛОВА, Б.Ф.МЯСОЕДОВ
АКТИНИЙ
Ac
ACTINIUM

Chemistry of Transuranium Elements

^{92}U $5f^36d^1$ 238.0289 Klaproth 1789	^{93}Np $5f^46d^1$ 237.048166 McMillan 1940	^{94}Pu $5f^6$ 244.064197 Seaborg 1940	^{95}Am $5f^7$ 243.061372 Seaborg 1945	^{96}Cm $5f^76d^1$ 247.070346 Seaborg 1944	^{97}Bk $5f^9$ 247.0702 Seaborg 1944	^{98}Cf $5f^{10}$ 249.0748 Seaborg 1950

- **Stabilization of Pu, Am, Bk in unstable oxidation states**
- **Extraction of TUE from acidic and alkaline solutions with organophosphorous compounds and in two-phase aqueous systems**
- **Sorption: concentration, separation of TUE on organic and inorganic sorbents**
- **Behavior of TPE in gas phase and in supercritical CO_2**
- **Methods of determination of TUE: radiometry, electrochemistry, luminescence**
- **Synthesis of solid compounds, including nanostructured materials**

Discovery of Heptavalent State of Np, Pu, Am

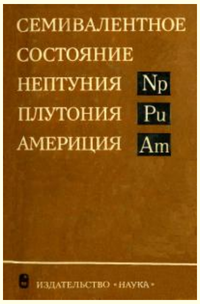

A.Gelman, G.Seaborg, V.Spitsin, N.Krot

Institute of Physical Chemistry (1969)

First Evidence of Existence Pu(VIII) in Alkaline Solutions (2007)

$$2Pu(VI) + O_3 = Pu(VII) + Pu(VIII)$$

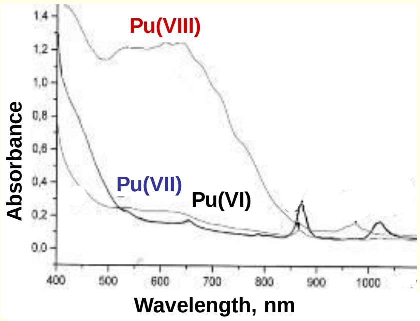

Absorption spectra of Pu in 2M NaOH solution

Products of reaction	Yield	ε ($L \cdot mole^{-1} \cdot cm^{-1}$) in 2M NaOH
Pu(VIII)	~15%	2600 at 607 nm
Pu(VII)	~85%	

Electrochemical oxidation

Oxidation potential of the couples, V	
Pu(VIII)/Pu(VII)	0,90
Pu(VII)/Pu(VI)	0,73

Interaction of Pu(VIII) with Pu(VI)

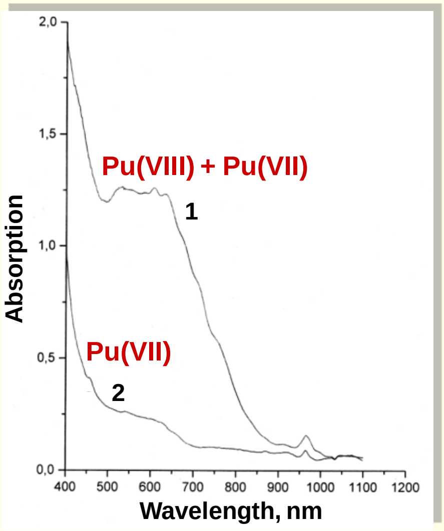

Pu(VIII) + Pu(VI) = 2Pu(VII)

Absorption spectra of:

1. Pu in 3,5M NaOH after ozonation of Pu(VI) for 40 min at 20°C
2. The same solution after interaction with $PuO_3 \cdot nH_2O$

Methods of separation and concentration

New Reagents for Extraction of Actinides

Organophosphorus compounds

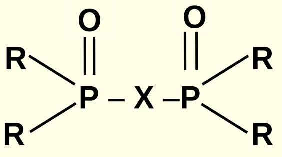

R = Ph, Bu;

X = $(CH)_2$; CHCl; CHBr;
CHJ; $CHC_{12}H_{25}$;
$CH\text{-}CH_2CH{=}CH_2$; $C{=}CH_2$

Dioxides of tetraaryl(alkyl)alkylenediphosphine

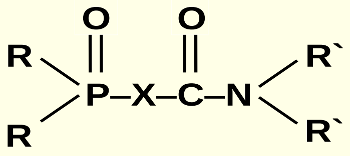

R = Tol, Ph, Hex, Bu, BuO;

R\` = Et, Bu;

X = CH_2, $CHCH_3$, CHC_7H_{15}
CHCl; CCl_2

Oxides of dialkyl(diaryl)[dialkylcarbamoylmethyl]phosphine («carbamoyls»)

Russian TRUEX Process

Extraction of Americium

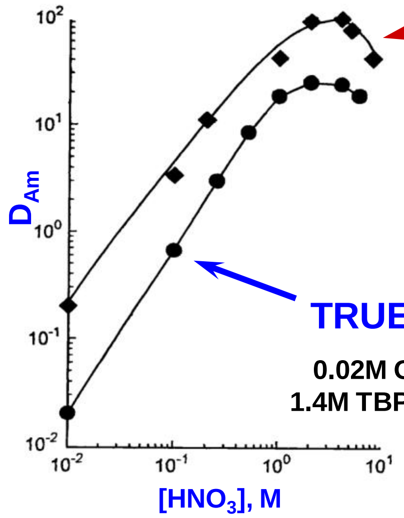

Russian TRUEX :

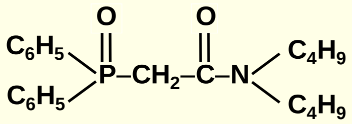

0.05M Ph_2Bu_2 – Fluoropol,
room temperature

TRUEX process:

0.02M OPhDiBCMPO –
1.4M TBP – Conoco, 30°C

New Reagents for Selective Extraction of Actinides

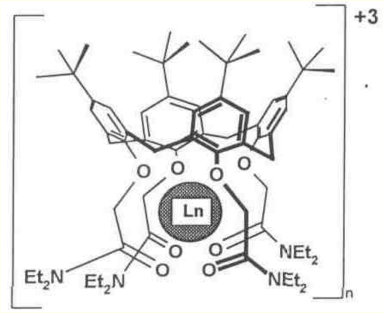

Calix[4]arenes for Tc(VII) extraction

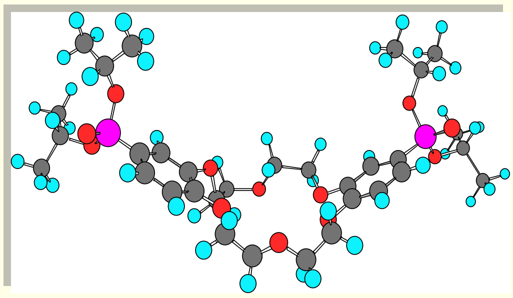

Phosphorinated Crown Ethers for separation of Am(III) and Eu(III)
f > 90

Fibrous “Filled” Sorbents

Novel type of sorption materials composed of two polymers:

Basis – porous polyacrylonitrile fiber
(inner diameter 30-40 μm)

Filler – high disperse powder of complexing or ion-exchange resin
(size of particles 5-10 μm)

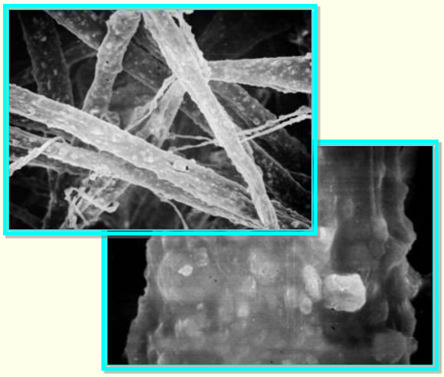


Forms of fibrous “filled” sorbents

Application of Fibrous «Filled» Sorbents for Radionuclide Preconcentration

Filler	Functional groups	Element recovery
POLYORGS 33, 34	Amidoxime and hydrazine	**Am, Pu, U, Th, Np, Pa** from natural waters
POLYORGS 4	3(5)-Methylpyrazole	**Pu** from 1-5M HNO_3
POLYORGS 17	1,3(5)-imethylpyrazole	**Tc** from natural and technological waters
Ionexchanger	Amine	

Countercurrent Chromatography for Separation of U, Pu, Am

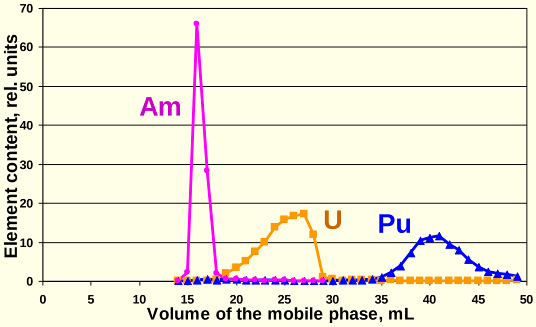

Planetary Centrifuge

- **Complete separation of Am from U and Pu is achieved in the system 0,075 M DMDOHTMA in dodecane – HNO_3**
- **Uranium fraction contains 100% of U and 0.7% of Pu**
- **Plutonium fraction contains 99.3% of pure Pu**

CCC Separation of ^{243}Am and ^{244}Cm

Stationary phase: 0.2 M DMDBDDEMA – tetrapropane
Moving phase: 3M HNO_3 (ω=660 rpm, F=0.5 mL/min, S_f =45%)

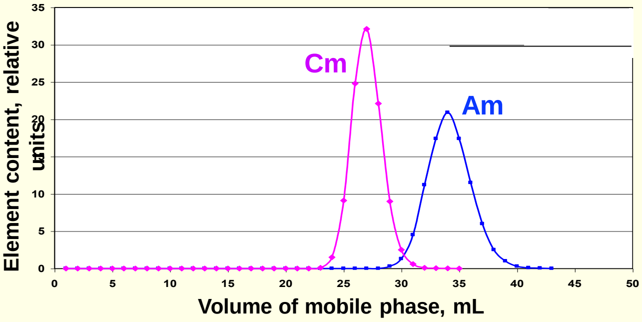

Fraction	Content, %	
	Cm	Am
Cm (9 mL)	**99.3**	**1.6**
Am (13 mL)	**0,7**	**98.4**

Radioanalytical Chemistry for Nuclear Fuel Cycle

Composition of Spent Nuclear Fuel

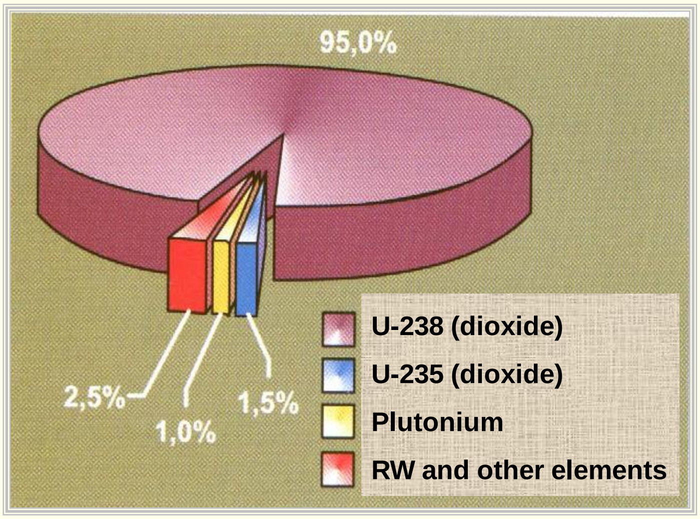

Ozersk City, Production Association “Mayak”

Spent Nuclear Fuel Reprocessing, PUREX-process

- Dissolution of SNF in nitric acid solutions
- Preparation of the solutions for extraction (organic flocculants and filtration)
- Extraction and separation of U, Pu, Np by 30% TBP in hydrocarbon solven

Main characteristics of the process

- Separation factor of U and Pu > $7{\cdot}10^5$
- Purification of U and Pu from fission products ~ 10^9.
- U, Pu and Np losses < 0.01%, 0.025%, 0.5%, respectively
- Large volumes of radioactive waste

Storage of Liquid High-level Radioactive Waste at "Mayak"

Storage type	Total volume, m^3	Filled volume, m^3	Radioactivity, MCi
Canyon 36 reservoirs with V=285 m^3	9120	7900	290
Canyon 5 reservoirs with V=1500 m^3 and V=500 m^3	5500	2800	57
Earth surface 20 reservoirs V=1170 m^3	23400	18400	146
Total	**38000**	**29000**	**500**

Amount of Vitrified Waste

Treated liquid waste – 11 460 m^3

Year	Weight, tons	Activity, MCi
1987-1990	162	3.96
1991	178	28.2
1992	563	77.7
1993	448	46.8
1994	407	57.4
1995	216	31.7
1996	270	38.2
1997-2004	>600	>76
Total	**>2830**	**>350**

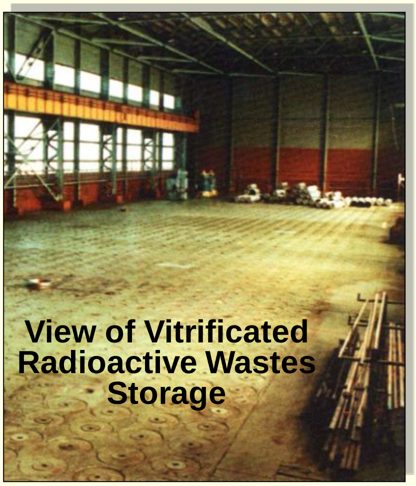

View of Vitrificated Radioactive Wastes Storage

Development of Modern Technologies for Spent Nuclear Fuel Reprocessing

REQUIREMENTS:

- **Safety of all the operations, connected with storage, transportation and utilization of SNF;**
- **Economy utilization of regenerated nuclear materials, taking into account the non-proliferation factor;**
- **Reduction of liquid HLW volume, demanded transportation and geological isolation;**
- **Transformation from modern nuclear energy to innovated systems of following generation**

New Approach for Reprocessing of Oxide Nuclear Fuel

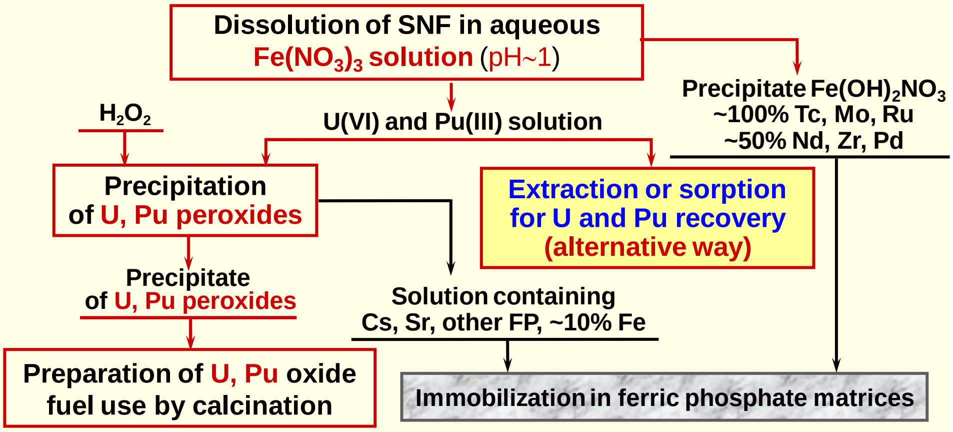

Dissolution of SNF in aqueous $Fe(NO_3)_3$ solution (pH~1)

Precipitate $Fe(OH)_2NO_3$
~100% Tc, Mo, Ru
~50% Nd, Zr, Pd

H_2O_2

U(VI) and Pu(III) solution

Precipitation of U, Pu peroxides

Extraction or sorption for U and Pu recovery (alternative way)

Precipitate of U, Pu peroxides

Solution containing Cs, Sr, other FP, ~10% Fe

Preparation of U, Pu oxide fuel use by calcination

Immobilization in ferric phosphate matrices

Advantages of proposed approach:

- **Decrease of the number of stages of SNF reprocessing**
- **Reduction of a volume of liquid radioactive wastes**
- **Decrease of Ecological Risks Arising on PUREX-process using**

Dissolution of Actinide Oxides by Supercritical CO_2 Containing $TBP \cdot HNO_3$

(t = 60°C, P = 250 atm)

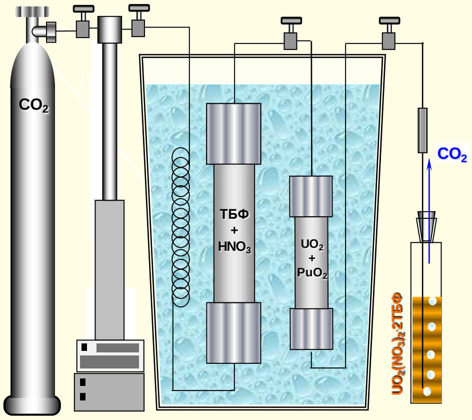

Scheme of Set-up for SFE

Compounds		Actinide (mg)	Extraction (%)
Oxides	UO_2	334.4	90
	UO_3	175.1	92
	U_3O_8	177.3	85
	PuO_2	50.1	<0.1
	NpO_2	55.0	<0.1
Mixture of dioxides	UO_2 PuO_2	150.5 37.4	87 <0.1
	UO_2 NpO_2	120.6 11.5	91 <0.1
Solid solution of dioxides	UO_2 PuO_2	4.7 0.25	94 90
	UO_2 PuO_2	6.14 2.15	89.6 93.1

Radioactive Waste Management

Peculiarities of Liquid Nuclear Waste

- Disposal of nuclear waste usually involves high ionic strength solutions (e.g., salts) and high temperatures
- Organic complexants are also present in the waste from processing systems
- Such complexants can increase solubility of actinides
- Ternary complexes (e.g., $Am(EDTA)(Ox)^{3-}$) likely to be present in waste systems
- Data of such complexation species are absent for the most part of liquid nuclear waste, which do not allow to do valid modeling for nuclear waste repositories

Solidification of Liquid HLRW

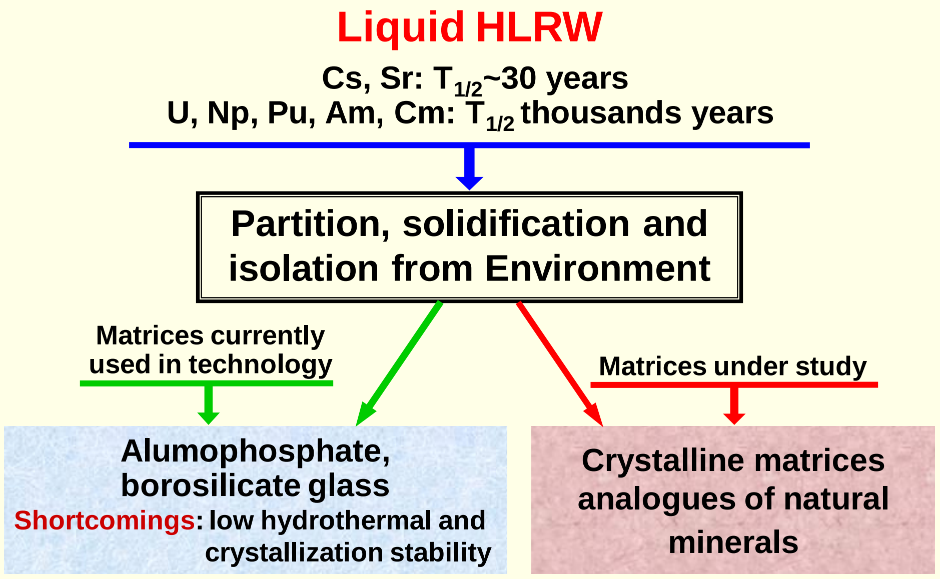

Liquid HLRW

Cs, Sr: $T_{1/2}$~30 years

U, Np, Pu, Am, Cm: $T_{1/2}$ thousands years

Partition, solidification and isolation from Environment

Matrices currently used in technology

Matrices under study

Alumophosphate, borosilicate glass

Shortcomings: low hydrothermal and crystallization stability

Crystalline matrices analogues of natural minerals

Recovery of TPE from HLRW with Ph_2Bu_2 in Fluoropol

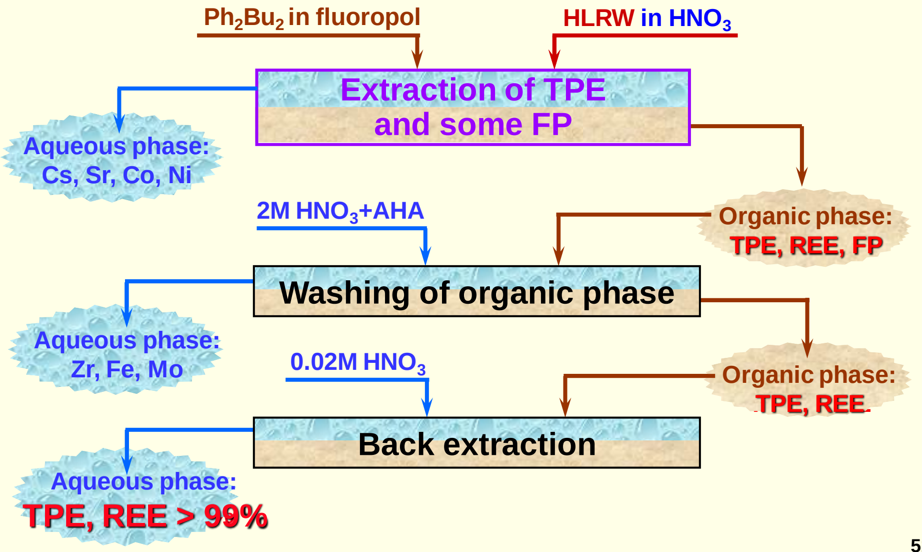

Ph_2Bu_2 in fluoropol

HLRW in HNO_3

Extraction of TPE and some FP

Aqueous phase: Cs, Sr, Co, Ni

Organic phase: TPE, REE, FP

2M HNO_3+AHA

Washing of organic phase

Aqueous phase: Zr, Fe, Mo

Organic phase: TPE, REE

0.02M HNO_3

Back extraction

Aqueous phase: TPE, REE > 99%

Basic Methods for Immobilization of Radionuclides in Mineral-like Matrices

- Cold pressing and sintering
- Hot pressing
- Induction melting in cold crucible

Shortcomings: laborious,
power-consuming,
high-tech operations

Alternative:

Self-propagating High-Temperature Synthesis

Self-propagating High-temperature Synthesis

Advantages:

- Simplicity of an equipment
- High synthesis rates (0.1-15 cm/s)
- High quality of products
- Absence of the large power expenses and fundamental scale restrictions

Ceramicrete Stabilization of Radioactive Liquid and Sludge Waste on “Mayak”

$MgO + KH_2PO_4 + 5H_2O = MgKPO_4{\cdot}6H_2O$

(at room temperature)

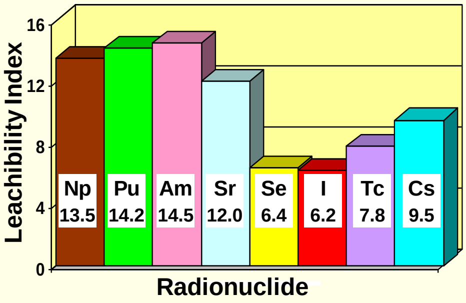

High resistance of the ceramicrete matrix to leaching of Np, Pu, Am and Sr by water

Recovery of Actinides from HLRW with Simultaneous Immobilization into the Matrix

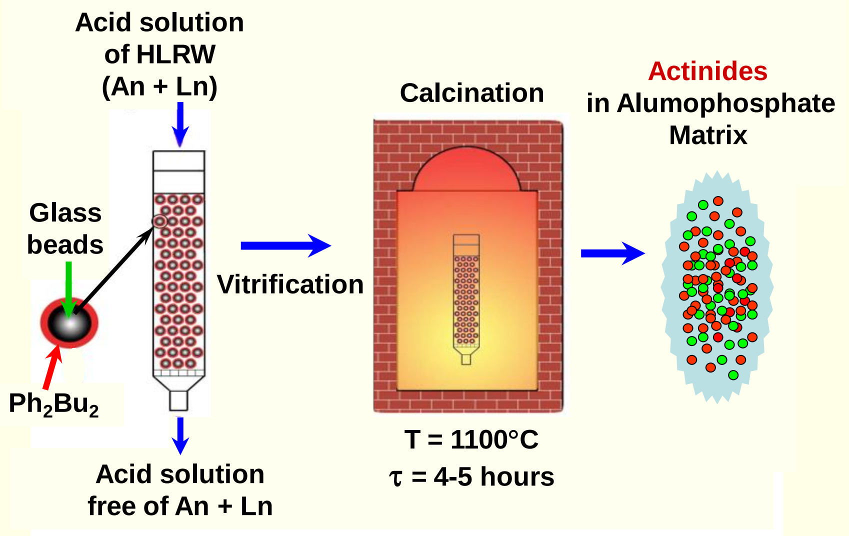

Acid solution of HLRW (An + Ln)

Glass beads

Ph_2Bu_2

Vitrification

Calcination

T = 1100°C

τ = 4-5 hours

Acid solution free of An + Ln

Actinides in Alumophosphate Matrix

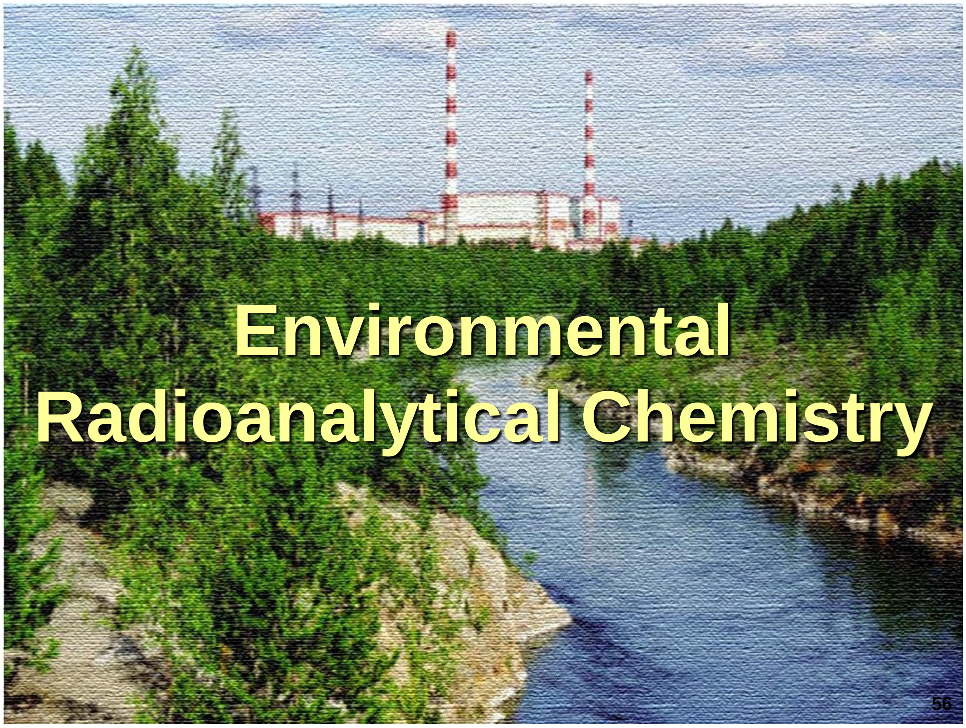

Environmental Radioanalytical Chemistry

Main Sources of Radionuclides Impact in the Environment

- Nuclear (thermonuclear) weapons tests
- Working of radiochemical plants supporting nuclear power cycle and production of plutonium for military purposes
- Dump of radioactive wastes into oceans
- Accidents on nuclear power plants

Actinides in the Environment

Purposes and tasks

- The study and estimation of sources of radioactive contamination
- Modern methods of determination of contents and speciation of actinides in the environmental samples
- Radioanalytical control for high-level radioactive waste management
- Monitoring in the sites of HLRW disposal
- Monitoring and remediation of contaminated territories

Radiochemical Procedures

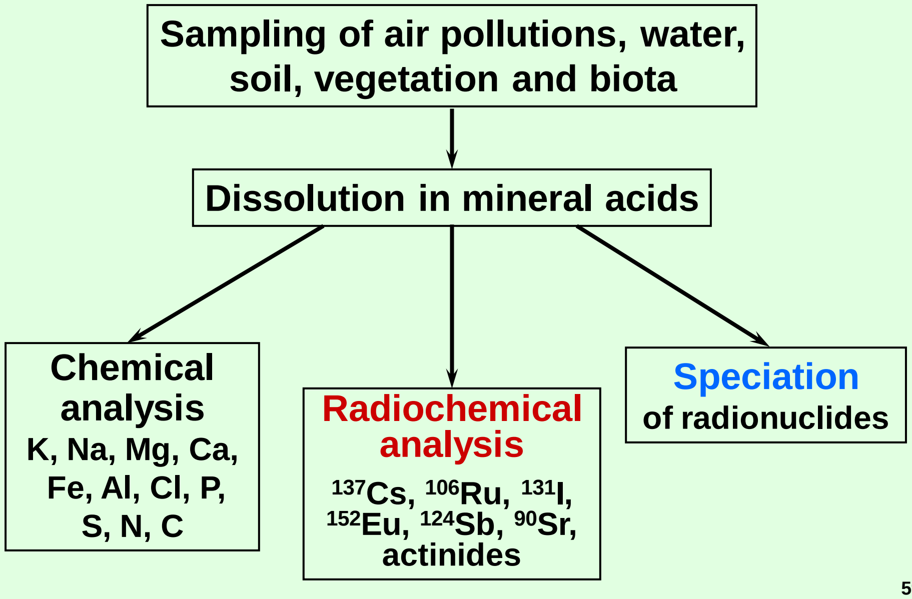

Sampling of air pollutions, water, soil, vegetation and biota

Dissolution in mineral acids

Chemical analysis
K, Na, Mg, Ca, Fe, Al, Cl, P, S, N, C

Radiochemical analysis
^{137}Cs, ^{106}Ru, ^{131}I, ^{152}Eu, ^{124}Sb, ^{90}Sr, actinides

Speciation of radionuclides

Novel Sorption Materials Based On Carbon Nanotubes (CNT)

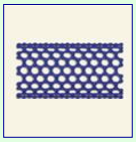

CNT «Taunit» without modification

Recovery of U, Pu, Am, Eu, Tc from natural and waste waters (pH=3-10)

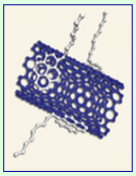

Solid-phase extractants

CNTs «Taunit» + organophosphorus ligands (e.g. CMPO, TOPO)

Recovery of U, Pu, Np, Am, Eu from nitric acid solutions (3-8M HNO_3)

Composite materials

CNTs «Taunit» + complexing polymers
CNTs «Taunit» + ferrocyanides of heavy metals

Recovery of Pd from nitric acid solutions
Recovery of Cs, Sr from neutral solutions

Sorption by Solid-phase Extractants Based on Carbon Nanotubes «Taunit» from 3M HNO_3

Impregnated ligands	Radionuclides	Distribution coefficients, mL/g
Diphenyldibutyl[carbamoyl-methyl]phosphine oxide **CMPO**	U(VI), Pu(IV), Np(V), Am(III), Eu(III)	$10^3 – 10^4$
Tri-*n*-octylphosphine oxide **TOPO**	U(VI), Pu(IV), Np(V)	10^3
Tri-*n*-butylphosphate **TBP**	Pu(IV)	10^2
N,N-Dimethyl-N,N-dioctylhexyletoximalonamide **DMDOHEMA**	U(VI), Pu(IV), Np(V)	$10^3 – 10^4$

Ligand content on the solid phase 0.7-1.3 mmole/g

Solid-phase Extractants with the Use of Ionic Liquids (IL)

Cations (R: $C_4 – C_{16}$):

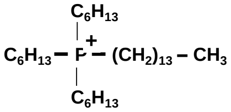

$$C_6H_{13}-\overset{\overset{C_6H_{13}}{|}}{\underset{\underset{C_6H_{13}}{|}}{\overset{+}{P}}}-(CH_2)_{13}-CH_3$$

phosphonium

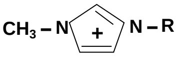

imidazolium

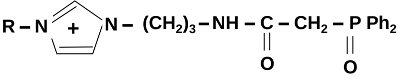

task-specific IL with CMPO groups

Anions: Cl^-, PF_6^-

Sorption Ability of Solid-phase Extractants in 3M HNO_3

ILs and reagents	Solid supports	Recovery
Cyphos IL-101	XAD-7, «Taunit», PAN-fiber	Pu(IV) 95-96 %
$[C_{16}MIm]^+PF_6^- + Ph_2Bu_2$	XAD-7, «Taunit»	U(VI), Pu(IV), Am(III), Eu(III) 90-99 %
Task-Specific IL $[C_{16}MIm]^+Ph_2CMPO\ PF_6^-$	«Taunit»	U(VI), Pu(IV), Am(III), Eu(III) 87-99 %

Ultrafiltration with Actinides Complex Formation

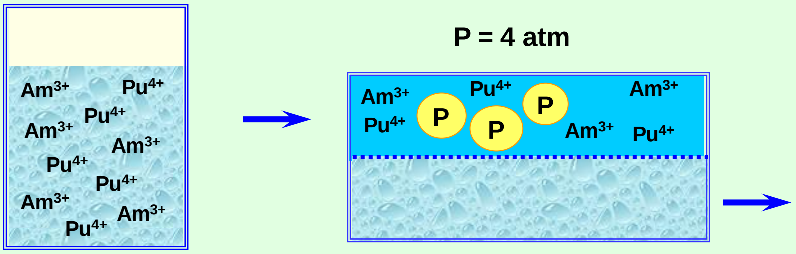

P – water soluble polymers with a molecular mass 20 000 – 50 000 D
(polyethylenamine; polyvinyl alcohol; poly[oxyn]; poly[amylphosphate]; poly[ethylene diamine tetraacetate])

Methods of Radiochemical Analysis

Preconcentration

γ-spectroscopy
^{137}Cs, ^{106}Ru, ^{131}I
^{152}Eu, ^{124}Sb

Samples

β-radiometry
^{90}Sr, ^{210}Pb

Purification and isolation

α-spectroscopy
Ra, Po, Th, Np, Pu, Am, Cm

Membrane Luminescence Determination of Trace Amounts of U, Np, Pu, Am

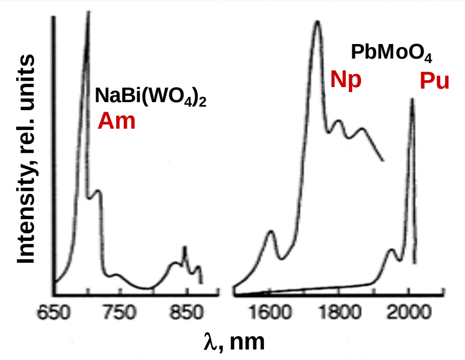

Luminescence Spectra of Crystal Phosphor with actinides

Membrane preconcentration

↓

Sample preparation

↓

Luminescent determination

Detection limit, g/g	
U $5 \cdot 10^{-12}$	Pu $2 \cdot 10^{-11}$
Np $5 \cdot 10^{-13}$	Am $2 \cdot 10^{-12}$

Speciation of Actinides in Aqueous Samples

Water Sample → **Ultrafiltration**

Ultrafiltration → Colloids, Suspended Matter, True Solution

Colloids → **Fractionation according to Particle Size**

True Solution → **Ion Exchange**, **Electrophoresis**

Ion Exchange → Cationic Species, Anionic Species, Neutral Species

Electrophoresis → Cationic Species, Anionic Species, Neutral Species

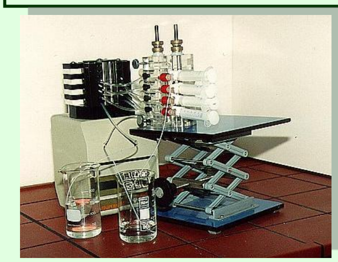

Methods of Colloids Partitioning

- Membrane micro- and ultra filtration
- Dialysis
- Sequential leaching
- Electrophoresis
- Membrane extraction
- Complex-forming ultra filtration

Distribution of Actinides During Membrane Size Fractionation

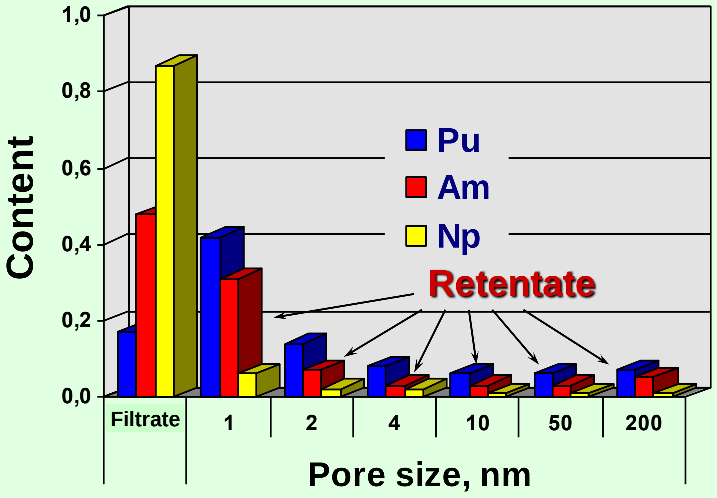

Speciation of Some Radionuclides in Sediments of Reservoir #10 “Mayak”

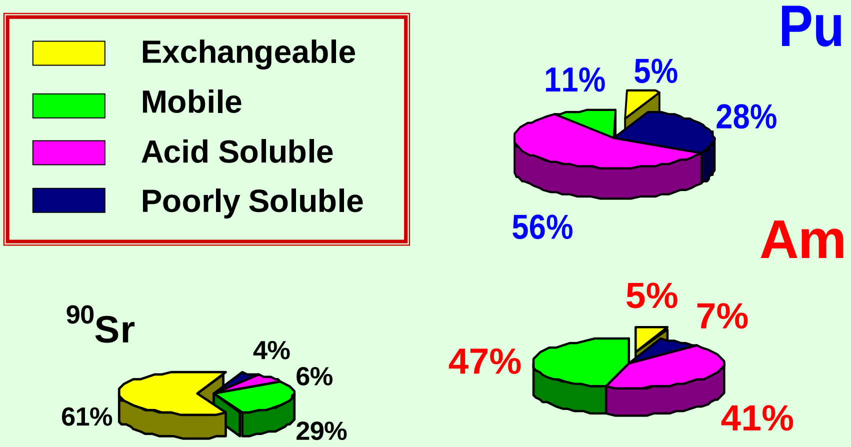

Nano-scale Distribution of U and Pu with Fe(III) Oxide Colloids

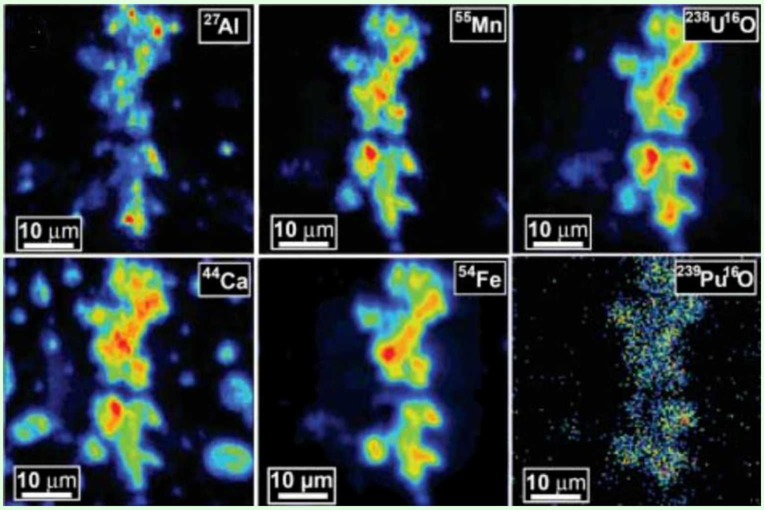

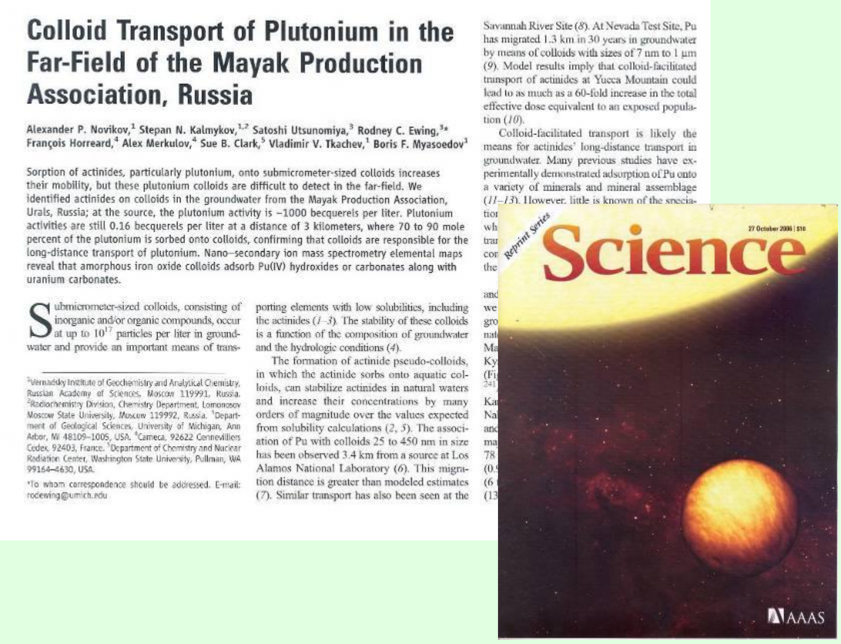

Colloid Transport of Plutonium in the Far-Field of the Mayak Production Association, Russia

Alexander P. Novikov,[1] Stepan N. Kalmykov,[1,2] Satoshi Utsunomiya,[3] Rodney C. Ewing,[3]* François Horreard,[4] Alex Merkulov,[4] Sue B. Clark,[5] Vladimir V. Tkachev,[1] Boris F. Myasoedov[1]

Sorption of actinides, particularly plutonium, onto submicrometer-sized colloids increases their mobility, but these plutonium colloids are difficult to detect in the far-field. We identified actinides on colloids in the groundwater from the Mayak Production Association, Urals, Russia; at the source, the plutonium activity is ~1000 becquerels per liter. Plutonium activities are still 0.16 becquerels per liter at a distance of 3 kilometers, where 70 to 90 mole percent of the plutonium is sorbed onto colloids, confirming that colloids are responsible for the long-distance transport of plutonium. Nano–secondary ion mass spectrometry elemental maps reveal that amorphous iron oxide colloids adsorb Pu(IV) hydroxides or carbonates along with uranium carbonates.

Submicrometer-sized colloids, consisting of inorganic and/or organic compounds, occur at up to 10^{17} particles per liter in groundwater and provide an important means of transporting elements with low solubilities, including the actinides (*1–3*). The stability of these colloids is a function of the composition of groundwater and the hydrologic conditions (*4*).

The formation of actinide pseudo-colloids, in which the actinide sorbs onto aquatic colloids, can stabilize actinides in natural waters and increase their concentrations by many orders of magnitude over the values expected from solubility calculations (*2*, *5*). The association of Pu with colloids 25 to 450 nm in size has been observed 3.4 km from a source at Los Alamos National Laboratory (*6*). This migration distance is greater than modeled estimates (*7*). Similar transport has also been seen at the Savannah River Site (*8*). At Nevada Test Site, Pu has migrated 1.3 km in 30 years in groundwater by means of colloids with sizes of 7 nm to 1 μm (*9*). Model results imply that colloid-facilitated transport of actinides at Yucca Mountain could lead to as much as a 60-fold increase in the total effective dose equivalent to an exposed population (*10*).

Colloid-facilitated transport is likely the means for actinides' long-distance transport in groundwater. Many previous studies have experimentally demonstrated adsorption of Pu onto a variety of minerals and mineral assemblage (*11–13*). However, little is known of the specia-

---

[1] Vernadsky Institute of Geochemistry and Analytical Chemistry, Russian Academy of Sciences, Moscow 119991, Russia. [2] Radiochemistry Division, Chemistry Department, Lomonosov Moscow State University, Moscow 119992, Russia. [3] Department of Geological Sciences, University of Michigan, Ann Arbor, MI 48109–1005, USA. [4] Cameca, 92622 Gennevilliers Cedex, 92403, France. [5] Department of Chemistry and Nuclear Radiation Center, Washington State University, Pullman, WA 99164–4630, USA.

*To whom correspondence should be addressed. E-mail: rodewing@umich.edu

Actual Basic Research in Radiochemistry

- **The study of chemical properties of actinides and fission products (speciation in solutions, new solid compounds, gas phase behavior; redox-reactions, complex formation reactions);**
- **Theory of extraction, sorption, precipitation and other methods for radionuclide isolation and separation;**
- **Synthesis of new effective, selective and radiation-resistant extractants, solvents and sorbents;**
- **The study on phase equilibriums in complex heterogeneous multicomponent systems;**
- **The study of nuclear-chemical processes in minerals, rocks and composite materials.**

Thank you very much for your attention

Japanese-Russian Workshop on Colloidal Transport of Radionuclides

Tokyo, 22-23 March 2006

“Selective recognition of imidazoles: an assembling tool for highly linear molecular wires".

Jean Weiss (Strasbourg, France)

Invited lecture

Trilateral seminar on supramolecular, intermolecular, interaggregate interactions and separation chemistry, IPCE RAS, Moscow, Russian Federation

20.-23.07.2012

SEVENTH EUROPEAN SUMMER
SCHOOL ON SUPRAMOLECULAR,
INTERMOLECULAR,
INTERAGGREGATE INTERACTIONS
AND
SEPARATION CHEMISTRY

Selective recognition of imidazoles: an assembling tool for highly linear molecular wires

Jean Weiss

C**himie des **L**igands à **A**rchitecture **C**ontrôlée **CLAC
***C**ontrolled **L**igand **A**rchitecture in **C**oordination chemistry*
UMR 7177 CNRS-UDS
1, rue Blaise Pascal 67070 Strasbourg, France.

jweiss@unistra.fr

Porphyrins as building blocks

A Natural choice :

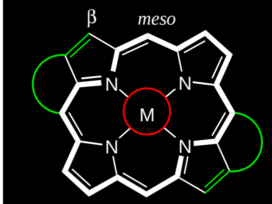

Highly stable: planar 18 π electrons aromatic [4 x 4 + 2]

Highly Colored: 400-450 nm ~ ε 300 000

500-700 nm ~ ε 30 000

Photo and electroactive species (depends usually on M)

Fonctionalization known => « Molecular Building Block »

…present in : enzymes, plants, bacterium

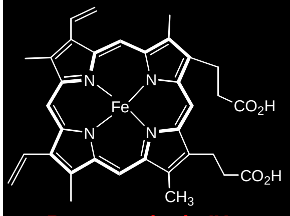

Protoporphyrin IX

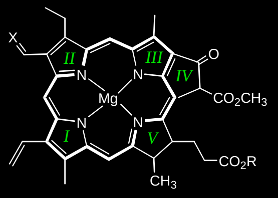

Chlorophyll

a: X=H_2
b: X=O
R= Phytyl

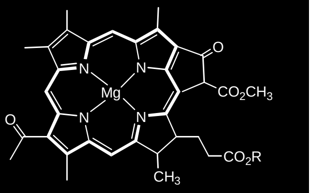

Bacteriochlorophyll a:
R= Phytyl
or Geranyl

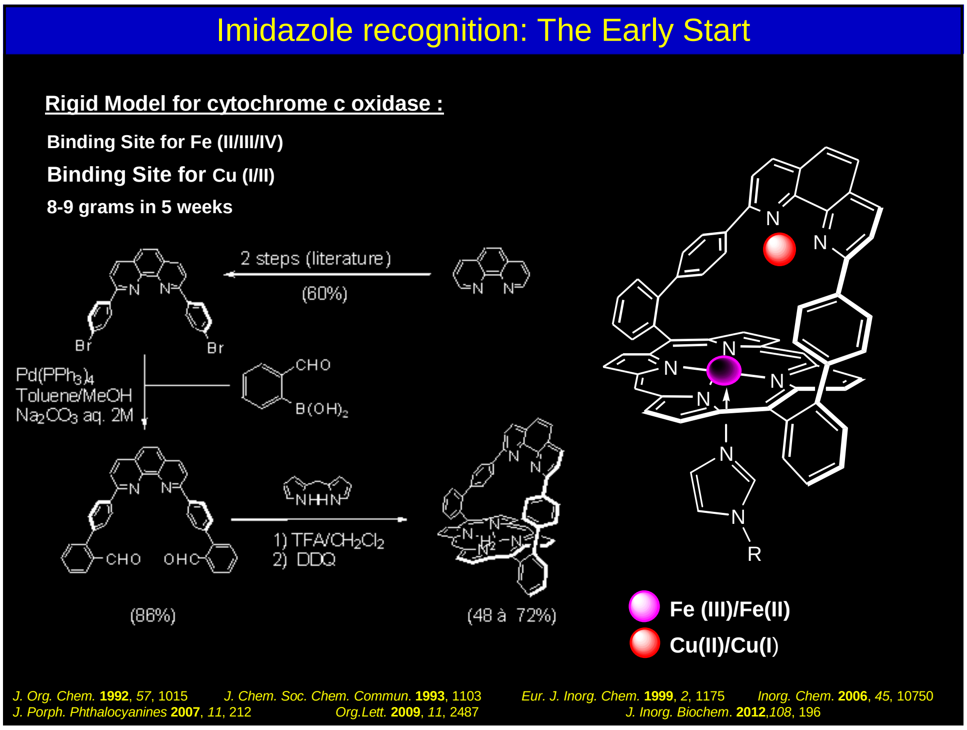

Imidazole recognition: The Early Start

Rigid Model for cytochrome c oxidase :

Binding Site for Fe (II/III/IV)

Binding Site for Cu (I/II)

8-9 grams in 5 weeks

● **Fe (III)/Fe(II)**

● **Cu(II)/Cu(I)**

J. Org. Chem. **1992**, *57*, 1015 *J. Chem. Soc. Chem. Commun.* **1993**, 1103 *Eur. J. Inorg. Chem.* **1999**, *2*, 1175 *Inorg. Chem.* **2006**, *45*, 10750
J. Porph. Phthalocyanines **2007**, *11*, 212 *Org.Lett.* **2009**, *11*, 2487 *J. Inorg. Biochem.* **2012**,*108*, 196

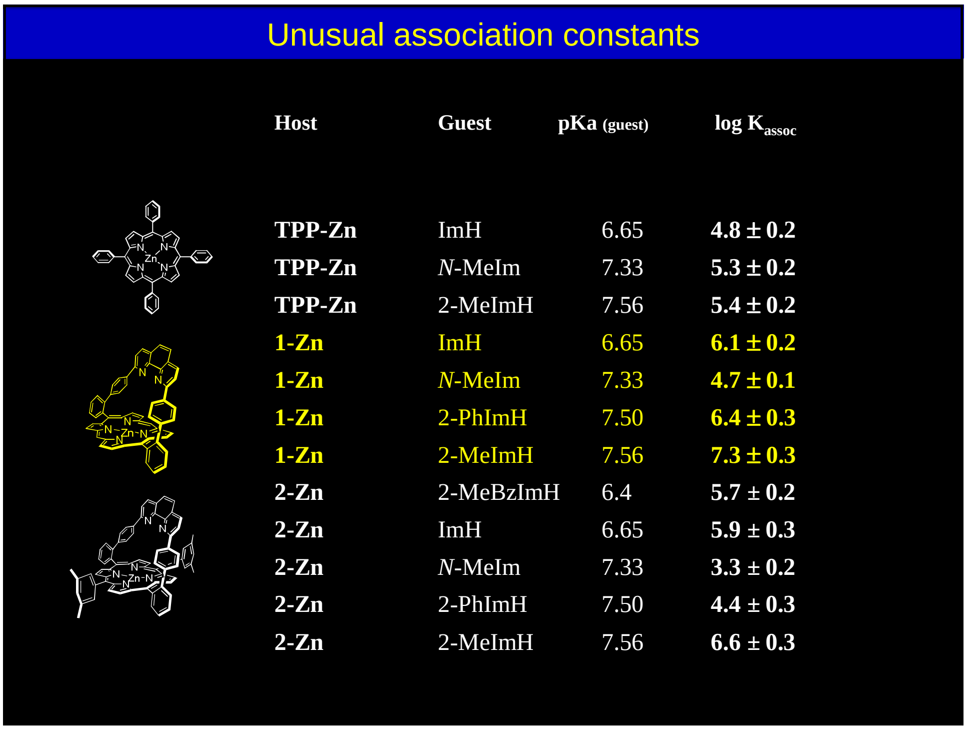

Unusual association constants

Host	Guest	pKa (guest)	log K_{assoc}
TPP-Zn	ImH	6.65	**4.8 ± 0.2**
TPP-Zn	*N*-MeIm	7.33	**5.3 ± 0.2**
TPP-Zn	2-MeImH	7.56	**5.4 ± 0.2**
1-Zn	ImH	6.65	**6.1 ± 0.2**
1-Zn	*N*-MeIm	7.33	**4.7 ± 0.1**
1-Zn	2-PhImH	7.50	**6.4 ± 0.3**
1-Zn	2-MeImH	7.56	**7.3 ± 0.3**
2-Zn	2-MeBzImH	6.4	**5.7 ± 0.2**
2-Zn	ImH	6.65	**5.9 ± 0.3**
2-Zn	*N*-MeIm	7.33	**3.3 ± 0.2**
2-Zn	2-PhImH	7.50	**4.4 ± 0.3**
2-Zn	2-MeImH	7.56	**6.6 ± 0.3**

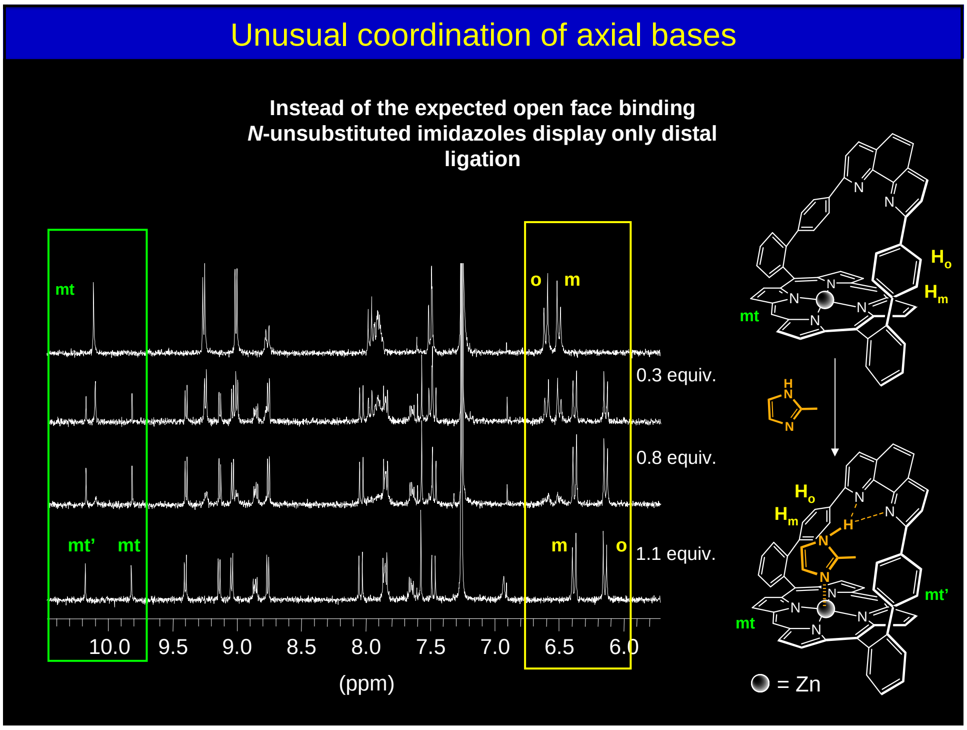

Unusual coordination of axial bases

Instead of the expected open face binding *N*-unsubstituted imidazoles display only distal ligation

---

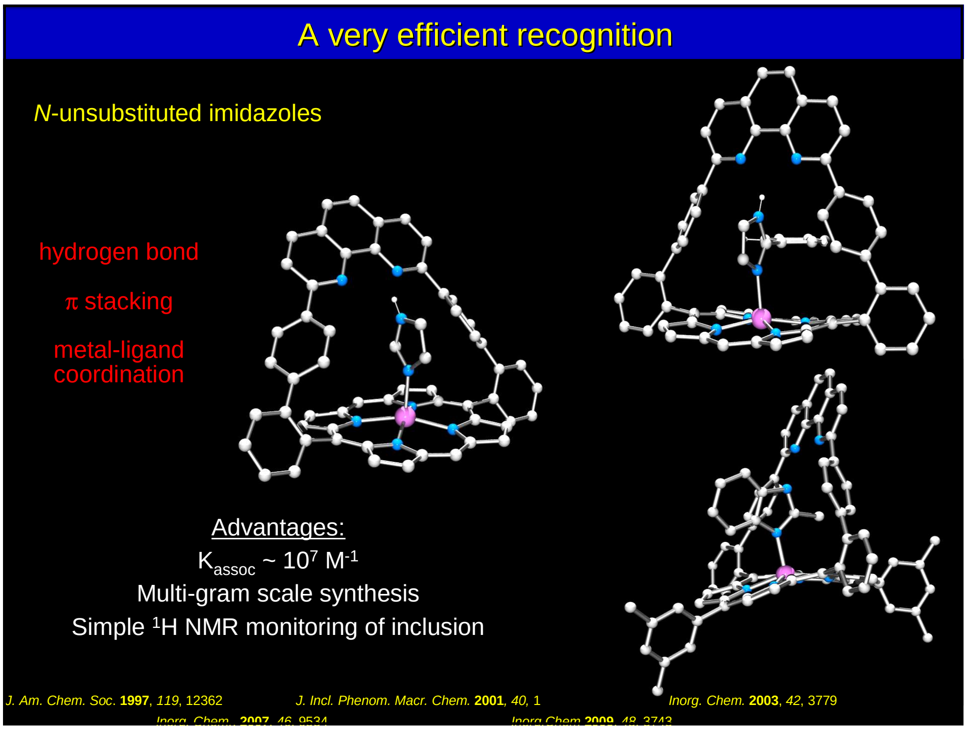

A very efficient recognition

N-unsubstituted imidazoles

hydrogen bond

π stacking

metal-ligand coordination

Advantages:

K_{assoc} ~ 10^7 M^{-1}

Multi-gram scale synthesis

Simple ^1H NMR monitoring of inclusion

J. Am. Chem. Soc. **1997**, *119*, 12362 *J. Incl. Phenom. Macr. Chem.* **2001**, *40*, 1 *Inorg. Chem.* **2003**, *42*, 3779

Inorg. Chem.. **2007**, *46*, 9534 *Inorg.Chem* **2009**, *48*, 3743

Iterative imidazole binding

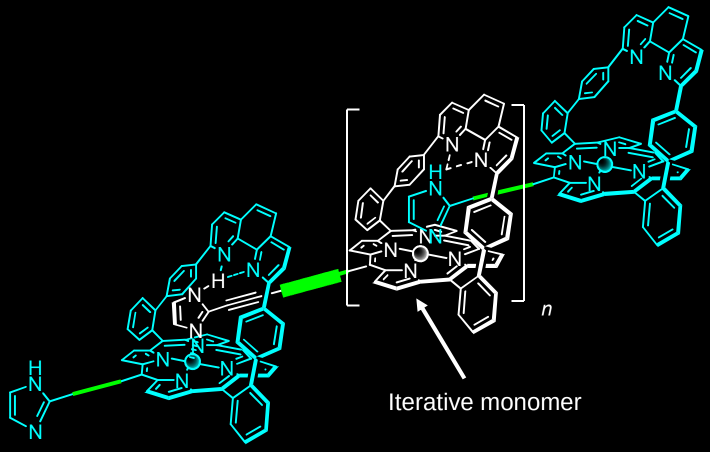

Iterative monomer

— Optimal spacer for communication ??

Molecular wires: inspiration

=> Covalent dyads, triads, tetrads,… Self-assembled wires

BChla arrangement

Rps. acidophila,

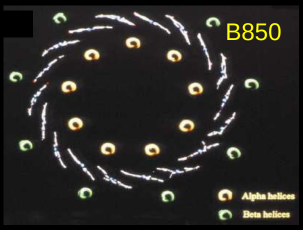

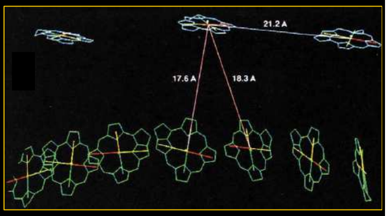

Reproduction of the B850's arrangement using synthetic approaches?

A review on « The structural basis of light-harvesting in purple bacteria »
Cogdell, R. J.; Isaacs Neil W.; Freer, A. A.; Howard, T. D. Gardiner, A. T.; Prince, S. M.; Papiz, M. Z.
FEBS Lett. **2003**, 555, 35.

Covalent synthesis and self-assembly of wires

Covalent Wires

Full geometric control over of the chromophore’s arrangement…
=> **Essential information** for the design of self-assembled wires…

Self-Assembled Wires

Concept: The final architecture is programmed in the monomer
Goals: Linearity, Orientation, Infinite Growth
(doping?...)

Covalent linear inspiration (and information)

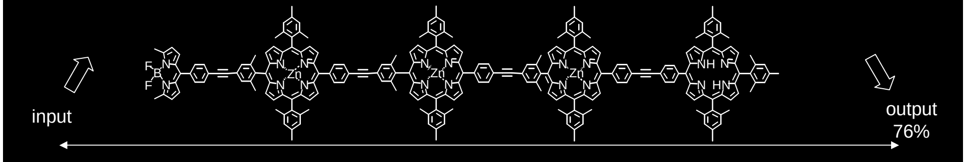

input

output
76%

90 Å

R.W. Wagner, J.S. Lindsey *J. Am. Chem. Soc.* 1994, 116, 9759.

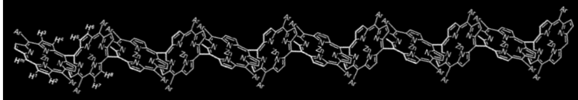

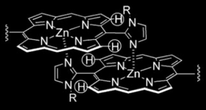

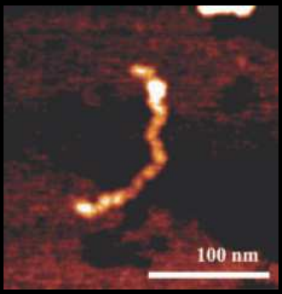

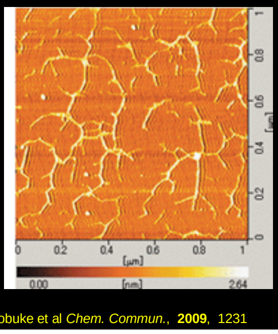

A. Osuka et al. *Chem. Eur. J.* **2005**, *11*, 3389

Y. Kobuke et al *Chem. Commun.*, **2009**, 1231

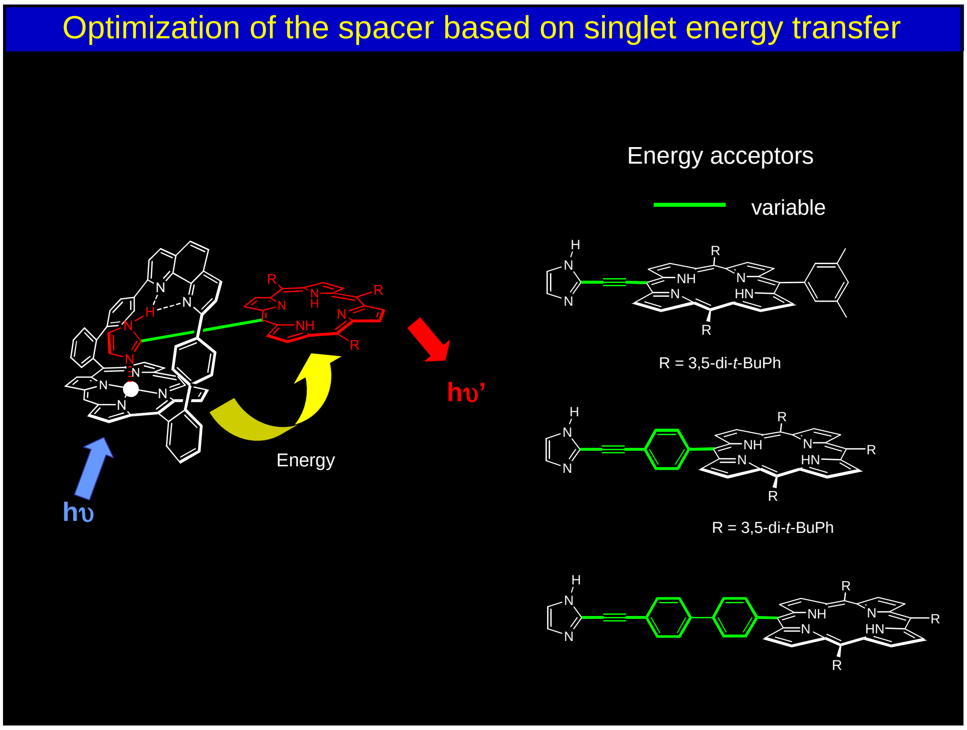

Optimization of the spacer based on singlet energy transfer

Energy acceptors

🟩 variable

R = 3,5-di-*t*-BuPh

R = 3,5-di-*t*-BuPh

Energy

hυ

hυ'

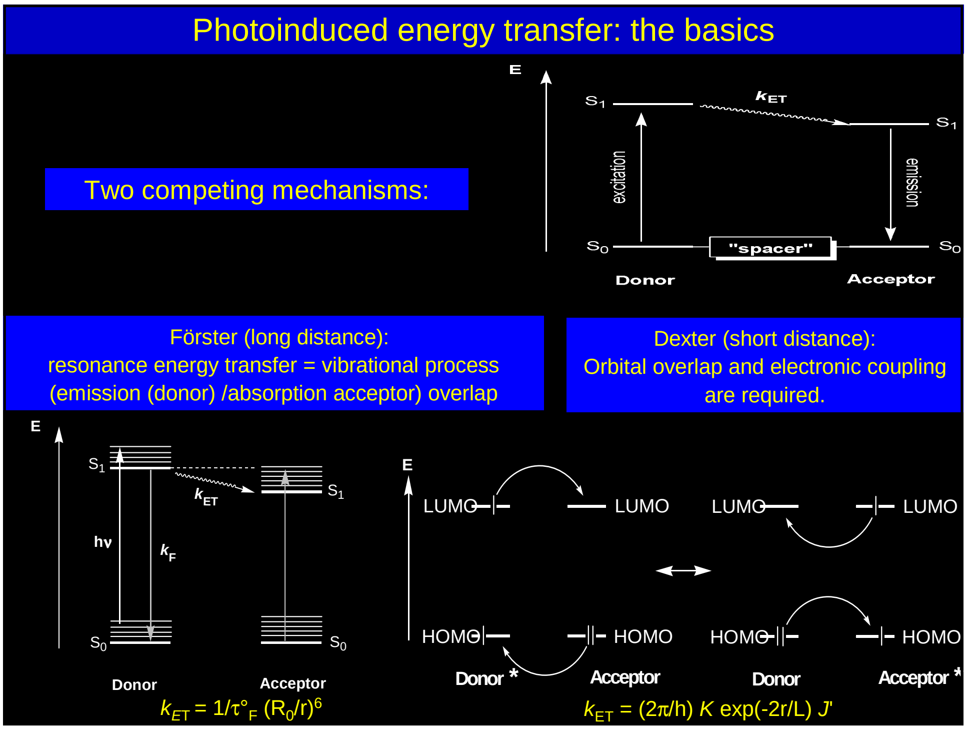

Photoinduced energy transfer: the basics

Two competing mechanisms:

Förster (long distance):
resonance energy transfer = vibrational process
(emission (donor) /absorption acceptor) overlap

Dexter (short distance):
Orbital overlap and electronic coupling
are required.

$k_{ET} = 1/\tau^{\circ}_{F}\,(R_0/r)^6$

$k_{ET} = (2\pi/h)\,K\,\exp(-2r/L)\,J'$

Fluorescence quenching

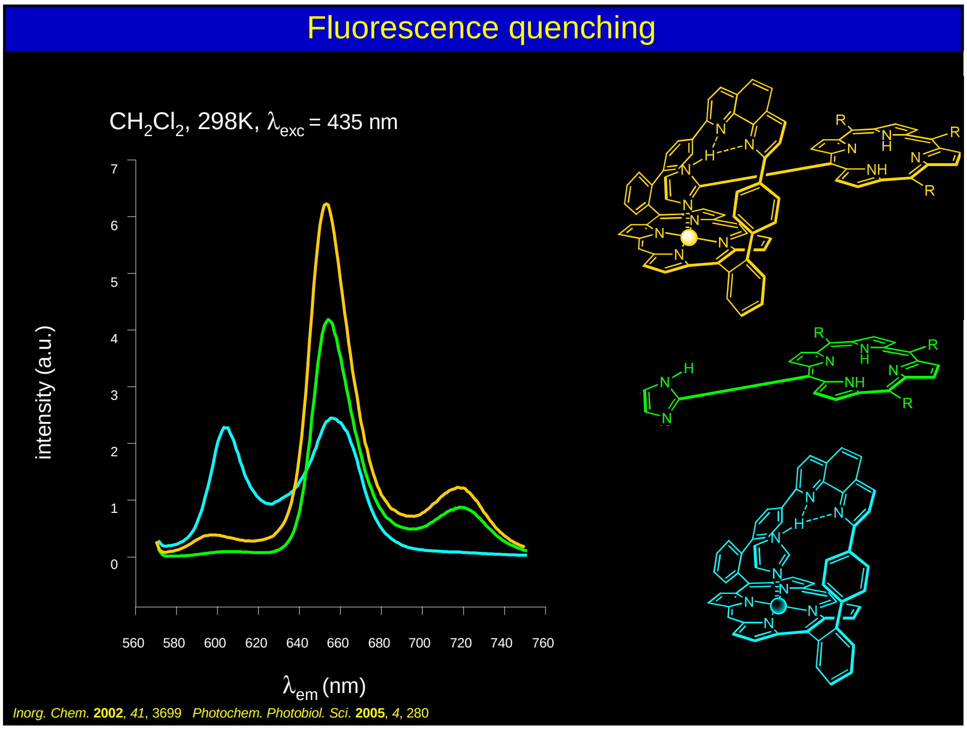

Inorg. Chem. **2002**, *41*, 3699 *Photochem. Photobiol. Sci.* **2005**, *4*, 280

Optimization of the Spacer for Singlet Energy Transfer

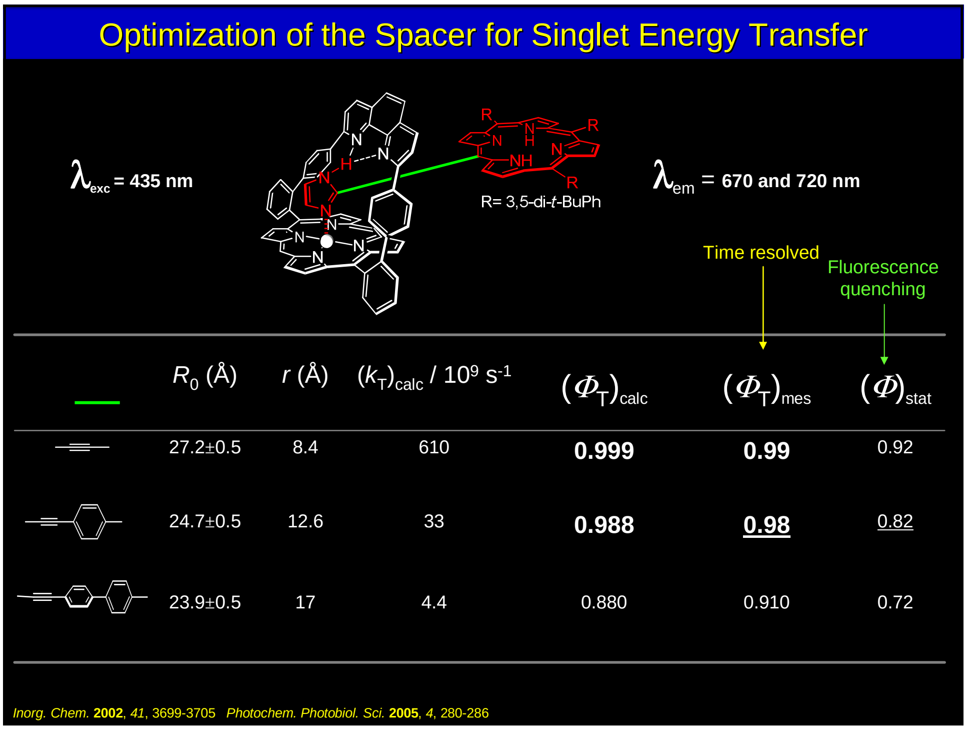

λ_{exc} = 435 nm

R= 3,5-di-*t*-BuPh

λ_{em} = 670 and 720 nm

Time resolved

Fluorescence quenching

	R_0 (Å)	r (Å)	$(k_T)_{calc}$ / 10^9 s^{-1}	$(\Phi_T)_{calc}$	$(\Phi_T)_{mes}$	$(\Phi)_{stat}$
	27.2±0.5	8.4	610	**0.999**	**0.99**	0.92
	24.7±0.5	12.6	33	**0.988**	**0.98**	0.82
	23.9±0.5	17	4.4	0.880	0.910	0.72

Inorg. Chem. **2002**, *41*, 3699-3705 *Photochem. Photobiol. Sci.* **2005**, *4*, 280-286

Förster resonance energy transfer in triads

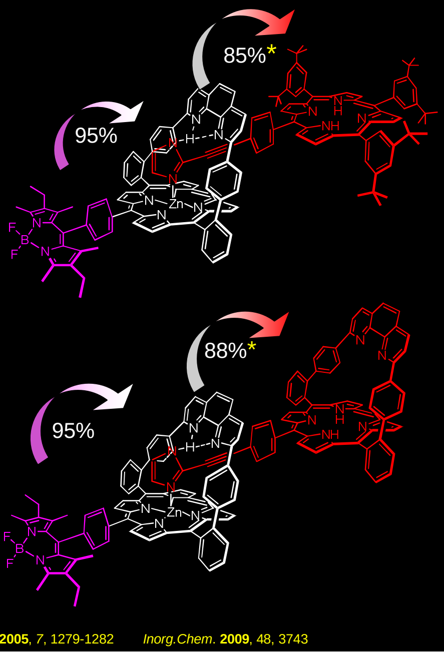

- *Fluorescence quenching measurements

- Only one geometry from ¹H NMR

- A candidate for coordination polymer formation

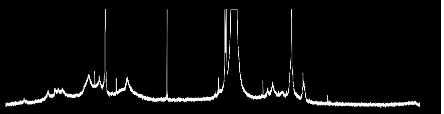

Org. Lett. **2005**, *7*, 1279-1282 *Inorg.Chem.* **2009**, 48, 3743

Synthesis of a soluble strapped porphyrin

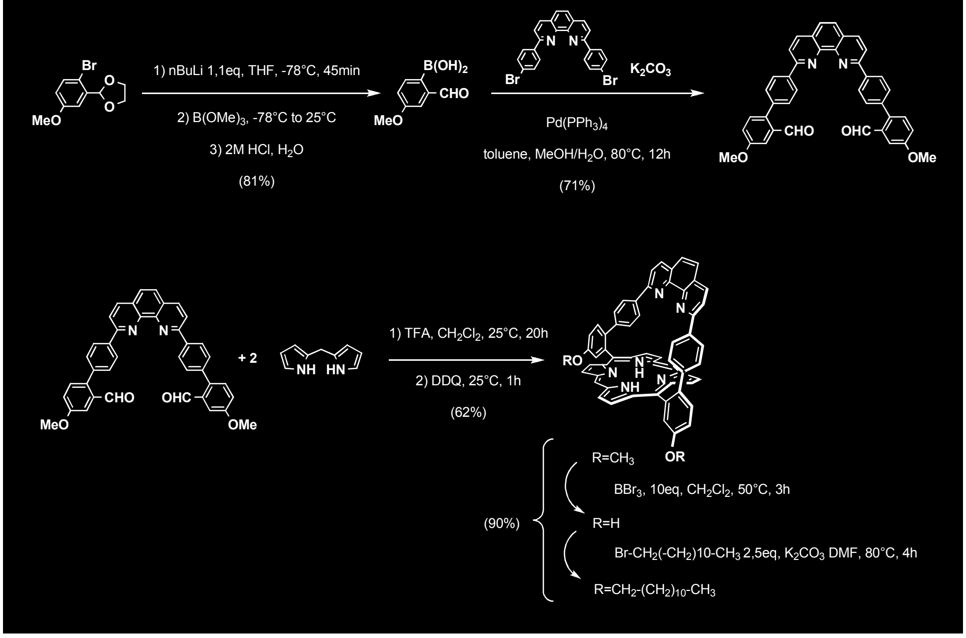

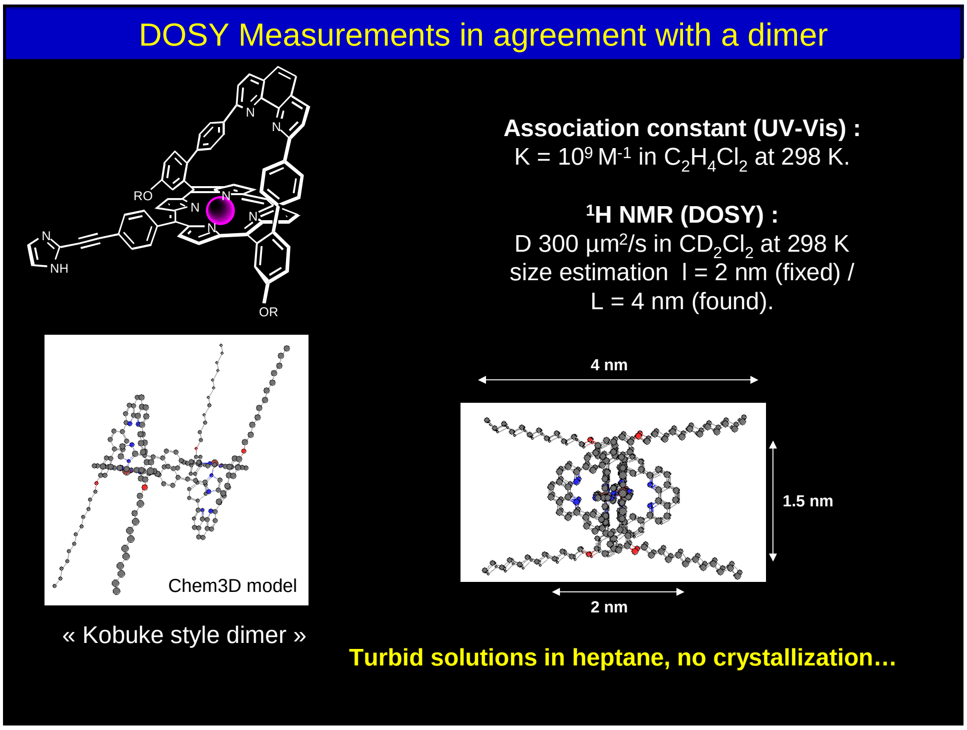

DOSY Measurements in agreement with a dimer

Association constant (UV-Vis) :
K = 10^9 M^{-1} in $C_2H_4Cl_2$ at 298 K.

^{1}H NMR (DOSY) :
D 300 μm^2/s in CD_2Cl_2 at 298 K
size estimation l = 2 nm (fixed) /
L = 4 nm (found).

Chem3D model

« Kobuke style dimer »

Turbid solutions in heptane, no crystallization…

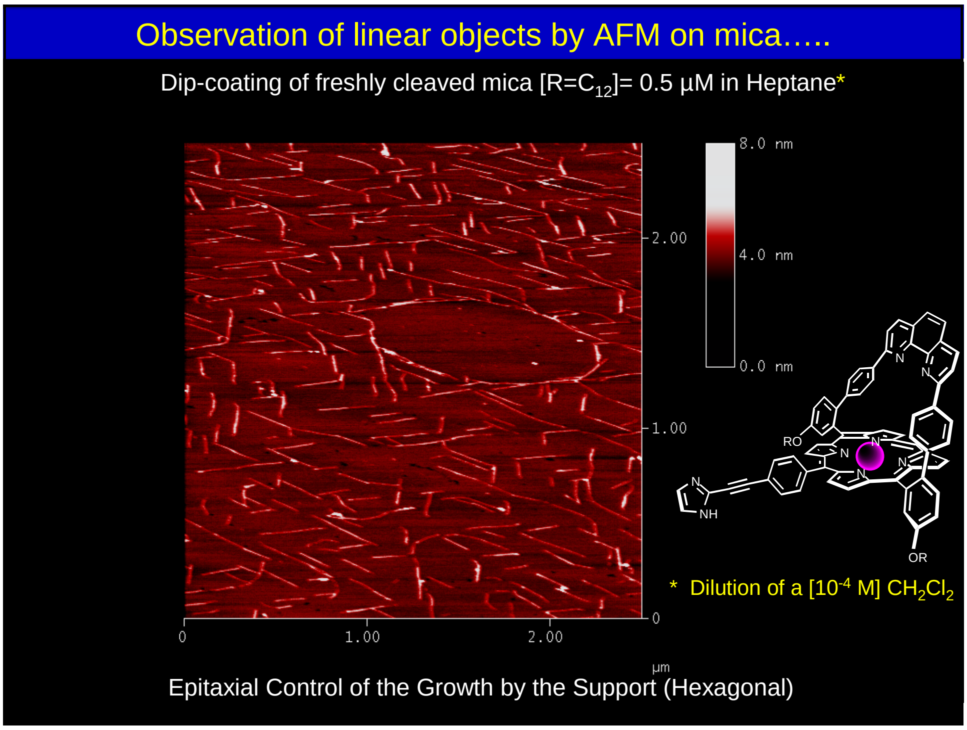

Observation of linear objects by AFM on mica…..

Dip-coating of freshly cleaved mica [R=C_{12}]= 0.5 µM in Heptane*

* Dilution of a [10^{-4} M] CH_2Cl_2

Epitaxial Control of the Growth by the Support (Hexagonal)

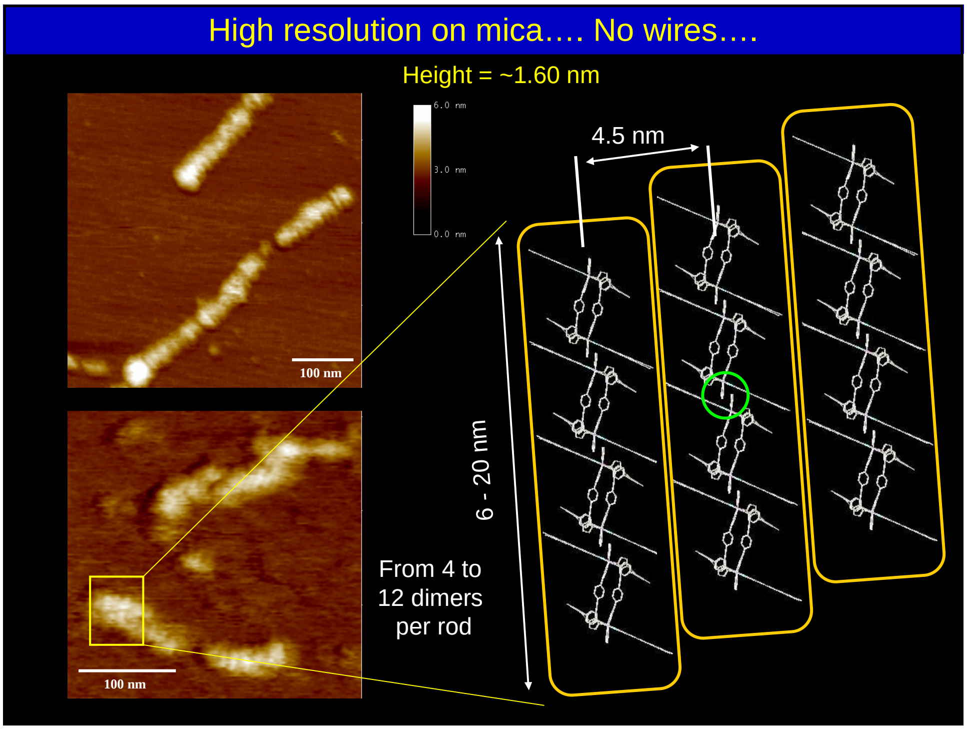

High resolution on mica…. No wires….

Height = ~1.60 nm

From 4 to 12 dimers per rod

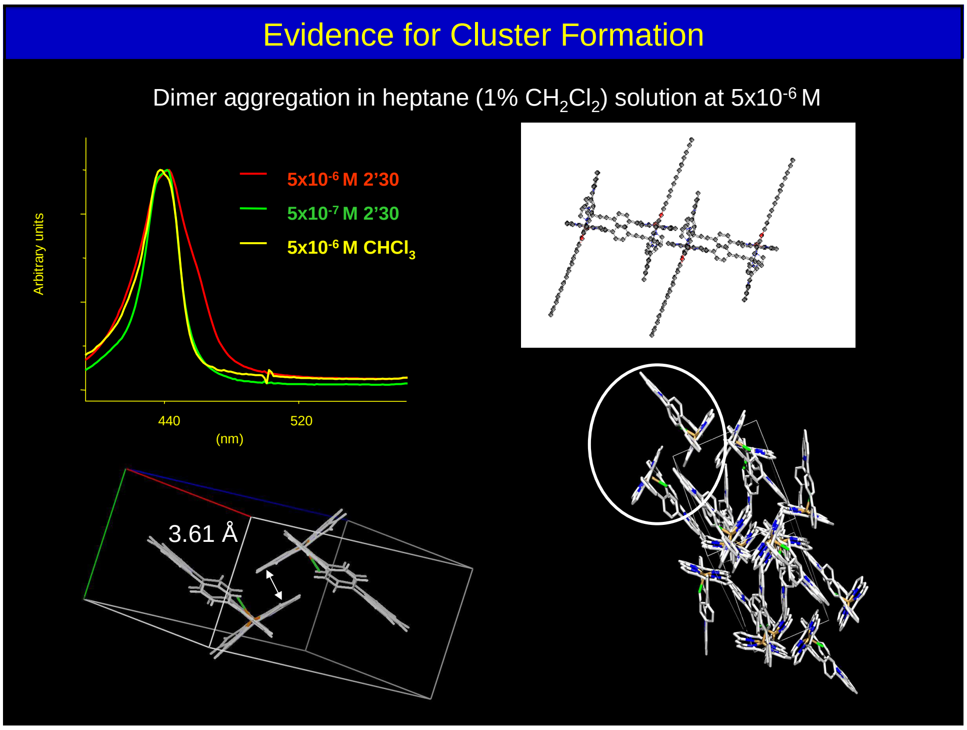

Evidence for Cluster Formation

Dimer aggregation in heptane (1% CH_2Cl_2) solution at $5x10^{-6}$ M

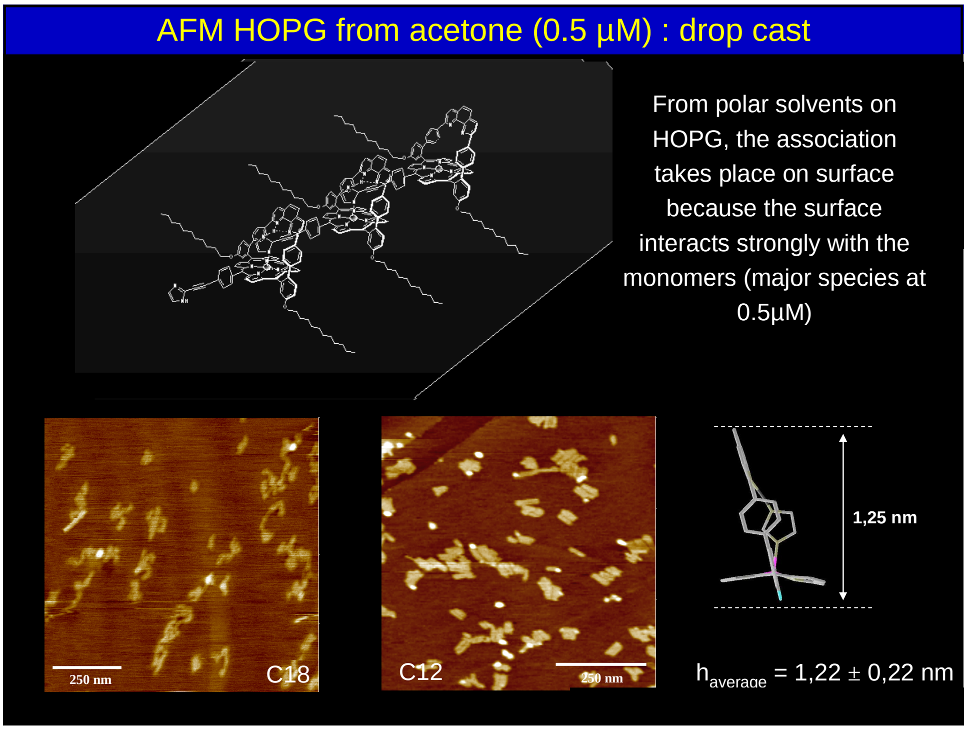

AFM HOPG from acetone (0.5 µM) : drop cast

From polar solvents on HOPG, the association takes place on surface because the surface interacts strongly with the monomers (major species at 0.5µM)

$h_{average}$ = 1,22 ± 0,22 nm

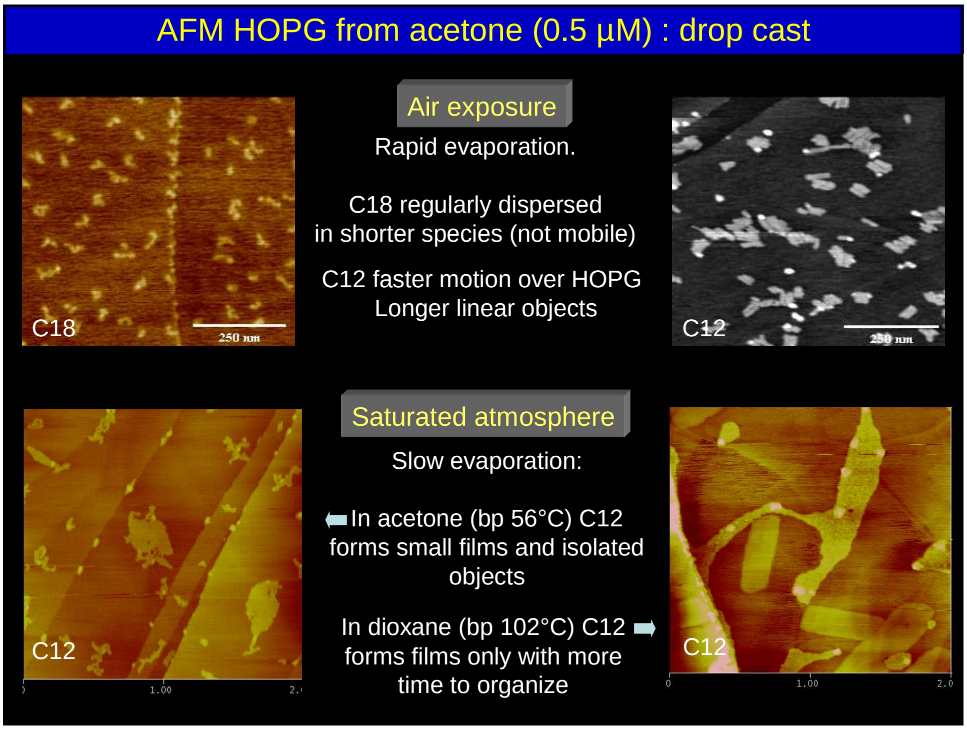

AFM HOPG from acetone (0.5 µM) : drop cast

Air exposure

Rapid evaporation.

C18 regularly dispersed
in shorter species (not mobile)

C12 faster motion over HOPG
Longer linear objects

Saturated atmosphere

Slow evaporation:

⬅In acetone (bp 56°C) C12 forms small films and isolated objects

In dioxane (bp 102°C) C12 ➡ forms films only with more time to organize

Does the surface matter ? (Barth, Kern, Ruben in Chemphyschem. 2008)

Source of ordering

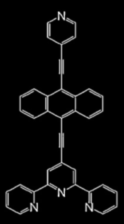

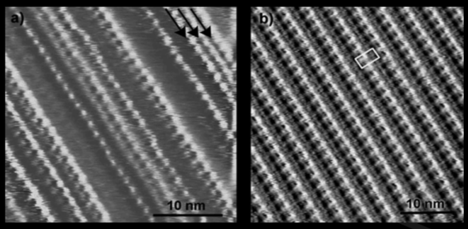

Co^{II} (apical Chlorine): Surface controls a 2D process

Pd^{II} (BF_4^- layer) : Surface controls a 1D process

M.W. Hosseini, P. Samori et al., *ACIE* **2007**

Source of atoms

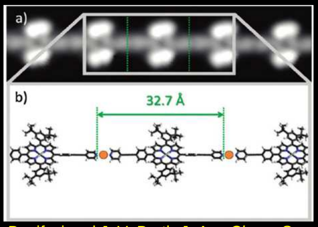

D. Bonifazi and J. V. Barth *J. Am. Chem. Soc.* **2010**

Source of reactivity

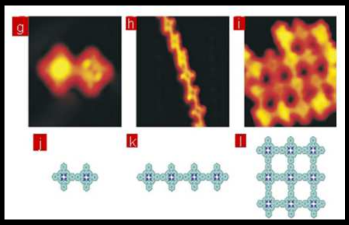

S. Hecht and L. Grill, *et al.Nat. Nanotechnolgy* **2007**

1D and 3D Surface assisted self-assembly Coord. Chem. Rev. ***2012***, in press

---

Summary of drop cast studies

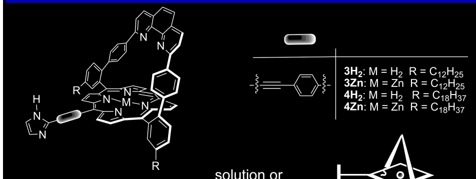

3H$_2$: M = H_2 R = $C_{12}H_{25}$
3Zn: M = Zn R = $C_{12}H_{25}$
4H$_2$: M = H_2 R = $C_{18}H_{37}$
4Zn: M = Zn R = $C_{18}H_{37}$

* Dillution of a [10^{-4} M] stock solution in CH_2Cl_2

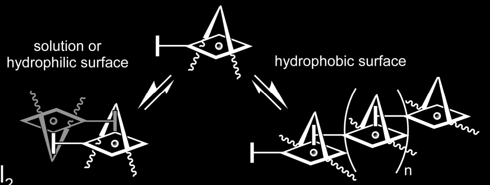

solution or
hydrophilic surface

hydrophobic surface

Mica CH_2Cl_2

HOPG Acetone

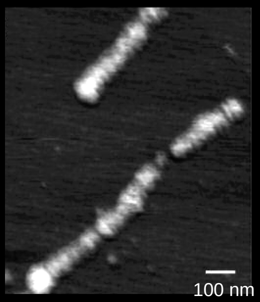

C_{18}

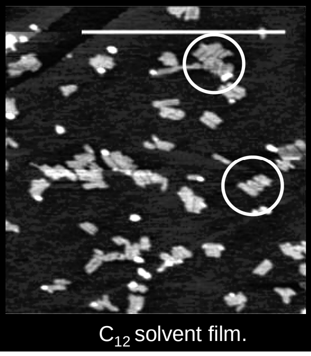

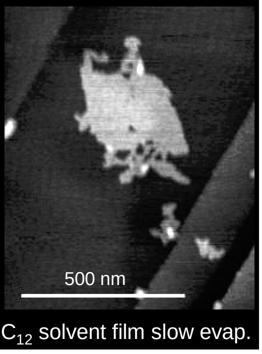

J. Am. Chem. Soc. **2008**, *130*, 9994

C_{12} solvent film.

C_{12} solvent film slow evap.

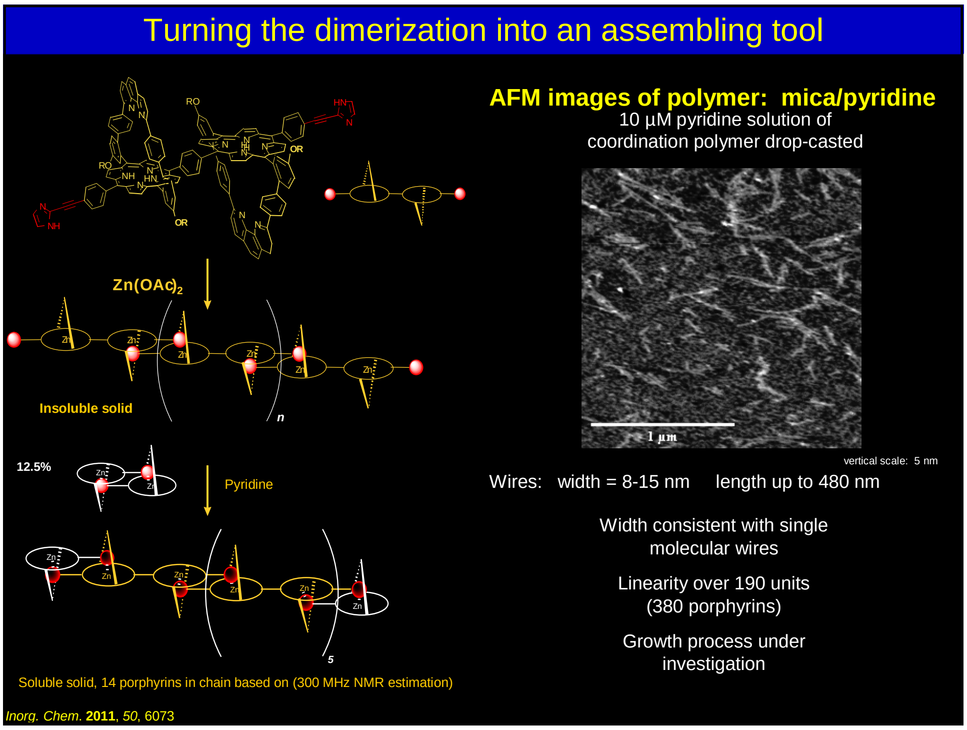

Turning the dimerization into an assembling tool

Insoluble solid

Soluble solid, 14 porphyrins in chain based on (300 MHz NMR estimation)

AFM images of polymer: mica/pyridine

10 µM pyridine solution of coordination polymer drop-casted

vertical scale: 5 nm

Wires: width = 8-15 nm length up to 480 nm

Width consistent with single molecular wires

Linearity over 190 units (380 porphyrins)

Growth process under investigation

Inorg. Chem. **2011**, *50*, 6073

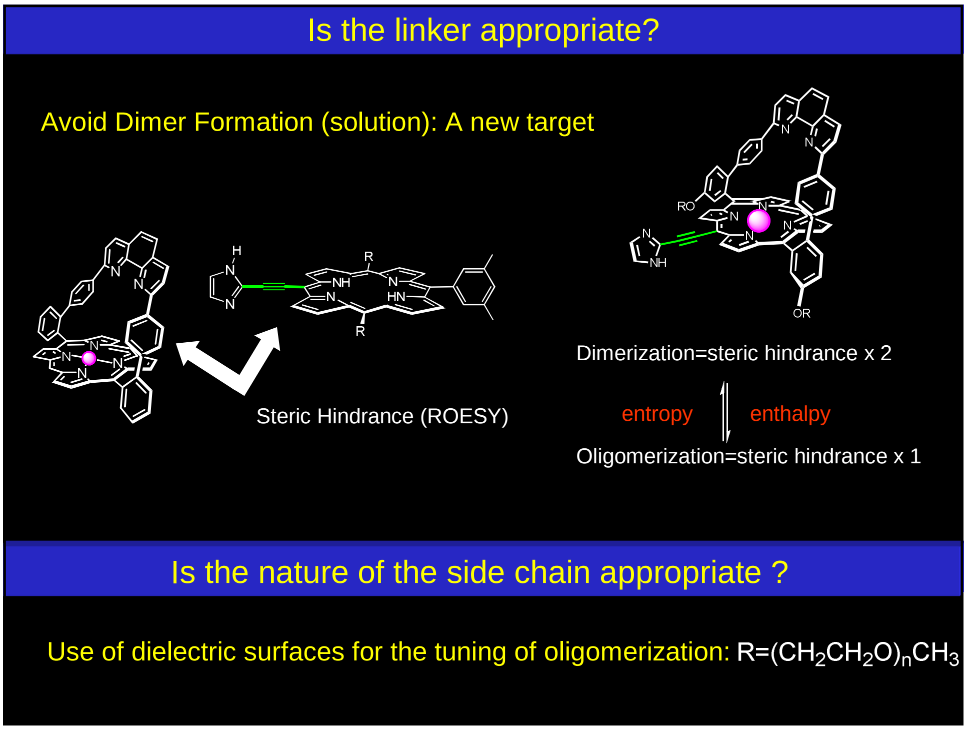

Is the linker appropriate?

Avoid Dimer Formation (solution): A new target

Steric Hindrance (ROESY)

Dimerization=steric hindrance x 2

entropy ⇅ enthalpy

Oligomerization=steric hindrance x 1

Is the nature of the side chain appropriate ?

Use of dielectric surfaces for the tuning of oligomerization: R=$(CH_2CH_2O)_nCH_3$

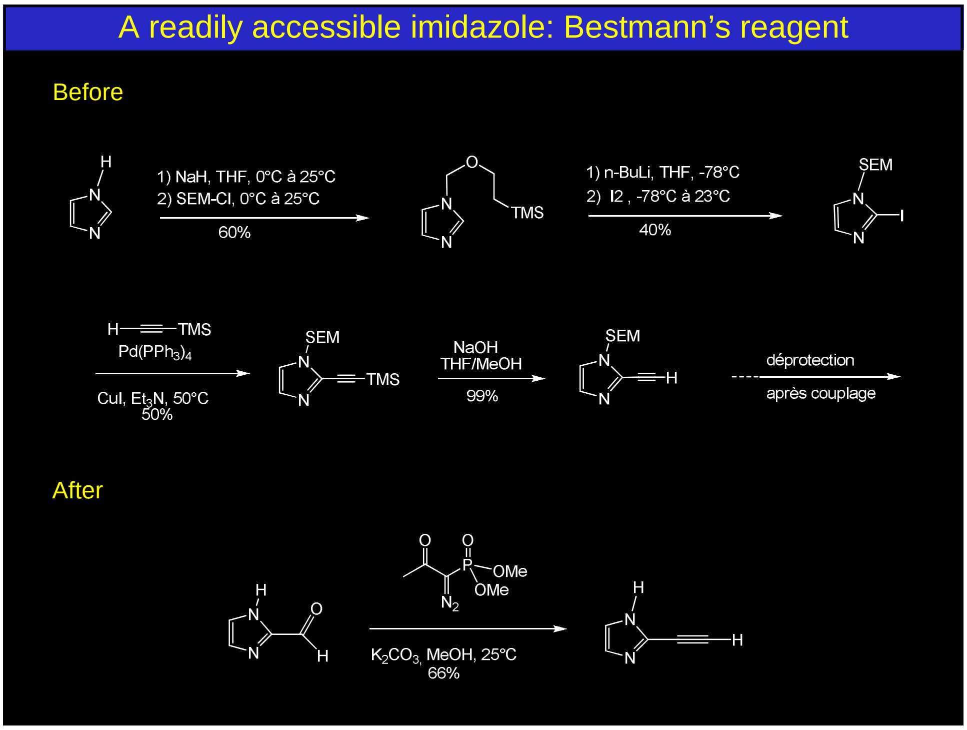

A readily accessible imidazole: Bestmann's reagent

Before

After

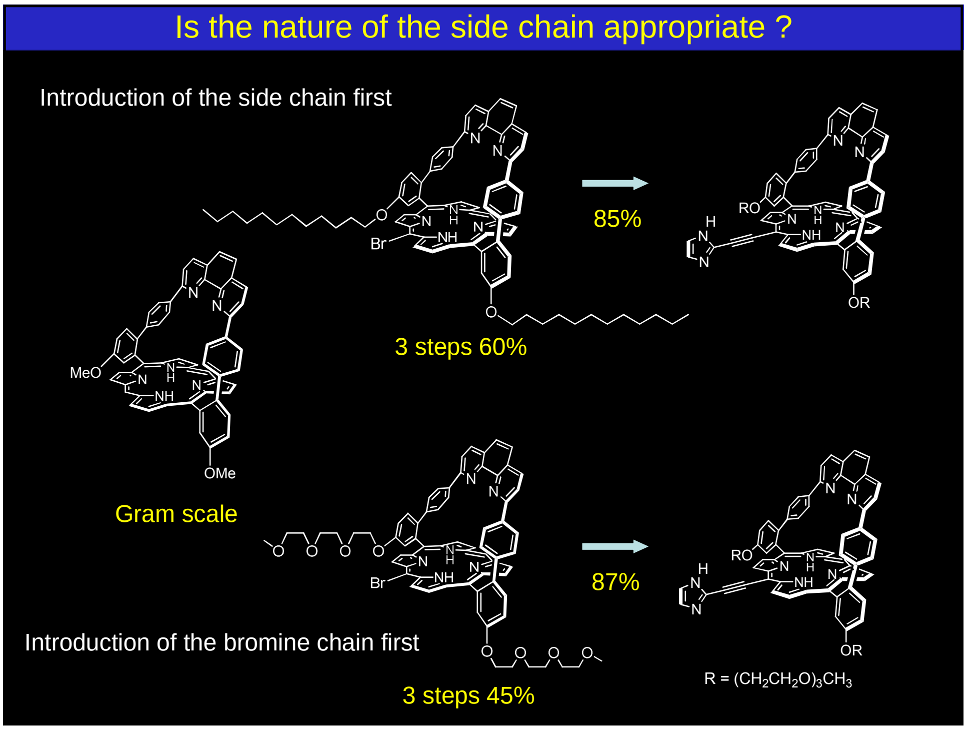

Is the nature of the side chain appropriate ?

Introduction of the side chain first

3 steps 60%

Gram scale

Introduction of the bromine chain first

3 steps 45%

R = $(CH_2CH_2O)_3CH_3$

Short spacer synthesis

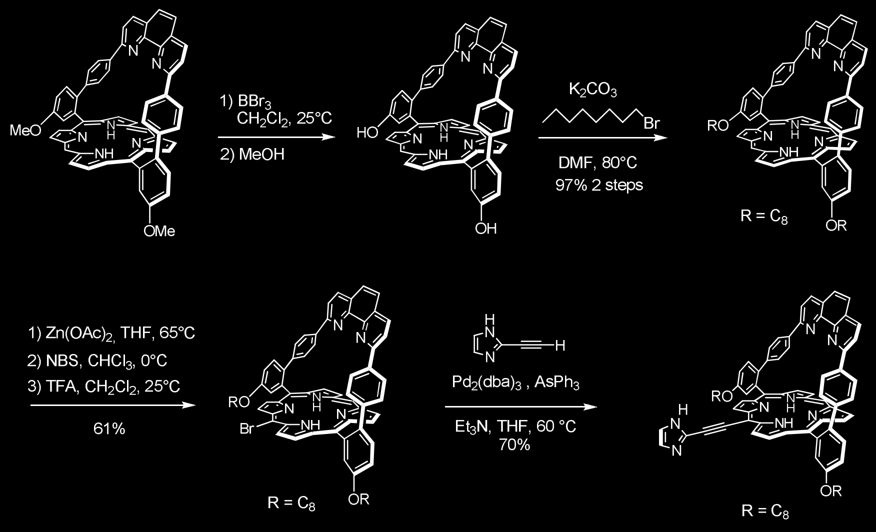

Dilution experiments in UV-vis: equilibration of solutions > one week

Stability of the dimer: comparison with literature

log K_{Dim}

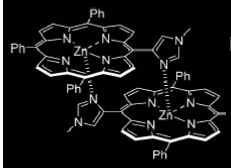

9.9

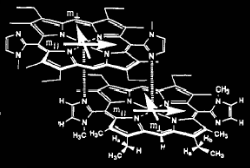

9.7

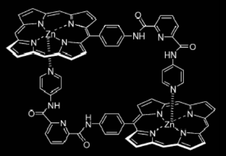

> 8

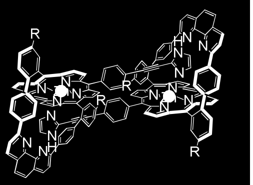

9.0(1)

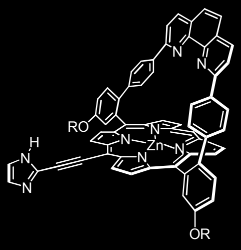

log K_{Dim} = 3.7 ± 0.2

$$ZnP + 2MeIm \rightleftharpoons ZnP.2MeIm$$

$$\log K_{Assoc} = 4.5 \pm 0.4\ M^{-1}$$

are all in the same range

⇒ The molecule-surface interactions can differenciate the association modes

Deposition on surfaces: C_8 and C_{12} on HOPG

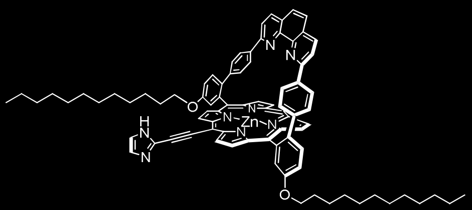

C8

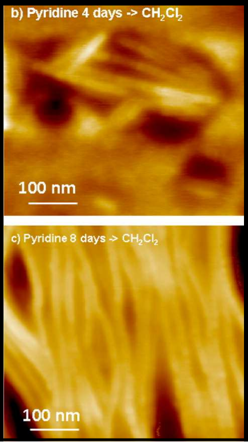

C18

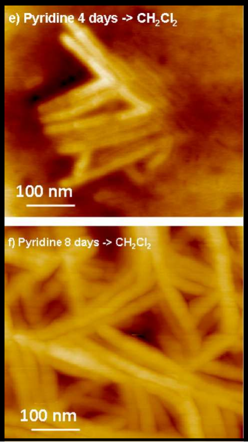

Org. Lett. **2012**, *14*, 1998

Deposition on CNTs

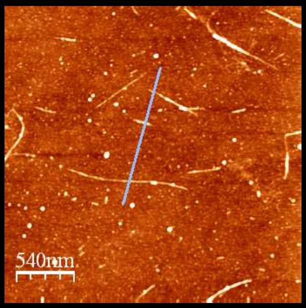

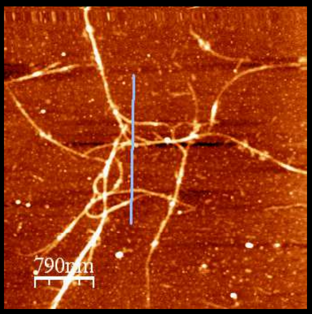

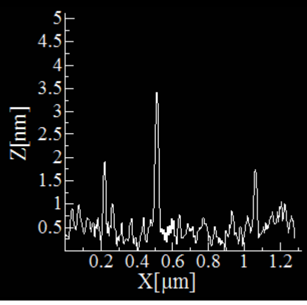

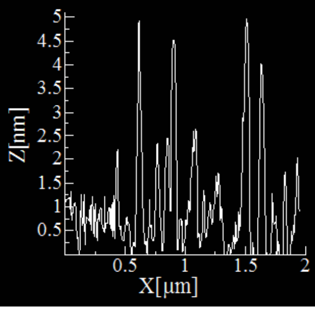

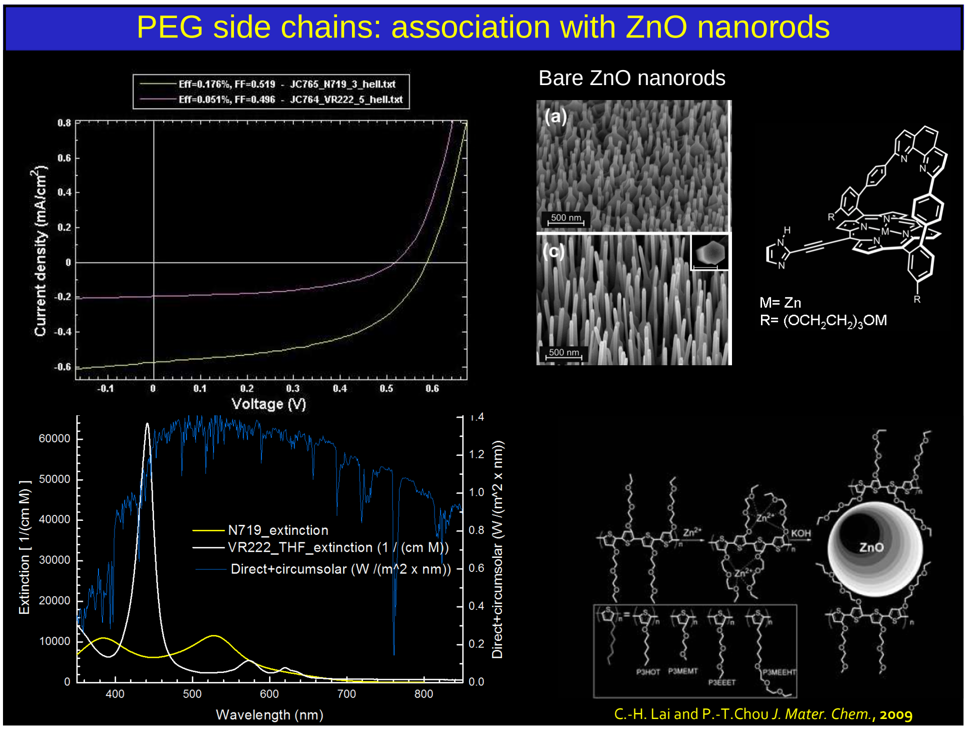

PEG side chains: association with ZnO nanorods

Bare ZnO nanorods

M= Zn
R= $(OCH_2CH_2)_3OM$

C.-H. Lai and P.-T.Chou *J. Mater. Chem.*, 2009

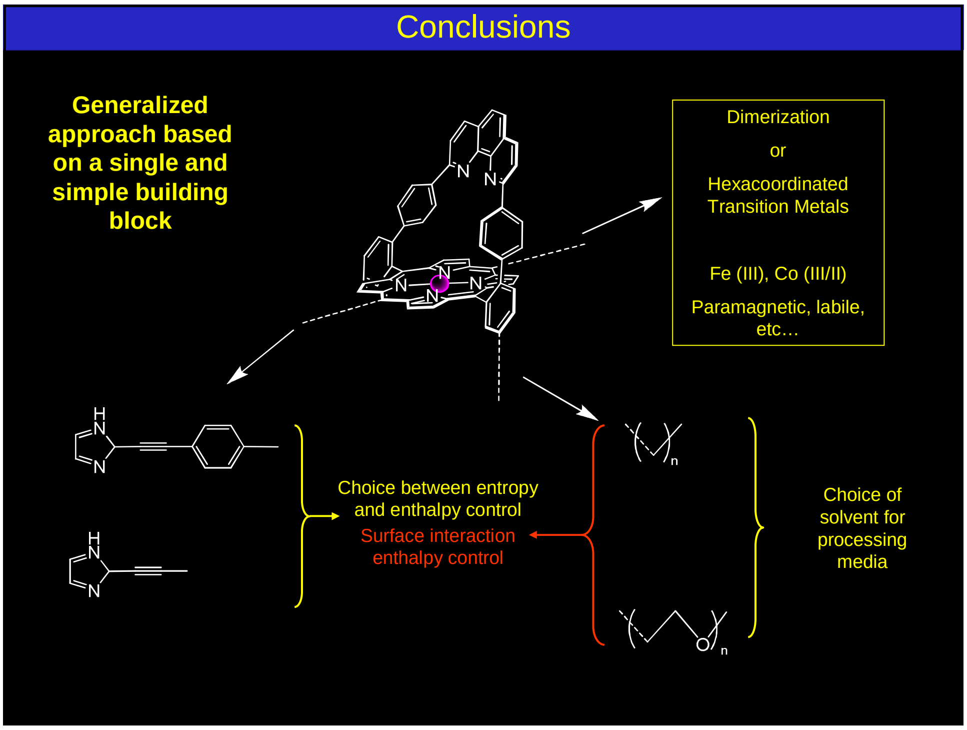

Conclusions

Generalized approach based on a single and simple building block

Dimerization

or

Hexacoordinated Transition Metals

Fe (III), Co (III/II)

Paramagnetic, labile, etc…

Choice between entropy and enthalpy control

Surface interaction enthalpy control

Choice of solvent for processing media

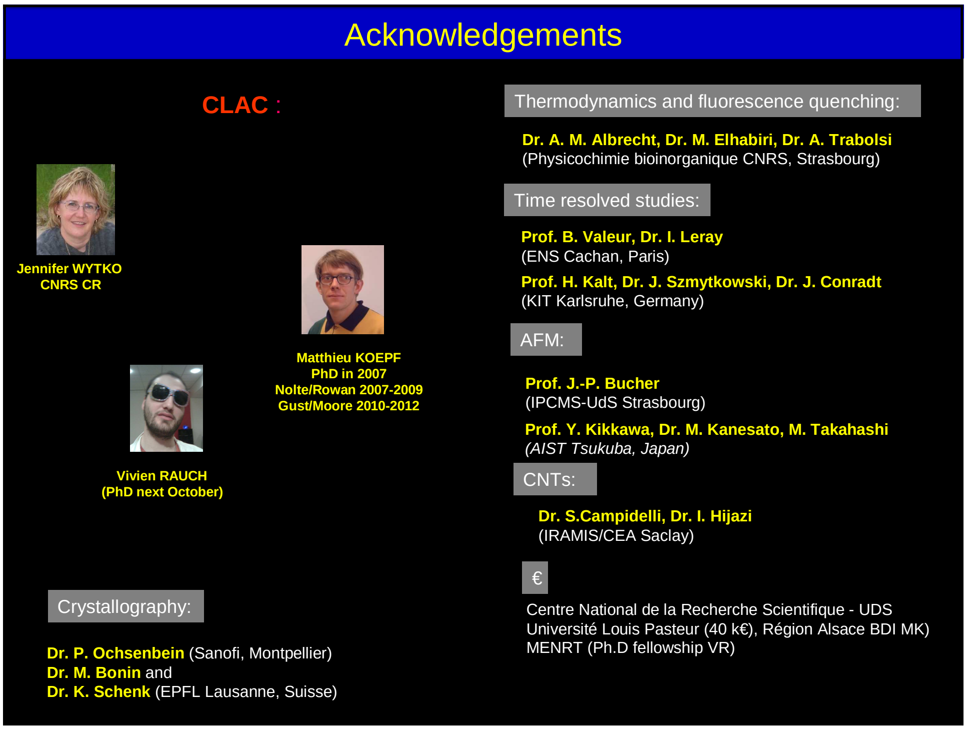

Acknowledgements

CLAC :

Jennifer WYTKO
CNRS CR

Matthieu KOEPF
PhD in 2007
Nolte/Rowan 2007-2009
Gust/Moore 2010-2012

Vivien RAUCH
(PhD next October)

Crystallography:

Dr. P. Ochsenbein (Sanofi, Montpellier)
Dr. M. Bonin and
Dr. K. Schenk (EPFL Lausanne, Suisse)

Thermodynamics and fluorescence quenching:

Dr. A. M. Albrecht, Dr. M. Elhabiri, Dr. A. Trabolsi
(Physicochimie bioinorganique CNRS, Strasbourg)

Time resolved studies:

Prof. B. Valeur, Dr. I. Leray
(ENS Cachan, Paris)

Prof. H. Kalt, Dr. J. Szmytkowski, Dr. J. Conradt
(KIT Karlsruhe, Germany)

AFM:

Prof. J.-P. Bucher
(IPCMS-UdS Strasbourg)

Prof. Y. Kikkawa, Dr. M. Kanesato, M. Takahashi
(AIST Tsukuba, Japan)

CNTs:

Dr. S.Campidelli, Dr. I. Hijazi
(IRAMIS/CEA Saclay)

€

Centre National de la Recherche Scientifique - UDS
Université Louis Pasteur (40 k€), Région Alsace BDI MK)
MENRT (Ph.D fellowship VR)

NanoScience in Nuclear Power Engineering & Radiochemical Technology

Ivan G. Tananaev

Frumkin Institute of Physical Chemistry & Electrochemistry RAS, Moscow
Ozyorsk Technical Institute National Scientific Nuclear University

---

“Nuclear Renaissance”

- In connection with growth of cost on hydrocarbon source of energy (gas, mineral oil, coal) the great interest on development of world nuclear energy is enlarged, called now as a “Nuclear Renaissance”.
- Many countries that do not have a nuclear power plant are considering building one.
- Many nations that already have one are considering expanding their nuclear enterprises.

Plans of Development of Nuclear Power Stations in the World

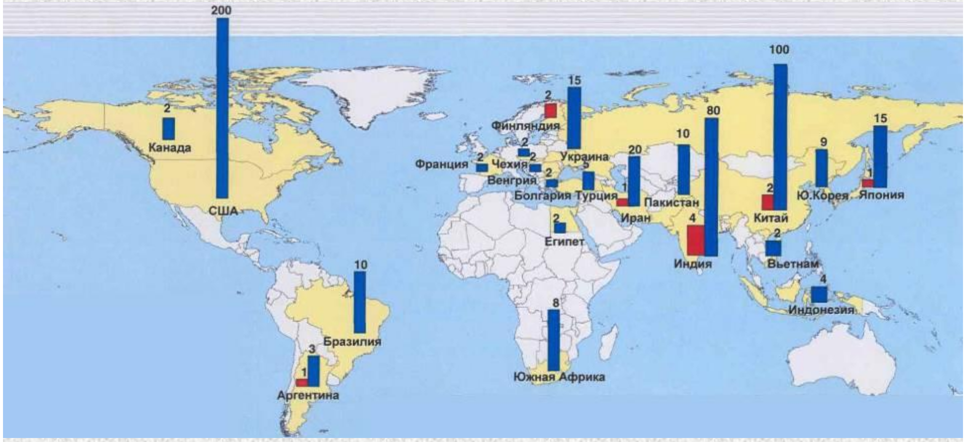

Program of putting into operation APP, GWatt:

🟦 - under construction

🟥 - prospects

In Russia: at present 31 power units operate at 10 Nuclear Power Plants

- **From 2012, at least two nuclear power units with a total capacity of 2 GW are to be founded annually.**
- **As a result, by 2018, 10 new power units will be put into operation, total installed capacity of which will make up 10 GW.**
- **Implementation of a special-purpose program will increase total installed capacity of all NPPs up to 33 GW (at present, it makes up 23 GW).**
- **It will lead to the increase of Nuclear Power Plant share in the total volume of generated electric power up to 18%.**

The ways of Production Magnification:

Extensive :

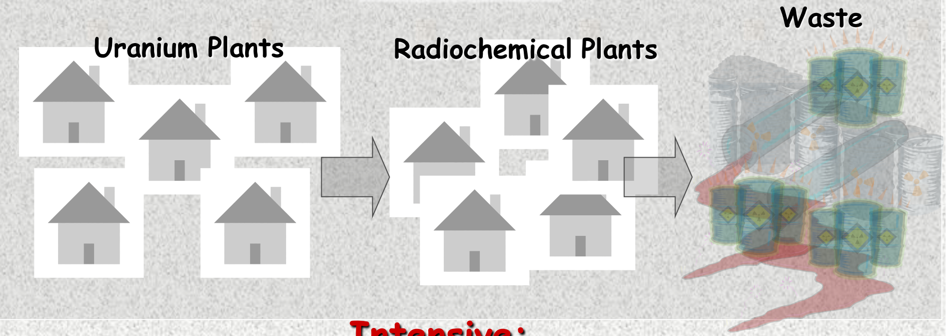

Intensive:

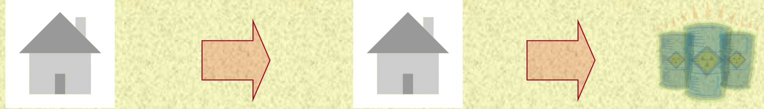

With Application of Innovative Nuclear Technologies

In our opinion, the best input on innovation on radiochemical technologies is feeding-in a nanomaterials and nanotechnologies.

Arises the First Question:

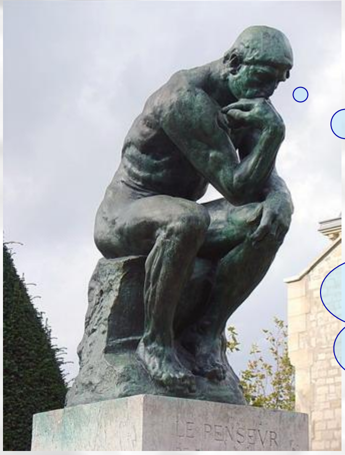

what is the best site for NanoTecnology implementation ?

Answer:

Production Association Mayak !

See photo

Ural Region

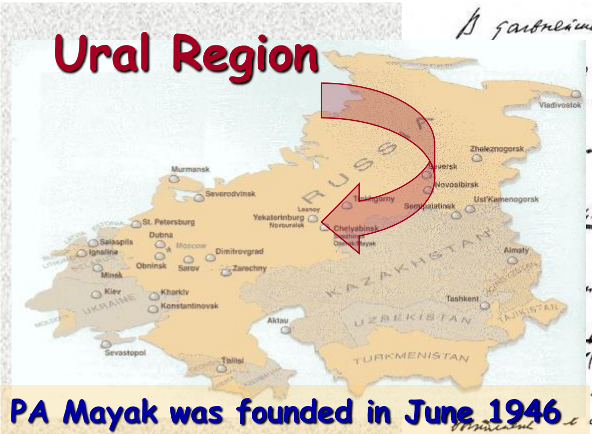

PA Mayak was founded in June 1946

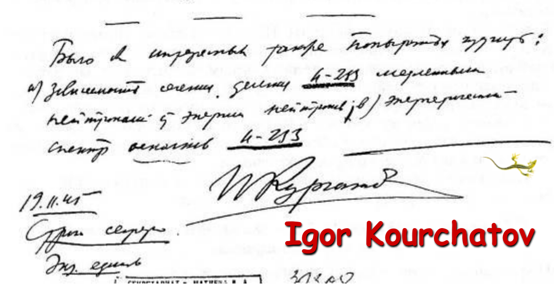

В главнейших образцах будет активирова[illegible]

[illegible] нейтронов, которые [illegible]

времени, благодаря малой доступности

4-213

(5 энергии нейтронов.

исследования будут начаты

в срок до 3 месяцев.

Было бы интересно также поставить опыты:
а) Зависимость сечения деления 4-213 медленными
нейтронами от энергии нейтронов; в) энергетический
спектр осколков 4-213

И. Курчатов

19.11.45

Срок секрет.

Экз. единств.

Igor Kourchatov

Arises the Second Question:

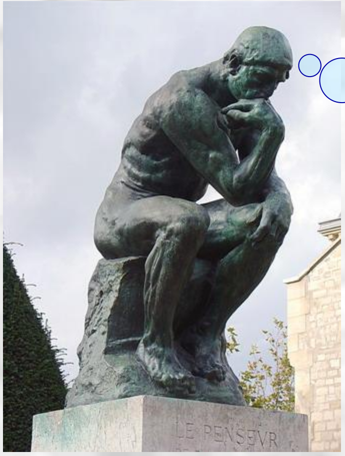

to find the
main directions in development of NanoScience for Radiochemistry.

Nuclear Fuel Cycle

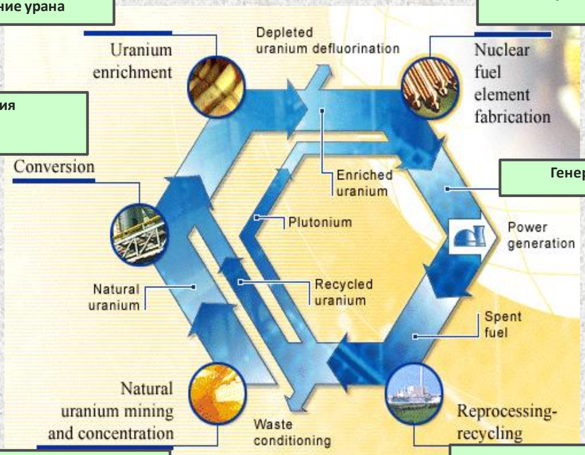

Обогащение урана

Фабрикация ТВЭЛов

Конверсия
(UF_6)

Генерация энергии

Добыча и получение урана

Обращение с радиоактивными отходами

Переработка ОЯТ

Technical properties of Fuel Element

Изменение механических свойств

Теплопроводимость
Thermal conductivity

Деформирование
Deformation

СТРУКТУРА

КИСЛОРОДНЫЙ ПОКАЗАТЕЛЬ

ПОРИСТОСТЬ

ГАЗОВЫДЕЛЕНИЕ

Распухание
Swelling-up

Окисление
Oxidation

Наводораживание
Hydrogen accumulation

Микроструктурные изменения
Microstructure changing

Радиационно-термическая ползучесть
Radiation & Thermal Creep

Результат: *изменения геометрических размеров твэлов и ТВС, взаимодействие топлива с оболочкой, рост давления ГПД*

Functional Fuel NanoCompositions

Введение 0.2-0.6 масс.% Er_2O_3 (РБМК) или 0.05-10% масс. Gd_2O_3 (ВВЭР) в качестве выгорающего поглотителя нейтронов позволяет значительно улучшить экономические показатели работы реактора (форсирование на 10%), повысить его безопасность за счет уменьшения реактивности топлива до роста выгорания до 55 МВт·сут/кг U.

Incorporation of 0.2-0.6 мas.% of Er_2O_3 (РБМК) of 0.05-10% мas. of Gd_2O_3 (ВВЭР) in to a nuclear fuel tablets as a burning down absorber goes to increasing of economic characteristics and safety of nuclear reactor.

New nuclear fuel compositions on the base of nanofractions of UO_2 was fabricated in the PA Mayak.

The physical-chemical properties and reactivity of nanoscale UO_2 are studied. It was found that incorporation of nanoscale UO_2 fractions (1-5%) goes to dramatic increasing of ceramic quality of fuel pills, homogeneity of solid solutions for dioxide mixture. This procedure raise of many times a quality of MOX-fuel for fast reactors.

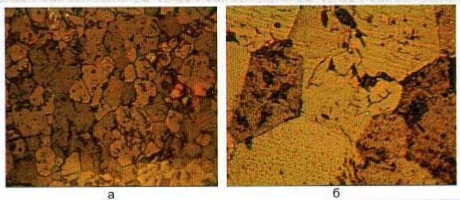

Standard microstructure (a) and microstructure of nuclear fuel, produced by incorporation of nano-additions (б)

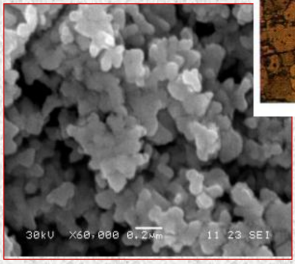

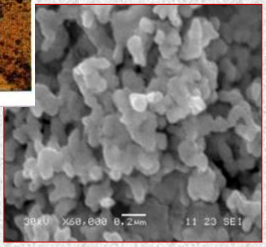

S_{BET} = 10 m²/g;
Ø 100-120 nm

Functional NanoMaterials for producing of Fuel Elements shells from oxides-dispersed steels

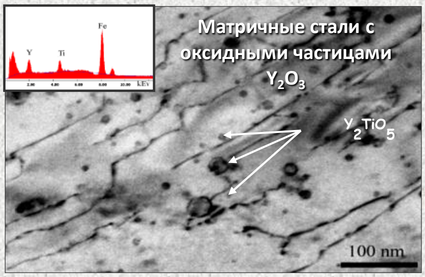

Матричные стали с оксидными частицами Y_2O_3

Y_2TiO_5

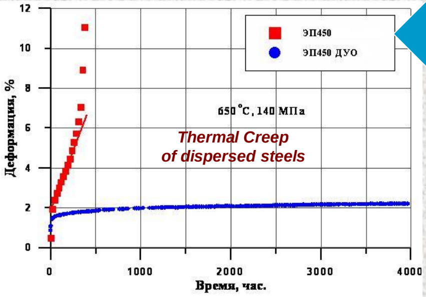

Thermal Creep of dispersed steels

Термическая ползучесть стали ЭП450 и дисперсно-упорядочной оксидами стали ЭП450 ДУО

Steels	Content of Sc, % mass.	Creep, %
ЭИ-847	0	12,8
ЭИ-847-Sc	0,13	0,50

NanoCatalysts

The NanoParticles of Pt, Pd, Rh, Ru, coated on a porous materials, are used as an heterogeneous catalysts in radiochemical technology for increasing of efficiency of chemical processes used, and for reducing of a volumes of radioactive waste.

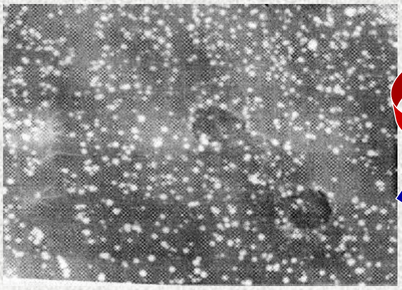

The morphology of a surface of catalysts (scan electronic microscope in a beams of secondary electrons of Pt granule)

Distribution of Pt particles sizes for 1% Pt/SiO_2 catalysts.
The middle Ø of a clusters is ~80 nm.

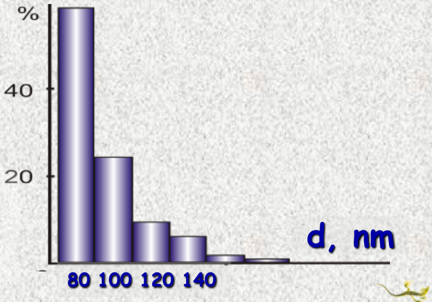

Effective methods of stabilization of actinides ions in given oxidation states were developed. The kinetic parameters of more 100 catalytic redox-reactions were calculated.

- Reduction of Uranium(VI) to (IV)
  - Reducing agents: H_2, N_2H_4, HCOOH, H_2CO, C_2H_5OH
- Reduction of Plutonium(IV) to (III), Neptunium(VI,V) to (IV)
  - Reducing agents: H_2, N_2H_4 , HCOOH
- Oxidation of Neptunium(IV)
  - Oxidizer: HNO_3

The main advantages of catalytic redox-processes: application of «not saline» reagents in technology.

The perspective methods of decomposition of organic radioactive waste were developed :

- Decomposition of oxalic acid, EDTA at so on;
- Decomposition of $N_2H_5NO_3$, HNO_3, NH_4NO_3, carbamide.

Examples of developed catalytic processes in radiochemical technology

Reduction U(VI) to U(IV) 0,1M $N_2H_5NO_3$ in 1M HNO_3 at 40°C	
In the present of 1% Pt/SiO_2	Without of a catalysts
Выход U(IV) 98% за 45 мин	Реакция не протекает
Results: a pilot device for fabrication of U(IV) at Siberian Chemical Combine (ОАО «СХК», Северск) 130 кg/day was created.	

Decomposition of oxalic acid	
1% Pt/SiO_2 50°C, 60 min in 1MHNO_3	Without a catalysts, 90°C, 48 hours in 8M HNO_3
100% Decomposition	80% Decomposition
Results: a pilot device for dynamic decomposition of oxalic acid was created	

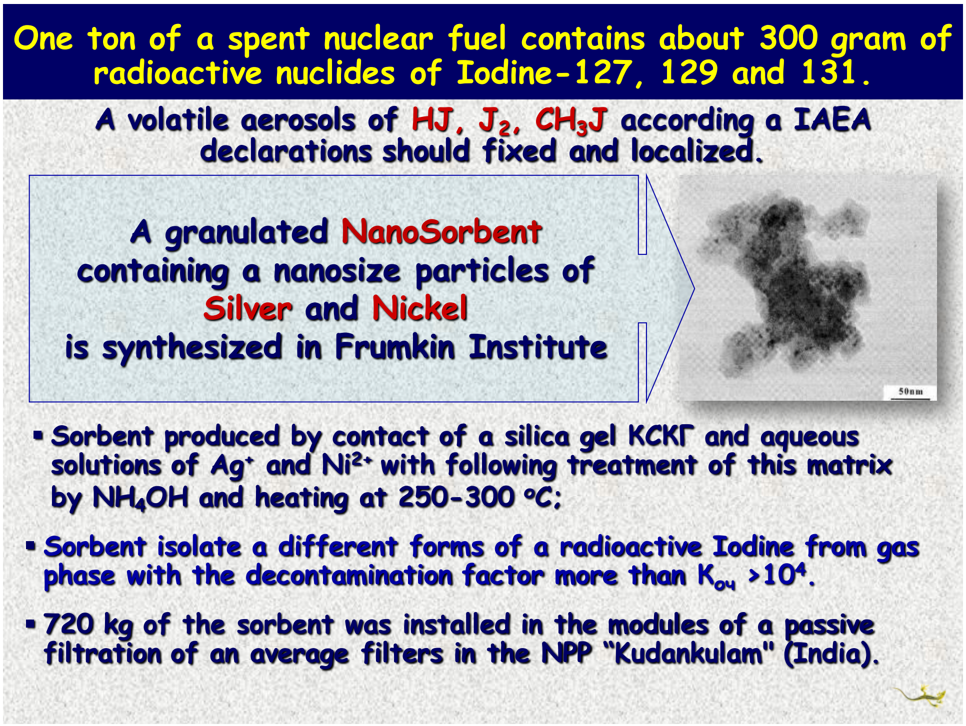

One ton of a spent nuclear fuel contains about 300 gram of radioactive nuclides of Iodine-127, 129 and 131.

A volatile aerosols of HJ, J_2, CH_3J according a IAEA declarations should fixed and localized.

A granulated **NanoSorbent** containing a nanosize particles of **Silver** and **Nickel** is synthesized in Frumkin Institute

50nm

- Sorbent produced by contact of a silica gel КСКГ and aqueous solutions of Ag^+ and Ni^{2+} with following treatment of this matrix by NH_4OH and heating at 250-300 °C;
- Sorbent isolate a different forms of a radioactive Iodine from gas phase with the decontamination factor more than $K_{оч} > 10^4$.
- 720 kg of the sorbent was installed in the modules of a passive filtration of an average filters in the NPP "Kudankulam" (India).

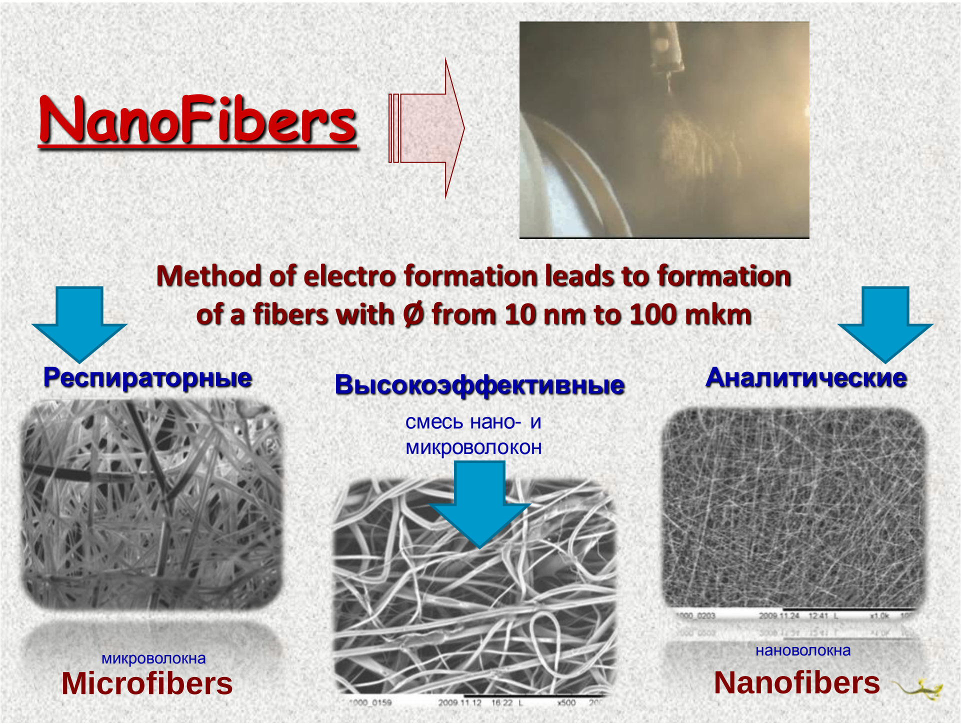

NanoFibers

Method of electro formation leads to formation of a fibers with Ø from 10 nm to 100 mkm

Респираторные

микроволокна

Microfibers

Высокоэффективные

смесь нано- и микроволокон

Аналитические

нановолокна

Nanofibers

NanoFibers ⇨ "Filled" Fibrous Complexing Sorbents

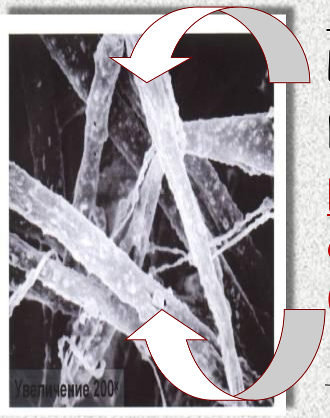

Basis:

Polyacrylonitrile
porous fiber (300-400 nm)

Filler:

Complexing Sorbents
(Ø ~100 nm)

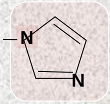

imidazole groups

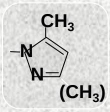

3(5)-methylpyrazole groups

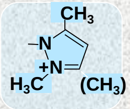

1,3(5)-dimethyl-pyrazole groups

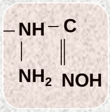

amidoxime and hydrazidine groups

Fibrous "Filled" Sorbents Application

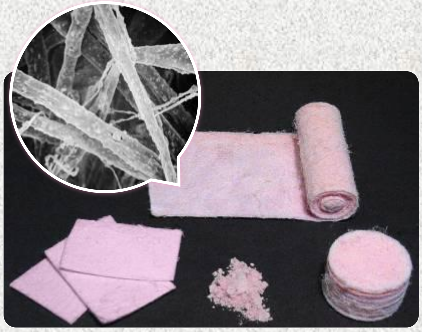

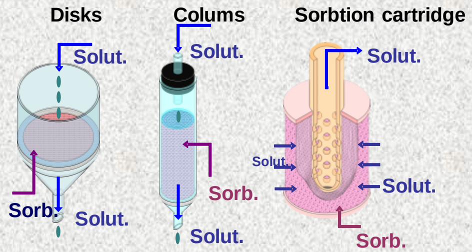

Tc(VII) sorption by fibrous sorbents from underground waters (20°C; time contact 2 h; V : m = 100 cm³/g)

Sorbent	K_d (cm³/g)
Poliorgs 17-n	$2{,}8 \cdot 10^5$
AB-17-н	$1{,}0 \cdot 10^4$

The radiometric map of Tc-99 contamination around the technical depositories were determined first time.

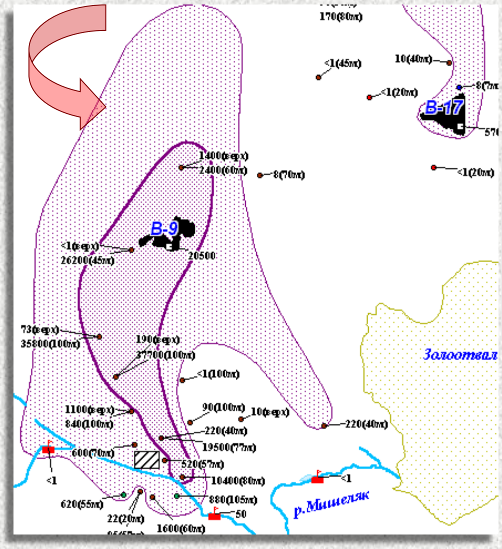

^{99}Tc contamination around **B-9:**
220 Bk/L - **11,7 км^2**,
2200 Bk/L - **2,9 км^2**;

around **B-17:**
220 Bk/L - **1,2 км^2**.

NanoMembranes

for discovery of radionuclide species migration

Device of multistage membrane filtration

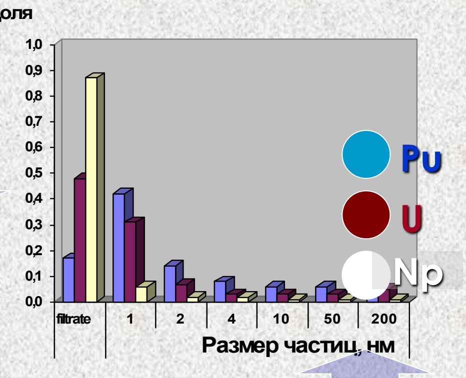

Distribution of actinides forms founded by membrane partitioning (GEOKHI RAS)

Pilot Installation of membrane cleaning of a natural water

Membrane «Trumem», Size from 2 to 250 nm.

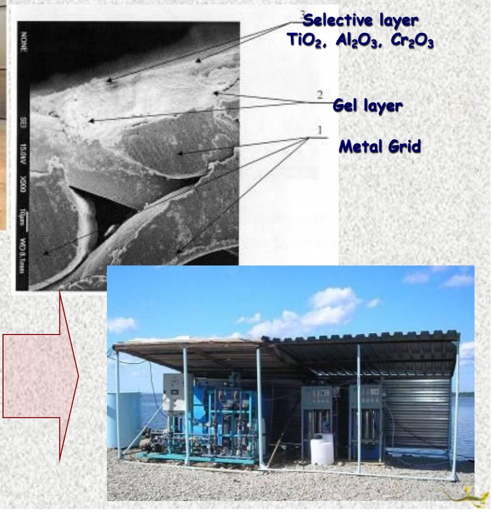

Decontamination factor for:

$\Sigma\alpha = 2 \bullet 10^3$;
$\Sigma\beta = 10^3$;
$^{90}Sr = 10^4$; $^{137}Cs = 90$

Carbonic NanoMaterials:

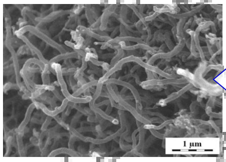

Taunit: 1D - NanoScale filous formations with inert Ø 5-8 nm as a powder

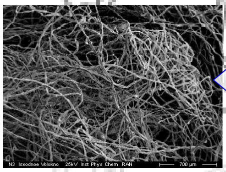

NanoPorous coals as a powder

- as a perspective sorbents for radwaste treatment;
- as an additive for hardening of solid matrixes;
- as a NanoFuel elements;
- as a matrixes for immobilization of organic waste.

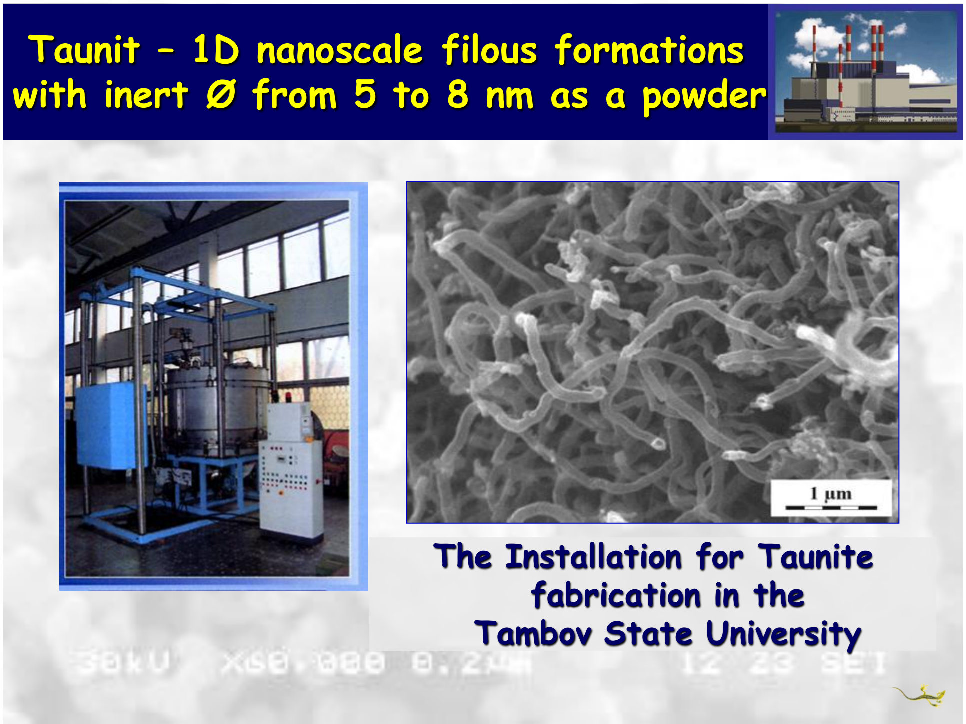

Taunit – 1D nanoscale filous formations with inert Ø from 5 to 8 nm as a powder

The Installation for Taunite fabrication in the Tambov State University

---

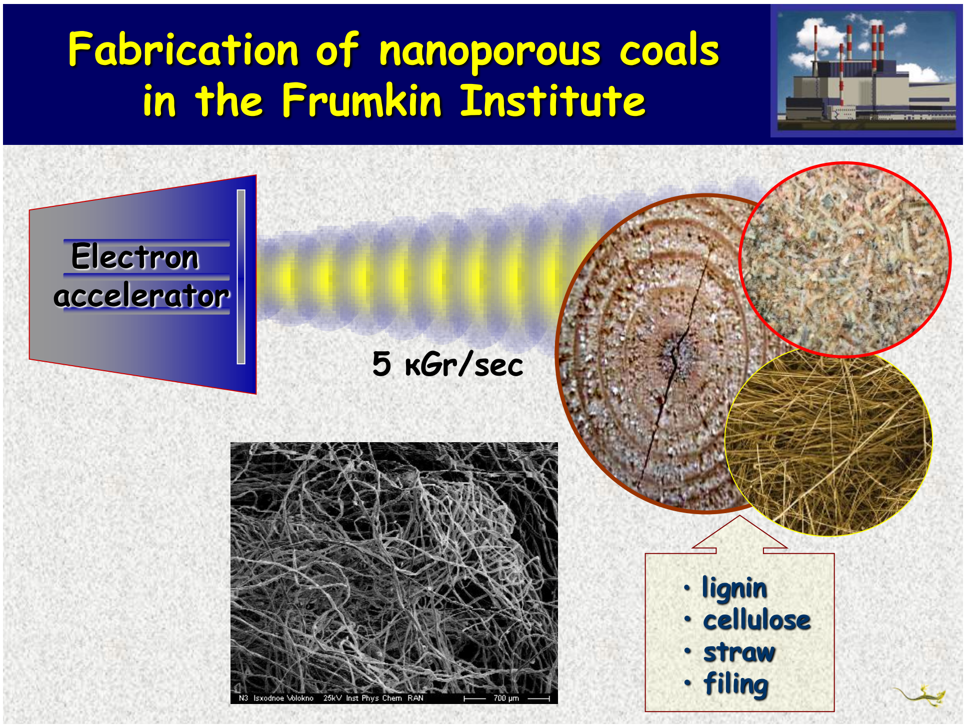

Fabrication of nanoporous coals in the Frumkin Institute

Electron accelerator

5 кGr/sec

- lignin
- cellulose
- straw
- filing

Charcoal structures

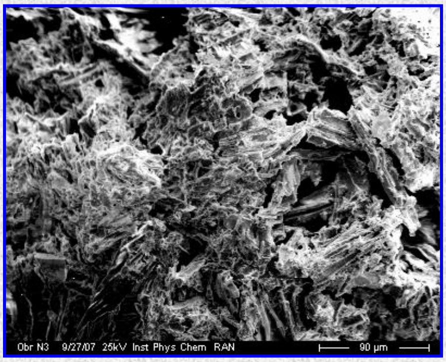

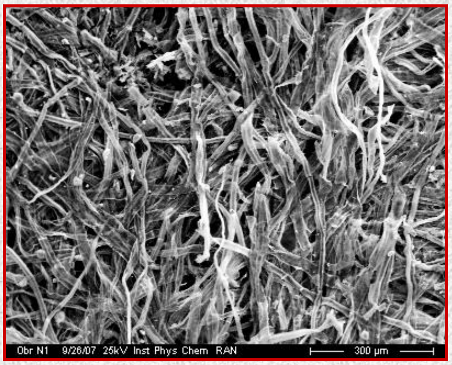

Conventional heating **Electron beam heating**

Atomic composition

C – 82.6 %
O – 16.0 %

C – 89.5 %
O – 9.6 %

Such processing conserves structure of feed stock fibrils.

The high sorption ability of «Taunit» with respect of a radionuclides was found.

The degree of radionuclides isolation from model solutions, %.
Sorbent mass 20 mg, V:m = 100, time contact 2 hour; [Me] = 10^{-6}M.

Content	Am(III)	Eu(III)	Pu(IV)	U(VI)	Tc(VII)
1mM HNO_3	99	99	96	99	99
Underground water	90	97	85	99	90

The effective sorbents based on the Fe,Ni ferrocyanides for Cs^{137} and Sr^{90} isolation from solutions were synthesized and tested

Distribution coefficient K_p Cs-137 on different sorbent, cm^3/g				
Type solution	ФЖ-Taunite	ФН-Taunite	ФЖ-NanoCoal	ФНС selling
Underground water	$3,2\times10^4$	$4,8\times10^4$	$3,8\times10^4$	$2,8\times10^4$
1M $NaNO_3$	$1,5\times10^5$	$3,1\times10^5$	$1,2\times10^5$	$4,8\times10^5$
Distillation residue from Kursk NPP	$1,6\times10^3$	$3,6\times10^3$	$4,1\times10^2$	$8,4\times10^3$

The high absorption ability of carbon nanomaterials with respect of technical oils or another organic compounds (TBP, hydrocarbon diluent) was found.

For "Taunite" – 4 g/g;
For coals – 19 g/g.

Effective method of fixation of technical oils on a carbon NanoMaterials with following solidification by epoxy-resin or cement was developed.

- Oil inclusion up to 25%;
- Compressing strength 570 kg/cm^2;
- Oil secession was not found;
- Oil Leaching Degree <0,01 %;
- Rate Oil Leaching <$1 \cdot 10^{-5}$ g/cm$^2 \cdot$day;
- Diffusion Coefficient of RN is 10^{-12} m^2/s

Chemically Bonded Phosphate Ceramics

Example: potassium-magnesium ceramic

$$MgO + KH_2PO_4 + 5H_2O = KMgPO_4 \cdot 6H_2O$$

- Formed at room temperature;
- Made by acid-base reactions;
- Hard, durable, dense, and hence
- the Ideal for macro-incorporation.

Addition of NanoSize of a nature minerals to the stock mix during solidification of a radioactive waste leads to increasing of compressive strength of a ceramic matrix :

Content composition, %					Compressive Strength, Kg/cm^2
MgO	KH_2PO_4	HLW	Wollastonite $CaSiO_3$	Asbestos	
14	43	43	0	0	41,7
12	40	43	0	5	364,1
12	40	43	5	0	321,1

Conclusion:

NanoMaterials and NanoTechnologies could be used in the field of radiochemical practice.

The Foreseeable Results are:

1. Nuclear Fuel Fabrication;
2. Development of modern Technologies for Spent Nuclear Fuel Reprocessing;
3. Radioactive Waste Handling;
4. Radioecology Development.

Arises the Third Question:

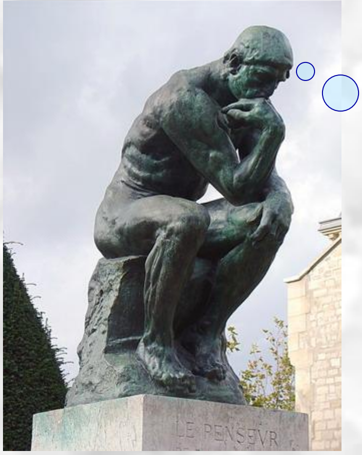

who will work?

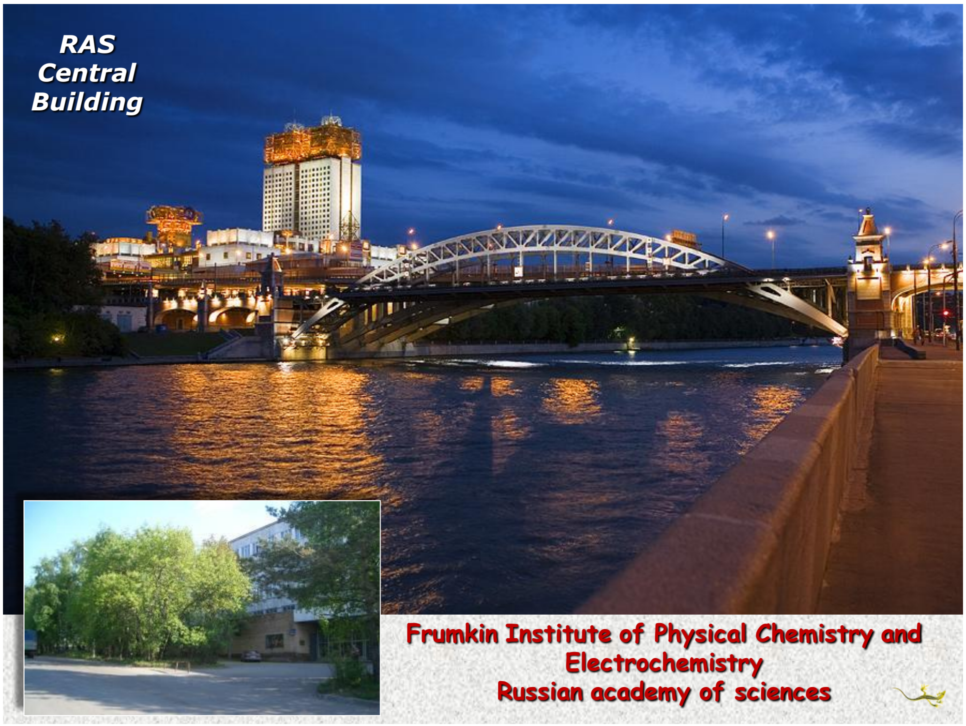

RAS Central Building

Frumkin Institute of Physical Chemistry and Electrochemistry
Russian academy of sciences

Central Plant Laboratory

PA Mayak

Ozyorsk Technological Institute found in September 1952

The First Symposium for «NanoIndustry and NanoMaterials in Radiochemical Technology»

PA Mayak, Ozyorsk, Chelyabinsk Region,

1-3 June 2009

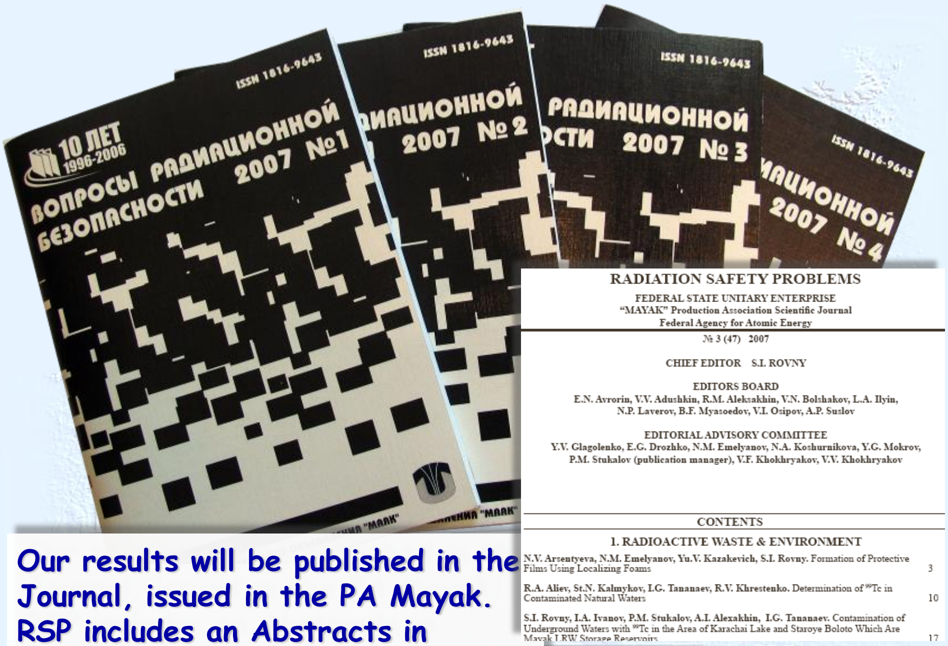

RADIATION SAFETY PROBLEMS

FEDERAL STATE UNITARY ENTERPRISE
“MAYAK” Production Association Scientific Journal
Federal Agency for Atomic Energy

№ 3 (47) 2007

CHIEF EDITOR S.I. ROVNY

EDITORS BOARD
E.N. Avrorin, V.V. Adushkin, R.M. Aleksakhin, V.N. Bolshakov, L.A. Ilyin, N.P. Laverov, B.F. Myasoedov, V.I. Osipov, A.P. Suslov

EDITORIAL ADVISORY COMMITTEE
Y.V. Glagolenko, E.G. Drozhko, N.M. Emelyanov, N.A. Koshurnikova, Y.G. Mokrov, P.M. Stukalov (publication manager), V.F. Khokhryakov, V.V. Khokhryakov

CONTENTS

1. RADIOACTIVE WASTE & ENVIRONMENT

Our results will be published in the Journal, issued in the PA Mayak. RSP includes an Abstracts in English, and has many subscribers.

All-Russian Youth Conference on Nuclear Technology
(around Ozersk) 2001-2009 гг.

Russian Summer School on Modern Radiochemistry.
Dalnaya Dacha (around Ozersk) 2004-2012 гг.

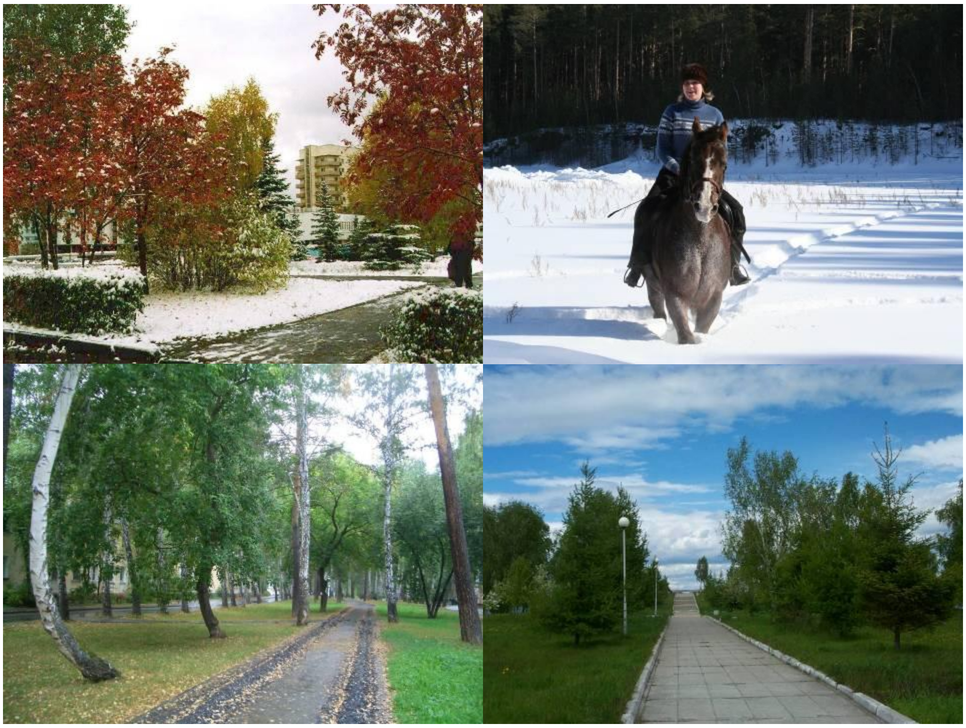

SPECIFIC ION EFFECTS IN SOLUTIONS, AT INTERFACES, AND IN COLLOIDAL SYSTEMS

Werner Kunz,
University of Regensburg, Institute of Physical and Theoretical Chemistry,
D-93040 Germany

In this presentation, I give a general overview about specific ion effects. In an introductory example I shortly present the complexity of so-called chemical gardens. I will then say a few words about general properties of ions, how they can be described and give a short historical background. After having introduced the Hofmeister series, Collins' law of matching water affinities are discussed as a first-order and qualitative model to understand a great number of specific ion effects. I stress that not a single model or even a single parameter can describe the effects of ions. The behaviour of an ion type will rather depend on its counterion and its environment. The task of the scientist will be to identify the most important effect in a given system and to select it out of a panoply of effects that are well-known and well-described today. Several examples will illustrate this approach.

Finally, I give examples of ion effects not following the Hofmeister series, for example the bubble-bubble coalescence in salt water or the spontaneous self-organisation of carboxylates and silicates to so-called biomorphs showing helical structures without any organic template.

SOLUTION CHEMISTRY

Specific Ion Effects in Solutions, at Interfaces and in Colloidal Systems

Werner Kunz
Institut für Physikalische und Theoretische Chemie
Fakultät für Chemie und Pharmazie

Universität Regensburg

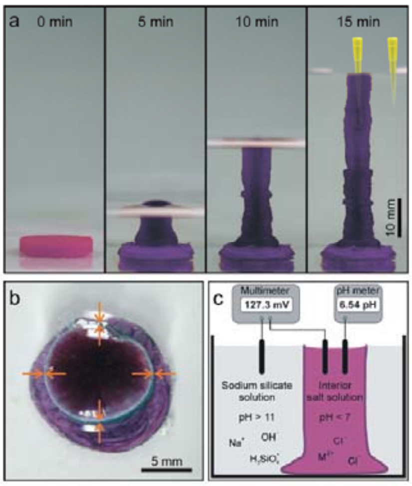

Figure 1. a) Formation of a tubular membrane with defined dimensions upon slow addition of silica solution to a tablet of $CoCl_2$. Pipette tips indicate sampling of the inner and outer solution. b) Top view of the tube, showing its open end. Arrows mark the tube wall. c) Scheme of the experimental setup used for pH and ΔE_h measurements.

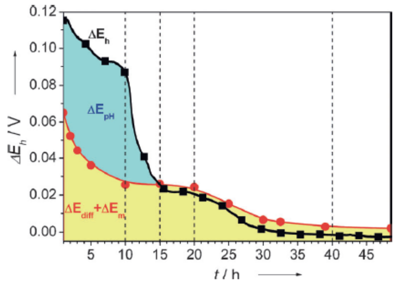

Figure 4. Electrochemical potentials in $CoCl_2$-based silica gardens. The overall cell potential (ΔE_h) results from a combination of diffusion (ΔE_{diff}) and membrane (ΔE_m) potentials as well as a third pH-induced contribution (ΔE_{pH}).

Thesis:
Fabian Glaab

Chemical garden ...

With Juan-Mauel Garcia Ruiz, Granada

... are beautiful structures that show fascinating membrane and diaphragm properties. In their Communication on page 4317 ff., W. Kunz, J. M. García-Ruiz, and co-workers reveal that, beyond beauty, this purely inorganic biomimetic phenomenon constitutes a complex out-of-equilibrium physicochemical system of two compartmentalized distinct solutions that creates measurable potential differences over extended periods of time (cover design: M. Wyrwoll).

WILEY-VCH

BASICS AND TRIVIALITIES

- **Ion specifities are everywhere (e.g. Na^+ versus K^+ in nature).**
- **Ions are everywhere.**
- **They interact via electrostatic interactions.**
- **At low concentrations (< 0.01 M) Debye-Hückel (DH) theory is adequate.**
- **In colloidal systems, the DLVO theory often properly reproduces interactions at long distances.**
- **Basically, the charge of the ion (or headgroup) is considered together with DH sceening.**

DEBYE-HÜCKEL

$$-\log \gamma_i = \frac{A z_i^2 \sqrt{I}}{1 + a_i B \sqrt{I}}$$

$$I = \frac{1}{2} \sum_i c_i z_i^2$$

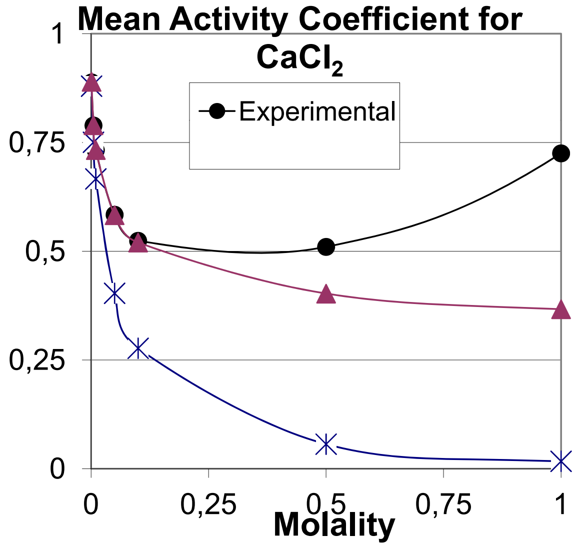

$$\mu_\mathrm{i} = \mu_\mathrm{i}^0 + RT \ln m_i \gamma_i$$

As long as activity coefficients are not too far from 1, they are not very relevant in real life.

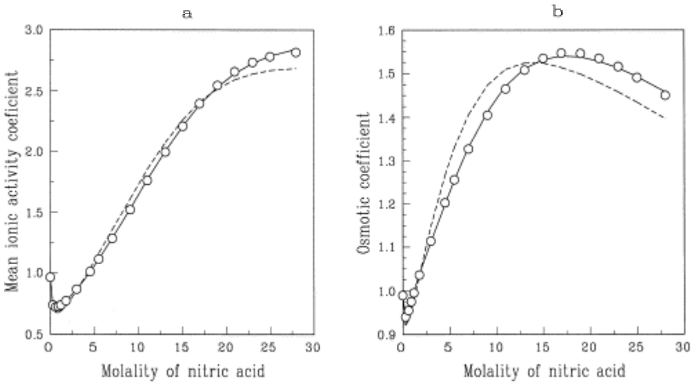

Osmotic Pressures of electrolyte solutions can be up to hundreds of bars!

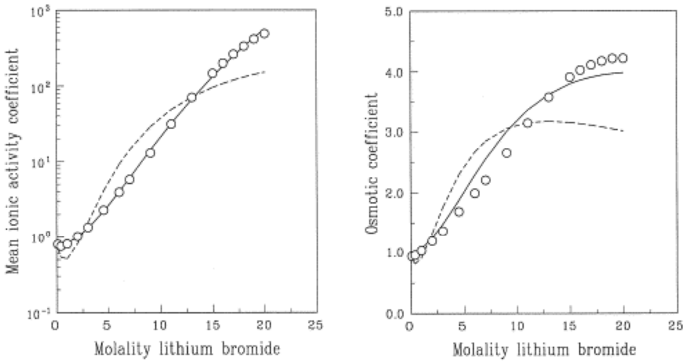

Electrical Conductivity can be very high

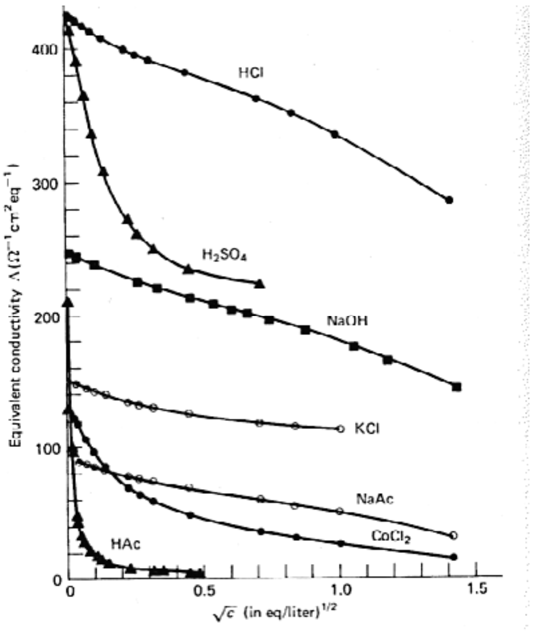

History

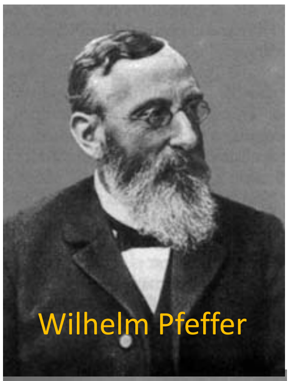
Wilhelm Pfeffer

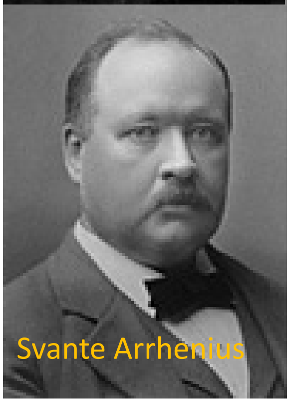
Svante Arrhenius


Professor Franz Hofmeister

Used with permission from the *Journal of Chemical Education*, Vol. 44, No.3, 1967, pp 177–180, copyright © 1967, Division of Chemical Education, Inc.

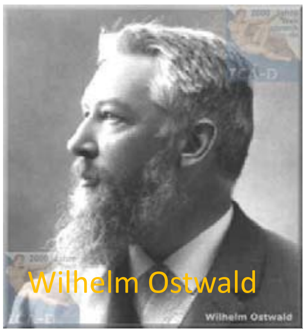
Wilhelm Ostwald


Jacobus H. van 't Hoff

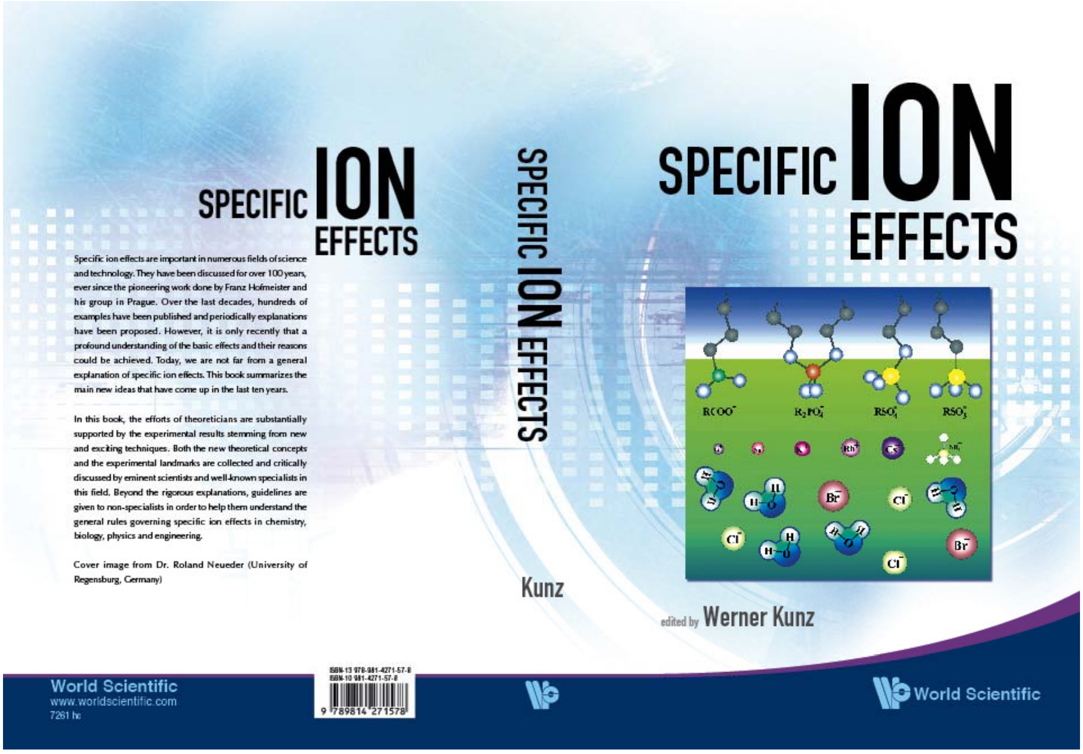
SPECIFIC ION EFFECTS

Specific ion effects are important in numerous fields of science and technology. They have been discussed for over 100 years, ever since the pioneering work done by Franz Hofmeister and his group in Prague. Over the last decades, hundreds of examples have been published and periodically explanations have been proposed. However, it is only recently that a profound understanding of the basic effects and their reasons could be achieved. Today, we are not far from a general explanation of specific ion effects. This book summarizes the main new ideas that have come up in the last ten years.

In this book, the efforts of theoreticians are substantially supported by the experimental results stemming from new and exciting techniques. Both the new theoretical concepts and the experimental landmarks are collected and critically discussed by eminent scientists and well-known specialists in this field. Beyond the rigorous explanations, guidelines are given to non-specialists in order to help them understand the general rules governing specific ion effects in chemistry, biology, physics and engineering.

Cover image from Dr. Roland Neueder (University of Regensburg, Germany)

World Scientific
www.worldscientific.com
7261 hc
ISBN-13 978-981-4271-57-8
ISBN-10 981-4271-57-8

SPECIFIC ION EFFECTS
Kunz

SPECIFIC ION EFFECTS

edited by Werner Kunz

World Scientific

Gibbs adsorption isotherm

@ liquid surface, surface and subphase are in equilibrium:exchange possible

Problem: Location of a surface at a liquid/vapor interface?

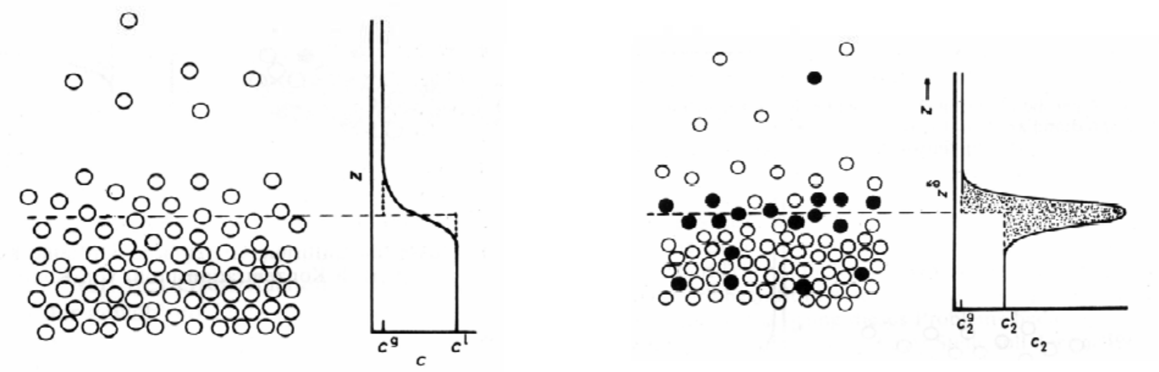

Liquid surface: interfacial region a few molecular diameters thick ***(nm)***
Solid surface: interfacial region on a Å scale

Gibbs adsorption equation

$$\Delta c(z) = c(z) - c_{liq} \qquad \Gamma = \int_{-\infty}^{\infty} \Delta c(z)dz$$

$$\Delta c(z) = c(z) - c_{vap} \qquad \Gamma = \int_{-\infty}^{\infty} (c(z) - c_{vap})dz + \int_{-\infty}^{\infty} (c(z) - c_{liq})dz$$

$$\Gamma_1 = \Gamma_{H_2O} = \int_{z_0}^{\infty} (c(z) - c_{H_2O,v})dz + \int_{-\infty}^{z_0} (c(z) - c_{H_2O,liq})dz = 0$$

$$\Gamma_2 = \Gamma_{SDS} = \int_{z_0}^{\infty} (c(z) - c_{SDS,v})dz + \int_{-\infty}^{z_0} (c(z) - c_{SDS,liq})dz$$

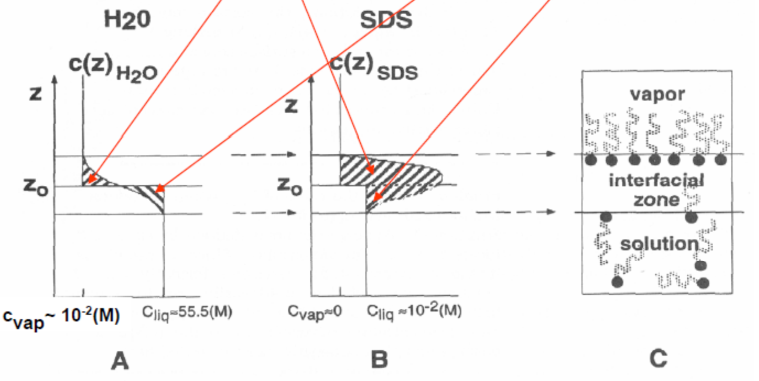

$$\frac{d\gamma}{d\mu} = -\Gamma_{SDS}$$

$$\Gamma_{SDS} = -\frac{1}{RT}\frac{d\gamma}{d\ln c_{SDS}}$$

10468 *J. Phys. Chem. B* **2001,** *105,* 10468−10472

Molecular Structure of Salt Solutions: A New View of the Interface with Implications for Heterogeneous Atmospheric Chemistry

Pavel Jungwirth[†,‡] and Douglas J. Tobias[*,§]

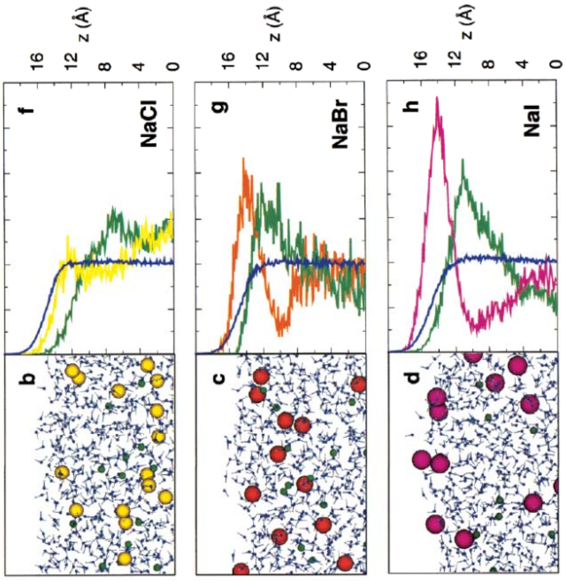

Surface Tensions of Aqueous Salt Solutions

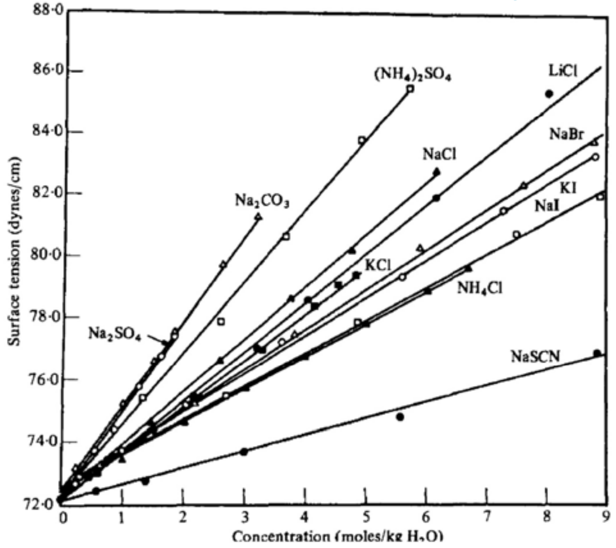

Jarvis and Scheiman, *JPC* 72, 77 (1968)

Weissenborn and Pugh →

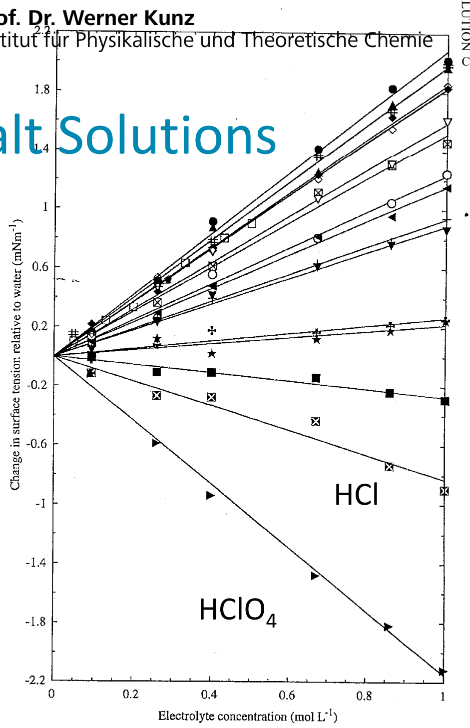

FIG. 3. Effect of electrolyte concentration on the change in surface tension relative to water for 1:1 electrolytes. Bubble interval, 1.5 s. Experimental error in data points is ±0.1 mN m^{-1}. HCl (■), LiCl (▲), NaCl (●), KCl (♦), CsCl (⊠), NaF (□), NaI (○), NH_4Cl (▽), NaBr (◇), HNO_3 (☒), $(CH_3)_4NCl$ (+), NH_4NO_3 (◀), $HClO_4$ (▶), $NaClO_3$ (▼), $LiClO_4$ (✢), $NaClO_4$ (★), KOH (#).

Activity coefficients of simple electrolyte solutions

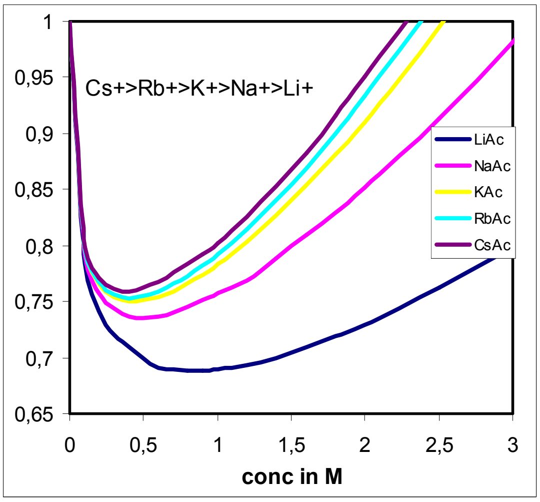

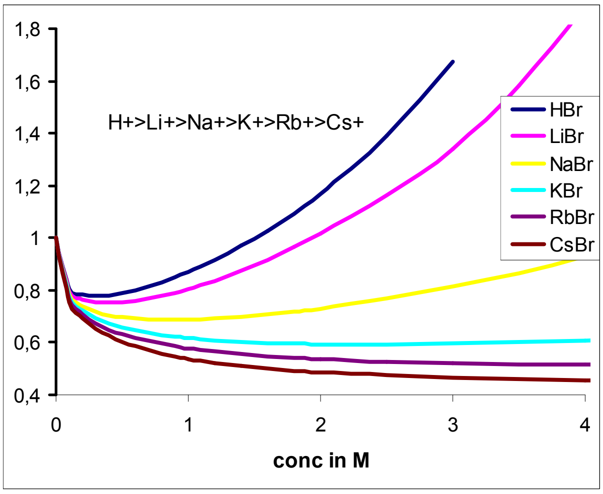

See book of Robinson and Stokes

HOFMEISTER SERIES

Cations

guanidinium — guanidinium

Chaotropic cations $N(CH_3)_4^+$ NH_4^+ Cs^+ Rb^+ K^+ Na^+ Li^+ Mg^{2+} Ca^{2+} **Kosmotropic cations**

organic ions of growing size

Kosmotropic anions SO_4^{2-} HPO_4^{2-} OAc^- cit^- OH^- Cl^- Br^- NO_3^- ClO_3^- BF_4^- I^- ClO_4^- SCN^- PF_6^- **Chaotropic anions**

Anions

↑surface tension
harder to make cavity
↓solubility hydrocarbons
salt out (aggregate)
↓protein denaturation
↑protein stability
weakly hydrated soft
cations of low
charge density
strongly hydrated hard
anions of high
charge density

↔

↓surface tension
easier to make cavity
↑solubility hydrocarbons
salt in (solubilize)
↑protein denaturation
↓protein stability
strongly hydrated hard
cations of high
charge density
weakly hydrated soft
anions of low
charge density

Why are the phase diagrams SDS/oil/water and DTAB/oil/water so different?

☞ Different hydration of the headgroups, as detected by Dielectric Relaxation Spectroscopy

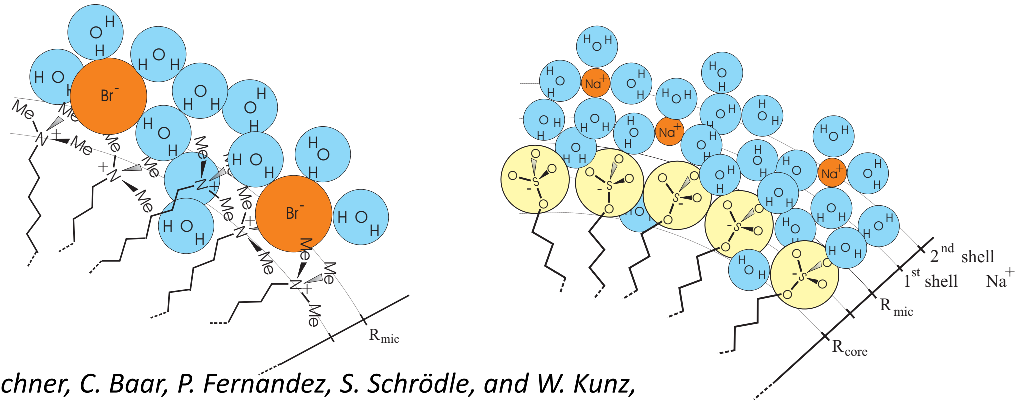

R. Buchner, C. Baar, P. Fernández, S. Schrödle, and W. Kunz,
Dielectric Spectroscopy of Micelle Hydration and Dynamics
in Aqueous Ionic Surfactant Solutions, *J. Molecular Liquids 118 (2005) 179–187.*

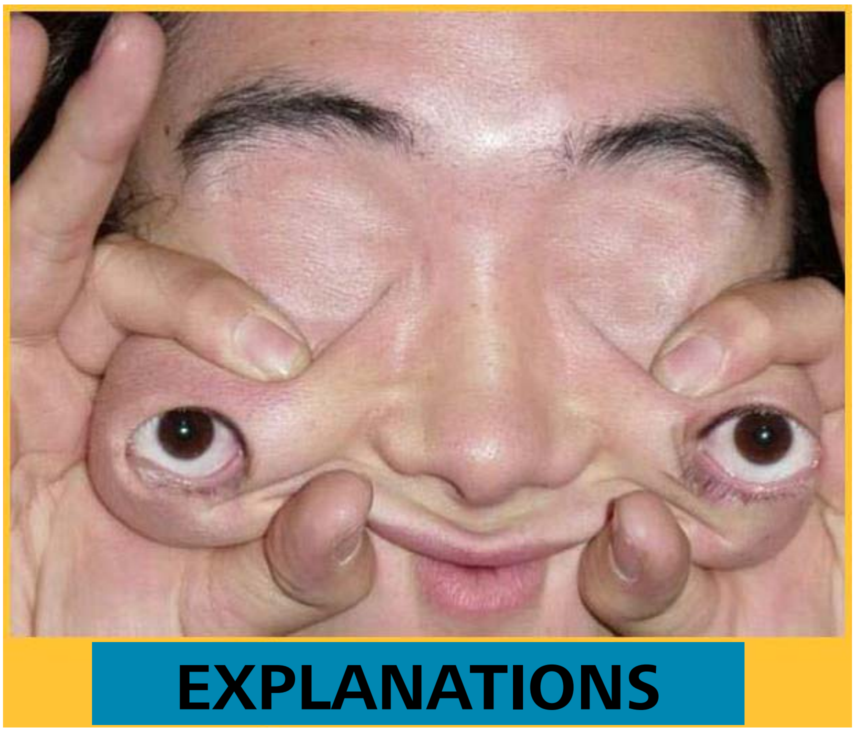

EXPLANATIONS

Kim D. Collins: the Debye-Hückel theory is misleading and slowed down the progress of understanding biological processes

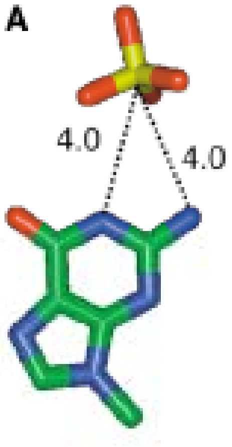

Anions can bind directly to electronegative pockets located around amino groups in nucleic acids: (A)N6 or (C)N4 in the deep/major groove of A-U and G+C pairs and (G)N2 in the shallow/ minor groove of G=C pairs.

Auffinger, Bielecki & Westhof (2004) Structure 12: 379-388.

Ions from the Hofmeister series and osmolytes: effects on proteins in solution and in the crystallization proces

Methods 34 (2004) 300–311

Kim D. Collins*

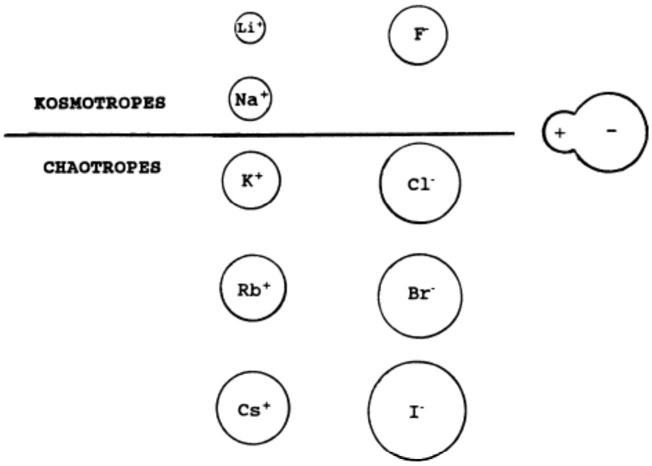

K.D. Collins / Methods 34 (2004) 300–311

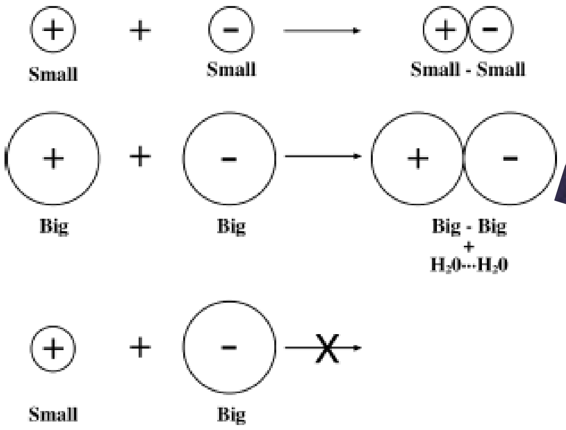

Ion Pairing as a Possible Clue for Discriminating between Sodium and Potassium in Biological and Other Complex Environments

Barbara Jagoda-Cwiklik,† Robert Vácha,† Mikael Lund,† Monika Srebro,‡ and Pavel Jungwirth*,†

THE JOURNAL OF PHYSICAL CHEMISTRY B LETTERS

2007, *111*, 14077–14079

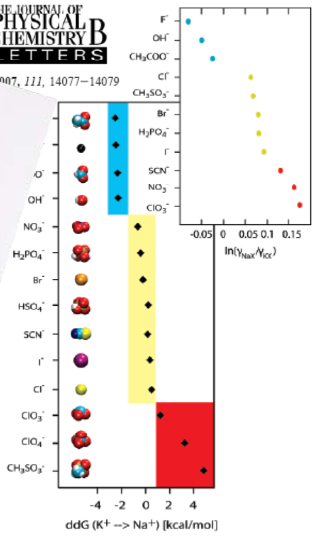

Figure 2. Free energy change upon replacing potassium with sodium in a contact ion pair with a series of anions. Inset: The corresponding differences in excess chemical potentials obtained experimentally for 0.7 M solutions.[16–18] Blue, red, or yellow color indicates anions preferring sodium, potassium, or having little preference between the two cations, respectively.

Activity coefficients of simple electrolyte solutions

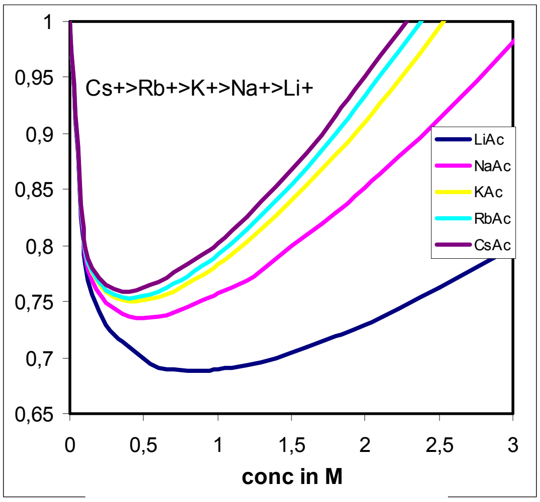

hard-hard → association

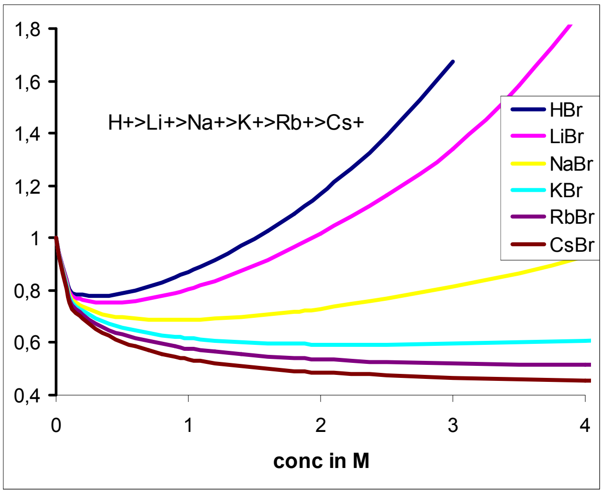

soft-soft → association

Hans Lyklema: “like seeks like”

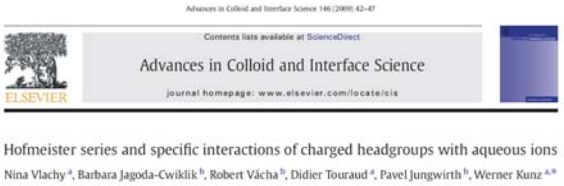

Advances in Colloid and Interface Science 146 (2009) 42–47

Contents lists available at ScienceDirect

ELSEVIER

Advances in Colloid and Interface Science

journal homepage: www.elsevier.com/locate/cis

Hofmeister series and specific interactions of charged headgroups with aqueous ions

Nina Vlachy [a], Barbara Jagoda-Cwiklik [b], Robert Vácha [b], Didier Touraud [a], Pavel Jungwirth [b], Werner Kunz [a,*]

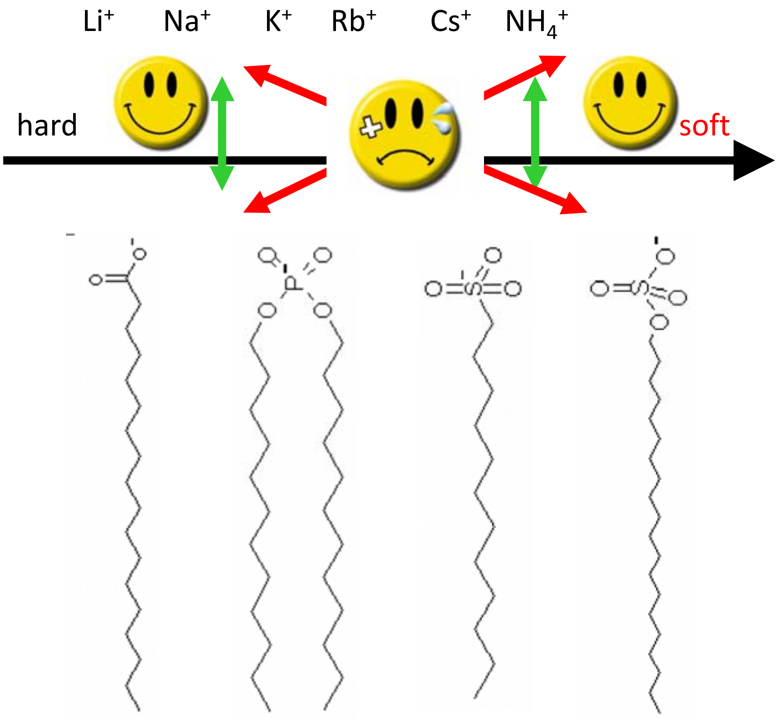

carboxylate phosphate sulphonate sulphate

Thesis
Nina Vlachy
Regensburg
2008

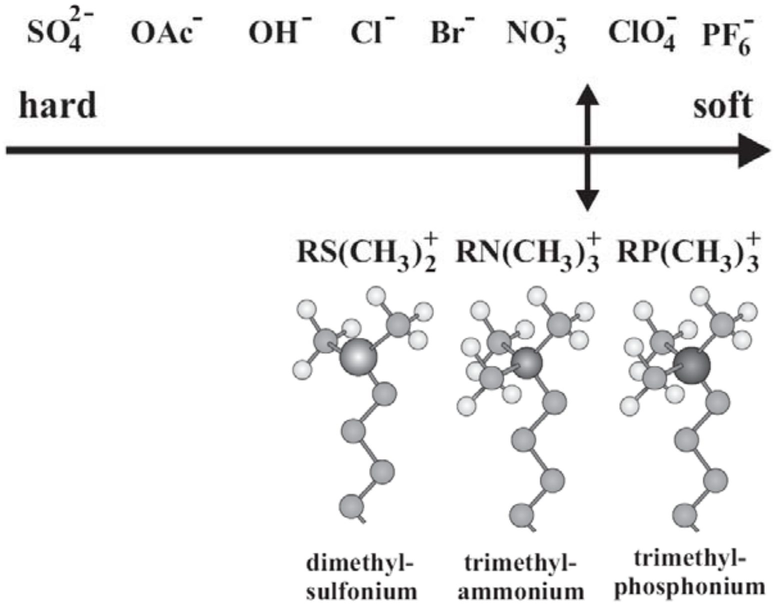

Dozens of experiments can be explained now and others predicted:

- cation affinity to ion-exchange resins
- membrane potentials
- electrophoretic mobilities of colloids
- ion-transport phenomena
- swelling of hydrogels
- counter-ion binding to fatty acids
- counter-ion binding to polyelectrolytes and phospholipids
- counter-ion binding to micelles

Example:

- B.W. Ninham, S. Hashimoto, J.K. Thomas
  Unusual behaviour of hydroxide surfactants
  Journal of Colloid & Interface Science 95 (1983) 594-596

  cmc (DDA^+ OH^-) ≈ 2 cmc (DDA^+ Br^-) explained with „hydration forces“.

Our explanation: OH^- does not come into close contact with DDA^+

Specific Anion and Cation Binding to Lipid Membranes Investigated on a Solid Supported Membrane

Juan J. Garcia-Celma,† Lina Hatahet,† Werner Kunz,‡ and Klaus Fendler*,†

Langmuir 23(20) (2007) 10074-80

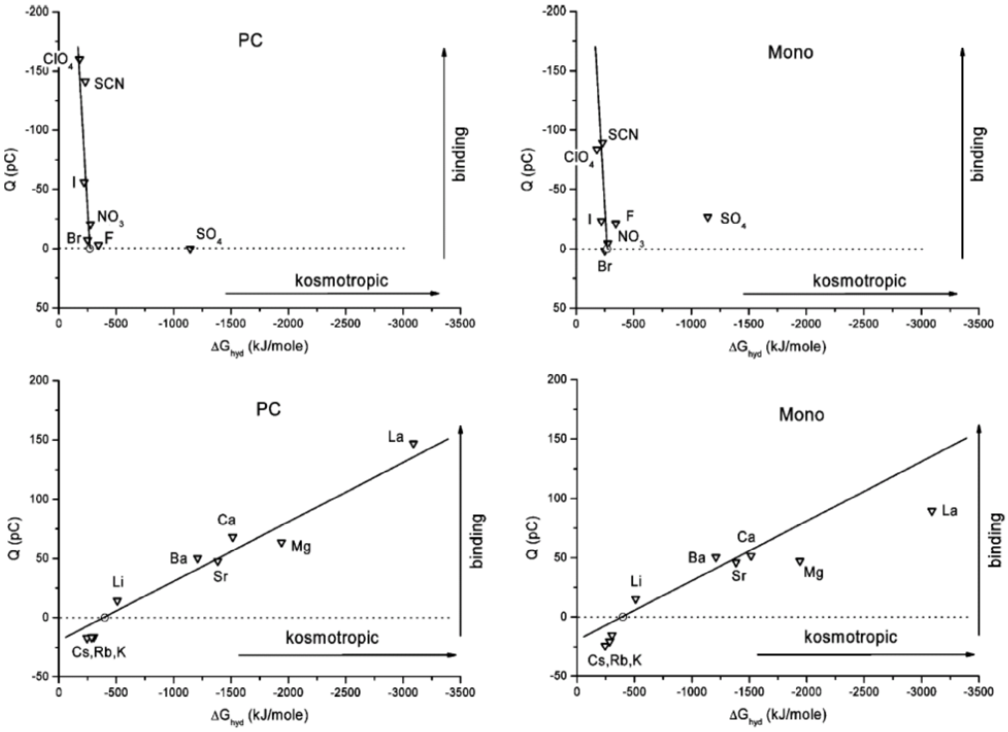

Figure 2. Charge displacements of different anions and cations on a PC (phosphatidylcholine) and a Mono (monoolein) membrane. The open circle indicates the reference ions Na or Cl. Ions are classified according to their Gibbs free energies of hydration ΔG_{hyd}.

Regina Klein

Prof. Dr. Werner Kunz

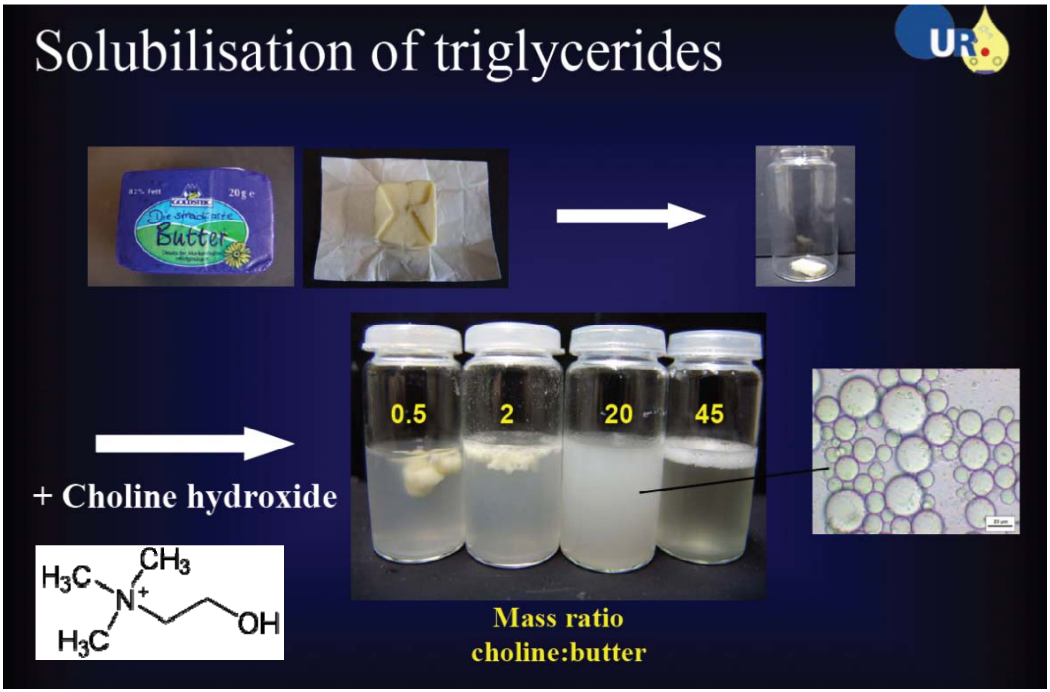

Solubilisation of triglycerides

+ Choline hydroxide

Mass ratio
choline:butter

Regina Klein, Didier Touraud, and Werner Kunz,
Choline Carboxylate Surfactants: Biocompatible and Highly Soluble in Water,
Green Chemistry 10(4) (2008) 433-435.

Reversed Anionic Hofmeister Series: The Interplay of Surface Charge and Surface Polarity

Nadine Schwierz,* Dominik Horinek, and Roland R. Netz*

Langmuir **2010,** *26(10)*, 7370–7379

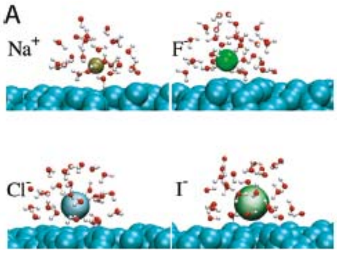

Simulation results at the hydrophobic CH_3-terminated SAM.

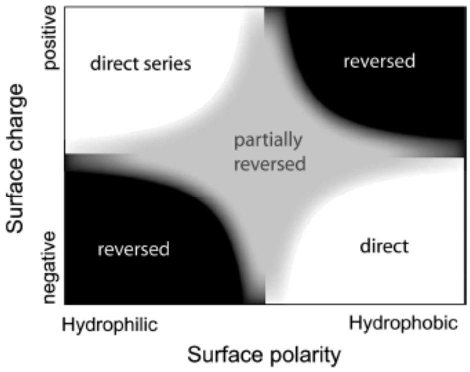

Figure 1. Schematic Hofmeister phase diagram as a function of surface charge and polarity, featuring direct and reversed (i.e., indirect) series as well as partial reversion (derived from our modeling results and in agreement with experimental results for colloids[23]).

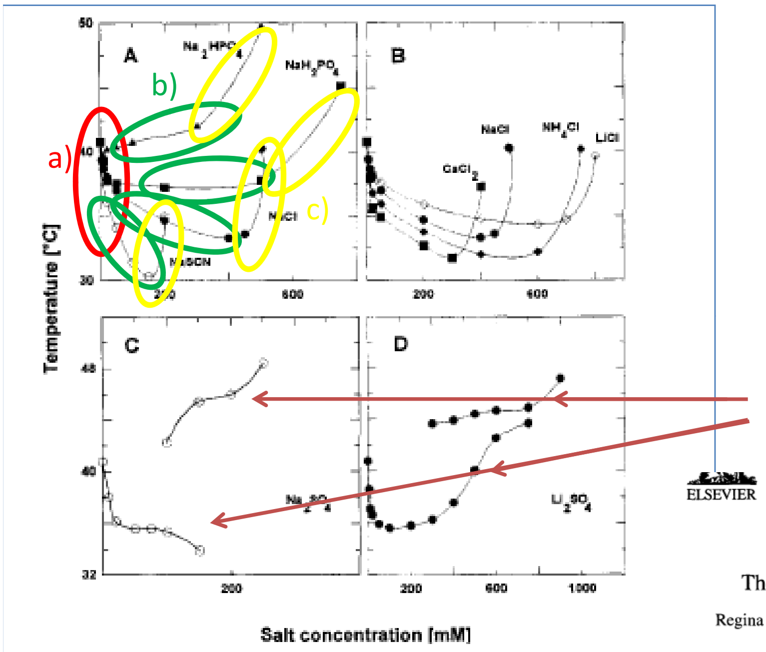

Fig. 5. Dependence of the denaturation temperature of calf skin collagen type I on the salt concentration: (A) selection of sodium salts; (B) selection of chloride salts; (C) Na_2SO_4, (D) Li_2SO_4.

a) small concentrations:
all salts are salting-in.
reason: electrostatic screening

b) intermediate concentrations:
ion specificity

c) „high“ concentration:
all salts salting-out

d) two types of denaturation
processes with sulfate ions !

ELSEVIER
Biochimica et Biophysica Acta 1297 (1996) 171–181
et Biophysica Ac

Thermal stability of calf skin collagen type I in salt solutions

Regina Komsa-Penkova [a], Rumiana Koynova [b], Georgi Kostov [b], Boris G. Tenchov [b,*]
[a] *Department of Biochemistry, Medical University of Pleven, 5802 Pleven, Bulgaria*
[b] *Institute of Biophysics, Bulgarian Academy of Sciences, 1113 Sofia, Bulgaria*

Received 20 May 1996; accepted 3 June 1996

“Sausage Casing”

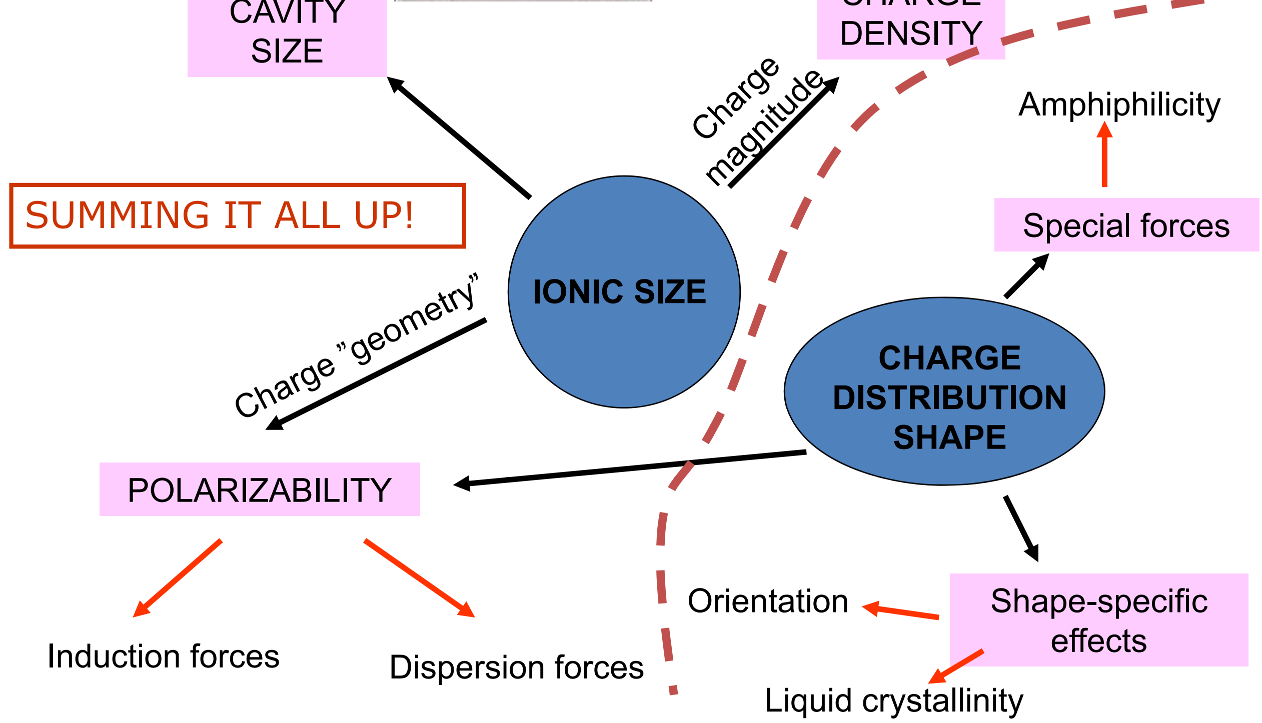

Partitioning phenomena

SOLVENT CAVITY SIZE

Solvation

Ion pairing

CHARGE DENSITY

Charge magnitude

Amphiphilicity

SUMMING IT ALL UP!

Special forces

IONIC SIZE

Charge ”geometry”

CHARGE DISTRIBUTION SHAPE

POLARIZABILITY

Orientation

Shape-specific effects

Induction forces

Dispersion forces

Liquid crystallinity

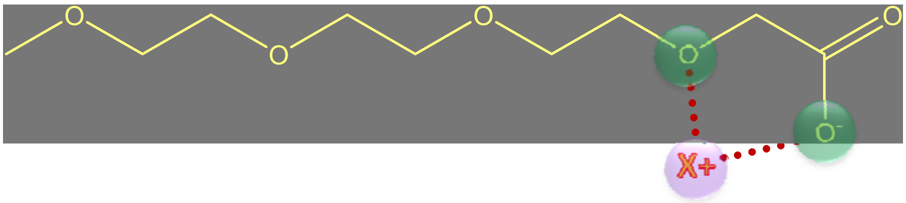

Cation	Melting- / Glass - point [°C]	H_2O [ppm]	Decomposition temperature [°C]
Li^+	-53	103	357
Na^+	-57	211	384
K^+	60	1292	369

O. Zech, M. Kellermeier, S. Thomaier, E. Maurer, R. Klein, C. Schreiner, W. Kunz, Chem. Eur. J., 15, 1341 (2009)

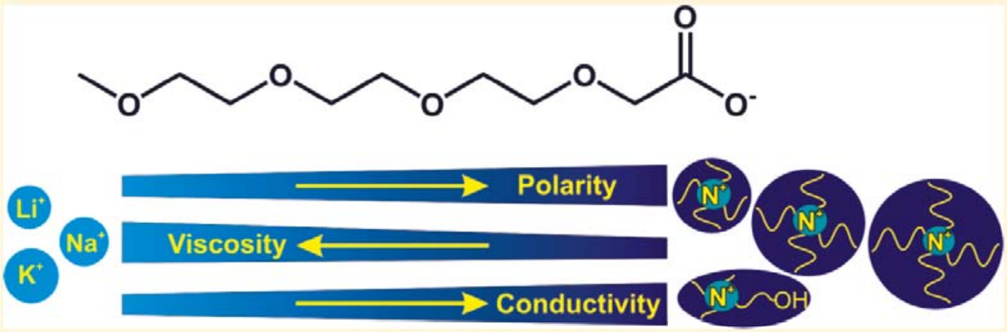

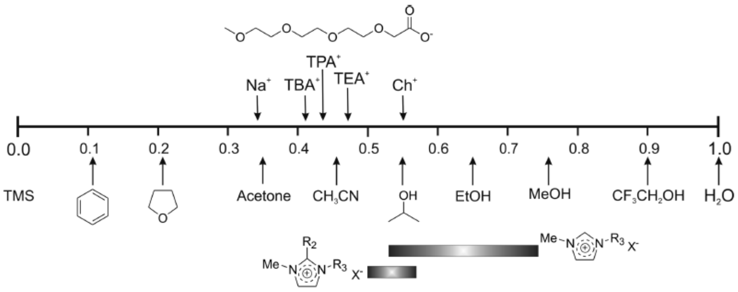

Figure 4. Classification of TOTO RTILs on the normalized E_T^N scale (25 °C) as compared with various molecular solvents and conventional ionic liquids. The scheme and the E_T^N range of imidazolium-typed ILs are partially based on a drawing by Reichardt in 2005.37 Values for the molecular solvents and Na−TOTO were adapted from refs 36 and 12, respectively.

Catanionics

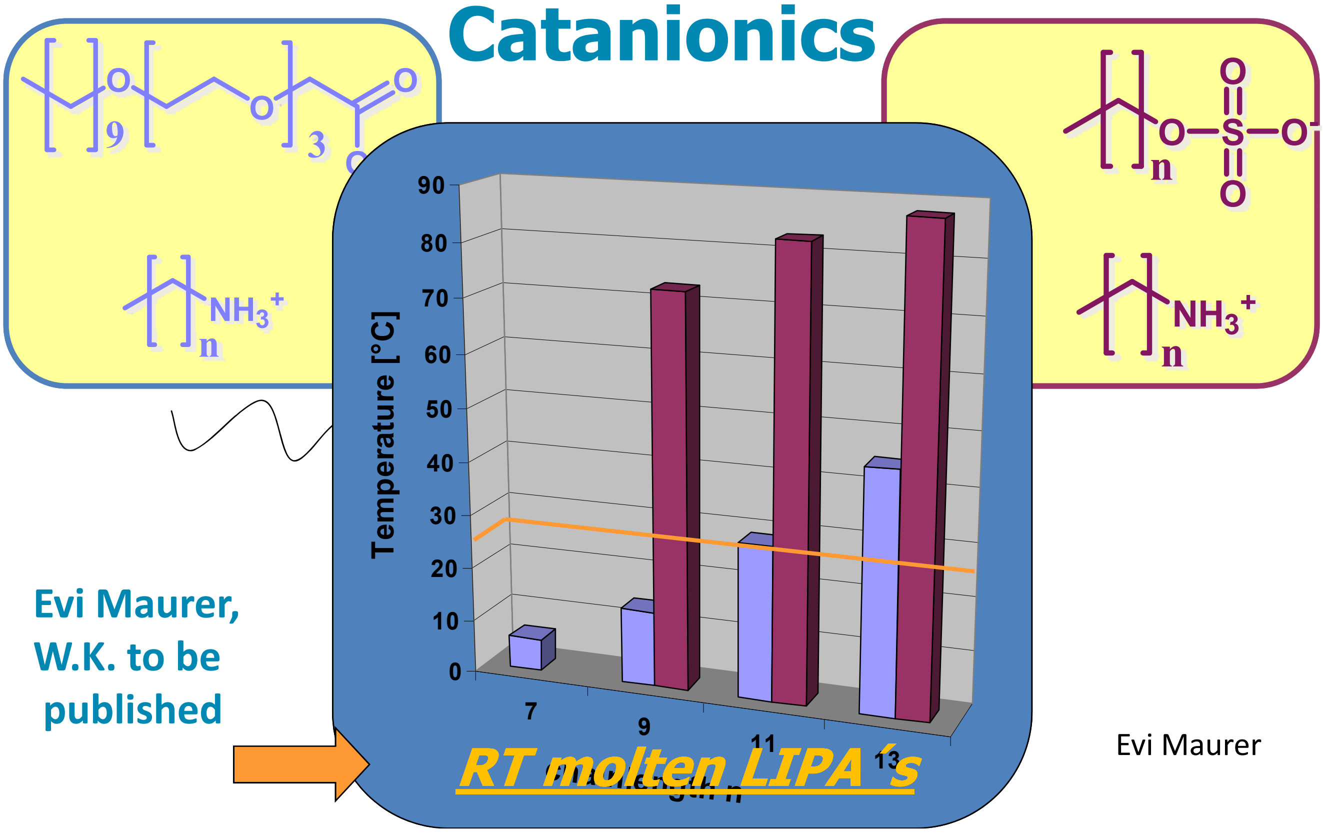

Evi Maurer, W.K. to be published

Evi Maurer

CONCLUSIONS AND SUMMARY

- At short distances electrostatic interactions are not always dominant, see example K.D. Collins.
- Ion specific effects occur at intermediate concentrations.
- The ion specificity depends on the counterpart.
- Ion specificities are usually amplified at interfaces.
- The law of matching water affinities is as useful first order approximation in biological systems.
- The appropriate explanation depends much on the given system (see Leontidis‘ scheme.

Specific-Ion Effects in Bubble Coalescence

Dr Vincent Craig
Department of Applied Mathematics
Research School of Physical Sciences
and Engineering
Australian National University

Vince Craig,
Current Opinion in Colloid and Interface Science (2011) 16(6), 597–600.

Nature 364 (1993) 317-319

αα , ββ	**Ions**	**Cations**	Na^+	H^+	αβ, βα
	**Anions**	*Assignment*	α	β	
	Cl^-	α	✓	×	
	ClO_4^-	β	×	✓	

Ions		Li^+	Na^+	K^+	Cs^+	Mg^{2+}	Ca^{2+}	NH_4^+	H^+	$(CH_3)NH_3^+$	$(CH_3)_2NH_2^+$	$(CH_3)_3NH^+$	$(CH_3)_4N^+$
Assignment		α	α	α	α	α	α	α	β	β	β	β	β
OH^-	α		✓	✓					×				
F^-	α		✓										
Cl^-	α	✓	✓	✓		✓	✓		×	×	×	×	×
Br^-	α		✓	✓	✓				×				×
I^-	α	✓	✓	✓									
NO_3^-	α	✓	✓	✓			✓		×				
SO_4^{2-}	α	✓	✓	✓		✓			×				
$(COO_2)^{2-}$	α			✓					×				
IO_3^-	α		✓										
ClO_3^-	β		×										
ClO_4^-	β		×			×		×	✓				
CH_3COO^-	β		×	×	×	×		×	✓				✓
SCN^-	β		×					×					

✓= inhibit coalescence
αα, ββ = ✓
×= no inhibition
αβ, βα = ×

[a] Based on Craig et al.[2] with additional results.

Vincent Craig

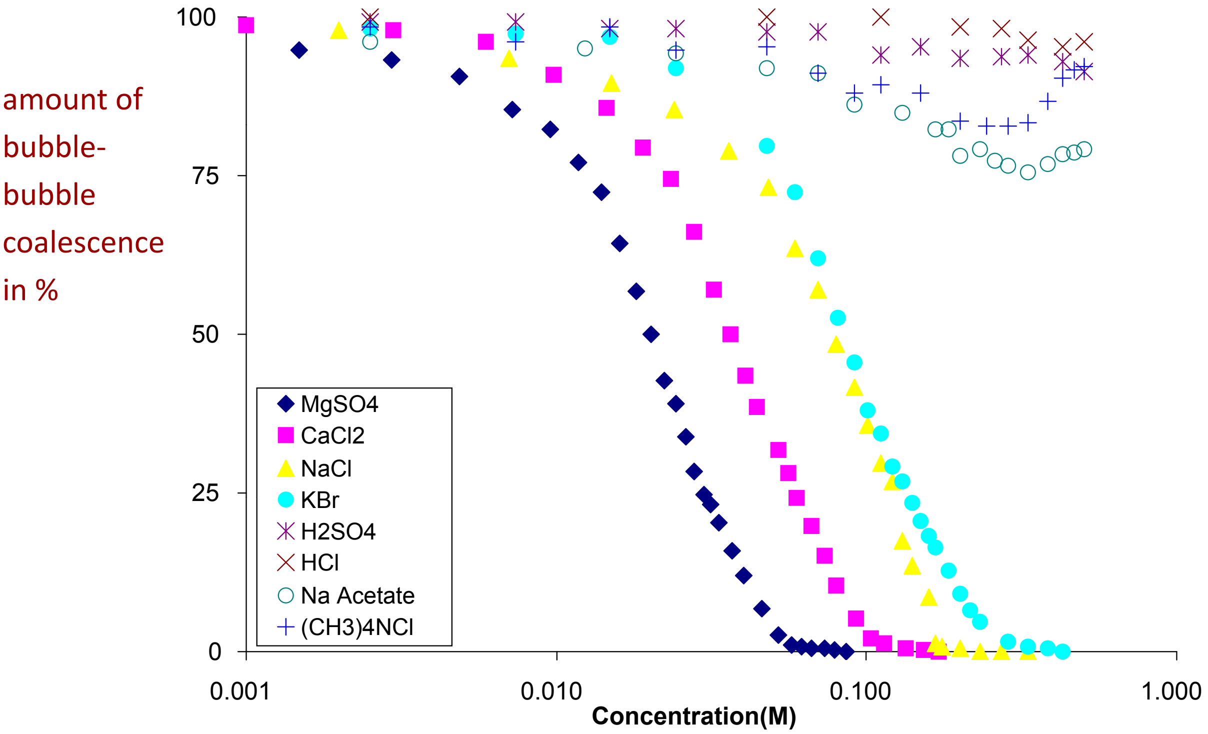

Origin of life

Cavitation and bubble fusion/growth inhibited above 0.175 M.

Eukaryotic life could not evolve until salt concentration reached 0.175 M.
This is the concentration of Permian ocean and in all land animals that emerged.
(Present ocean ≥ 0.3 M)

Ninham, Craig et al.

in Evolution:

- Ediacara extinction 570 million years before present: Worldwide all multicelled animals died.
- Burgess Shales extinction 530 million years before present.
- Permian extinction 230 million years before present .
  95% of all species disappeared.

- All coincide with known CO_2 cycle; consequent ice ages; precipitation and removal of salt. Followed by reduction of salinity below 0.175 M after ice melts.
- Massive extinction of phytoplankton.

Simple Experiment

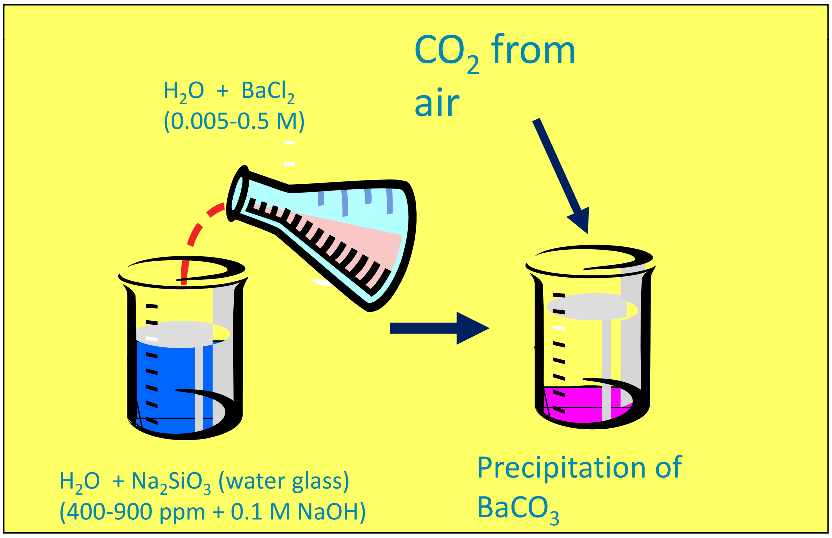

H_2O + $BaCl_2$
(0.005-0.5 M)

CO_2 from air

H_2O + Na_2SiO_3 (water glass)
(400-900 ppm + 0.1 M NaOH)

Precipitation of $BaCO_3$

first discovered by Juan Manuel Garcia-Ruiz about 15 years ago

---

$BaCO_3$ + Silicate

Matthas Kellermeier, Stephen Hyde and W.K. 2005

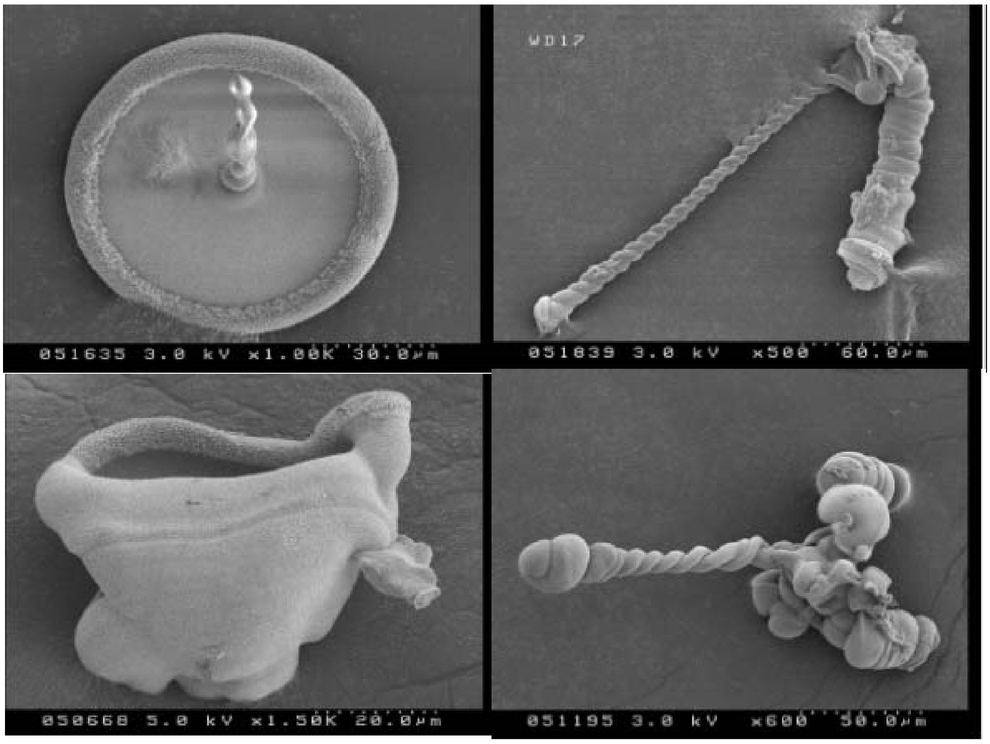

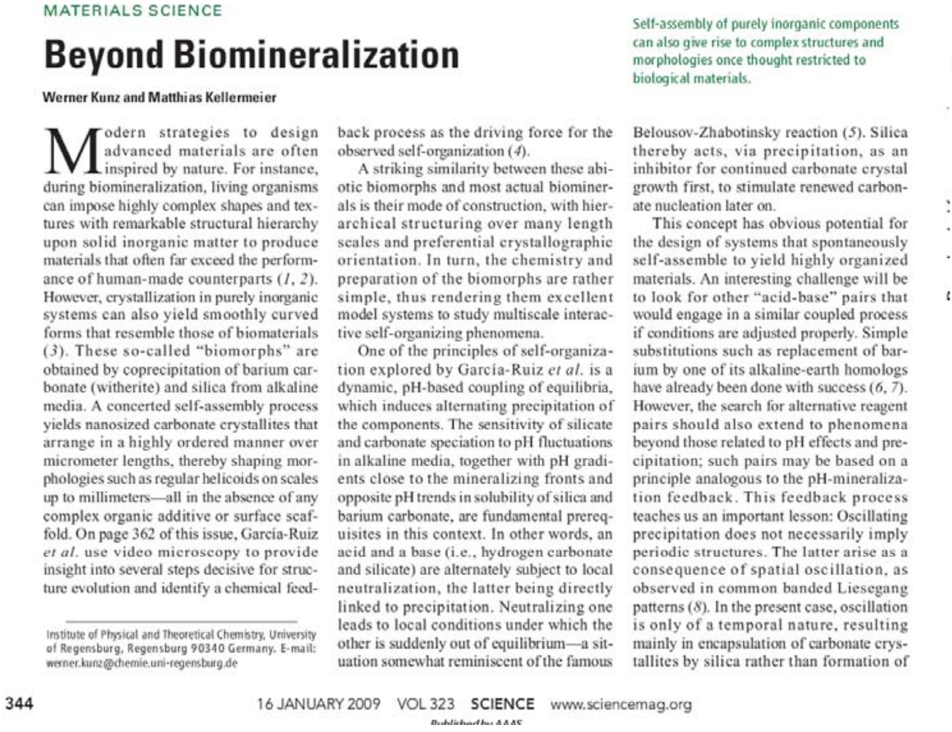

MATERIALS SCIENCE

Beyond Biomineralization

Werner Kunz and Matthias Kellermeier

Self-assembly of purely inorganic components can also give rise to complex structures and morphologies once thought restricted to biological materials.

Modern strategies to design advanced materials are often inspired by nature. For instance, during biomineralization, living organisms can impose highly complex shapes and textures with remarkable structural hierarchy upon solid inorganic matter to produce materials that often far exceed the performance of human-made counterparts (*1*, *2*). However, crystallization in purely inorganic systems can also yield smoothly curved forms that resemble those of biomaterials (*3*). These so-called "biomorphs" are obtained by coprecipitation of barium carbonate (witherite) and silica from alkaline media. A concerted self-assembly process yields nanosized carbonate crystallites that arrange in a highly ordered manner over micrometer lengths, thereby shaping morphologies such as regular helicoids on scales up to millimeters—all in the absence of any complex organic additive or surface scaffold. On page 362 of this issue, García-Ruiz *et al.* use video microscopy to provide insight into several steps decisive for structure evolution and identify a chemical feedback process as the driving force for the observed self-organization (*4*).

A striking similarity between these abiotic biomorphs and most actual biominerals is their mode of construction, with hierarchical structuring over many length scales and preferential crystallographic orientation. In turn, the chemistry and preparation of the biomorphs are rather simple, thus rendering them excellent model systems to study multiscale interactive self-organizing phenomena.

One of the principles of self-organization explored by García-Ruiz *et al.* is a dynamic, pH-based coupling of equilibria, which induces alternating precipitation of the components. The sensitivity of silicate and carbonate speciation to pH fluctuations in alkaline media, together with pH gradients close to the mineralizing fronts and opposite pH trends in solubility of silica and barium carbonate, are fundamental prerequisites in this context. In other words, an acid and a base (i.e., hydrogen carbonate and silicate) are alternately subject to local neutralization, the latter being directly linked to precipitation. Neutralizing one leads to local conditions under which the other is suddenly out of equilibrium—a situation somewhat reminiscent of the famous Belousov-Zhabotinsky reaction (*5*). Silica thereby acts, via precipitation, as an inhibitor for continued carbonate crystal growth first, to stimulate renewed carbonate nucleation later on.

This concept has obvious potential for the design of systems that spontaneously self-assemble to yield highly organized materials. An interesting challenge will be to look for other "acid-base" pairs that would engage in a similar coupled process if conditions are adjusted properly. Simple substitutions such as replacement of barium by one of its alkaline-earth homologs have already been done with success (*6*, *7*). However, the search for alternative reagent pairs should also extend to phenomena beyond those related to pH effects and precipitation; such pairs may be based on a principle analogous to the pH-mineralization feedback. This feedback process teaches us an important lesson: Oscillating precipitation does not necessarily imply periodic structures. The latter arise as a consequence of spatial oscillation, as observed in common banded Liesegang patterns (*8*). In the present case, oscillation is only of a temporal nature, resulting mainly in encapsulation of carbonate crystallites by silica rather than formation of

---

Institute of Physical and Theoretical Chemistry, University of Regensburg, Regensburg 90340 Germany. E-mail: werner.kunz@chemie.uni-regensburg.de

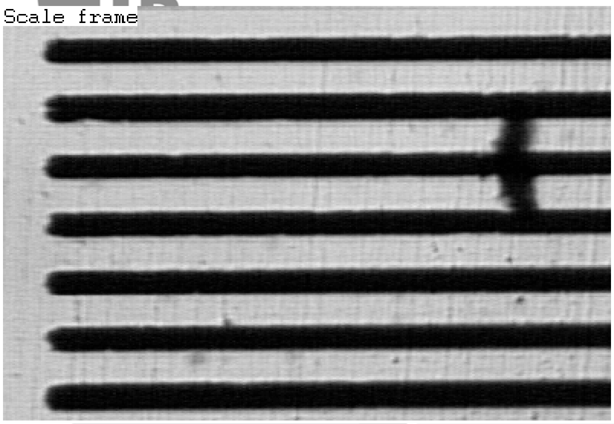

With Juan-Mauel García Ruiz, Granada

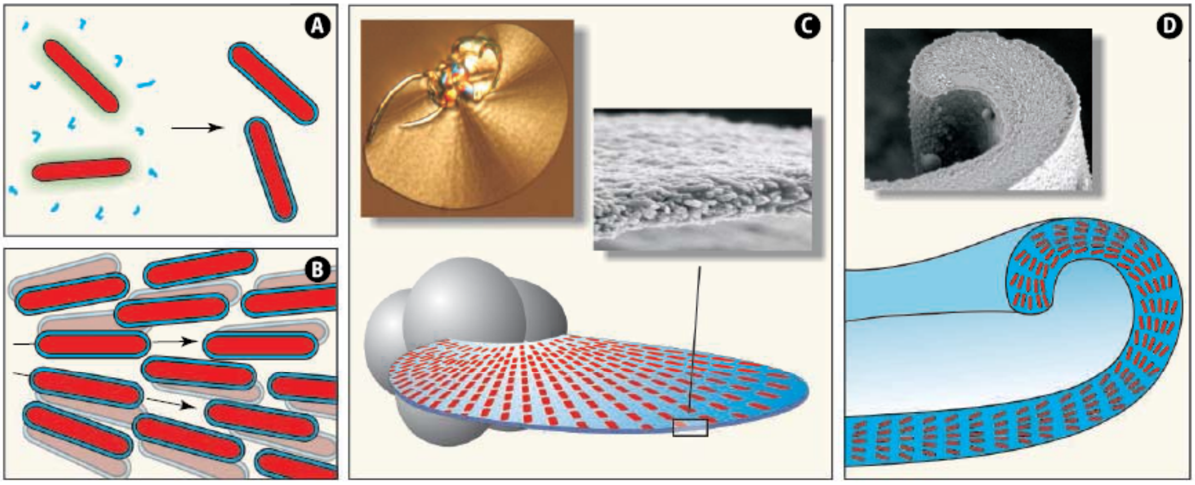

Thank you
for your attention!

Merci!

DANKE !

Спасибо!

A.N. Frumkin INSTITUTE OF PHYSICAL CHEMISTRY AND ELECTROCHEMISTRY
RUSSIAN ACADEMY OF SCIENCES
Laboratory of new physico-chemical problems

Anna Sinelshchikova

Self-assembling of transition *d*-metals complexes with *meso*-polyphosphoryl porphyrins

Supervisors
Full member of RAS Aslan Yu. Tsivadze
Prof. Yulia G. Gorbunova

Moscow 2012

Noncovalent architectures – self-assembling

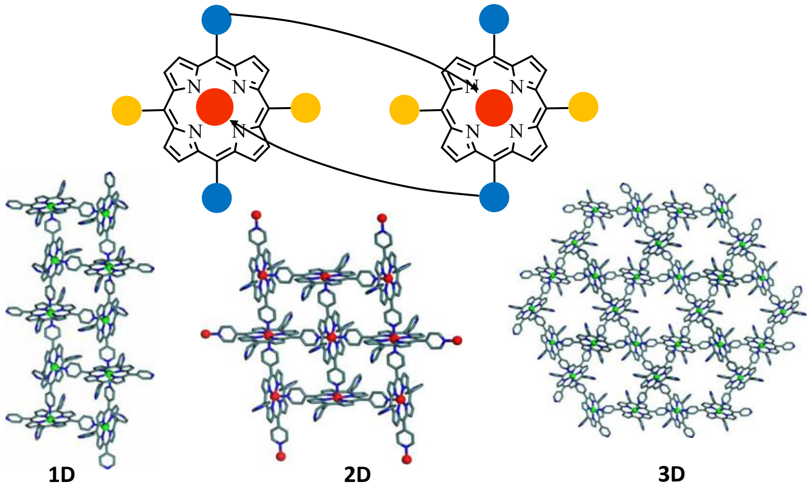

DeVries L.D., Choe W. *J. Chem. Crystallogr.*, **2009**, 39, 229
Deiters E., Bulach V., Hosseini M.W. *New J. Chem.*, **2008**, 32, 99.

Supramolecular assemblies

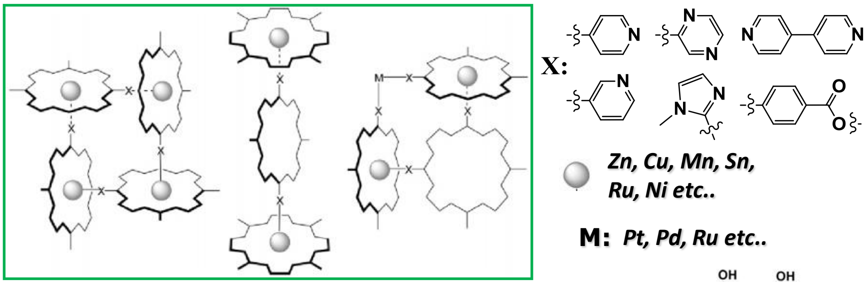

Beletskaya I., Tyurin V., Tsivadze A. et al. *Chem. Rev.*, **2009**, 109, 1659.

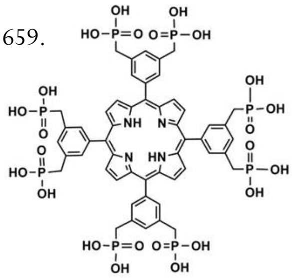

- Phosphorous porphyrins are less investigated
- -R-P(O)$(OH)_2$ form hydrogen and coordination bonds

Meso-polyphosphorylporphyrins

- *Meso*-polyphosphorylporphyrins were synthesised earlier in our group
- Self-assembling of zinc (II) porphyrin was demonstrated

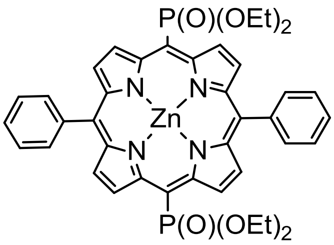

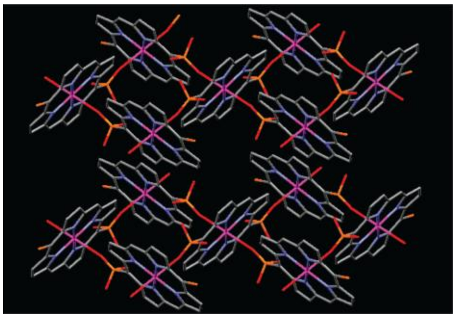

Y.Y. Enakieva et al. *Org. Lett.* **2009**, 11, 3842.

Objective

- Investigation of influence of *d*-metals nature on ability of *meso*-diphosphorylporphyrinates towards supramolecular self-assembling in solution and solid state

Meso-diphosphorylporphyrins

$1H_2$=

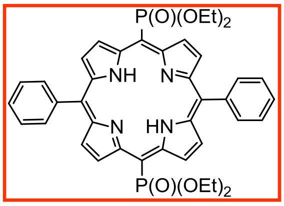

$2H_2$=

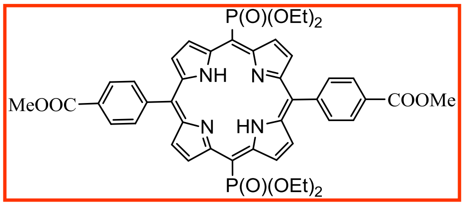

Synthesis of free-base diphosphorylporphyrins

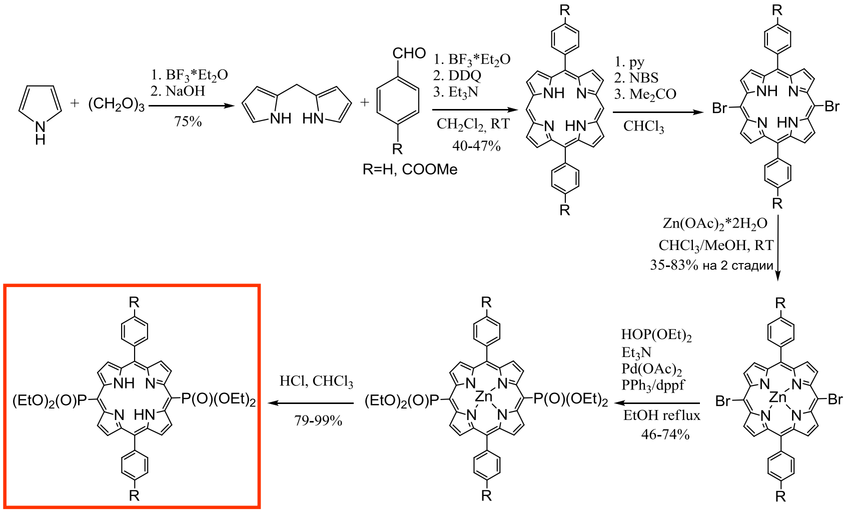

Y. Y. Enakieva et al. *Org. Lett.* **2009**, 11, 3842.

d-metal complexes

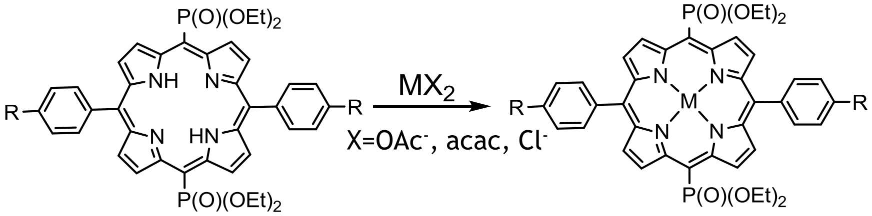

1M - R=H, 2M - R=COOMe

M = Cu(II), Cd(II), Co(II), Ni(II), Pd(II), Pt(II)

Self-assembling in solution

1Ni

CHCl$_3$ c=3.3*10^{-5}-3.3*10^{-3} mol/L

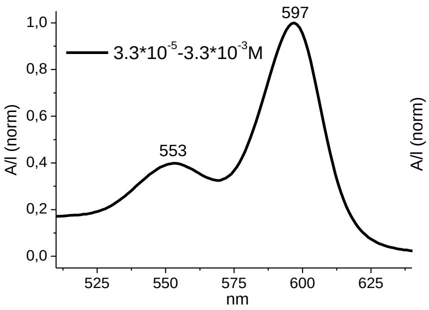

No changes in UV-vis spectra at different concentrations => no aggregation in solution

1Cd

CHCl$_3$ c=9.5*10^{-6}-1.1*10^{-3} mol/L

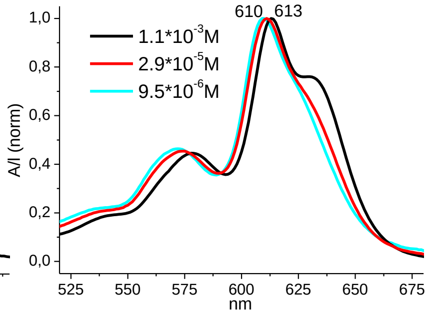

Changes in UV-vis spectra indicate aggregation in solution

^{1}H NMR **1Ni** (CDCl$_3$)

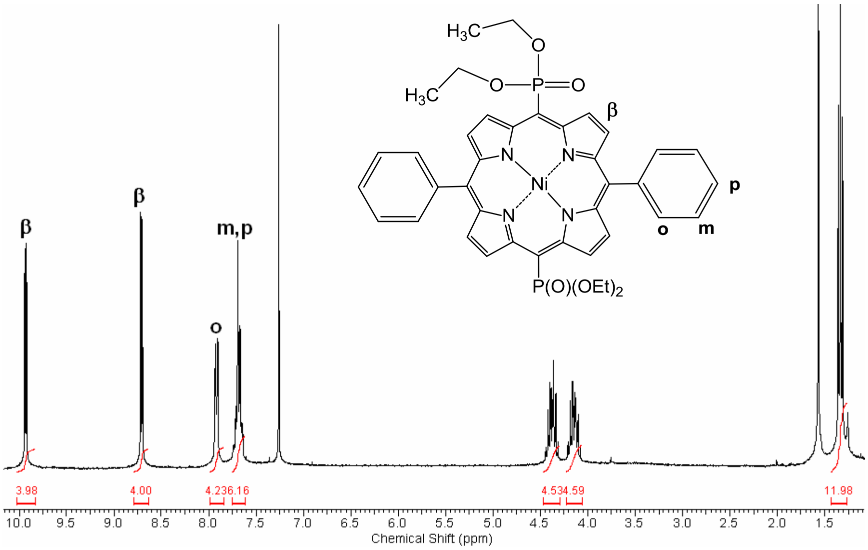

^{1}H NMR **1Cd** (CDCl$_3$)

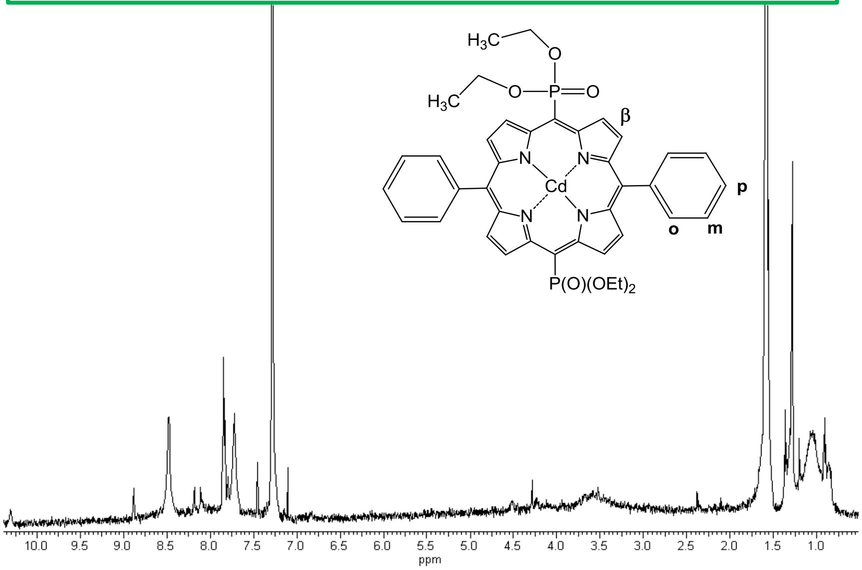

^{1}H NMR **1Cd** (CDCl$_3$:CD$_3$OD=5:1)

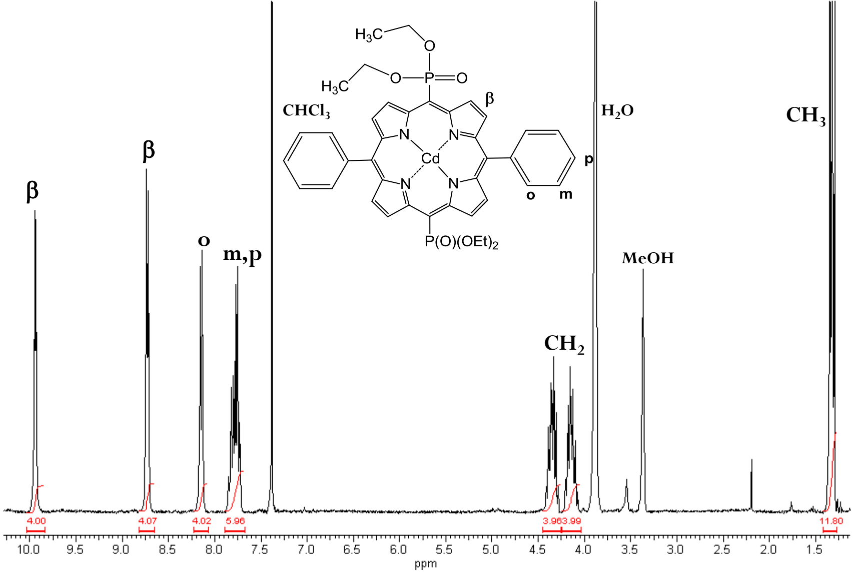

DOSY-NMR ($CDCl_3$)

DOSY → D → R

	C, mol/L	D, cm^2/sec	R, Å
1Ni	$1.04 \cdot 10^{-2}$	$7.3 \cdot 10^{-6}$	11.9
1Pd	$1.04 \cdot 10^{-2}$	$7.2 \cdot 10^{-6}$	12.0
1Cd	$1.04 \cdot 10^{-2}$	$5.5 \cdot 10^{-6}$	15.6

- The complex of UV-vis and NMR data can indicate the ability of porphyrins to self-assembling

XRD **1Cd**

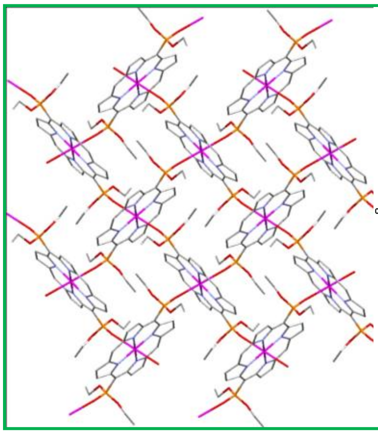

2D coordination polymer

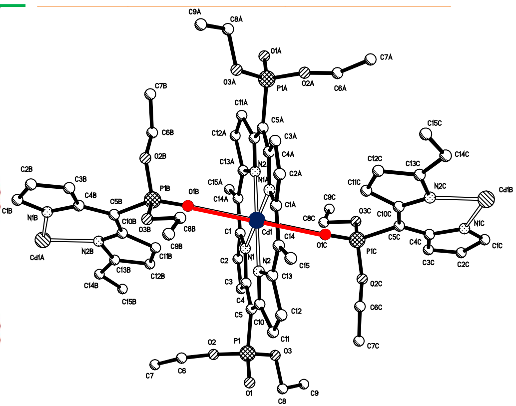

[1]Y.Y. Enakieva et al. *Org. Lett.* **2009**, 11, 3842.

XRD **1Cu**

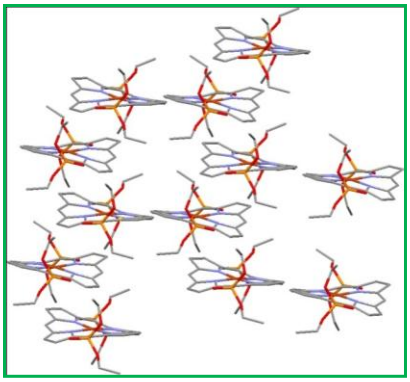

The packing of individual molecules

parameter	**1Cu**
	C2/c
a	19.565(6)
b	20.676(7)
c	9.063(3)
b	94.445(5)
V	3655(2)
N-M	1.993(3)-2.005(3)
∠CuN(1)N(2)/CuN(1A) N(2A)	8.2°
Displacement of N from N4 plane	+/-0.100Å
Displacement of C from N4 plane	+/-0.665Å

XRD **1Cu**

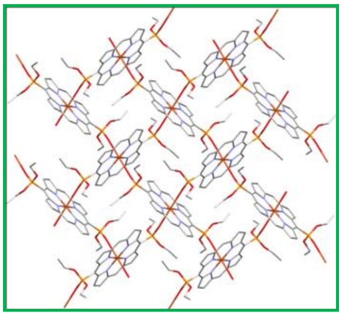

Para-meter	**1Cu**	**1Cd**	**1Zn**
	P 21/c	P 21/c	P 21/c
a	12.3787(6)	12.4567(16)	12.4759(5)
b	11.7319(5)	11.7829(15)	11.4931(4)
c	12.2028(6)	12.1147(16)	12.1459(4)
b	91.8580(10)	91.889(2)	91.4240(10)
V	1771.23(14)	1777.2(4)	1741.02(11)
N-M, Å	2.0146(16)-2.0220(15)	2.1402(16)-2.1517(15)	2.061(3)-2.062(3)
M…O, Å	2.649(3)	2.6253(14)	2.467(3)

2D coordination polymer

Electrochemistry of **1Cu**

(prof. K.Kadish)

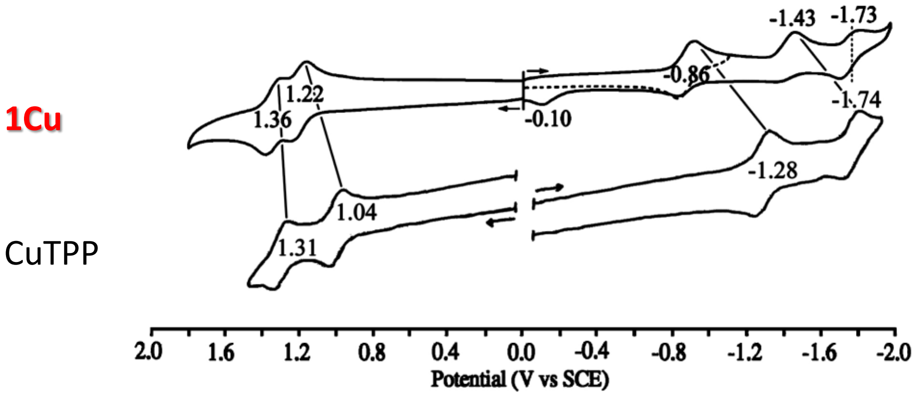

PhCN, 0.1 M TBAP
Three-electrode cell:
working glassy carbon electrode,
platinum counter electrode,
saturated calomel reference electrode

XRD **1Ni**

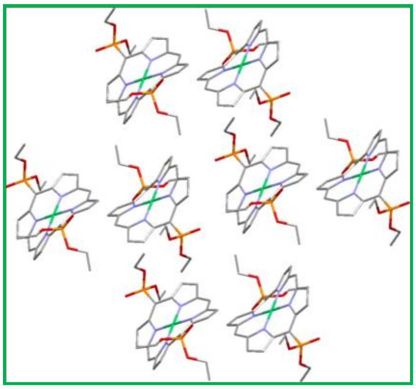

The packing of individual molecules

parameter	**1Ni**
	P -1
a	13.152(6)
b	13.183(7)
c	13.284(8)
a	91.407(7)
b	110.863(6)
g	107.160(6)
V	2034.7(18)
N-M	1.888(8) -1.913(7)
∠NiN1N2/NiN3N4	1.9°
Displacement of Ni from N4 plane	+/-0.022Å
Displacement of C from N4 plane	-0.288 ÷ +0.499Å

XRD **1Pd** and **2Pd**

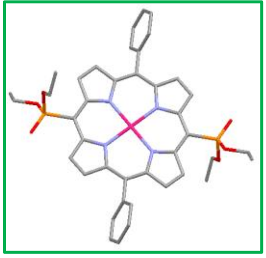

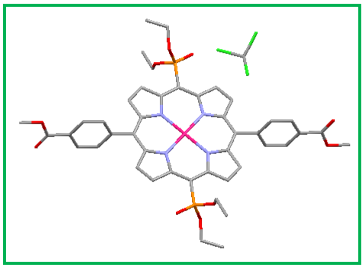

The packing of individual molecules

Parameter	**1Pd**	**2Pd**
	C2/c	P -1
a	16.128(4)	10.7994(17)
b	18.158(5)	10.9564(17)
c	13.503(3)	11.7583(18)
a	90	75.860(3)
b	113.570(3)	85.800(3)
g	90	70.708(2)
V	3624.3(16)	1273.3(3)
N-M	2.019(2)	2.019(5) - 2.025(4)

XRD **1Pt**

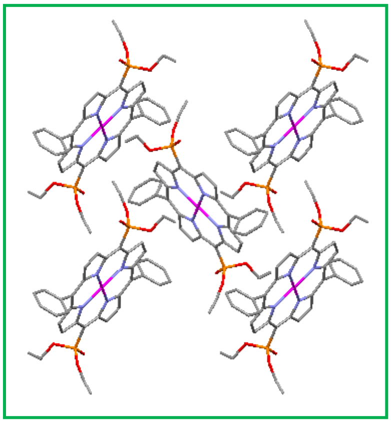

The packing of individual molecules

Parameter	**1Pt**
	P 21/c
a	12.0856(13)
b	13.6274(15)
c	11.4059(13)
b	91.489(2)
V	1877.9(4)
N-M	2.017(2)-2.018(2)

Conclusion

- *d*-metal complexes with *meso*-diphosphorylporphyrins were obtained with high yields (77-99%)

- Self-assembling in solution was detected for Cd complexes

- The single crystals of 6 compound were obtained. The self-assembling in solid state is typical for Cd and Cu complex. Ni, Pd and Pt complexes with *meso*-diphosphorylporphyrins do not form supramolecular assembly.

Acknowledgments

- Russian-French laboratory LAMREM
  - A. Lemeune, Prof. R. Guilard
- Collaboration in synthesis and MALDI-Tof MS– Enakieva Yu.
- NMR – Birin K.
- XRD – Nefedov S.
- Financial support – Russian Foundation for Basic Research, ARCUS

Calix[4]arene-Based Tetrapodal Ligand Incorporating Cyclic Hydroxamic Acids as Chelating Units

Pawel JEWULA

Institut de Chimie Moléculaire de
l'Université de Bourgogne (ICMUB)
UMR CNRS 6302
9 avenue Alain Savary 21078 DIJON
FRANCE

Summer School 21 – 23 July 2012 Moscow

Objective

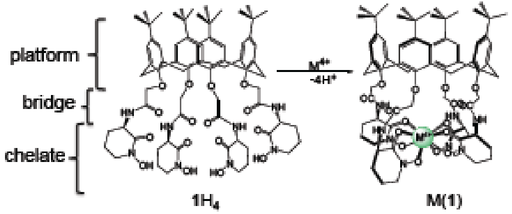

M = Zr, Hf, U

Synthesis of $1H_4$

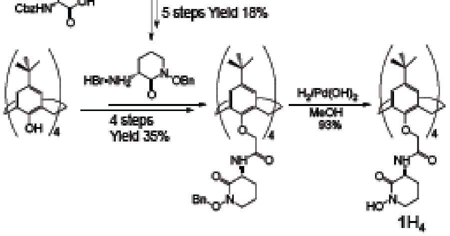

Complexes
$[Zr_2 1_2 K]^+$
$[Hf_2 1_2 K]^+$

Confirmed by

- MALDI – TOF
- ESI Analysis
- 1D and 2D NMR
- DOSY-NMR

Simple models

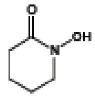
2H

2 steps
Y = 18%
pKa = 8.86

Complexes:
Zr(**2**)$_4$ Y = 57%
Hf(**2**)$_4$ Y = 38%
U(**2**)$_4$ Y = 90%
Fe(**2**)$_3$ Y = 41%
Ga(**2**)$_3$ Y = 54%

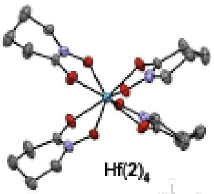
Hf(2)$_4$

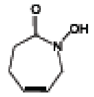
3H

4 steps
Y = 12%
pKa = 9.08

Complex:
Zr(3)$_4$ Y = 59%

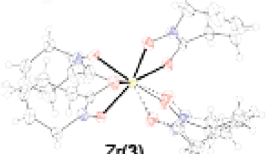
Zr(3)$_4$

Acknownledgements

- Dr. Michel MEYER: Supervisor
- Dr. Jean-Claude CHAMBRON: Supervisor (Synthesis)
- Dr. Jean-Claude Berthet: Uranium Chemistry
- Dr. Pierre Thuéry: Uranium X-Ray Crystallography
- Dr. Yoann Rousselin: X-ray Crystallography
- Marie-José Penouilh: NMR Spectroscopy and Mass Spectrometry

COMPREHENSION OF SYNERGISTIC MECHANISMS FOR URANIUM EXTRACTION FROM PHOSPHORIC MEDIA

7th European Summer School on Supramolecular, Intermolecular,
Interaggregate, Interactions and Separation Chemistry
ICPE RAS – Moscow, Russia

O.Pecheur[a], D.Guillaumont[a], S.Dourdain[b], F.Testard[c], H.Mokhtari[d]

[a]CEA, DEN/DRCP/SCPS/LILA, 30207 Bagnols-sur-Cèze, France.
[b]UMR 5257, ICSM, CEA/CNRS/universités, 30207 Bagnols-sur-Cèze, France.
[c]CEA, DSM/IRAMIS/SCM/LIONS, 91191 Gif-sur-Yvette, France.
[d]AREVA Mines-SEPA, 87250 Bessines sur Gartempe, France.

Summer School 2012 | Olivia Pecheur

JULY 20TH-23RD 2012

COMPREHENSION OF SYNERGISTIC MECHANISMS FOR URANIUM EXTRACTION FROM PHOSPHORIC MEDIA

Context: Recovering uranium from phosphoric ores

Process: designed in the 80's, two molecules (HDEHP/TOPO) extracting uranium in synergism, reference system, based on liquid-liquid extraction

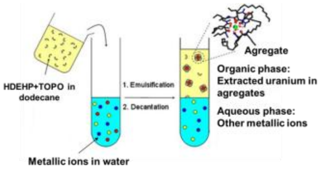

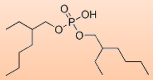

HDEHP
Bis(2-ethylhexyl) phosphoric acid

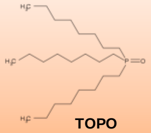

TOPO
Tri-n-octylphosphine oxide

$$D_U = \frac{[U_{org}]}{[U_{aq}]}$$

Synergism : $D_{U\text{-HEDHP/TOPO}} >> D_{U\text{-HEDHP}} + D_{U\text{-TOPO}}$

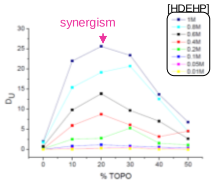

Objectives: Get a better comprehension of the mechanisms of synergism

MOLECULAR SCALE

SUPRAMOLECULAR SCALE

Possible improvements:
- Increase D_U for a one-step extraction cycle
- Avoid the extraction of iron as a by-product

COMPREHENSION OF SYNERGISTIC MECHANISMS FOR URANIUM EXTRACTION FROM PHOSPHORIC MEDIA

MOLECULAR SCALE

During liquid-liquid extraction process, extractant molecules form several complexes with uranium, water, acid and other ions inside. The aim of the molecular approach is to study the structure of such complexes.

Objective: What is the influence of synergism on the complexation ?

EXPERIMENTAL APPROACH

Methods used to probe the complexes stoichiometry:

- Raman/Infra-Red spectroscopy; fonctional groups responsible for the extraction. Study of the changes in the chemical bondings when the extractants are put together with ions.
- NMR (Nuclear Magnetic Resonance); interactions between the particles (by studying the auto-diffusion coefficients of ^{31}P)
- ESI-MS (Electro-Spray Ionisation Mass Spectroscopy); stoichiometry of species
- EXAFS (Extended X-ray Absorption Fine Structure); local structure and neighbour atoms around one peculiar element

Theoretical chemistry is complementary to the experiments:

- by molecular dynamics, investigation on the molecular organisation, optimization of molecular structures
- then molecular structures are used to interpret experimental data such as IR-Spectra

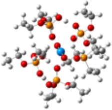

Uranyl surrounded by 2 (HDEHP-DEHP) and 1 TOPO (optimized structure):

SUPRAMOLECULAR SCALE

The complexes formed by HDEHP, TOPO and the cations are considered as small aggregates with peculiar properties :

- CAC (Critical Aggregation Concentration): Concentration of extractants above which aggregates form.
- N_{ag} (Aggregation number): Number of molecules in one aggregate
- d (diameter of the chore) and D (diameter of the aggregate)

Objective: What is the influence of synergism on these properties ?

EXPERIMENTAL APPROACH

Several methods are used to investigate these properties:

- SAXS: Small-Angle X-ray Scattering; study of the polar core of the aggregates
- SANS : Small-Angle Neutron Scattering; study of the non-polar shell of the aggregates

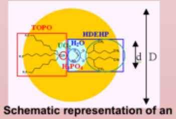

Schematic representation of an aggregate

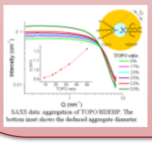

SAXS data: aggregation of TOPO/HDEHP. The bottom inset shows the deduced aggregate diameter.

SANS experiments performed at the Laboratoire Léon Brillouin (CEA Saclay)

A.N.Frumkin Institute of Physical Chemistry and Electrochemistry

Surface forces as the basis for the analysis of interparticle and interaggregate interactions

Ludmila Boinovich

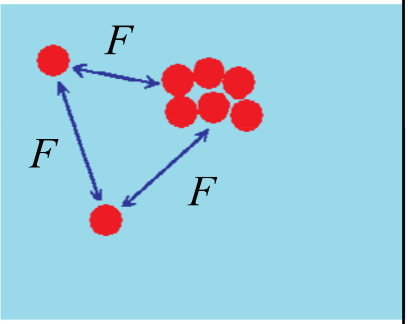

Disjoining pressure in thin liquid films

(B.V.Derjaguin, Acta Physico-Chim.URSS, 1939, v.10, №1, p. 25-44)

$$\Pi(h) = P_N - P_0$$

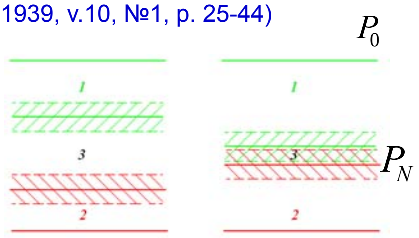

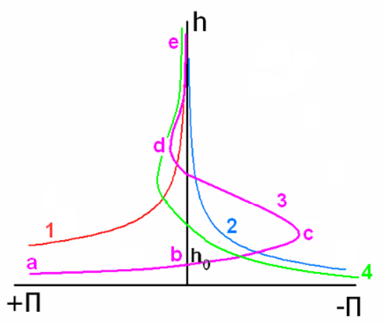

The dependence of the disjoining pressure on the thickness of the liquid film is the key thermodynamic characteristic of thin interlayer that differentiates it with the bulk liquid.

$$\Pi(h) = \Pi_{vdw} + \Pi_{ion-electr} + \Pi_{steric} + \Pi_{phonon} + \ldots$$

Derjaguin's approximation

(B.V.Derjaguin, **Kolloidn.Z**, 1934, v.69, p. 155)

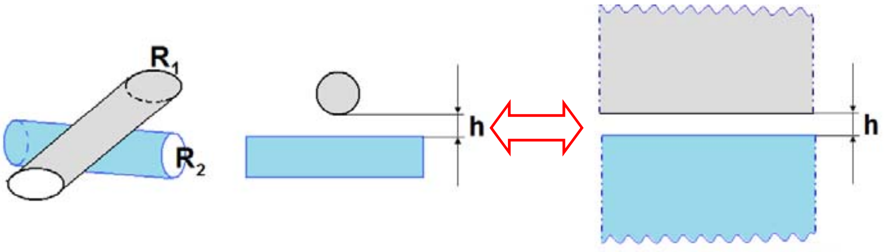

$$U(h) = \frac{2\pi}{\sqrt{\varepsilon\varepsilon'}} \int_h^\infty f(H)dH$$

$$f(H) = \int_H^\infty \Pi(h')dh'$$

For R_1, R_2 >> range of action of surface forces

Π_{vdw}, $\Pi_{ion-electr}$, Π_{steric}, Π_{phonon}

The interaction between similar cubic nanoparticles

(microscopic approaches)

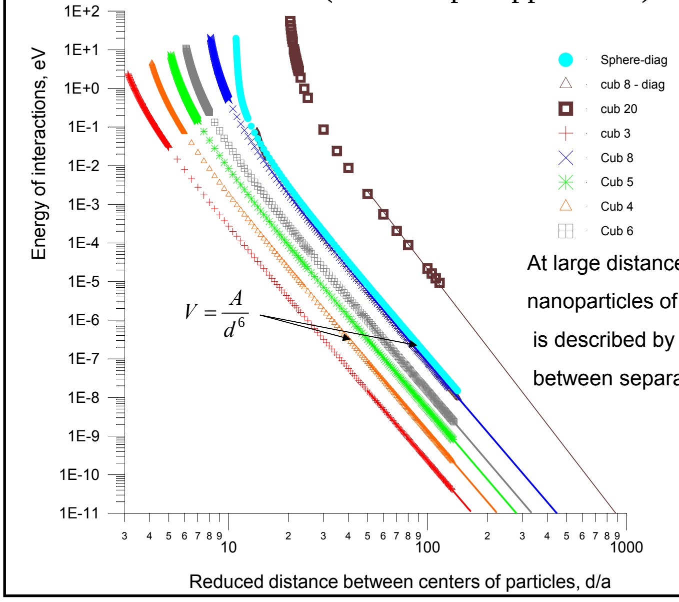

At large distances the interaction between nanoparticles of various shapes and sizes is described by the same law as between separate atoms.

Van der Waals interactions in nanosystems

Character of the dependence of the energy of the van der Waals interaction on separation, *h*, for various systems in non-retarded and retarded limits

system	non-retarded limit	retarded limit
crossed nanowires	**$1/h^4$**	**$1/h^5$**
parallel nanowires (per unit length)	**$1/h^5$**	**$1/h^6$**
nanoparticle / half-space	**$1/h^3$**	**$1/h^4$**
nanoparticle / nanoparticle	**$1/h^6$**	**$1/h^7$**
foil / foil (per unit area)	**$1/h^{5/2}$**	**$1/h^{7/2}$**
parallel macrocylinders (per unit length), for $h<<R$, where R is cylinders radius	**$1/h^{3/2}$**	**$1/h^{5/2}$**
large (compared to separation *h*) spherical particle / large spherical particle	**$1/h$**	**$1/h^2$**
large spherical particle / half-space	**$1/h$**	**$1/h^2$**
half-space / half-space	**$1/h^2$**	**$1/h^3$**

L.B. Boinovich, A.M.Emelyanenko, Langmuir (2009)

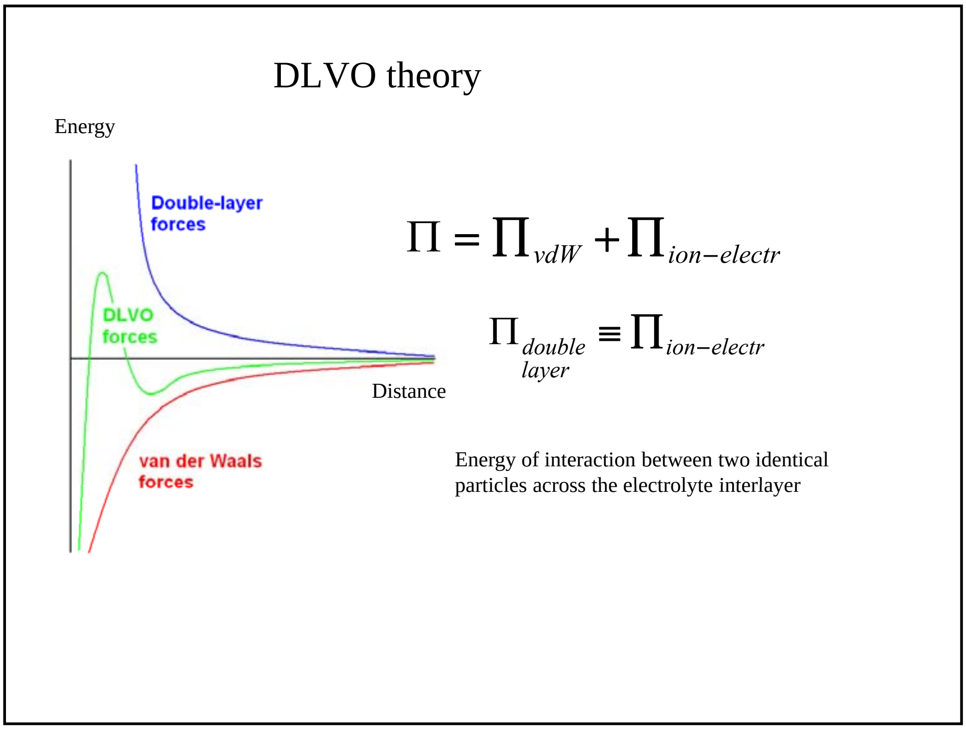

DLVO theory

$$\Pi = \Pi_{vdW} + \Pi_{ion-electr}$$

$$\Pi_{\substack{double\\layer}} \equiv \Pi_{ion-electr}$$

Energy of interaction between two identical particles across the electrolyte interlayer

van der Waals forces in electrolyte interlayers

1. Screening of zero frequency contribution of forces

$$G_{\xi=0}(h)=\frac{k_BT}{4\pi}\int_0^\infty k\ln\left[1-\left(\frac{\varepsilon_1-\varepsilon_3}{\varepsilon_1+\varepsilon_3}\right)\left(\frac{\varepsilon_2-\varepsilon_3}{\varepsilon_2+\varepsilon_3}\right)\exp(-2hk)\right]dk \qquad \varepsilon_i=\varepsilon_i(\xi=0)$$

$$G_{\xi=0}(h)=\frac{k_BT}{4\pi}\int_0^\infty k\ln\left[1-\left(\frac{\varepsilon_1 k-\varepsilon_3\sqrt{k^2+\kappa^2}}{\varepsilon_1 k+\varepsilon_3\sqrt{k^2+\kappa^2}}\right)\left(\frac{\varepsilon_2 k-\varepsilon_3\sqrt{k^2+\kappa^2}}{\varepsilon_2 k+\varepsilon_3\sqrt{k^2+\kappa^2}}\right)\exp(-2h\sqrt{k^2+\kappa^2})\right]dk$$

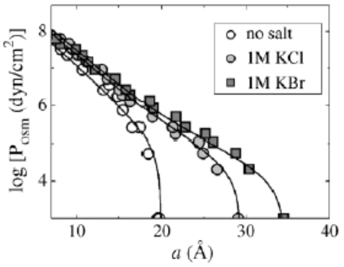

Osmotic pressure of multilamellar DLPC samples versus the water spacing (a) that was determined for that sample as the D-spacing minus the steric bilayer thickness

Horia I. Petrache et al. J. Lipid Research 2006, 47, 302

van der Waals forces in electrolyte interlayers

Effects of ions on the behavior of dielectric permittivity

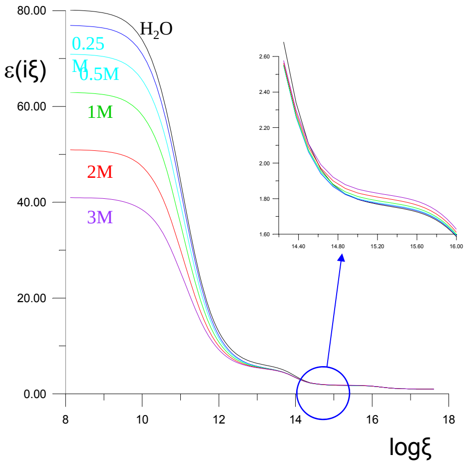

Dielectric permittivities of aqueous NaCl solutions

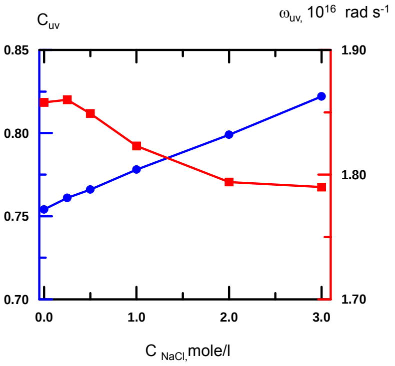

The parameters of effective ultraviolet oscillators in NaCl aqueous solutions. C_{uv} (circles) is the constant associated with the strength of oscillator in ultraviolet (UV) region, ω_{uv} (squares) is the characteristic relaxation frequency in UV region.

Boinovich LB, Emelyanenko AM. Adv Colloid Interface Sci 2009;147–148:44.

Distribution of potential in the vicinity of interface

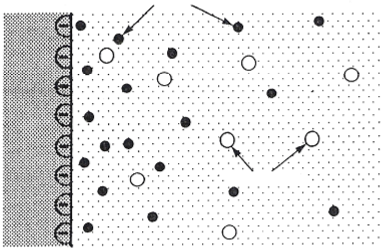

$$\mathrm{div}(\varepsilon\,\mathrm{grad}\,\psi) = -4\pi\rho$$

$$\rho = \sum_i e z_i \tilde{n}_i \qquad \tilde{n}_i = n_i \exp(-z_i e\psi / kT)$$

Poisson-Boltzmann equation:

$$\boxed{\Delta\psi = -\frac{4\pi}{\varepsilon}\sum_i z_i e n_i \exp\left(-\frac{z_i e\psi}{kT}\right)}$$

$$\boxed{\Delta\psi = -\frac{4\pi}{\varepsilon}\sum_i z_i e n_i \exp\left(-\frac{z_i e\psi + U_{vdW} + U_{ion-ion} + U_{ion-solv} + U_{specific} + U_{image}}{kT}\right)}$$

Ion-electrostatic interactions beyond conventional consideration

$$\boxed{\Delta\psi = -\frac{4\pi}{\varepsilon}\sum_i z_i e n_i \exp\left(-\frac{z_i e\psi + U_{vdW} + U_{ion-ion} + U_{ion-solv} + U_{specific} + U_{image}}{kT}\right)}$$

1. charge inversion
2. presence of DEL near uncharged interfaces
3. attraction of likely charged surfaces
4. ion specific effects
5. image charge forces

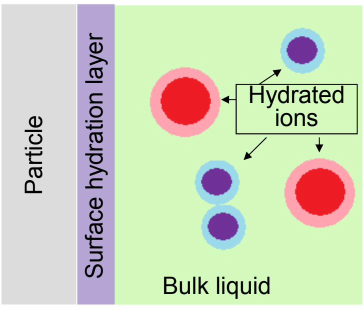

Boinovich L.B., COCIS 2010

Discrete charges
and their influence on surface forces

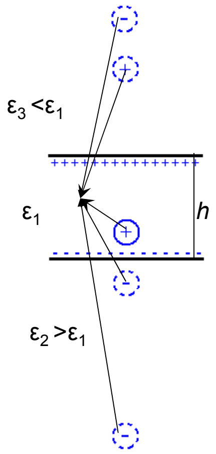

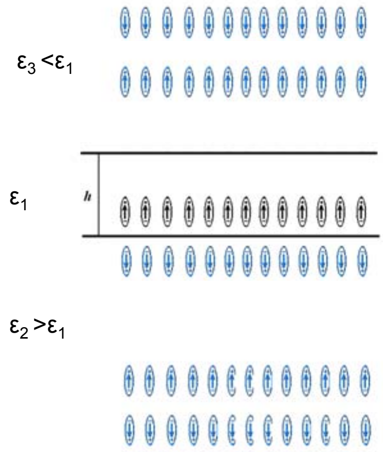

Boinovich LB, Emelyanenko AM. Adv Colloid Interface Sci 2003, 104,93

Discreteness of surface charge. Image forces

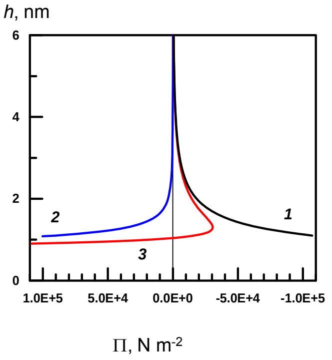

Contribution of van der Waals (1) and image charge (2) components to the isotherm of total disjoining pressure Π (3) of heptane wetting films on the surface of 3M NaCl aqueous solution.

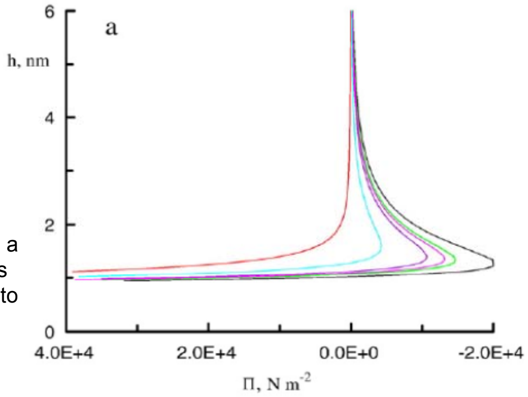

$\Pi(h)$ in pentane wetting films atop a surface of *NaCl* aqueous solutions with various concentrations (right to left:

0, 0.25, 0.5, 1, 2, 3 M)

Boinovich L, Emelyanenko A. J Phys Chem B,2007,111,10217

Interaction forces, caused by modified structure of liquid interlayer

Forces due to static and dynamic structure of liquid in the film

Boinovich LB, Emelyanenko AM Z.Phys.Chem. 1992, 178, 229

Forces, associated with the presence of long-chain surfactants and high molecular mass polymers inside the liquid film

For review of experiments see:
Kleshchanok D, Tuinier R, Lang PR. J Phys Condens Matter 2008, 20,073101.

Forces due to nonhomogeneous distribution of solution components across the film

Derjaguin B.V., Churaev N.V. J. Coll.Interf.Sci., 1977, 62,369

Boinovich LB, Adv.Coll.Int.Sci.1992. 37, 177

Surface induced dynamic structuring

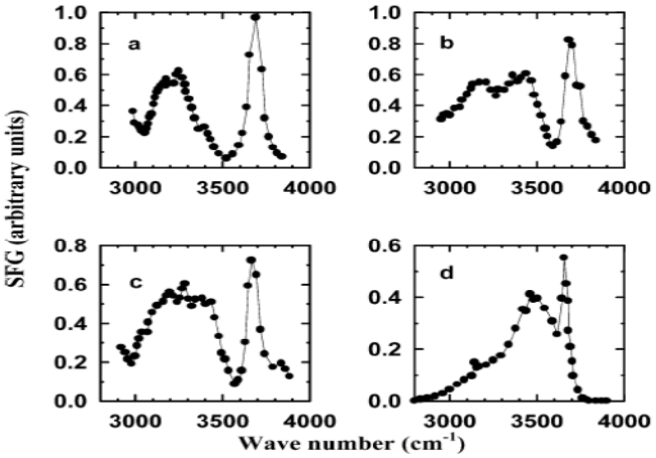

Sum-frequency-generation (SFG) spectra from (**a**) the quartz–octadecyl-trichlorosilane–water interface, (**b**) the air–water interface, **(c**) the hexane–water interface and (**d**) the carbon tetrachloride– water interface
Quan Du, Freysz E, Shen YR Science, 1994, 264:826,
Scatena LF, Brown MG, Richmond GL, Science, 2001 292:908

Surface induced dynamic structuring

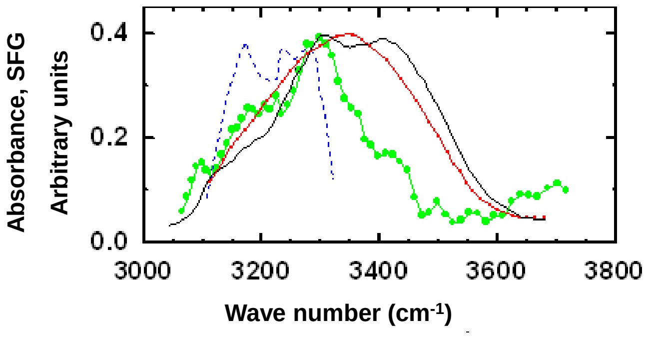

IR spectra for ethanol in the OH stretch region. The red and blue curves are the bulk liquid and the bulk crystalline phases, respectively; the solid curve corresponds to the 25-nm film of liquid ethanol, confined by fluorite plates. The green curve represents SFG spectrum for the liquid surface.

Boinovich LB, Gagina IA,Emelyanenko AM Colloid J, 1995, 57:851

Phonon component of disjoining pressure

The dynamic structure difference between bulk liquid and the liquid in the film are related to the facts that:
localization of collective motions,
mutual orientations of molecules and relative to interface,
intermolecular distances in thin layer
are changed due to the interaction between molecules and surfaces.
In addition, the confining surfaces induce changes in the conformational states of molecules.
All these factors affect the normal-mode spectrum and give rise to an additional contribution to the film energy, which depends on the film thickness *H*

$$F^E = \sum_j \int_0^\infty kT \ln \frac{\mathrm{sh}(\hbar\omega/kT)}{\mathrm{sh}(\hbar\omega_{j0}/kT)} Z_j(\omega)\exp\left(-H/L_j(\omega)\right)\mathrm{d}\omega$$

Boinovich LB, Emelyanenko AM. Adv Colloid Interface Sci 2002,96:37

Phonon component of disjoining pressure in thin liquid films

$$\Pi(h)=\sum_j\int_0^\infty\left[-\frac{dK_j}{dh}-\frac{K_jh}{L_j^2(\omega)}\frac{dL_j(\omega)}{dh}+\frac{K_j}{L_j(\omega)}\right]\exp(-h/L_j(\omega))d\omega$$

$$K_j=Z_j(\omega)k_BT\cdot\ln\frac{\mathrm{sh}(\hbar\omega\ /2k_BT)}{\mathrm{sh}(\hbar\omega_{j0}/2k_BT)}$$

$$\Pi_1(h)=\sum_j\frac{\overline{K}_j}{\overline{L}_j}\exp(-h/\overline{L}_j)\quad(thick\ films)$$

$$\Pi_2(h)=\sum_j-\frac{d\overline{K}_j}{dh}\exp(-h/\overline{L}_j)\quad(thin\ films)$$

$$\Pi_3(h)=\sum_j-\frac{\overline{K}_jh}{\overline{L}_j^2(\omega)}\frac{d\overline{L}_j}{dh}\exp(-h/\overline{L}_j)$$

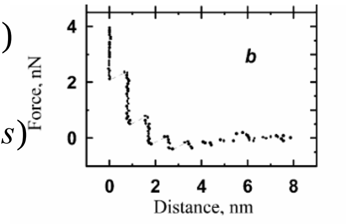

Boinovich LB, Emelyanenko AM. Adv Colloid Interface Sci 2002,96:37

Repulsive and attractive exponential forces

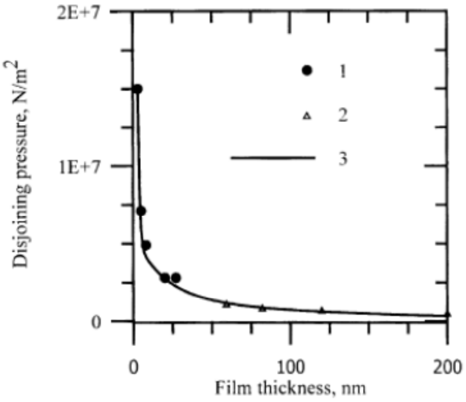

$$\Pi(H)=2\cdot10^7e^{\frac{-H}{1.0}}+4\cdot10^5e^{\frac{-H}{20}}+1.5\cdot10^5e^{\frac{-H}{130}}$$

Three-exponential fit for experimental data of
R.M. Pashley, J.A. Kitchener, J. Colloid Interf. Sci. 1979, 71, 491
L.R. Fisher, R.A. Gamble, J. Middlehurst, Nature 1981, 290, 575.
for the disjoining pressure of water wetting films on quartz

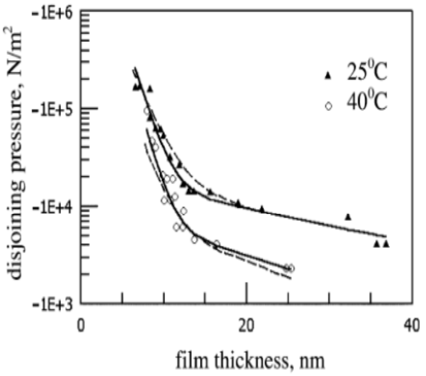

Interaction between mica surfaces covered by dihexadecyldimethilammonium acetate in water.
Y. Tsao, S.X.et al, Langmuir, 1991, 7, 3154.
Solid lines: fits obtained as a result of minimization of root-mean-square difference between the experimental points and biexponential curves:

for 25C $\Pi(H)=-2\cdot10^7e^{\frac{-H}{1.5}}-2.4\cdot10^4e^{\frac{-H}{23}}$

for 40C $\Pi(H)=-2.2\cdot10^7e^{\frac{-H}{1.3}}-10^4e^{\frac{-H}{17}}$

Surface forces in complex fluids

$$\Pi(h) = \Pi_{vdw} + \Pi_{ion-electr} + \Pi_{steric} + \Pi_{phonon} + \ldots$$

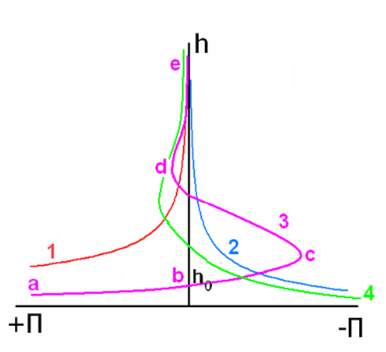

Thank you

for the

attention!

Oscillating behaviour of the force–distance curve

$$\Pi_2(h) = \sum_j -\frac{d\overline{K}_j}{dh}\exp(-h/\overline{L}_j)$$

Boinovich LB. Prog Colloid Polym.Sci 2004;128:44–51.

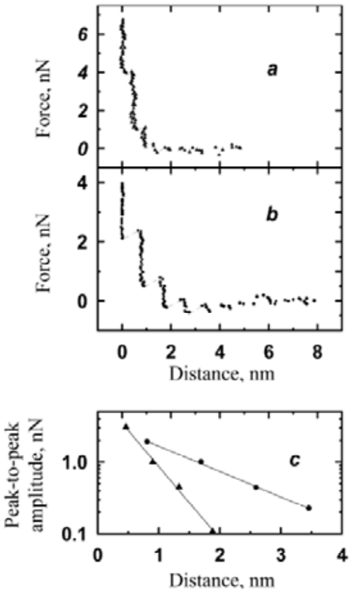

The force–distance curves for
a) highly oriented pyrolytic graphite and
b) mica substrates immersed in n-dodecanol and
c) peak-to-peak amplitudes versus distance on a log scale. The exponential decay length is 1.23 nm for mica (circles) and 0.43 nm for HOPG (triangles)

Nakada T, et al, Jpn J Appl Phys 1996 35:52

Trilateral Seminar on supramolecular, intermolecular, interaggregate interactions and separation chemistry

Control in selective ion separation in molecular systems *via* supramolecular and colloidal interactions

S. Pellet-Rostaing

Moscow, 20 – 23 July 2012

Optimize the Separation Processes for decontamination and recycling

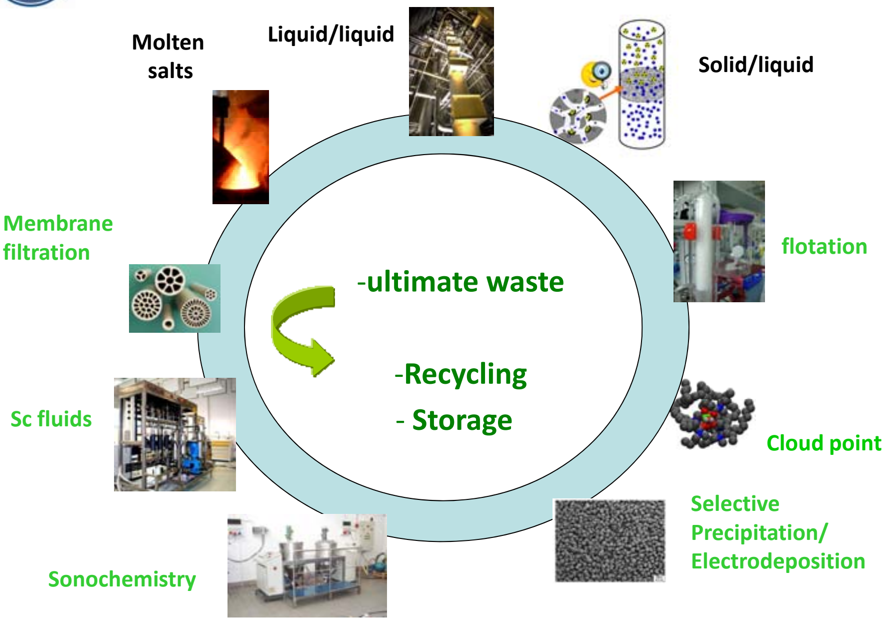

Molten salts

Liquid/liquid

Solid/liquid

Membrane filtration

flotation

-ultimate waste

-Recycling

- Storage

Sc fluids

Cloud point

Selective Precipitation/ Electrodeposition

Sonochemistry

Alfred Werner – late 1800's the father of coordination chemistry

- **Studied in Switzerland at the University of Zurich**
- **He lectured in both organic and inorganic chemistry**
- **He developed the theory of coordination chemistry**
- **He prepared and studied coordination compounds and discovered optically active forms of 6-coordinate octahedral complexes**
- **His coordination chemistry extended through a whole range of systematic inorganic chemistry and into organic chemistry and he was awarded the** Nobel Prize in Chemistry in 1913

1949: first successful solvent extraction for recovery of both uranium and plutonium (PUREX process) at Oak Ridge National Laboratory

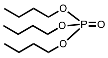

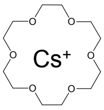

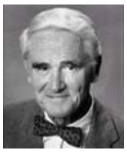

D. J. Cram

J.-L. Lehn

C.J. Pedersen

Nobel prize awarded in 1987

Macrocyclic chemistry

Current simplified fuel cycle in France

Liquid/liquid extraction

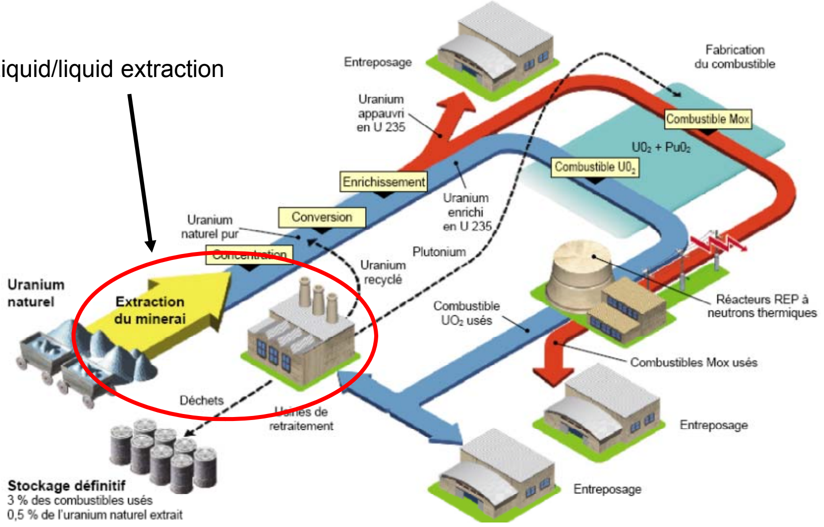

Nuclear waste reprocessing

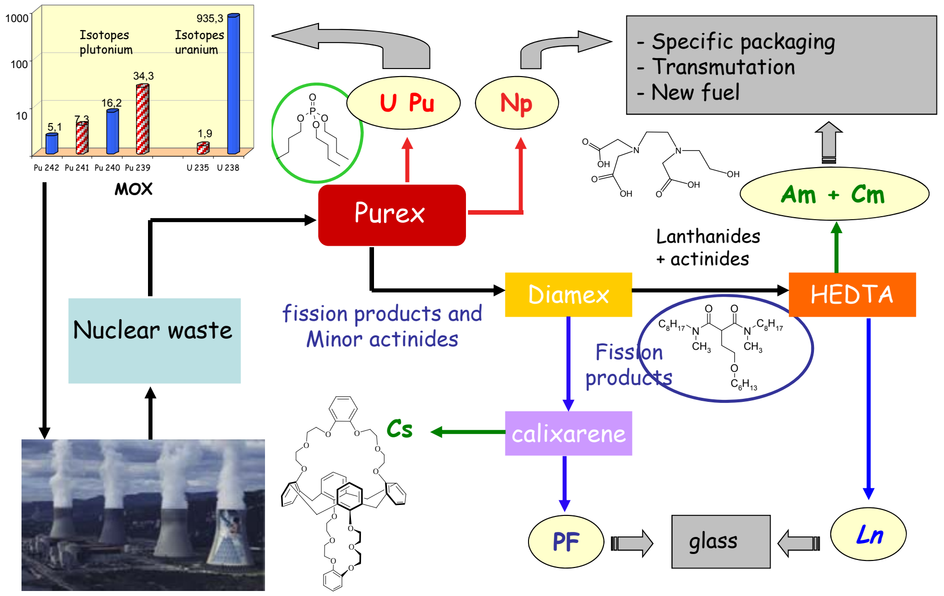

U Pu

Np

- Specific packaging
- Transmutation
- New fuel

Am + Cm

Purex

Lanthanides
+ actinides

Diamex

HEDTA

Nuclear waste

fission products and
Minor actinides

Fission
products

Cs

calixarene

PF

glass

Ln

Aggregation in solvent extraction

1987 : Musikas recognized the importance of aggregation in solvent extraction systems and assumed that the mechanism of extraction of f-block elements with aliphatic malonamide involves « both inner-sphere and outer-sphere extractant-metal complex interactions ».

Musikas, C.; Hubert, H. « N,N’-tetraalkylmalonamides. II. Extraction of metallic ions. » *Solvent Extr. Ion Exch.* **1987**, 5, 877-93

1991: Osseo-Asare introduced the micellar model to solvent extraction systems.

Extractant-acid/metal ion complexes self-assemble into higher-order architectures where the extractants and solutes are aggregated in the form of reverse micelles.

Osseo-Asare, K. « Aggregation, reverse micelles, and micro-emulsion in liquid-liquid extraction: the tri-n-butyl phosphate-diluent-water-electrolyte system. » *Adv. Colloïd Interface Sci.* **1991**, 37, 123-73.

Then Erlinger, Chiarizia, Antonio, …

In liquid/liquid separation the question is

What drives ion selectively from a concentrated solution into an organic solvent?

- **binding sites (hard/soft, solvating, ion exchange)**
- **Ligand/metal interactions (electrostatic…)**
- **Volume/steric hindrance**
- **Structure of the complex**

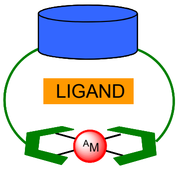

But also : hydrophobic/hydrophylic (amphiphilic)

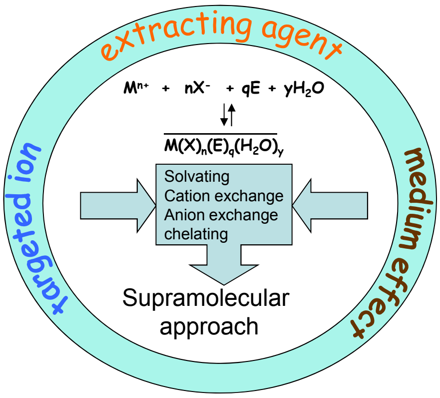

extracting agent

targeted ion

medium effect

M^{n+} + nX^- + qE + yH_2O ⇄ $M(X)_n(E)_q(H_2O)_y$

Solvating
Cation exchange
Anion exchange
chelating

Supramolecular approach

- **Valency**
- **Oxidation state**
- **Size**
- **Hydration number**
- **Hard/Soft**
- **Counter ion**

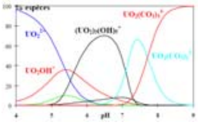

- **pH (neutral/acidic/basic)**
- **nature of the acid**
- **Ionic strenght**
- **Solvent/co-solvent**
- **Temperature**

Molecular scale approach of Solvent extraction

Design and synthesis of the ligand

From the knowledge of the binding sites

Chelating sites for Uranyl

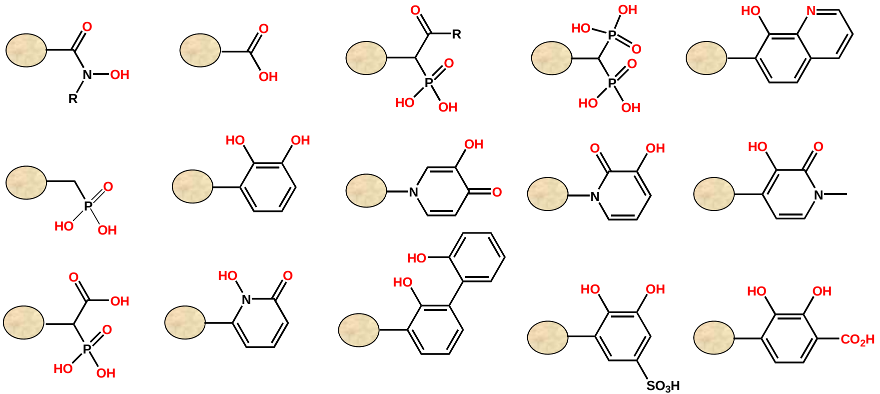

A. E. V. Gorden, J. Xu, K. N. Raymond, and P. Durbin, *Chemical Reviews* **103**, (11), 4207-4282 (2003)

M. Sawicki, J.-M. Siaugue, C. Jacopin, C. Moulin, T. Bailly, R. Burgada, S. Meunier, P. Baret, J.-L. Pierre, and F. Taran, *Chemistry--A European Journal* **11**, (12), 3689-3697 (2005)

A. Leydier, Y. Lina, G. Arrachart, R. Turgis, D. Lecerclé, A. Favre-Reguillon, F. Taran, M. Lemaire, S. Pellet-Rostaing Tetrahedron **2012**, 68, 1163-1170.

then

Molecular scale approach of Solvent extraction

Synthesis and screening

Déplacement du complexe SCP/UO$_2$ (%)

○ 0-20% ▨ 20-40% ◔ 40-60% ◑ 60-80% ● 80-100%

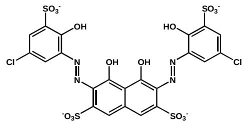

SCP

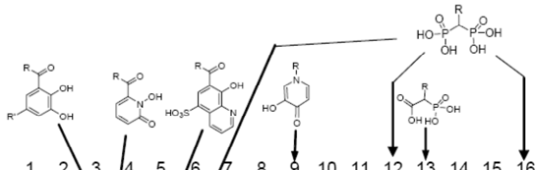

300 molecules

pH=5.5

	1	2	3	4	5	6	7	8	9	10	11	12	13	14	15	16	17
A	○	○	◔	○	○	○	○	○	○	○	○	●	○	○	○	●	○
B	○	○	▨	○	○	◔	○	○	○	○	○	●	▨	○	○	●	○
C	○	●	○	○	○	◑	○	○	▨	○	○	●	▨	○	○	●	○
D	○	○	◑	▨	○	●	○	○	▨	○	○	●	◔	○	○	●	○
E	○	○	◑	◔	◑	●	○	○	◔	○	○	◑	▨	○	○	●	○
F	○	○	○	▨	○	●	○	○	▨	○	○	●	▨	○	○	●	○
G	○	○	○	○	○	◑	○	○	○	○	○	●	◔	○	▨	●	○

○ $\log K_{cond} < 10.65$

▨ $10.65 < \log K_{cond} < 11.50$

◔ $11.50 < \log K_{cond} < 12.20$

◑ $12.20 < \log K_{cond} < 13.05$

● $\log K_{cond} > 13.05$

M. Sawicki, D. Lecerclé, G. Grillon, B. Le Gall, A.-L. Sérandour, J.-L. Poncy, T. Bailly, R. Burgada, M. Lecouvey, V. Challeix, A. Leydier, S. Pellet-Rostaing, E. Ansoborlo, F. Taran *European Journal of Medicinal Chemistry* **2008**, 43, 2768-2777.

A. Leydier, D. Lecerclé, S. Pellet-Rostaing, A. Favre-Reguillon, F. Taran, Marc Lemaire tetrahedron 2008, 64, 11319-11324.

Molecular scale approach of Solvent extraction

Design and synthesis of the ligand

Or Combinatorial Chemistry

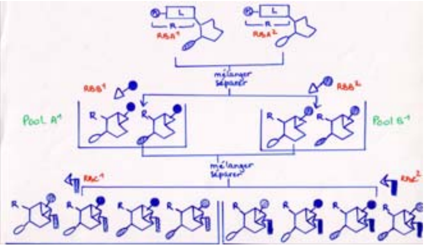

Scheme 1. Modular Synthesis of Multidentate Ligands

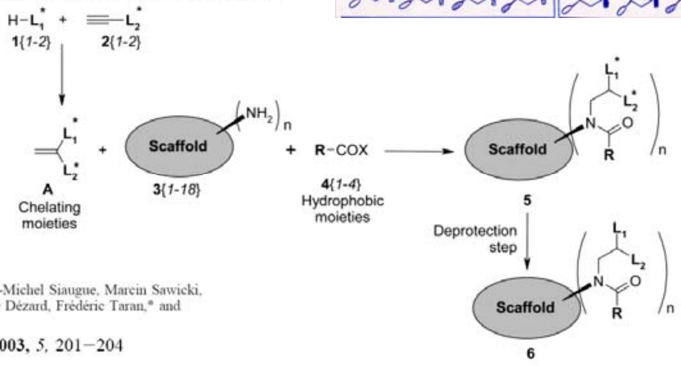

Stéphane Meunier, Jean-Michel Siaugue, Marcin Sawicki, Fabrice Calbour, Sophie Dézard, Frédéric Taran,* and Charles Mioskowski†

J. Comb. Chem. **2003**, *5*, 201–204

L* and L are respectively protected and unprotected chelating functions. Library size (2 × 2 × 18 × 4 = 288).

Molecular scale approach of Solvent extraction

Or Combinatorial Chemistry

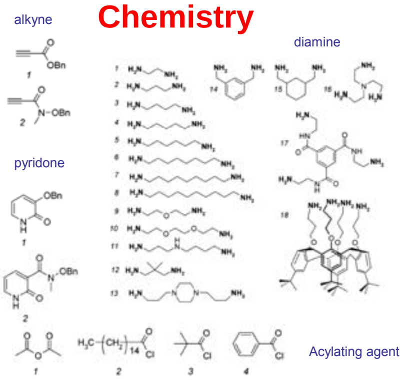

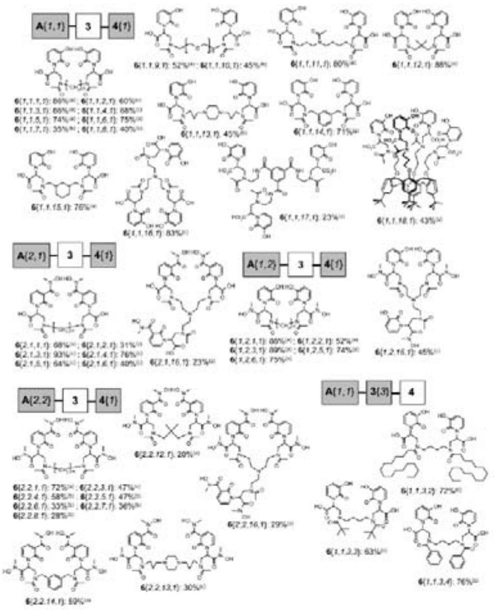

Modular synthesis of **288 new multidentate** metal ligands, incorporating four sources of diversity.

Modulation of:
- Architecture
- Denticity
- Nature of the chelating functions
- lipophilicity

Molecular scale of Solvent extraction

Quantitative Structure-Property Relationships (QSPR)

Y = f (structure) = f (descriptors)

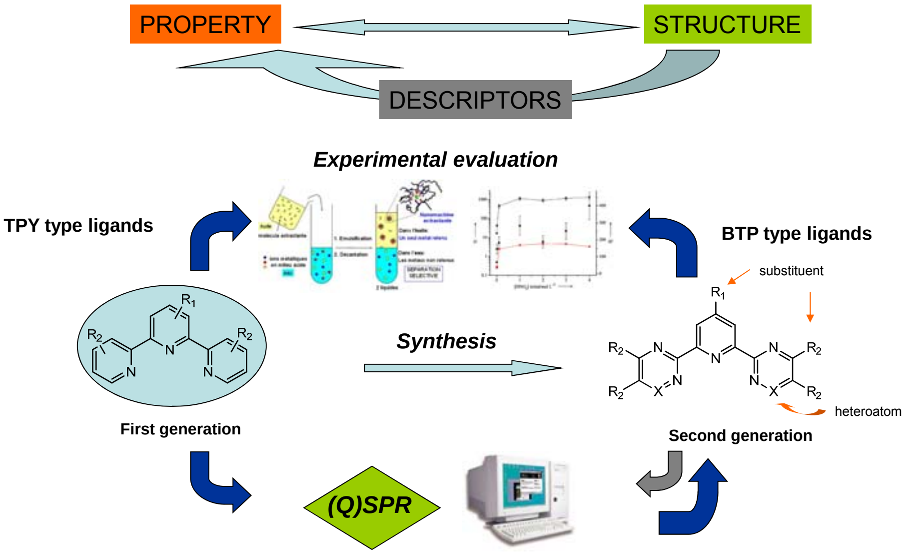

PROPERTY

STRUCTURE

DESCRIPTORS

Experimental evaluation

TPY type ligands

BTP type ligands

substituent

heteroatom

First generation

Synthesis

Second generation

(Q)SPR

Molecular scale of Solvent extraction

Quantitative Structure-Property Relationships (QSPR)

Descriptors

Constitutional	(mol. Weight, number of N, S, O…)
Topological	(cyclic, bicyclic…)
Geometrical	(molecular size, distances between functional groups…)
Electrostatic	(electrostatic potential, charges…)
Quantum-Chemical	(énergies of molecular orbitals, reactivity index…)
Thermodynamical	(heat of formation, logP…)
Fragments	(sequences of atoms and bonds, number of atoms…)

Ligand behavior

Hancock equation $\log K(ML) = E_A E_B + C_A C_B - D_A D_B$

electrostatic
electronic

covalent

Steric hindrance

Drug activity

Hansch Equation $\text{Log}\,(1/C) = -k_1(\log P)^2 + k_2 \log P + k_3\pi + k_4\sigma + k_5 ES + k_6$

A. VARNEK *(ULP, Strasbourg)* → CoMet PREDICTOR 1.0

Molecular scale of Solvent extraction

Quantitative Structure-Property Relationships (QSPR)

Extraction of UO_2^{2+} by monoamides

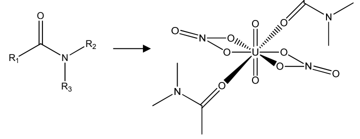

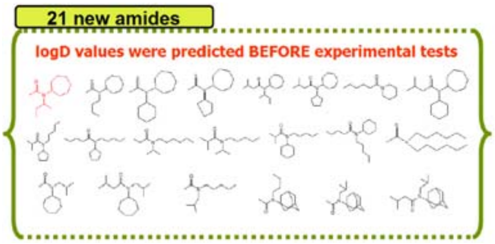

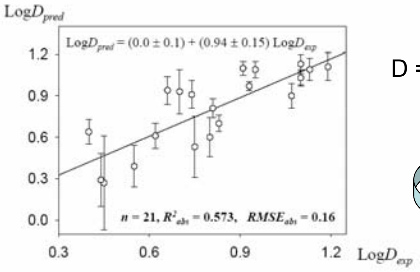

$$D = \frac{[U]_{org}}{[U]_{aq}}$$

Experimental conditions

Solvent: Toluene
Temperature: 22°C
Metal: UO_2^{2+}
HNO_3: 3M

What happens when the conditions Change ?

A. Varnek, D. Fourches, V. Solov'ev, O. Klimchuk, A. Ouadi, I. Billard *J. Solv. Extr. Ion Exch., 2007,* ***25,*** *N°4,* 433–462

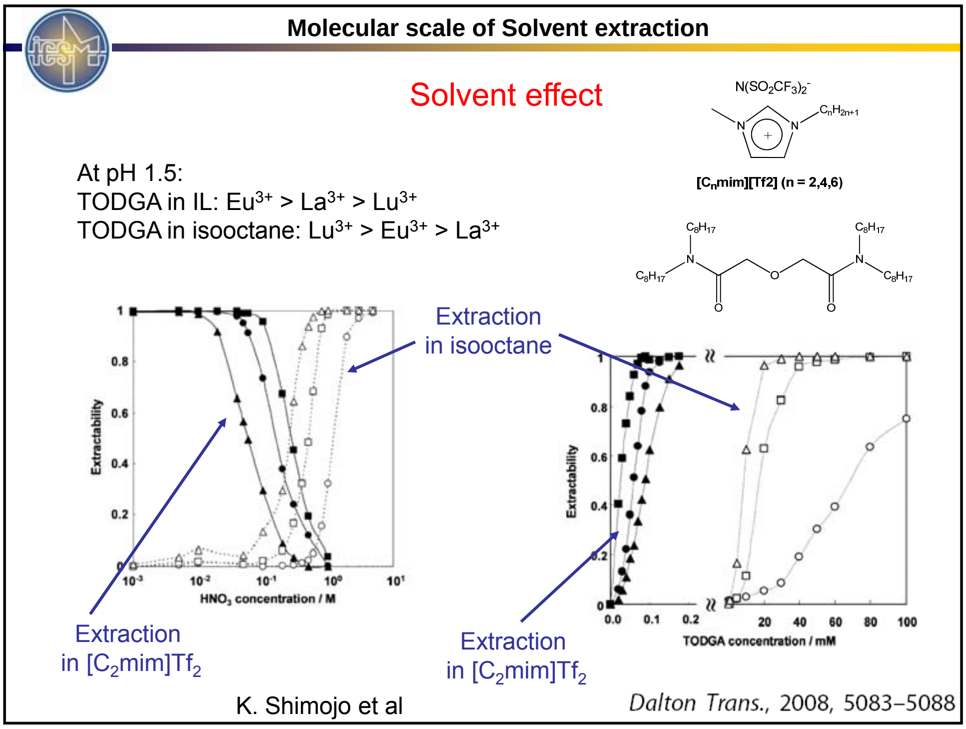

Molecular scale of Solvent extraction

Solvent effect

At pH 1.5:
TODGA in IL: $Eu^{3+} > La^{3+} > Lu^{3+}$
TODGA in isooctane: $Lu^{3+} > Eu^{3+} > La^{3+}$

$[C_nmim][Tf2]$ (n = 2,4,6)

Extraction in isooctane

Extraction in $[C_2mim]Tf_2$

Extraction in $[C_2mim]Tf_2$

K. Shimojo et al

Dalton Trans., 2008, 5083–5088

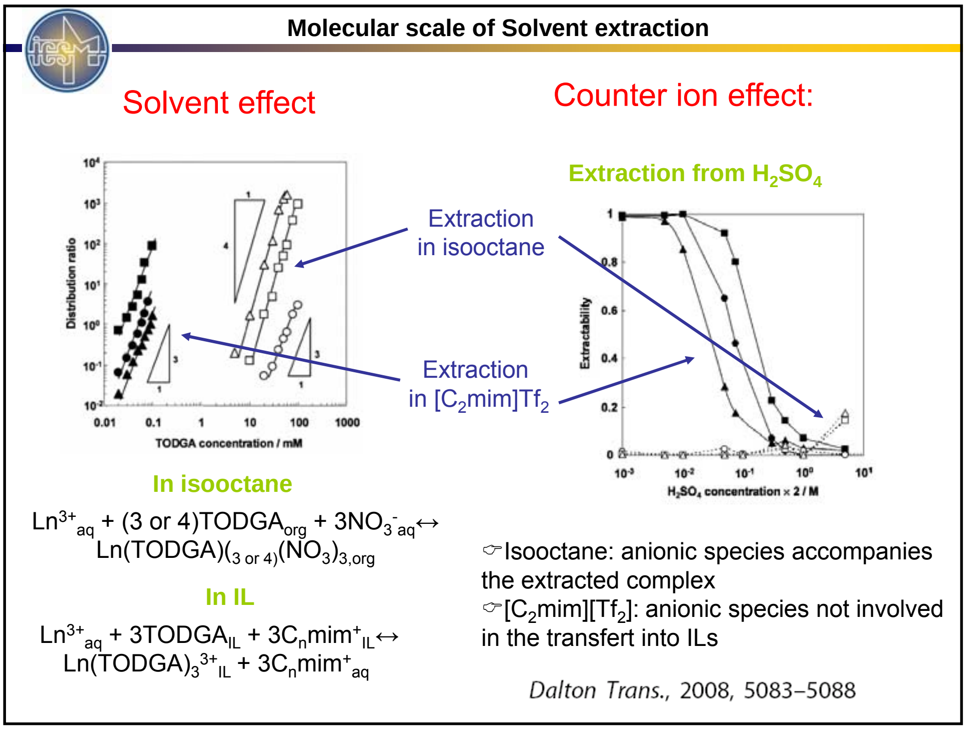

Molecular scale of Solvent extraction

Solvent effect

Counter ion effect:

Extraction from H_2SO_4

Extraction in isooctane

Extraction in $[C_2mim]Tf_2$

In isooctane

Ln^{3+}_{aq} + (3 or 4)$TODGA_{org}$ + $3NO_3^-{}_{aq} \leftrightarrow$
$Ln(TODGA)_{(3\text{ or }4)}(NO_3)_{3,org}$

In IL

Ln^{3+}_{aq} + $3TODGA_{IL}$ + $3C_nmim^+_{IL} \leftrightarrow$
$Ln(TODGA)_3{}^{3+}_{IL}$ + $3C_nmim^+_{aq}$

☞Isooctane: anionic species accompanies the extracted complex
☞$[C_2mim][Tf_2]$: anionic species not involved in the transfert into ILs

Dalton Trans., 2008, 5083–5088

Coordination Structures and Supramolecular Architectures in a Cerium(III)–Malonamide Solvent Extraction System

Ross J. Ellis and Mark R. Antonio*

Supramolecular Structures based on

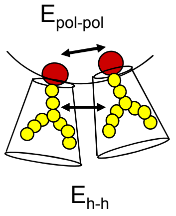

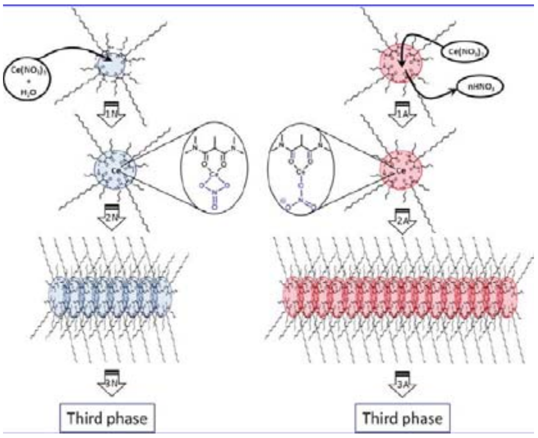

Tools:
- ICP-AOS
- FT-IR
- EXAFS
- SAXS

Langmuir 2012, 28, 5987–5998

Molecular and supra-molecular scales of Solvent extraction

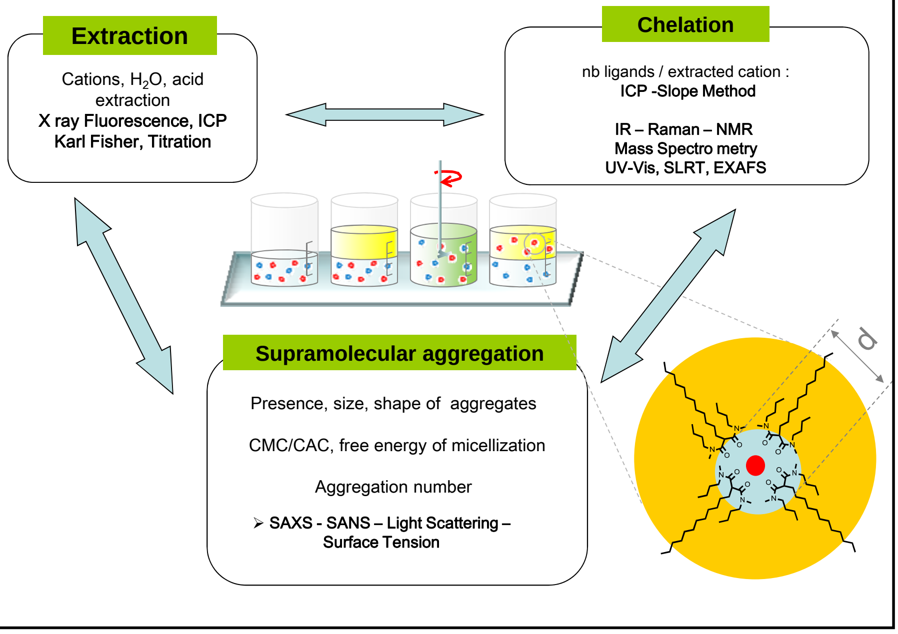

Extraction

Cations, H_2O, acid extraction
X ray Fluorescence, ICP
Karl Fisher, Titration

Chelation

nb ligands / extracted cation :
ICP -Slope Method

IR – Raman – NMR
Mass Spectro metry
UV-Vis, SLRT, EXAFS

Supramolecular aggregation

Presence, size, shape of aggregates

CMC/CAC, free energy of micellization

Aggregation number

- SAXS - SANS – Light Scattering – Surface Tension

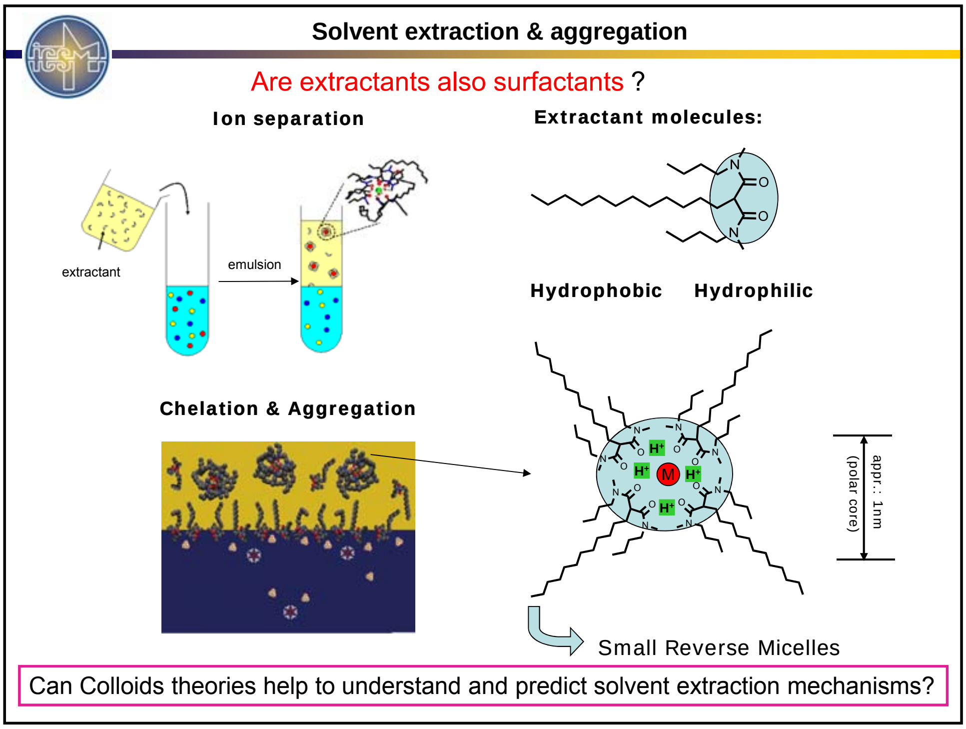

Solvent extraction & aggregation

Are extractants also surfactants ?

Ion separation

Extractant molecules:

Hydrophobic **Hydrophilic**

Chelation & Aggregation

Small Reverse Micelles

Can Colloids theories help to understand and predict solvent extraction mechanisms?

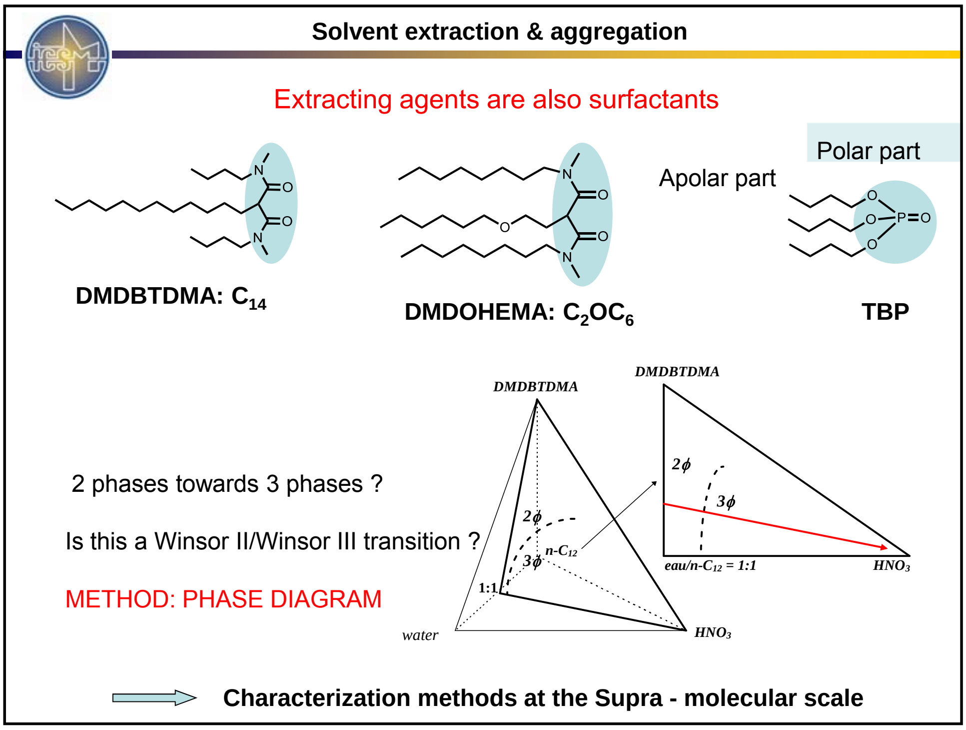

Solvent extraction & aggregation

Extracting agents are also surfactants

DMDBTDMA: C_{14}

DMDOHEMA: C_2OC_6

TBP

2 phases towards 3 phases ?

Is this a Winsor II/Winsor III transition ?

METHOD: PHASE DIAGRAM

Characterization methods at the Supra - molecular scale

Characterization methods at the Supra - molecular scale

Organisation

Surface tension γ

$$\boxed{\gamma = (\rho_{org}-\rho_{aq})Vg / (2\pi r\, f)}$$

f : shape of the droplet ~ r/V

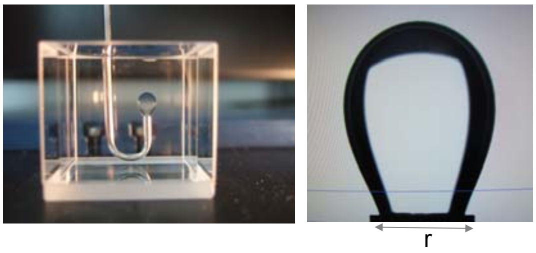

Drop of oil in water: organic phase in aqueous phase

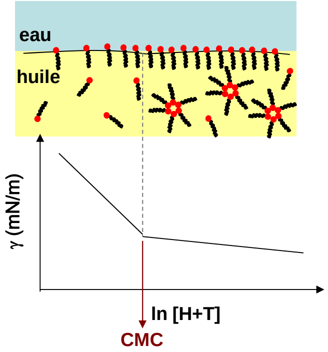

Gibbs Micellisation energy:

$$\Delta G^0_{micellisation} = RT \ln CMC$$

Characterization methods at the Supra - molecular scale

DMDOHEMA is a surfactant :

Organic phase (DMDOHEMA+dodecane) pre-equilibrated with HNO_3 (2M)

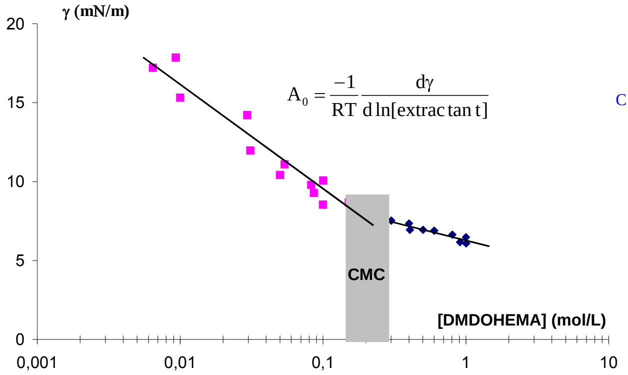

$$A_0 = \frac{-1}{RT}\frac{d\gamma}{d\ln[\text{extractant}]}$$

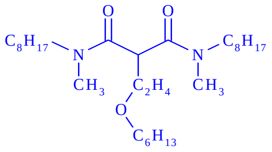

- γ decreases : adsorption at w:o interface ⟶ A_0 = 138 $Å^2$
- break-point : ΔG of micellar formation ⟶ CMC = 0.22 ± 0.07 $mol.L^{-1}$

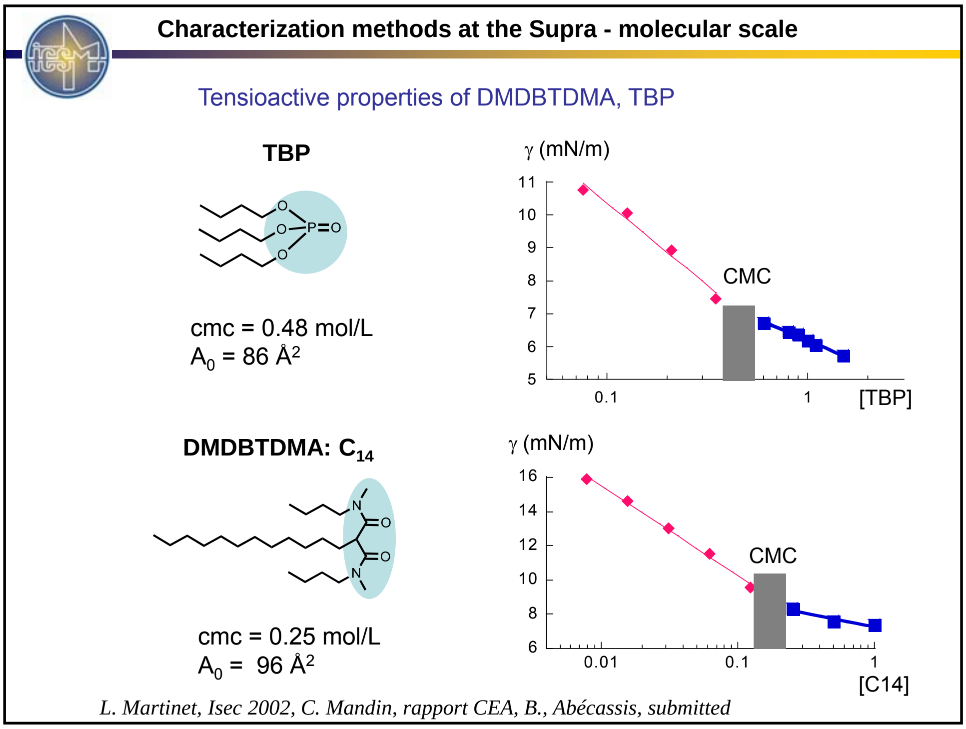

Characterization methods at the Supra - molecular scale

Tensioactive properties of DMDBTDMA, TBP

TBP

cmc = 0.48 mol/L
A_0 = 86 Å^2

DMDBTDMA: C_{14}

cmc = 0.25 mol/L
A_0 = 96 Å^2

L. Martinet, Isec 2002, C. Mandin, rapport CEA, B., Abécassis, submitted

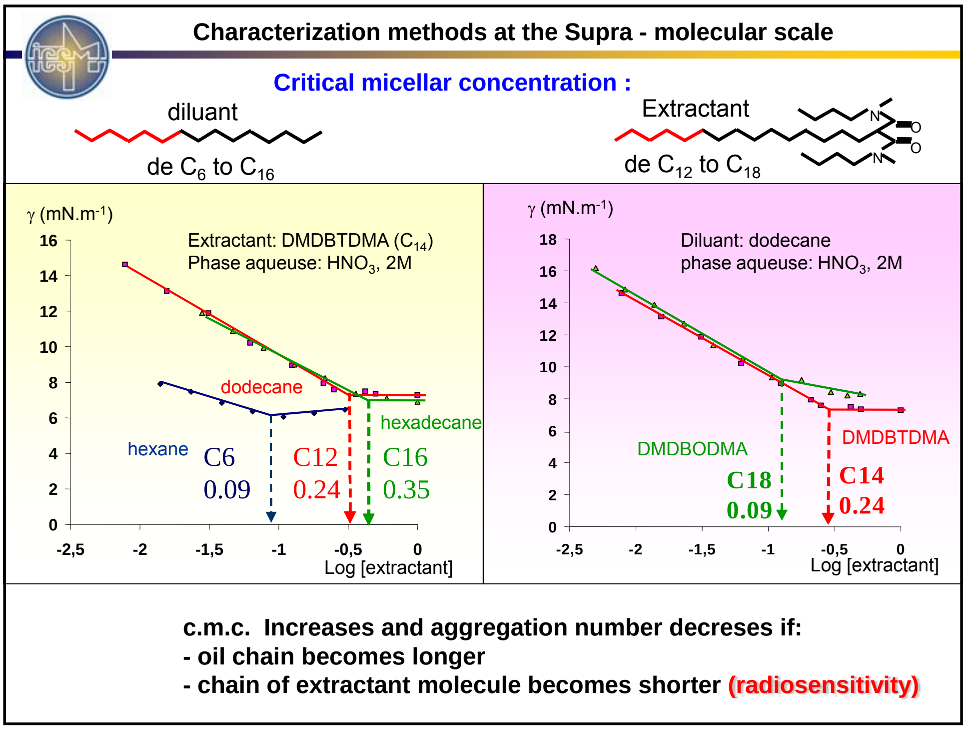

Characterization methods at the Supra - molecular scale

Critical micellar concentration :

diluant
de C_6 to C_{16}

Extractant
de C_{12} to C_{18}

Extractant: DMDBTDMA (C_{14})
Phase aqueuse: HNO_3, 2M

Diluant: dodecane
phase aqueuse: HNO_3, 2M

c.m.c. Increases and aggregation number decreses if:
- oil chain becomes longer
- chain of extractant molecule becomes shorter (radiosensitivity)

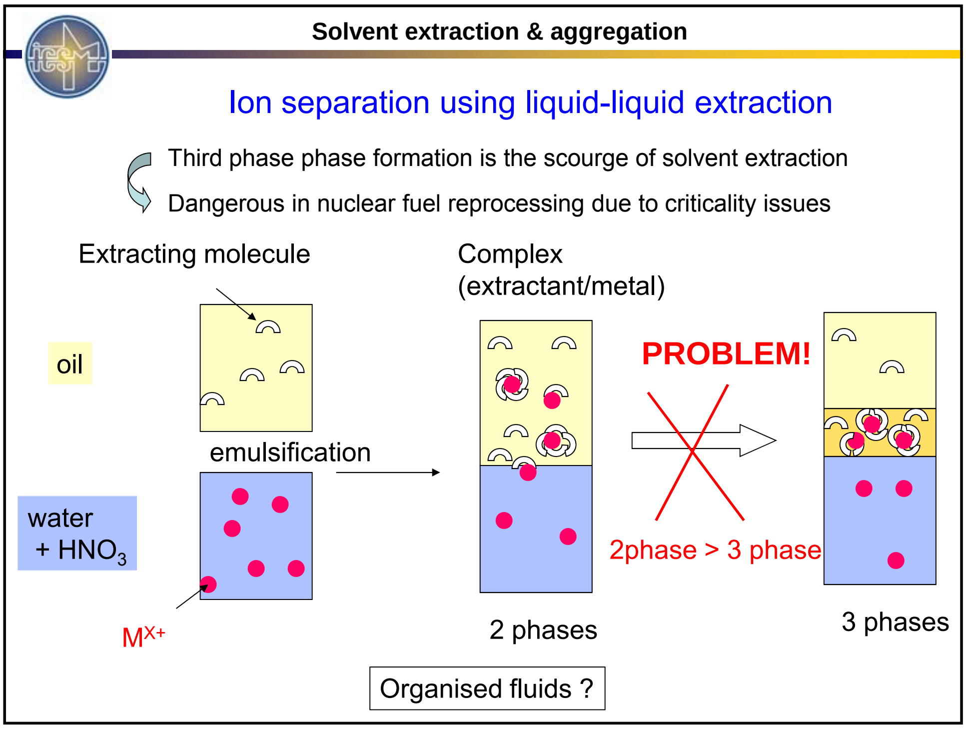

Solvent extraction & aggregation

Ion separation using liquid-liquid extraction

Third phase phase formation is the scourge of solvent extraction

Dangerous in nuclear fuel reprocessing due to criticality issues

Extracting molecule

Complex (extractant/metal)

oil

water + HNO_3

M^{X+}

emulsification

PROBLEM!

2phase > 3 phase

2 phases

3 phases

Organised fluids ?

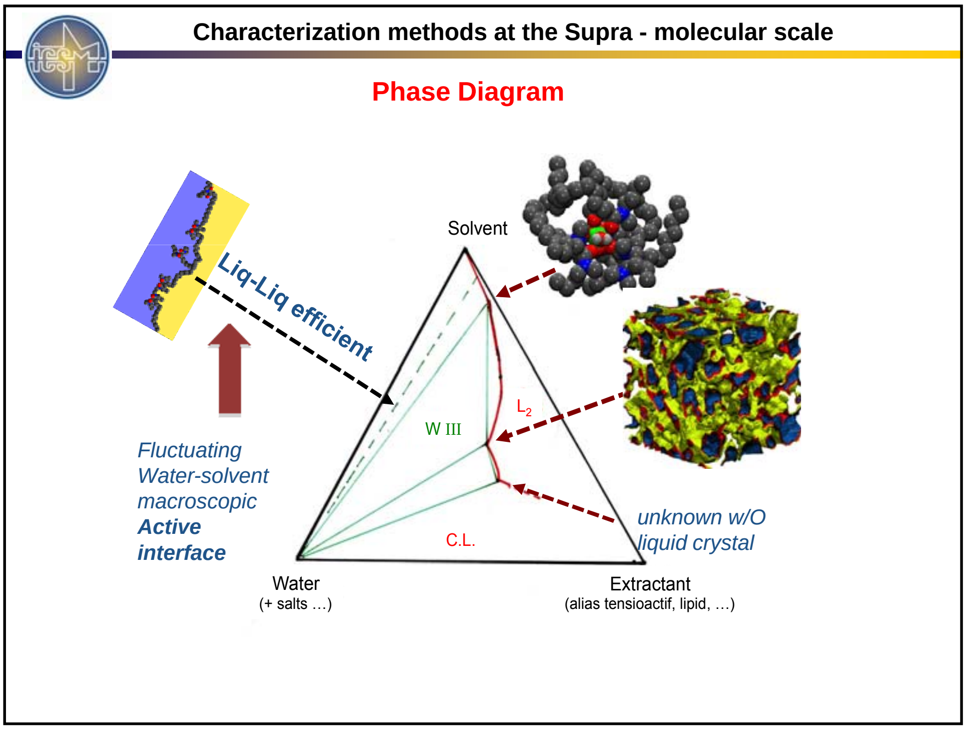

Characterization methods at the Supra - molecular scale

Phase Diagram

Fluctuating Water-solvent macroscopic ***Active interface***

unknown w/O liquid crystal

Characterization methods at the Supra - molecular scale

Third phase instability limit

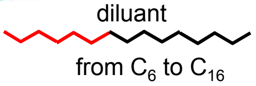

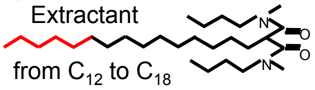

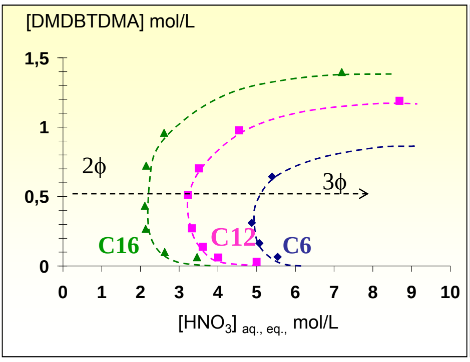

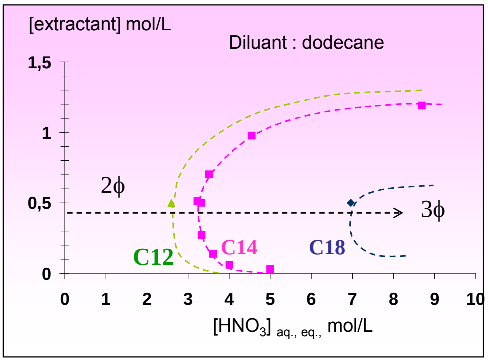

Stability increased if:
- **oil chain length decreases (or ramification)**
- **Extractant chain length increases**

L. Martinet et al, ISEC, 2002

Characterization methods at the Supra - molecular scale

Liquid-gas transition due to short-range attractions only

Sticky spheres (Baxter) model gives the composition where instability occurs

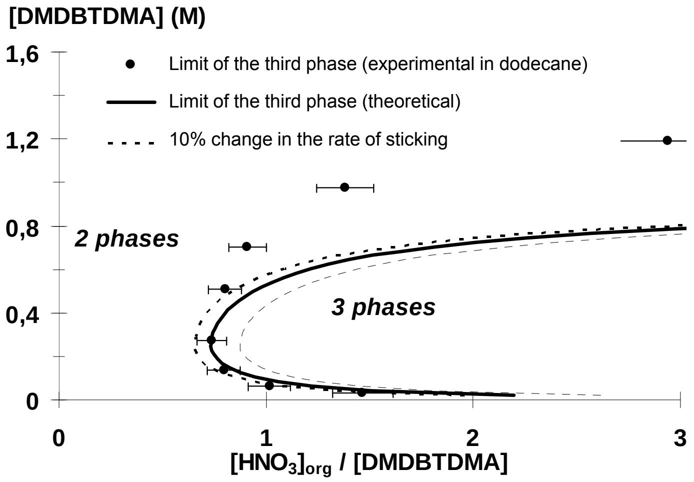

*C. Erlinger et al, Langmuir, **1999**, 15, 2290.;*

Characterization methods at the Supra - molecular scale

DMDBTDMA

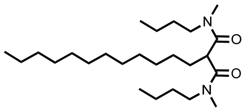

[Ce] in third phase

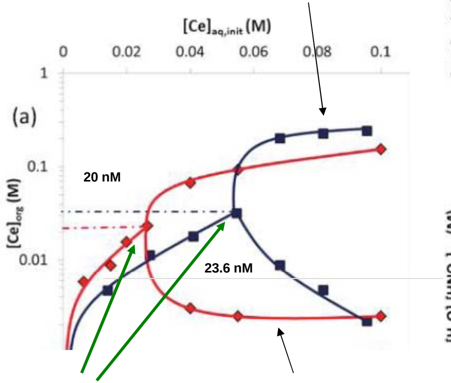

LOC point

Limiting organic concentration

[Ce] in light organic phase

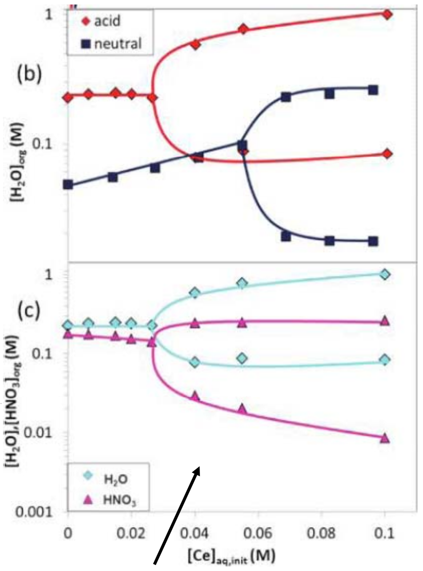

Langmuir 2012, 28, 5987−5998

$H_2$0 and HNO_3 extracted in acidic conditions

Characterization methods at the Supra - molecular scale

Supramolecular Organization : SAXS - SANS

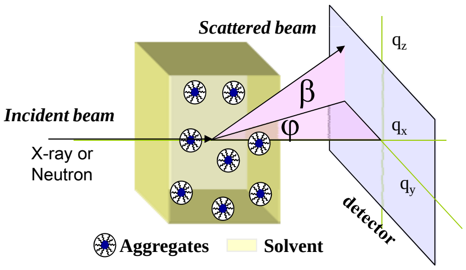

Scattering patterns are dependent on the structure of the solution

Proof of aggregation…or not

- ➢ **Shape**, **Size** et **organization** of aggregates

X-rays

see **electrons** → big Z (metals,…) → diameter **d**

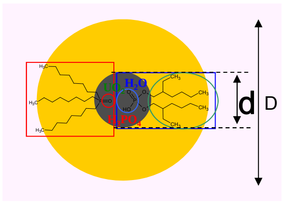

Neutrons

see **protons** → deuterated solvent → diameter **D**

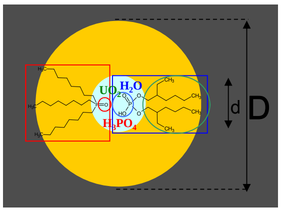

Characterization methods at the Supra - molecular scale

DMDOHEMA aggregate in dodecane

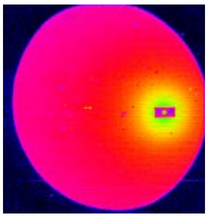

Diamide in dodecane

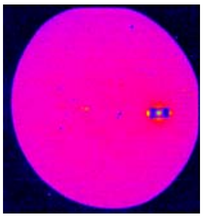

Dodecane

Absolutely scaled intensity:

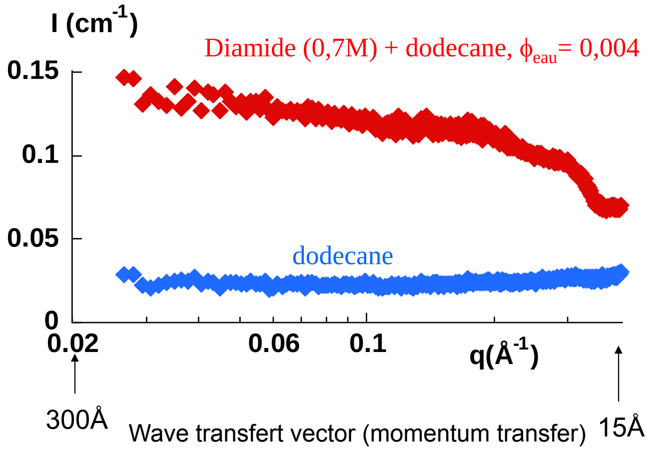

Wave transfert vector (momentum transfer)

Q = 4πsin2θ/λ

λ = wavelenght
θ = scattering angle

*C. Erlinger et al, Langmuir, **1999**, 15, 2290.; L. Martinet, Isec 2002,*

Characterization methods at the Supra - molecular scale

Small angle scattering

<u>Centrosymmetric monodisperse hypothesis:</u>

I(q) = n. P(q). S(q)

n: nb of micelles/unit volume

- P(q) : form factor, coming from micellar size, shape

-S(q) : structure factor, interaction

Statistical mechanics of liquids

S(q) =1 when micelles independant

$$I(Q)=\frac{N_a(C-CAC)}{N}V^2(\Delta\rho)^2P(Q)S(Q)$$

Total concentration

Concentration of Critical aggregation

Aggregation number

Volume of the aggregate

density

DMDBTDMA - 0,5 M
diphasique - phase organique - effet du pH

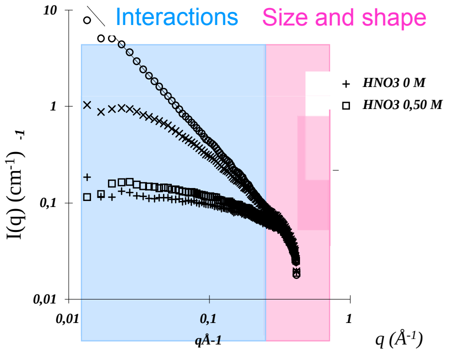

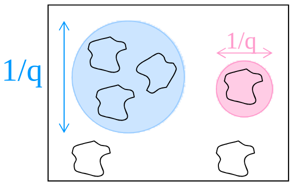

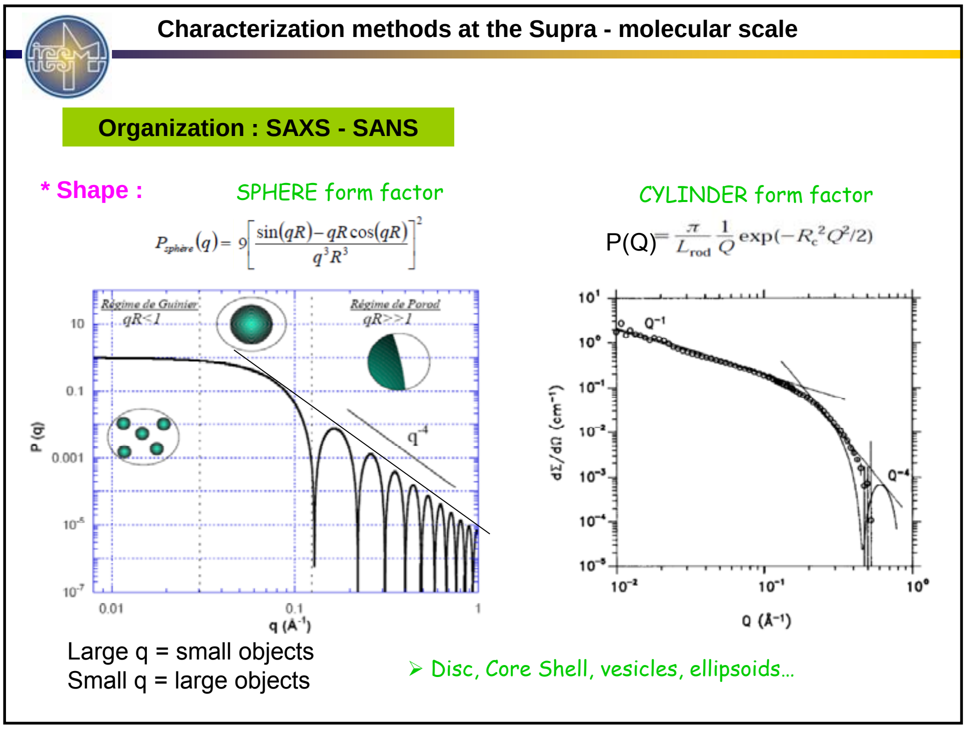

Characterization methods at the Supra - molecular scale

Organization : SAXS - SANS

*** Shape :**

SPHERE form factor

$$P_{sphère}(q) = 9\left[\frac{\sin(qR) - qR\cos(qR)}{q^3R^3}\right]^2$$

CYLINDER form factor

$$P(Q) = \frac{\pi}{L_{rod}}\frac{1}{Q}\exp(-R_c^2Q^2/2)$$

Large q = small objects
Small q = large objects

- Disc, Core Shell, vesicles, ellipsoids…

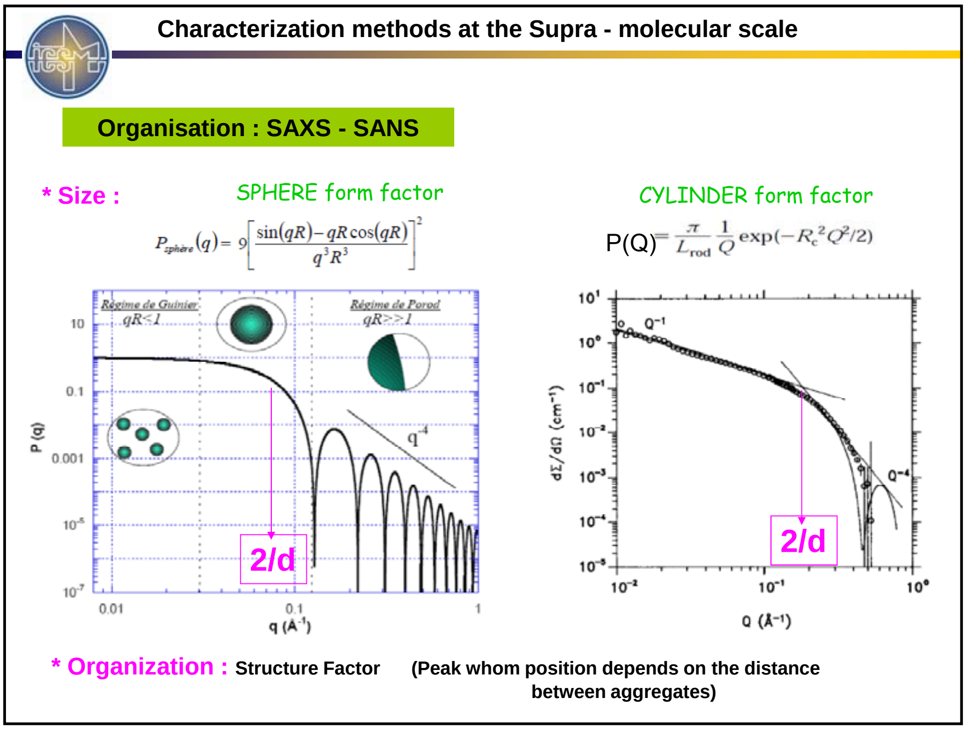

Characterization methods at the Supra - molecular scale

Organisation : SAXS - SANS

*** Size :**

SPHERE form factor

$$P_{sphère}(q) = 9\left[\frac{\sin(qR) - qR\cos(qR)}{q^3R^3}\right]^2$$

CYLINDER form factor

$$P(Q) = \frac{\pi}{L_{rod}}\frac{1}{Q}\exp(-R_c^2Q^2/2)$$

*** Organization :** **Structure Factor** **(Peak whom position depends on the distance between aggregates)**

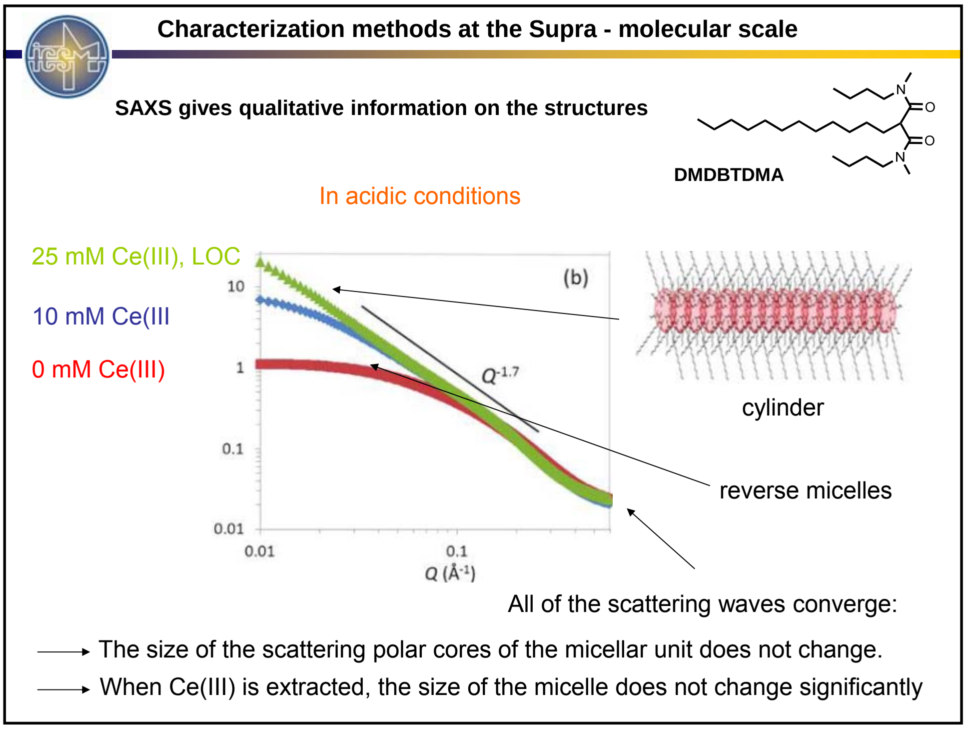

Characterization methods at the Supra - molecular scale

SAXS gives qualitative information on the structures

DMDBTDMA

In acidic conditions

All of the scattering waves converge:

→ The size of the scattering polar cores of the micellar unit does not change.

→ When Ce(III) is extracted, the size of the micelle does not change significantly

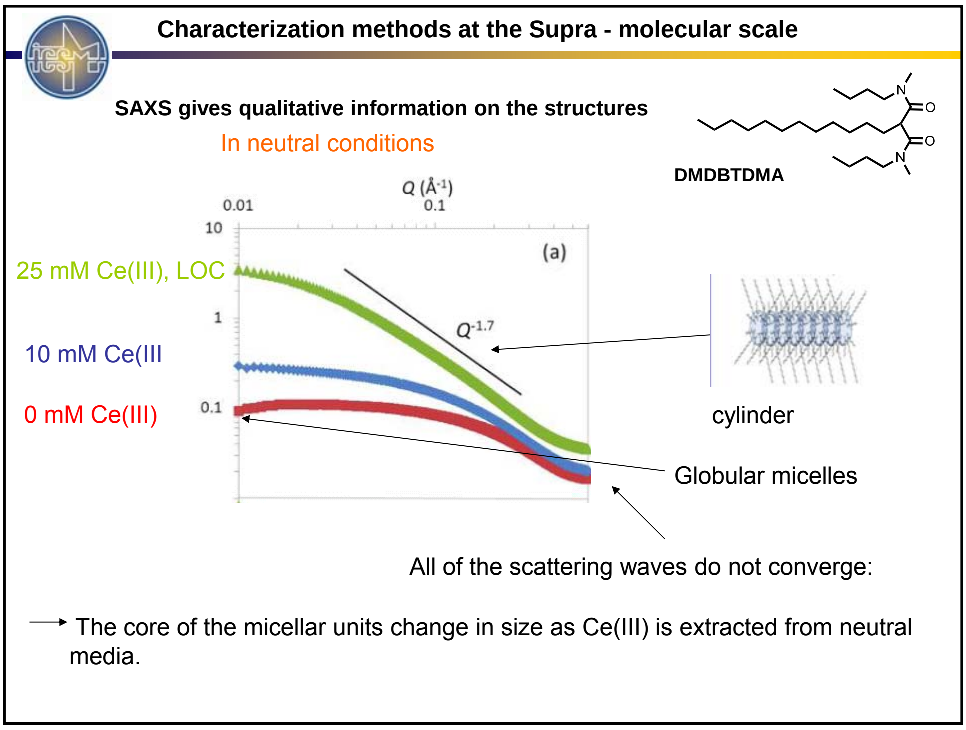

Characterization methods at the Supra - molecular scale

SAXS gives qualitative information on the structures

In neutral conditions

DMDBTDMA

All of the scattering waves do not converge:

→ The core of the micellar units change in size as Ce(III) is extracted from neutral media.

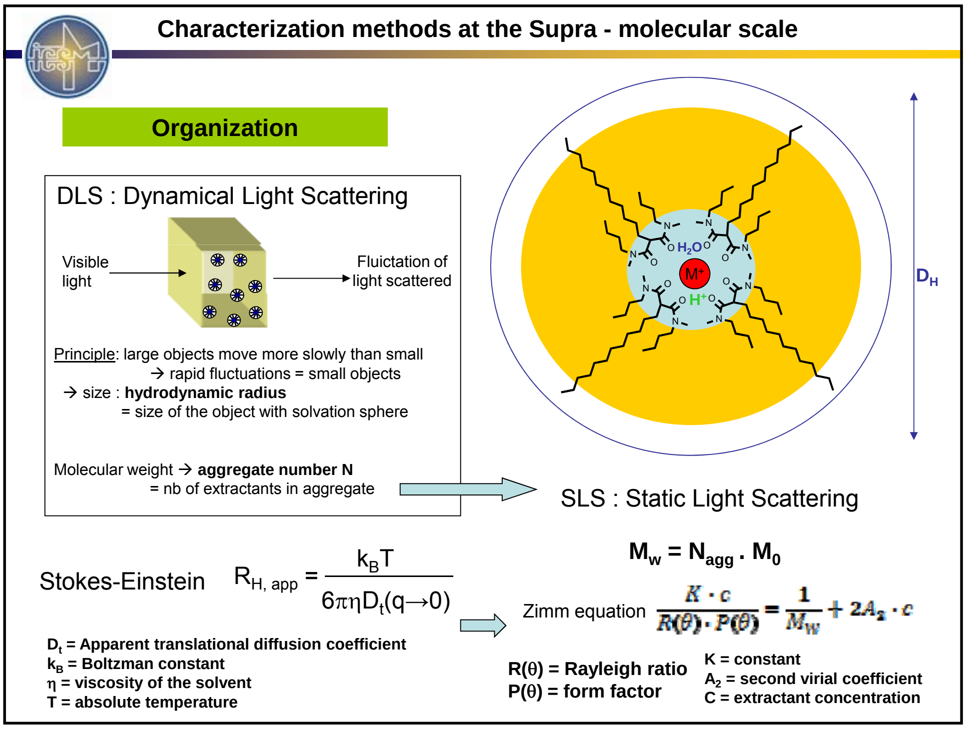

Characterization methods at the Supra - molecular scale

Organization

DLS : Dynamical Light Scattering

Visible light → Fluictation of light scattered

Principle: large objects move more slowly than small
→ rapid fluctuations = small objects
→ size : **hydrodynamic radius**
= size of the object with solvation sphere

Molecular weight → **aggregate number N**
= nb of extractants in aggregate

SLS : Static Light Scattering

$$\mathbf{M_w = N_{agg} \, . \, M_0}$$

Zimm equation $$\frac{K \cdot c}{R(\theta) \cdot P(\theta)} = \frac{1}{M_W} + 2A_2 \cdot c$$

R(θ) = Rayleigh ratio
P(θ) = form factor

K = constant
A_2 = second virial coefficient
C = extractant concentration

Stokes-Einstein $$R_{H,\,app} = \frac{k_B T}{6\pi\eta D_t(q\rightarrow 0)}$$

D_t = Apparent translational diffusion coefficient
k_B = Boltzman constant
η = viscosity of the solvent
T = absolute temperature

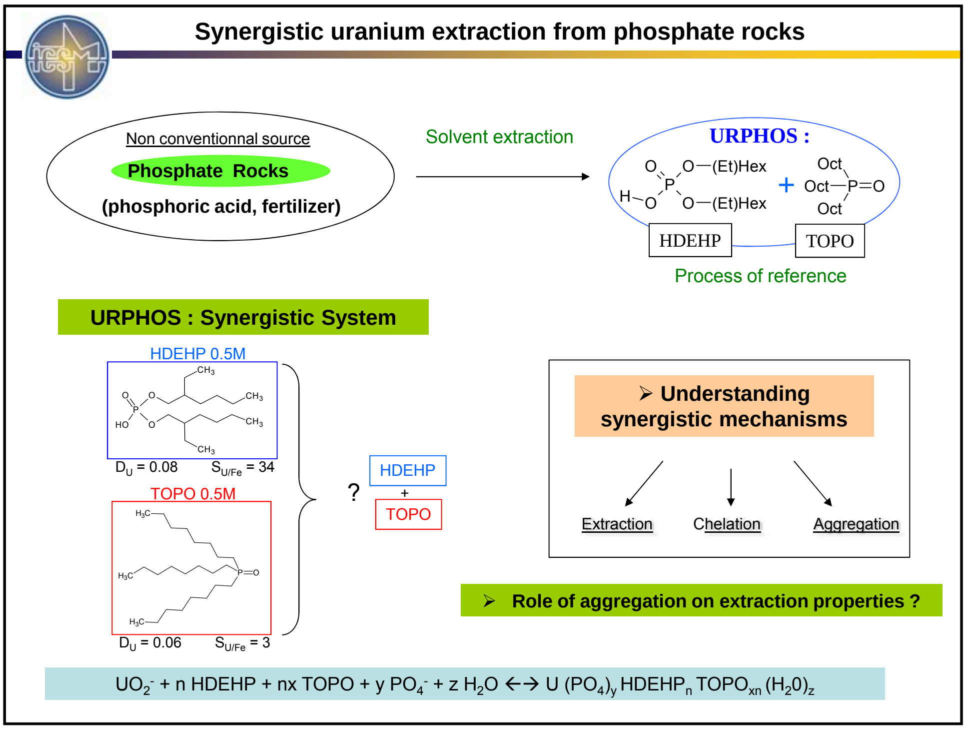

Synergistic uranium extraction from phosphate rocks

Non conventionnal source
Phosphate Rocks
(phosphoric acid, fertilizer)

Solvent extraction →

URPHOS :

HDEHP TOPO

Process of reference

URPHOS : Synergistic System

HDEHP 0.5M

D_U = 0.08 $S_{U/Fe}$ = 34

TOPO 0.5M

D_U = 0.06 $S_{U/Fe}$ = 3

? HDEHP + TOPO

➢ Understanding synergistic mechanisms

Extraction Chelation Aggregation

➢ Role of aggregation on extraction properties ?

$$UO_2^- + n\ HDEHP + nx\ TOPO + y\ PO_4^- + z\ H_2O \leftrightarrow U\,(PO_4)_y\,HDEHP_n\,TOPO_{xn}\,(H_20)_z$$

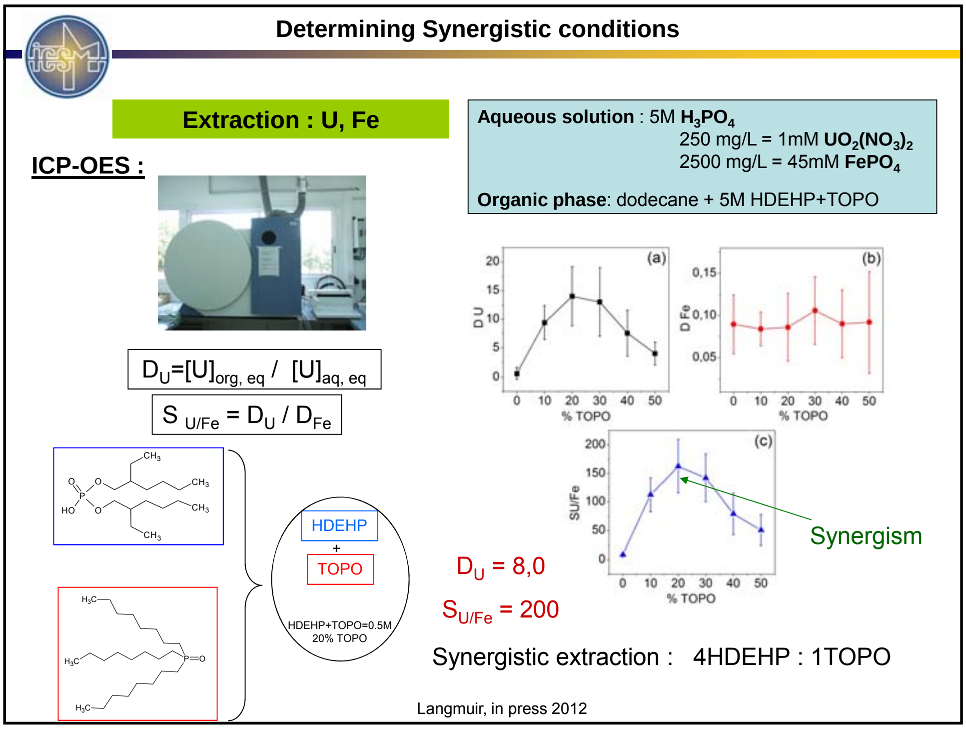

Determining Synergistic conditions

Extraction : U, Fe

ICP-OES :

$D_U = [U]_{org, eq} / [U]_{aq, eq}$

$S_{U/Fe} = D_U / D_{Fe}$

Aqueous solution : 5M $\mathbf{H_3PO_4}$
250 mg/L = 1mM $\mathbf{UO_2(NO_3)_2}$
2500 mg/L = 45mM $\mathbf{FePO_4}$

Organic phase: dodecane + 5M HDEHP+TOPO

$D_U = 8,0$

$S_{U/Fe} = 200$

Synergistic extraction : 4HDEHP : 1TOPO

Langmuir, in press 2012

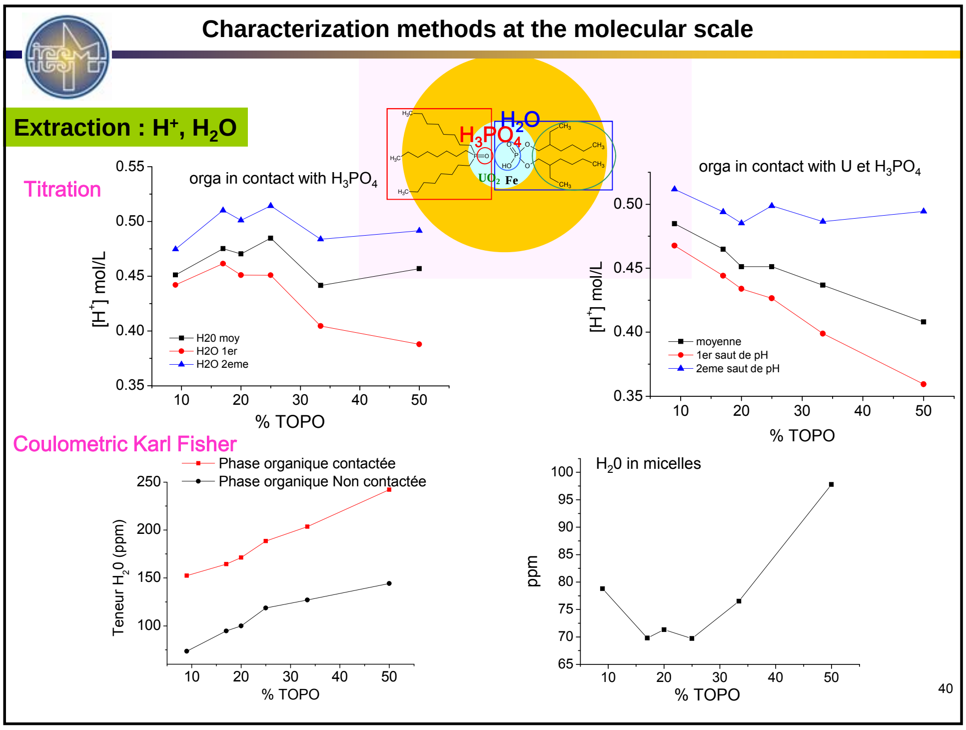

Characterization methods at the molecular scale

Extraction : H^+, H_2O

Titration

Coulometric Karl Fisher

Characterization methods at the molecular scale

Chelation The Slope Method

$UO_2^- + n\ HDEHP + nx\ TOPO + y\ PO_4^- + z\ H_2O \leftrightarrow U(PO_4)_y HDEHP_n TOPO_{xn}(H_20)_z$

$K = [U(PO_4)_y HDEHP_n TOPO_{xn}(H_20)_z]_{eq,\,org} / [HDEHP]^n [TOPO]^{nx} [UO_2^-]_{eq,aq} [PO_4-]^y$

$D_U = [UO_2^+]_{eq,\,org} / [UO_2^+]_{eq,\,aq}$

$\ln D_U = \ln K + n \ln [ligands]$

n = 5 for 20% of TOPO (1 : 4 ratio)

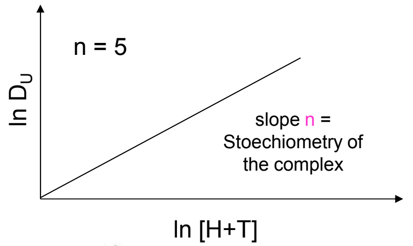

n : number of ligand per U

⇩

Molecular modeling →

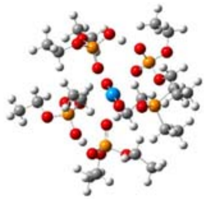

2(HDEHP-DEHP) andt 1TOPO (1st sphere)

Guillaumont, CEA/DEN/DRCP

Aggregation in the organic phase

SAXS spectra

[HDEHP+TOPO]= 0.5M

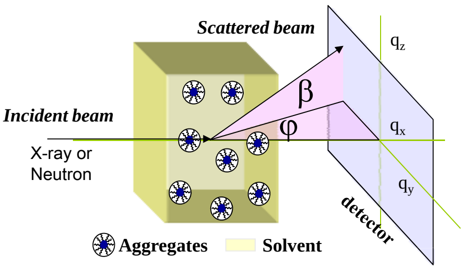

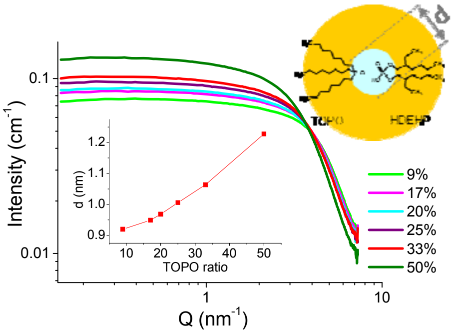

$$I(Q) = \phi_v V(\Delta\rho)^2 P(Q) S(Q)$$

- ➢ **Globular aggregates**
- ➢ **Core size increase gradually with the TOPO ratio :** I(0) increase due to V increase
- ➢ **No Synergistic effect on the core size of the aggregates (water and acid)**

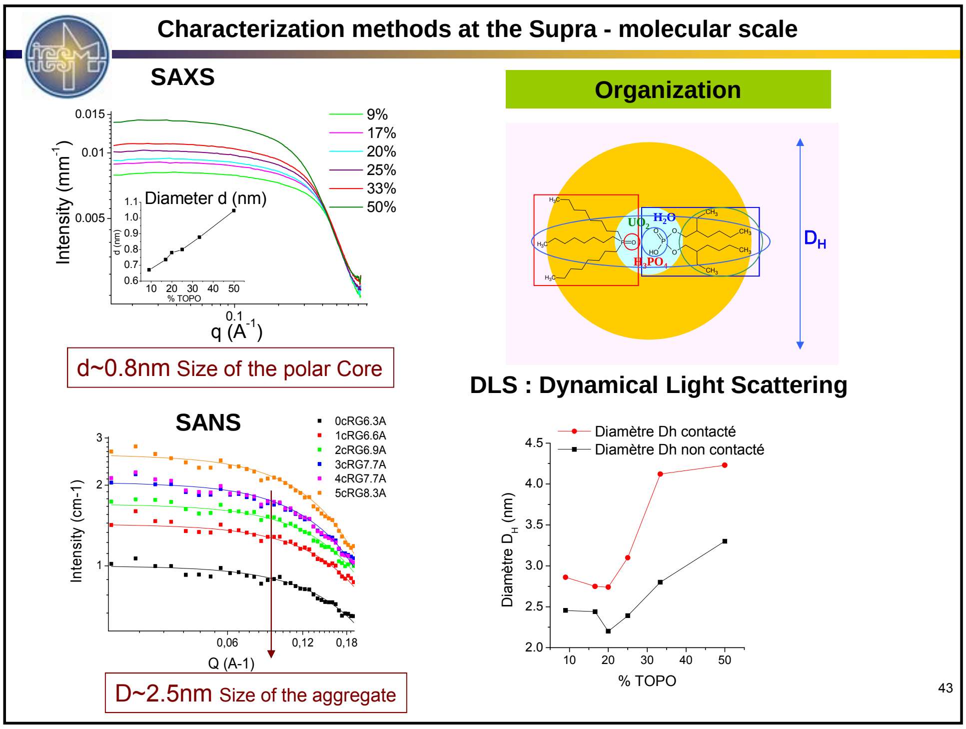

Characterization methods at the Supra - molecular scale

SAXS

d~0.8nm Size of the polar Core

SANS

D~2.5nm Size of the aggregate

Organization

DLS : Dynamical Light Scattering

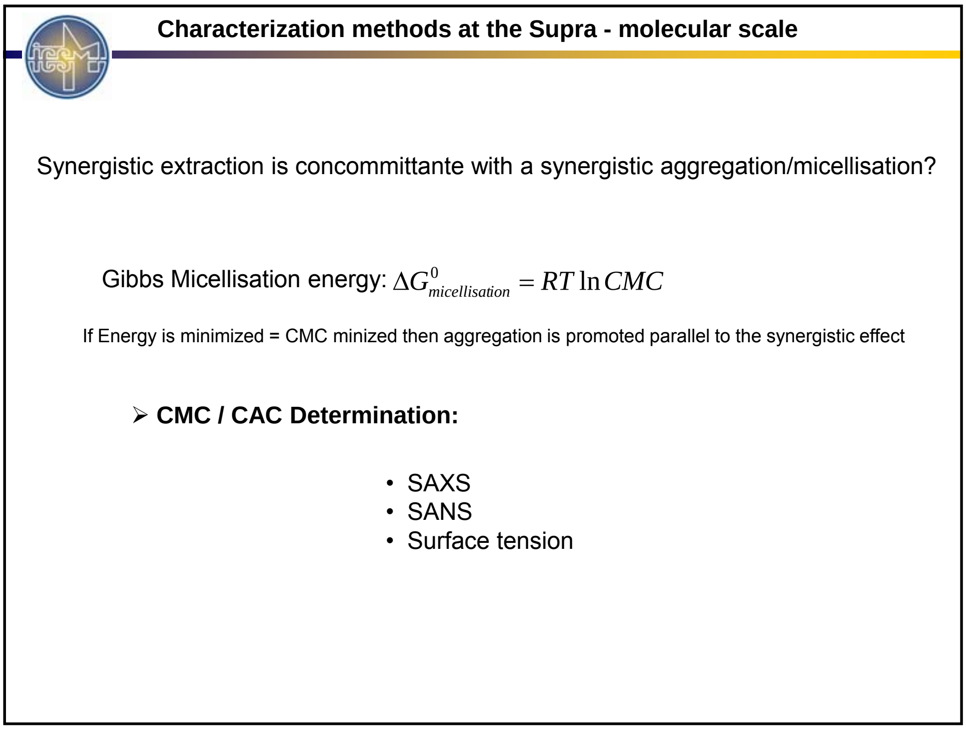

Characterization methods at the Supra - molecular scale

Synergistic extraction is concommittante with a synergistic aggregation/micellisation?

Gibbs Micellisation energy: $\Delta G^0_{micellisation} = RT \ln CMC$

If Energy is minimized = CMC minized then aggregation is promoted parallel to the synergistic effect

- **CMC / CAC Determination:**
  - SAXS
  - SANS
  - Surface tension

Characterization methods at the Supra - molecular scale

CAC : Tensiometry

Surface tension γ

$$\gamma = (\rho_{org}-\rho_{aq})Vg / (2\pi r\, f)$$

f : drop shape ~ r/V

Harkins and Brown empirical correction factor

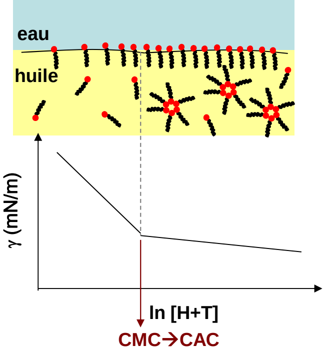

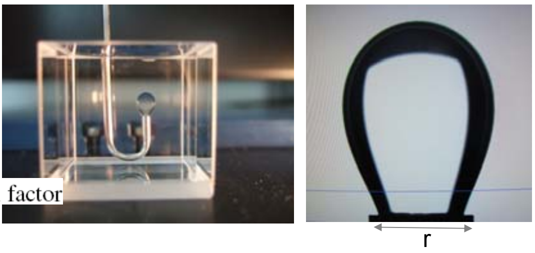

Drop of organic phase in aqueous phase

- **CAC Comparison with different TOPO ratios**
- **In contact with acidic aqueous solutions of U/Fe**

Characterization methods at the Supra - molecular scale

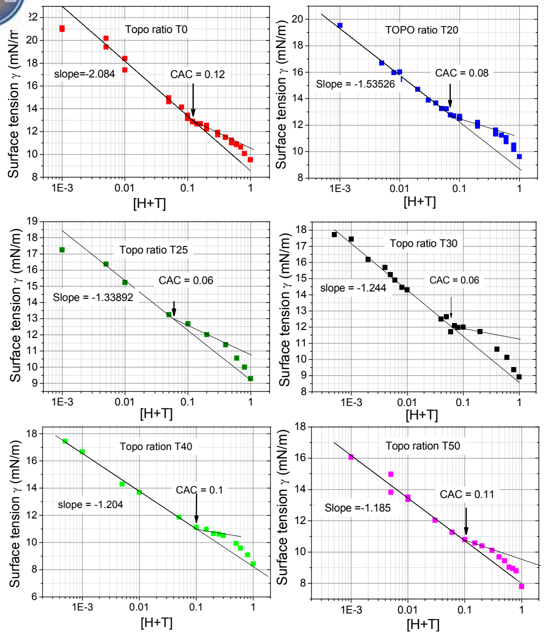

CAC : Tensiometry

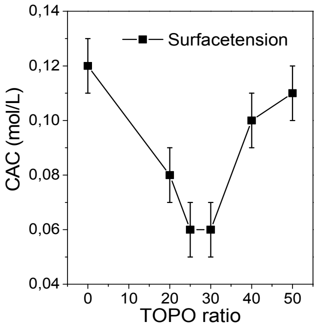

Characterization methods at the Supra - molecular scale

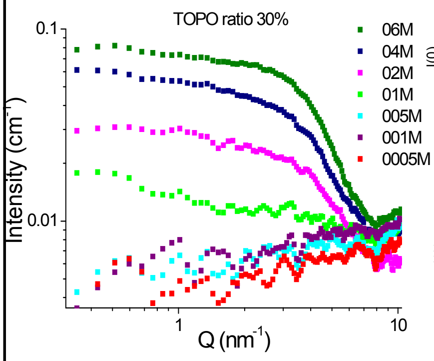

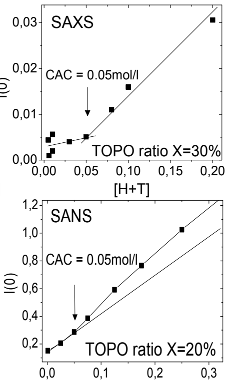

CAC : SAXS - SANS

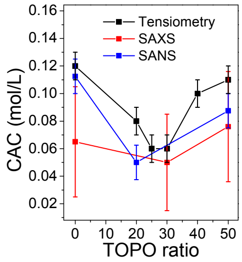

- ➢ Minimization of Micellisation energy for synergistic extraction

Synergistic extraction is concomitant with an easier aggregation of the two extractant molecules in a mixed reverse micelle

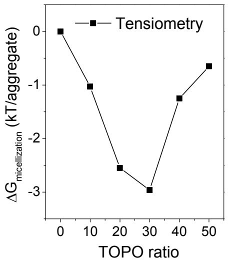

Conclusion

- **Synergistic extraction is concomitant to a synergistic aggregation**

  Is it controlling the extraction?

  Can it be generalized to other synergistic systems?

$LiNO_3$ in excess; $[UO_2^{2+}] = 2.10^{-2}$ M, [extractant] ≈ 4.10^{-2} M
[extractant] / [cation] = 2

% UO_2^{2+} extracted

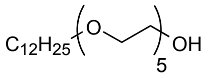

3,7

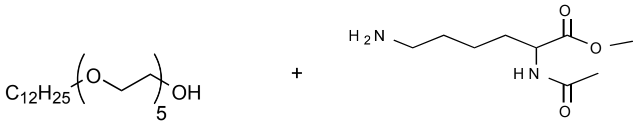

≈ 0

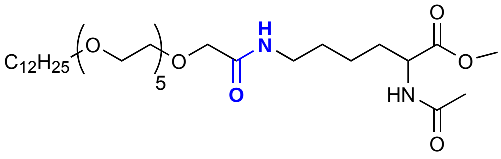

48

Synergy brought by di-bloc structure

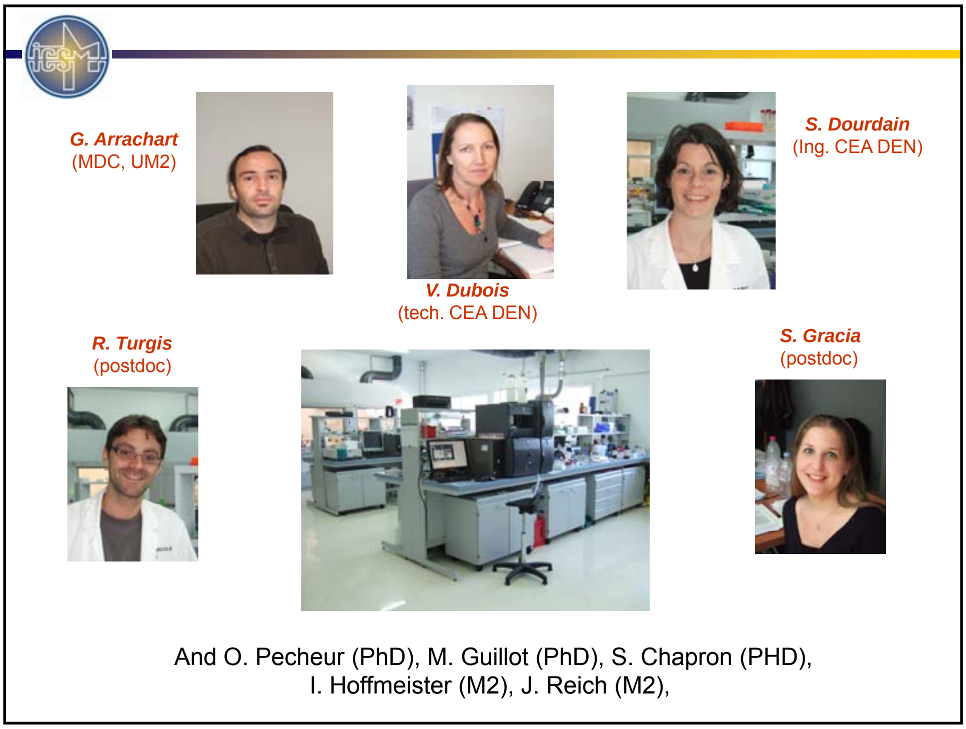

G. Arrachart
(MDC, UM2)

V. Dubois
(tech. CEA DEN)

S. Dourdain
(Ing. CEA DEN)

R. Turgis
(postdoc)

S. Gracia
(postdoc)

And O. Pecheur (PhD), M. Guillot (PhD), S. Chapron (PHD),
I. Hoffmeister (M2), J. Reich (M2),

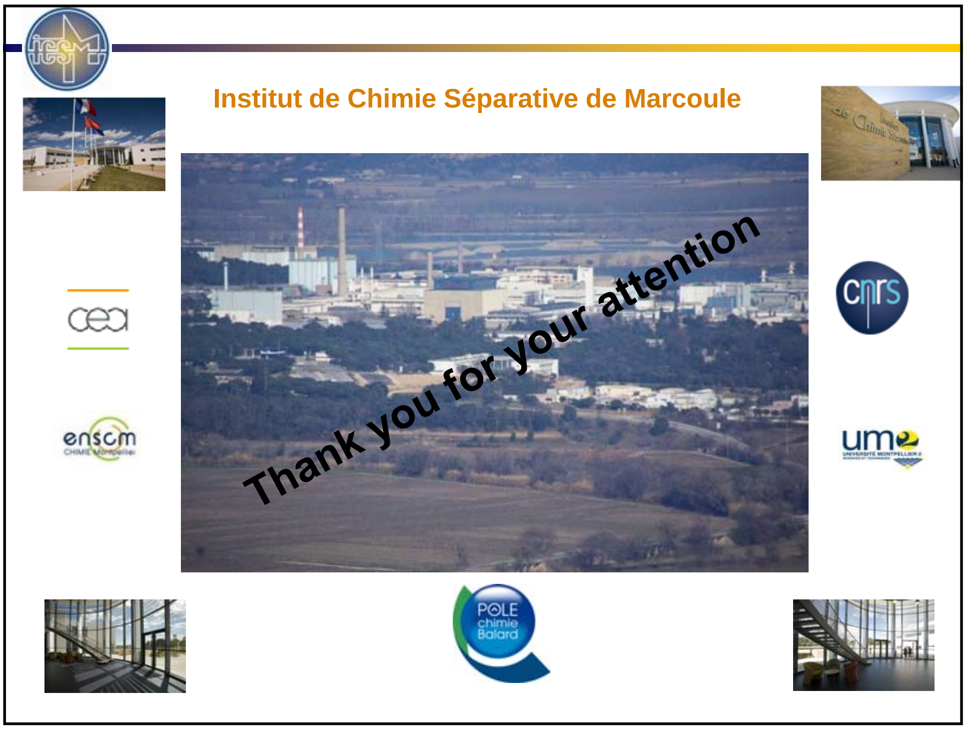

Institut de Chimie Séparative de Marcoule

Thank you for your attention

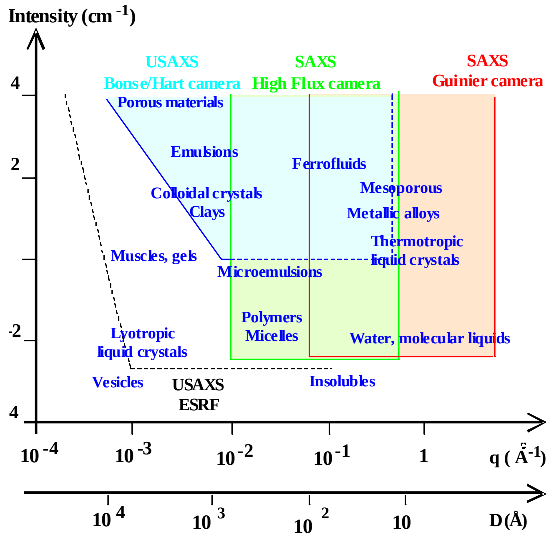
Intensity (cm -1)
USAXS
Bonse/Hart camera
SAXS
High Flux camera
SAXS
Guinier camera
4
2
-2
4
Porous materials
Emulsions
Ferrofluids
Colloidal crystals
Clays
Mesoporous
Metallic alloys
Thermotropic
liquid crystals
Muscles, gels
Microemulsions
Polymers
Micelles
Lyotropic
liquid crystals
Water, molecular liquids
Vesicles
USAXS
ESRF
Insolubles
10 -4
10 -3
10 -2
10 -1
1
q (Å-1)
10 4
10 3
10 2
10
D(Å)

Sorption and diffusion of actinides in clays

Tobias Reich, Samer Amayri, Daniel R. Fröhlich, Ugras Kaplan

Johannes Gutenberg University Mainz
Institute of Nuclear Chemistry

7th European Summer School on Supramolecular, Intermolecular, Interaggregate Interactions and Separation Chemistry
Moscow, Russia, July 20-23, 2012

JOHANNES GUTENBERG UNIVERSITÄT MAINZ

Institute of Nuclear Chemistry

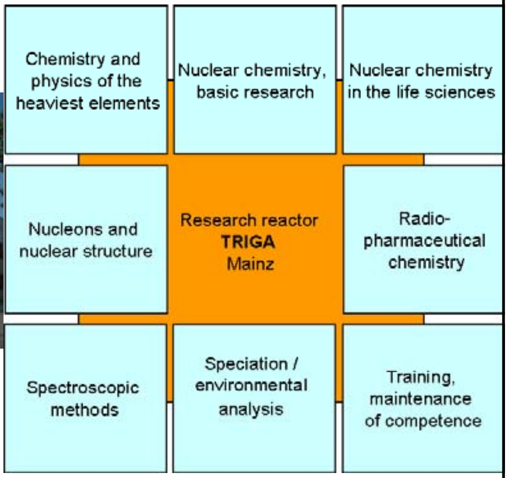

Chemistry and physics of the heaviest elements

Nuclear chemistry, basic research

Nuclear chemistry in the life sciences

Nucleons and nuclear structure

Research reactor **TRIGA** Mainz

Radio-pharmaceutical chemistry

Spectroscopic methods

Speciation / environmental analysis

Training, maintenance of competence

Institute of Nuclear Chemistry

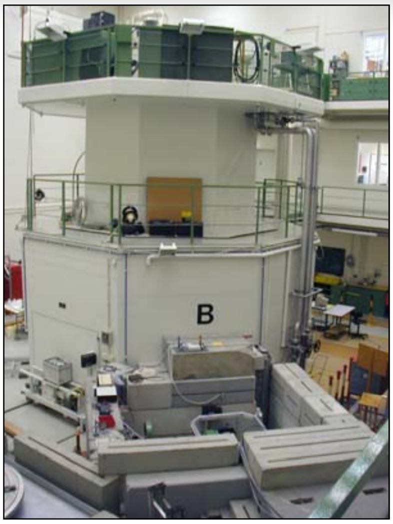

Research reactor TRIGA Mainz

Outline

- Motivation
- Introduction to X-ray Absorption Fine Structure (XAFS) spectroscopy
- Overview of EXAFS studies on U, Np, and Pu sorption on clay minerals
  - Kaolinite
  - Montmorillonite
- Np and Pu interaction with Opalinus Clay (OPA)
  - Sorption and diffusion experiments
  - Spectroscopic investigations
    - XAFS
    - µ-XAFS, µ-XRF, µ-XRD
- Summary

Motivation

- The radiotoxicity of spent nuclear fuel after a storage time >1,000 years will be determined by Np, Pu, Am and Cm

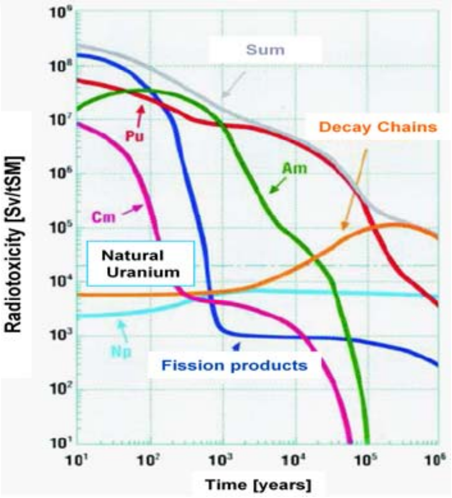

Radiotoxicity of 1 ton burned nuclear fuel (4 % ^{235}U, 40 GWd/t burn up

K. Gompper et al. (2001), Radioaktivität und Kernenergie, FZK

Motivation

- Clay formations are discussed as potential host rock formations
- Migration behaviour of long-lived radionuclides in the host rock has to be studied in detail
- Retardation and transport of the actinides in clay rock are dominated by sorption and diffusion
- X-ray absorption spectroscopy is a powerful tool to provide information about the interaction mechanisms on a molecular level

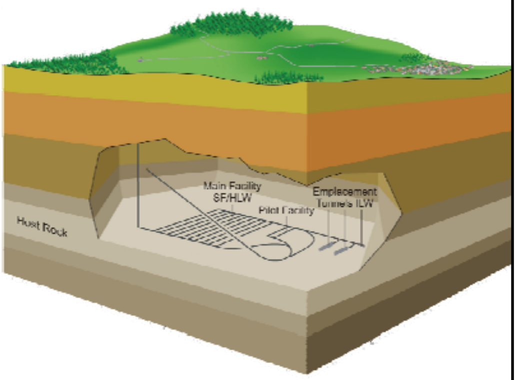

Nagra, NTB 02-03, 2002

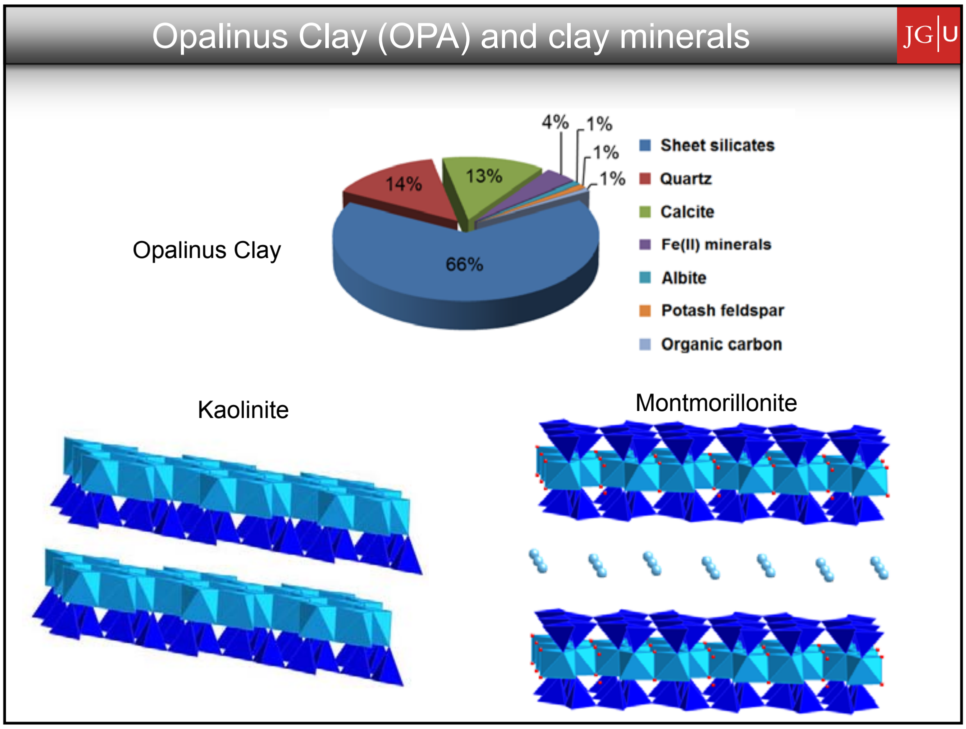

Opalinus Clay (OPA) and clay minerals

JG|U

Opalinus Clay

Kaolinite

Montmorillonite

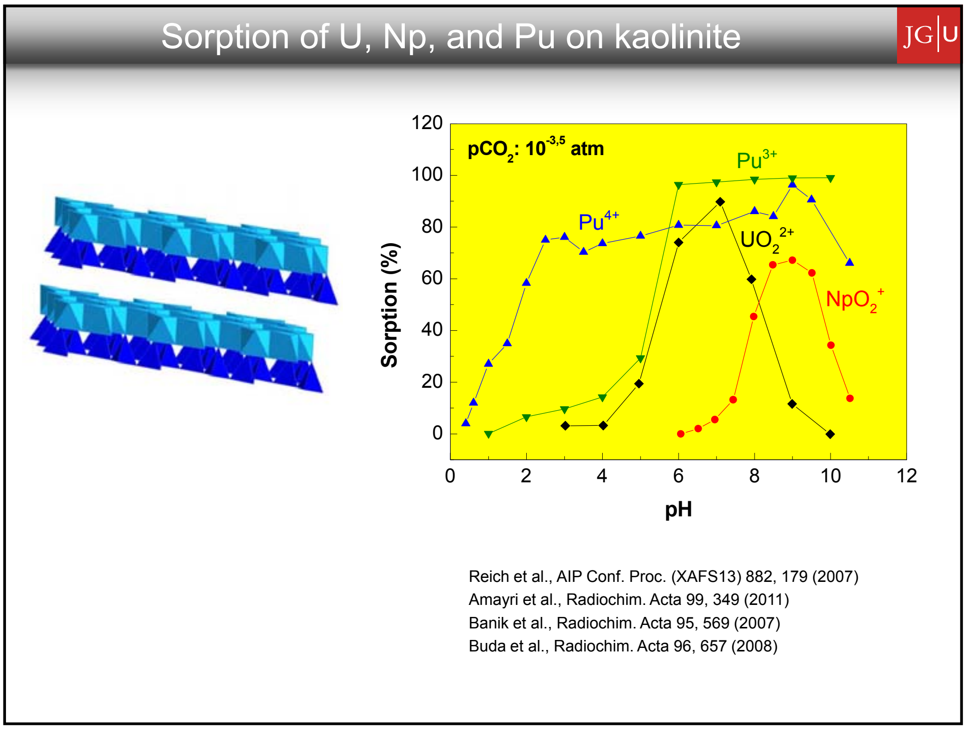

Sorption of U, Np, and Pu on kaolinite

JG|U

Reich et al., AIP Conf. Proc. (XAFS13) 882, 179 (2007)
Amayri et al., Radiochim. Acta 99, 349 (2011)
Banik et al., Radiochim. Acta 95, 569 (2007)
Buda et al., Radiochim. Acta 96, 657 (2008)

Interactions of metal ions with mineral surfaces

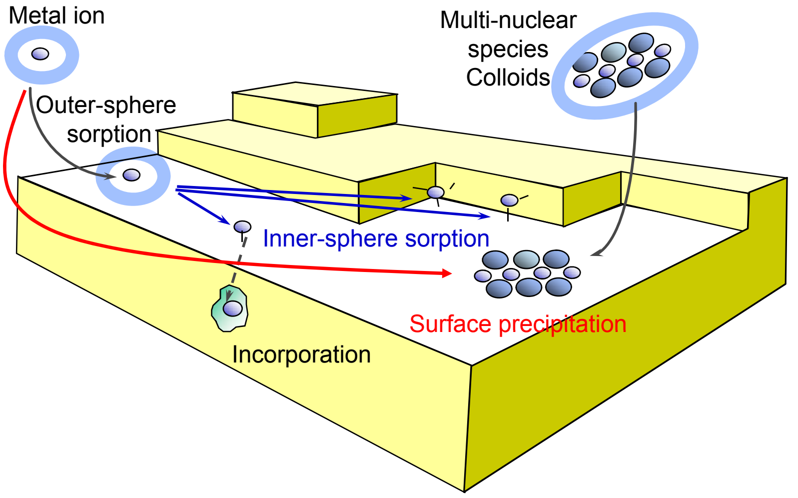

Manceau et al., Rev. Mineral. Geochem. 49, 344 (2002)

Introduction to XAFS spectroscopy

- XAS is often artificially divided into two experiments:
  - XANES - X-ray absorption near-edge structure
  - EXAFS - Extended X-ray absorption fine structure.

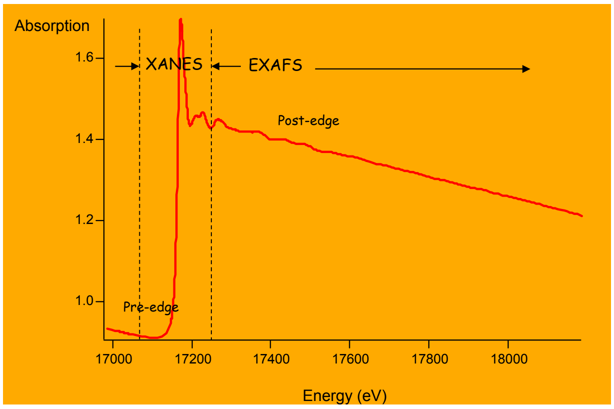

Main features of XANES

- XANES provides information about the valence of the central ion by comparison to standards of known oxidation state.

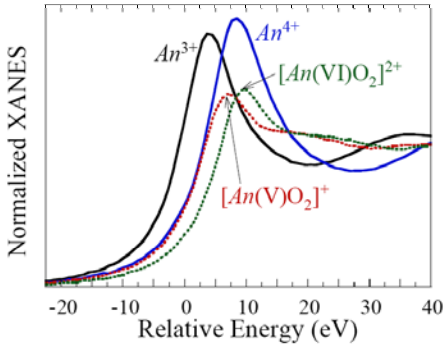

Representative XANES spectra as function of oxidation state and coordination environment (Antonio and Soderholm, 2006).

Sample	2nd der. crossing (eV)
Pu^{3+}	18060.1
Pu^{4+}	18063.2
$Pu(V)O_2^{+}$	18062.6
$Pu(VI)O_2^{2+}$	18064.8

Conradson et al., Polyhedron Vol. 17, No. 4, 599 (1998)

U L_{III}-edge XANES of mixtures of U(IV) and U(VI)

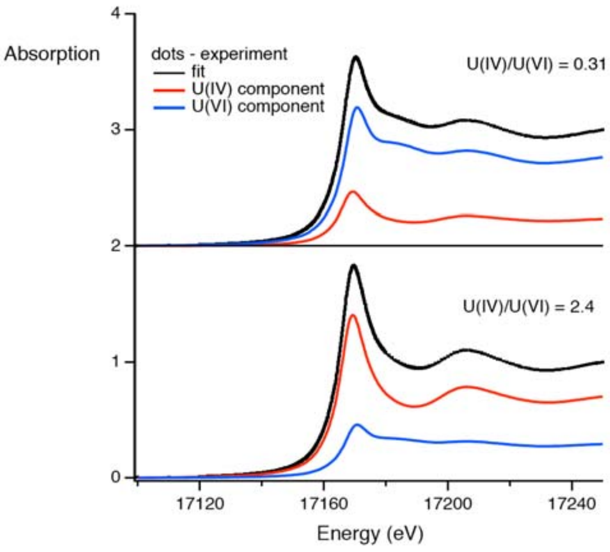

Absorption spectrum of a uranium complex

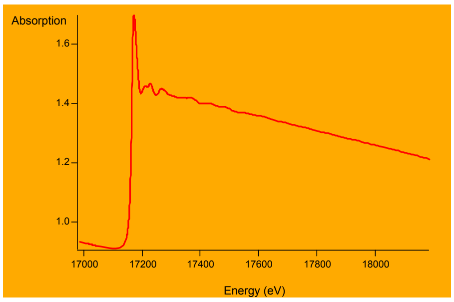

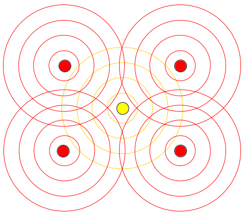

Oscillations in the absorption spectrum above the absorption edge

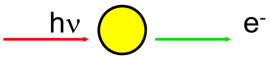

Scattering of photoelectrons at neighboring atoms

Interference between outgoing and backscattered electron waves

EXAFS data analysis

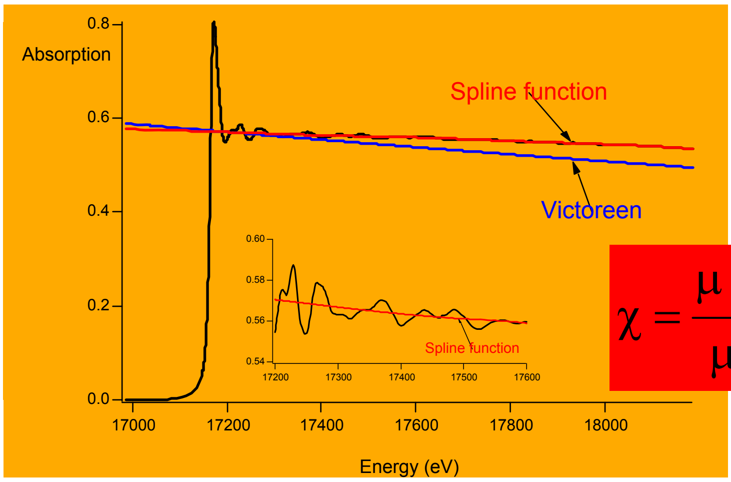

$$\chi = \frac{\mu - \mu_{\mathrm{Spline}}}{\mu_{\mathrm{Victoreen}}}$$

EXAFS spectrum and Fourier transform magnitude

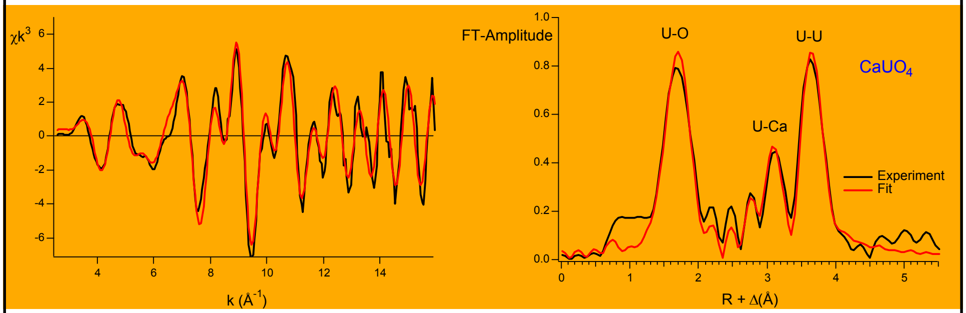

Aim of EXAFS measurement

Determination of structural parameters for the neighboring atoms

• Coordination number	N (± 20%)
• Interatomic distance	R (± 0,02 Å)
• Debye-Waller factor	σ^2 (± 0,005 Å^2)
• Type of neighboring atom	Z (± 4)

Condition for the interpretation:	Species is present in the sample to > 80%

Concentration limits:

• XANES spectroscopy	10^{-5} mol/L
• EXAFS spectroscopy	5×10^{-4} mol/L / 50-100 ppm

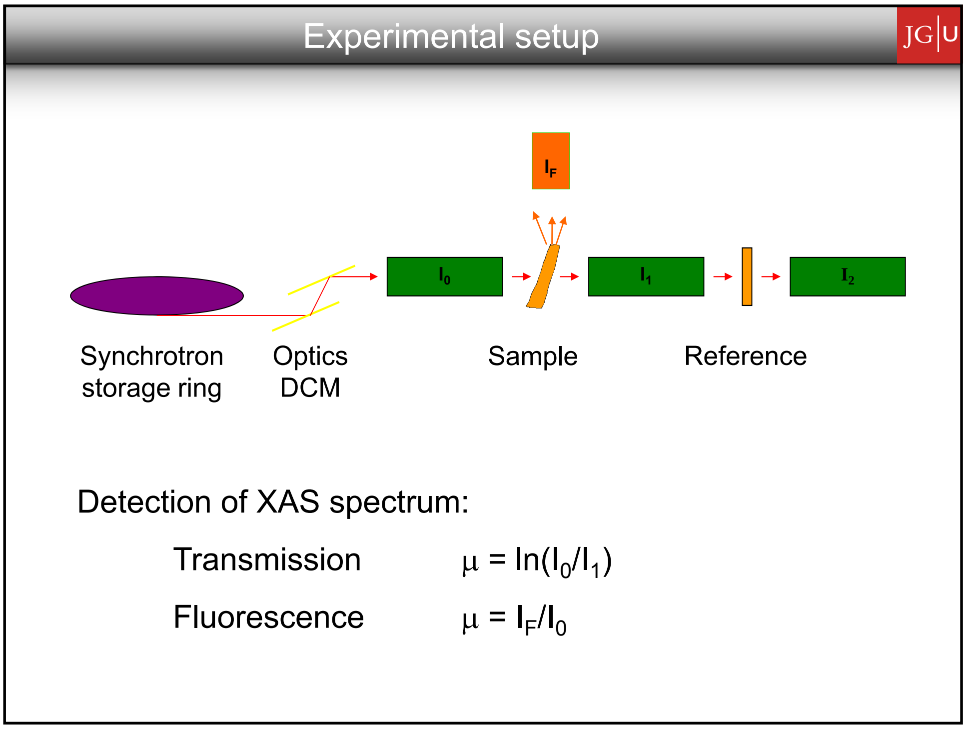

Experimental setup

I_F

I_0 I_1 I_2

Synchrotron
storage ring

Optics
DCM

Sample

Reference

Detection of XAS spectrum:

Transmission $\mu = \ln(I_0/I_1)$

Fluorescence $\mu = I_F/I_0$

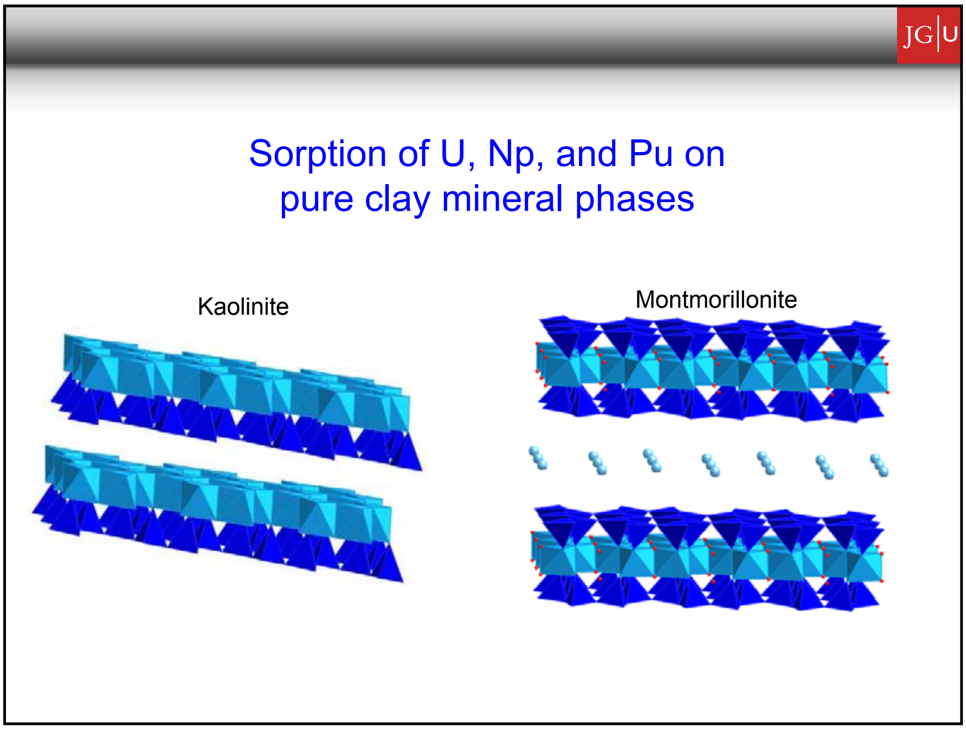

Sorption of U, Np, and Pu on pure clay mineral phases

Kaolinite

Montmorillonite

Sorption of U(VI) on kaolinite

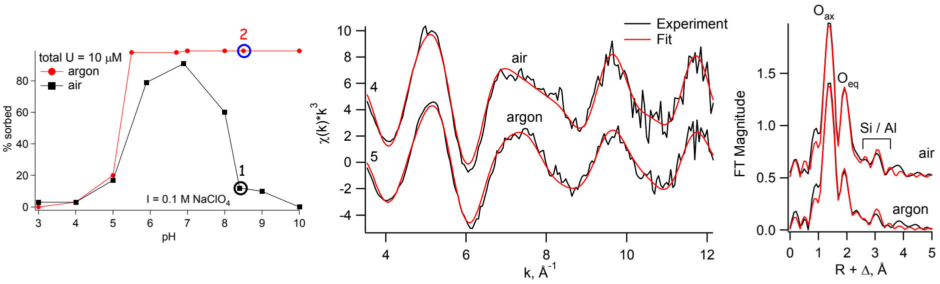

Sample		2 x O_{ax}		5 x O_{eq}		1 x Si / Al		1 x Si / Al	
		R(Å)	σ^2(Å^2)	R(Å)	σ^2(Å^2)	R(Å)	σ^2(Å^2)	R(Å)	σ^2(Å^2)
1	air	1.81	0.0023	2.41	0.0094	3.07	0.0010	3.28	0.0022
2	argon	1.80	0.0024	2.36	0.0155	3.09	0.0040	3.30	0.0047
$[UO_2(CO_3)_3]^{4-}$		1.80	0.0010	2.44	0.0050	-	-	-	-

$\Delta R = \pm\ 0.02$ Å, $\Delta\sigma^2 = 0.001$ Å^2

Reich et al., AIP Conf. Proc. (XAFS13) 882, 179 (2007)

Sorption of U(VI) on kaolinite

	Argon	Air
EXAFS [1]	U-O_{eq}: ≈ 2.36 Å < UO_2^{2+}(aq.) no change with pH	U-O_{eq}: 2.36 – 2.41 Å increase with pH
	U-Al/Si interactions at 3.1 and 3.3 Å	
Conclusions Estimates [2]	inner-sphere sorption of UO_2^{2+} edge-sharing with [SiO_4] and or [AlO_6] 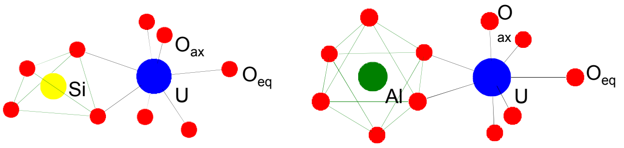 U-Si: 2.7 – 3.1 Å	U-Al: 3.2 – 3.4 Å

[1] Reich et al., AIP Conf. Proc. (XAFS13) 882, 179 (2007)

[2] Hennig, Reich et al., Radiochim. Acta 90, 653 (2002)

Quantum chemical modeling of U(VI) on kaolinite

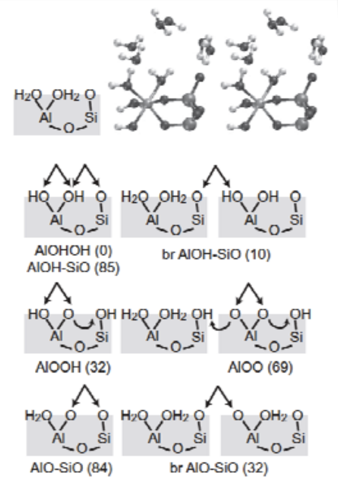

Sketches of various sites of bidentate U(VI) sorption on solvated (010) edge surface sites [2]

A few conclusions from [1]:

- Sorption on the (010) surface is energetically favorable compared to sorption on equivalent sites at the Al(o) (001) surface.
- Bidentate sorption at alumina related sites is favored over adsorption complexes that involve silica tetrahedra (AlOH-SiO).
- U(VI) hydroxide was obtained as adsorbed species.
- Several sorption complexes may be consistent with EXAFS data.

[1] Kremleva et al., Radiochim. Acta 99, 635 (2010)

[2] Kremleva et al., GCA 75, 706 (2011)

Sorption of Np(V) on kaolinite

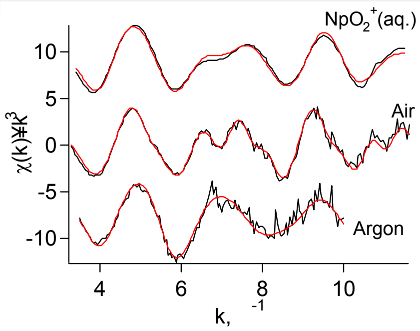

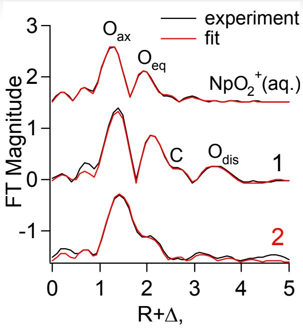

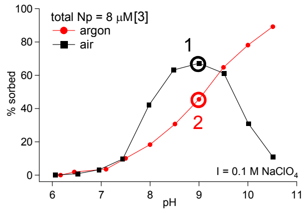

Sample	pH	CO_2	2 x O_{ax}	4 x O_{eq}	2 x C	2 x O_{dis}
1	9.0	yes	1.85	2.57	2.97	4.28
2	9.0	no	1.85	2.45		
$NpO_2(CO_3)_3^{5-}$ (aq.) [1]			1.86	2.53	2.98	4.22
NpO_2^+ (aq.) [2]	0		1.82	2.49		

[1] Clark et al., JACS 118, 2089 (1996)

[2] Reich et al., Radiochim. Acta 88, 633 (2000)

[3] Amayri et al., Radiochim. Acta 99, 349 (2011)

Sorption of Np(V) on kaolinite

	Argon	Air
EXAFS [1]	Np-O_{eq} distance similar to or shorter than in NpO_2^+(aq.), Np-Al/Si at 3.2 and 3.8 Å	bidentate coordination of two CO_3^{2-} ligands
Conclusions	inner-sphere sorption of NpO_2^+ 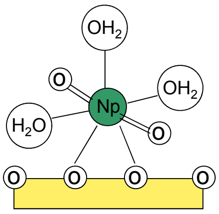 	inner-/outer-sphere sorption of $NpO_2(CO_3)_2^{3-}$ 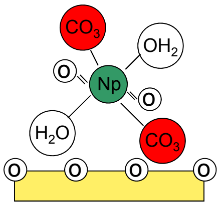

Reich et al., AIP Conf. Proc. (XAFS13) 882, 179 (2007)

Sorption of Pu(III) and Pu(IV) on kaolinite

Partial pair distribution functions

Sample 1 – Pu(III)

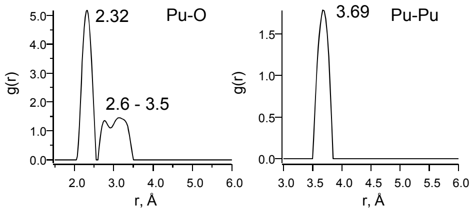

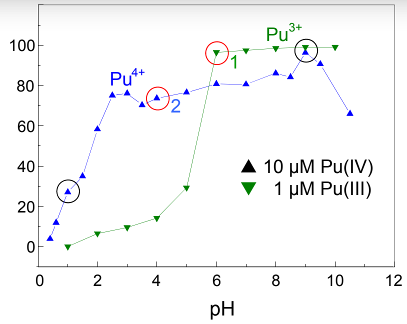

Sample 2 – Pu(IV)

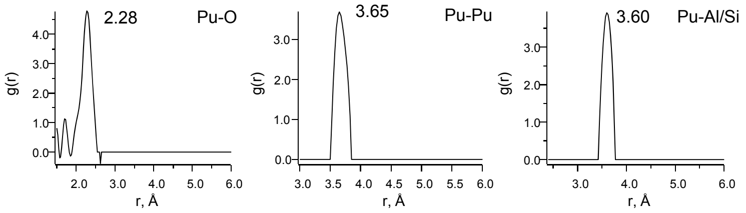

- Oxidation of Pu(III) to Pu(IV)
- Pu(IV): inner-sphere sorption of polynuclear Pu(IV) species

Ta. Reich, Dissertation, Johannes Gutenberg University Mainz (2008)

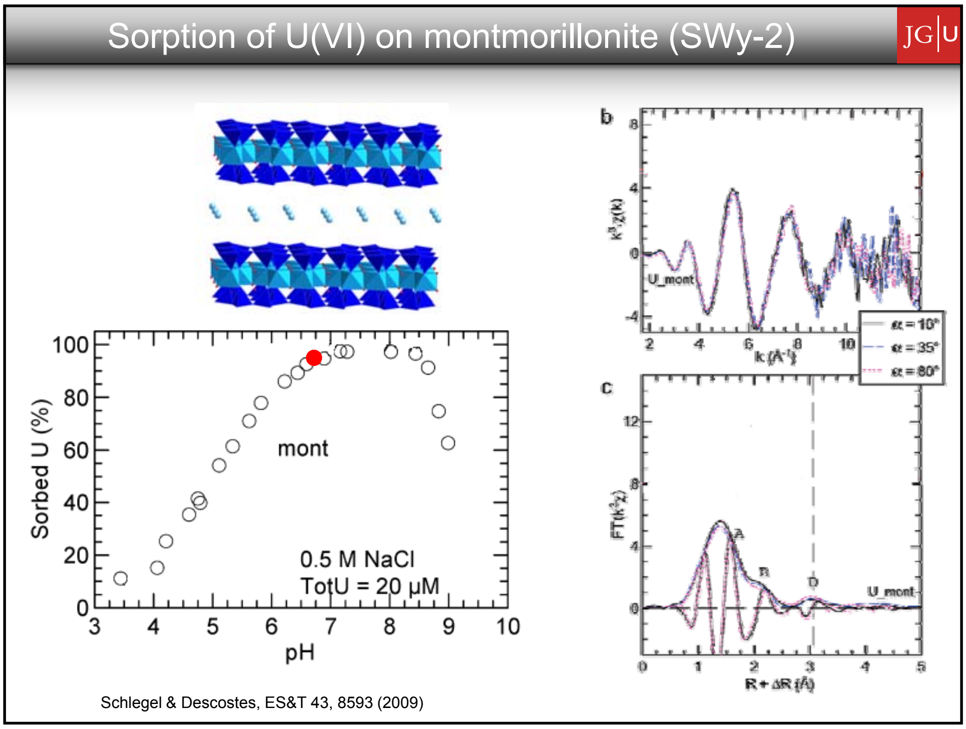

Sorption of U(VI) on montmorillonite (SWy-2)

Schlegel & Descostes, ES&T 43, 8593 (2009)

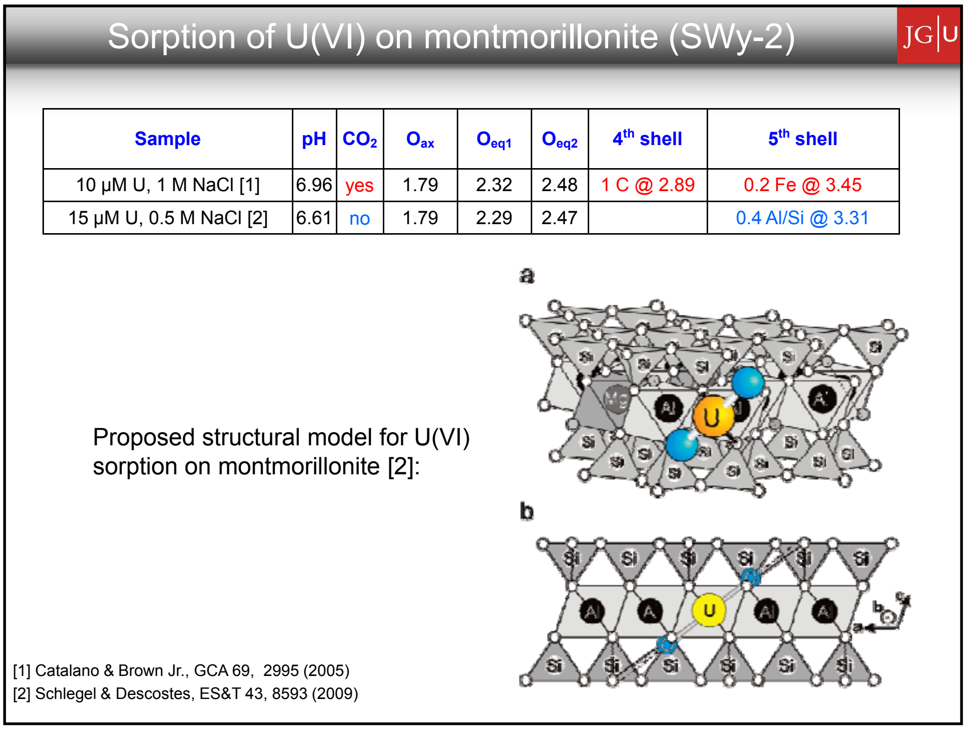

Sorption of U(VI) on montmorillonite (SWy-2)

Sample	**pH**	**CO_2**	**O_{ax}**	**O_{eq1}**	**O_{eq2}**	**4th shell**	**5th shell**
10 µM U, 1 M NaCl [1]	6.96	yes	1.79	2.32	2.48	1 C @ 2.89	0.2 Fe @ 3.45
15 µM U, 0.5 M NaCl [2]	6.61	no	1.79	2.29	2.47		0.4 Al/Si @ 3.31

Proposed structural model for U(VI) sorption on montmorillonite [2]:

[1] Catalano & Brown Jr., GCA 69, 2995 (2005)
[2] Schlegel & Descostes, ES&T 43, 8593 (2009)

Sorption of Np(V) on montmorillonite / without CO_2

Cation exchange: Na-mont. + NpO_2^+ ⇔ NpO_2-mont. + Na^+ $K_c = 1.1$

Surface complexation: $\equiv SOH + NpO_2^+ \Leftrightarrow \equiv SONpO_2^0 + H^+$ $\log K_1 = -2.2$

$\equiv SOH + NpO_2^+ + H_2O \Leftrightarrow \equiv SONpO_2OH^- + 2H^+$ $\log K_2 = -12.0$

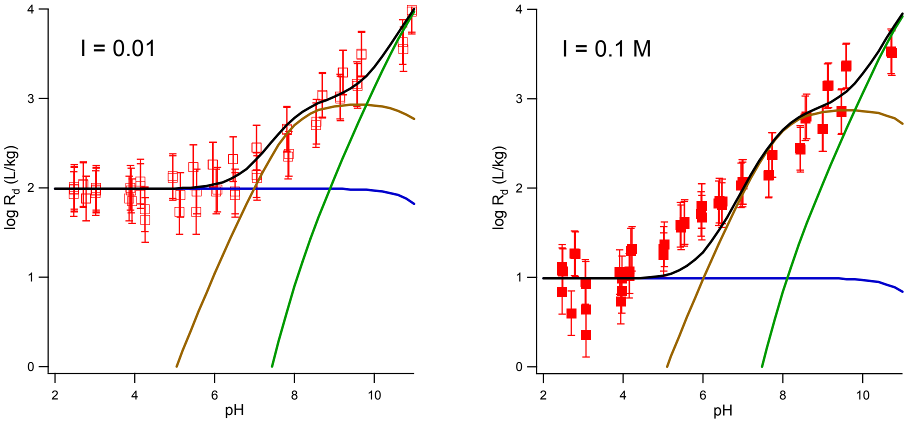

Black solid lines represent the overall model

Bradbury & Baeyens, J. Contam. Hydrol. 27, 223 (1997)

Sorption of Np(V) on montmorillonite / $p_{CO2} = 10^{-3.5}$ atm

Cation-exchange and surface-complexation constants: $K_c = 1.1$

$\log K_1 = -2.2$

Black solid line represents the model $\log K_2 = -12.0$

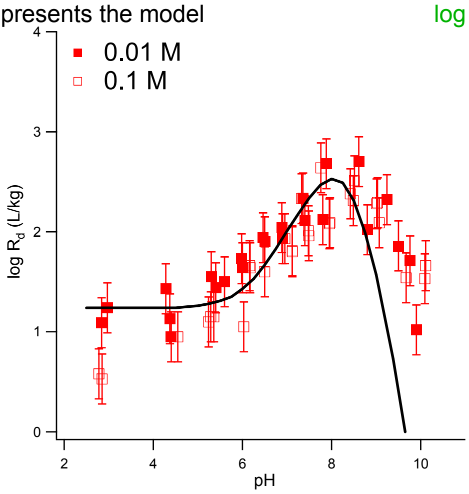

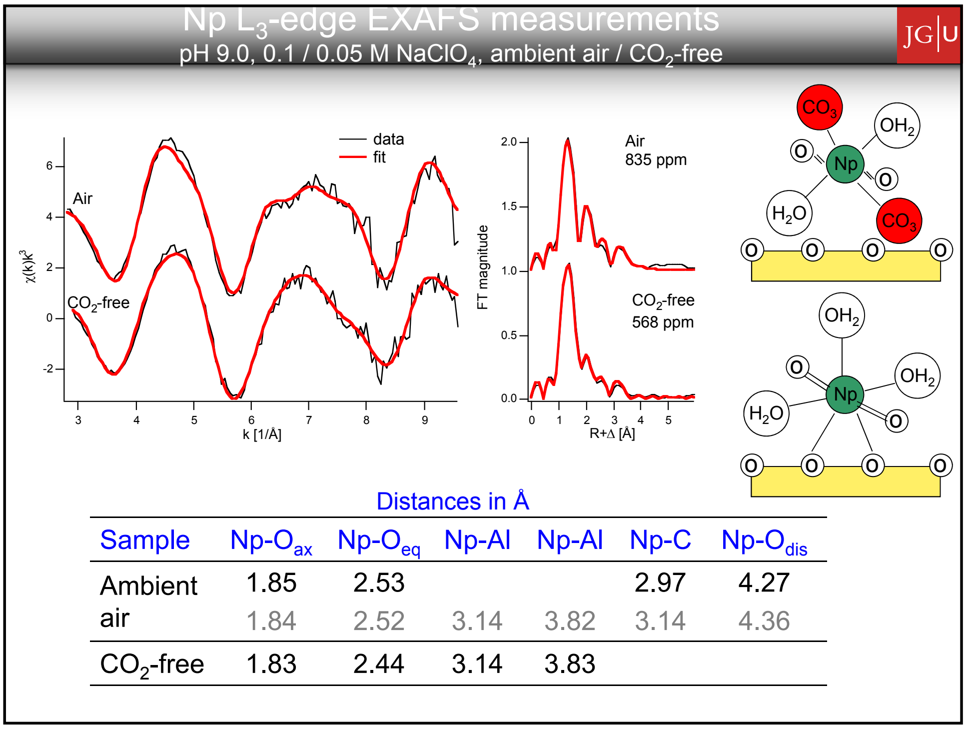

Np L_3-edge EXAFS measurements

pH 9.0, 0.1 / 0.05 M $NaClO_4$, ambient air / CO_2-free

Distances in Å

Sample	Np-O_{ax}	Np-O_{eq}	Np-Al	Np-Al	Np-C	Np-O_{dis}
Ambient air	1.85 1.84	2.53 2.52	 3.14	 3.82	2.97 3.14	4.27 4.36
CO_2-free	1.83	2.44	3.14	3.83		

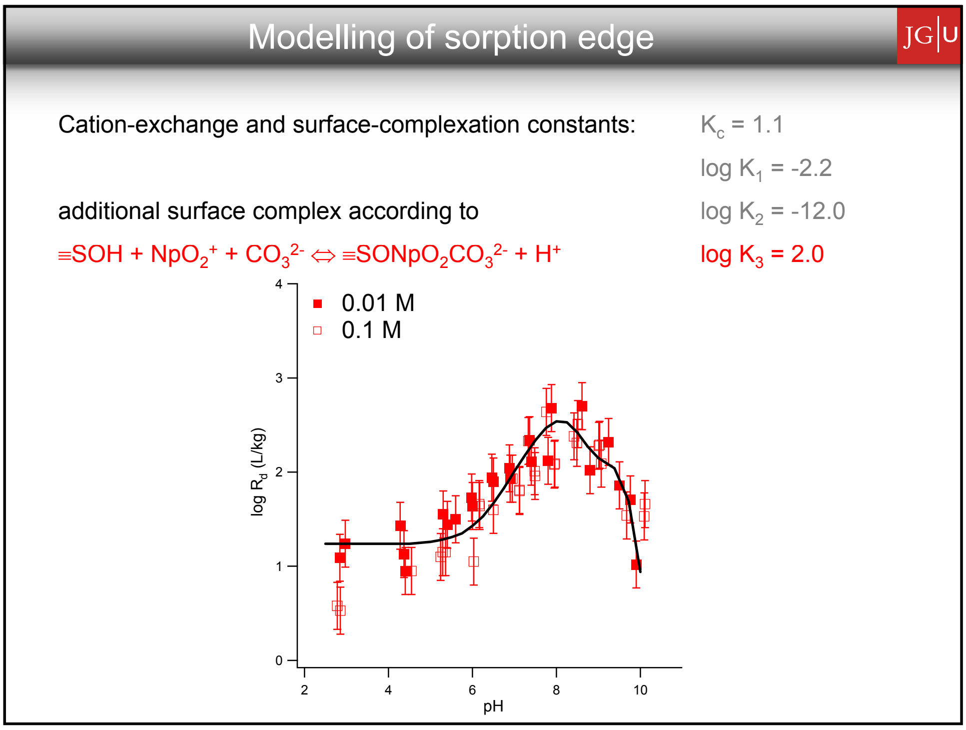

Modelling of sorption edge

Cation-exchange and surface-complexation constants:

$K_c = 1.1$

$\log K_1 = -2.2$

$\log K_2 = -12.0$

additional surface complex according to

$\equiv SOH + NpO_2^+ + CO_3^{2-} \Leftrightarrow \equiv SONpO_2CO_3^{2-} + H^+$ $\log K_3 = 2.0$

Sorption of Np(V) and Pu(V) on montmorillonite (SWy-1)

Dependence of apparent sorption rate constant on mol fraction of exchangeable H⁺ for Pu(V) sorption

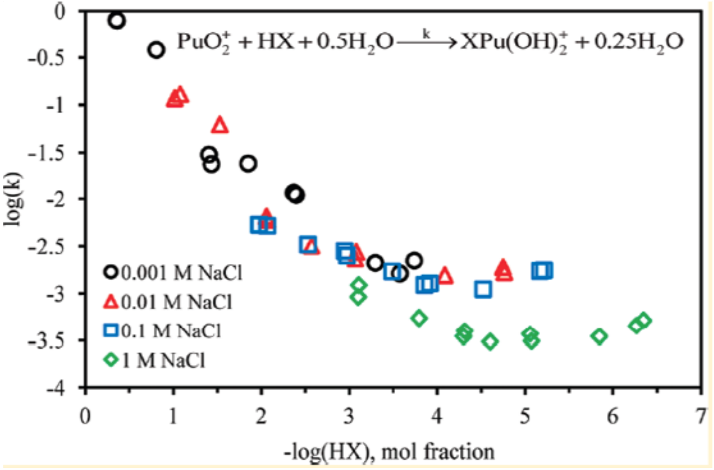

Differences in Np(V) and Pu(V) sorption behavior are indicative of surface-mediated transformation of Pu(V) to Pu(IV).

Zavarin et al., ES&T 46, 2692 (2012)

Characterization of OPA

OPA from Mont Terri (Switzerland) was used as a reference for natural clays.

- ✓ Low hydraulic conductivity
- ✓ Strong retention of RN
- ✓ Selfsealing

Average mineralogy of OPA [1]

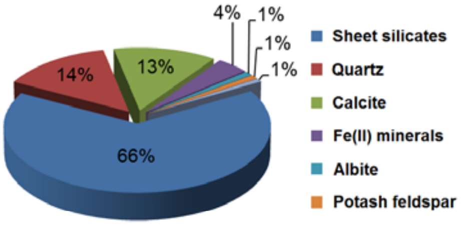

[1] Nagra, NTB 02-03, 2002

OPA
•CEC: 9 ± 2 meq/100 g
•Spec. surf. area: 38.0 m²/g
•TOC: ≤ 1%

OPA pore water [2]
pH 7.6
I = 0.39 M

[2] Pearson (1998), PSI Technical Report TM-44-98-07.

Diffusion experiments with Np(V)

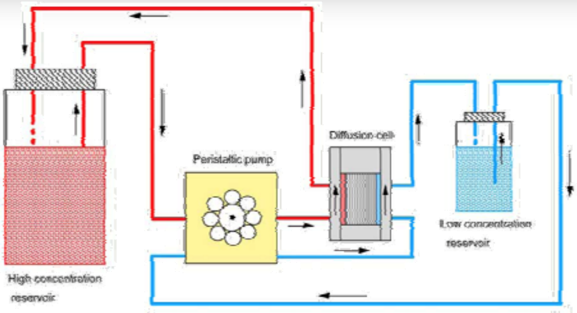

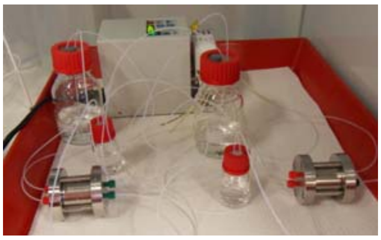

Wu et al., Environ. Sci. Technol., 43, 6567 (2009)

Diffusion experiments with ^{237}Np(V) and ^{22}Na

Synth. pore water, pH 7.6, $p_{CO_2} = 10^{-3.5}$ atm

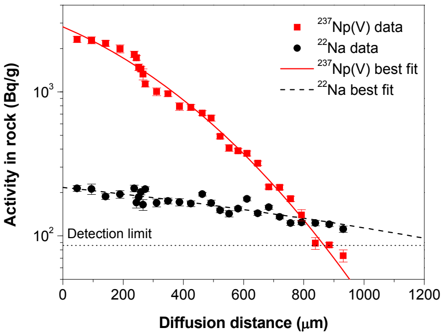

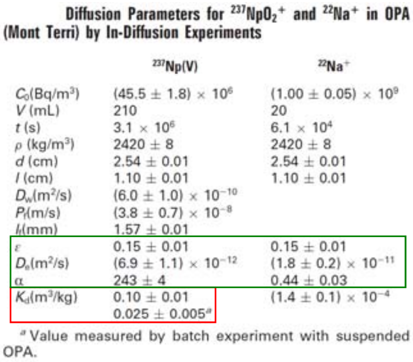

Diffusion Parameters for $^{237}NpO_2^+$ and $^{22}Na^+$ in OPA (Mont Terri) by In-Diffusion Experiments

	^{237}Np(V)	$^{22}Na^+$
C_0(Bq/m^3)	$(45.5 \pm 1.8) \times 10^6$	$(1.00 \pm 0.05) \times 10^9$
V (mL)	210	20
t (s)	3.1×10^6	6.1×10^4
ρ (kg/m^3)	2420 ± 8	2420 ± 8
d (cm)	2.54 ± 0.01	2.54 ± 0.01
l (cm)	1.10 ± 0.01	1.10 ± 0.01
D_w(m^2/s)	$(6.0 \pm 1.0) \times 10^{-10}$	
P_f(m/s)	$(3.8 \pm 0.7) \times 10^{-8}$	
l_f(mm)	1.57 ± 0.01	
ε	0.15 ± 0.01	0.15 ± 0.01
D_e(m^2/s)	$(6.9 \pm 1.1) \times 10^{-12}$	$(1.8 \pm 0.2) \times 10^{-11}$
α	243 ± 4	0.44 ± 0.03
K_d(m^3/kg)	0.10 ± 0.01 0.025 ± 0.005[a]	$(1.4 \pm 0.1) \times 10^{-4}$

[a] Value measured by batch experiment with suspended OPA.

Very slow diffusion of Np in OPA under aerobic conditions in comparison with ^{22}Na or HTO ⇨ clay formations are suitable materials for high level waste repository

Wu et al., Environ. Sci. Technol., 43, 6567 (2009)

Sorption of Np(V) on OPA

[Np(V)] = 8×10^{-6} M, S/L = 15 g/L, saturated calcite solution

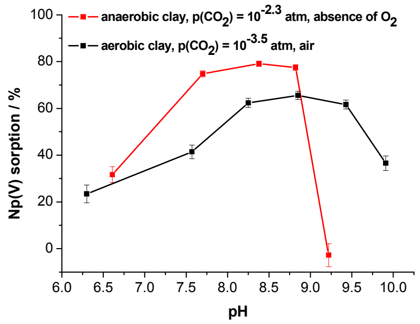

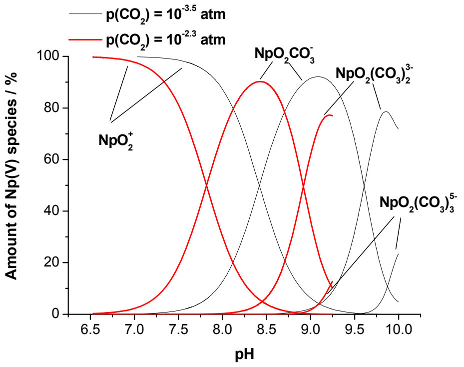

- Sorption edge is shifted due to changes in Np(V) speciation
- An increase in sorption between pH 7-9 is caused by partial reduction of Np(V) to Np(IV)

Fröhlich et al., Radiochim. Acta 99, 71 (2011)

Spectroscopic methods

XAFS (X-ray absorption fine-structure)

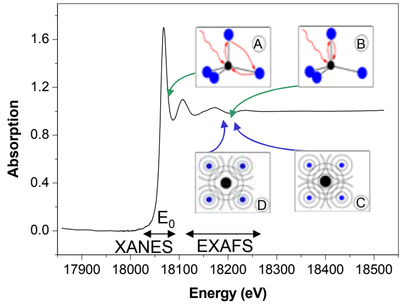

ESRF, ROBL BM 20

OPA powder sample

µ-XAFS (X-ray absorption fine-structure)
- Actinide speciation

µ-XRF (X-ray fluorescence)
- Elemental distributions

µ-XRD (X-ray diffraction)
- Crystalline phases

PSI, SLS, microXAS

OPA thin section

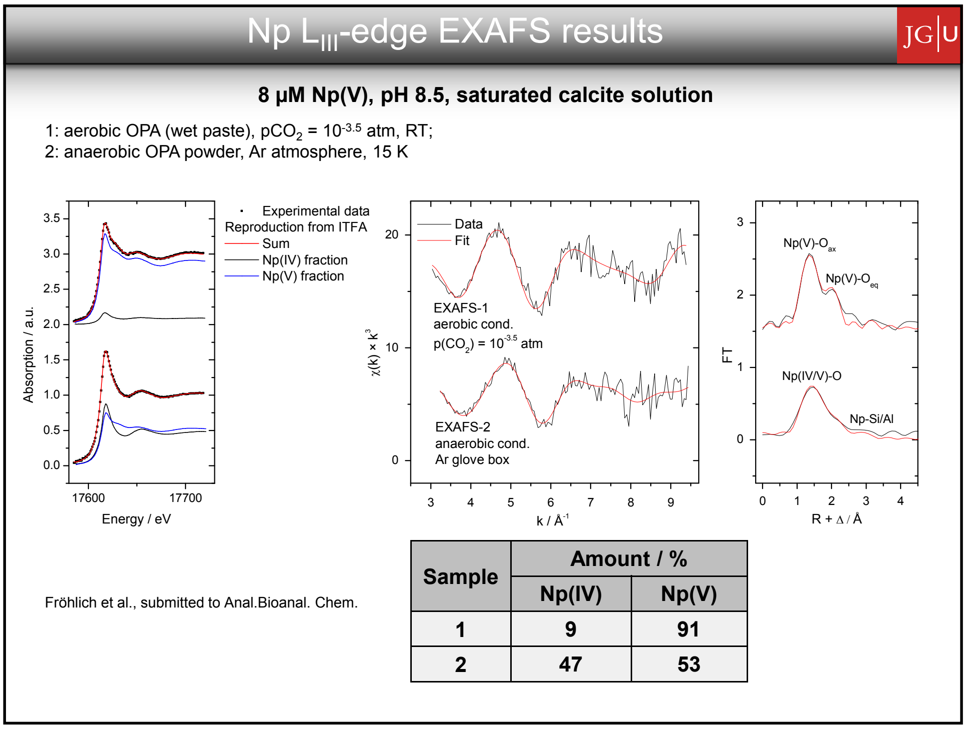

Np L_{III}-edge EXAFS results

8 µM Np(V), pH 8.5, saturated calcite solution

1: aerobic OPA (wet paste), $pCO_2 = 10^{-3.5}$ atm, RT;
2: anaerobic OPA powder, Ar atmosphere, 15 K

Fröhlich et al., submitted to Anal.Bioanal. Chem.

Sample	Amount / %	
	Np(IV)	Np(V)
1	9	91
2	47	53

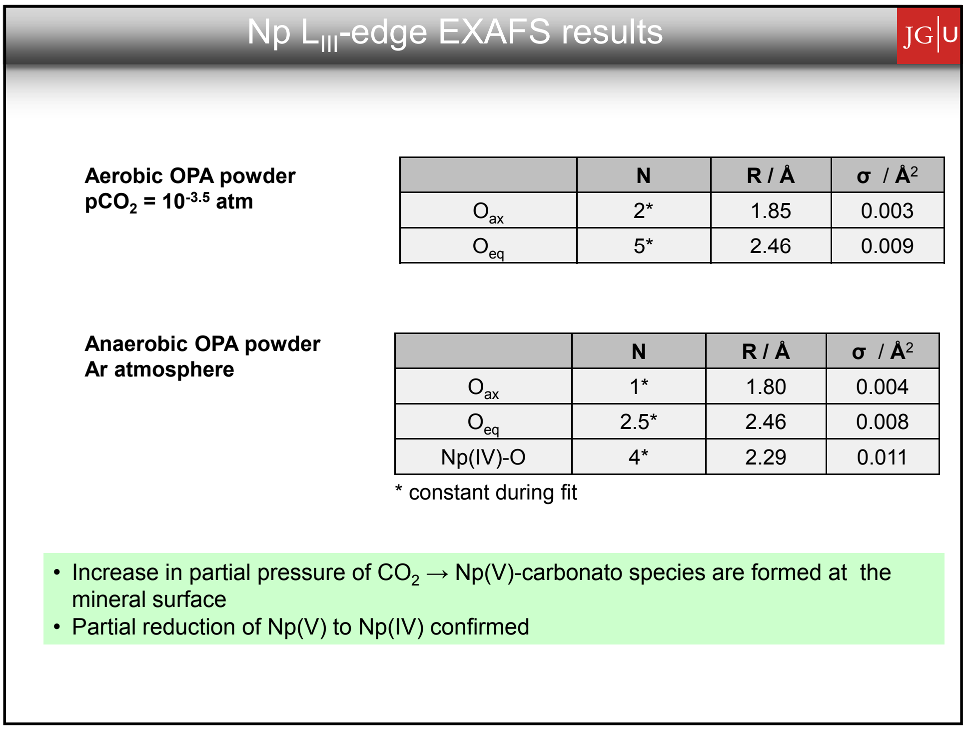

Np L_{III}-edge EXAFS results

Aerobic OPA powder
$pCO_2 = 10^{-3.5}$ atm

	N	R / Å	σ / Å²
O_{ax}	2*	1.85	0.003
O_{eq}	5*	2.46	0.009

Anaerobic OPA powder
Ar atmosphere

	N	R / Å	σ / Å²
O_{ax}	1*	1.80	0.004
O_{eq}	2.5*	2.46	0.008
Np(IV)-O	4*	2.29	0.011

* constant during fit

- Increase in partial pressure of CO_2 → Np(V)-carbonato species are formed at the mineral surface
- Partial reduction of Np(V) to Np(IV) confirmed

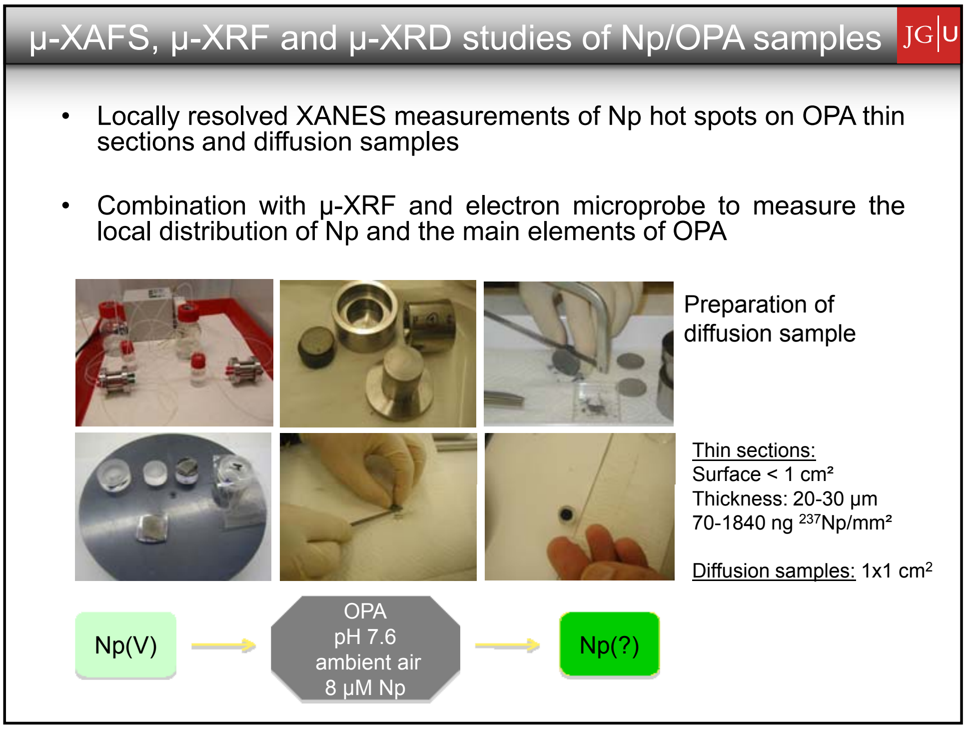

μ-XAFS, μ-XRF and μ-XRD studies of Np/OPA samples

- Locally resolved XANES measurements of Np hot spots on OPA thin sections and diffusion samples
- Combination with μ-XRF and electron microprobe to measure the local distribution of Np and the main elements of OPA

Preparation of diffusion sample

Thin sections:
Surface < 1 cm²
Thickness: 20-30 μm
70-1840 ng ^{237}Np/mm²

Diffusion samples: 1x1 cm^2

Np(V) → OPA pH 7.6 ambient air 8 μM Np → Np(?)

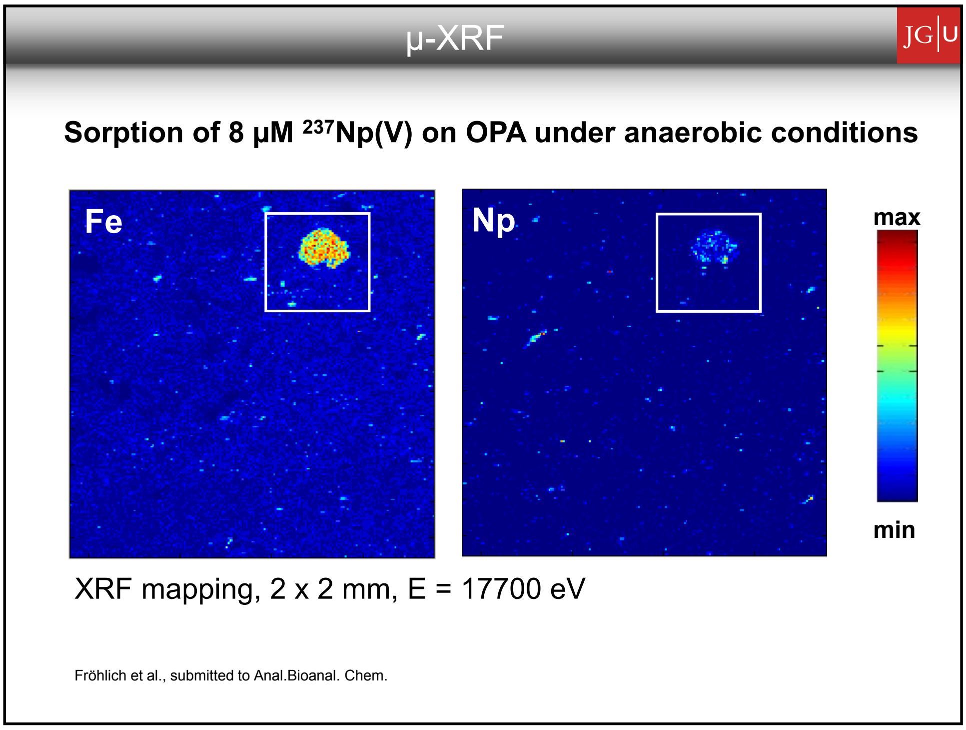

μ-XRF

Sorption of 8 μM ^{237}Np(V) on OPA under anaerobic conditions

XRF mapping, 2 x 2 mm, E = 17700 eV

Fröhlich et al., submitted to Anal.Bioanal. Chem.

µ-XRF

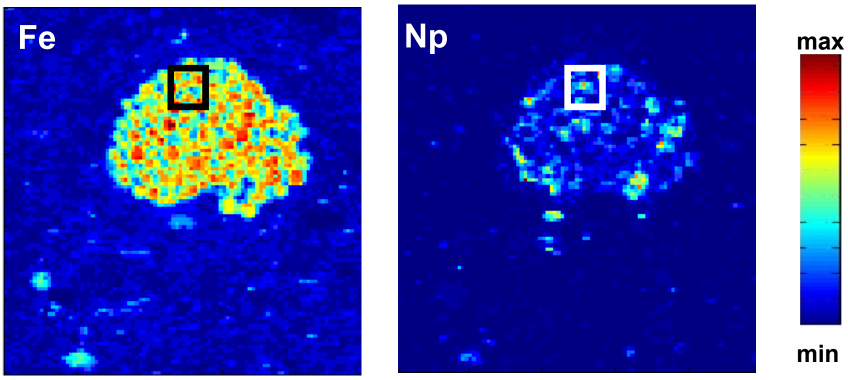

XRF mapping, 500 x 500 µm, E = 17700 eV

→ µ-XRD und µ-XANES

µ-XANES

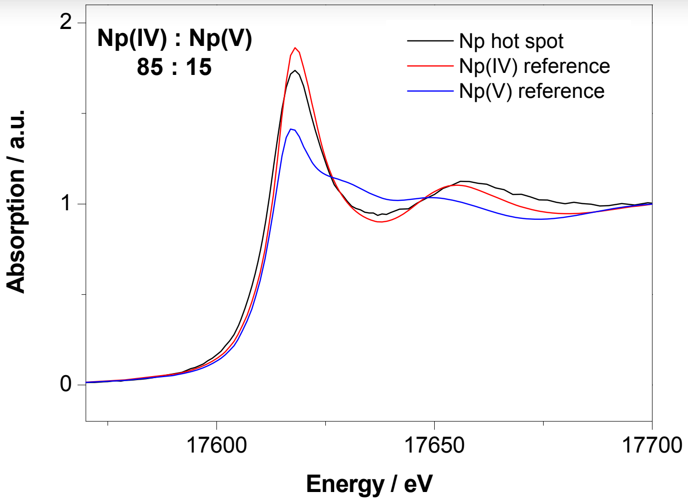

- Most of Np(V) has been reduced to Np(IV)
- Enrichments of Np(IV) are located near areas of high iron content, indicating that reduction is caused by Fe(II) minerals

μ-XRD – comparison with pyrite

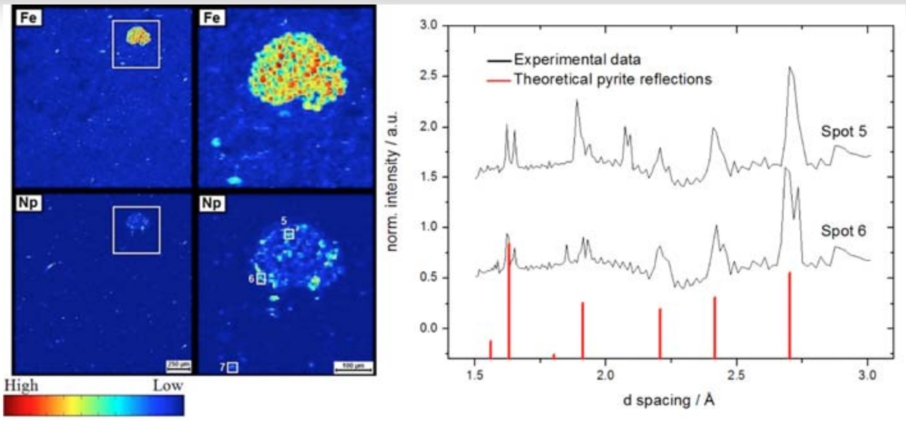

XRD mapping, 20 x 20 µm, E = 17700 eV

- Pyrite is one of the redox-active mineral phase of OPA determining the speciation of Np after uptake on OPA
- Reduction process of Np takes place on the OPA surface and not in solution
- Immobilization of Np by OPA

Sorption experiments of Pu(VI) on OPA

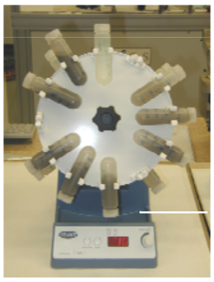

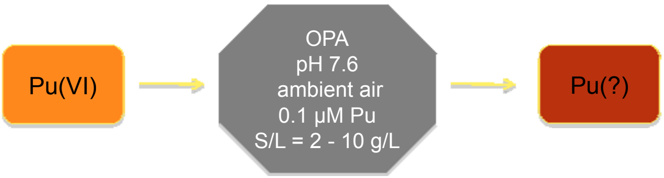

Pu(VI)

OPA
pH 7.6
ambient air
0.1 µM Pu
S/L = 2 - 10 g/L

Pu(?)

Summary

- Wet-chemistry experiments are useful for obtaining K_d values or diffusion parameters that are needed for the safety assessment of future nuclear waste repositories.

- However, these experiments cannot provide a molecular-lever understanding of the underlying processes.

- Natural clays are heterogeneous with respect to mineralogy. Therefore, synchrotron radiation is a unique tool for determining chemical speciation with high spatial resolution.

- Sorption of Np on OPA

  The increase in K_d under anaerobic conditions is caused by partial reduction of Np(V) to Np(IV).

Acknowledgement

J. Drebert, A. Jermolajev, S. Wendt

D. Banerjee, H. Funke, Ch. Hennig, A. Roßberg,
A.C. Scheinost

B. Baeyens, C. Borca, M.H. Bradbury, D. Grolimund

Ch. Marquardt

Working group at Mainz

Working group at Mainz

Institute of Nuclear Chemistry

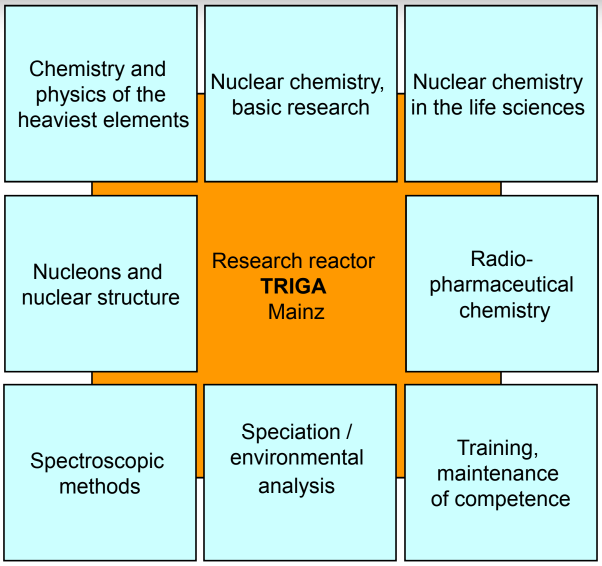

Chemistry and physics of the heaviest elements

Nuclear chemistry, basic research

Nuclear chemistry in the life sciences

Nucleons and nuclear structure

Research reactor **TRIGA** Mainz

Radio-pharmaceutical chemistry

Spectroscopic methods

Speciation / environmental analysis

Training, maintenance of competence

Resonance ionization mass spectrometry (RIMS) - a powerful tool for ultratrace analysis of long-lived radionuclides

N. Stöbener[1], P. Schönberg[1], G. Passler[2], T. Reich[1], N. Trautmann[1],

[1]University of Mainz, Institute of Nuclear Chemistry, 55099 Mainz, Germany
[2]University of Mainz, Institute of Physics, 55099 Mainz, Germany

Trilateral seminar on supramolecular, intermolecular, interaggregate interactions and separation chemistry, IPCE RAS, Moscow, Russian Federation
20.-23.07.2012

Outline

- Introduction
  - Long-lived radionuclides
  - Motivation
  - Challenges for analytical chemistry
- RIMS
  - Idea
  - Setup
- Applications
  - $^{239-242}$Pu, ^{237}Np, ^{99g}Tc

Introduction

- Nuclear energy (civil/military) produces radionuclides (RN):
  - Short-lived: ^{131}I ($T_{1/2}$ ~8 d)
  - Long-lived: ^{239}Pu ($T_{1/2}$ ~2×10^4 a)
    ^{99g}Tc ($T_{1/2}$ ~2×10^5 a)
    ^{237}Np ($T_{1/2}$ ~2×10^6 a)

long half-lives
+ high mobility in aquatic systems

→ long term hazards for the environment

Motivation

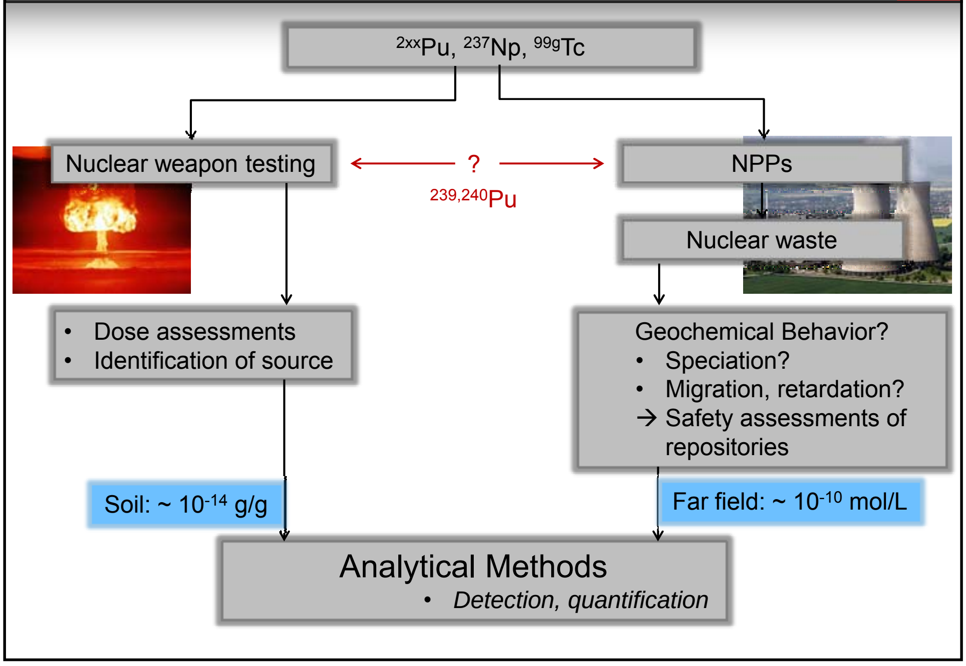

^{2xx}Pu, ^{237}Np, ^{99g}Tc

Nuclear weapon testing ← ? → NPPs

^{239,240}Pu

Nuclear waste

- Dose assessments
- Identification of source

Geochemical Behavior?
- Speciation?
- Migration, retardation?

→ Safety assessments of repositories

Soil: ~ 10^{-14} g/g

Far field: ~ 10^{-10} mol/L

Analytical Methods
- *Detection, quantification*

Detection of long lived RN

- Ultratrace analysis of long lived radionuclides:

mass spectrometry (ICP-MS, TIMS, …)

- Problem: isobaric Interferences

ICP-MS standard
4×10^{-8} M uranium

RIMS: Principle

- RIMS: Resonance ionization mass spectrometry
  Introduces element selectivity ionization

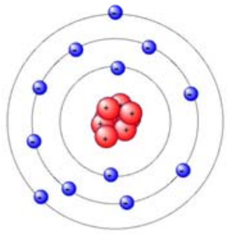

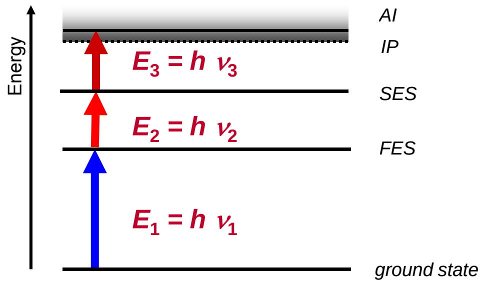

$E_3 = h\,\nu_3$

$E_2 = h\,\nu_2$

$E_1 = h\,\nu_1$

- Resonant, multistep excitation and ionization of sample atoms with laser radiation
- Uniqueness of optical transitions → element selectivity

RIMS: Principle

- RIMS: Resonance ionization mass spectrometry
  Introduces element selectivity ionization

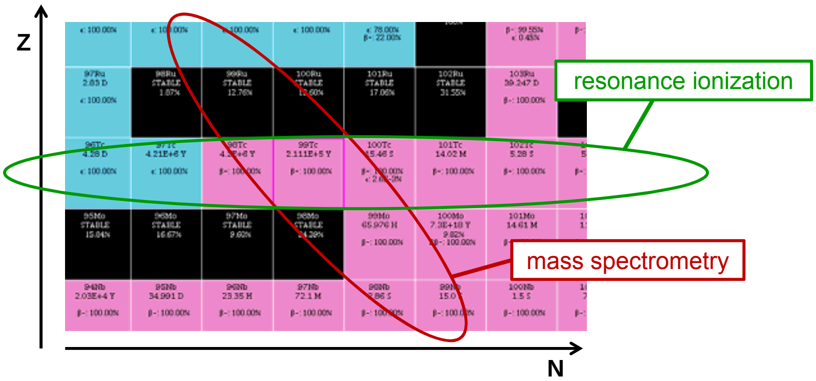

- No isobaric interferences!

RIMS: Setup

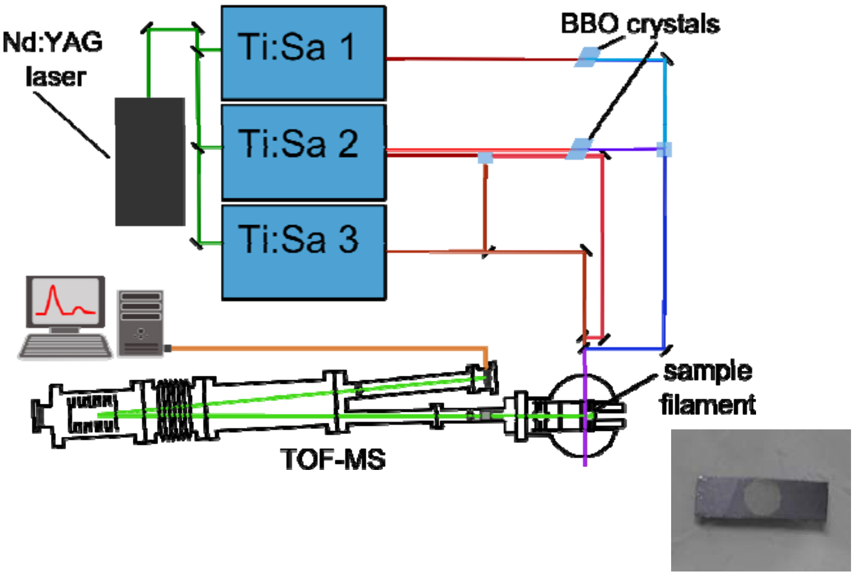

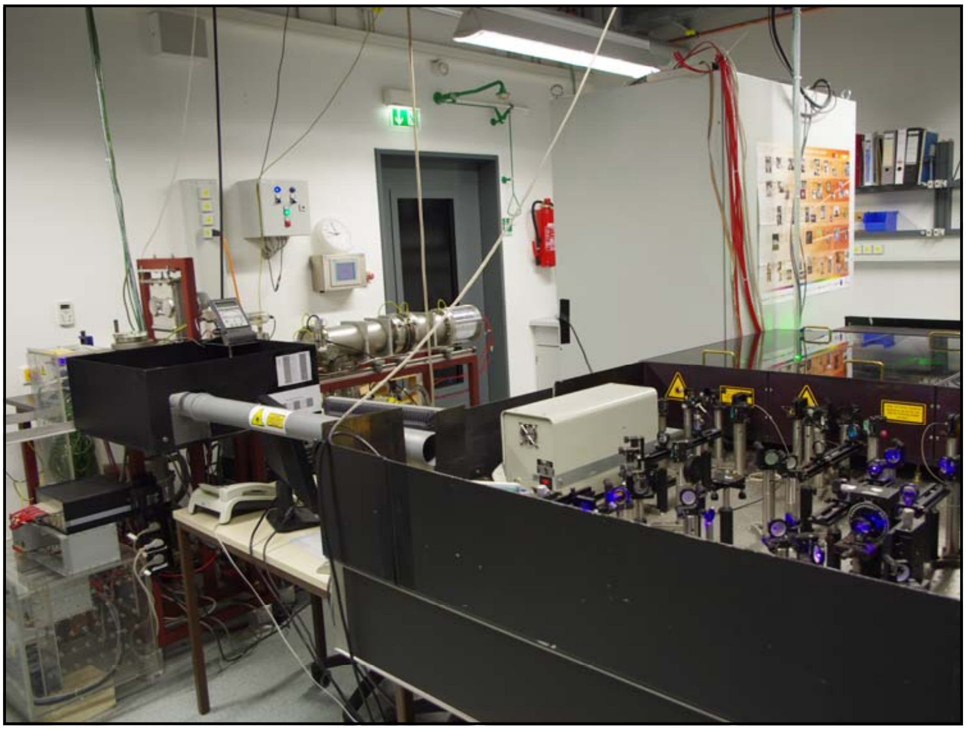

Plutonium isotopes ($^{239-242}$Pu)

- Application:
  - Identification of Pu sources
  - Dose assessment for fallout Pu
- Tracer: ^{244}Pu
- Limit of detection (LOD): 1×10^{6} atoms (< 1 fg) / 2 g sample

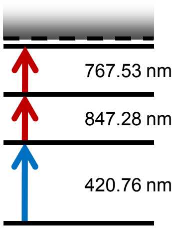

Excitation scheme for ^{239}Pu
IP = 6.03 eV

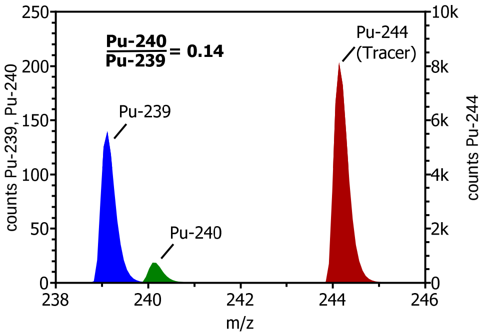

Mass spectrum showing fallout plutonium in a soil sample

$\varepsilon = 3\times10^{-6}$

Neptunium-237

- Application:
  - Migration studies
  - Np(IV,V) redox speciation studies (CE-RIMS)
- Tracer: ^{235}Np (under development)
- LOD: 2×10^{7} atoms (< 10 fg)

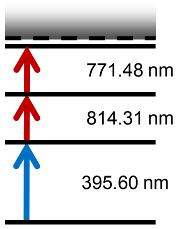

Excitation scheme for ^{237}Np
IP = 6.27 eV

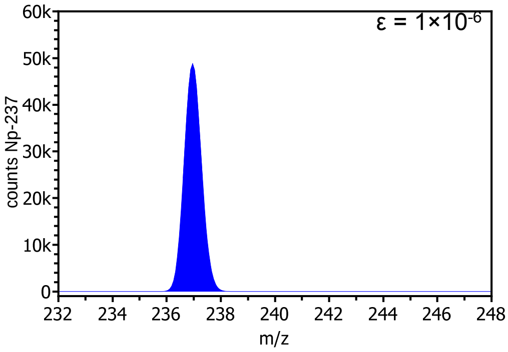

Mass spectrum of 4x10^{11} atoms ^{237}Np

Technetium-99g

- Application:
  - Migration studies
- Tracer: ^{97}Tc?
- LOD: 3×10^{6} atoms (< 1 fg)

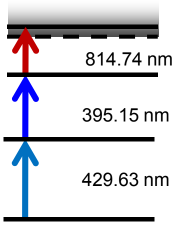

Excitation scheme for ^{99g}Tc
IP = 7.12 eV

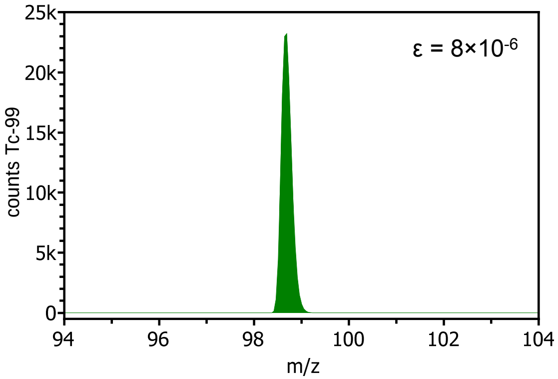

Mass spectrum of 2x10^{10} atoms ^{99g}Tc

Conclusion

- RIMS: Sensitive Method for the detection of stable or long-lived isotopes
- Element selective mass spectrometric method due to optical ionization
- Strength: Suppression of isobaric interferences

Acknowledgement

Deutsche Forschungsgemeinschaft
DFG
GRK 826

Bundesministerium
für Wirtschaft
und Technologie

… and you for your kind attention!

Interaction of Plutonium with Natural Clay

U. Kaplan[1], S. Amayri[1], J. Drebert[1], D.R. Fröhlich[1], D. Grolimund[2], T. Reich[1]

[1]Johannes Gutenberg University Mainz, Institute of Nuclear Chemistry
[2]Paul Scherrer Institute, Swiss Light Source

7th European Summer School on Supramolecular, Intermolecular, Interaggregate Interactions and Separation Chemistry
Moscow, Russia, July 20-23, 2012

Outline

- Motivation
- Characteristics of Opalinus Clay (OPA)
- Aqueous chemistry of Pu
- Pu interaction with OPA
  - Sorption experiment
  - Spectroscopic investigations
    - ➢ µ-XANES [X-ray Absorption Near Edge Structure]
    - ➢ µ-XRF [X-ray fluorescence analysis]
    - ➢ µ-XRD [X-ray diffraction analysis]
- Summary

Motivation

- ❖ Repository based on a multi-barrier concept
  - i-) Technical barrier [spent nuclear fuel, container and glass-HLW].
  - ii-) Geotechnical barrier [depending on the geological repository].
  - iii-) Geological barrier [salt, granite or clay].

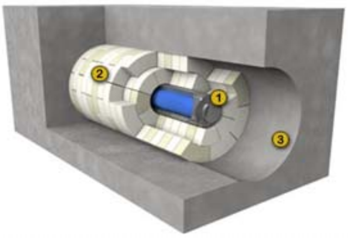

1-technical barrier
2-geotechnical barrier
3-geological barrier

- ❖ Detailed sorption studies of Pu are needed to predict its migration behaviour in the geological barrier after a leakage of Pu from the repository.

- ❖ Macroscopic experiment (sorption and diffusion) within microscopic investigations combined to determine the speciation of Pu.

[1] K. Gompper et al., Radioaktivität und Kernenergie, FZK (2001)

Characteristics of Opalinus Clay (OPA)

OPA from Mont Terri, Switzerland was chosen as a representative natural clay to study the migration behaviour of Pu.

Average mineralogy of OPA [2]

Mineral	Amount / %
Sheet silicates	66 ± 11
Quartz	14 ± 4
Calcite	13 ± 8
Fe(II)-bearing minerals	4.1 ± 2.3
Albite, feldspars, org. matter	2.8 ± 3.1

- ➢ high sorption capacity
- ➢ low hydraulic conductivity
- ➢ very low permeability

- CEC: 9 ± 2 meq/100 g
- Spec. surf. area: 38.0 m^2/g
- TOC: ≤ 1%

[2] Nagra (2002), NTB 02-03

Chemical properties of plutonium

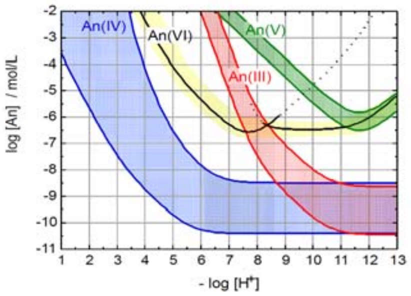

[3] Neck et al., C. R. Chimie 10 (2007) 959

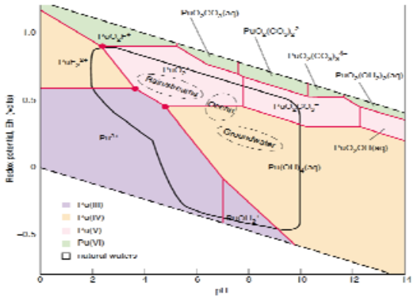

[4] Runde, Los Alamos Sci. 26 (2000) 392

- ❖ In solution, up to three oxidation states of Pu can coexist.
- ❖ Pu(III) and Pu(IV) have quite high sorption ability and low dissolution properties.
- ❖ Pu(V) and Pu(VI) have low sorption and higher dissolution properties.

Sorption of ^{238}U(VI) and ^{239}Pu(VI) on OPA

Ambient air, OPA pore water (pH 7.6)

[Pu(VI)] = 1×10^{-7} M, S/L = 2 - 10 g/L

[U(VI)] = 2×10^{-4} - 1×10^{-7} M, S/L = 15 g/L

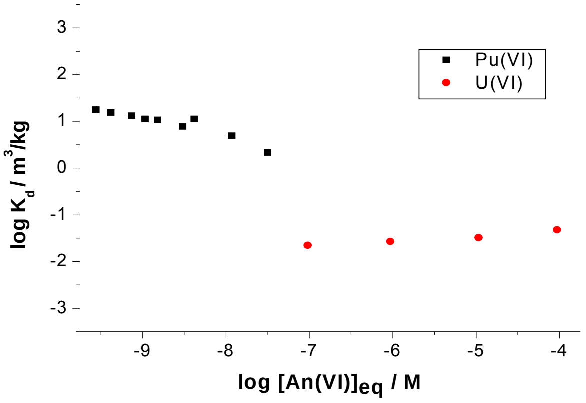

Pu(VI)

K_d = 13 ± 3 m³/kg

U(VI)

K_d = 0.03 ± 0.01 m³/kg

The uptake of Pu by OPA is more than 400 times higher than for U(VI), indicating a change in Pu oxidation state.

Micro beam studies at SLS

μ-XAS Beamline Environmental & Materials Sciences [5].

Investigation methods:

- ✓ μ-XRF → Distribution of elements [Pu and other elements contained in OPA]?
- ✓ μ-XRD → Correlation between Pu and OPA-mineral phases?
- ✓ μ-XANES → Oxidation state of sorbed Pu?

[5] www.psi.ch

Diffusion and thin section samples

Samples	**Method**	**^{242}[Pu] (VI) in Mol/L**	**Contact time**	**^{242}Pu (ng/mm^2)**
μ-XAFS 1	Sorption, Millipore water, pH=7.6	20 μM	5 days	311
μ-XAFS 2	Deposition, Millipore water, pH=7.6	20 μM	-	96
μ-XAFS 3	Diffusion, OPA/Pore water, pH=7.6	20 μM	30 days	7

OPA thin section

→

Thin section thickness= 20 - 30 μm

Surface area < 1 cm^2

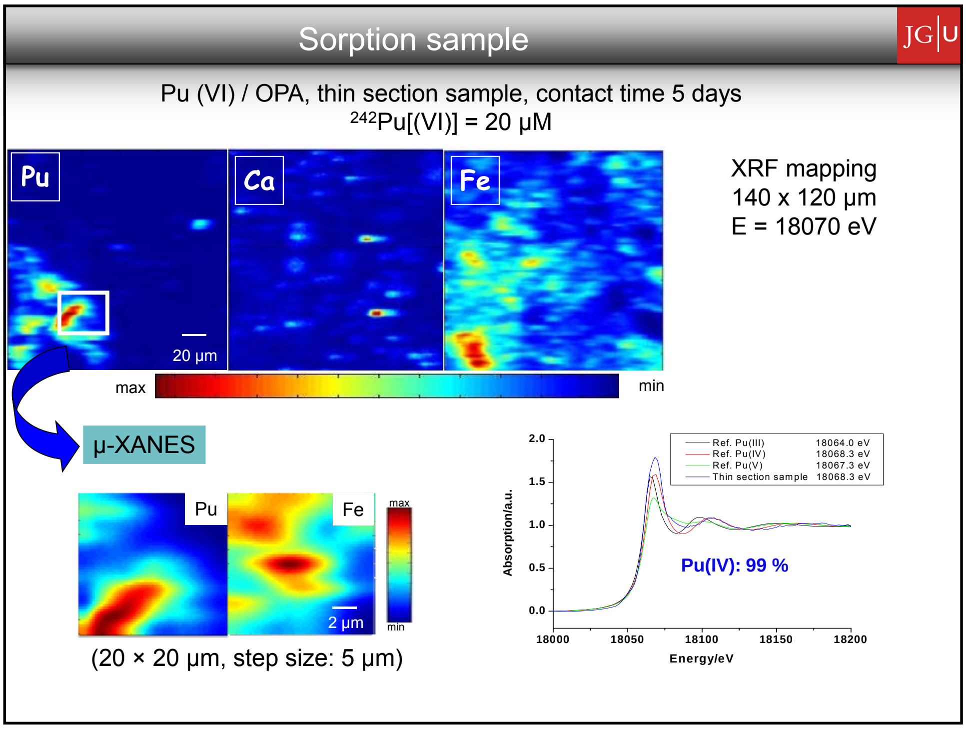

Sorption sample

Pu (VI) / OPA, thin section sample, contact time 5 days

^{242}Pu[(VI)] = 20 µM

XRF mapping
140 x 120 µm
E = 18070 eV

µ-XANES

(20 × 20 µm, step size: 5 µm)

Pu(IV): 99 %

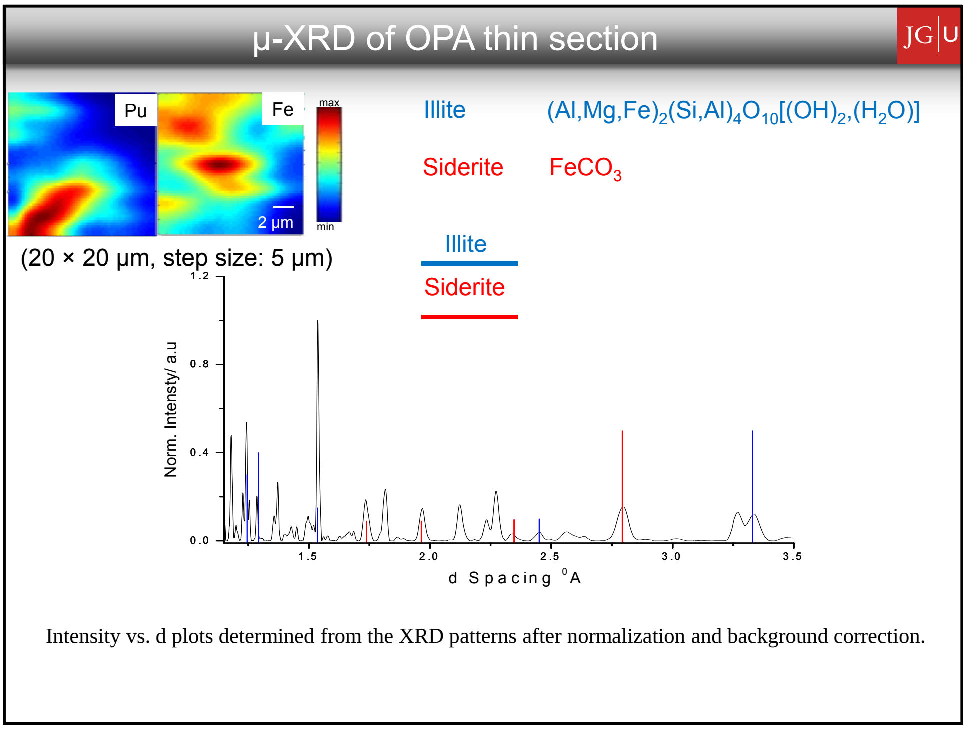

µ-XRD of OPA thin section

Illite $(Al,Mg,Fe)_2(Si,Al)_4O_{10}[(OH)_2,(H_2O)]$

Siderite $FeCO_3$

(20 × 20 µm, step size: 5 µm)

Intensity vs. d plots determined from the XRD patterns after normalization and background correction.

Conclusions

Pu(VI) → OPA pH 7.6 air 20 µM Pu → Pu(IV)

Mobile

İmmobile

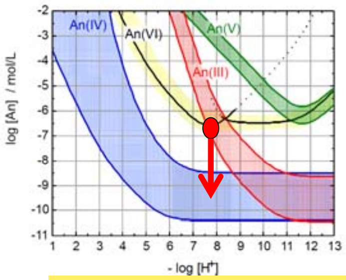

- ❖ Pu is retained by OPA in the reduced and less mobile tetravalent oxidation state of Pu.
- ❖ Pu is localized on or in close vicinity of the Fe(II) mineral siderite and the clay mineral illite.

Chemical information on trace elements in heterogeneous media can be obtained with high spatial resolution using synchrotron radiation based µ-XAFS, µ-XRF and µ-XRD.

Acknowledgement

M. Biegler, J. Huth

C. Borca

Ch. Marquardt

“Chemoinformatics: time to predict”. Selective recognition of imidazoles: an assembling tool for highly linear molecular wires".

Alexandre Varnek (Strasbourg, France)

Trilateral seminar on supramolecular, intermolecular, interaggregate interactions
and separation chemistry, IPCE RAS, Moscow, Russian Federation
20.-23.07.2012

Actinide environmental behavior- role of nanoparticle formation

Horst Geckeis

MOSCOW, JULY 20-23, 2012

7-th ESSSIISC
Moscow, 20-23 July 2012

INSTITUT FÜR NUKLEARE ENTSORGUNG (INE)

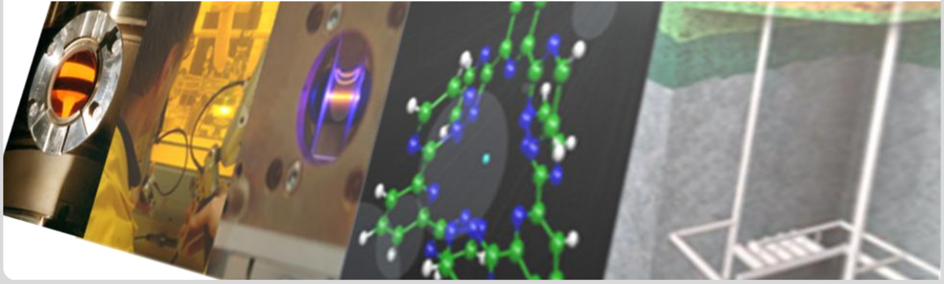

The relevance to study actinide nanoparticles/colloids in natural systems:

Novikov, Kalmykov et al.:
Colloid Transport of Plutonium in the Far-Field of the Mayak Production Association, Russia, Science, 314, 2006

Kersting et al.:
Migration of plutonium in groundwater at the Nevada Test Site, Nature, 397, 1999

Kim:
Actinide colloid generation in groundwater. Radiochim. Acta, 52/53, 1991

…

Topics

- Some aspects of aquatic AN chemistry
- AN polymerization reactions and properties of AN nanoparticles
- AN interaction with naturally abundant colloids/nanoparticles
- Parameters determining AN-colloid/nanoparticle mobility
    - Colloid stability
    - Colloid/nanoparticle surface interaction
    - AN desorption from colloids/nanoparticles

Actinide redox chemistry

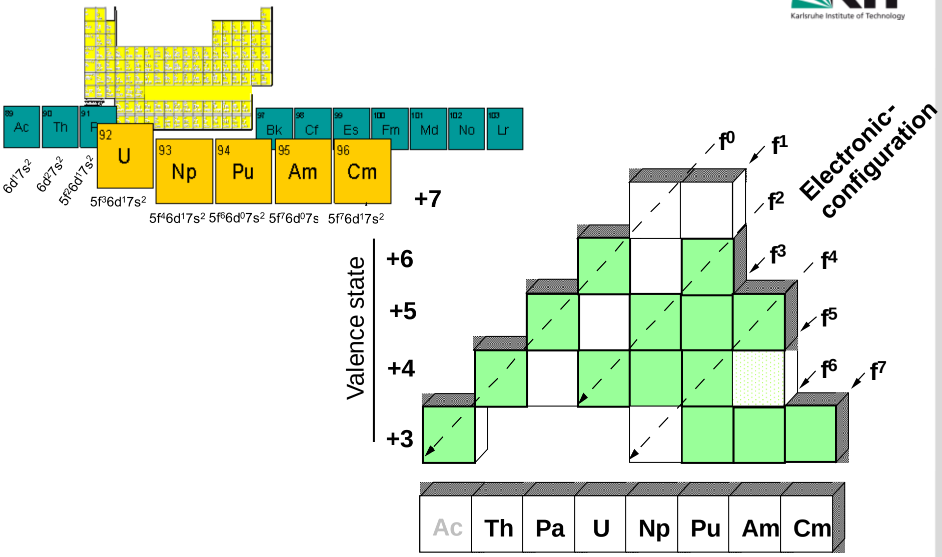

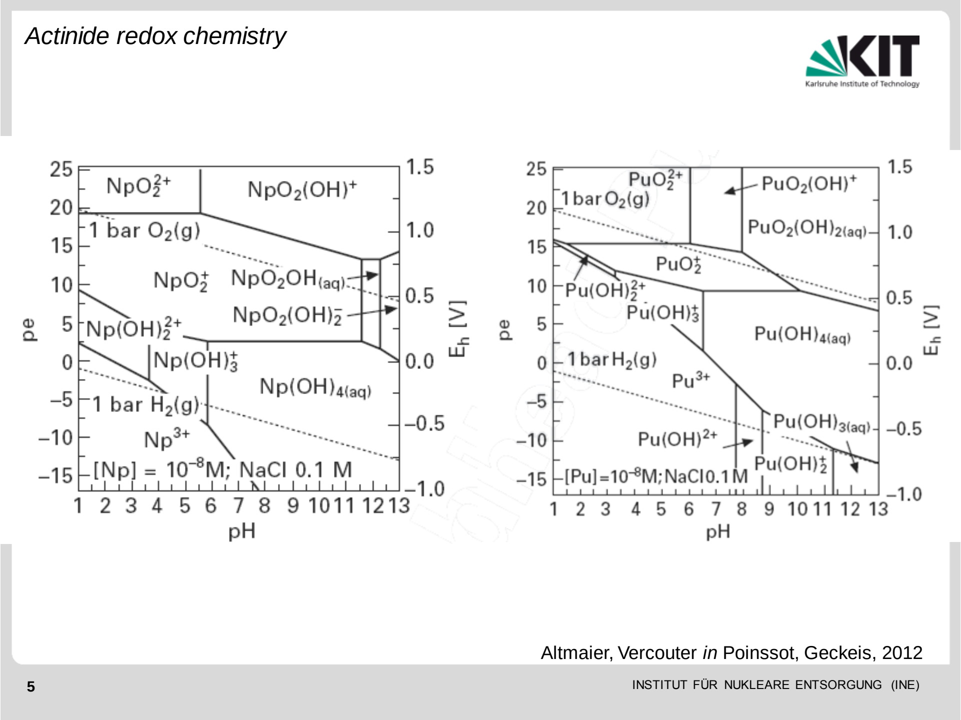

Actinide redox chemistry

Altmaier, Vercouter *in* Poinssot, Geckeis, 2012

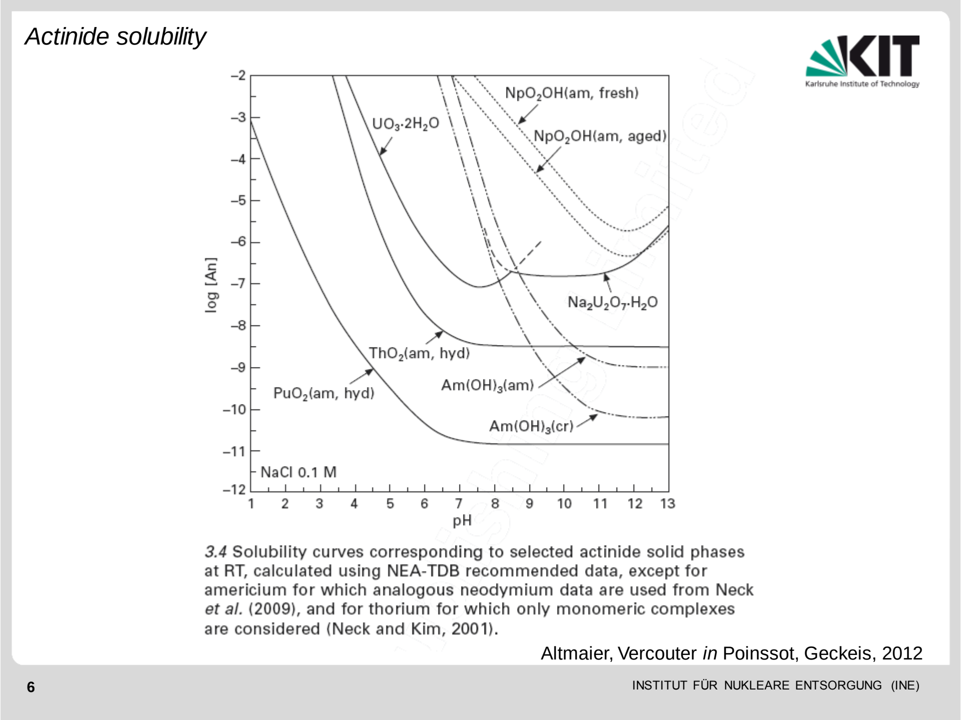

Actinide solubility

3.4 Solubility curves corresponding to selected actinide solid phases at RT, calculated using NEA-TDB recommended data, except for americium for which analogous neodymium data are used from Neck *et al.* (2009), and for thorium for which only monomeric complexes are considered (Neck and Kim, 2001).

Altmaier, Vercouter *in* Poinssot, Geckeis, 2012

Topics

- Some aspects of aquatic AN chemistry
- AN polymerization reactions and properties of AN nanoparticles
- AN interaction with naturally abundant colloids/nanoparticles
- Parameters determining AN-colloid/nanoparticle mobility
  - Colloid stability
  - Colloid/nanoparticle surface interaction
  - AN desorption from colloids/nanoparticles

Colloid-mediated RN migration
Observation at the Nevada Test Site (NTS)

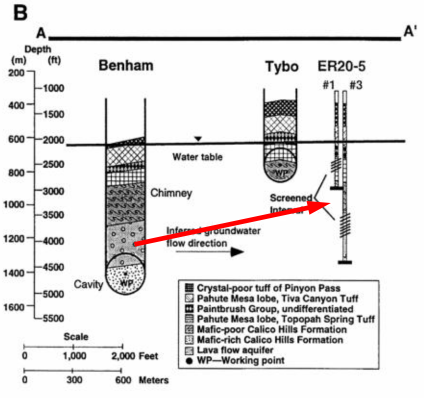

^{60}Co, ^{137}Cs, $^{154/155}$Eu, $^{239/240}$Pu have been analyzed in the groundwater as colloid-borne

Kersting et al. (1999) Nature 397, 56.

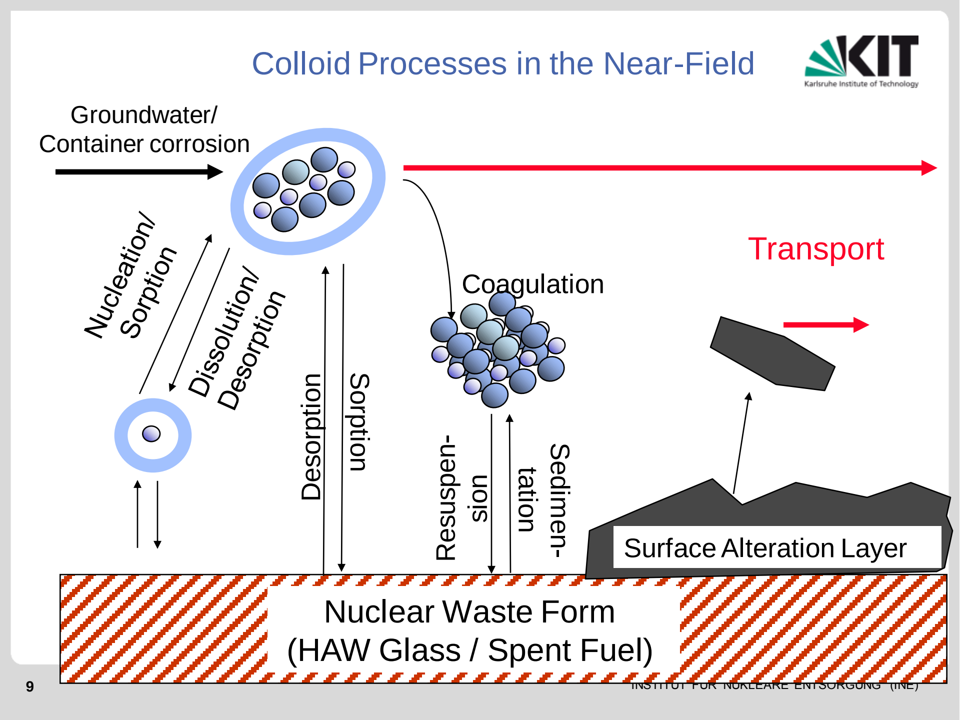

Colloid Processes in the Near-Field

9

INSTITUT FÜR NUKLEARE ENTSORGUNG (INE)

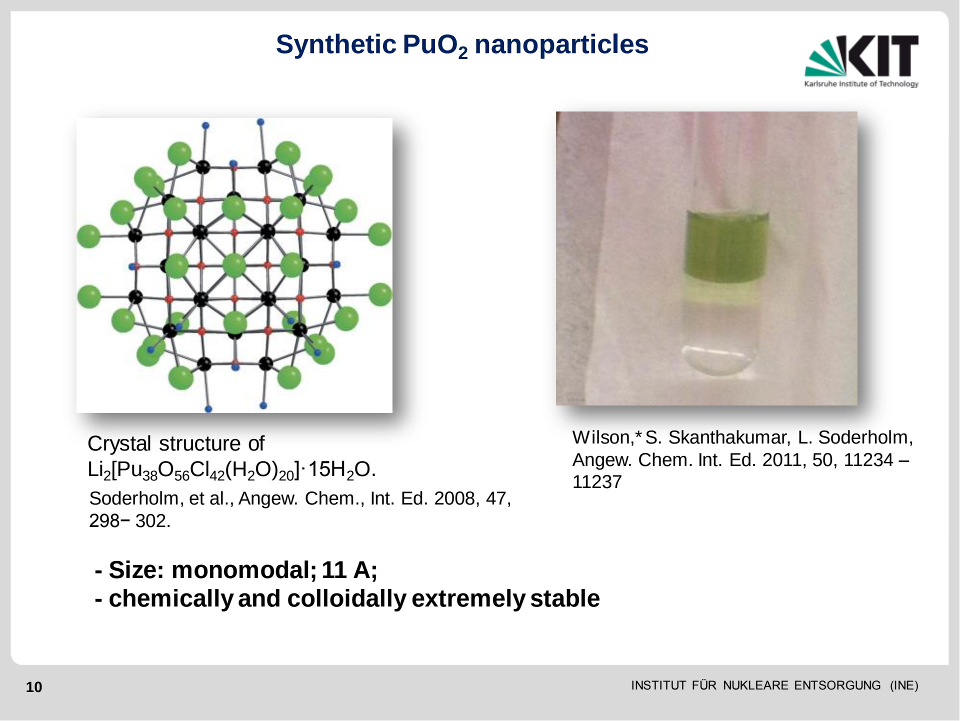

Synthetic PuO_2 nanoparticles

Crystal structure of $Li_2[Pu_{38}O_{56}Cl_{42}(H_2O)_{20}]\cdot 15H_2O$.
Soderholm, et al., Angew. Chem., Int. Ed. 2008, 47, 298– 302.

Wilson,* S. Skanthakumar, L. Soderholm, Angew. Chem. Int. Ed. 2011, 50, 11234 – 11237

- Size: monomodal; 11 A;
- chemically and colloidally extremely stable

10

INSTITUT FÜR NUKLEARE ENTSORGUNG (INE)

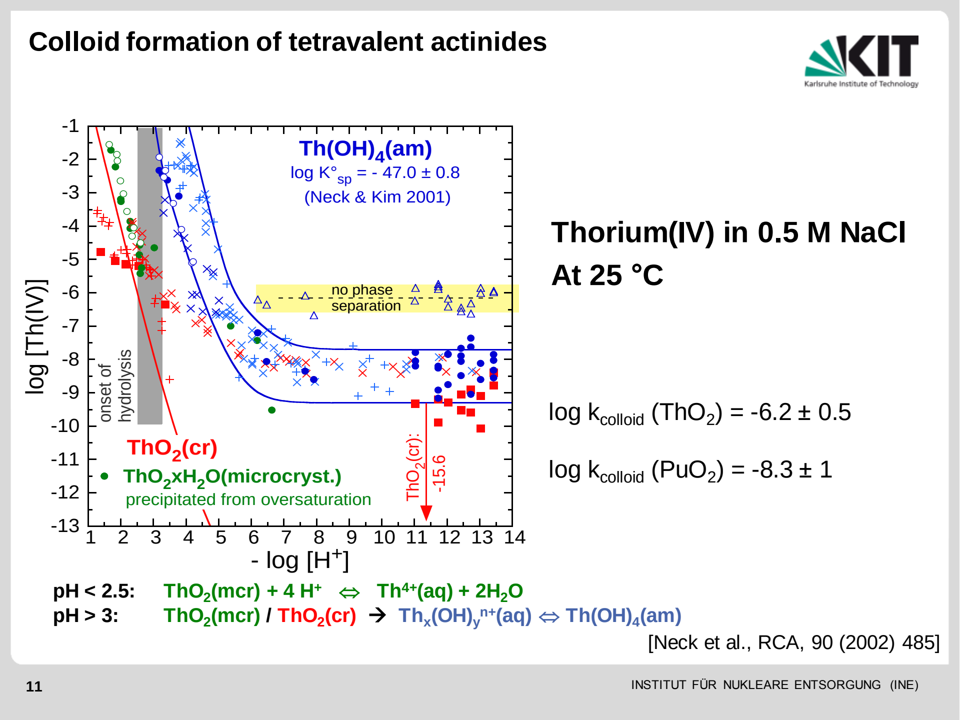

Colloid formation of tetravalent actinides

Thorium(IV) in 0.5 M NaCl

At 25 °C

log $k_{colloid}$ (ThO_2) = -6.2 ± 0.5

log $k_{colloid}$ (PuO_2) = -8.3 ± 1

pH < 2.5: **$ThO_2(mcr) + 4 H^+ \Leftrightarrow Th^{4+}(aq) + 2H_2O$**

pH > 3: **$ThO_2(mcr)$ / $ThO_2(cr)$ → $Th_x(OH)_y^{n+}(aq) \Leftrightarrow Th(OH)_4(am)$**

[Neck et al., RCA, 90 (2002) 485]

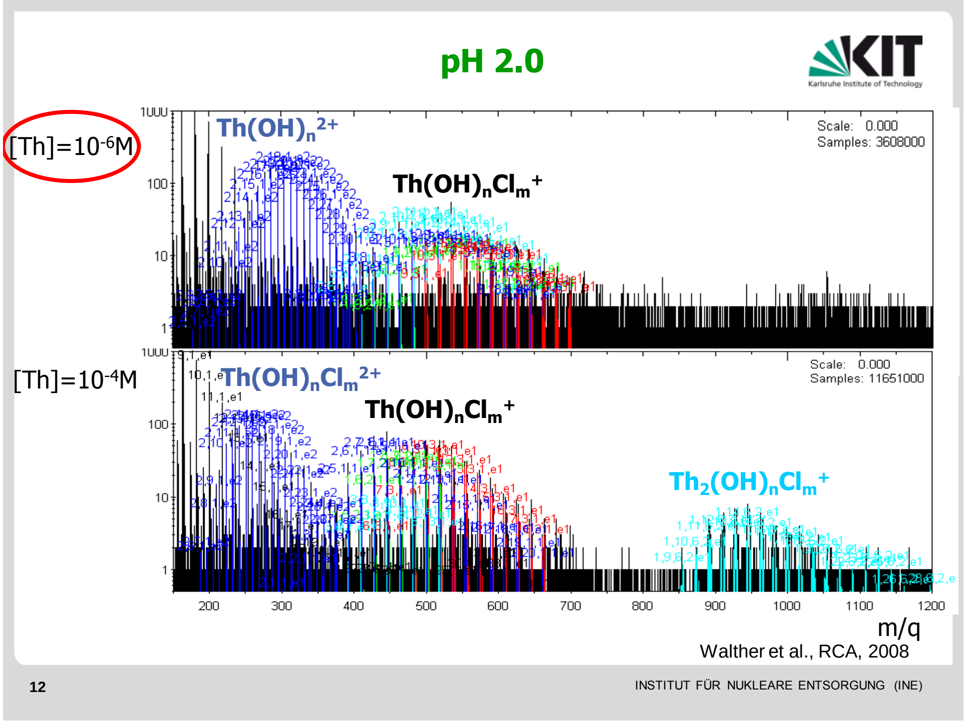

pH 2.0

[Th]=10^{-6}M

[Th]=10^{-4}M

Walther et al., RCA, 2008

Colloid formation of tetravalent actinides
- By polymerization -

[Th]= 0.1mM

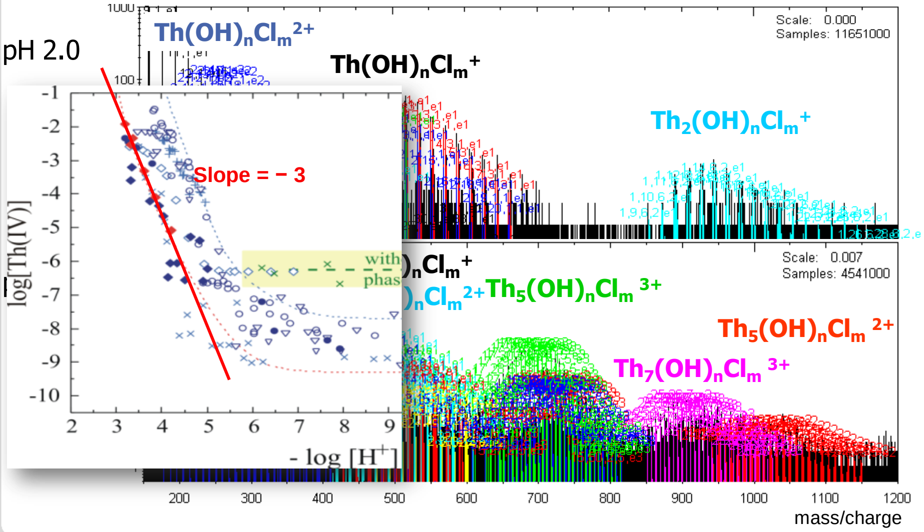

Colloid formation of tetravalent actinides
- By polymerization -

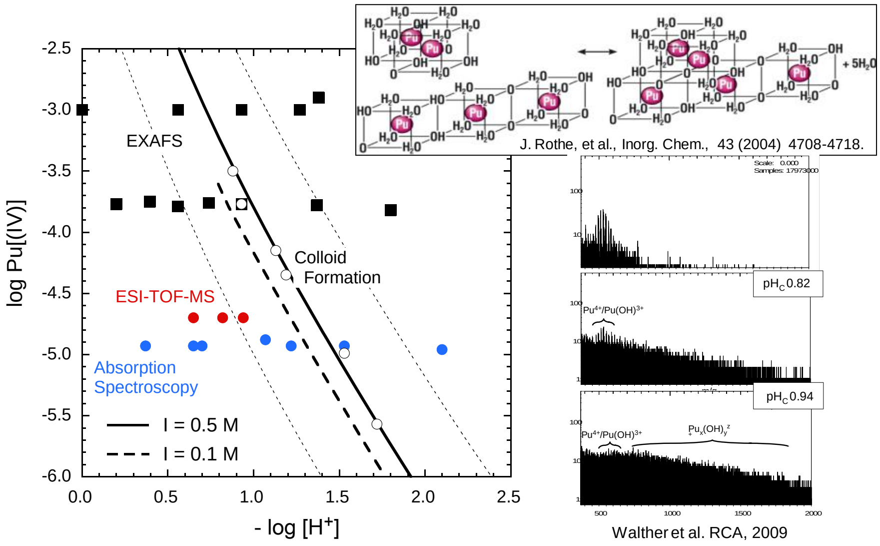

J. Rothe, et al., Inorg. Chem., 43 (2004) 4708-4718.

Walther et al. RCA, 2009

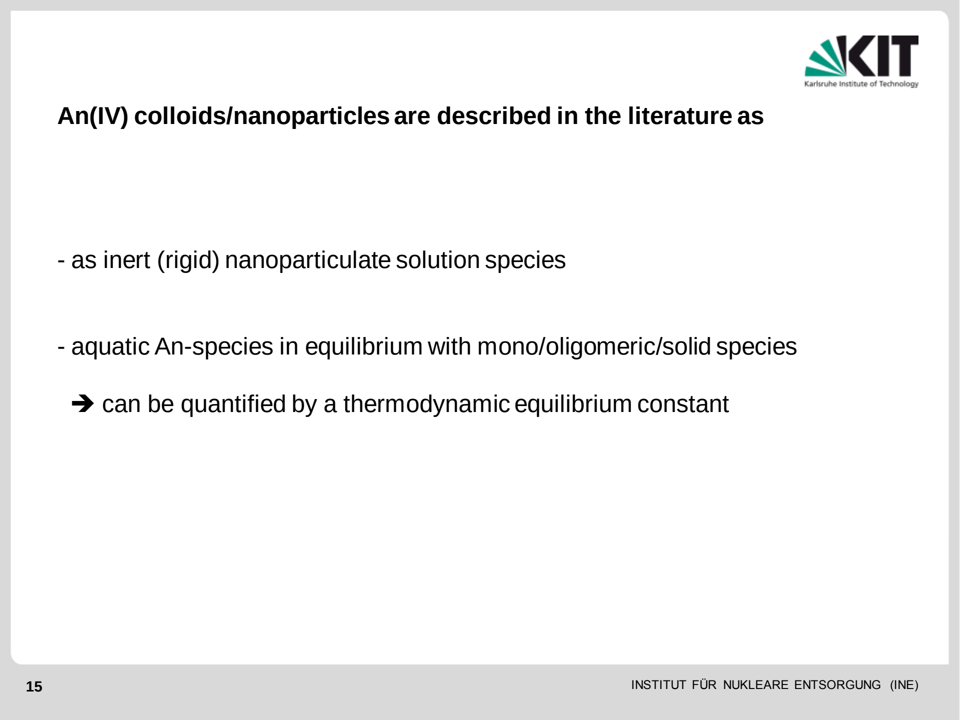

An(IV) colloids/nanoparticles are described in the literature as

- as inert (rigid) nanoparticulate solution species

- aquatic An-species in equilibrium with mono/oligomeric/solid species

  ➔ can be quantified by a thermodynamic equilibrium constant

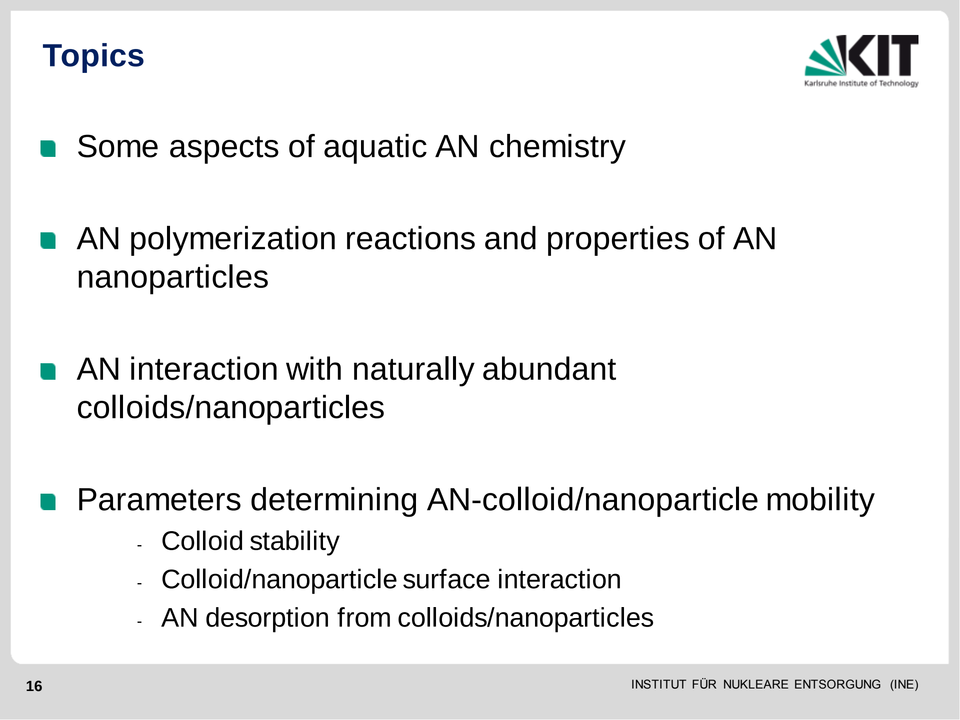

Topics

- Some aspects of aquatic AN chemistry
- AN polymerization reactions and properties of AN nanoparticles
- AN interaction with naturally abundant colloids/nanoparticles
- Parameters determining AN-colloid/nanoparticle mobility
  - Colloid stability
  - Colloid/nanoparticle surface interaction
  - AN desorption from colloids/nanoparticles

Aquatic colloids

Diameter

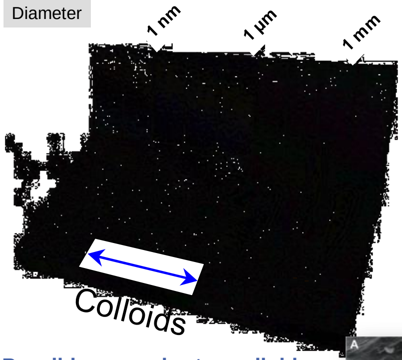

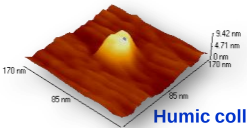

Humic colloids in a sandy aquifer
(Gorleben, Germany)
[M. Plaschke et al, Environ. Sci. Technol. (2002)]

Colloidal Particles
in a granitic groundwater
(Grimsel, Switzerland)

[Degueldre et al., Appl. Geochem, (1996)]

Possible groundwater colloids:
Mineral particles (FeOOH, Clay etc.)
Humic matter, bacteria, virus

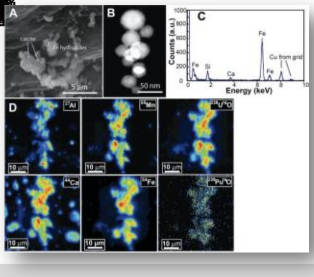

Amorphous iron hydroxide colloids
(Mayak, Russia)

[Novikov et al., Science, 314, (2006)]

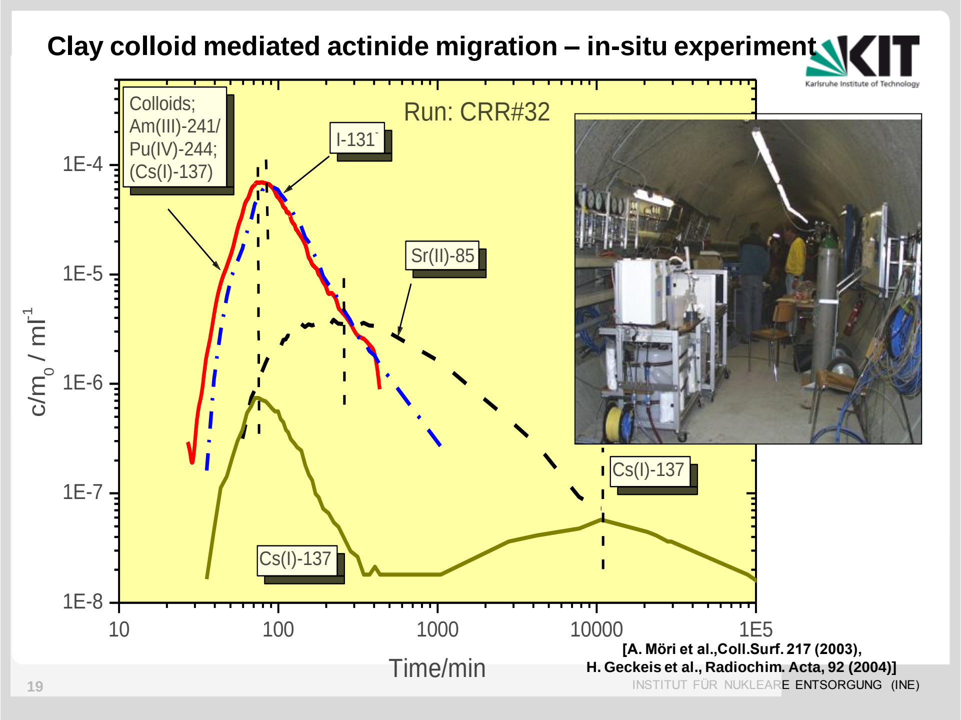

Clay colloid mediated actinide migration – in-situ experiment

**[A. Möri et al.,Coll.Surf. 217 (2003),
H. Geckeis et al., Radiochim. Acta, 92 (2004)]**

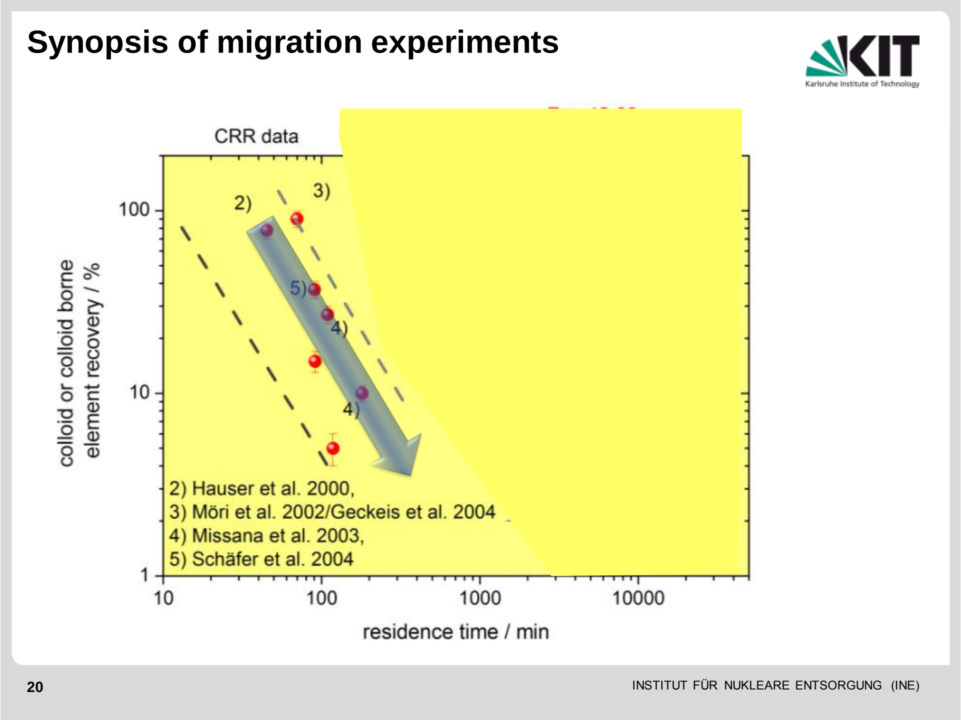

Synopsis of migration experiments

2) Hauser et al. 2000,
3) Möri et al. 2002/Geckeis et al. 2004
4) Missana et al. 2003,
5) Schäfer et al. 2004

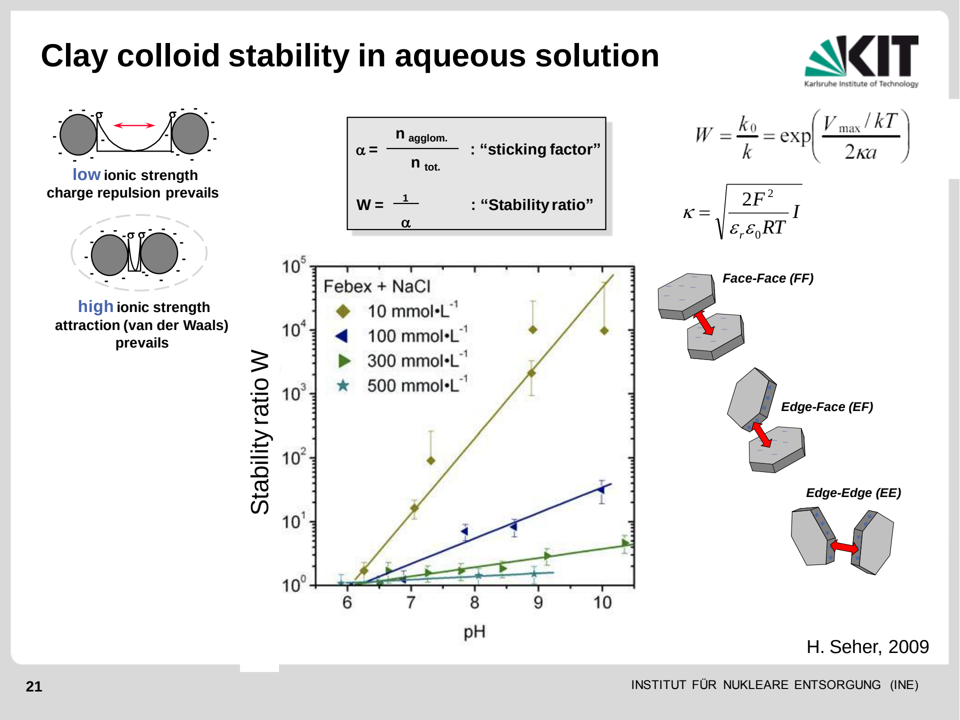

Clay colloid stability in aqueous solution

low ionic strength
charge repulsion prevails

high ionic strength
attraction (van der Waals) prevails

$\alpha = \frac{n_{\text{agglom.}}}{n_{\text{tot.}}}$: "sticking factor"

$W = \frac{1}{\alpha}$: "Stability ratio"

$$W = \frac{k_0}{k} = \exp\left(\frac{V_{\max}/kT}{2\kappa a}\right)$$

$$\kappa = \sqrt{\frac{2F^2}{\varepsilon_r \varepsilon_0 RT} I}$$

H. Seher, 2009

21

INSTITUT FÜR NUKLEARE ENTSORGUNG (INE)

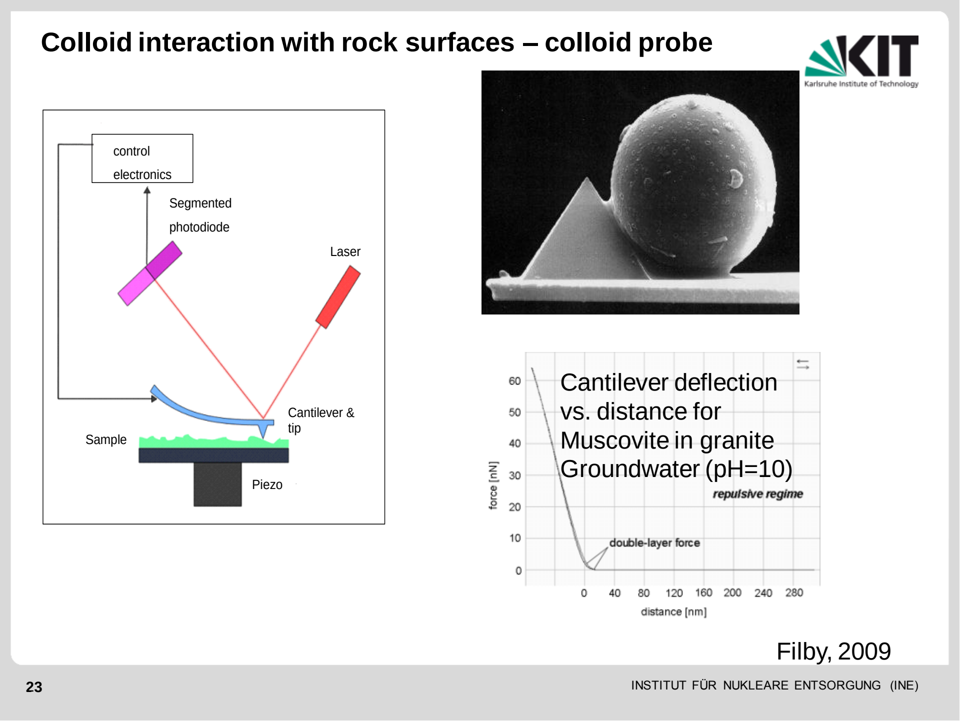

Colloid interaction with rock surfaces – colloid probe

Cantilever deflection vs. distance for Muscovite in granite Groundwater (pH=10)

Filby, 2009

23

INSTITUT FÜR NUKLEARE ENTSORGUNG (INE)

Table 1: Grimsel granodiorite bulk composition

Mineral	Vol.-%	pH_{pzc}
quartz, SiO_2	15	2^{a} - 3.8
plagioclase/albite, $CaAl_2Si_2O_8/NaAlSi_3O_8$	28	2^{a}, $5.25^{b,c}$
K-feldspar, $KAlSi_3O_8$	7	2-2.4 ^{a}, 5.6^{b}
biotite, $K(Mg,Fe)_3\ [(OH)_2/Si_3AlO_{10}]$	41	6.5^{d}
muscovite, $KAl_2[(OH)_2/Si_3AlO_{10}]$	4	4^{d}, 6.6^{c}
epidote, $Ca_2Al_2(Al, Fe^{3+})OOH[Si_2O_7][SiO_4]$	3	?
titanite, $CaTiOSiO_4$	2	?
chlorite, $(Mg,Fe,Al)_3(Si,Al)_4O_{10}(OH)_2(Mg,Fe,Al)_3(OH)_6$	< 1	?
apatite, $Ca_5[(F,Cl,OH)/(PO_4)_3]$	trace	7.6^{e},8.1^{f}
rutile, TiO_2	trace	?
zircon, $ZrSiO_4$	trace	?
ilmenite, $FeTiO_3$	trace	?
orthite, $(Ca,Mn,Ce,La,Y,Th)_2Al(Al,Fe^{3+})(Fe^{2+},Fe^{3+},Ti)OOH[Si_2O_7][SiO_4]$	< 1	?
Clay minerals	0-1	5-6 (edges)

Filby, 2009

Electrostatic attachment of PuO_2 nanoparticles at the muscovite surface

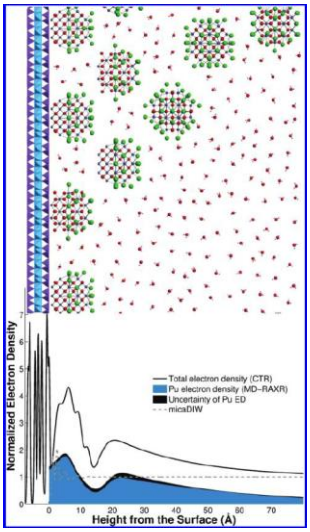

- studied by resonant anomalous X-ray reflectivity (RAXR)

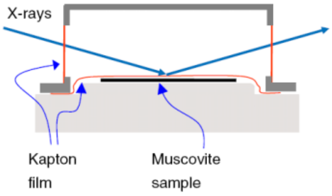

Schmidt et al., Langmuir, 2012, 28, 2620

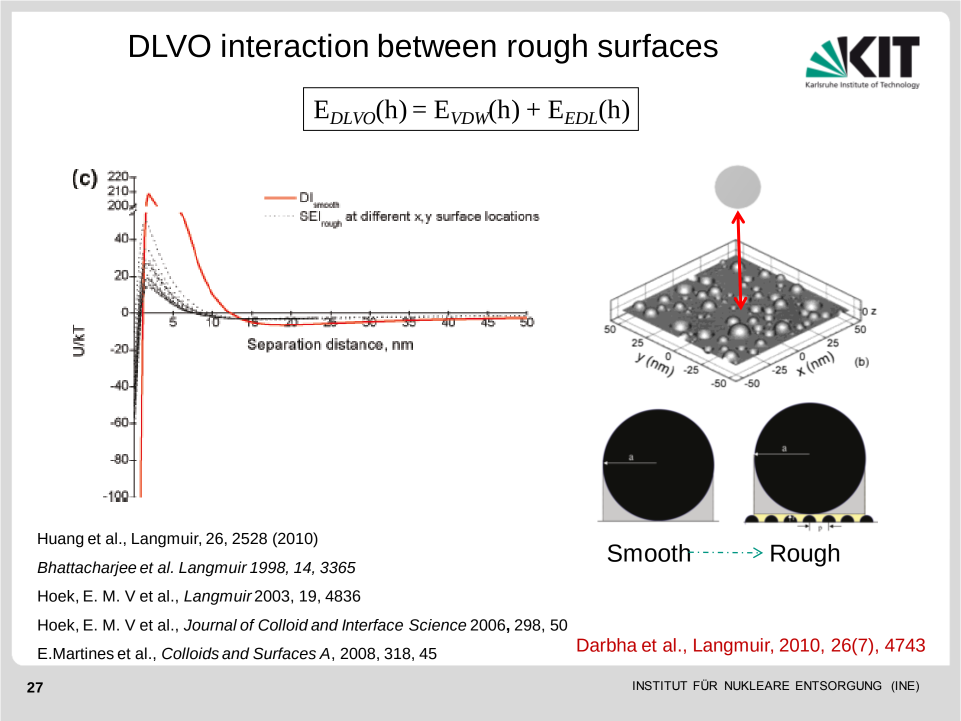

DLVO interaction between rough surfaces

$$E_{DLVO}(h) = E_{VDW}(h) + E_{EDL}(h)$$

Huang et al., Langmuir, 26, 2528 (2010)

Bhattacharjee et al. Langmuir 1998, 14, 3365

Hoek, E. M. V et al., *Langmuir* 2003, 19, 4836

Hoek, E. M. V et al., *Journal of Colloid and Interface Science* 2006, 298, 50

E.Martines et al., *Colloids and Surfaces A*, 2008, 318, 45

Smooth ---> Rough

Darbha et al., Langmuir, 2010, 26(7), 4743

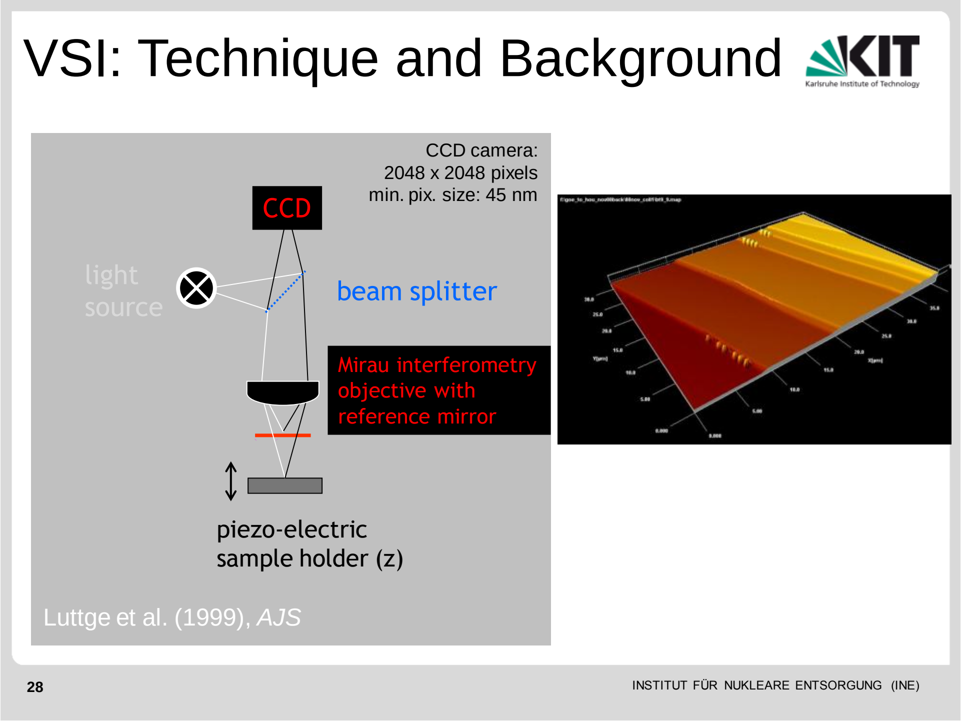

VSI: Technique and Background

CCD camera:
2048 x 2048 pixels
min. pix. size: 45 nm

Luttge et al. (1999), *AJS*

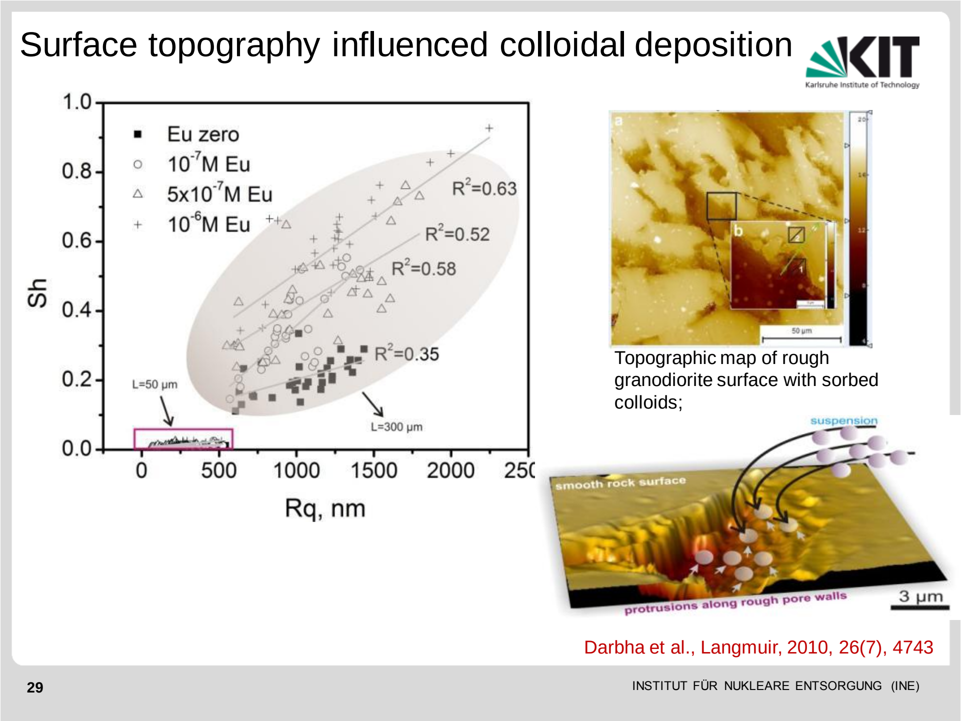

Surface topography influenced colloidal deposition

Topographic map of rough granodiorite surface with sorbed colloids;

Darbha et al., Langmuir, 2010, 26(7), 4743

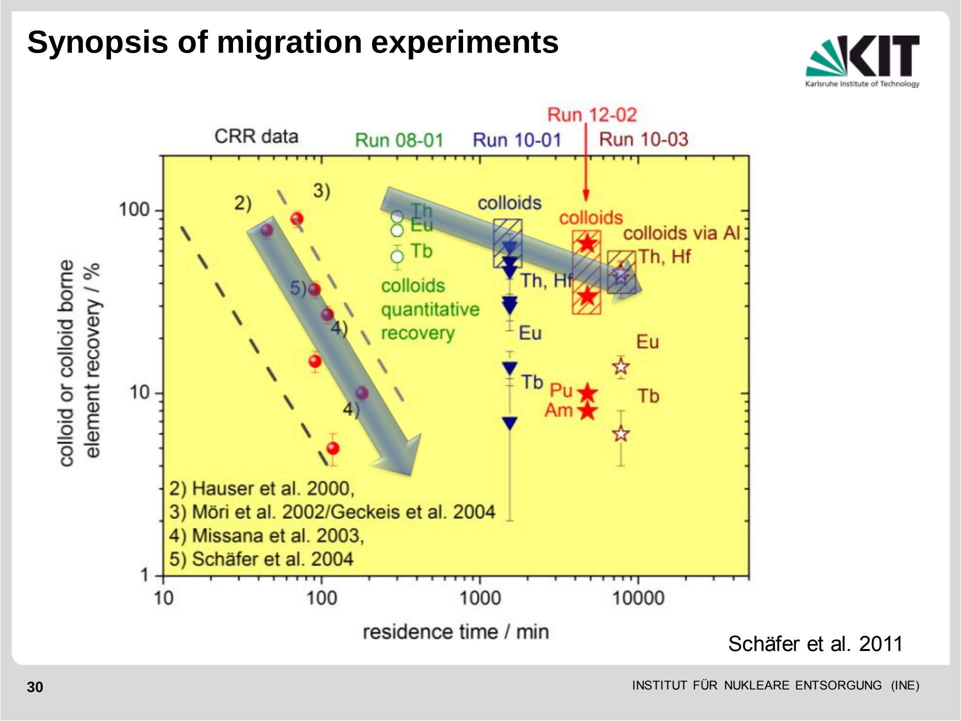

Synopsis of migration experiments

2) Hauser et al. 2000,
3) Möri et al. 2002/Geckeis et al. 2004
4) Missana et al. 2003,
5) Schäfer et al. 2004

Schäfer et al. 2011

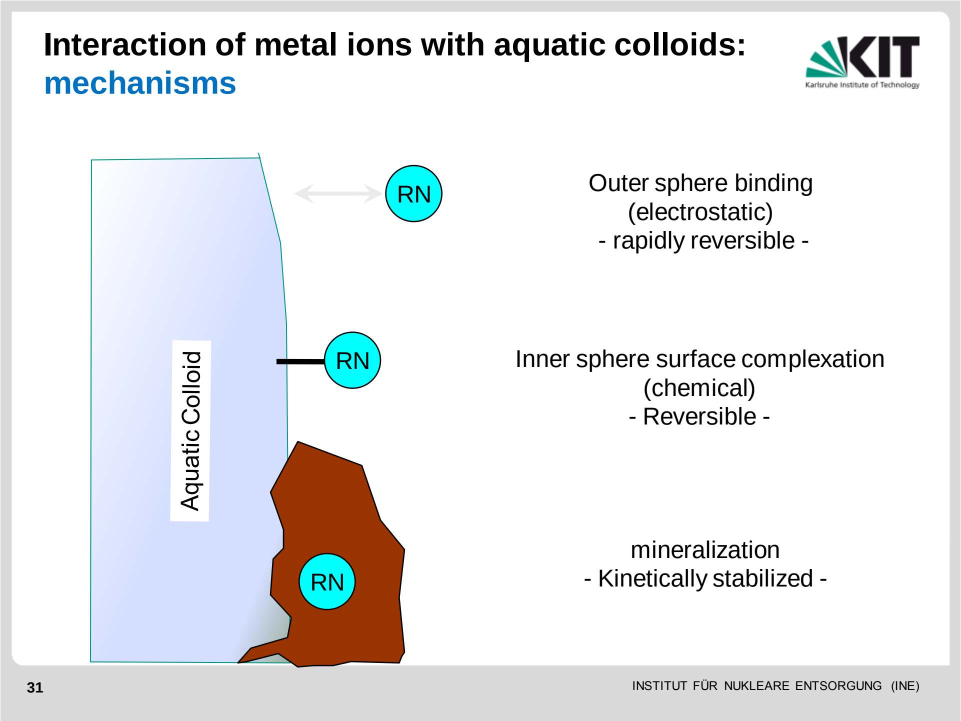

Interaction of metal ions with aquatic colloids: mechanisms

Outer sphere binding
(electrostatic)
- rapidly reversible -

Inner sphere surface complexation
(chemical)
- Reversible -

mineralization
- Kinetically stabilized -

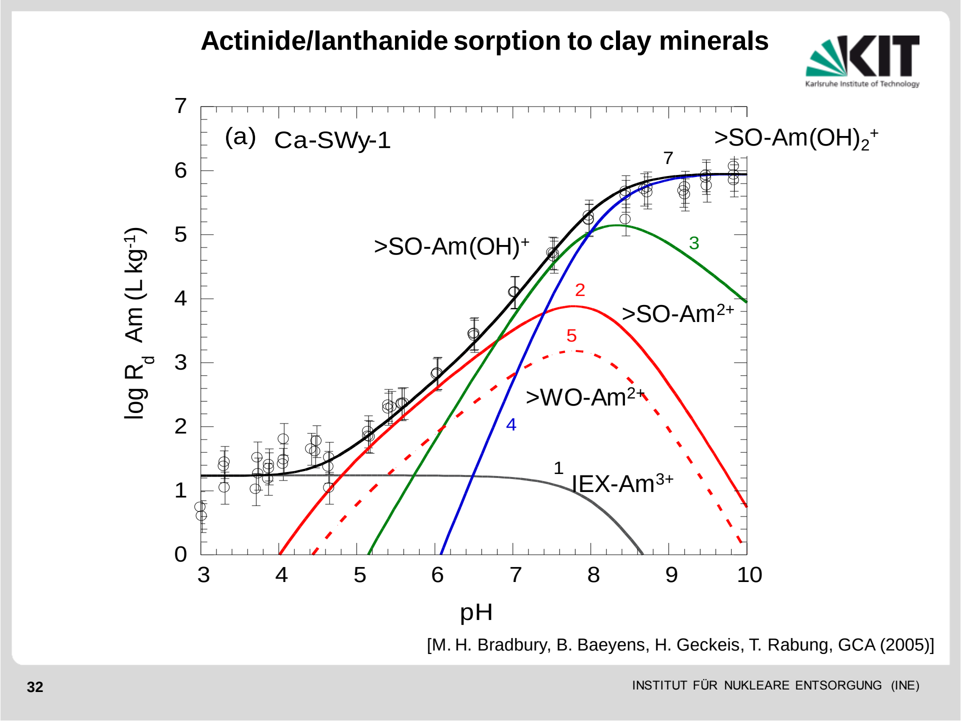

Actinide/lanthanide sorption to clay minerals

[M. H. Bradbury, B. Baeyens, H. Geckeis, T. Rabung, GCA (2005)]

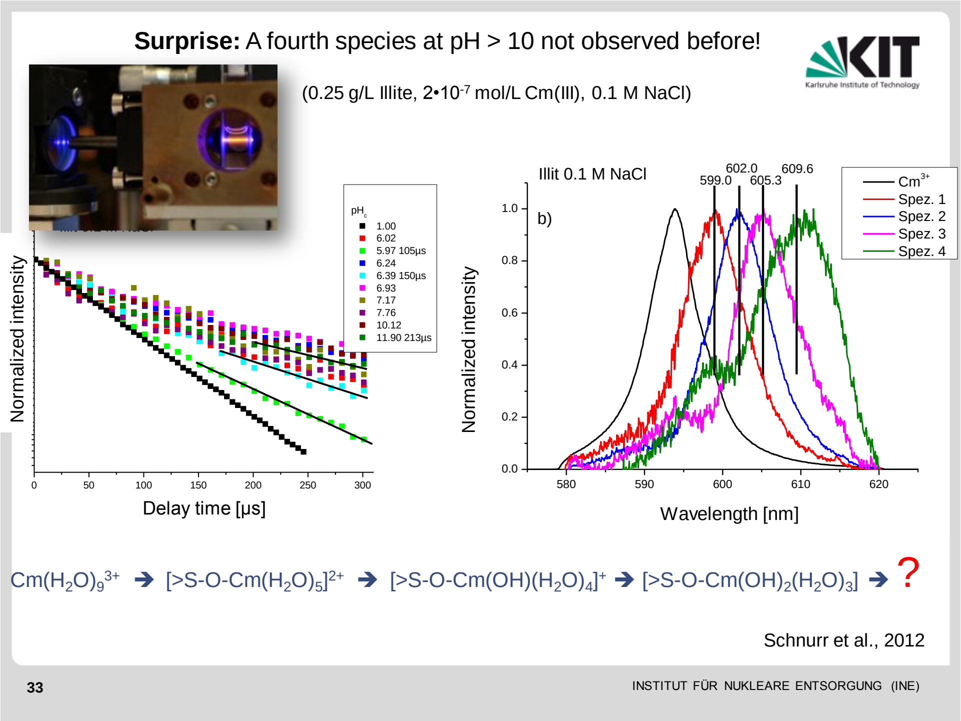

Surprise: A fourth species at pH > 10 not observed before!

(0.25 g/L Illite, $2 \cdot 10^{-7}$ mol/L Cm(III), 0.1 M NaCl)

$Cm(H_2O)_9^{3+}$ ➔ $[>S\text{-}O\text{-}Cm(H_2O)_5]^{2+}$ ➔ $[>S\text{-}O\text{-}Cm(OH)(H_2O)_4]^{+}$ ➔ $[>S\text{-}O\text{-}Cm(OH)_2(H_2O)_3]$ ➔ ?

Schnurr et al., 2012

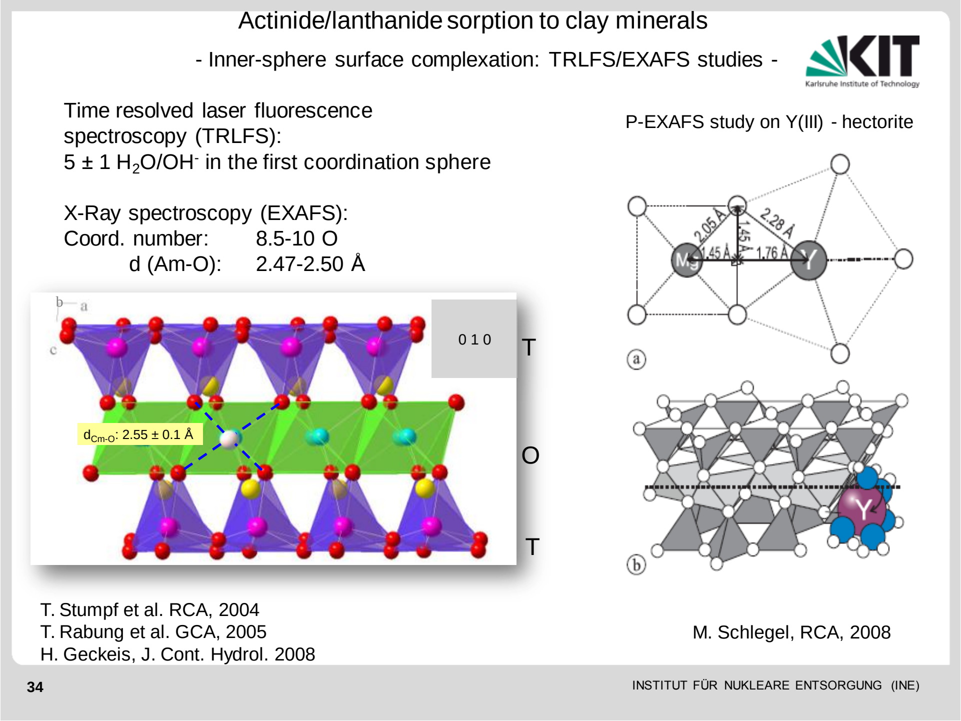

Actinide/lanthanide sorption to clay minerals

- Inner-sphere surface complexation: TRLFS/EXAFS studies -

Time resolved laser fluorescence spectroscopy (TRLFS):
5 ± 1 H_2O/OH^- in the first coordination sphere

X-Ray spectroscopy (EXAFS):
Coord. number: 8.5-10 O
d (Am-O): 2.47-2.50 Å

P-EXAFS study on Y(III) - hectorite

T. Stumpf et al. RCA, 2004
T. Rabung et al. GCA, 2005
H. Geckeis, J. Cont. Hydrol. 2008

M. Schlegel, RCA, 2008

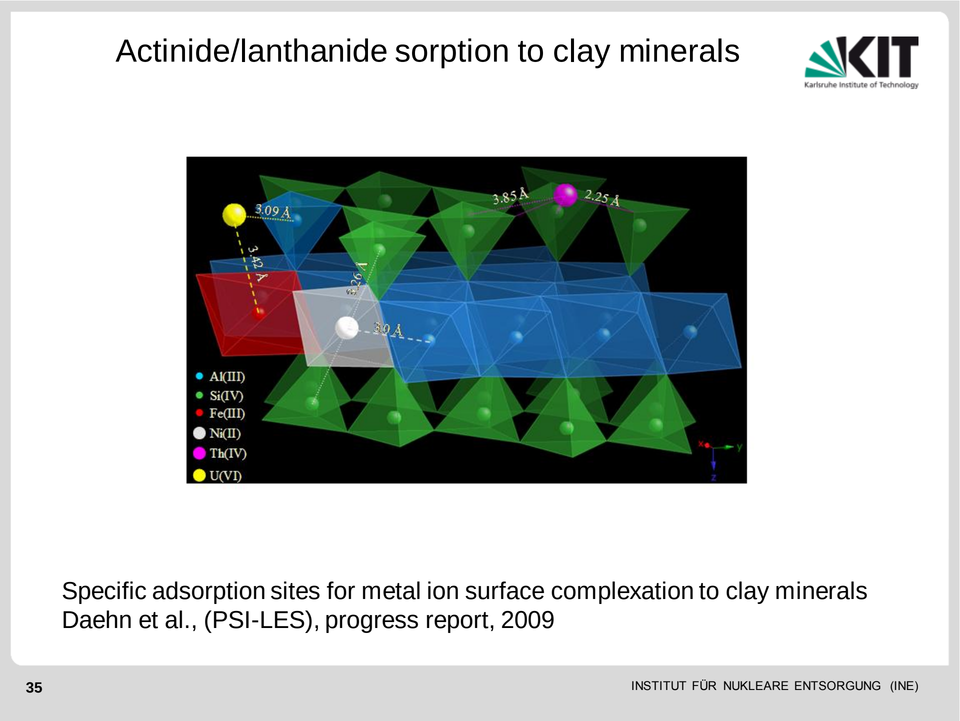

Actinide/lanthanide sorption to clay minerals

Specific adsorption sites for metal ion surface complexation to clay minerals
Daehn et al., (PSI-LES), progress report, 2009

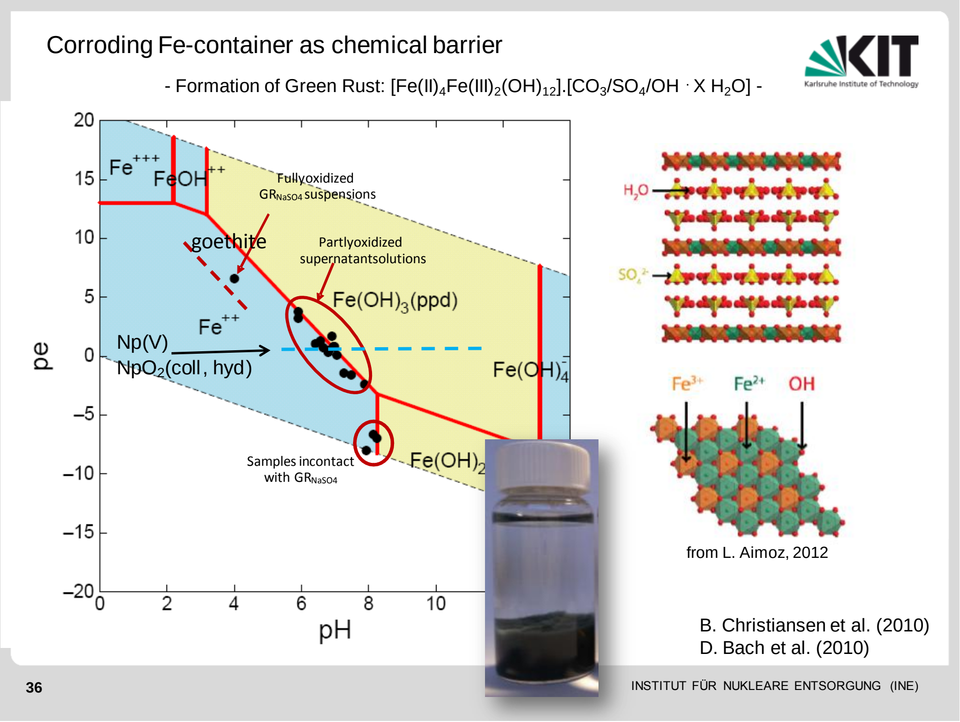

Corroding Fe-container as chemical barrier

- Formation of Green Rust: $[Fe(II)_4Fe(III)_2(OH)_{12}].[CO_3/SO_4/OH \cdot X\ H_2O]$ -

from L. Aimoz, 2012

B. Christiansen et al. (2010)
D. Bach et al. (2010)

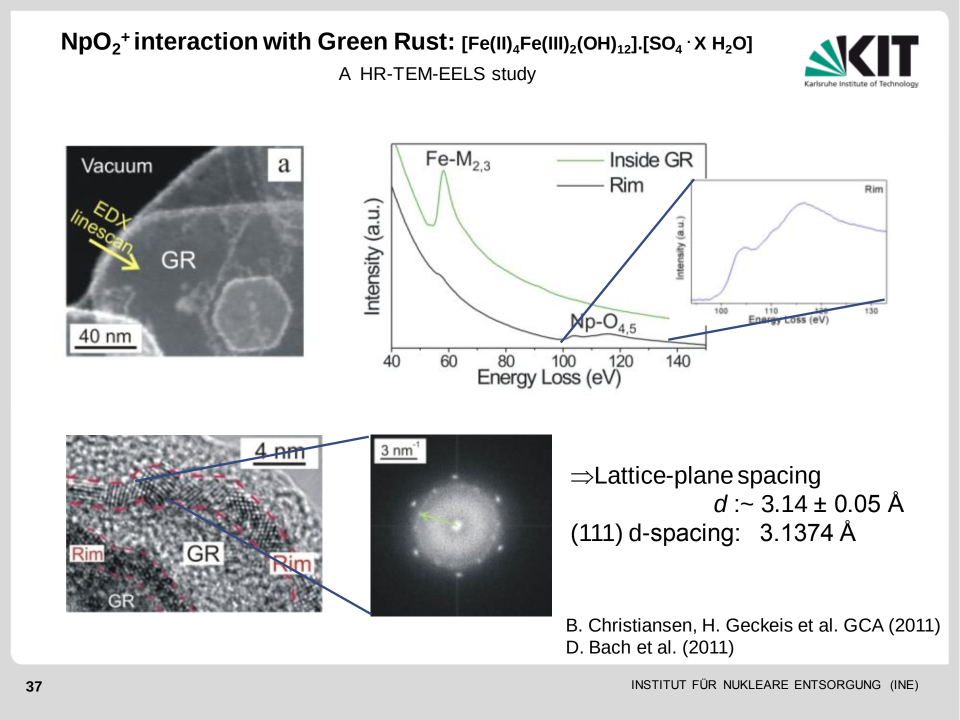

NpO_2^+ interaction with Green Rust: $[Fe(II)_4Fe(III)_2(OH)_{12}].[SO_4 \cdot X\ H_2O]$

A HR-TEM-EELS study

⇒Lattice-plane spacing
d :~ 3.14 ± 0.05 Å
(111) d-spacing: 3.1374 Å

B. Christiansen, H. Geckeis et al. GCA (2011)
D. Bach et al. (2011)

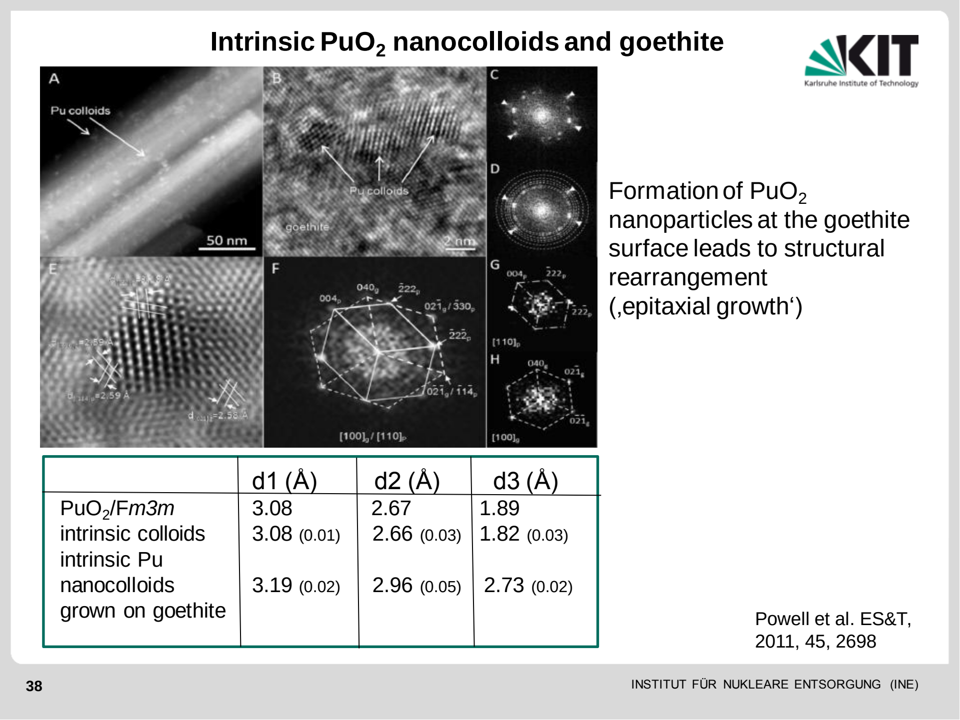

Intrinsic PuO_2 nanocolloids and goethite

Formation of PuO_2 nanoparticles at the goethite surface leads to structural rearrangement (‚epitaxial growth‘)

	d1 (Å)	d2 (Å)	d3 (Å)
PuO_2/F*m3m*	3.08	2.67	1.89
intrinsic colloids	3.08 (0.01)	2.66 (0.03)	1.82 (0.03)
intrinsic Pu nanocolloids grown on goethite	3.19 (0.02)	2.96 (0.05)	2.73 (0.02)

Powell et al. ES&T, 2011, 45, 2698

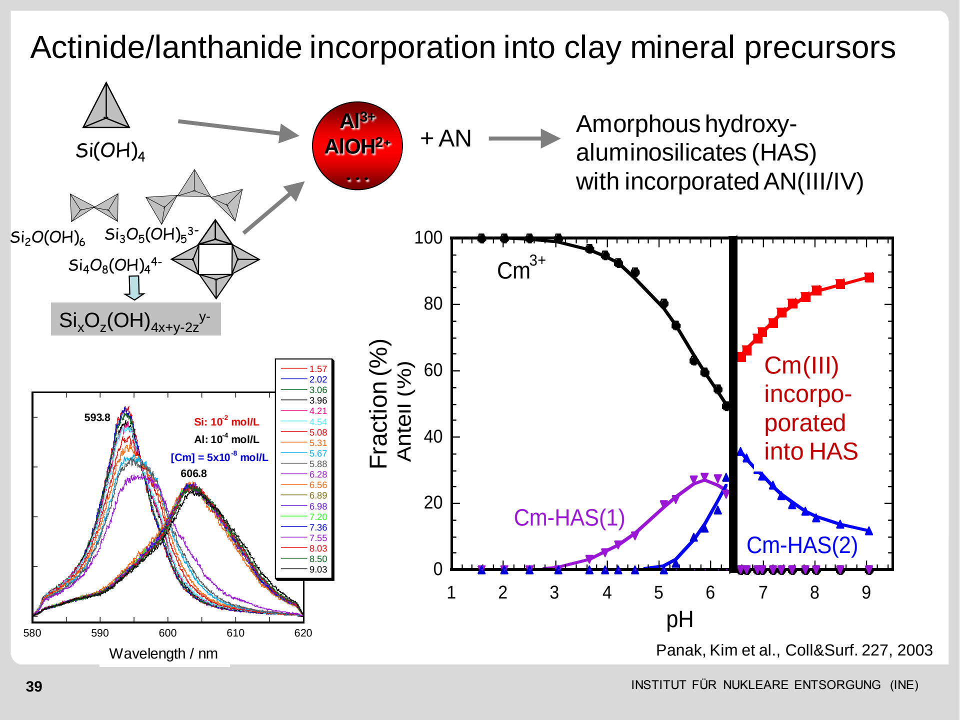

Actinide/lanthanide incorporation into clay mineral precursors

$Si(OH)_4$ → Al^{3+}, $AlOH^{2+}$ … + AN → Amorphous hydroxy-aluminosilicates (HAS) with incorporated AN(III/IV)

$Si_2O(OH)_6$ $Si_3O_5(OH)_5^{3-}$ $Si_4O_8(OH)_4^{4-}$

$Si_xO_z(OH)_{4x+y-2z}^{y-}$

Panak, Kim et al., Coll&Surf. 227, 2003

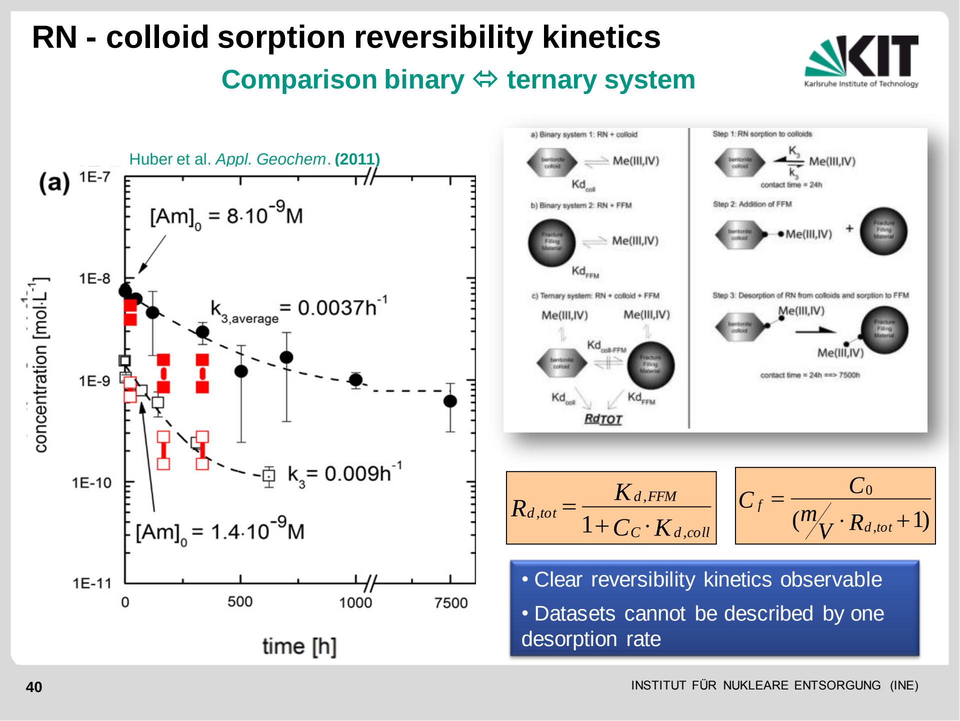

RN - colloid sorption reversibility kinetics

Comparison binary ⇔ ternary system

Huber et al. *Appl. Geochem*. **(2011)**

$$R_{d,tot} = \frac{K_{d,FFM}}{1 + C_C \cdot K_{d,coll}}$$

$$C_f = \frac{C_0}{\left({}^{m}\!/\!_{V} \cdot R_{d,tot} + 1 \right)}$$

- Clear reversibility kinetics observable
- Datasets cannot be described by one desorption rate

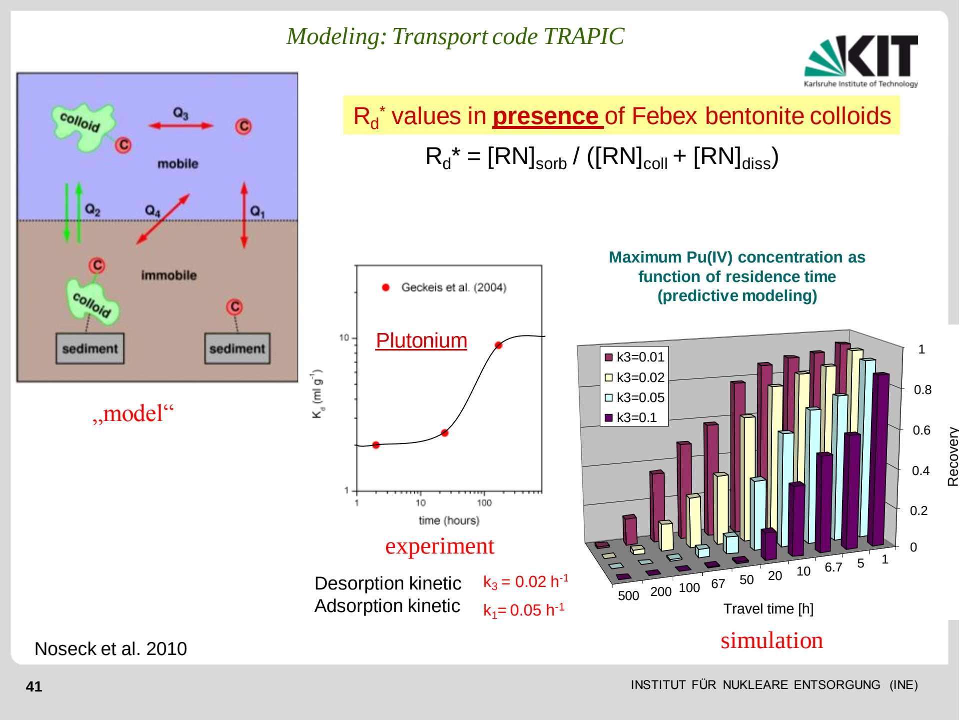

Modeling: Transport code TRAPIC

R_d^* values in **presence** of Febex bentonite colloids

$R_d^* = [RN]_{sorb} / ([RN]_{coll} + [RN]_{diss})$

„model“

experiment

Desorption kinetic $k_3 = 0.02\ h^{-1}$
Adsorption kinetic $k_1 = 0.05\ h^{-1}$

Maximum Pu(IV) concentration as function of residence time (predictive modeling)

simulation

Noseck et al. 2010

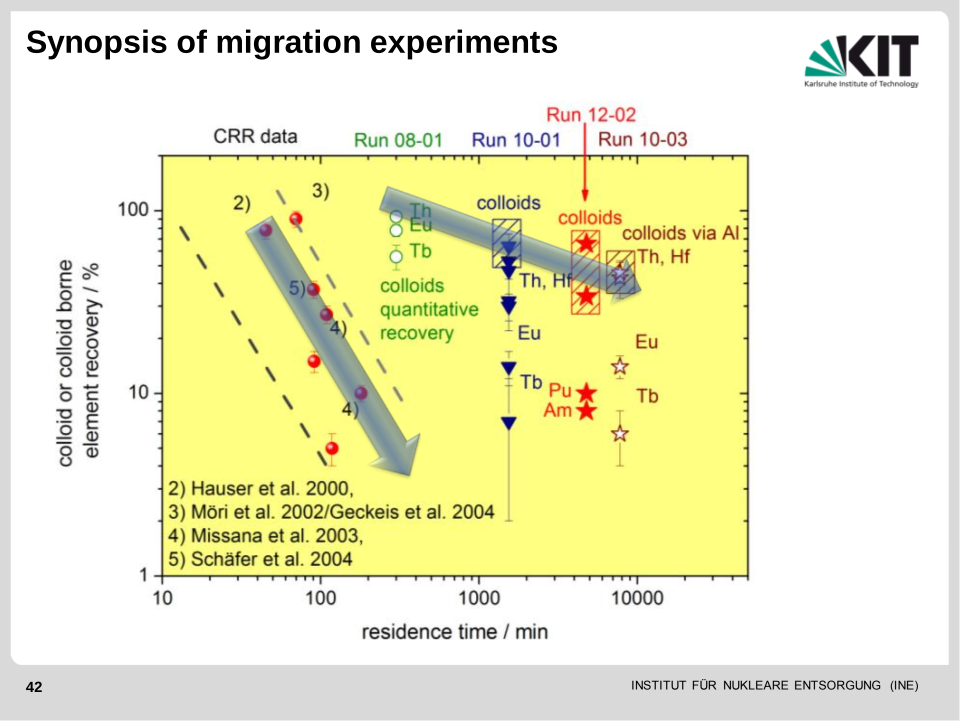

Synopsis of migration experiments

2) Hauser et al. 2000,
3) Möri et al. 2002/Geckeis et al. 2004
4) Missana et al. 2003,
5) Schäfer et al. 2004

Short conclusions

- AN nanoparticles have different properties depending on their generation (or synthesis mode)
- Mobility of AN bearing colloid/nanoparticles decreases
  - depending on pH/ionic strength conditions which determine colloid/nanoparticle stability and surface attachment due to electrostatic attraction
  - with increasing surface roughness (even under unfavorable conditions)
  - with decreasing strength of AN binding (incorporation/surface induced redox/surface sorption)

KIT - Institute for Nuclear Waste Disposal

“Specific ion effects in solutions, at interfaces, and in colloidal systems”.

Invited lecture

Werner Kunz (Regensburg, Germany)

Trilateral seminar on supramolecular, intermolecular, interaggregate interactions
and separation chemistry, IPCE RAS, Moscow, Russian Federation
20.-23.07.2012

SPECIATION AND SEPARATION CHEMISTRY OF Tc FOR SNF REPROCESSING

Yana Obruchnikova, Konstantin German, Vladimir Peretrukhin
IPCE RAS, Moscow

One of the most important stages of reprocessing of spent nuclear fuel is uranium – plutonium separation. In this stage there are the following substances: U, Pu, Np, Tc, nitric acid, hydrazine and other fission products.

As is known Tc catalyzes the oxidation reaction of hydrazine by nitric acid. And of course that influence is negative because the reductive separation of uranium and plutonium in PUREX-process can be disturbed.

For successful separation of uranium and plutonium in PUREX-process technetium must be in its reduced condition Tc(IV). But somehow Tc comes with U(VI) in organic phase.

Intermediate oxidation states Tc(VI) and Tc(V) and various corresponding species also participates in catalytic cycles. However they rest inidentified due to small ε or lifetimes and the information about their behavior in such systems can hardly be found in the available literature or is contadictory. Tc influence is a real disaster for reprocessing of spent nuclear fuel. Its harmful effect lead to closure of Sellafield for several years and operation problems on Mayak and French UP-plant. Using spectrophotometric method we have found out what happens among Tc, Zr or Th, nitric acid and reducing agent, e.g. hydrazine nitrate in the stage of reductive separation of U and Pu. It takes us more than 2 hours to get the equilibrium state. Tc(IV) was measured by the shoulder at 400 nm. And for the first time the peak at 470 nm probably corresponding to Tc(V) complex was observed in such a system due to its important time needed for reaction complete development that was missed by previous researchers.

The reaction consists of 3 stages. On addition of hydrazine to Tc(VII)+Th(IV) solution in nitric acid the reaction first proceeds as a Tc(VII) reduction to Tc(IV) thus developing the shoulder at 400 nm and following the zero order kinetics, initiating the hydrazine decomposition with gas evolution. Then, the decomposition of Tc(IV) takes place in similar zero order kinetics with formation of *unidentified TcX species*. Then finally Tc(V)-Th(IV) complex is formed characterized with a peak at 470 - 475 nm in first order kinetics.

Obtained solutions are pink or brown depending on Tc concentration. It is necessary to emphasize that this complex rests stable for several days at 55 ^{o}C.

We can see that this system forms a quite stable compound with Tc(V). Because of the presence of different species, to analyze all spectra we used deconvolution method. Hundreds spectra were deconvolved during the investigation. On the right side a wide variety of reactions taking place in studied system could be found.

The influence of zirconium was studied as well. Since the kinetics has been studied by example of thorium, we decided to consider equilibrated solutions. And it helped us to find out the ratio between Tc and Zr in the complex at 470 nm which is 2 to 1.

In the case of Zr - Tc diagram, concentration of Tc(V) complex increases in these limits of Tc concentration to be boud in the complex. But further increase of Tc concentration leads to appearance of excess Tc(IV) which restars the catalytic decomposition of hydrazine providing forming oxidizing conditions in the finally resulting solution. So oxidation of the Tc(V) complex to Tc(VII) occurs at the excess of Tc.

The ratio between Tc and Th in a complex was also found as 2 to 1. After such a complicated separation of U and Pu it's still needed to get rid of Tc from obtained solutions.

For this purpose its precipitation in form of Pr_4NTcO_4 (pertechnetate tetrapropylammonium) was suggested. It's possible to use this compound to convert Tc into slightly soluble form and remove Tc from the solution. The obtained data on the coefficients of Tc purification from ^{239}Pu and ^{106}Ru also suggest Pr_4NTcO_4, as a promising precipitating agent in technology of Tc transmutation.

Speciation and separation of Tc for SNF reprocessing

K.E. German, Ya.A. Obruchnikova,
V.F. Peretrukhin
IPCE RAS

2

Technetium interfering role in the scenario of PUREX development

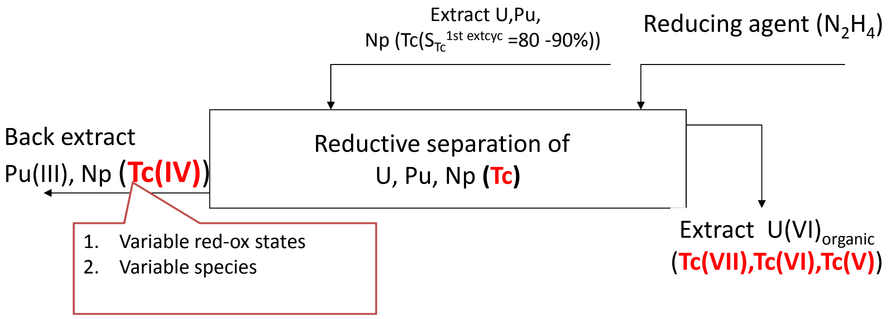

Extract U,Pu, Np (Tc($S_{Tc}^{1st\ extcyc}$ =80 -90%))

Reducing agent (N_2H_4)

Reductive separation of U, Pu, Np (**Tc**)

Back extract Pu(III), Np (**Tc(IV)**)

1. Variable red-ox states
2. Variable species

Extract U(VI)$_{organic}$ (**Tc(VII),Tc(VI),Tc(V)**)

- Pu(IV) + U(IV) → U(VI)$_{org}$ + Pu(III)$_{H2O}$
- Difficulties in stability of U/Pu separation at UK, Russian and French facilities
- Catalytic Tc effects in many chem. reactions
- Variable Tc redox states
- Tc - Waste problems

Sellafield (UK)

Mayak (Russia)

Kinetics of Tc(VII) reduction with $N_2H_5NO_3$ in presence of Th(4+)

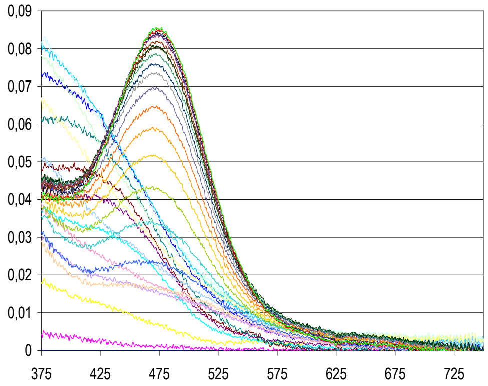

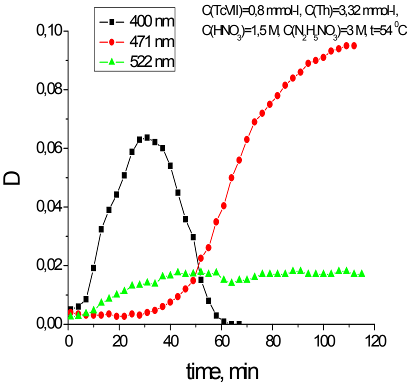

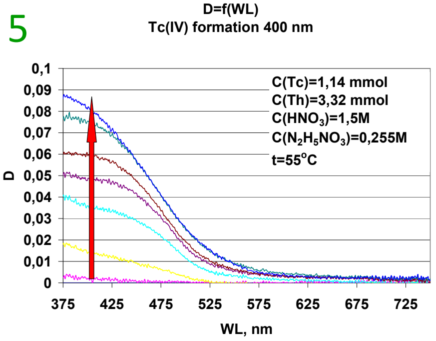

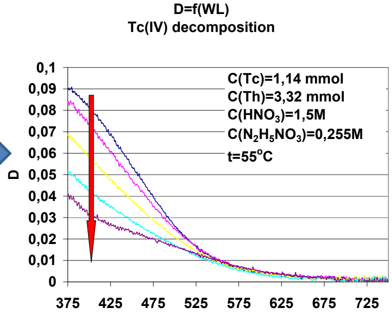

First stage: Tc(VII) → Tc(IV)
quantified by the shoulder at 400 nm
Reaction order n=0

Second stage : Tc(IV) →Tc(X) 400 nm
Reaction order n=0

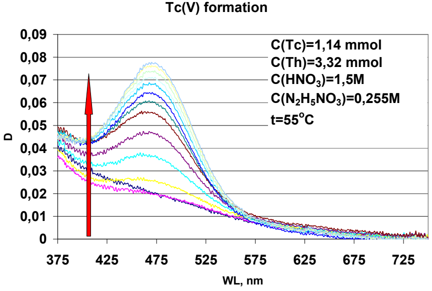

The third stage: Tc(X)→Tc(V)
470 nm
evolution of N_2 followed by Tc(V)
formation
Reaction order n = 1

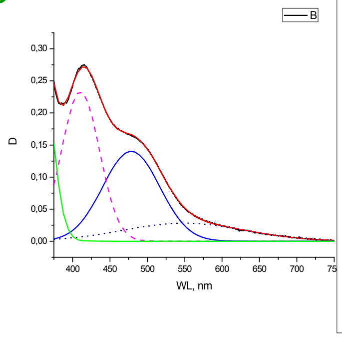

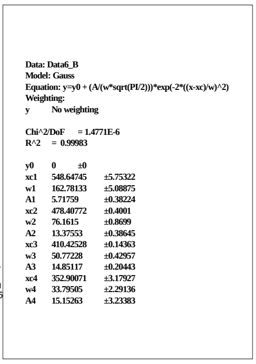

```
Data: Data6_B
Model: Gauss
Equation: y=y0 + (A/(w*sqrt(PI/2)))*exp(-2*((x-xc)/w)^2)
Weighting:
y         No weighting

Chi^2/DoF     = 1.4771E-6
R^2    =  0.99983

y0      0          ±0
xc1     548.64745       ±5.75322
w1      162.78133       ±5.08875
A1      5.71759         ±0.38224
xc2     478.40772       ±0.4001
w2      76.1615         ±0.8699
A2      13.37553        ±0.38645
xc3     410.42528       ±0.14363
w3      50.77228        ±0.42957
A3      14.85117        ±0.20443
xc4     352.90071       ±3.17927
w4      33.79505        ±2.29136
A4      15.15263        ±3.23383
```

Reactions taking place in $Tc-HNO_3-N_2H_5NO_3$ system

$TcVII+N_2H_5^+ \rightarrow TcVI+N_2H_3\cdot+H^+$
$TcV+N_2H_5^+ \rightarrow TcIV+N_2H_3\cdot+H^+$
$TcIV+TcVII \rightarrow TcVI+TcV$
$TcIV+NO_3^- \rightarrow TcVI+NO_2^-$
$TcVI+N_2H_5^+ \rightarrow TcIV+N_2H_2^++3H^+$
$TcVI+NO_3^- \rightarrow TcVII+NO_2^-$
$TcV+NO_3^- \rightarrow TcVI+HNO_2$
$HNO_2+N_2H_5^+ \rightarrow HN_3+2H_2O+H^+$
$HN_3+HNO_2 \rightarrow N_2+N_2O+H_2O$
$2N_2H_3\cdot \rightarrow N_4H_6 \rightarrow 2NH_3+N_2$
$2N_2H_2 \rightarrow N_4H_4 \rightarrow HN_3+NH_3$

- Every spectrum was analyzed by deconvolution, otherwise the analysis would be impossible

1) 600 nm – Tc(III)
2) 470 nm – Tc(Y)
3) 420 nm – complex with products of hydrazine oxidation
4) 400 nm – Tc(IV)

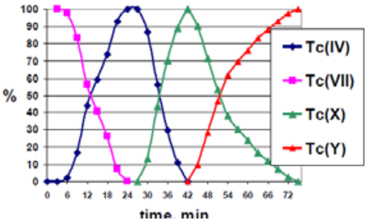

7

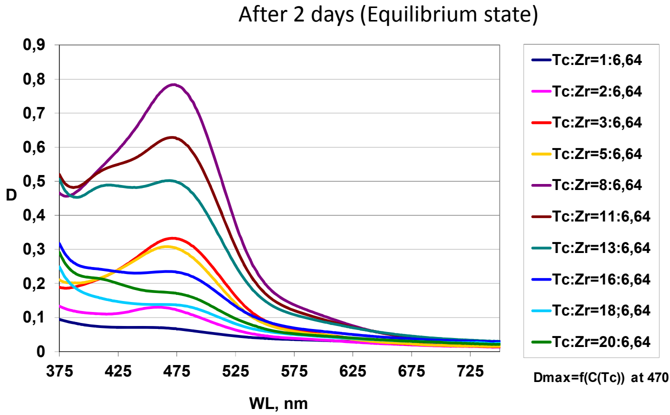

Zirconium c(Zr)=6,64 mmol/l

t = 60°C

Dmax=f(C(Tc)) at 470 nm

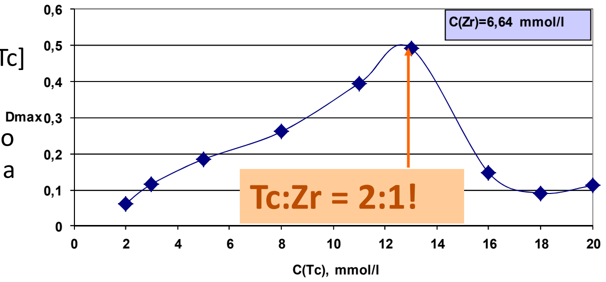

Concentration of the Tc(V) complex is increasing at the [Tc] from 2 up to 13 mM.

Futher increase of [Tc] leads to appearance of Tc(IV) which is a catalytic agent for decomposition of hydrazine.

8

Pr_4NTcO_4 structure and solubility study for Tc separation from High level radioactive wastes

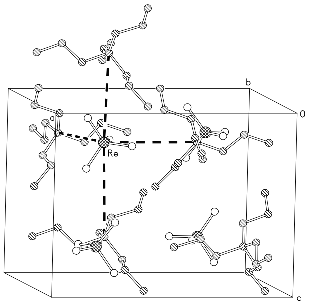

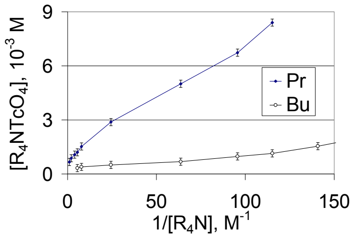

C(Pr4N+)	C(TcO4-)	γ±	Ks	G298, kJ/mol
0,0087	0,0087	0,904489	6,19221E-05	24,02
0,014	0,006	0,882947	6,5486E-05	23,88
0,0172	0,005	0,872475	6,54643E-05	23,88
0,041	0,0029	0,820264	7,99998E-05	23,38

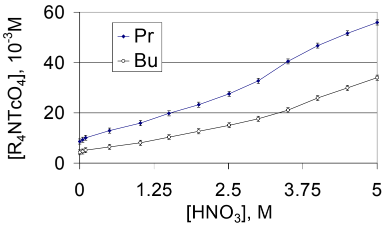

Conclusions

- 4 Tc species were characterized kinetically and spectrophotometrically in PUREX-like solutions. Tc(V) forms stable complexes with M(IV) (M=Th,Zr) in 1.3 M HNO_3 when Tc:Zr(Th)=2:1
- The system Th(Zr)-Tc-$N_2H_5NO_3$ (NH_2OH*HCl)-HNO_3 is so complicated that to answer all the questions we need supplementary study of the solid phases
- Pr_4NTcO_4 can be used to precipitate Tc from solutions to further transmutation. We have determined ΔG as 23 kJ/M. For TdS term temperature dependence is needed.

Thank you for attention!

And be careful with Technetium!

DEEP EUTECTIC SOLVENTS

Veronika Fischer, Werner Kunz

Institute of Physical and Theoretical Chemistry, University of Regensburg,
D-93053 Regensburg, Germany

Mixtures of environmentally friendly salts, sugars and urea form deep eutectic solvents (DES) with melting points below 25 °C. These are completely new, green solvents whose properties are widely unexplored. In general, the structure of DES depends on the formation of hydrogen bonds between the molecules[1,2]. These mixtures offer certain advantages. They are easy to prepare by simply mixing the components[3]. The purity is only dependent on the purity of its individual components[4]. Furthermore the mixtures are biodegradable, non-toxic, non-volatile, non-reactive with water and can be accomplished with low cost materials[1,3,4]. In our study, we examine ternary mixtures with high sugar contents. The sugar causes a further depression of freezing point compared to the binary mixture.

References:

(1) Abbott, A. P.; Boothby, D.; Capper, G.; Davies, D. L.; Rasheed, R. K. *Journa of the American Chemical Society* **2004**, *126*, 9142.
(2) Abbott, A. P.; Capper, G.; Davies, D. L.; Rasheed, R. K.; Tambyrajah, V. *Chemical Communications* **2003**, 70.
(3) Abbott, A. P.; Capper, G.; Gray, S. *ChemPhysChem* **2006**, *7*, 803.
(4) Carriazo, D.; Serrano, M. C.; Gutierrez, M. C.; Ferrer, M. L.; del Monte, F. *Chemical Society Reviews* **2012**, *41*, 4996.

Universität Regensburg

Veronika Fischer
Lehrstuhl für Physikalische Chemie II
FAKULTÄT FÜR CHEMIE UND PHARMAZIE

Deep Eutectic Solvents

V. FISHER

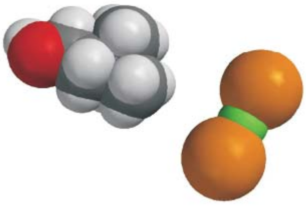

7th European Summer School
Moscow, 20-23 July 2012

Universität Regensburg

Veronika Fischer
Lehrstuhl für Physikalische Chemie II
FAKULTÄT FÜR CHEMIE UND PHARMAZIE

General Information

- The term deep eutectic solvents (DESs) has been coined as the mixtures are effectively eutectics formed between two components → very large depression of the melting point in the region of 200 °C[1]
- Eutectic mixtures of salts: Formed to decrease the temperature for molten salt applications (e.g. mixing quaternary ammonium salts with metal salts)[1]
- The deep eutectic results from the formation of complex anions → depression of the lattice energy → depression of the melting point[1]

Advantages

- Easy to produce [1,2]
- Purity of the resulting DES simply depends on the purity of its individual components[1, 2]
- Low costs[1, 2]
- Nonreactive with water[1, 2]
- Non-volatile, non-inflammable and biodegradable[1, 2]

Types of DES

There are three types of DES [1]

- Type 1: Metal salt + organic salt
- Type 2: Metal salt hydrate + organic salt
- Type 3: Hydrogen bond donor + organic salt

First deep eutectic solvent without metal salt[1]:

Hydrogen bond donor (HBD) = Urea (mp = 133 °C)

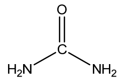

Organic salt = Choline chloride (ChCl) (mp = 302 °C)

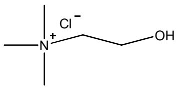

→ Liquid at ambient temperature

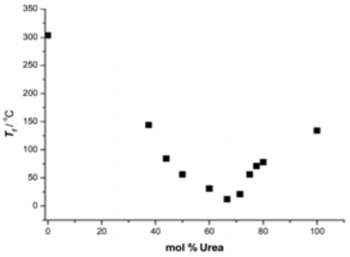

Figure 1. Melting point of choline chloride/urea mixtures as a function of composition[1].

- Depression of the melting point must arise from an interaction between urea molecules and the chloride ion[1]

- Homogeneous liquids are only formed with compounds capable of forming hydrogen bonds with chloride ions[1]

Universität Regensburg

Veronika Fischer
Lehrstuhl für Physikalische Chemie II
FAKULTÄT FÜR CHEMIE UND PHARMAZIE

Other DES

The principle of DES is not limited to amides. It can be applied to a wide variety of other HBD such as acids, amines and alcohols[1, 3].

HBD	T_m in °C	$T_m{}^*$ in °C
Urea, $(NH_2)_2CO$	12	134
1-Methyl urea, $CH_3NHCONH_2$	29	93
Acetamide, CH_3CONH_2	51	80
Malonic acid, $CH_2(COOH)_2$	10	135
Oxalic acid, HO_2CCO_2H	34	190
Phenylacetic acid, $C_6H_5CH_2CO_2H$	25	77
Ethylene glycol, $HOCH_2CH_2OH$	-91	-13

Table 1. Melting point temperature of various ChCl:HBD DES at eutectic composition together with the melting point of the pure HBDs

Universität Regensburg

Veronika Fischer
Lehrstuhl für Physikalische Chemie II
FAKULTÄT FÜR CHEMIE UND PHARMAZIE

DES with sugar content

Ternary mixtures of sugar/sugar alcohol-urea-inorganic salt as a solvent for organic transformations[4, 5].

But: Melting points in the range of 65 to 85 °C

↓

Optimization of the melting point by varying the components and the composition of the mixtures

Universität Regensburg

Veronika Fischer
Lehrstuhl für Physikalische Chemie II
FAKULTÄT FÜR CHEMIE UND PHARMAZIE

Mixture	Molar ratio	Melting point
Urea-ChCl	2:1	12 °C
Glucose-Urea-NaCl	2:1.3:1	78 °C
Glucose-Urea- ChCl	1:1:1	< 0 °C
Sorbitol-DMU-NH_4Cl	2:1.2:1	67 °C
Sorbitol-Urea-ChCl	1:1:1	< 0 °C

Table 2. Melting points of mixtures containing glucose/sorbitol, urea/DMU and salt

→ The melting point decreases by changing the composition and replacing the inorganic salt with ChCl

→ The sugar/sugar alcohol causes a further depression of melting point compared to the binary mixture

---

Thank you for your Attention

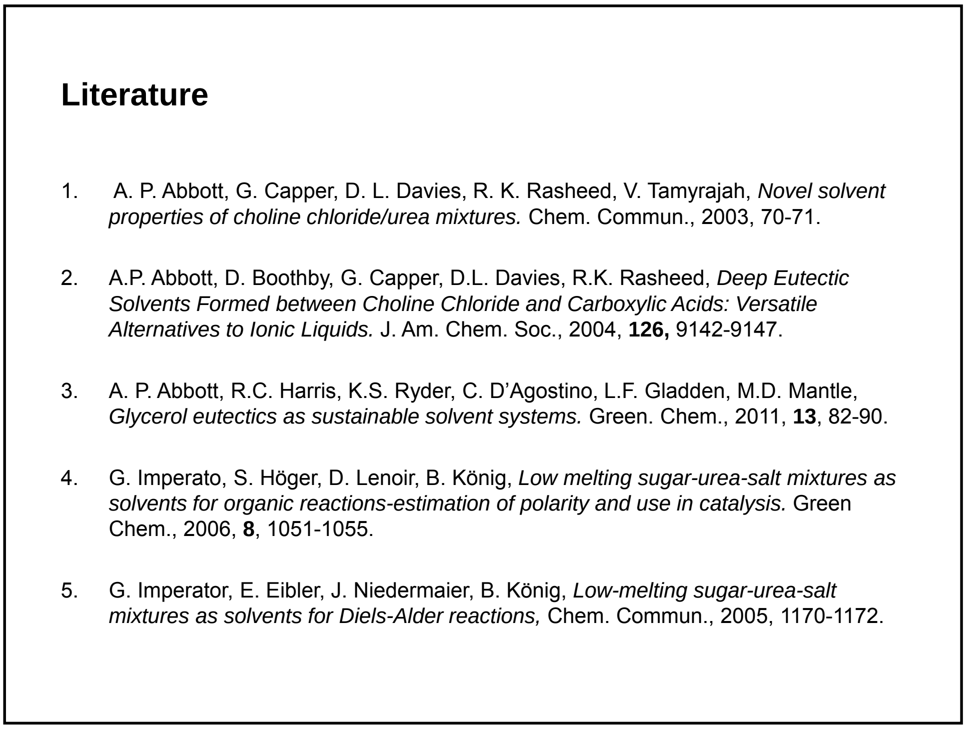

Literature

1. A. P. Abbott, G. Capper, D. L. Davies, R. K. Rasheed, V. Tamyrajah, *Novel solvent properties of choline chloride/urea mixtures.* Chem. Commun., 2003, 70-71.

2. A.P. Abbott, D. Boothby, G. Capper, D.L. Davies, R.K. Rasheed, *Deep Eutectic Solvents Formed between Choline Chloride and Carboxylic Acids: Versatile Alternatives to Ionic Liquids.* J. Am. Chem. Soc., 2004, **126,** 9142-9147.

3. A. P. Abbott, R.C. Harris, K.S. Ryder, C. D'Agostino, L.F. Gladden, M.D. Mantle, *Glycerol eutectics as sustainable solvent systems.* Green. Chem., 2011, **13**, 82-90.

4. G. Imperato, S. Höger, D. Lenoir, B. König, *Low melting sugar-urea-salt mixtures as solvents for organic reactions-estimation of polarity and use in catalysis.* Green Chem., 2006, **8**, 1051-1055.

5. G. Imperator, E. Eibler, J. Niedermaier, B. König, *Low-melting sugar-urea-salt mixtures as solvents for Diels-Alder reactions,* Chem. Commun., 2005, 1170-1172.

NANOSTRUCTURED LIQUIDS, COLLOIDS AND ENVIRONMENTALLY ACCEPTABLE LIQUID MEDIA

Michael Klossek, Didier Touraud and Werner Kunz*

Institute of Physical and Theoretical Chemistry University of Regensburg,
93040 Regensburg, Germany
** e-mail: werner.kunz@chemie.uni-regensburg.de*

In order to investigate the influence of the chemical structure of renewable feedstock oils (RFOs) on the domains of existence and nanostructure of microemulsions we have chosen to study the pseudo-ternary system water/SDS/1-Pentanol/renewable oil.

The domains of existence were determined by recording pseudo-ternary phase diagrams (PTPD) with a melt of SDS/1-Pentanol as pseudo component in a constant mass ratio of 1:2 and limonene and/or rapeseed biodiesel as renewable oil. The nanostructures of the formulated microemulsions were studied using conductivity measurements.

All the results were compared to those obtained by using n-alkanes as oils with a carbon chain length between 6 and 16.

We can show that the use of limonene gives a similar phase diagram as octane or nonane. The domain of existence of the microemulsion obtained with rapeseed biodiesel is more like the one observed in presence of hexadecane.

By mixing both oils we were able to screen more or less the whole spectrum of phase diagrams beginning with octane and ending with hexadecane. For this reason we examined the phase diagrams for the limonene-to-biodiesel mixtures with the mass ratios 1:3, 1:1 and 3:1 further to those with pure components. For the behavior of the oil not the hydrophobicity plays an important role on the domain of existence of the microemulsion but the number of carbon atoms in the molecule.

The ultimate goal of this study is the proposition of “green” alternatives to alkanes that are still widely used in product formulations.

7-th ESSSIISC
Moscow, 20-23 July 2012

Nanostructured Liquids, Colloids and Environmentally Acceptable Liquid Media

M. Sc. Michael Klossek
Institute of Physical and Theoretical Chemistry
Faculty of Chemistry & Pharmacy

Universität Regensburg

Content

- Introduction
  - What are Microemulsions
  - Pseudo-Ternary Phase Diagrams (PTPDs)
- Green Microemulsions
  - With Renewable Feedstock Oils
  - With Green Surfactants
  - With Green Co-Surfacants
- Conclusion

What are Microemulsions

Microemulsions are thermodynamically stable, isotropic, transparent mixtures of at least one hydrophilic, one hydrophobic, and one amphiphilic component.
A great variety of structures of single phase microemulsions is known in literature ranging from water-in-oil (w/o) over bicontinuous to oil-in-water (o/w) structures. In the case of a w/o microemulsion, oil is the continuous phase with water droplets stabilized by surfactant molecules and vice versa for o/w structures. Bicontinuous structures, which are networks of oil and water nanodomains separated and stabilized by a surfactant interfacial film with a net curvature close to zero can be found at almost equal amounts of water and oil.[1]

---

[1] Agnes Harrar, Dissertation, 2011, Regensburg

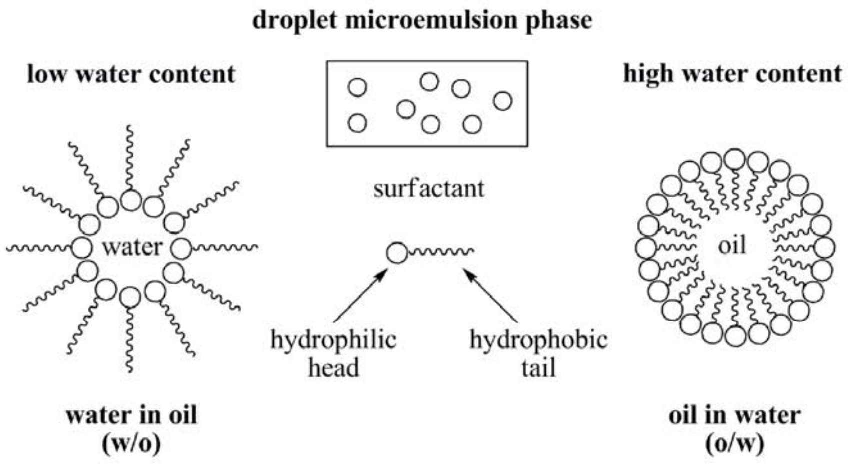

Universität Regensburg

M. Sc. Michael Klossek
Institute of Physical and Theoretical Chemistry
Faculty of Chemistry & Pharmacy

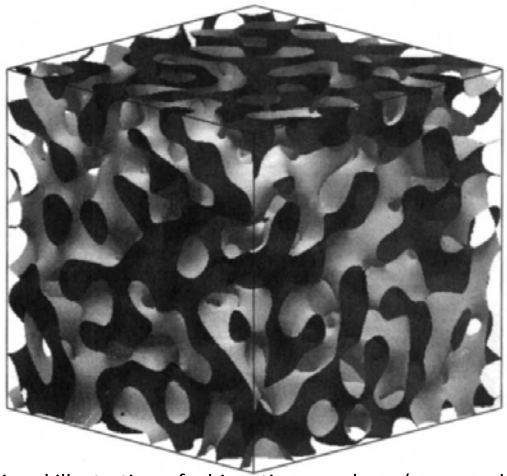

3-Dimensional illustration of a bicontinuous phase (sponge phase)[2]

[2] Pieruschka, P.; Marcelja, S., *Langmuir* ,1994, **10**, 345

Universität Regensburg

M. Sc. Michael Klossek
Institute of Physical and Theoretical Chemistry
Faculty of Chemistry & Pharmacy

Pseudo-Ternary Phase Diagrams

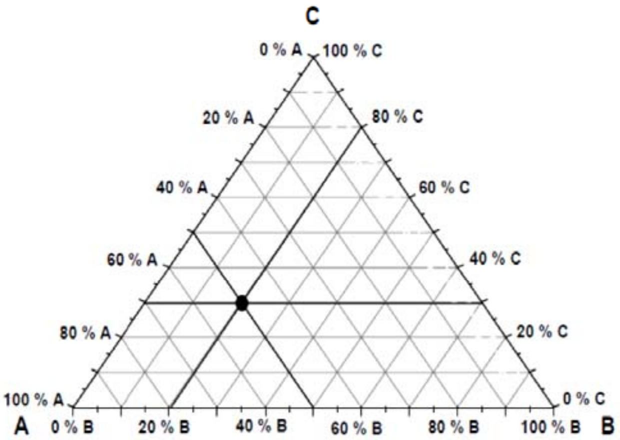

M. Sc. Michael Klossek
Institute of Physical and Theoretical Chemistry
Faculty of Chemistry & Pharmacy

Green Microemulsions with Renewable Feedstock Oils

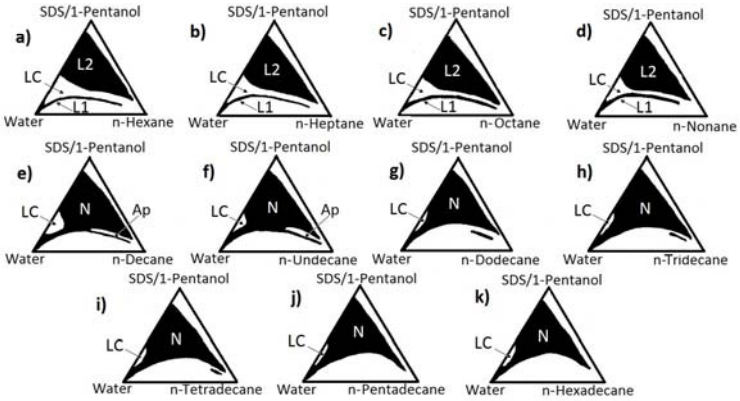

Homologous series of pseudo-ternary phase diagrams for the water/SDS/1-Pentanol/n-alkanes systems. The domains of existence of the microemulsions are represented in black. All these phase diagrams were determined during an anterior work[4]. Temperature was kept constant at 25°C and the weight ratio of SDS-to-1-Pentantol (1:2) as well.

M. Sc. Michael Klossek
Institute of Physical and Theoretical Chemistry
Faculty of Chemistry & Pharmacy

Green Microemulsions with Renewable Feedstock Oils

- Biodiesel
  - Rapeseed Biodiesel
    Obtained by transesterification of rapessed oil with methanol to give fatty acid methyl esters (FAME)
  - TBK Biodiesel
    TBK-Biodiesel is made by partial transesterification of triglycerides with alkyl esters of carboxylic acids
  - Cuphea Biodiesel
    Cuphea is proposed as a source of fatty acids with medium chain length, mostly decanoic acid

- Limonene (1-methyl-4-(1-methylethenyl)-cyclohexane)
  - major constituent in citrus oils (peel oil contains 95% R-Limonene)
  - nowadays widely used as biogenic solvent (e.g can be used to dissolve polystyrene, and is a more ecologically friendly substitute for acetone or toluene)
  - Limonene is considered as a skin irritant and sensitizer in high concentrations but not allergenic

Brassica napus
Origin: Mediterranean Area

Cuphea ignea A. DC., Origin: South America

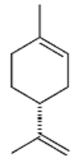

R-Limonene

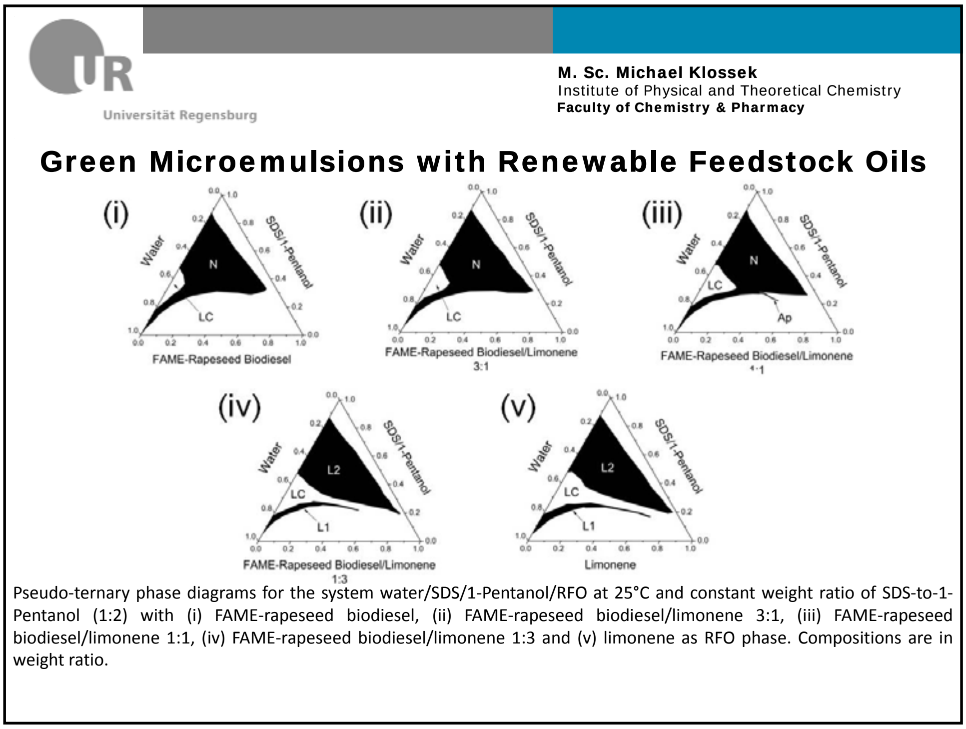

Universität Regensburg

M. Sc. Michael Klossek
Institute of Physical and Theoretical Chemistry
Faculty of Chemistry & Pharmacy

Green Microemulsions with Renewable Feedstock Oils

Pseudo-ternary phase diagrams for the system water/SDS/1-Pentanol/RFO at 25°C and constant weight ratio of SDS-to-1-Pentanol (1:2) with (i) FAME-rapeseed biodiesel, (ii) FAME-rapeseed biodiesel/limonene 3:1, (iii) FAME-rapeseed biodiesel/limonene 1:1, (iv) FAME-rapeseed biodiesel/limonene 1:3 and (v) limonene as RFO phase. Compositions are in weight ratio.

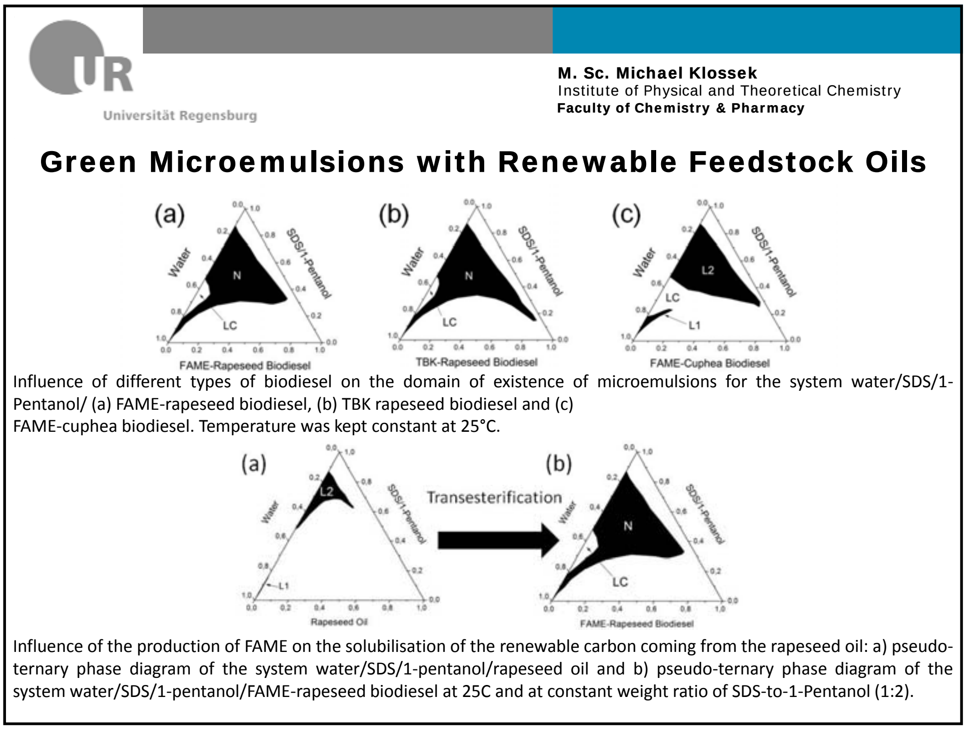

Universität Regensburg

M. Sc. Michael Klossek
Institute of Physical and Theoretical Chemistry
Faculty of Chemistry & Pharmacy

Green Microemulsions with Renewable Feedstock Oils

Influence of different types of biodiesel on the domain of existence of microemulsions for the system water/SDS/1-Pentanol/ (a) FAME-rapeseed biodiesel, (b) TBK rapeseed biodiesel and (c) FAME-cuphea biodiesel. Temperature was kept constant at 25°C.

Influence of the production of FAME on the solubilisation of the renewable carbon coming from the rapeseed oil: a) pseudo-ternary phase diagram of the system water/SDS/1-pentanol/rapeseed oil and b) pseudo-ternary phase diagram of the system water/SDS/1-pentanol/FAME-rapeseed biodiesel at 25C and at constant weight ratio of SDS-to-1-Pentanol (1:2).

M. Sc. Michael Klossek
Institute of Physical and Theoretical Chemistry
Faculty of Chemistry & Pharmacy

Green Microemulsions with Renewable Feedstock Oils

Characterization of Microemulsions – Electrical Conductivity

Measurement of electrical conductivity is one of the key methods to study the microstructure of microemulsions, especially in the case of w/o systems. In this case conductivity shows a significant change over many orders when the volume fraction of dispersed matter, here water, is increased above a certain value. Corresponding to several studies this sharp increase is the consequence of the percolative behavior of formed nanostructure in the system[5]. The percolation is induced when droplets in the microemulsion come close enough for an ion exchange from one to another or when the droplets coalesce and from clusters leading to an exchange of material[6]. This phenomenon can be observed when the specific conductivity of the polar phase is some orders of magnitude higher than the one of the oil.

[5] Lagues, M. *J. Phys. Lett.* 1979, **40**, 331
[6] Alexandridis, P., Holzwarth, J. F. and Alan Hatton, T., *J. Phys. Chem.* 1995, **99**, 8222-8232

M. Sc. Michael Klossek
Institute of Physical and Theoretical Chemistry
Faculty of Chemistry & Pharmacy

Green Microemulsions with Renewable Feedstock Oils

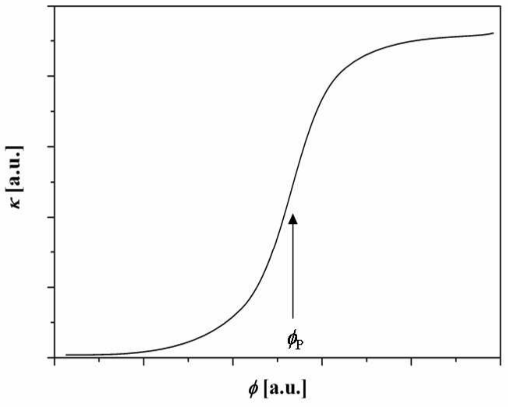

Universität Regensburg

M. Sc. Michael Klossek
Institute of Physical and Theoretical Chemistry
Faculty of Chemistry & Pharmacy

Green Microemulsions with Renewable Feedstock Oils

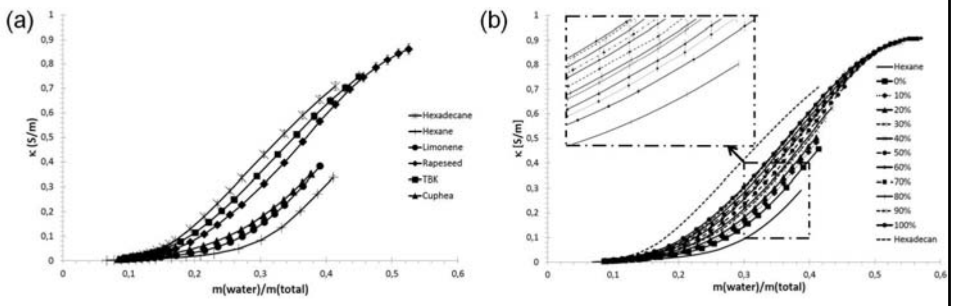

The specific conductivity of the microemulsions as a function of water weight ratio for the pseudo-ternary system water/SDS/1-Pentanol/oil with a constant weight ratio of SDS-to-1-Pentanol (1:2) is shown. As oil phase either hexadecane, or hexane, or limonene, or FAME-rapeseed, or TBK-rapeseed, or FAME-cuphea biodiesels were used. (b) The specific conductivity of the microemulsions as a function of water weight content for the pseudo-ternary system water/SDS/1-Pentanol/oil with a constant weight ratio of SDS-to-1-Pentanol (1:2) is shown. As oil phase mixtures of FAME-rapeseed biodiesel and limonene were used. The experimental path of the conductivity measurements is the same as already shown and explained in Figure 1. All experiments were recorded at 25°C.

Universität Regensburg

M. Sc. Michael Klossek
Institute of Physical and Theoretical Chemistry
Faculty of Chemistry & Pharmacy

Microemulsions with Green Surfactants

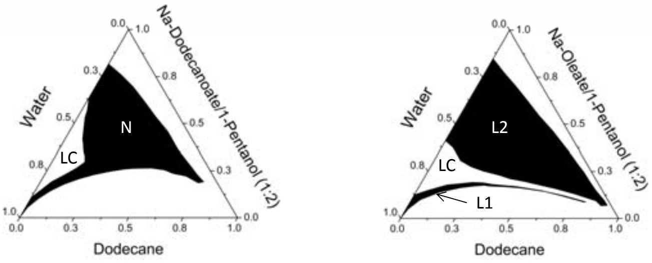

Influence of different green surfactant on the domain of existence of microemulsions for the system water/Na-Oleate/1-Pentanol/ Dodecane. Temperature was kept constant at 25°C and the surfactant-to-cosurfactant weight ratio at 1:2.

M. Sc. Michael Klossek
Institute of Physical and Theoretical Chemistry
Faculty of Chemistry & Pharmacy

RFO-Microemulsions with Green Co-Surfactants

- Heptanol/Ethanol Mixtures
- Citronellol/Ethanol Mixtures
- *Replace Ethanol by 1,5-Pentanediol (Planned)*
- Dodecanol/Ethanol Mixtures
- Guerbet-Alcohols

M. Sc. Michael Klossek
Institute of Physical and Theoretical Chemistry
Faculty of Chemistry & Pharmacy

Conclusion

- Replacing of NFOFS by pure or ROF mixtures is possible
- Limonene and Cuphea Biodiesel act like short-chain alkanes
- TBK- and FAME-rapeseed biodiesel oil can substitute long-chain
- The extent of the microemulsion domains and the organization of the nano-droplets could be predicted by the average number of carbon pro molecules (or the average molecular volume) of the RFO or RFOs mixtures.
- Percolative behaviour of the studied systems is kept whatever the molecular volume or the polarity of the oil

M. Sc. Michael Klossek
Institute of Physical and Theoretical Chemistry
Faculty of Chemistry & Pharmacy

Thank You For Your Attention !!

SYNTHESIS AND CONFORMATIONAL BEHAVIOUR OF PHTHALOCYANINES, BEARING LATERAL COORDINATING MACROCYCLIC SUBSTITUENTS

Martynov A.G., Gorbunova Yu.G.,
Tsivadze A.Yu., Sauvage J.-P.

A.N. Frumkin Institute of Physical Chemistry and Electrochemistry RAS, Moscow, Russia
N.S. Kurnakov Institute of General and Inorganic Chemistry RAS, Moscow, Russia
Institut de Science et d'Ingénierie Supramoléculaires, Strasbourg, France

---

Heterotopic tetrapyrrolic compounds

Molecular building blocks of supramolecular assemblies

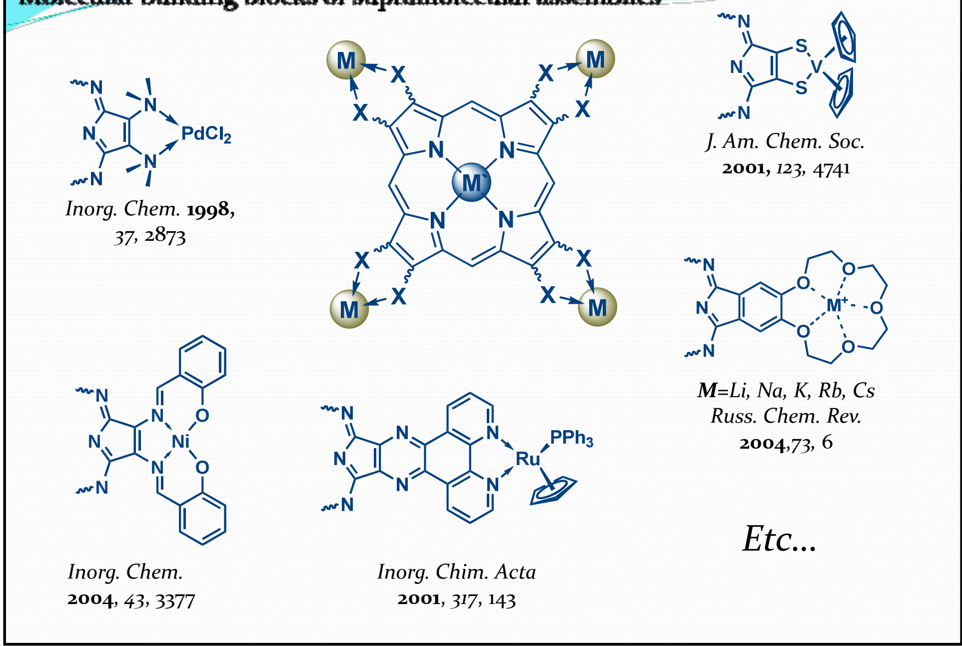

Inorg. Chem. **1998**, *37*, 2873

J. Am. Chem. Soc. **2001**, *123*, 4741

M=*Li, Na, K, Rb, Cs*
Russ. Chem. Rev.
2004,*73*, 6

Inorg. Chem.
2004, *43*, 3377

Inorg. Chim. Acta
2001, *317*, 143

Etc…

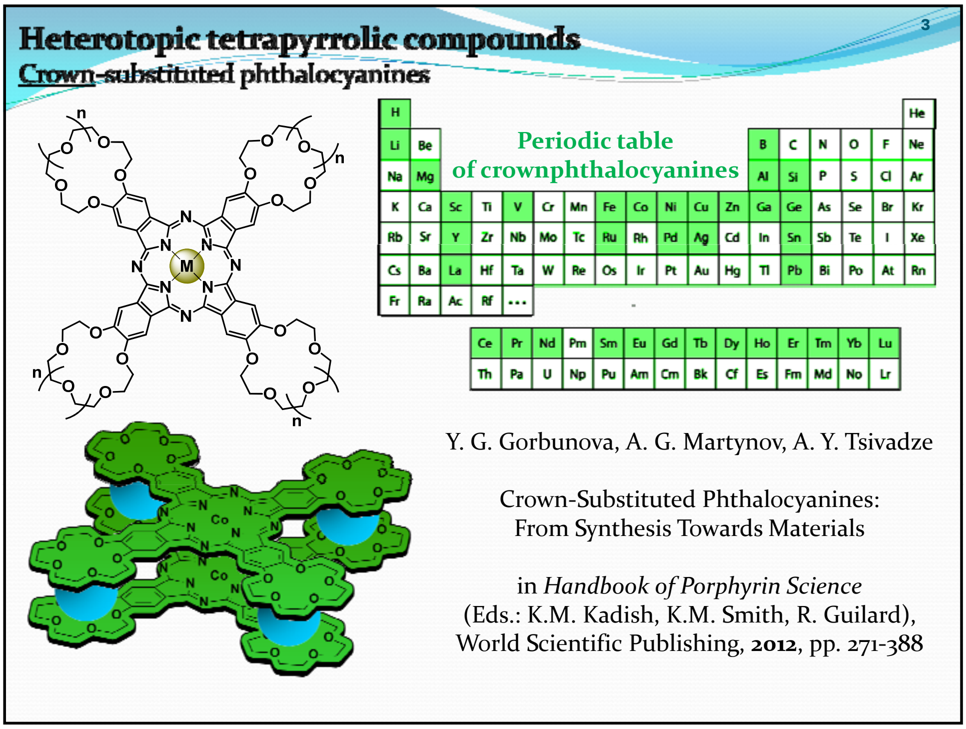

Heterotopic tetrapyrrolic compounds

Crown-substituted phthalocyanines

Periodic table of crownphthalocyanines

H																	He
Li	Be											B	C	N	O	F	Ne
Na	Mg											Al	Si	P	S	Cl	Ar
K	Ca	Sc	Ti	V	Cr	Mn	Fe	Co	Ni	Cu	Zn	Ga	Ge	As	Se	Br	Kr
Rb	Sr	Y	Zr	Nb	Mo	Tc	Ru	Rh	Pd	Ag	Cd	In	Sn	Sb	Te	I	Xe
Cs	Ba	La	Hf	Ta	W	Re	Os	Ir	Pt	Au	Hg	Tl	Pb	Bi	Po	At	Rn
Fr	Ra	Ac	Rf	...													
			Ce	Pr	Nd	Pm	Sm	Eu	Gd	Tb	Dy	Ho	Er	Tm	Yb	Lu	
			Th	Pa	U	Np	Pu	Am	Cm	Bk	Cf	Es	Fm	Md	No	Lr	

Y. G. Gorbunova, A. G. Martynov, A. Y. Tsivadze

Crown-Substituted Phthalocyanines:
From Synthesis Towards Materials

in *Handbook of Porphyrin Science*
(Eds.: K.M. Kadish, K.M. Smith, R. Guilard),
World Scientific Publishing, **2012**, pp. 271-388

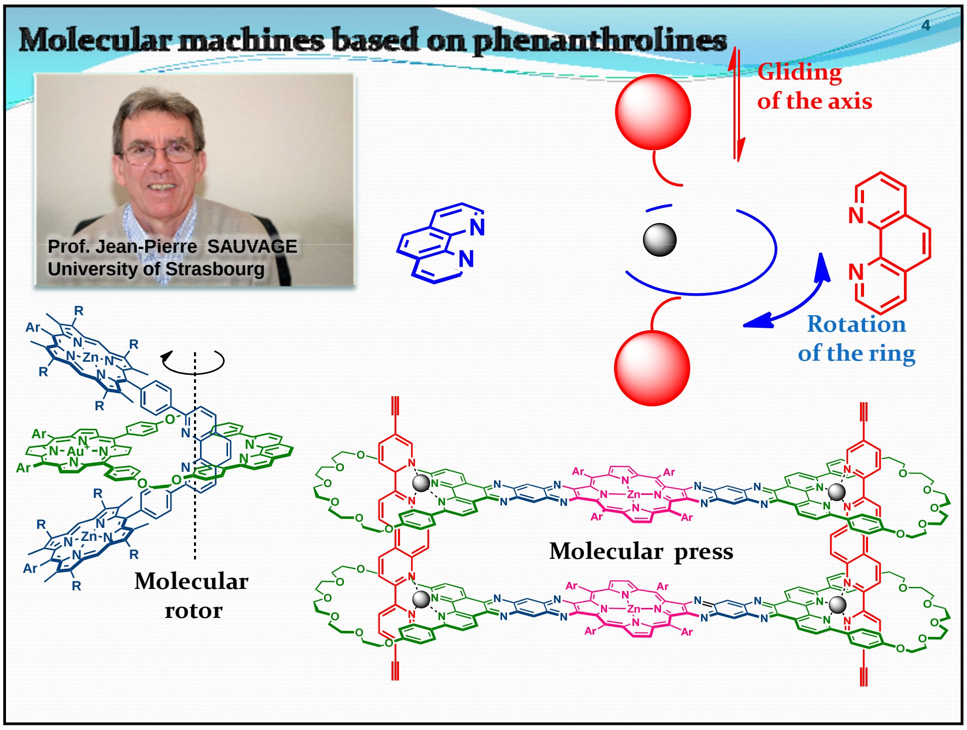

Molecular machines based on phenanthrolines

Prof. Jean-Pierre SAUVAGE
University of Strasbourg

Gliding of the axis

Rotation of the ring

Molecular rotor

Molecular press

JOINT RUSSIAN-FRENCH PROJECT: Phthalocyanines with latheral phenanthroline-containing macrocycles

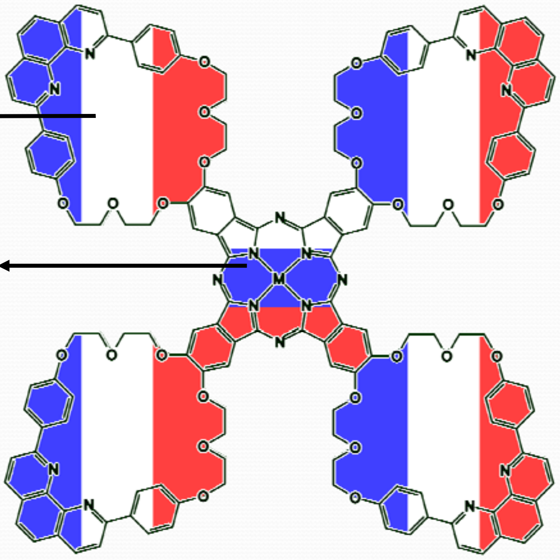

Macrocyclic phenanthroline-containing substituents

Phthalocyanine

Supported by grants
RFBR 09-03-93117,
MK-3595.2011.3 and
European research
association SUPRACHEM

Cu$^+$-templated molecular assembly

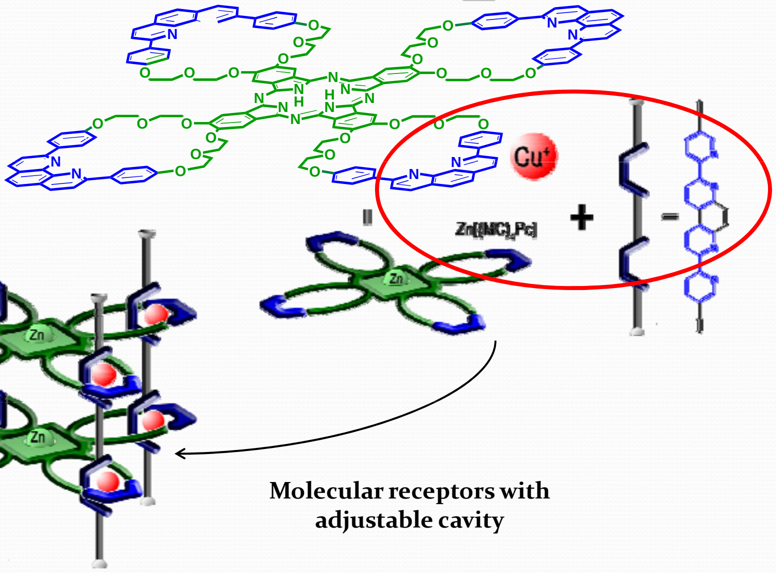

Molecular receptors with adjustable cavity

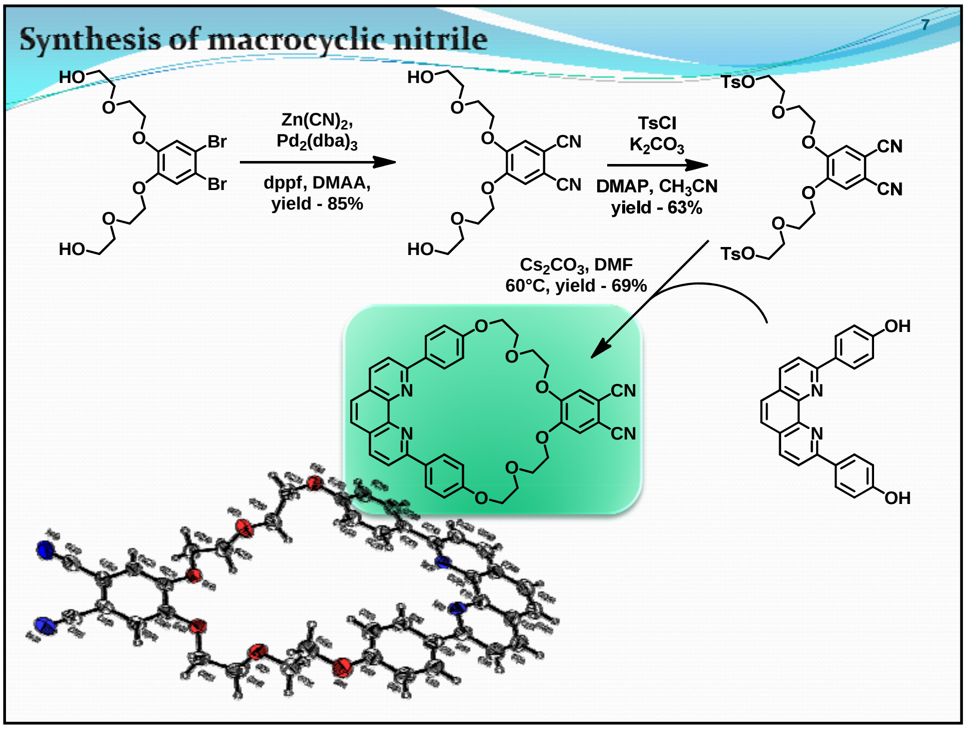

Synthesis of macrocyclic nitrile

$Zn(CN)_2$, $Pd_2(dba)_3$

dppf, DMAA, yield - 85%

TsCl K_2CO_3

DMAP, CH_3CN yield - 63%

Cs_2CO_3, DMF 60°C, yield - 69%

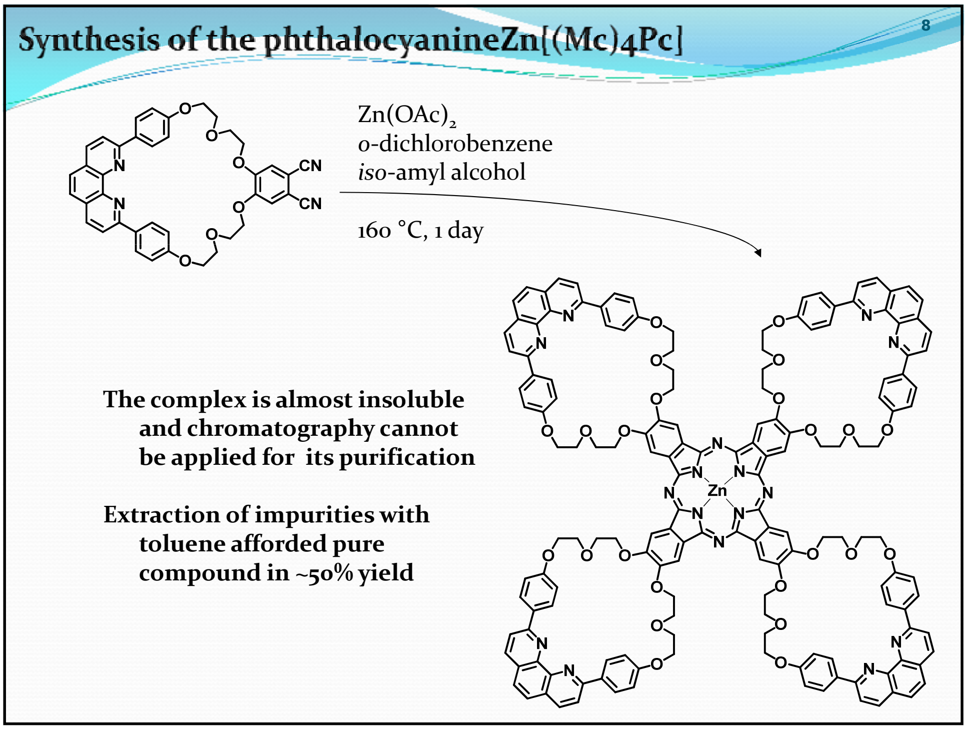

Synthesis of the phthalocyanineZn[(Mc)4Pc]

$Zn(OAc)_2$
o-dichlorobenzene
iso-amyl alcohol

160 °C, 1 day

The complex is almost insoluble and chromatography cannot be applied for its purification

Extraction of impurities with toluene afforded pure compound in ~50% yield

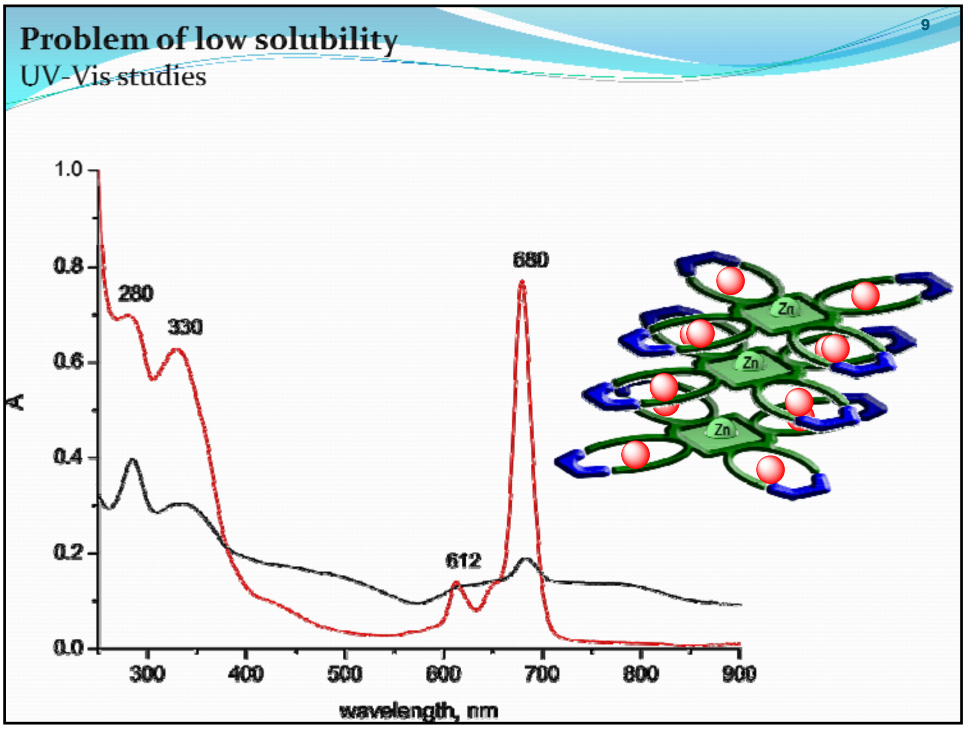

Problem of low solubility

UV-Vis studies

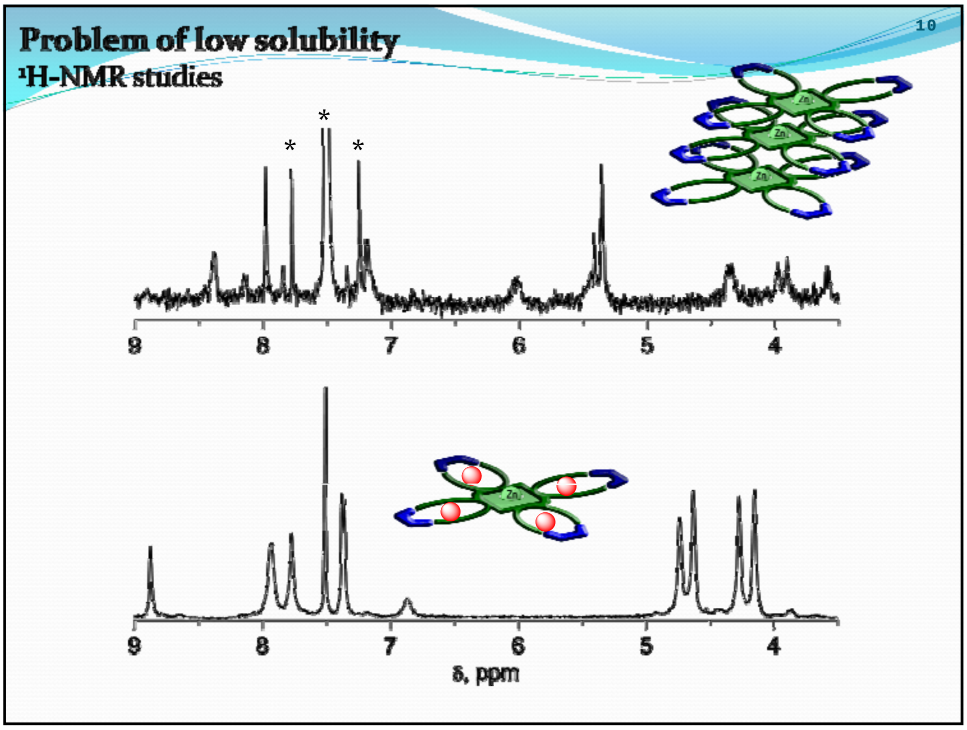

Problem of low solubility

^{1}H-NMR studies

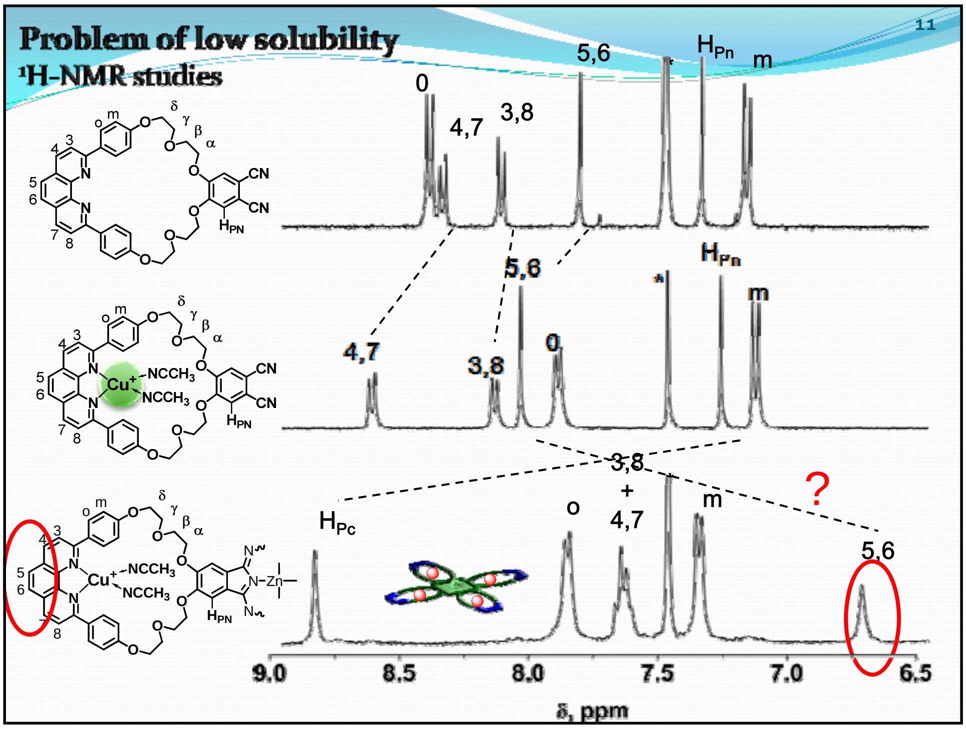

Problem of low solubility
¹H-NMR studies

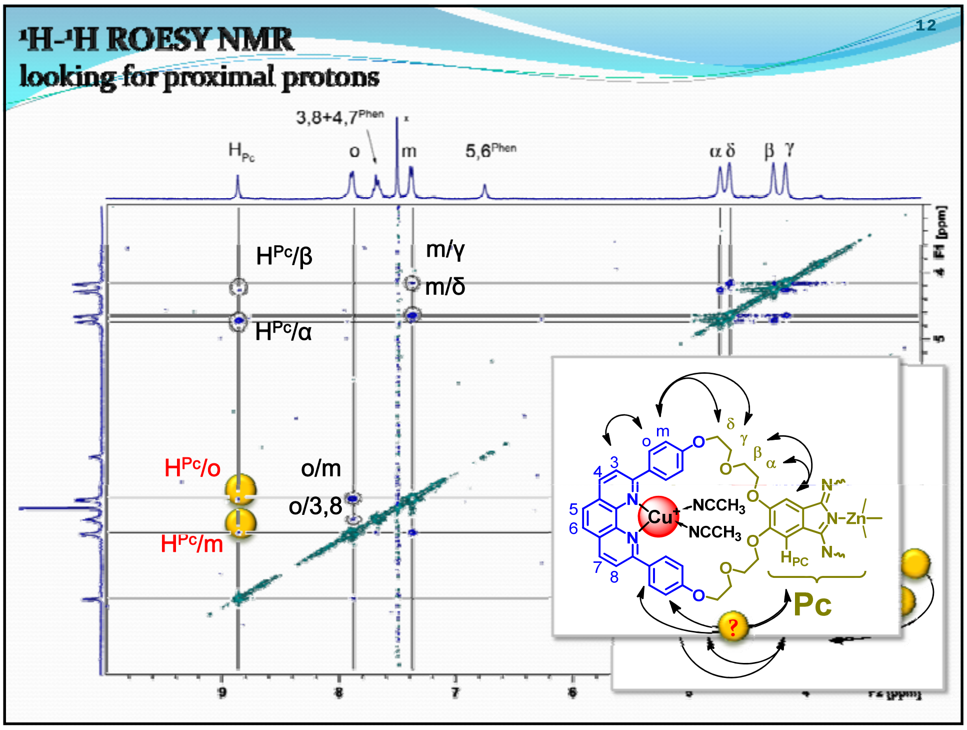

¹H-¹H ROESY NMR
looking for proximal protons

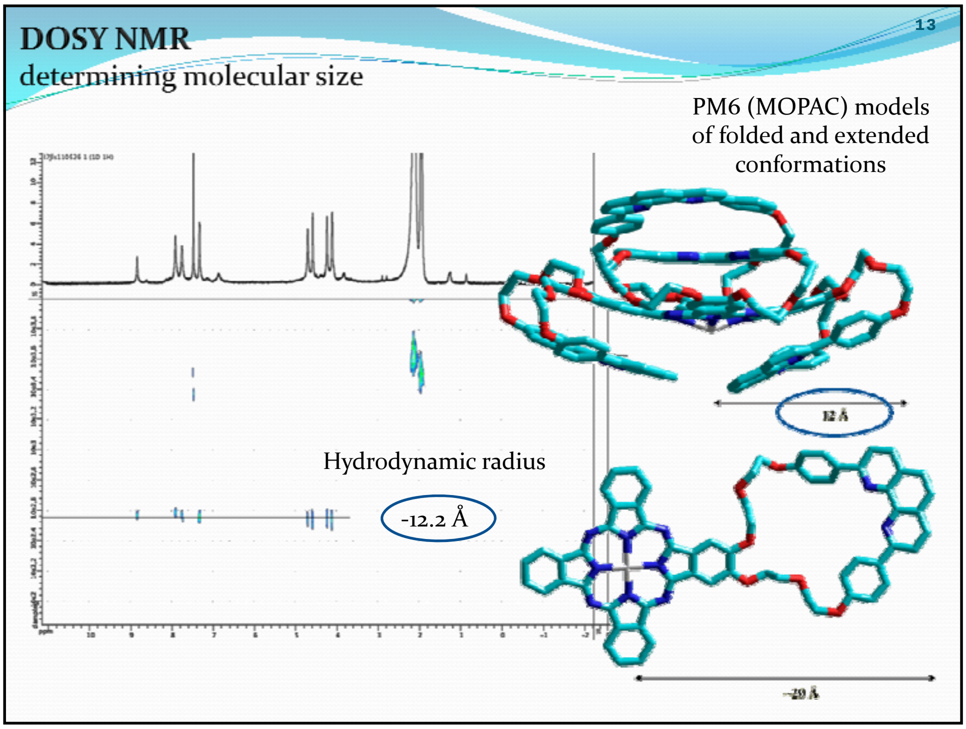

DOSY NMR

determining molecular size

PM6 (MOPAC) models of folded and extended conformations

Hydrodynamic radius

-12.2 Å

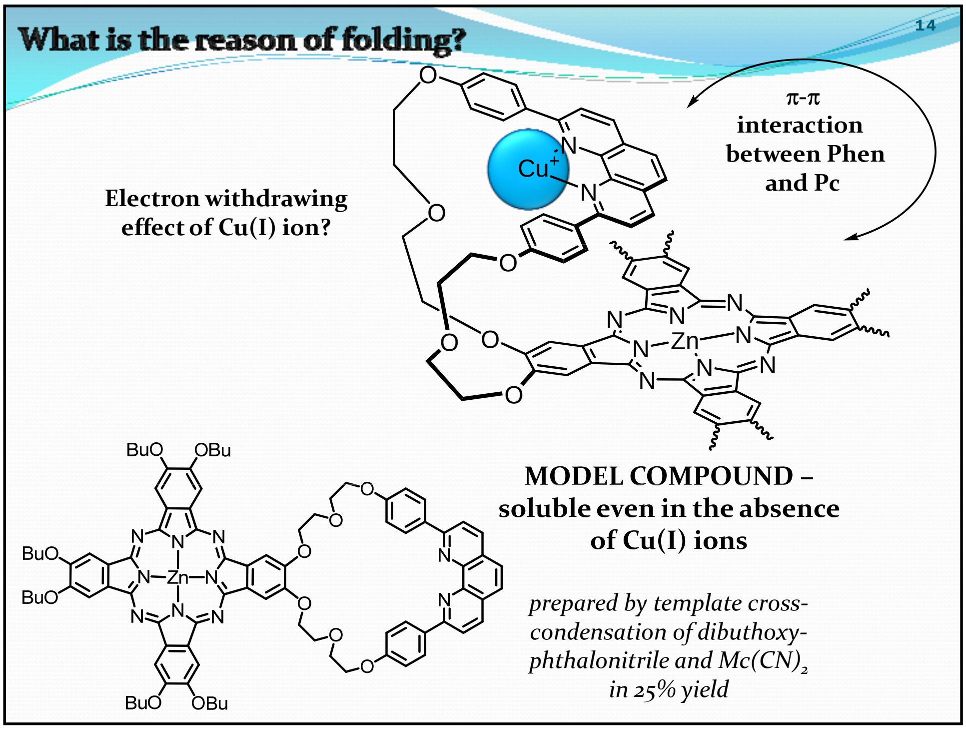

What is the reason of folding?

Electron withdrawing effect of Cu(I) ion?

π-π interaction between Phen and Pc

MODEL COMPOUND – soluble even in the absence of Cu(I) ions

prepared by template cross-condensation of dibuthoxy-phthalonitrile and Mc(CN)$_2$ in 25% yield

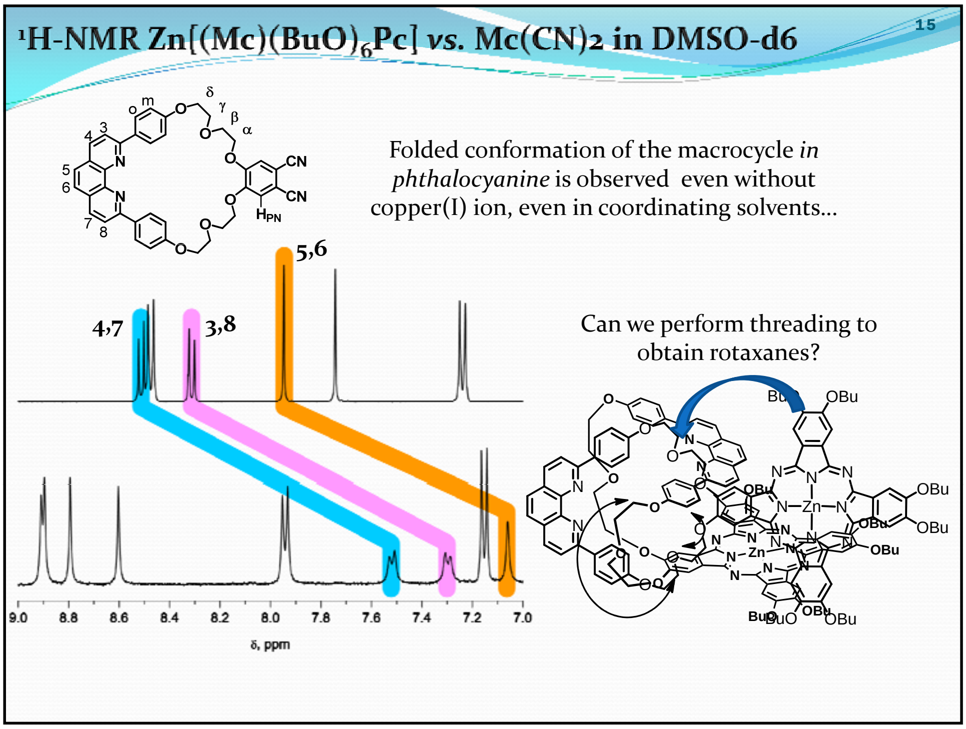

¹H-NMR Zn[(Mc)(BuO)$_6$Pc] *vs.* Mc(CN)2 in DMSO-d6

Folded conformation of the macrocycle *in phthalocyanine* is observed even without copper(I) ion, even in coordinating solvents…

Can we perform threading to obtain rotaxanes?

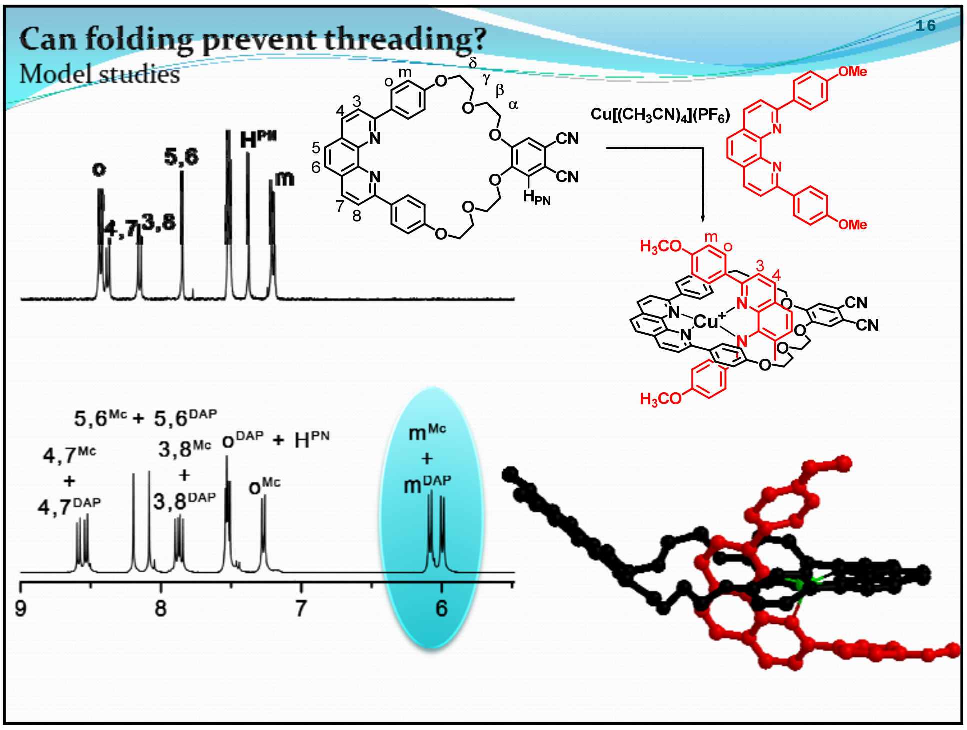

Can folding prevent threading?

Model studies

Cu[(CH$_3$CN)$_4$](PF$_6$)

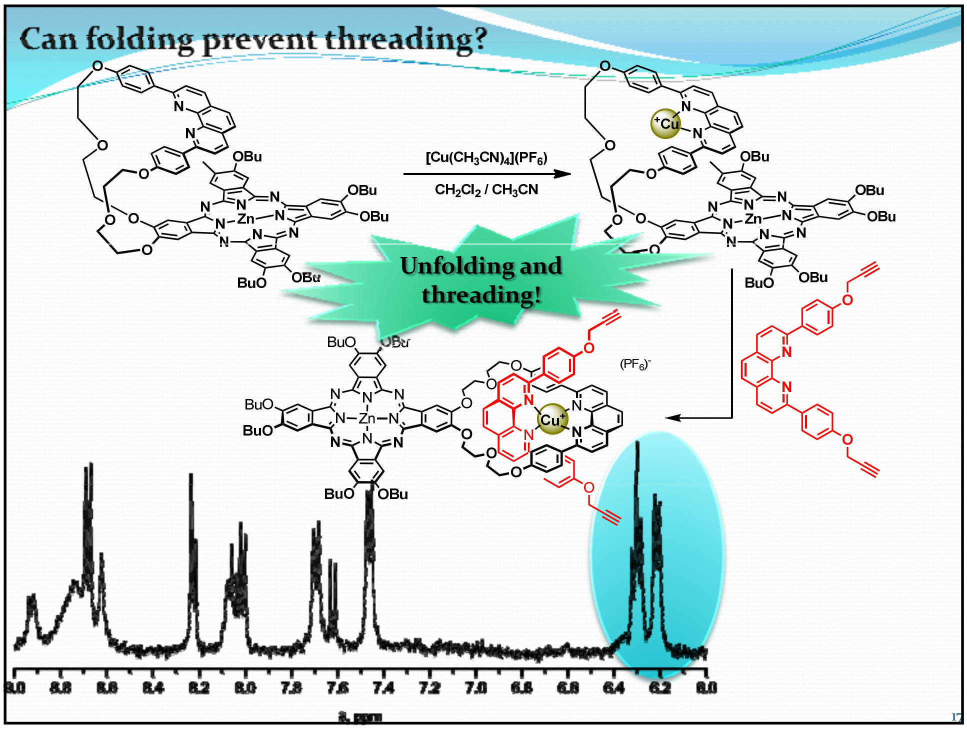

Can folding prevent threading?

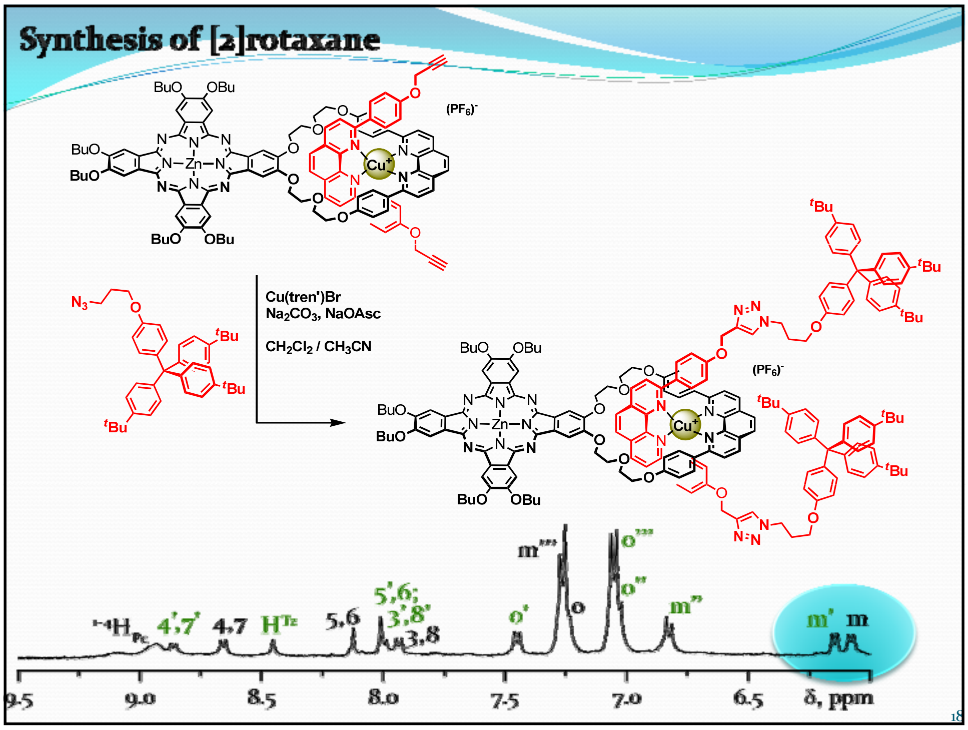

Synthesis of [2]rotaxane

Conclusions and perspectives…

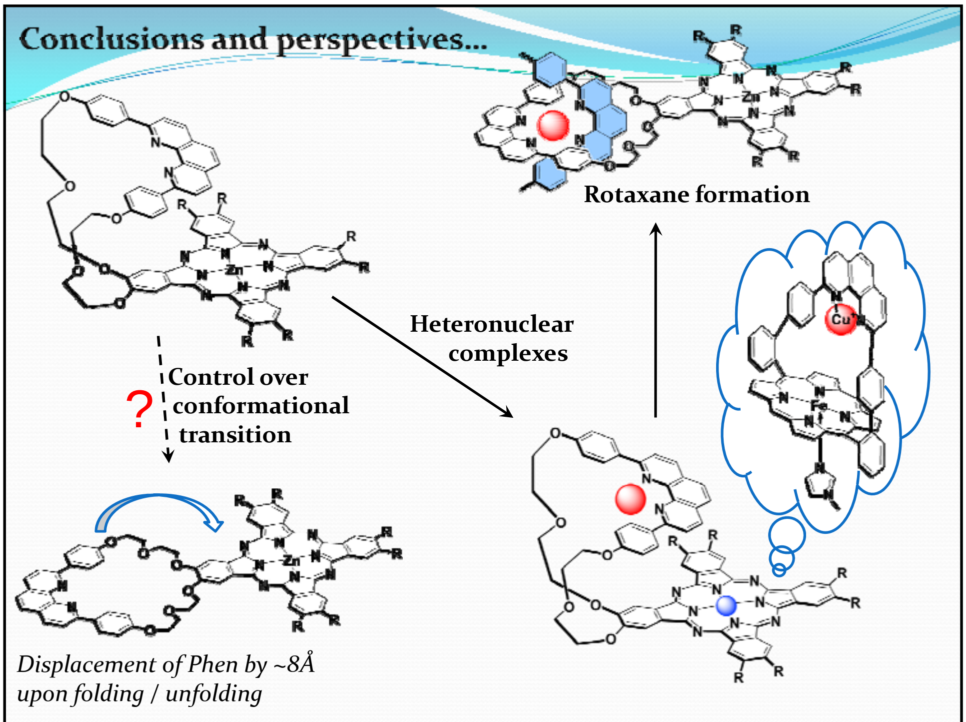

Rotaxane formation

Heteronuclear complexes

? Control over conformational transition

Displacement of Phen by ~8Å upon folding / unfolding

Thank you for your kind attention!

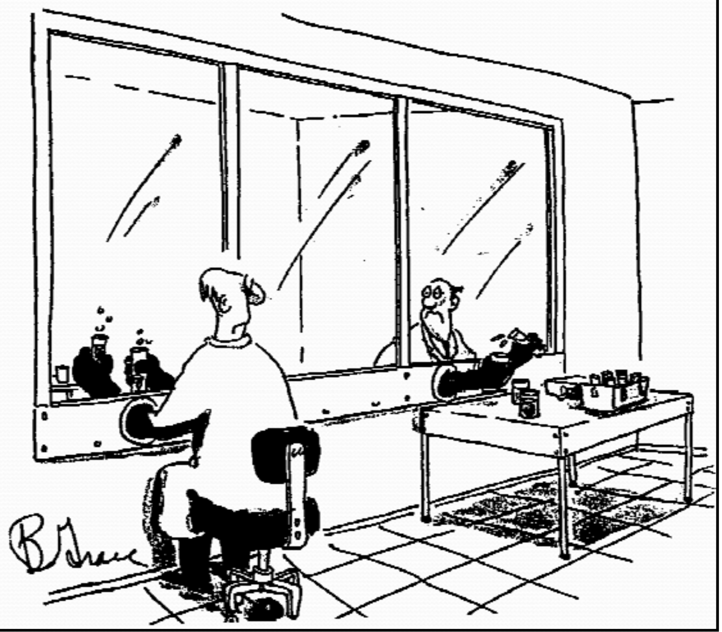

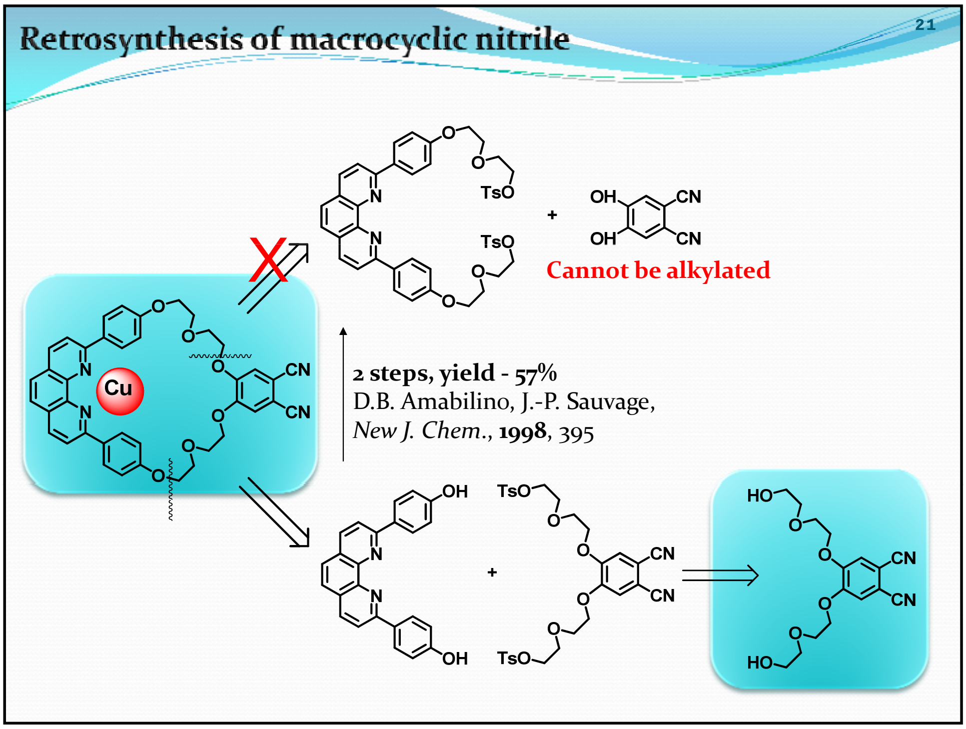

Retrosynthesis of macrocyclic nitrile

Cannot be alkylated

2 steps, yield - 57%
D.B. Amabilino, J.-P. Sauvage,
New J. Chem., **1998**, 395

MOSCOW STATE UNIVERSITY
CHEMISTRY DEPARTMENT, DIVISION OF RADIOCHEMISTRY
LABORATORY OF DOSIMETRY AND ENVIRONMENTAL RADIOACTIVITY

ENVIRONMENTAL CHEMISTRY OF ACTINIDES IN NANO- AND MICROPARTICLES FROM DIFFERENT NUCLEAR SITES

Stepan N. Kalmykov

stepan@radio.chem.msu.ru

Radiotoxicity as Ingestion Hazard

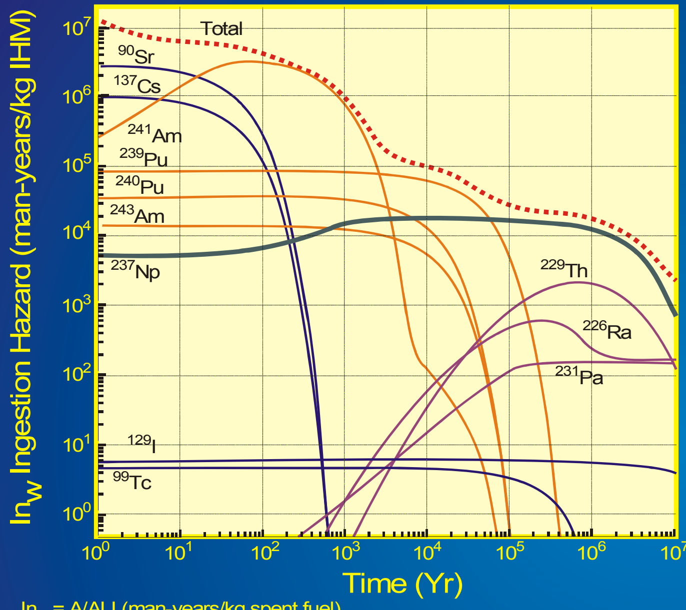

In_w = A/ALI (man-years/kg spent fuel)
where A is activity in Bq and ALI is the Annual Limit for Ingestion)

Taken from
Ken Nash

Radionuclide speciation / partitioning needs:

Development of spent nuclear fuel (SNF) or nuclear wastes (NW) geological disposal

Very different in geology/geochemistry
Granites vs. Tuffs vs. Clays vs. Salts unoxic vs. oxic

Clays

Switzerland,
Mont Terri (Opalinus Clays)

France,
Bure, Mudstone

Granites

Switzerland,
Grimsel Test Site

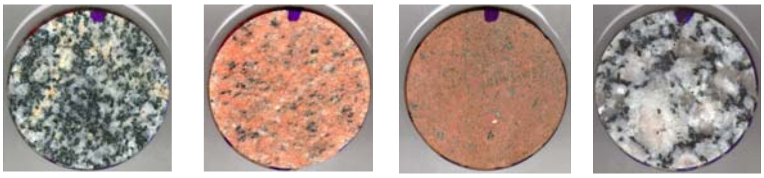

Russia,
Granite samples from Niznekansk Rock Massif near Karasnoyarsk

Tuffs

Yucca Mountain, USA,
project stopped in 2010

Salts

Germany,
Gorleben, (moratorium)

Radionuclide speciation / partitioning needs:

Remediation of radionuclide contaminated sites:

“Mayak” area, Russia,
Hanford, USA
Rocky Flats,
Old uranium mines – East Germany, Czech Rep., Tajikistan, etc.

Rocky Flats

In 1995, DOE estimated that the cleanup for Rocky Flats would cost in excess of $37 billion and take 70 years to complete. By 1996, DOE and Kaiser-Hill initiated a massive accelerated closure effort that resulted in a plan to reach closure by December 31, 2006, at a contracted cost of $7 billion.

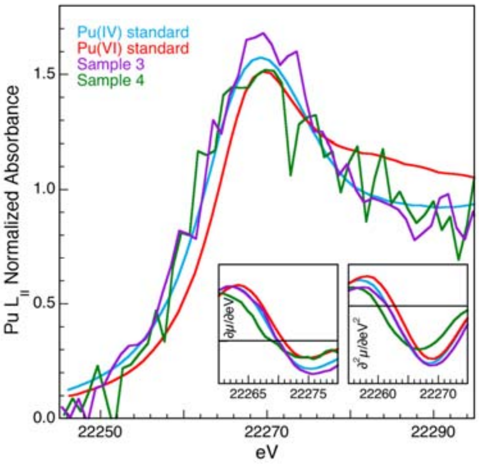

XAFS was used to determine the speciation and the remediation strategy was based on these data

“Mayak” site

Sources of radioactive contamination of South Ural

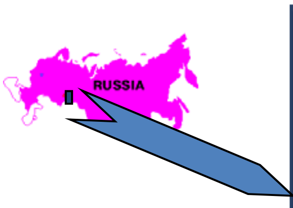

Dec. 22, 1948 – the plant to separate weapon grade Pu from irradiated uranium was launched

Production capacity was around 1 ton of U blocks per day

about 10^5 Ci of wastes

Year before the plant was launched, complex “C” was constructed that is the assembly of tanks for HLW. The capacity was estimated around 15000 m^3 per year. However the real volume of wastes was 200 m^3 per day.

All tanks were filled with HLW before 1950 (about a year after the plant was launched).
The construction of new tanks for HLW was too expensive.

From 1949 till 1951 wastes were disposed to Techa river. During this period c.a. 76 Mm^3 of waste solutions were disposed equal to 2.8 MCi.

Industrial reservoirs at PA “Mayak”

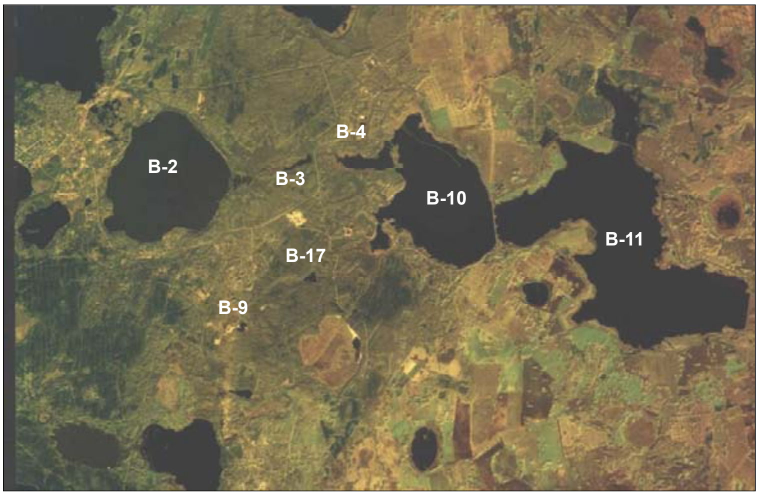

Actinide speciation basics

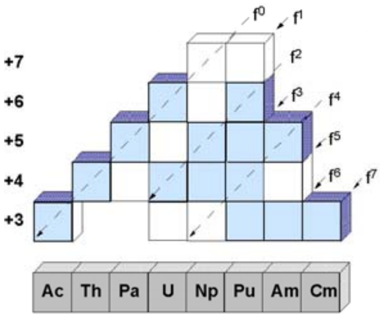

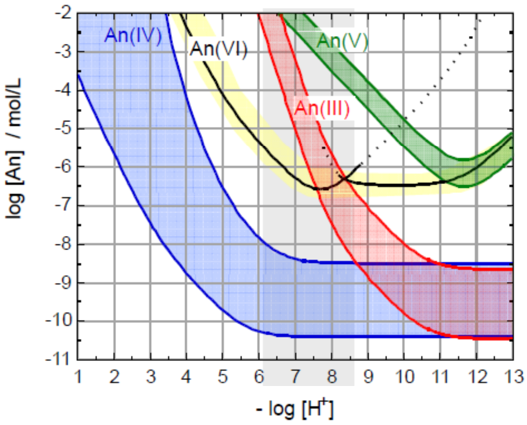

V. Neck et al. Comptes Rendus Chimie, 10, 2007

Actinide speciation basics

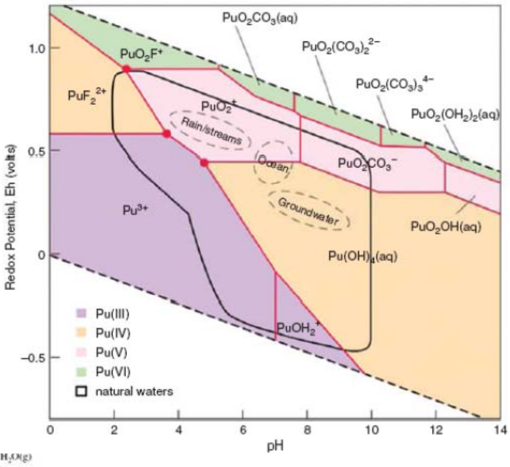

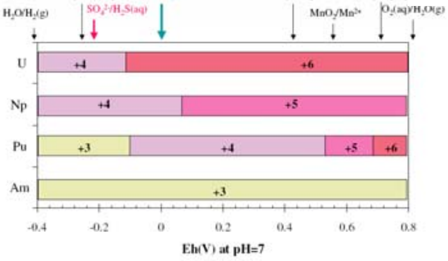

R.Ewing et al. MRS Bulletin, 35, 2010

Reduced species, An(III), An(IV) have low solubility and strong sorption affinity

⬇

Their migration in geologic conditions is defined by PARTICLES:

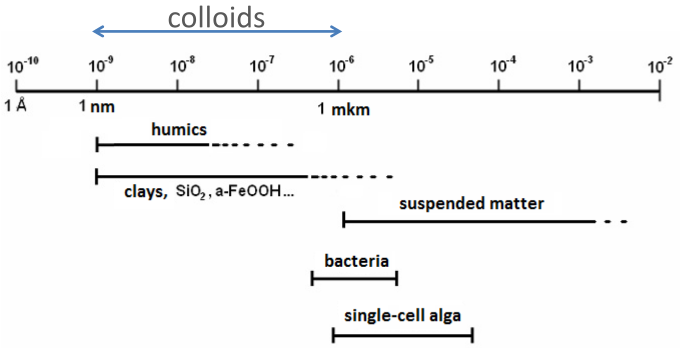

Nanoparticles – particles with the size in the order of 10^{-9} m for which size effects are observed (difference in properties with larger size particles)

Example of nano

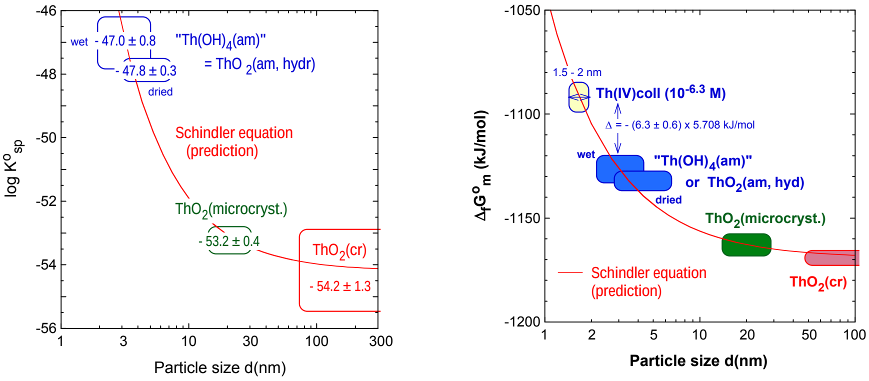

$$\Delta(\Delta_f G^\circ_m) = RT \ln \frac{K^\circ_{sp}(S)}{K^\circ_{sp}(S \rightarrow 0)} = \frac{2}{3}\gamma S$$

Neck et al.

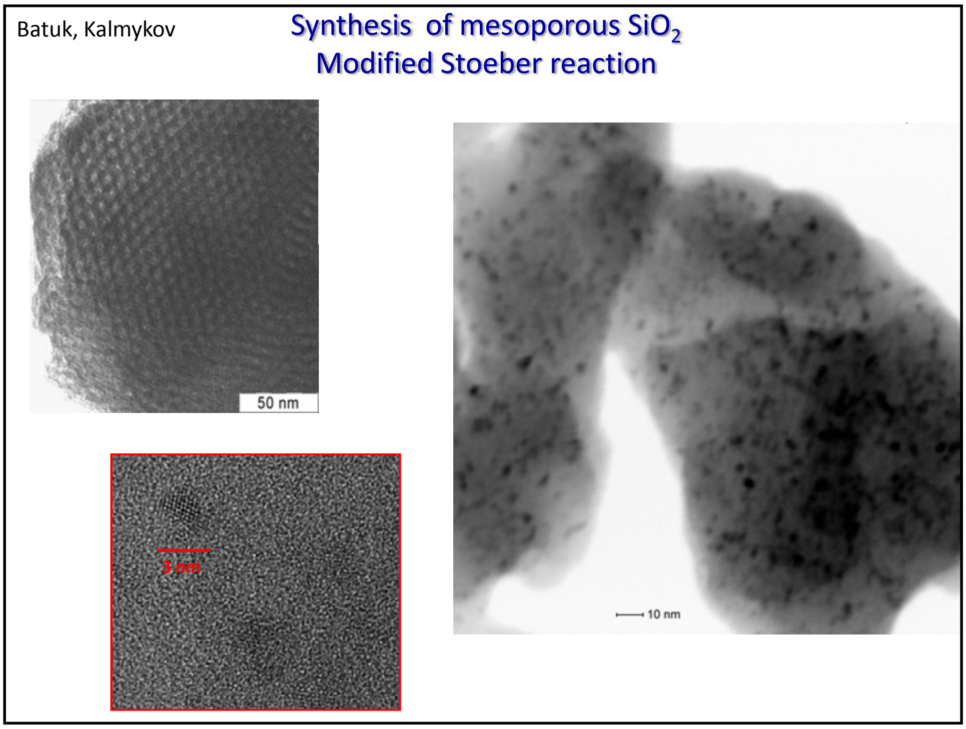

Batuk, Kalmykov

Synthesis of mesoporous SiO_2
Modified Stoeber reaction

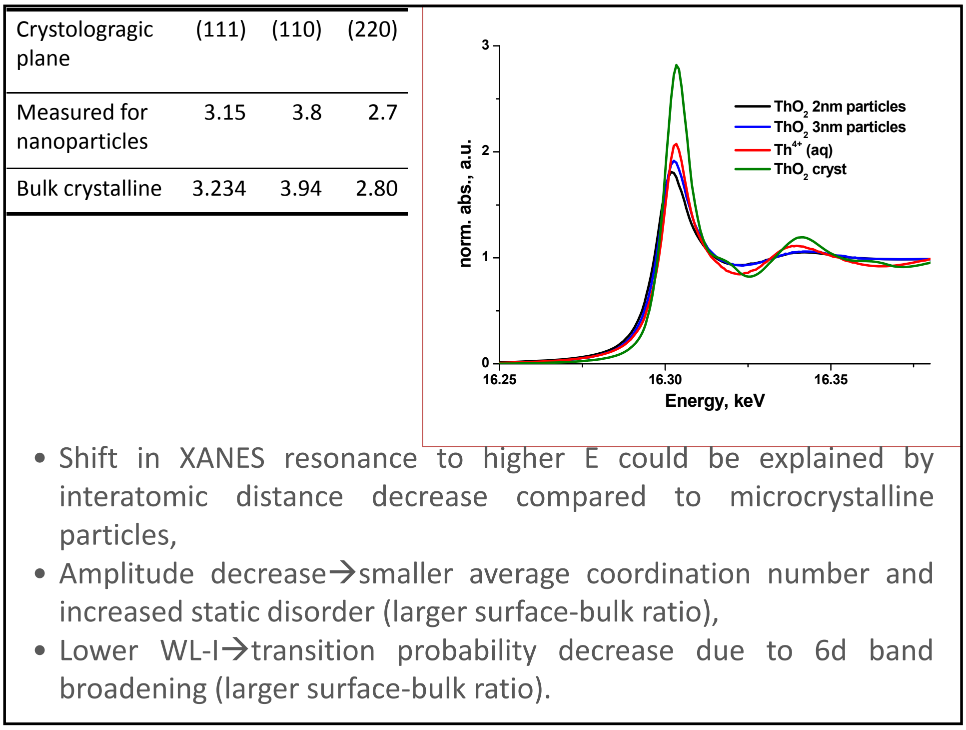

Crystologragic plane	(111)	(110)	(220)
Measured for nanoparticles	3.15	3.8	2.7
Bulk crystalline	3.234	3.94	2.80

- Shift in XANES resonance to higher E could be explained by interatomic distance decrease compared to microcrystalline particles,
- Amplitude decrease→smaller average coordination number and increased static disorder (larger surface-bulk ratio),
- Lower WL-I→transition probability decrease due to 6d band broadening (larger surface-bulk ratio).

Radionuclide transport with particles

Sorption mechanisms:

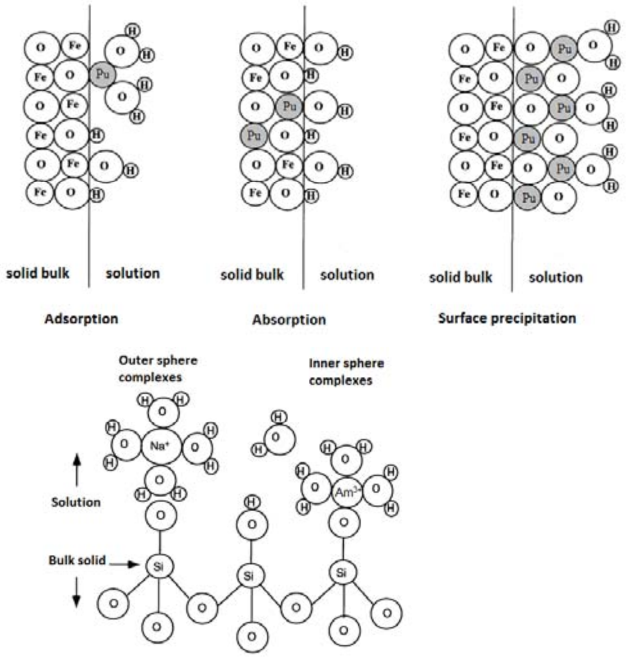

Surface complexation vs. ion exchange

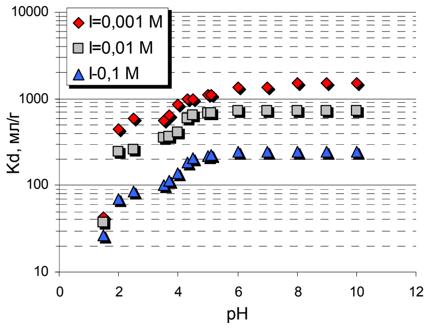
Cs(I) sorption onto bentonite

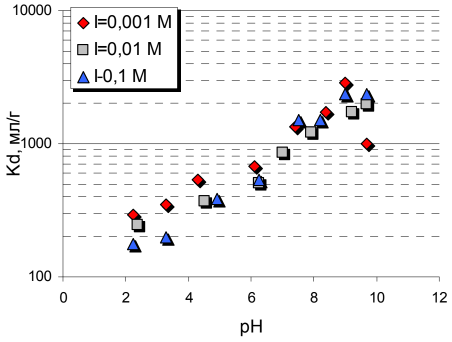
Np(V) sorption onto bentonite

Various mineral particles have different properties (pHiep, ξ-potential, ΔG of “XO-Cat” bond formation, …) the distribution of radionuclides is very heterogeneous.

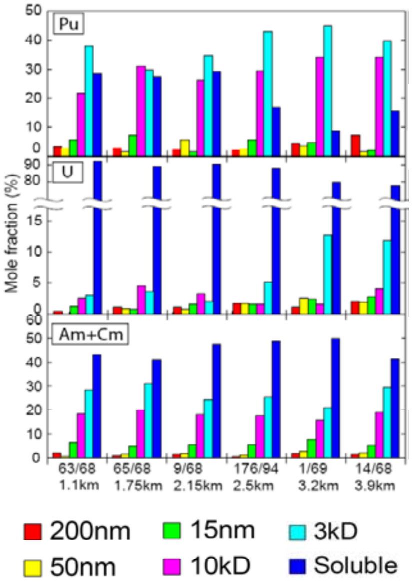

Novikov A.P., Kalmykov St.N., Utsunomiya S., Ewing R.C., Horreard F., Merkulov A., Clark S.B., Tkachev V.V., Myasoedov B.F. Colloid Transport of Plutonium in the Far-field of the Mayak Production Association, Russia. // Science, Vol. 314, 2006, p. 638-641

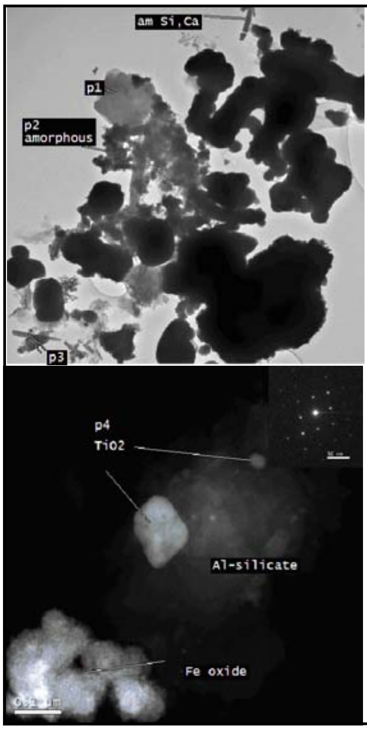

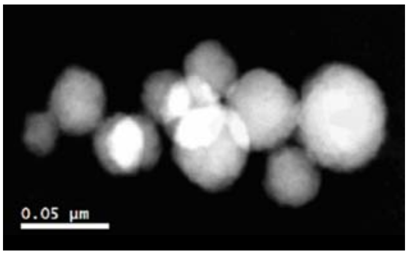

Kalmykov et al.

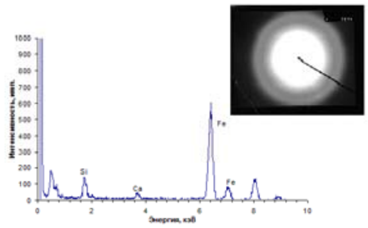

nano-SIMS elemental maps

Kalmykov et al.

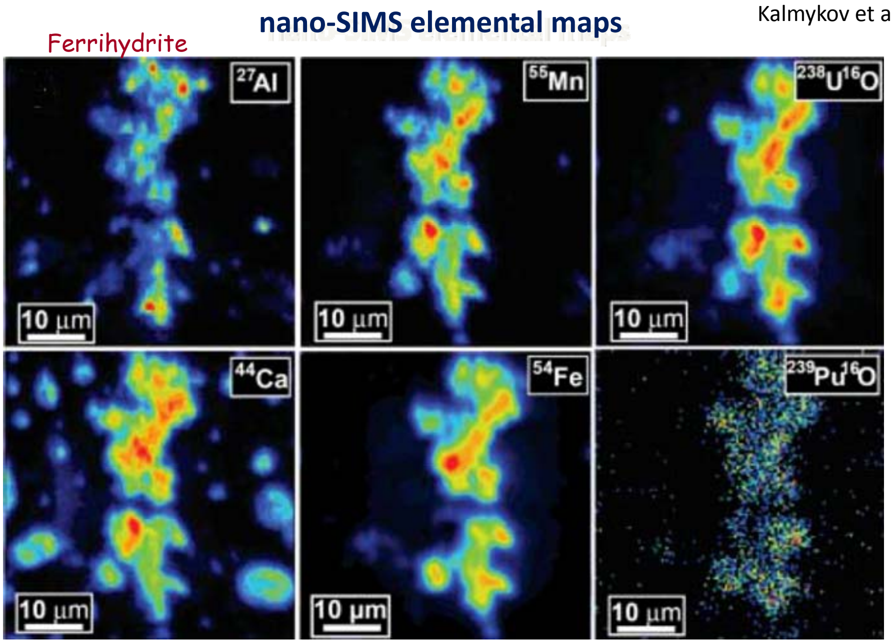

Novikov A.P., Kalmykov S.N., Utsunomiya S., Ewing R.C., Horreard F., Merkulov A., Clark S.B., Tkachev V.V., Myasoedov B.F., Colloid transport of plutonium in the far-field of the Mayak Production Association, Russia, Science 2006, v. 314, p. 638-641

Mechanisms of actinide interaction with mineral phases

Surface complexation modeling *vs.* Kd

$$Kd = \frac{C_{sorbed}}{C_{solution}}$$

Surface complexation

$$Met^{3+} + \equiv X-OH \xleftrightarrow{\beta_1} \equiv X-O-Met^{2+} + H^+$$

$$MetOH^{2+} + \equiv X-OH \xleftrightarrow{\beta_2} \equiv X-O-MetOH^{+} + H^+$$

$$Met(OH)_2^+ + \equiv X-OH \xleftrightarrow{\beta_3} \equiv X-O-Met(OH)_2 + H^+$$

Hydrolysis

$$Met^{3+} + OH^- \xleftrightarrow{\beta_4} MetOH^{2+}$$

$$Met^{3+} + 2OH^- \xleftrightarrow{\beta_5} Met(OH)_2^+$$

$$Met^{3+} + 3OH^- \xleftrightarrow{\beta_6} Met(OH)_3$$

$$Kd = \frac{[\equiv X-OH]\{\beta_1 + \beta_2\beta_4[OH^-] + \beta_3\beta_5[OH^-]^2\}}{[H^+]\{1 + \beta_4[OH^-] + \beta_5[OH^-]^2 + \beta_6[OH^-]^3\}}$$

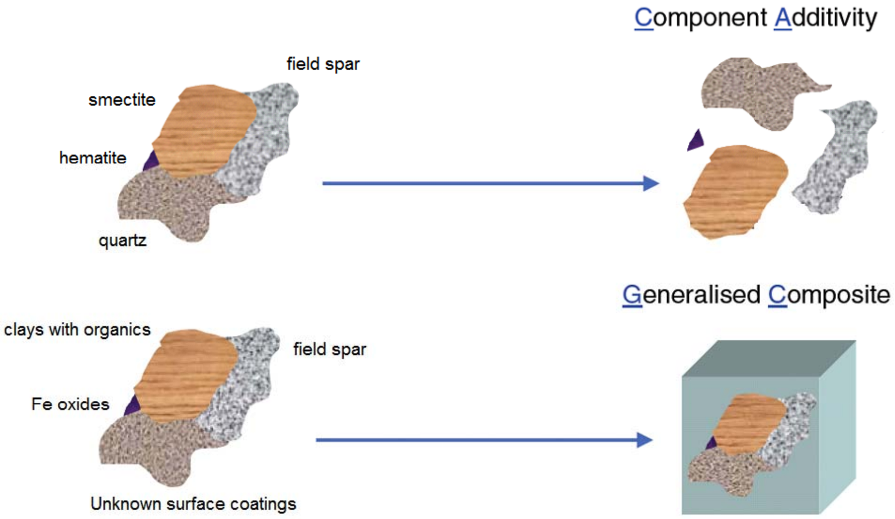

Surface complexation modeling for actinide/colloid interaction

Model experiments under well-defined laboratory conditions

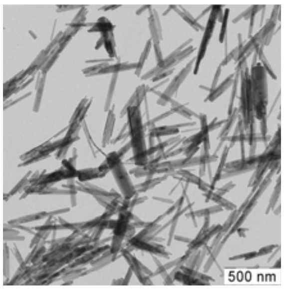

Goethite, α-FeOOH

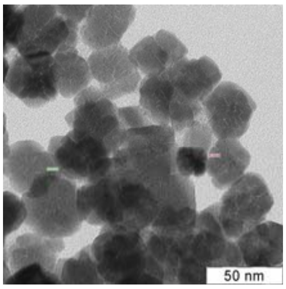

Hematite, α-Fe_2O_3

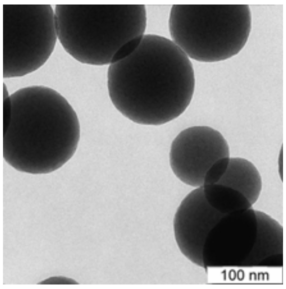

Amorphous SiO_2 microspheres

Sorption pH edges at different total actinide concentrations, various Eh and ionic strangths

Spectroscopic characterization of surface species (XAFS, XPS, TRLIF for U(VI), Eu(III))

Surface complexation modeling

Molecular-level understanding of the surface reactions and fundamental thermodynamic data for migration modeling

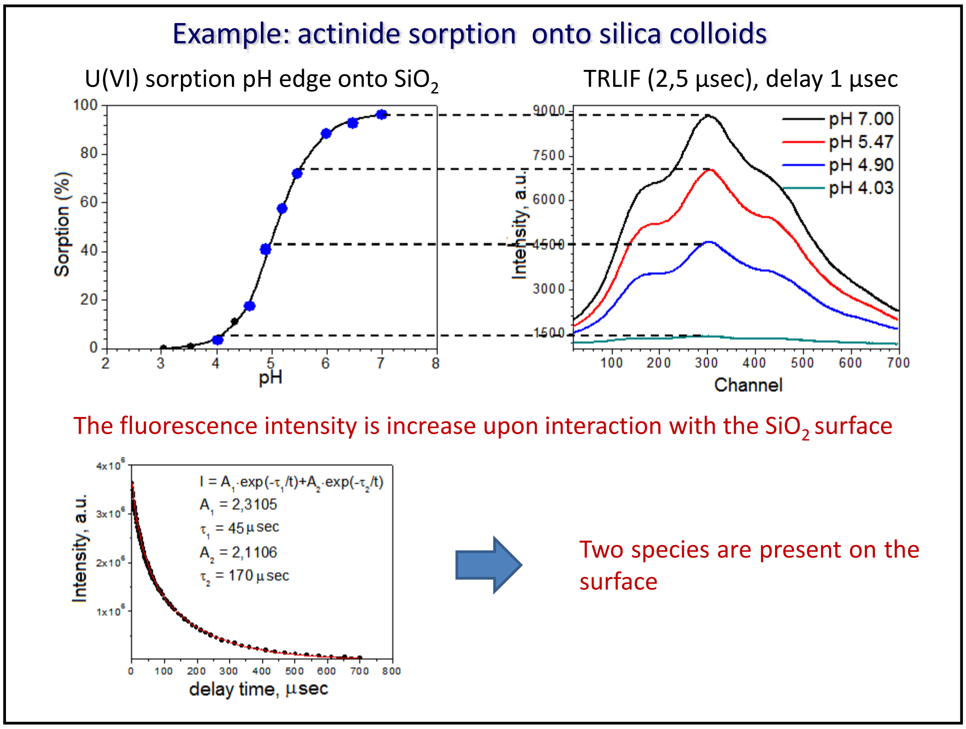

Example: actinide sorption onto silica colloids

U(VI) sorption pH edge onto SiO_2

TRLIF (2,5 µsec), delay 1 µsec

The fluorescence intensity is increase upon interaction with the SiO_2 surface

$I = A_1 \cdot \exp(-\tau_1/t) + A_2 \cdot \exp(-\tau_2/t)$
$A_1 = 2{,}3105$
$\tau_1 = 45\,\mu sec$
$A_2 = 2{,}1106$
$\tau_2 = 170\,\mu sec$

Two species are present on the surface

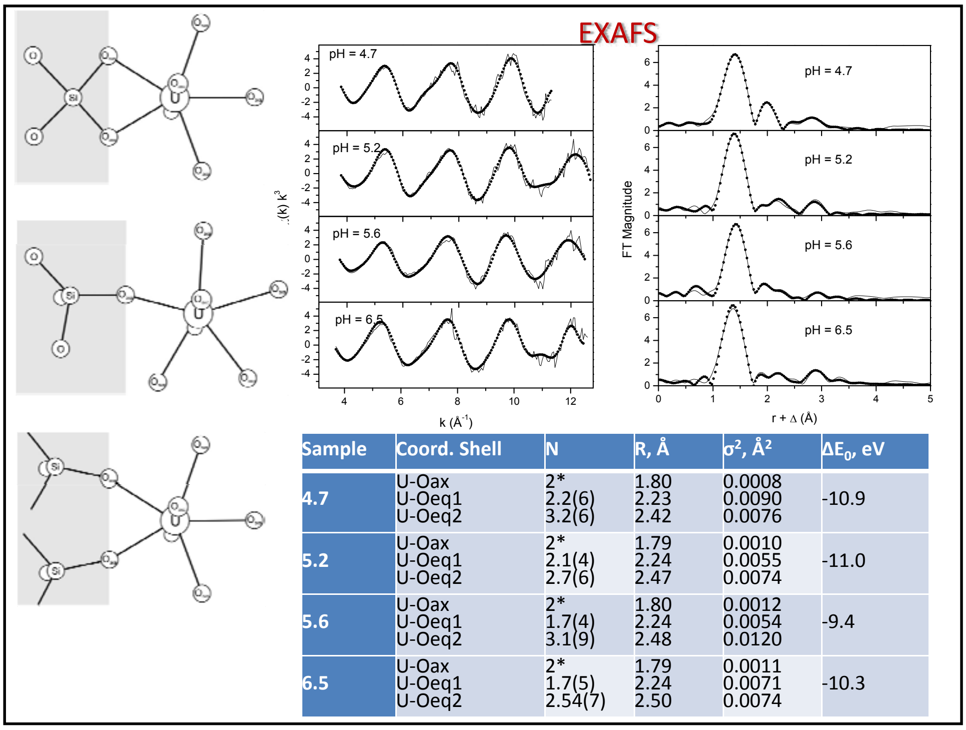

EXAFS

Sample	Coord. Shell	N	R, Å	σ^2, Å^2	ΔE_0, eV
4.7	U-Oax U-Oeq1 U-Oeq2	2* 2.2(6) 3.2(6)	1.80 2.23 2.42	0.0008 0.0090 0.0076	-10.9
5.2	U-Oax U-Oeq1 U-Oeq2	2* 2.1(4) 2.7(6)	1.79 2.24 2.47	0.0010 0.0055 0.0074	-11.0
5.6	U-Oax U-Oeq1 U-Oeq2	2* 1.7(4) 3.1(9)	1.80 2.24 2.48	0.0012 0.0054 0.0120	-9.4
6.5	U-Oax U-Oeq1 U-Oeq2	2* 1.7(5) 2.54(7)	1.79 2.24 2.50	0.0011 0.0071 0.0074	-10.3

$2\ \equiv SiOH + UO_2^{2+} \leftrightarrows (\equiv SiO)_2UO_2 + 2H^+$, $\boldsymbol{K_1}$

$2\ \equiv SiOH + UO_2^{2+} + H_2O \leftrightarrows (\equiv SiO)_2UO_2OH^- + 3H^+$, $\boldsymbol{K_2}$.

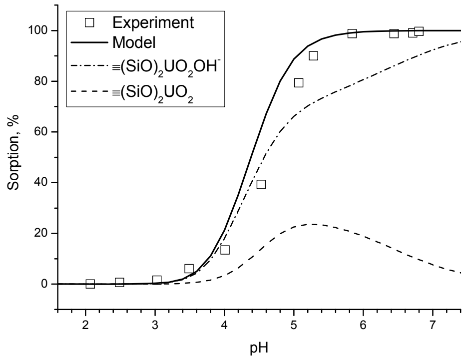

$\log K_1 = -2.22 \pm 0.03$

$\log K_2 = -5.85 \pm 0.05$

Free energy linear relationship

Analogy of hydrolysis and sorption:

$Cat^n + \equiv FeOH \leftrightarrows \ \equiv FeO\text{-}Cat^{\ n-1} + H^+$

$Cat^n + \quad HOH \leftrightarrows \ HO\text{-}Cat^{\ n-1} + H^+$

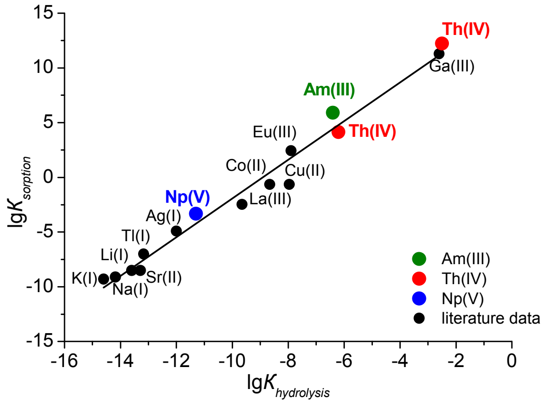

Where is Pu(IV)?

Pu interaction with hematite

Average particle size, nm	20-40
Lattice parameters, Å	a = 5.031(1) c = 13.78(1)
Surface area, m^2/g	35
pH_{pzc}	8.0

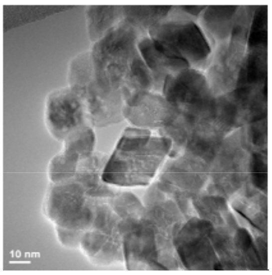

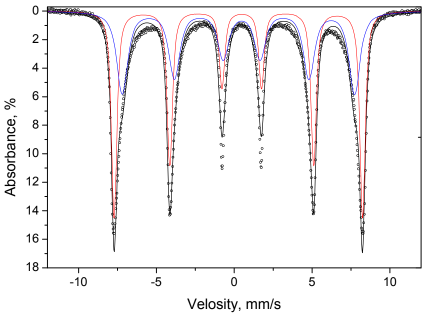

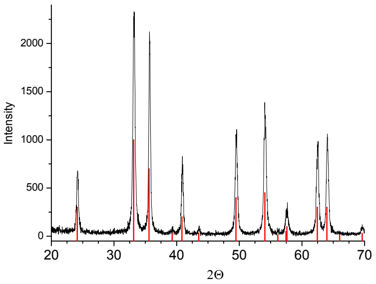

Different total concentrations of Pu

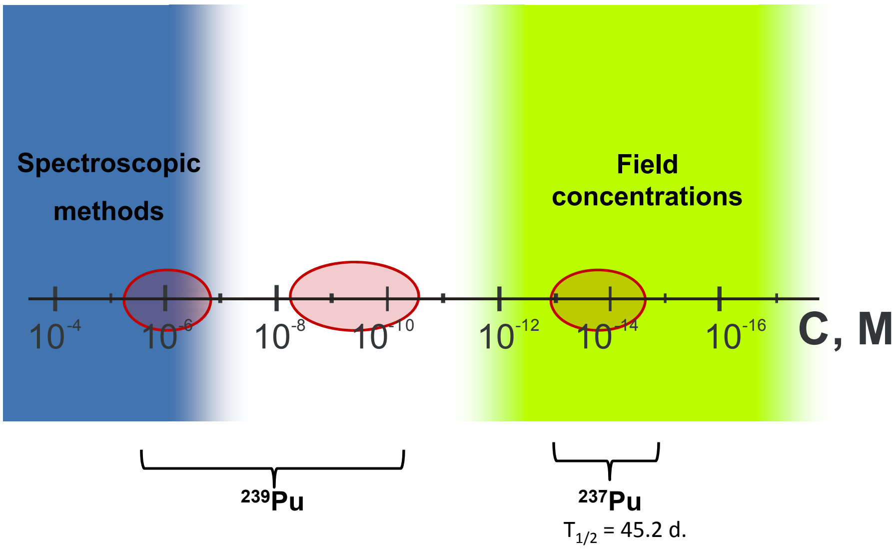

Spectroscopic methods

Field concentrations

^{239}**Pu**

^{237}**Pu**

$T_{1/2}$ = 45.2 d.

Reduction of Pu(V,VI) to Pu (IV) upon sorption onto hematite surface

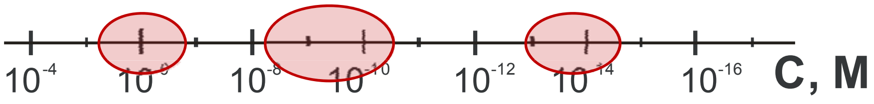

Stabilization of Pu(IV) onto hematite surface upon sorption is observed at different Pu total concentrations

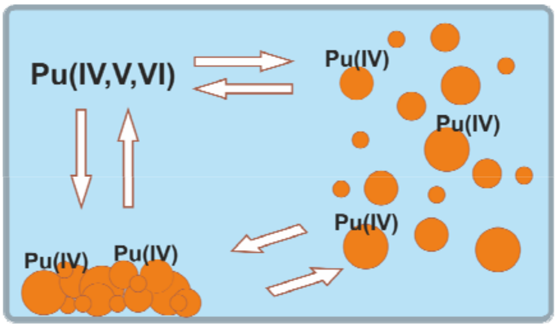

Experiment: Starting from soluble Pu(VI) at $C_{tot}(Pu) > 10^{-9}$ M

Blank experiments at C(Pu) = 10^{-6} M

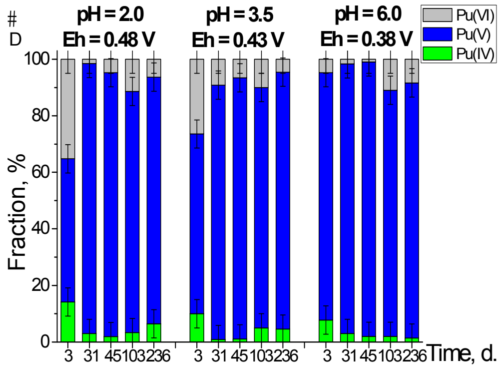

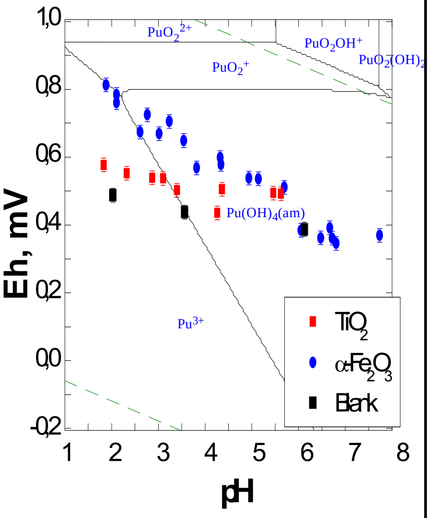

Pu(V) shows high **kinetic** stability **in pure solution** (despite thermodynamics)

Pu L_{III} XANES

Pu(VI). $2\cdot10^{-6}$ M

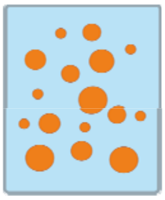

Eh = 400 – 600 мВ

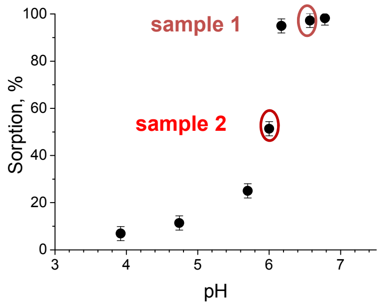

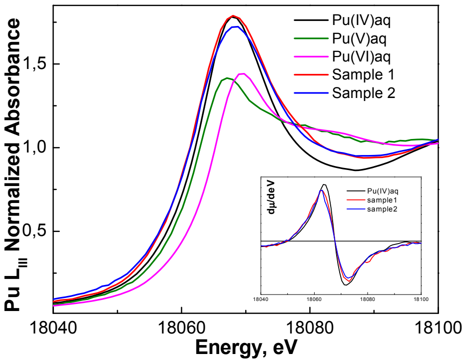

Stabilization of Pu(IV) on hematite surface

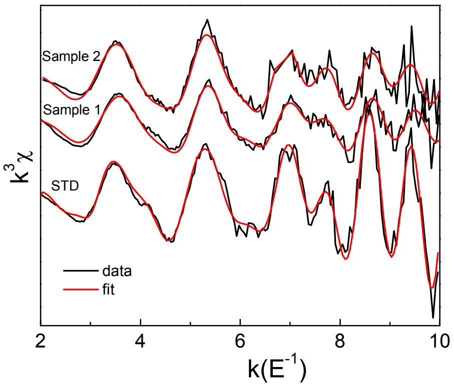

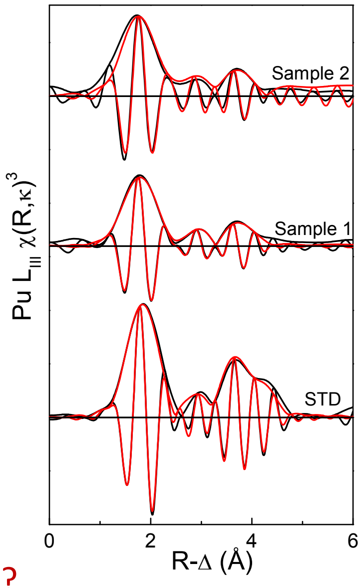

$PuO_{2+x}\cdot nH_2O$ - like species ???

HR-TEM

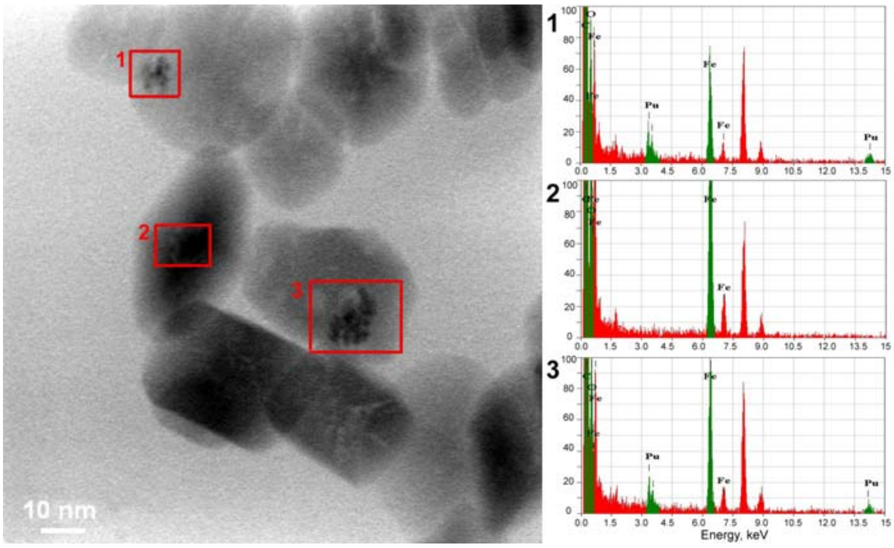

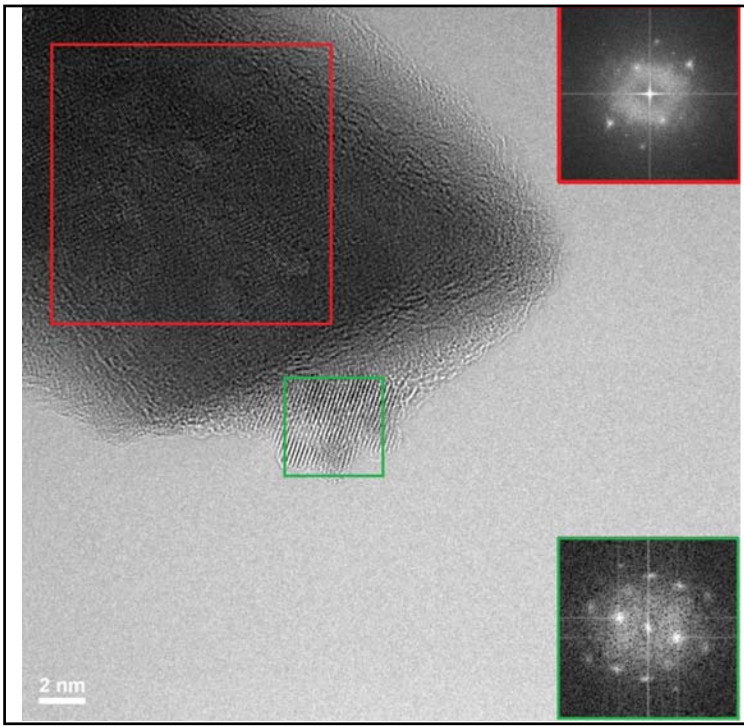

hematite

$PuO_{2+x}\cdot nH_2O$ nanoparticles

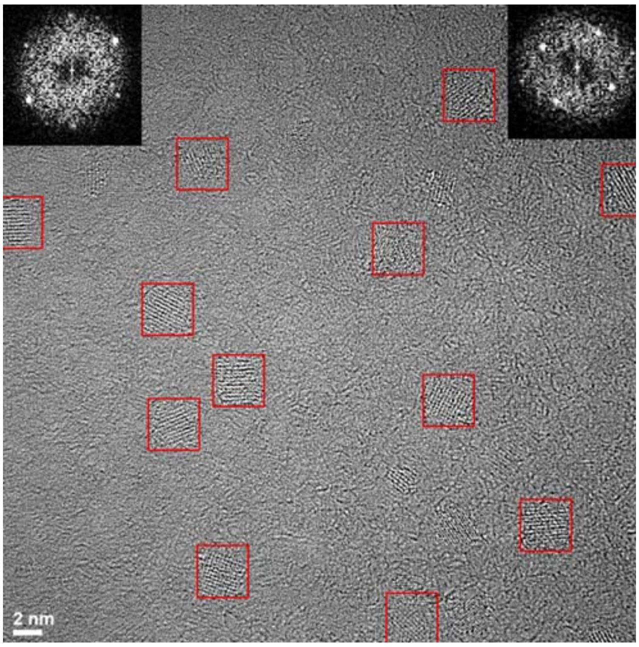

$[Pu]_{tot}=10^{-9}$ M

Kinetics of Pu(IV,VI) sorption on hematite at different $C_{tot}(Pu)$

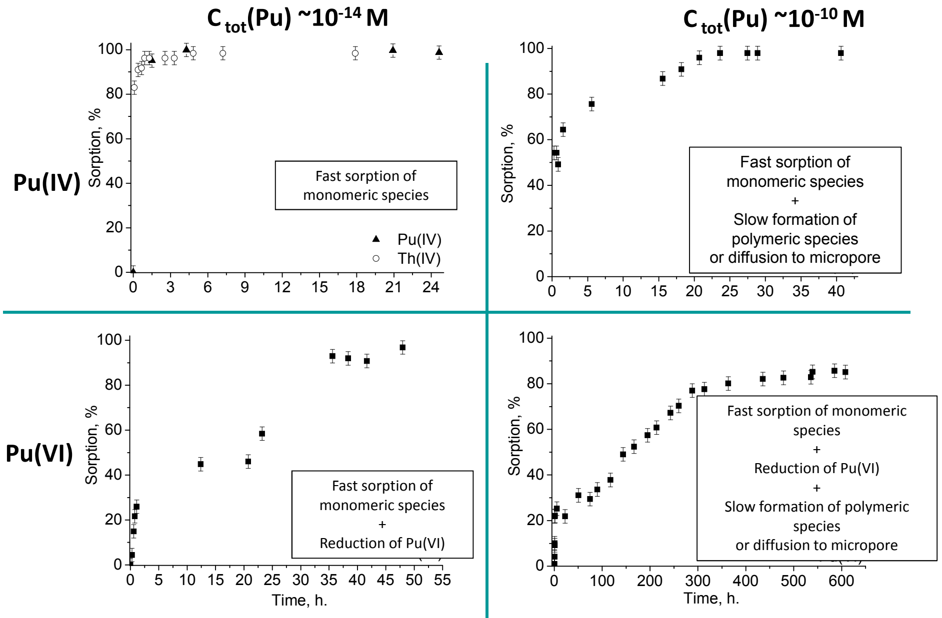

Romanchuk et al., Radiochim. Acta, 2011

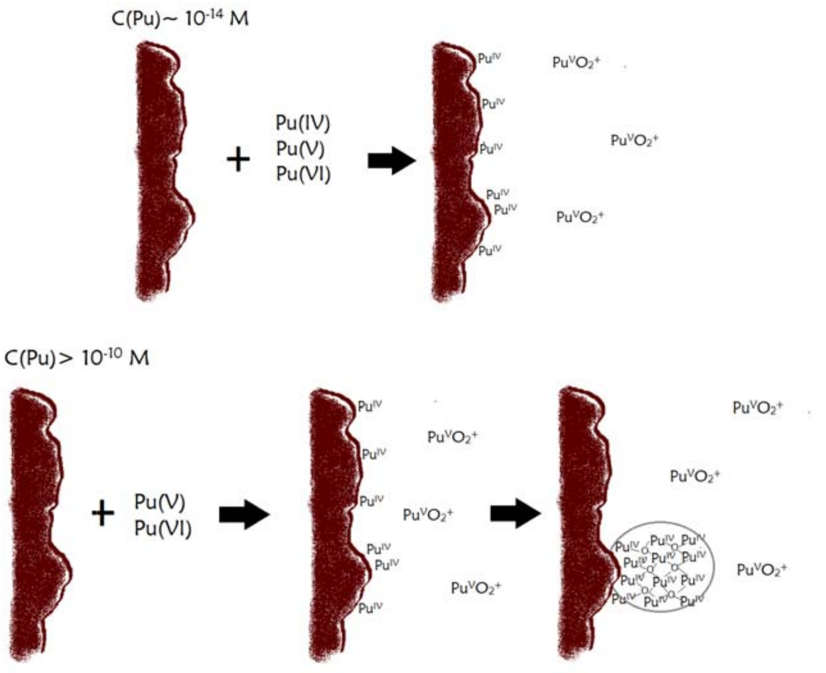

What is the mechanism of reduction of Pu(VI)?

Possible mechanism of Pu(V,VI) reduction onto hematite:

- ~~Disproportionation~~ in EDL of hematite
- ~~Self-reduction~~
- Trace amount of Fe(II)
- Semiconductors properties of hematite
- ……

Romanchuk et al., RCA, 2011

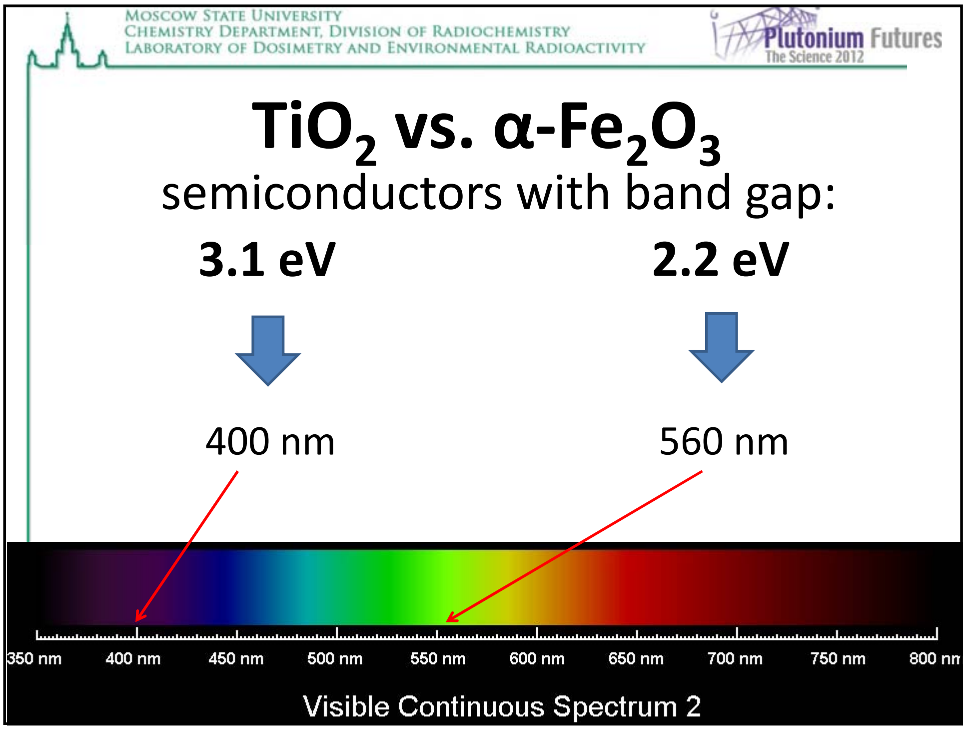

MOSCOW STATE UNIVERSITY
CHEMISTRY DEPARTMENT, DIVISION OF RADIOCHEMISTRY
LABORATORY OF DOSIMETRY AND ENVIRONMENTAL RADIOACTIVITY

Plutonium Futures
The Science 2012

TiO_2 vs. α-Fe_2O_3

semiconductors with band gap:

3.1 eV **2.2 eV**

400 nm 560 nm

Visible Continuous Spectrum 2

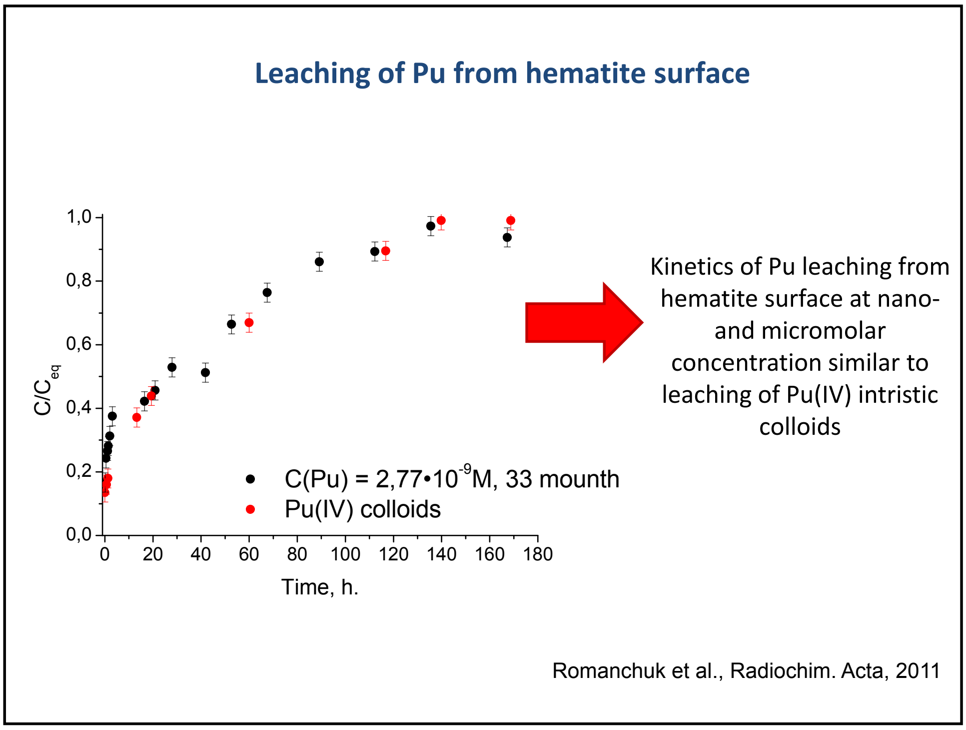

Leaching of Pu from hematite surface

● C(Pu) = 2,77•10^{-9}M, 33 mounth
● Pu(IV) colloids

Kinetics of Pu leaching from hematite surface at nano- and micromolar concentration similar to leaching of Pu(IV) intristic colloids

Romanchuk et al., Radiochim. Acta, 2011

Radionuclide transport with particles

particle transport vs. ionic transport

sorption-desorption mechanism

Source dependent

species are not at thermodynamic equilibrium with their surroundings but remain in forms that are influenced by the source

"Hot particles"

Source independent

Pseudo-colloids

Intrinsic colloids

Kinetically very stable forms which behavior in the time scale of years or even decades is defined by their pre-history (origin). Important to develop remediation strategies.

Source dependent species

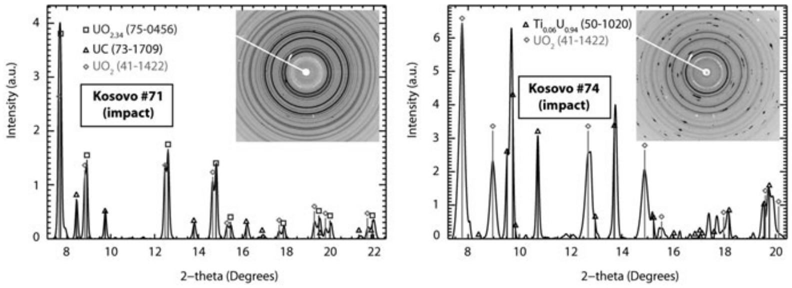

Lind et al. (2009) J Environ Radioact 100:301–307

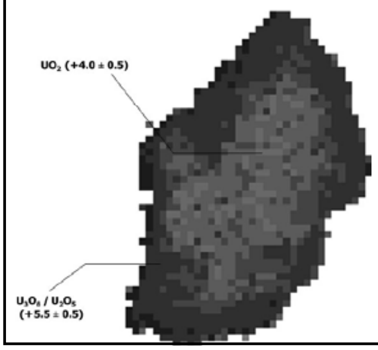

Salbu B et al. (2004) J Environ Radioact 74:233–242

“Hot” particle characterization

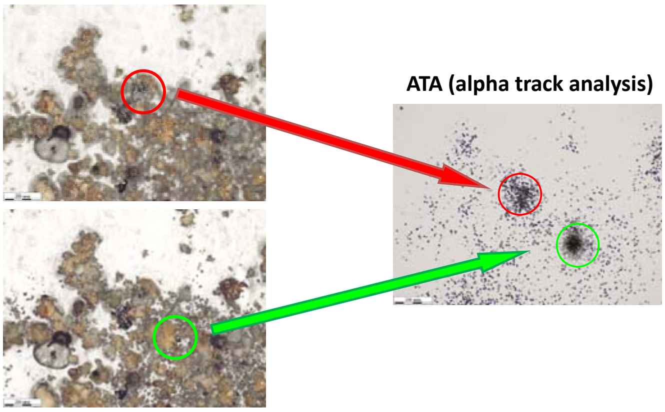

Optical microscope

Bottom sediments from “Mayak”

ATA (alpha track analysis)

Lot of discrete alpha-containing particles were found

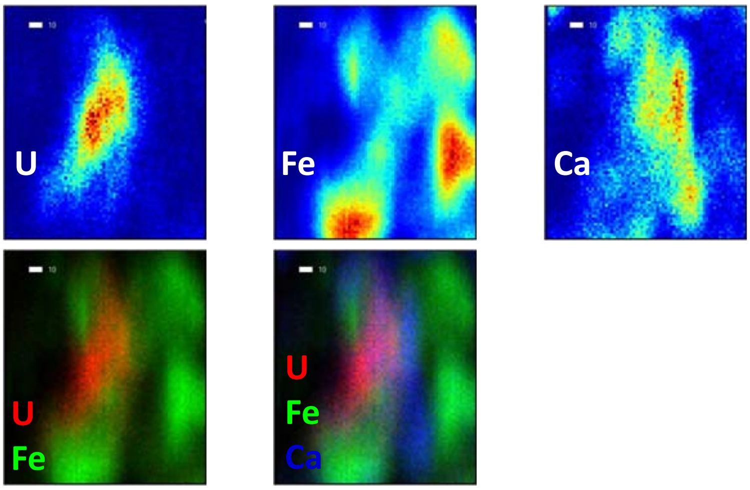

Elemental mapping shows only isolated uranium particles with no associations with other elements ≥Ca, neither evenly distributed within the particles nor as an agglomerate that would imply U sorption on a mineral surface that nucleated further growth of a U-containing precipitate on the surface.

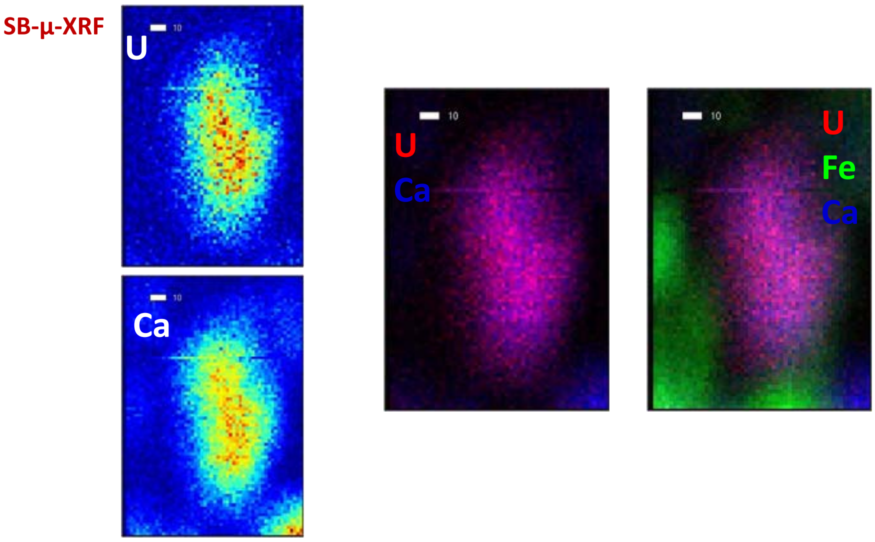

Particles consist of chemically homogeneous
UO_{2+x}
U_3O_8 and
schoepite
$(UO_2)_8O_2(OH)_{12}(H_2O)_{12}$

SB-µ-EXAFS

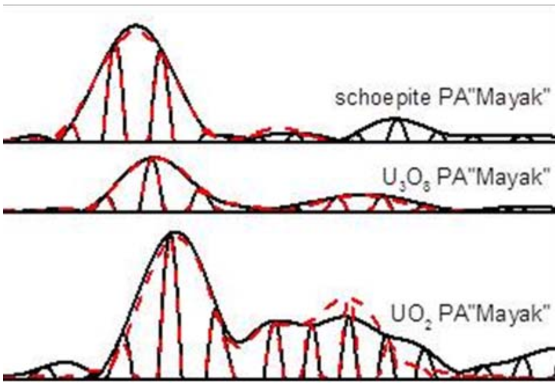

Particle characterization

Alpha track analysis	Search for HP
SEM/ EDX	Morphology, major element composition
SIMS	Isotope composition
SB-µ-XRF	Elemental mapping
µ-XANES/EXAFS	Chemical speciation
µ-XRD	Phase composition
Single particle chemical analysis	Trace element, radionuclide composition

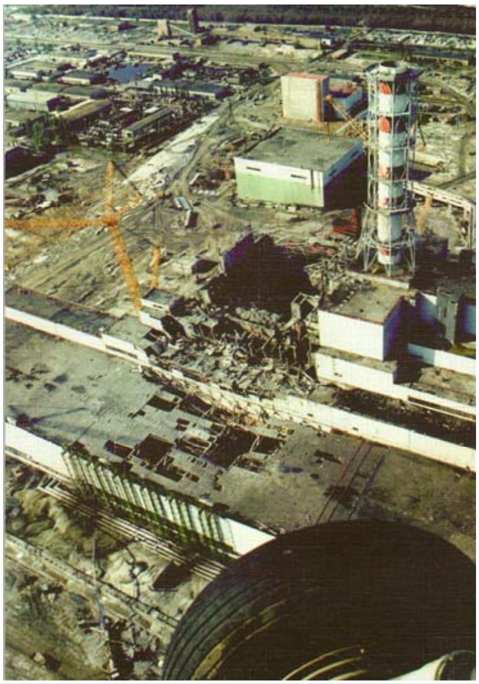

EXAMPLE 1
“Hot” particles from Chernobyl

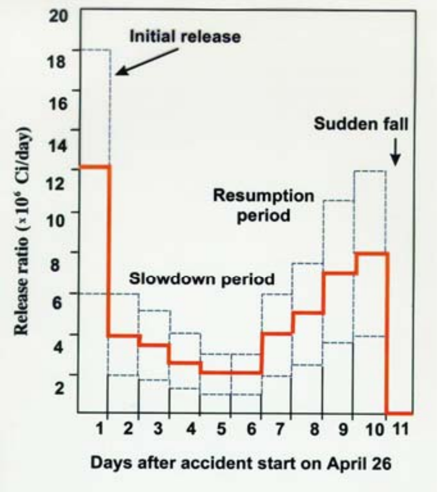

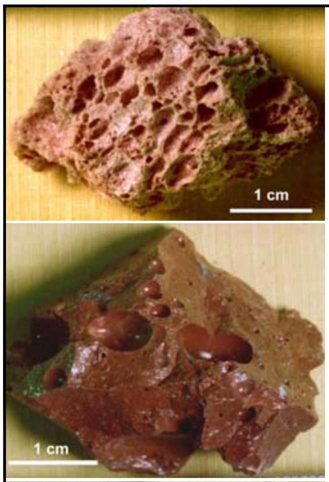

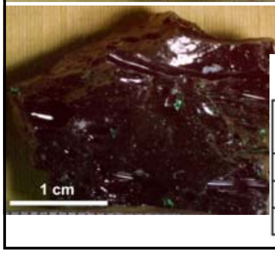

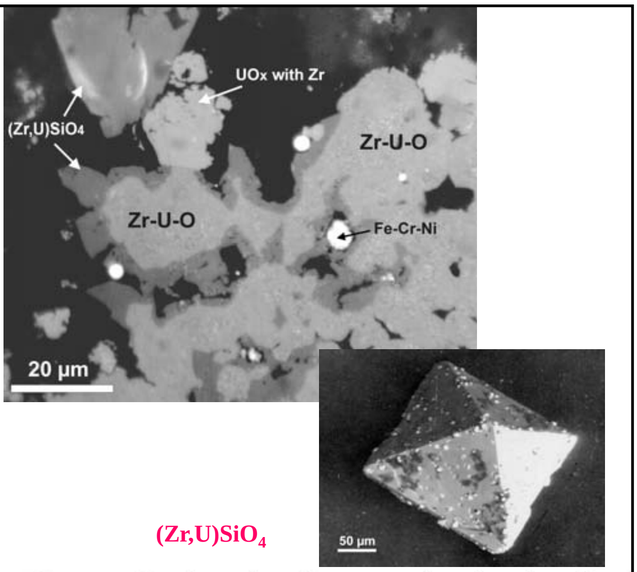

$(Zr,U)SiO_4$

Type of “lava”	Fe	Na	Si	Al	Mg	K	Ca	Zr	U
porous	0.2	0.5	35.2	3.8	4.5	2.3	7.5	4.0	2.9
brown	0.2	0.6	36.6	4.0	4.4	2.3	7.2	2.9	2.0
black	0.3 to 6.7	0.4	37.2	3.8	1.3 to 3.2	2.7	8.2	3.7	3.2

Alpha track analysis / fission track analysis

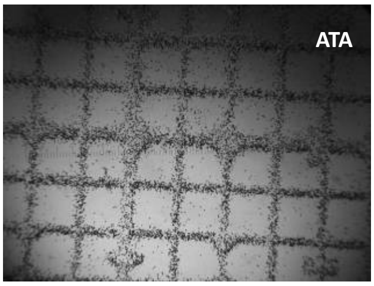

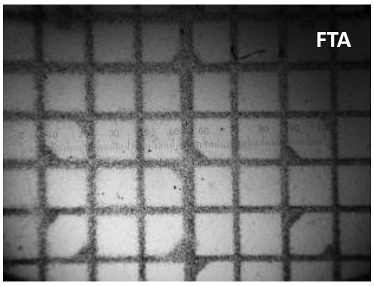

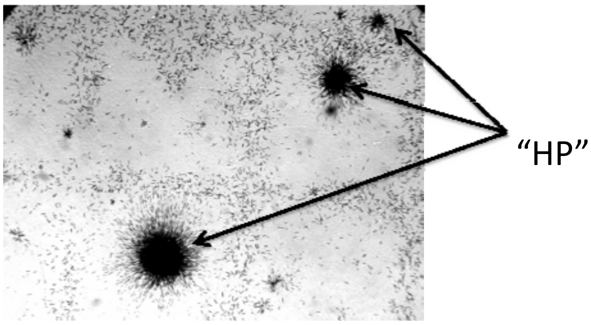

SEM-EDX

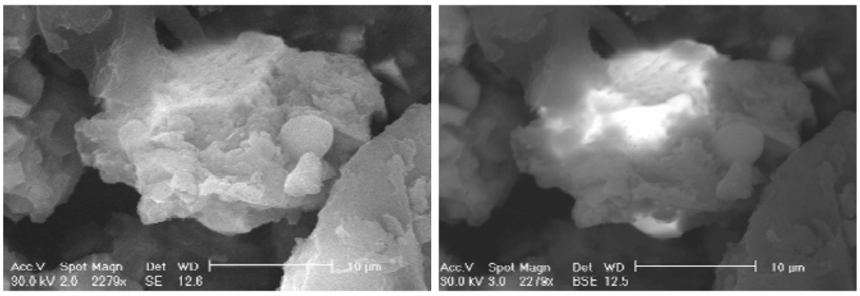
Acc.V Spot Magn Det WD 10 µm
30.0 kV 2.0 2279x SE 12.6
Acc.V Spot Magn Det WD 10 µm
30.0 kV 3.0 2279x BSE 12.5

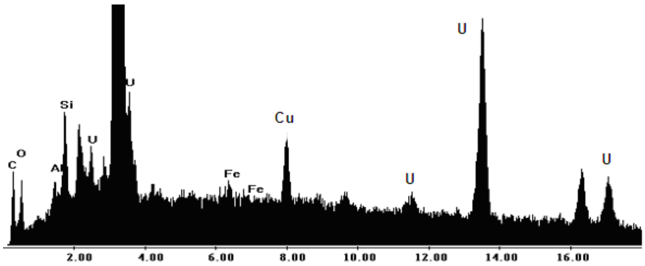
C
O
Al
Si
U
U
Cu
Fe
Fe
U
U
U
2.00
4.00
6.00
8.00
10.00
12.00
14.00
16.00

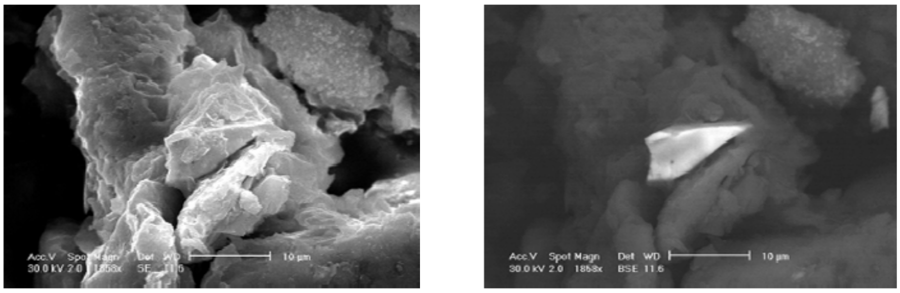
Acc.V Spot Magn Det WD 10 µm
30.0 kV 2.0 1858x SE 11.6
Acc.V Spot Magn Det WD 10 µm
30.0 kV 2.0 1858x BSE 11.6

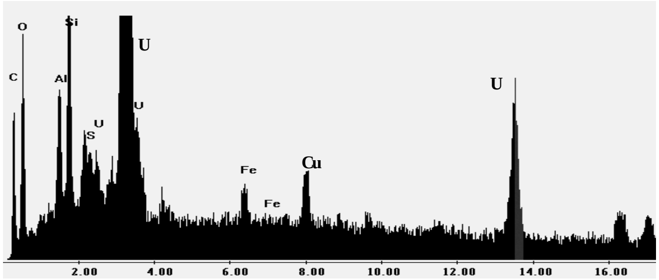
O
Si
U
C
Al
U
S
U
Fe
Cu
Fe
U
2.00
4.00
6.00
8.00
10.00
12.00
14.00
16.00

SIMS

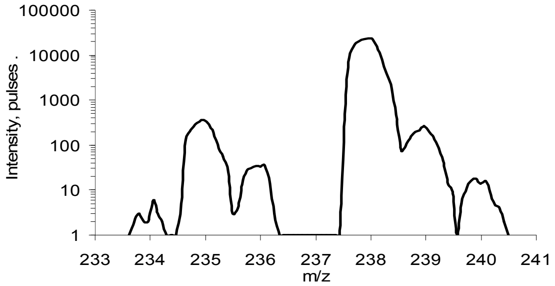

Particle	^{234}U	^{235}U	^{236}U	^{238}U
1--1	0.016 ± 0.004	1.35 ± 0.04	0.12 ± 0.02	98.51 ± 0.05
1--2		0.60 ± 0.15	0.2 ± 0.1	99.2 ± 0.25
1--3	0.012 ± 0.009	0.98 ± 0.09	0.18 ± 0.04	98.83 ± 0.14
9--1	0.022 ± 0.011	1.7 ± 0.2	0.06 ± 0.02	98.2 ± 0.2
11--1	0.016 ± 0.009	0.93 ± 0.07	0.20 ± 0.04	98.85 ± 0.12

SB-µ-XRF

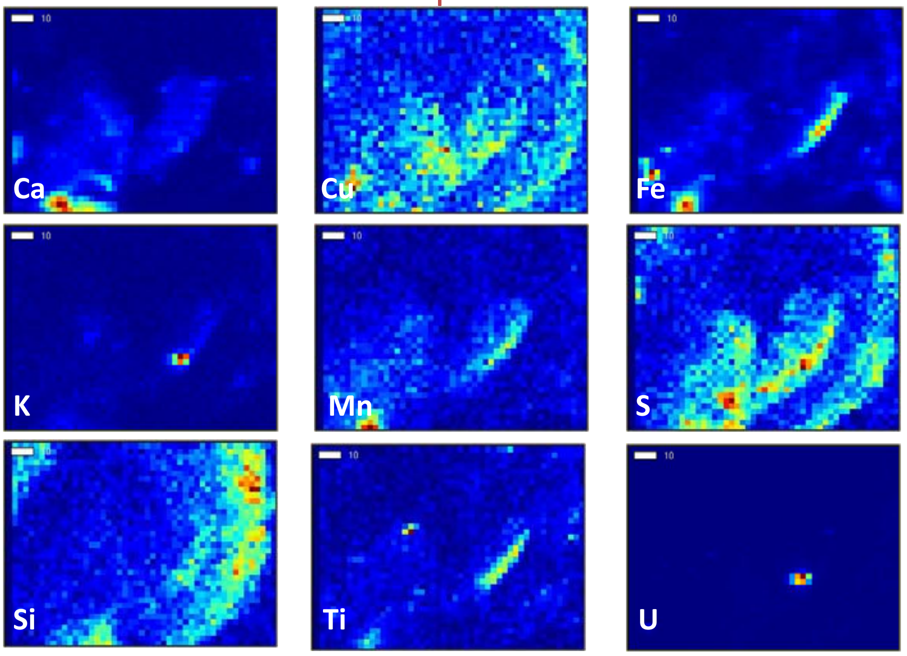

μ-XAFS

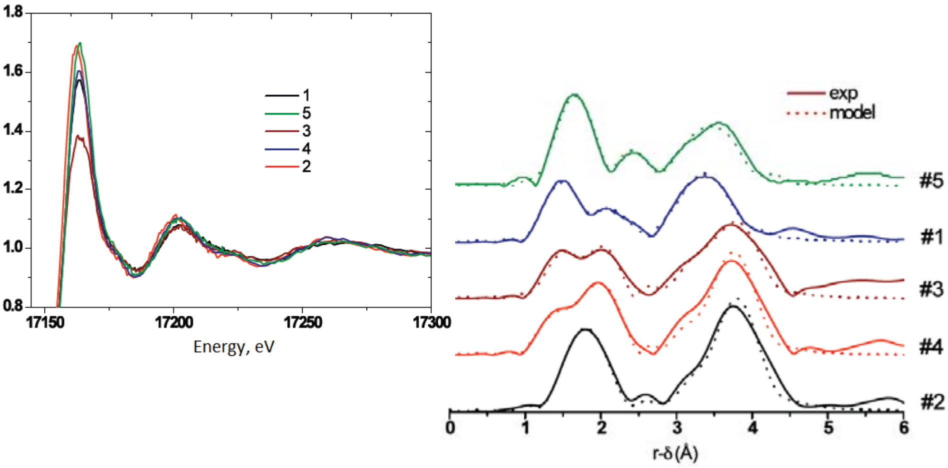

Despite of oxidation conditions – presence of oxygen, atmospheric precipitations , HP remain unoxidized (mostly in UO_2 form)

Conclusions

The need for molecular-scale radionuclide speciation is needed for performance assessment of geological repositories of SNF or NW,

Generally radionuclide behavior (sorption, precipitation, complexation) could be relatively easily described thermodynamically,

Plutonium – “the element of surprise” could form oxide-like particles even in diluted solutions that show high kinetic stability,

In the environment, actinide speciation could be governed by their origin rather than (or as well as) local geochemical conditions. This remains a huge field of research on formation and properties of actinide containing particles, their kinetic stability.

PARTITIONING AND TRANSMUTATION – BTP-TYPE N-DONOR LIGANDS IN THE SANEX PROCESS

Björn B. Beele[a,b*], Udo Müllich[b], Andreas Geist[b], Petra J. Panak[a,b]

[a] *University of Heidelberg, Department of Physical Chemistry, Im Neuenheimer Feld 253, 69120 Heidelberg*
[b] *Karlsruhe Institute of Technology (KIT), Institut für Nukleare Entsorgung (INE), Postfach 3640, 76021 Karlsruhe*

Dr. Björn Beele, Research Associate since 07.2010, Dept. of Physical Chemistry, University of Heidelberg 2002-2006, chemistry undergraduate studies, University of Heidelberg; 2006, Diploma thesis in organic chemistry, University of Heidelberg; 2006-2009, graduate studies in chemistry, University of Heidelberg / Texas A&M University, College Station, TX, USA; 2009-2010, postdoctoral research associate, Texas A&M University, College Station, TX, USA.

** Corresponding author Tel.: 0049-721-608-24550*
E-mail address: Bjoern.Beele@partner.kit.edu

Abstract:

Partitioning and transmutation (P&T) is a strategy to reduce the long-term radiotoxicity and heat load of waste generated in nuclear power facilities.[1,2] Hereby Plutonium and the minor actinides are separated from the nuclear waste (partitioning) and converted into shorter-lived or stable elements (transmutation).

The long-term toxicity of nuclear waste and how the residual toxicity of nuclear waste is reduced by removing Plutonium and the MA from nuclear waste is shown in fig. 1, left.

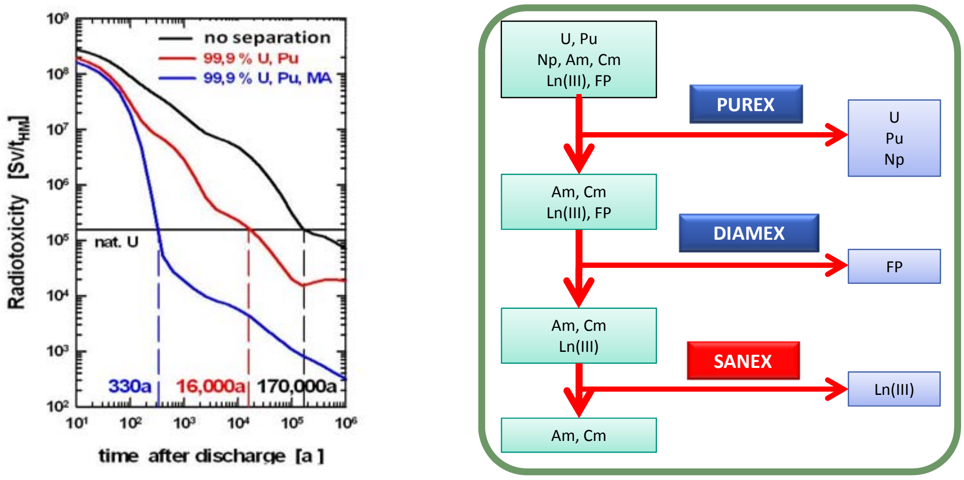

***Fig. 1**. left: Development of the radiotoxicity of spent fuel with time. Right: Schematic draft of the P&T strategy.*

The separation of trivalent actinides, An(III), from the lanthanides, Ln(III), in the so-called SANEX (*Selective* ActiNide EXtraction) process is a crucial part of the partitioning process. This separation is extremely demanding due to the high similarity of An(III) and Ln(III) in both chemical property and ionic radius.

It has been demonstrated that this separation can be realized by selective liquid-liquid extraction using soft donor ligands such as aromatic, N-heterocyclic compounds. Among these ligands 2,6-bis(1,2,4-triazin-3-yl)pyridines (BTPs) are promising compounds.[3-5] They act as tridentate ligands and form 1:3 complexes with both An(III) and Ln(III). For an application in an industrial process these ligands require optimization and the driving force behind the selectivity for An(III) and Ln(III) has not yet been completely understood.

In a synthetic approach the number of nitrogen atoms in the lateral rings of the BTP ligand is changed and the resulting effect on extraction properties is studied. 2,6-bis(4-ethyl-pyridazinyl)pyridine (Et-BDP) with a lower amount of nitrogen atoms in the aromatic ring of the substituents has already been synthesized at University of Reading and tested at CEA-Marcoule. Extraction tests have been performed in 1,1,2,2,-tetrachloroethane as solvent within the EUROPART project. The second ligand (2,6-bis(4-*n*propyl-2,3,5,6-tetrazine-1-yl)pyridine, *n*Pr-Tetrazine) is synthesized as a BTP-type ligand containing a higher number of nitrogen atoms in the lateral rings (fig. 2).

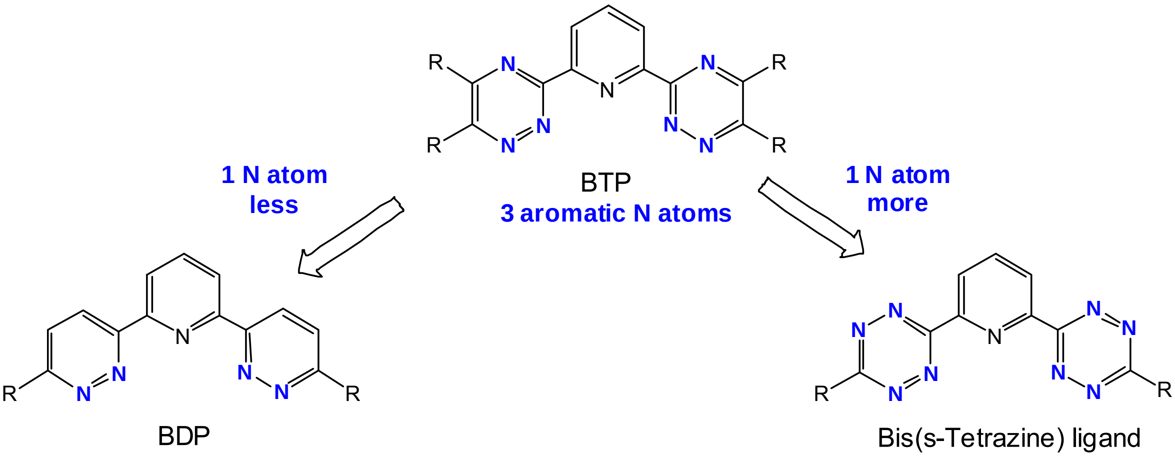

***Fig. 2**. Molecular structures of Et-BDP (**1**)[6] (left), ^{n}Pr-BTP (middle)[3,7] and ^{n}Pr-Tetrazine (**2**) (right).*

The separation of Am(III) from Eu(III) using both ligands is tested by two phase liquid-liquid separation tests. For both ligands significantly smaller separation factors $SF_{Am/Eu}$ in comparison to ^{n}Pr-BTP ($SF_{Am/Eu} \approx 130$) are observed using Et-BDP ($SF_{Am/Eu} \approx 5$) or ^{n}Pr-tetrazine ($SF_{Am/Eu} \approx 9$), respectively. Furthermore, in liquid-liquid extraction tests with Et-BDP protonation of the ligand and dissolution in the organic phase is observed (Fig. 3).

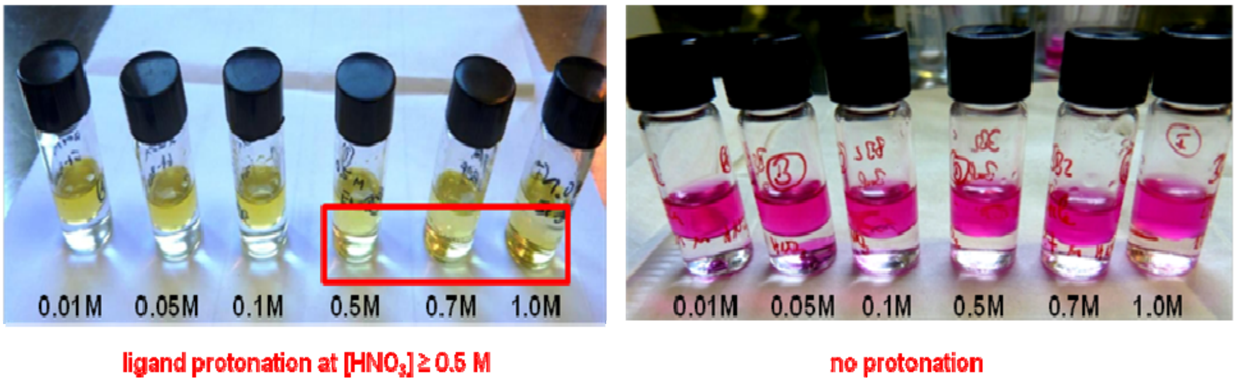

Fig. 3 Two phase liquid-liquid extraction experiments of Am(III) and Eu(III) using 3.2 mM Et-BDP (left) and 6.5 mM ^{n}Pr-Tetrazine, (right) respectively, in kerosene/0.5 M 2-bromodecanoic acid and various concentrations of nitric acid.[8]

These extraction studies in combination with theoretic, thermodynamic and spectroscopic studies endeavor to give a detailed understanding about the extraordinary selectivity of the ^{n}Pr-BTP ligand.

References

(1) Status and Assessment Report on Actinide and Fission Product Partitioning and Transmutation; OECD-NEA, Paris, **1999**.

(2) J. Magill, V. Berthou, D. Haas, J. Galy, R. Schenkel, H.-W. Wiese, G. Heusener, J. Tommasi, G. Youinou, *Nuclear Energy* **2003**, *42*, 263-277.

(3) Z. Kolarik, U. Müllich, F. Gassner, *Solvent Extr. Ion Exch.* **1999**, *17*, 1155-1170.
(4) M. A. Denecke, A. Rossberg, P. J. Panak, M. Weigl, B. Schimmelpfennig, A. Geist, *Inorg. Chem.* **2005**, *44*, 8418-8425.
(5) M. A. Denecke, P. J. Panak, F. Burdet, M. Weigl, A. Geist, R. Klenze, M. Mazzanti, K. Gompper, *C. R. Chim.* **2007**, *10*, 872-882.

(6) EUROPART project: Synthesis at University of Reading, Extraction at CEA-Marcoule.

(7) S. Trumm et al. *Eur. J. Inorg. Chem.* **2010**, 3022-3028.

(8) B. B. Beele, U. Müllich, F. Schwörer, A. Geist, P. J. Panak, *Proc. Chem.* **2012**, *accepted*.

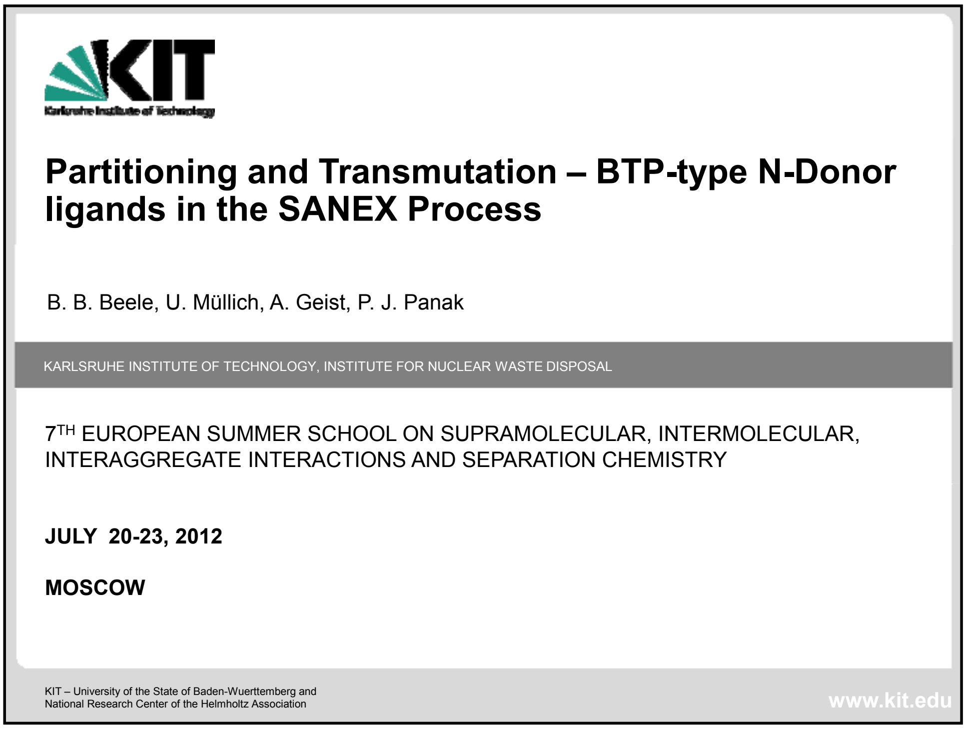

Partitioning and Transmutation – BTP-type N-Donor ligands in the SANEX Process

B. B. Beele, U. Müllich, A. Geist, P. J. Panak

KARLSRUHE INSTITUTE OF TECHNOLOGY, INSTITUTE FOR NUCLEAR WASTE DISPOSAL

7TH EUROPEAN SUMMER SCHOOL ON SUPRAMOLECULAR, INTERMOLECULAR, INTERAGGREGATE INTERACTIONS AND SEPARATION CHEMISTRY

JULY 20-23, 2012

MOSCOW

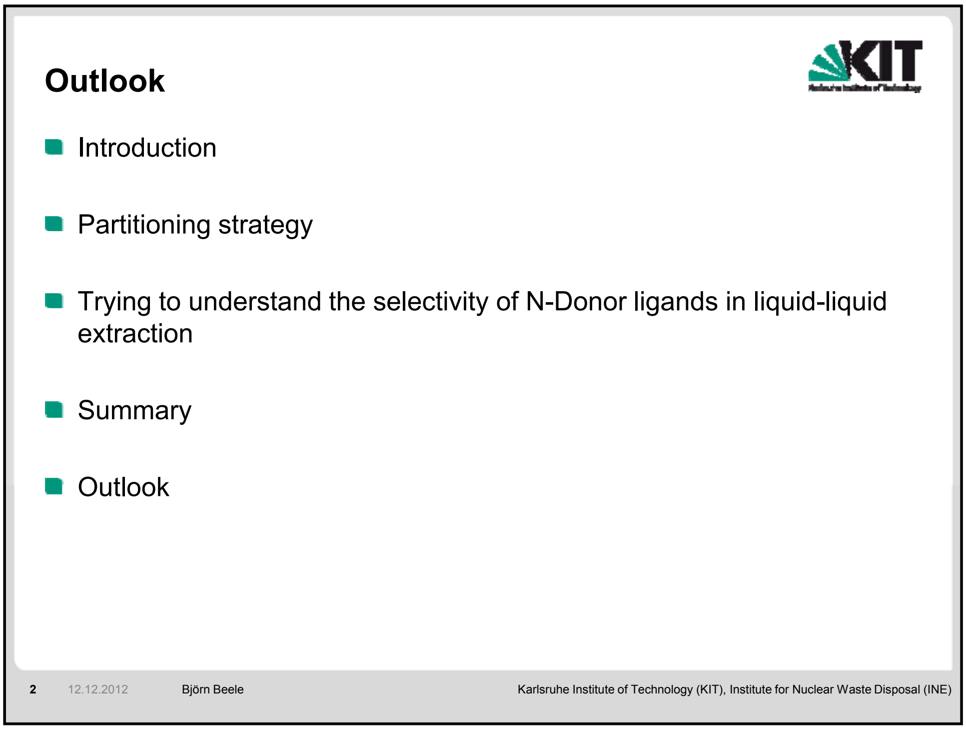

Outlook

- Introduction
- Partitioning strategy
- Trying to understand the selectivity of N-Donor ligands in liquid-liquid extraction
- Summary
- Outlook

Introduction

- **Radiotoxicity of spent nuclear fuel is governed over long periods of time by plutonium and the minor actinides (neptunium, americium, curium).**
- **The content of these elements in the spent fuel is altogether in the range of 1 %.**
- **The partitioning & transmutation concept aims at separating plutonium and the minor actinides and transmuting them into short-lived or stable nuclides.**
- **This would lead to a drastic reduction of the radiotoxicity and the heat load of the nuclear waste.**

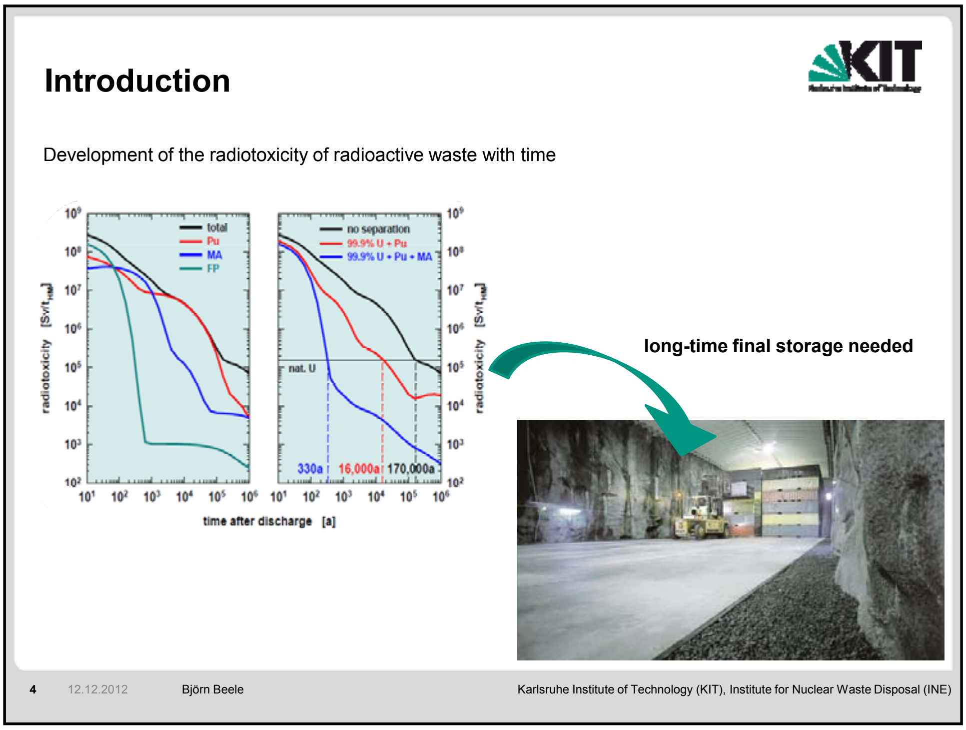

Introduction

Development of the radiotoxicity of radioactive waste with time

long-time final storage needed

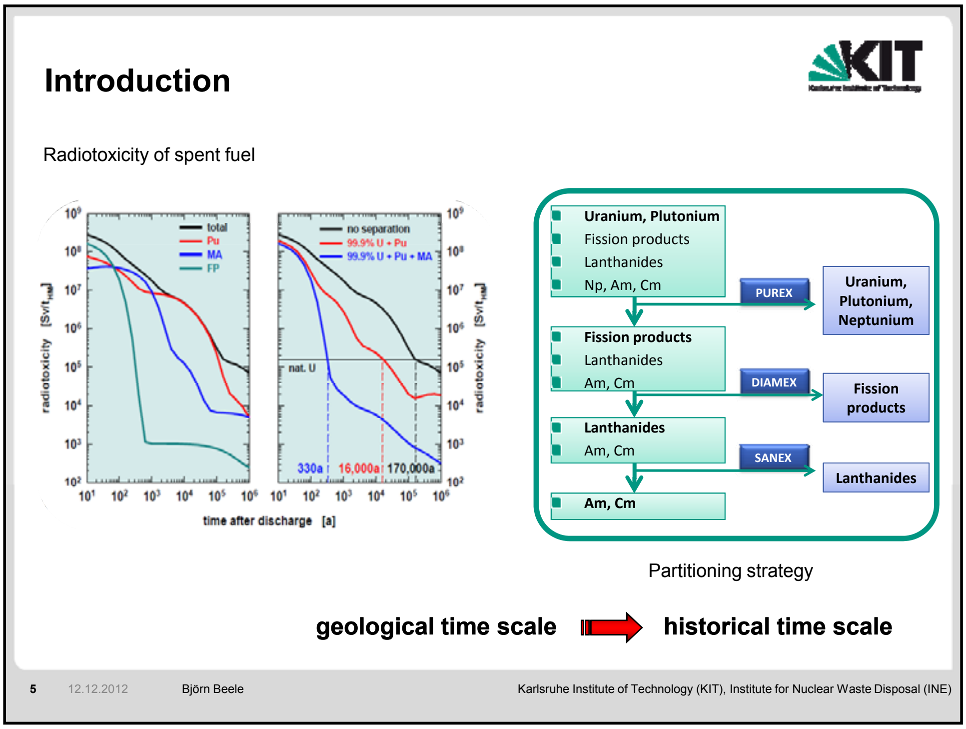

Introduction

Radiotoxicity of spent fuel

- Uranium, Plutonium
- Fission products
- Lanthanides
- Np, Am, Cm

PUREX → Uranium, Plutonium, Neptunium

- Fission products
- Lanthanides
- Am, Cm

DIAMEX → Fission products

- Lanthanides
- Am, Cm

SANEX → Lanthanides

- Am, Cm

Partitioning strategy

geological time scale ➡ **historical time scale**

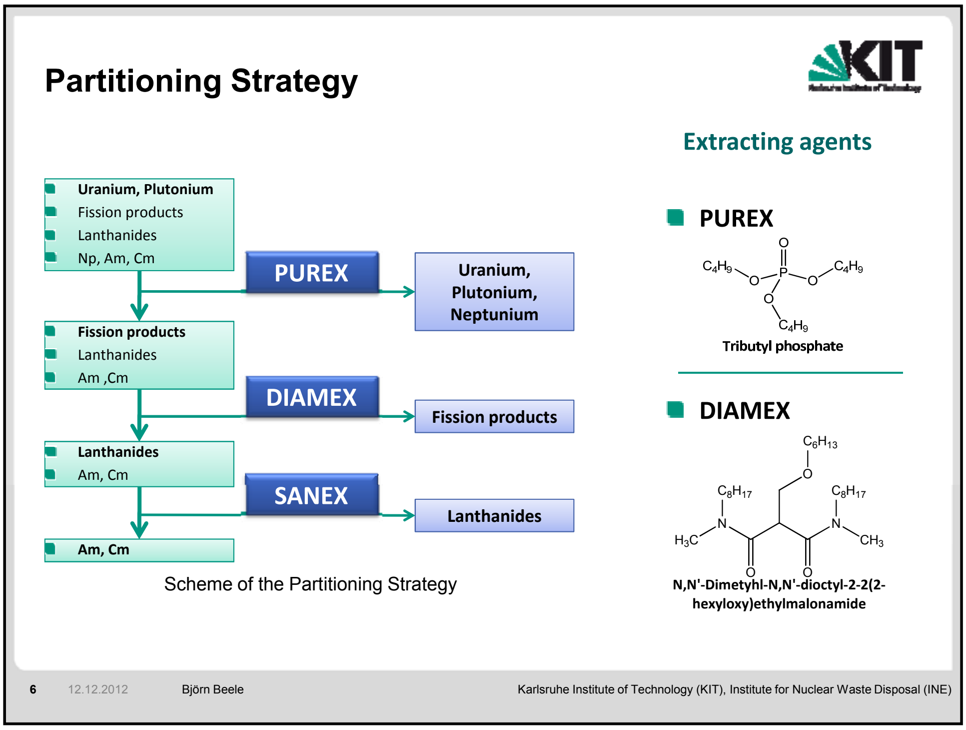

Partitioning Strategy

- Uranium, Plutonium
- Fission products
- Lanthanides
- Np, Am, Cm

PUREX → Uranium, Plutonium, Neptunium

- Fission products
- Lanthanides
- Am ,Cm

DIAMEX → Fission products

- Lanthanides
- Am, Cm

SANEX → Lanthanides

- Am, Cm

Scheme of the Partitioning Strategy

Extracting agents

- PUREX

Tributyl phosphate

- DIAMEX

N,N'-Dimetyhl-N,N'-dioctyl-2-2(2-hexyloxy)ethylmalonamide

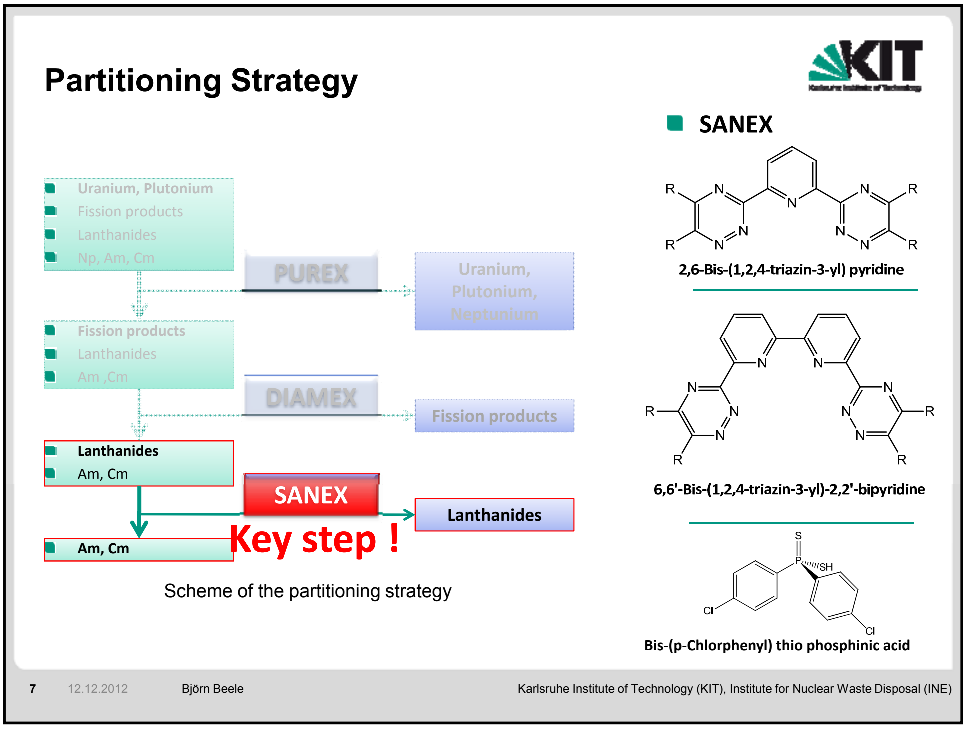

Partitioning Strategy

- Uranium, Plutonium
- Fission products
- Lanthanides
- Np, Am, Cm

PUREX

Uranium, Plutonium, Neptunium

- Fission products
- Lanthanides
- Am ,Cm

DIAMEX

Fission products

- Lanthanides
- Am, Cm

SANEX

Lanthanides

- Am, Cm

Key step !

Scheme of the partitioning strategy

- SANEX

2,6-Bis-(1,2,4-triazin-3-yl) pyridine

6,6'-Bis-(1,2,4-triazin-3-yl)-2,2'-bipyridine

Bis-(p-Chlorphenyl) thio phosphinic acid

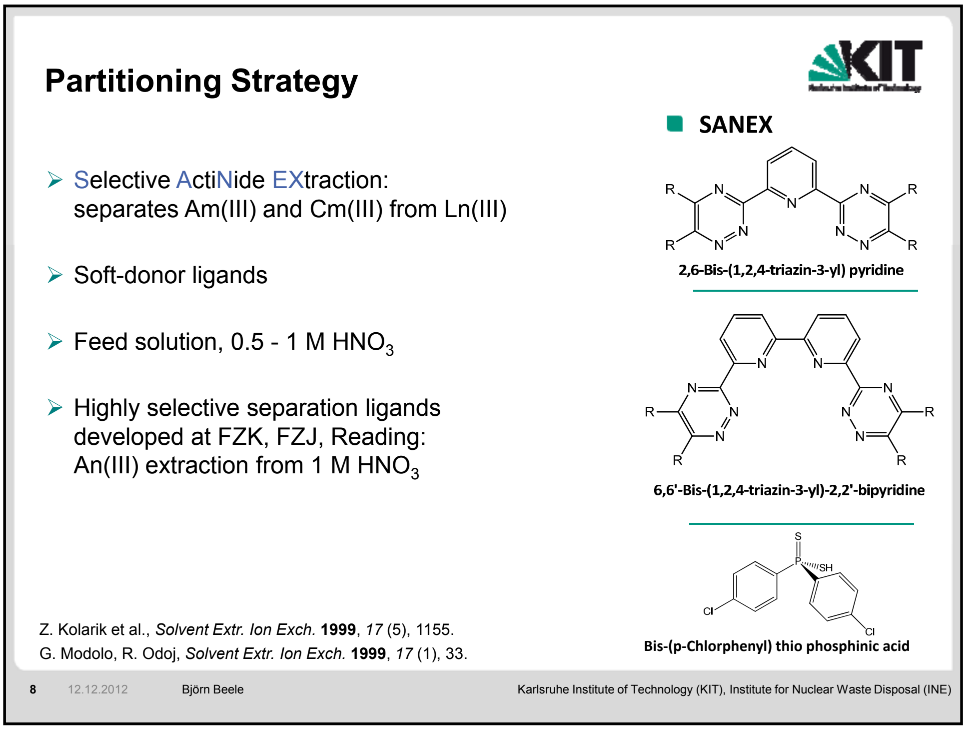

Partitioning Strategy

- Selective ActiNide EXtraction: separates Am(III) and Cm(III) from Ln(III)
- Soft-donor ligands
- Feed solution, 0.5 - 1 M HNO_3
- Highly selective separation ligands developed at FZK, FZJ, Reading: An(III) extraction from 1 M HNO_3

Z. Kolarik et al., *Solvent Extr. Ion Exch.* **1999**, *17* (5), 1155.
G. Modolo, R. Odoj, *Solvent Extr. Ion Exch.* **1999**, *17* (1), 33.

- SANEX

2,6-Bis-(1,2,4-triazin-3-yl) pyridine

6,6'-Bis-(1,2,4-triazin-3-yl)-2,2'-bipyridine

Bis-(p-Chlorphenyl) thio phosphinic acid

Partitioning Strategy

Does P&T replace the need for a final repository ?

NO

BUT P&T eases the requirements of a final repository

Selectivity of N-Donor Ligands

- ✓ Fast kinetics
- ✓ High complexation constant (14.4 in H_2O:MeOH)
- ✓ High seperation factor SF(D_{Am}/D_{Eu}) > 130
- ✓ Modifications possible at many positions
- ✓ Synthesis in multi 100g scale
- ✗ Instability against hydrolysis and radiolysis
- ✗ Synthesis requires 6 (2) steps

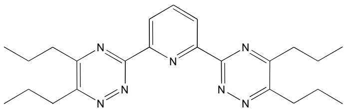

^{n}Pr-BTP

→ Breakthough in the field of actinide separation

Z. Kolarik et al., *Solvent Extr. Ion Exch.*, **1999**, 17(1), 23.
Z. Kolarik et al., *Solvent Extr. Ion Exch.* **1999**, *17* (5), 1155.
M. A. Denecke et al., *Inorg. Chem.* **2005**, *44*, 8418.
S. Trumm et al., *Eur. J. Inorg. Chem.* **2010**, 3022.

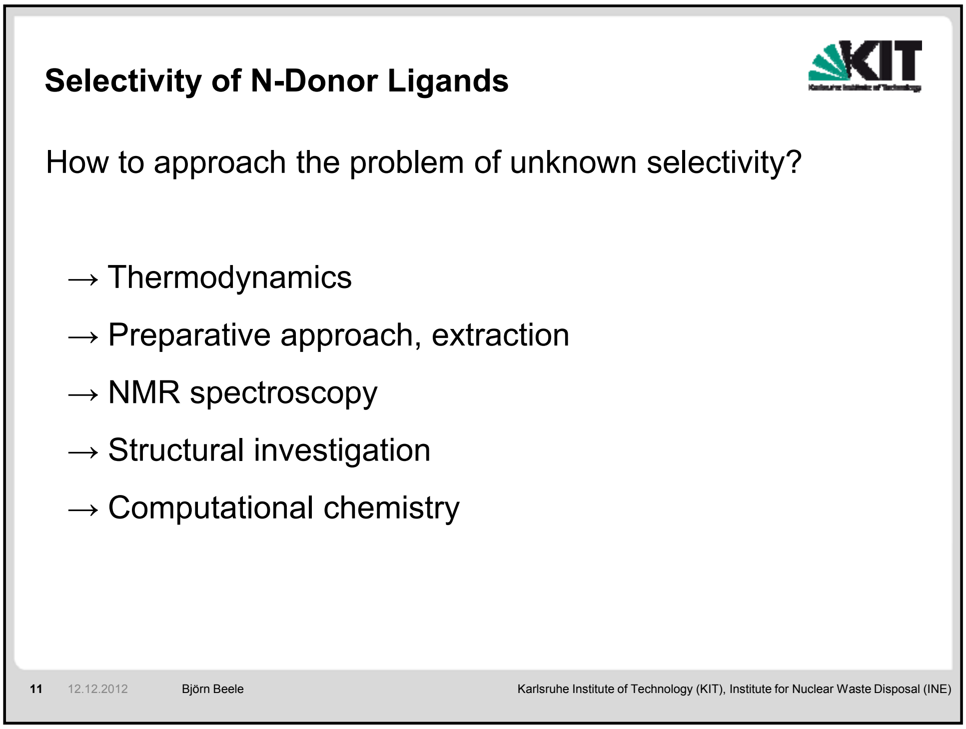

Selectivity of N-Donor Ligands

How to approach the problem of unknown selectivity?

→ Thermodynamics

→ Preparative approach, extraction

→ NMR spectroscopy

→ Structural investigation

→ Computational chemistry

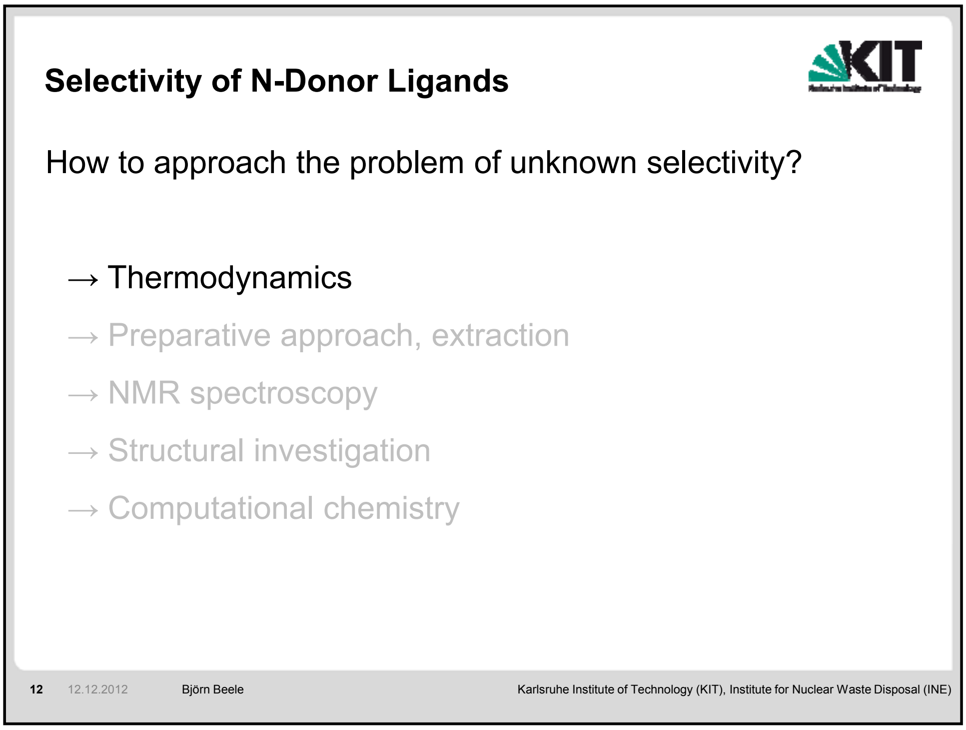

Selectivity of N-Donor Ligands

How to approach the problem of unknown selectivity?

→ Thermodynamics

→ Preparative approach, extraction

→ NMR spectroscopy

→ Structural investigation

→ Computational chemistry

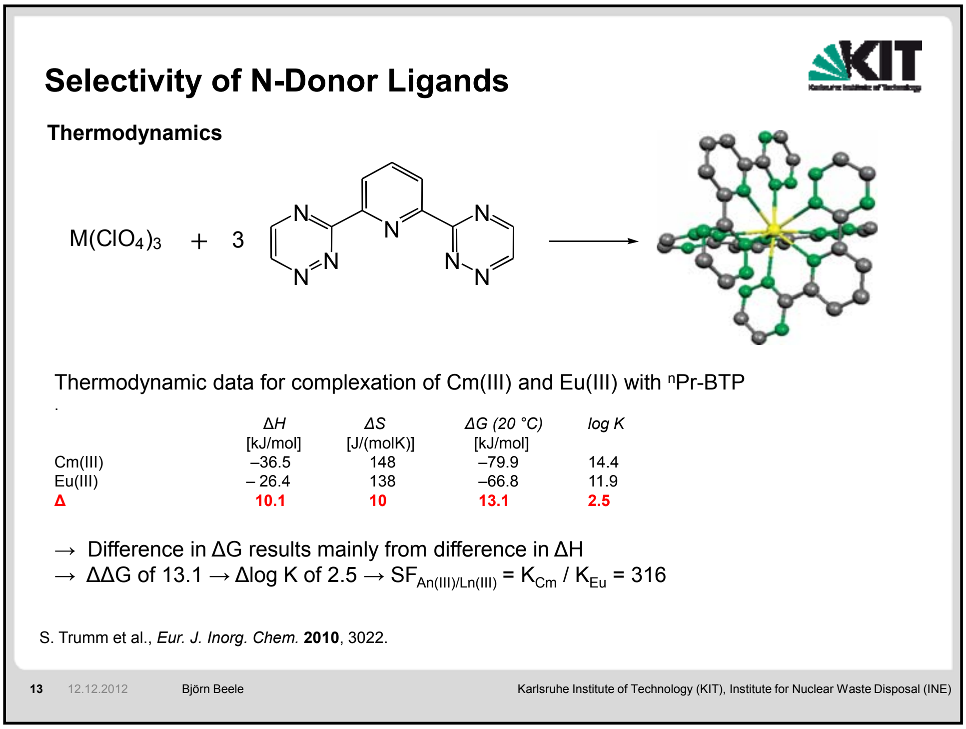

Selectivity of N-Donor Ligands

Thermodynamics

Thermodynamic data for complexation of Cm(III) and Eu(III) with ⁿPr-BTP

	ΔH [kJ/mol]	ΔS [J/(molK)]	ΔG (20 °C) [kJ/mol]	log K
Cm(III)	–36.5	148	–79.9	14.4
Eu(III)	– 26.4	138	–66.8	11.9
Δ	**10.1**	**10**	**13.1**	**2.5**

→ Difference in ΔG results mainly from difference in ΔH

→ ΔΔG of 13.1 → Δlog K of 2.5 → $SF_{An(III)/Ln(III)} = K_{Cm} / K_{Eu} = 316$

S. Trumm et al., *Eur. J. Inorg. Chem.* **2010**, 3022.

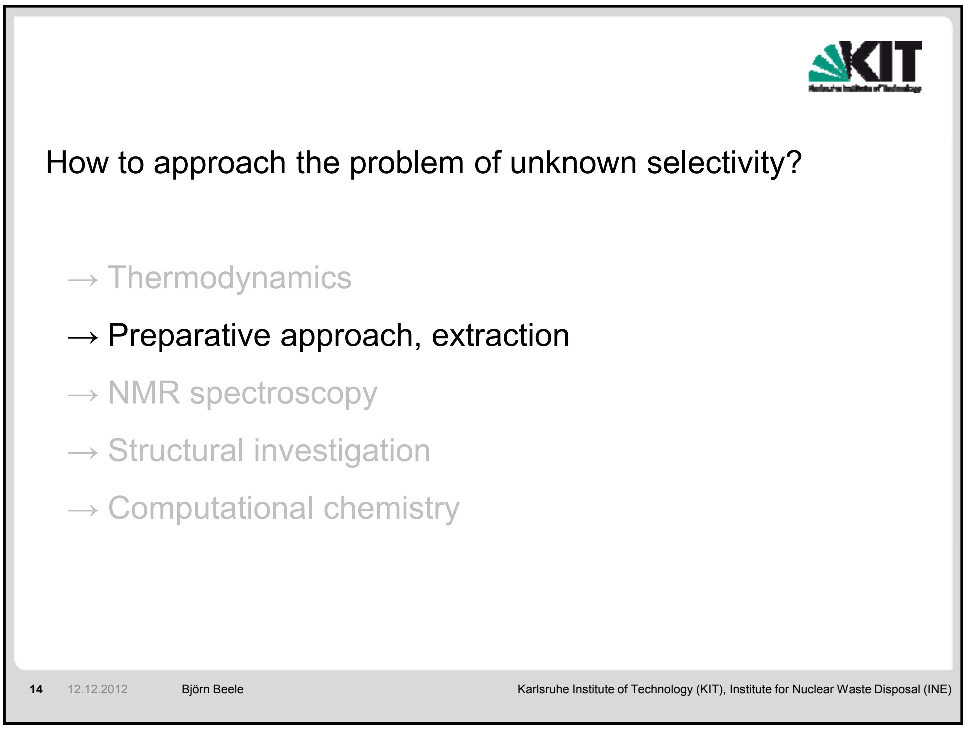

How to approach the problem of unknown selectivity?

→ Thermodynamics

→ Preparative approach, extraction

→ NMR spectroscopy

→ Structural investigation

→ Computational chemistry

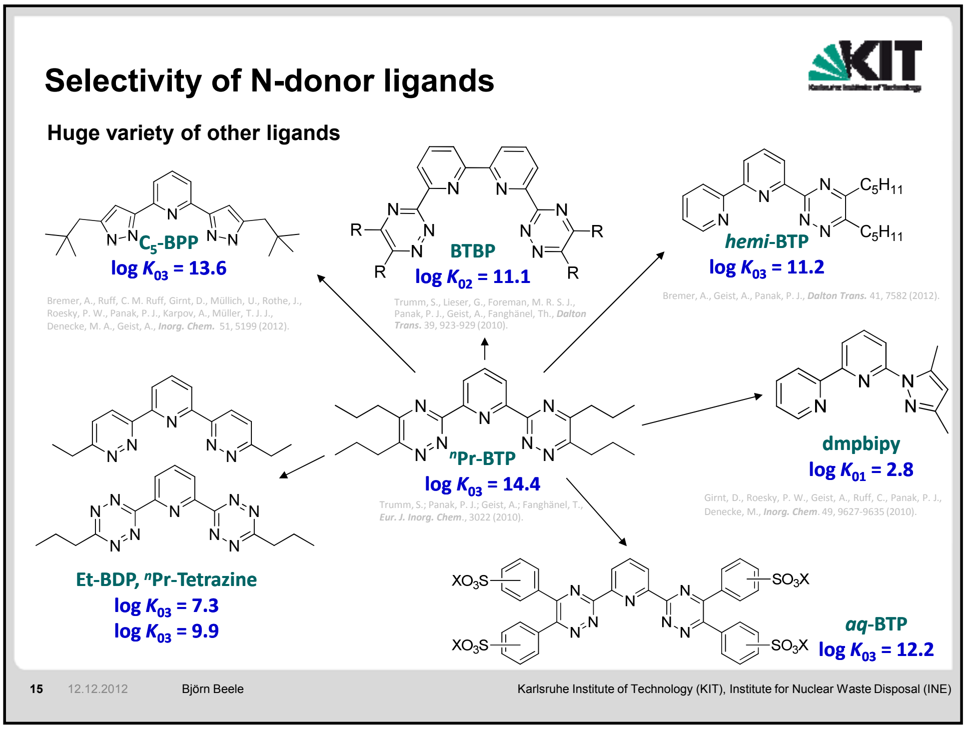

Selectivity of N-donor ligands

Huge variety of other ligands

C_5-BPP
log K_{03} = 13.6

Bremer, A., Ruff, C. M. Ruff, Girnt, D., Müllich, U., Rothe, J., Roesky, P. W., Panak, P. J., Karpov, A., Müller, T. J. J., Denecke, M. A., Geist, A., ***Inorg. Chem.*** 51, 5199 (2012).

BTBP
log K_{02} = 11.1

Trumm, S., Lieser, G., Foreman, M. R. S. J., Panak, P. J., Geist, A., Fanghänel, Th., ***Dalton Trans.*** 39, 923-929 (2010).

***hemi*-BTP**
log K_{03} = 11.2

Bremer, A., Geist, A., Panak, P. J., ***Dalton Trans.*** 41, 7582 (2012).

^{n}Pr-BTP
log K_{03} = 14.4

Trumm, S.; Panak, P. J.; Geist, A.; Fanghänel, T., ***Eur. J. Inorg. Chem.***, 3022 (2010).

dmpbipy
log K_{01} = 2.8

Girnt, D., Roesky, P. W., Geist, A., Ruff, C., Panak, P. J., Denecke, M., ***Inorg. Chem.*** 49, 9627-9635 (2010).

Et-BDP, ^{n}Pr-Tetrazine
log K_{03} = 7.3
log K_{03} = 9.9

***aq*-BTP**
log K_{03} = 12.2

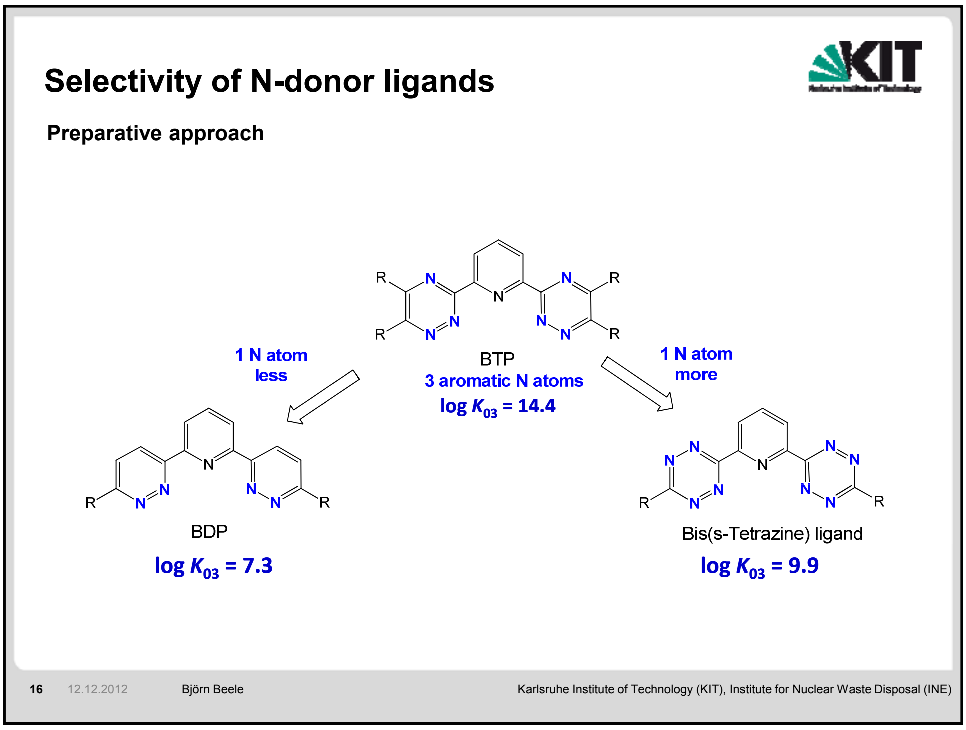

Selectivity of N-donor ligands

Preparative approach

BTP
3 aromatic N atoms
log K_{03} = 14.4

1 N atom less

1 N atom more

BDP
log K_{03} = 7.3

Bis(s-Tetrazine) ligand
log K_{03} = 9.9

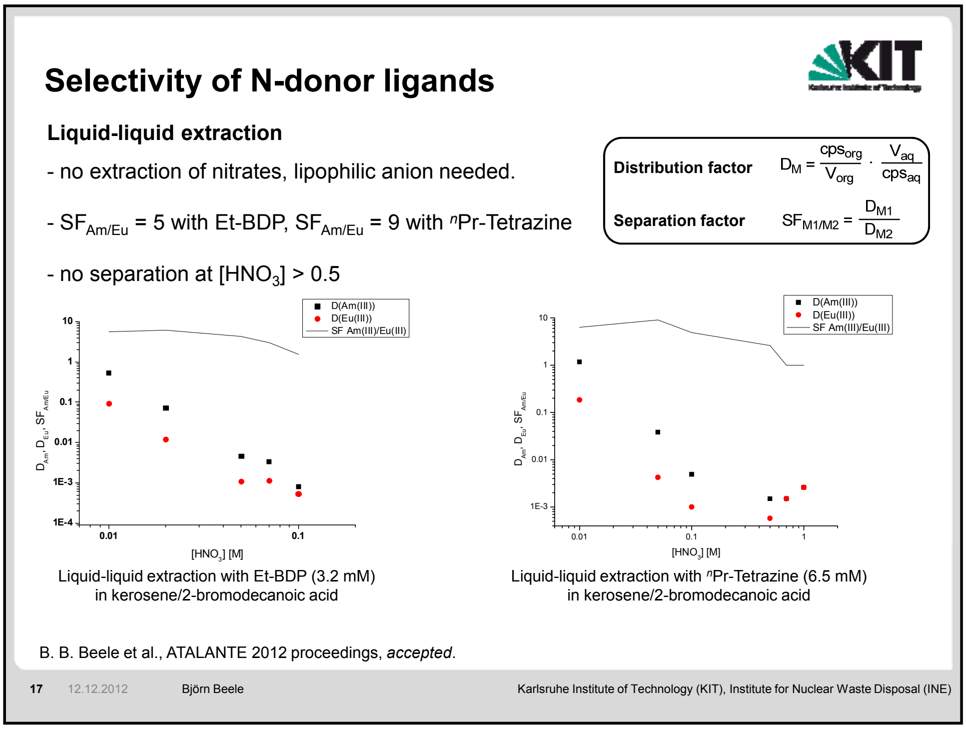

Selectivity of N-donor ligands

Liquid-liquid extraction

- no extraction of nitrates, lipophilic anion needed.

- $SF_{Am/Eu} = 5$ with Et-BDP, $SF_{Am/Eu} = 9$ with ^{n}Pr-Tetrazine

- no separation at $[HNO_3] > 0.5$

Distribution factor $D_M = \frac{cps_{org}}{V_{org}} \cdot \frac{V_{aq}}{cps_{aq}}$

Separation factor $SF_{M1/M2} = \frac{D_{M1}}{D_{M2}}$

Liquid-liquid extraction with Et-BDP (3.2 mM)
in kerosene/2-bromodecanoic acid

Liquid-liquid extraction with ^{n}Pr-Tetrazine (6.5 mM)
in kerosene/2-bromodecanoic acid

B. B. Beele et al., ATALANTE 2012 proceedings, *accepted*.

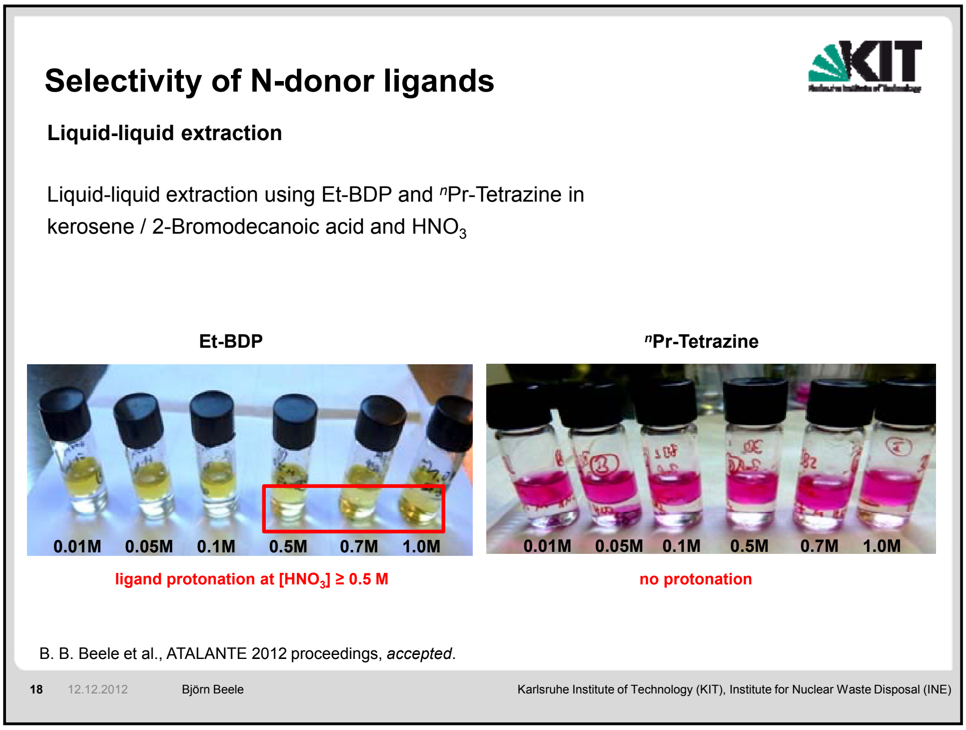

Selectivity of N-donor ligands

Liquid-liquid extraction

Liquid-liquid extraction using Et-BDP and ^{n}Pr-Tetrazine in kerosene / 2-Bromodecanoic acid and HNO_3

Et-BDP

ligand protonation at $[HNO_3] \geq 0.5$ M

^{n}Pr-Tetrazine

no protonation

B. B. Beele et al., ATALANTE 2012 proceedings, *accepted*.

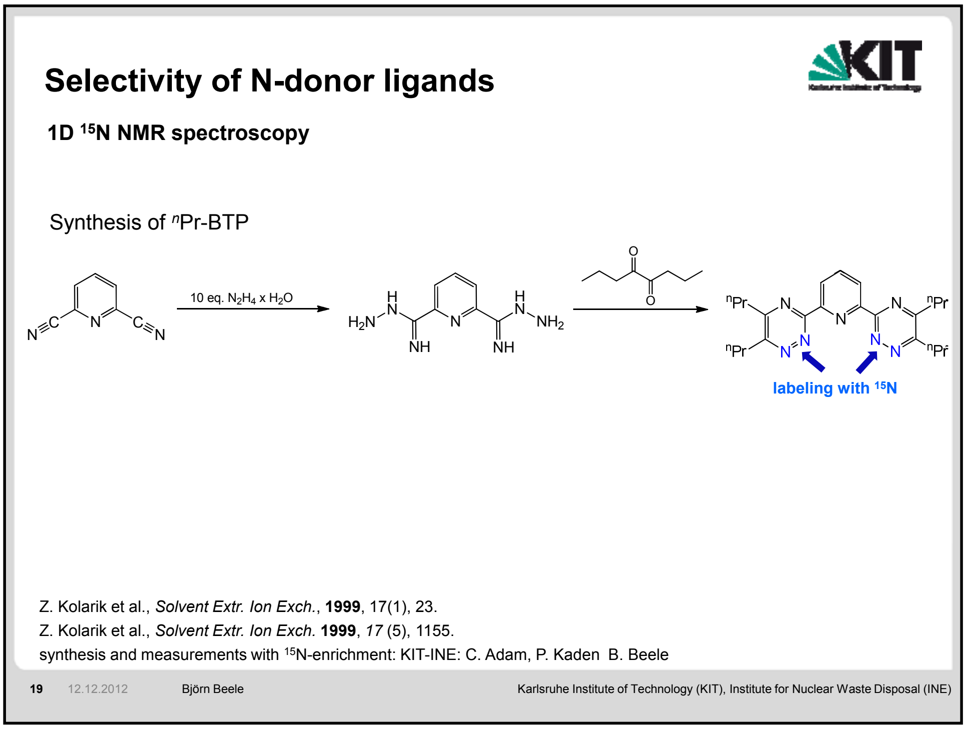

Selectivity of N-donor ligands

1D ^{15}N NMR spectroscopy

Synthesis of ^{n}Pr-BTP

labeling with ^{15}N

Z. Kolarik et al., *Solvent Extr. Ion Exch.*, **1999**, 17(1), 23.
Z. Kolarik et al., *Solvent Extr. Ion Exch.* **1999**, *17* (5), 1155.
synthesis and measurements with ^{15}N-enrichment: KIT-INE: C. Adam, P. Kaden B. Beele

19 12.12.2012 Björn Beele Karlsruhe Institute of Technology (KIT), Institute for Nuclear Waste Disposal (INE)

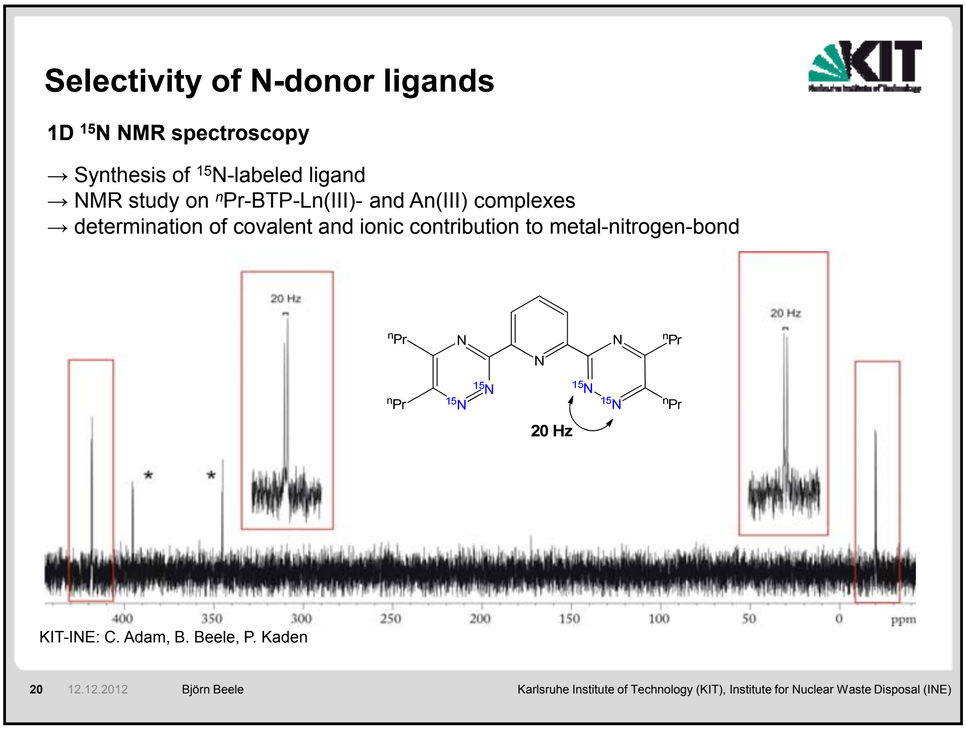

Selectivity of N-donor ligands

1D ^{15}N NMR spectroscopy

→ Synthesis of ^{15}N-labeled ligand
→ NMR study on ^{n}Pr-BTP-Ln(III)- and An(III) complexes
→ determination of covalent and ionic contribution to metal-nitrogen-bond

KIT-INE: C. Adam, B. Beele, P. Kaden

20 12.12.2012 Björn Beele Karlsruhe Institute of Technology (KIT), Institute for Nuclear Waste Disposal (INE)

How to approach the problem of unknown selectivity?

→ Thermodynamics

→ Preparative approach, extraction

→ NMR spectroscopy

→ Structural investigation

→ Computational chemistry

Selectivity of N-Donor Ligands

EXAFS study of An(BTP)$_3$ and Ln(BTP)$_3$

M(III)	$R_{M(III)-N}$	$r_{M(III)}$	$R - r$ [Å]
U(III)	2.57	1.214	1.356
Pu(III)	2.561	1.177	1.384
Am(III)	2.562	1.160	1.402
Cm(III)	2.568	1.148	1.420
Eu(III)	2.559	1.120	1.439
Gd(III)	2.554	1.107	1.447

Cm(III) → U(III);
increasing softness

→ Ln(III) and An(III) show essentially the same coordination structure

→ An(III)-N distances are slightly shorter

→ evidence of bond length contraction ?

Quantumchemical calculations

- Experimental structure and bond lengths are obtained on DFT level

- No obvious indications for differences in the bonding for Eu(III) and Cm(III) complexes (difference under 0.01 Å)

- Data in good agreement with EXAFS

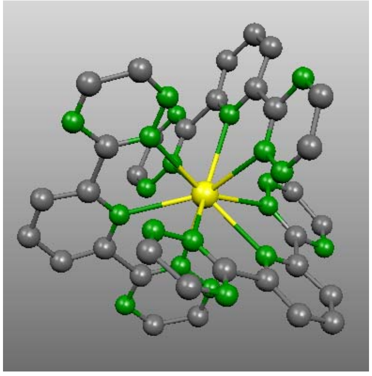

M. Denecke et al., *Inorg. Chem.* **2005**, 8418.

Summary

- P&T is a strategy to reduce radiotoxicity of radioactive waste.

- Most demanding task: Separating Ln(III) from An(III) in the SANEX process

- The reason for the N-donor ligands' selectivity is still not understood.

- Complexation of Cm(III) and Eu(III) with ^{n}Pr-BTP:
  - Complexation with Cm(III) is more exergonic.
  - Difference in ΔG results mainly from difference in ΔH

- Changing the lateral rings of the ^{n}Pr-BTP ligand severely degredates complexation and extraction properties

- Theoretic calculations and EXAFS give access to bond length and complex symmetry

- NMR experiments and theoretic calculations can give an insight into the covalent and ionic nature of the nitrogen-metal bond.

Outlook

Sounds easier than it is:

Combining results from synthesis, liquid-liquid extraction, spectroscopy and theoretical calculation to a general understanding of the relationship of molecular structure and extraction properties.

Some things are comprehended, yet the big picture is still not understood.

Acknowledgement

Christian Adam
Nidhu Banik
Antje Bremer
Sebastian Büchner
Melissa Denecke
Horst Geckeis
Andreas Geist
Peter Kaden
Carsten Koke
Udo Müllich
Petra Panak
Christian Ruff
Jörg Rothe
Bernd Schimmelpfennig
Felicitas Schwörer
Sascha Trumm
Tonya Vitova

JP 03-11 and JP 06-14 ACTINET
FI6W-CT-2003-508854 EuroPart
FP7-CP-2007-211267 ACSEPT
BMBF 2020+ Bundesministerium für Bildung und Forschung

Working at INE

Thank you for your kind attention

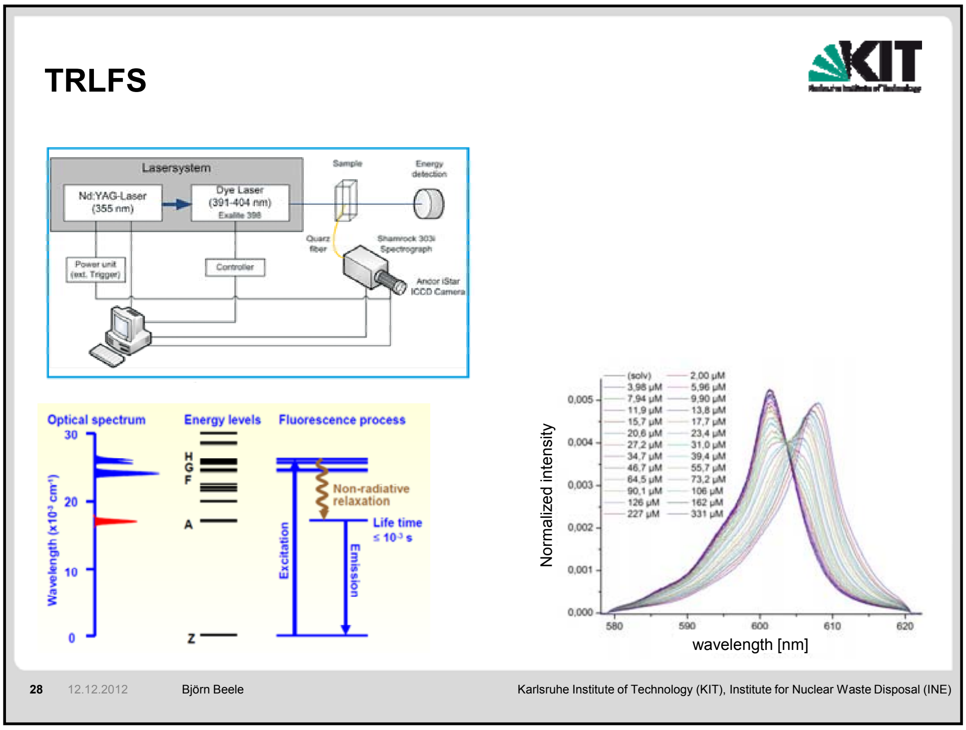

TRLFS

Artificial receptors for TcO_4^- , ReO_4^- recognition

(Selected works)

G.V. Kolesnikov, K.E. German, E.A. Kataev, G.A. Kirakosyan,
Khrustalev , Yu. A. Ustynyuk, I.G. Tananaev, B.F. Myasoedov

Problem of Tc binding is urgent
TcO_4^- is the most stable form

- **Nuclear fuel cycle**:
  - high yields, more then 800 g per 1 t ^{235}U
  - facilitates reductant decomposition during treatment
  - forms precipitates

TcO_4^- needs to be extracted before treatment

- **Ecology**:
  - ^{99}Tc ($E_{\beta-}$= 293.8 keV, $\lambda_{1/2}$ = 2.13×10^5 years)
  - TcO_4^- salts are poorly fixed with natural minerals
  - $NaTcO_4$ solubility in water — 11.3 M

Concentration control is necessary

TcO_4^- и ReO_4^- are extensively used in nuclear medicine

- ^{99m}Tc (E_γ = 141.0 keV, $\lambda_{1/2}$ = 6 h)

  Diagnostic application

  80% from 30 mln. injections yearly

- ^{188}Re ($E_{\beta-}$= 763.9 keV, $\lambda_{1/2}$ = 17 h)

  Therapeutic application

- **W**hat is common for both nuclides:

  are produced as MO_4^- (M = Tc, Re)

  then reduced with $SnCl_2$, $NaBH_4$

  injected as M(III)–(V) complexes

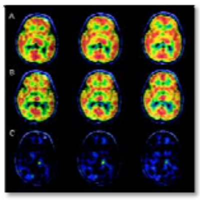

It is difficult to bind hydrophobic TcO_4^- и ReO_4^-

Anion	ΔH^0_{hydr} kJ/mol*	R_{H2O}, nm	S_{ion}, Å^2	Q/S×10^2, Å^{-2}
$H_2PO_4^-$	-522	0.20	50.3	2.0
H_3CCOO^-	-425	0.16	33.0	3.0
Cl^-	-367	0.18	41.2	2.4
NO_3^-	-312	0.18	40.3	2.5
I^-	-291	0.22	60.8	1.6
ClO_4^-	-246	0.25	78.5	1.3
ReO_4^-	-244	0.26	85.0	1.2
TcO_4^-**	-247	0.25	78.5	1.3
MnO_4^-	-250	0.24	72.4	1.4

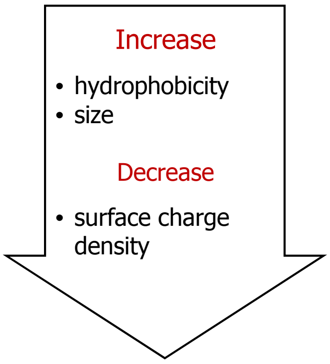

Increase

- hydrophobicity
- size

Decrease

- surface charge density

R_{H20} – ionic radius in water
S_{ion} – surface of an ion
Q/S – surface charge density of an ion

* ΔH^0_{hydr} и R_{H2O} obtained experimentally. Other data is calculated.
** for TcO_4^- data was produced by linear interpolation in the row: MnO_4^- - TcO_4^- - ReO_4^-.

Marcus Y. The thermodynamics of solvation of ions. Part 2. // J.Chem.Soc.Faraday Trans. 1. – 1987.

Approaches for binding of TcO_4^- and ReO_4^-

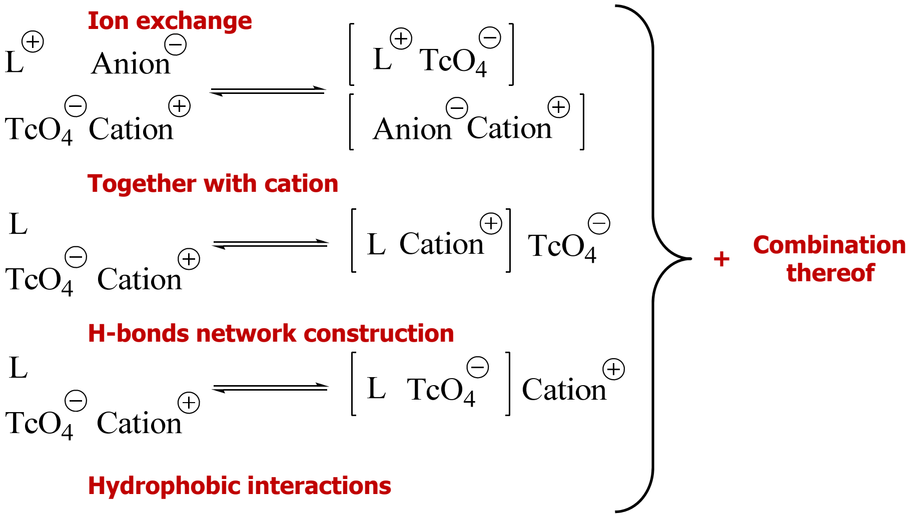

Ion exchange

Together with cation

H-bonds network construction

Hydrophobic interactions

+ Combination thereof

Some organic moieties for binding of TcO_4^- and ReO_4^-

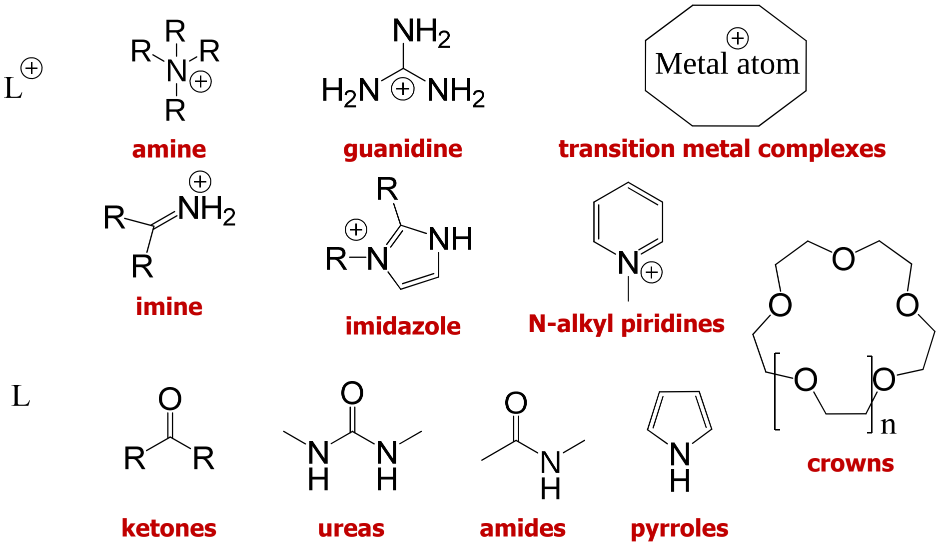

amine **guanidine** **transition metal complexes**

imine **imidazole** **N-alkyl piridines** **crowns**

ketones **ureas** **amides** **pyrroles**

Known methods for investigating interactions between TcO_4^- and ReO_4^- and organic receptors

- **E**xtraction – the most popular method
- **U**V-Vis – easy to do, but Tc and Re are UV active
- ^{1}H-NMR – precise, but concentration must be higher then in objects of interest
- **X**-ray – luck is needed
- ^{99}Tc-NMR – exotic

Solubility* of some TcO_4^- salts in H_2O

- **More hydrophobic cation produces less soluble salt with TcO_4^-**

$^{99}TcO_4Na$	11.3	Cl (NBu_4)	20.53
$^{99}TcO_4(NMe_4)$	0.14	Br (NBu_4)	21.48
$^{99}TcO_4(NBu_4)$	4×10^{-3}	I (NBu_4)	7×10^{-2}
$^{99}TcO_4$(**TPG**)	**4×10^{-3}**		
$^{99}TcO_4(NHept_4)$	**1×10^{-5}**		

TPG = triphenylguanidinium

*the concentration is given in mol/L

Rard J.A., Rand M.H., Anderegg G., Wanner H. Chemical thermodynamics Vol. 3. Chemical thermodynamics of Technetium. Sandino M.C.A., Osthols E., Eds.; Elsevier, 1999.

Imidazole based smaller organic receptor

- **Positive charge from N-alkyl imidazole**
- **Acidic N-H from imidazole**

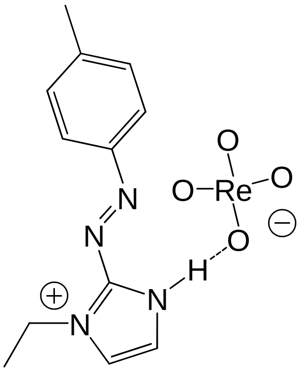

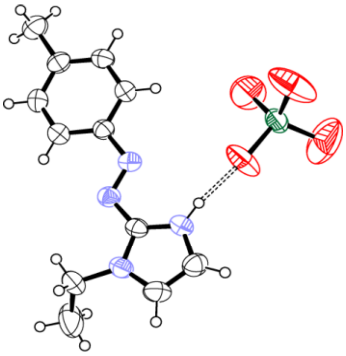

Ray U., Mostafa G., Lu T., Sinha C. Hydrogen bonded perrhenate-azoimidazoles. // Cryst.Eng. – 2002.
Ray U., Chand B., Dasmahapatra A., Mostafa G., Lu T., Sinha C. // Inorg.Chem.Commun. – 2003.

Phosphineimine bearing organic receptor

- **Positive charge from protonated imine**
- **Acidic N-H from protonated imine**

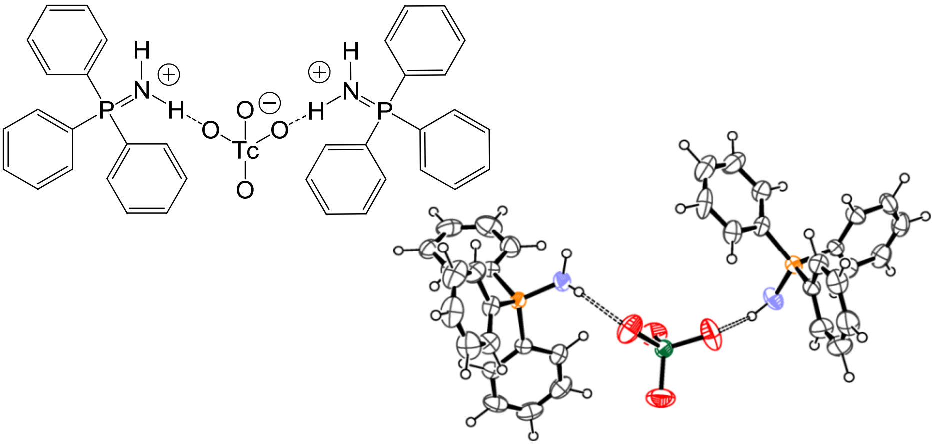

Eble B., Berning D., Barnes C.L., Katti K.V., Jurisson S. // J.Chem.Cryst. – 1999.

Guanidinium tetraoxidorhenate(VII)

- **Protonated guanidinium bears positive charge**
- **3 oxygen atoms of ReO_4^- are coordinated**

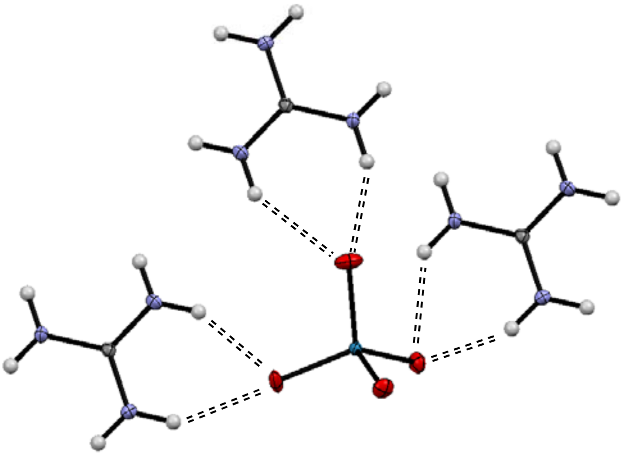

Grigoriev M.S., German K.E., Maruk A.Ya. // Acta Crystallogr., Sect. E. – 2007.

Metal complexes bind ReO_4^-. Re-complex.

- **Positive charge from metal**
- **Acidic N-H from organic moiety**

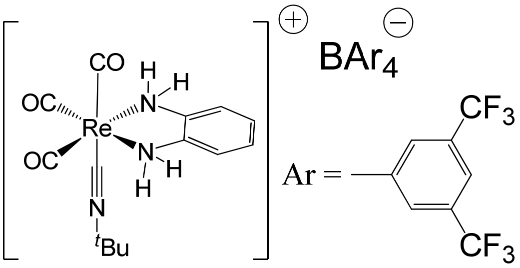

K_a, ^{1}H-NMR in MeCN	HSO_4^-	Cl^-	Br^-	NO_3^-	ClO_4^-	ReO_4^-
	19	77	48	26	18	**24**

Nieto S., Pérez J., Riera L., Riera V., Miguel D. // New J.Chem. – 2006.

Metal complexes bind ReO_4^-. Pt-complex.

- **Positive charge on metal**
- **Acidic N-H from amide**

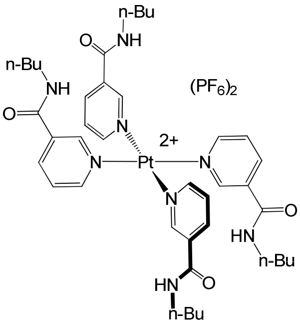

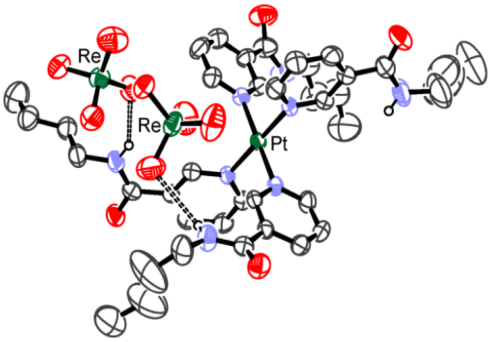

	HSO_4^-	$CF_3SO_3^-$	H_3CCOO^-	NO_3^-	ReO_4^-
K_a, ^1H-NMR in MeCN	149	129	230 (1:1) 491 (1:2)	526 (1:1) 132 (1:2)	**150**

Bondy C.R., Gale P.A., Loeb S.J. // Chem.Comm. – 2001.

More complicated compounds for TcO_4^- and ReO_4^-

Extraction
0.9% NaCl in H_2O
into $MeNO_2$
88% TcO_4^-

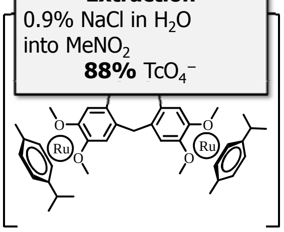

Extraction
1M NaOH in H2O
into dichloroethane
100% TcO_4^-

aqueous 1M HNO_3
into dichloroethane
80% TcO_4^-

^1H NMR CDCl3
$K(ReO_4^-)$ = 40 M^{-1}
$K(ReO_4^-)$ = 840 M^{-1}(+Na^+)

Extraction
aqueous NaOH, pH 11
into CH_2Cl_2
70% TcO_4^-

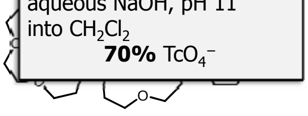

^1H NMR MeCN
$K(ReO_4^-)$ = **112** M^{-1}

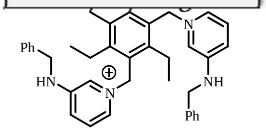

Extraction
HEPES/NaOH, pH 7.4
into $CHCl_3$
10% TcO_4^-

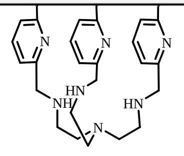

Extraction
HEPES/NaOH, pH 7.4
into $CHCl_3$
50% TcO_4^-

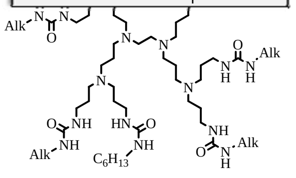

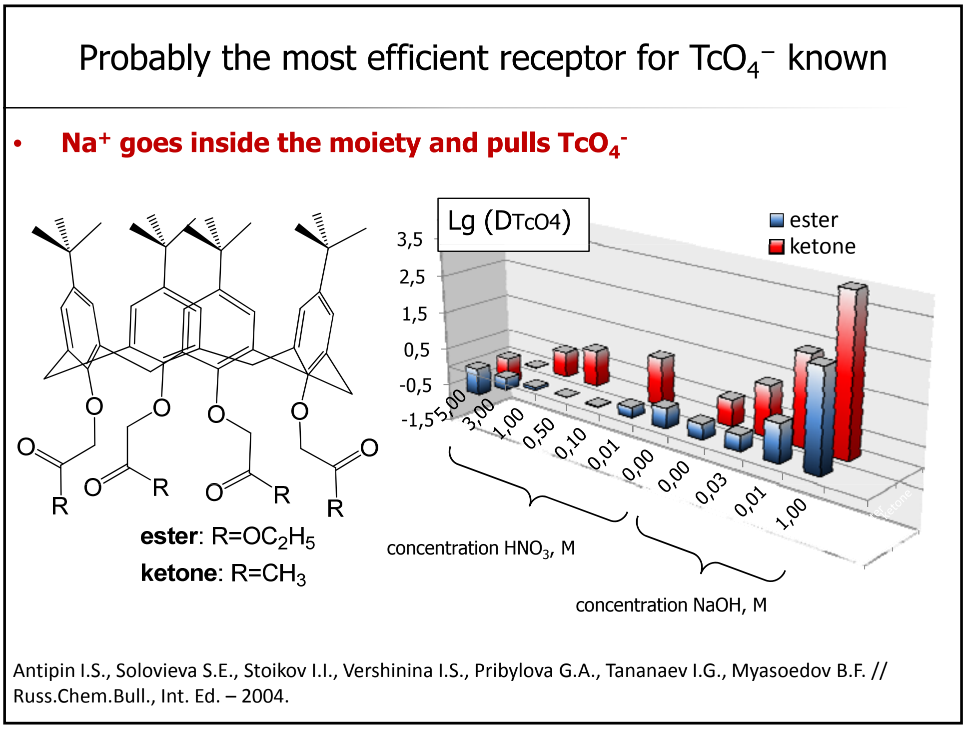

Probably the most efficient receptor for TcO_4^- known

- **Na⁺ goes inside the moiety and pulls TcO_4^-**

Antipin I.S., Solovieva S.E., Stoikov I.I., Vershinina I.S., Pribylova G.A., Tananaev I.G., Myasoedov B.F. // Russ.Chem.Bull., Int. Ed. – 2004.

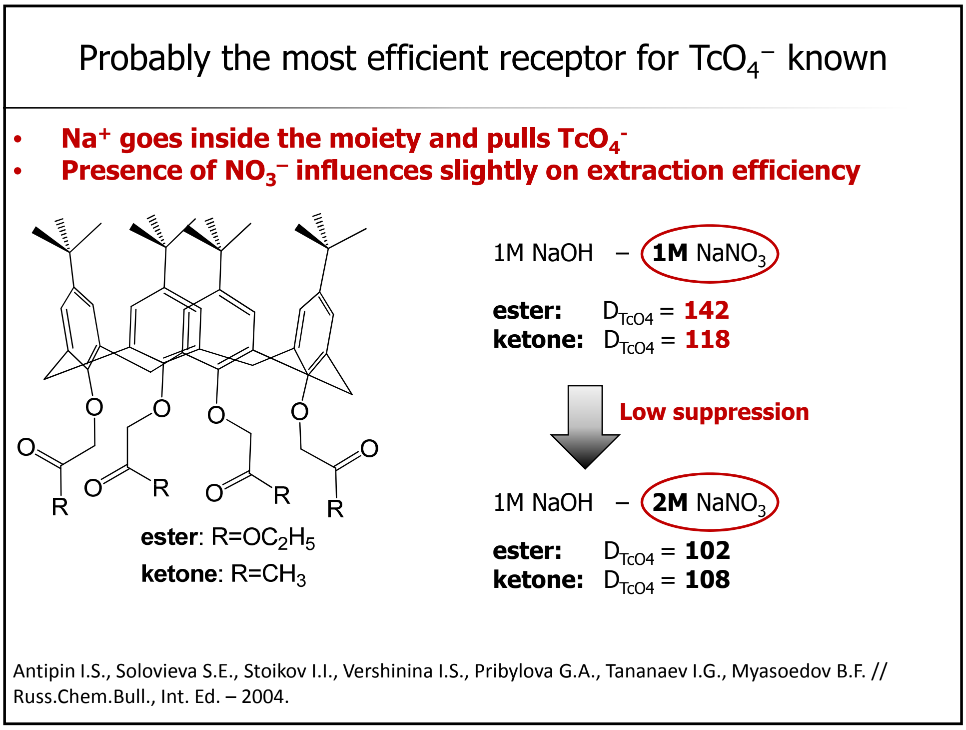

Probably the most efficient receptor for TcO_4^- known

- **Na⁺ goes inside the moiety and pulls TcO_4^-**
- **Presence of NO_3^- influences slightly on extraction efficiency**

1M NaOH – **1M** $NaNO_3$

ester: D_{TcO4} = **142**
ketone: D_{TcO4} = **118**

Low suppression

1M NaOH – **2M** $NaNO_3$

ester: D_{TcO4} = **102**
ketone: D_{TcO4} = **108**

Antipin I.S., Solovieva S.E., Stoikov I.I., Vershinina I.S., Pribylova G.A., Tananaev I.G., Myasoedov B.F. // Russ.Chem.Bull., Int. Ed. – 2004.

Effect of Na$^+$ precoordination is substantial

Na$^+$ coordination with receptor influences greatly:
- **K_a increased**
- **Selectivity improved**

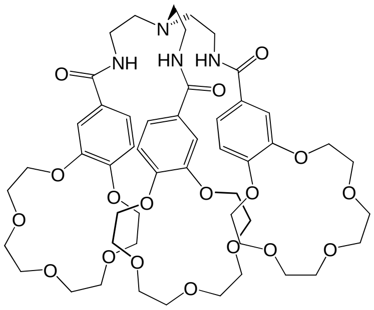

K_a, ^{1}H-NMR in MeCN	**Cl$^-$**	**I$^-$**	**ReO$_4^-$**
	60	30	40

1 eq.: Na$^+$

K_a, ^{1}H-NMR in MeCN	**Cl$^-$**	**I$^-$**	**ReO$_4^-$**
	520	390	**840**

Beer P.D., Hopkins P.K., McKinney J.D. // Chem.Comm. – 1999.

Hydrophobic cavitand with positively charged fragments

- **4$^+$ charge from two ruthenium atoms**
- **Hydrophobic cavity**

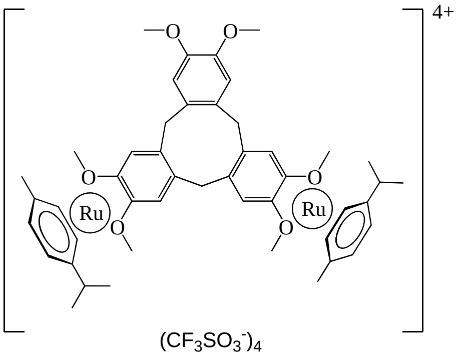

Extraction	**TcO$_4^-$**	**ReO$_4^-$**
0.9% NaCl in H$_2$O	12%	29%
MeNO$_2$	**88%**	**71%**

20 eq.: Cl$^-$, HSO$_4^-$, NO$_3^-$

No suppression

20 eq.: ClO$_4^-$

Extraction	**TcO$_4^-$**	**ReO$_4^-$**
0.9% NaCl in H$_2$O	---	94%
MeNO$_2$	---	**6%**

TcO$_4^-$ > ReO$_4^-$ > ClO$_4^-$ >> NO$_3^-$ > SO$_4^{2-}$ > Cl$^-$

Holman K.T., Halihan M.M., Jurisson S.S., Atwood J.L., Burkhalter R.S., Mitchell A.R., Steed J.W. // J.Am.Chem.Soc. – 1996.

Hydrophobic cavitand with positively charged fragments

- **4^+ charge from two ruthenium atoms**
- **Coordination due to hydrophobic cavity and π interactions**

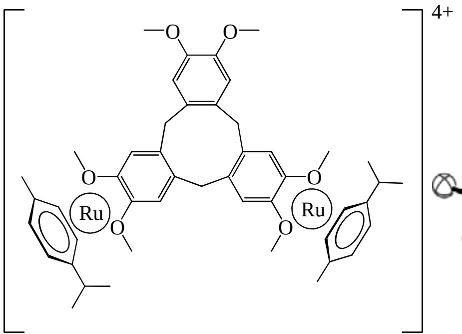

$(ReO_4^-)_3(CF_3SO_3^-)$

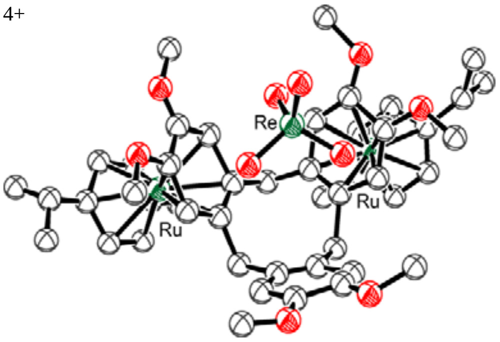

Holman K.T., Halihan M.M., Jurisson S.S., Atwood J.L., Burkhalter R.S., Mitchell A.R., Steed J.W. // J.Am.Chem.Soc. – 1996.

Hydrophobic cavitand with positively charged fragments

- **3^+ charge from three iron atoms**
- **More uniform charge distribution**
- **The same hydrophobicity**

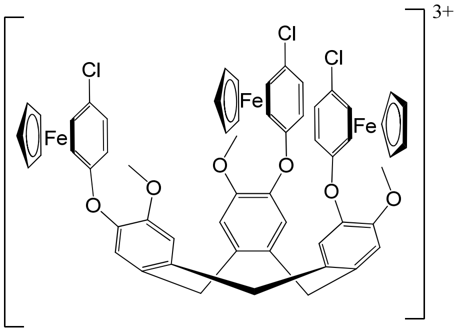

$(PF_6^-)_3$

Extraction	TcO_4^-	ReO_4^-
0.9% NaCl in H_2O	< 10%	< 10%
$MeNO_2$	> 90%	> 90%

20 eq.: Cl^-, HSO_4^-, NO_3^-

No suppression

This receptor is more efficient and more selective than Ru-based predecessor

Gawenis J.A., Holman K.T., Atwood J.L., Jurisson S.S. // Inorg.Chem. – 2002.

C_3-symmetric ligands bind ReO_4^- after protonation

- **Protonation makes the receptor more rigid**
- **ReO_4^- coordinates with amino NH- and benzylic CH-groups**

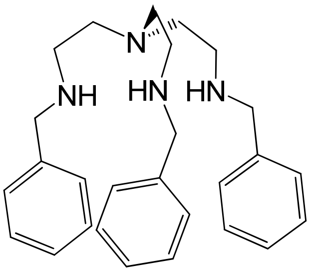

Extraction	TcO_4^-	ReO_4^-
H_2O, pH 5.5	18%	24%
$CHCl_3$	82%	76%

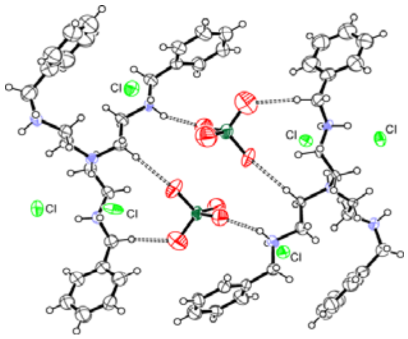

L•$(HReO_4)(HCl)_3$

Antonioli B., Gloe K., Gloe K., Goretzki G., Grotjahn M., Heßke H., Langer M., Lindoy L.F., Mills A.M., Söhnel T. // Z.Anorg.Allg.Chem. – 2004.

C_3-symmetric macrobicycles bind ReO_4^- outside cavity

- **Protonation of receptor is important for strong binding**
- **ReO_4^- coordinates outside the cavity**

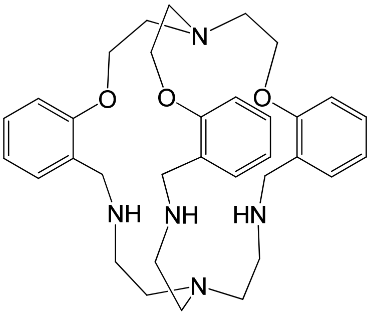

Extraction	TcO_4^-	ReO_4^-
H_2O, pH 7.4	18%	24%
$CHCl_3$	82%	76%

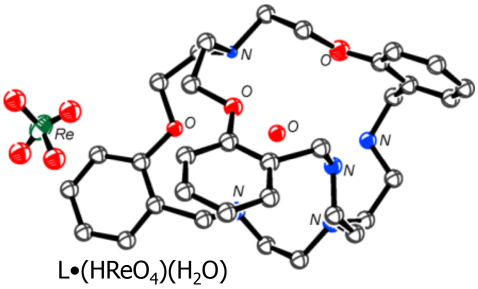

L•$(HReO_4)(H_2O)$

Stephan H., Gloe K., Kraus W., Spies H., Johannsen B., Wichmann K., Chand D.K., Bharadwaj P.K., Muller U., Muller W.M., Vogtle F. In «Fundamentals and applications of anion separations». Ed. by Singh R.P., Moyer B.A. Kluwer: New York; 2004.

C_3-symmetric macrobicycles bind ReO_4^- outside cavity

- **Larger cavity still does not allow TcO_4^- to go inside**
- **More hydrophilic ligand extracts worse**

Extraction	TcO_4^-	ReO_4^-
H_2O, pH 7.4	86%	90%
$CHCl_3$	14%	10%

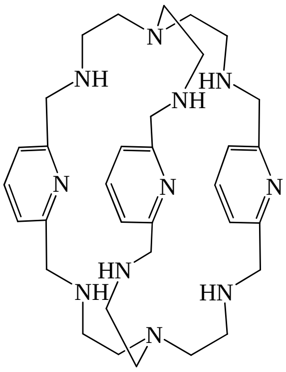

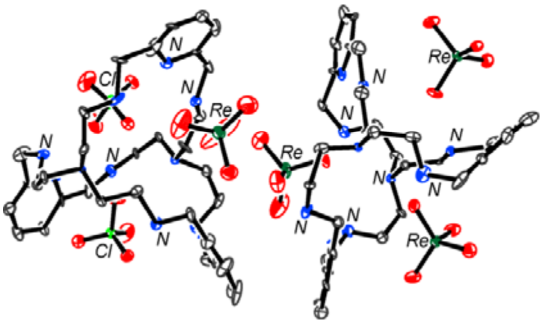

$[L\bullet(HMO_4)_3]_2(H_2O)_3$, M=Cl, Re

It is rational to reduce macrobicycle cavity to macrocyclic

- **Amino groups are protonated but…**
- **Amides coordinate ReO_4^-**

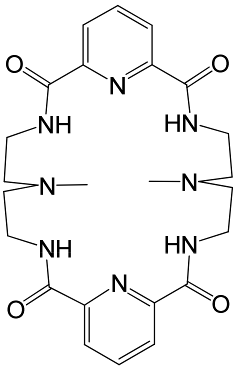

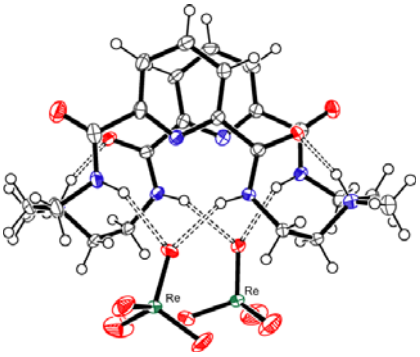

$L\bullet(HReO_4)_2$

Ghosh S., Roehm B., Begum R.A., Kut J., Hossain Md.A., Day V.W., Bowman-James K. // Inorg.Chem. – 2007.

Guanidinium tetraoxidorhenate(VII)

- **Protonated guanidinium bears positive charge**
- **3 oxygens of ReO_4^- are coordinated**

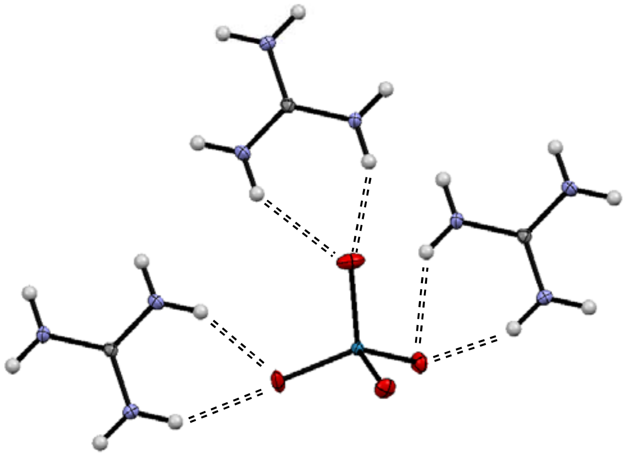

Grigoriev M.S., German K.E., Maruk A.Ya. // Acta Crystallogr., Sect. E. – 2007.

Rigid macrocyclic receptors are promising

- **Two positive charges, three H-bonds for each ReO_4^-**
- **Rigid planar macrocyclic core**

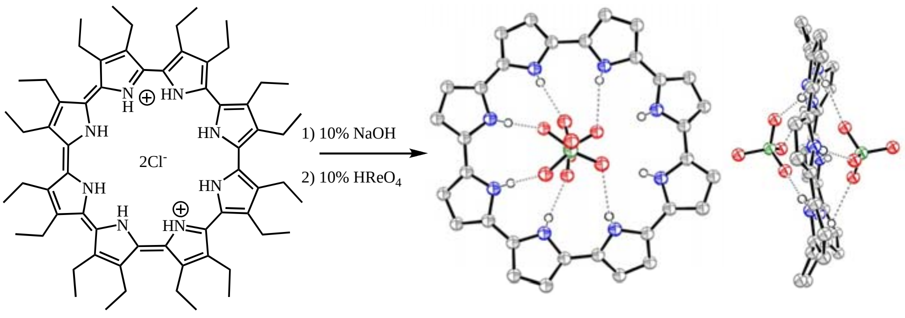

K_a, ^1H-NMR in MeCN	$H_2PO_4^-$	HSO_4^-	OAc^-	NO_3^-	I^-	ReO_4^-	TcO_4^-
	9.7	6.5	6.7	9.8	**5.0**	**5.9**	**6.0**

Seidel D., Lynch V., Sessler J.L. // Angew.Chem.Int.Ed. – 2002.
Kolesnikov G. PhD Thesis. 2011.

$HReO_4$ as a good template for macrocycle synthesis

- **Chloride is small and volatile, anything suits**
- **ReO_4^- is highly complementary to the rigid macrocyclic core**

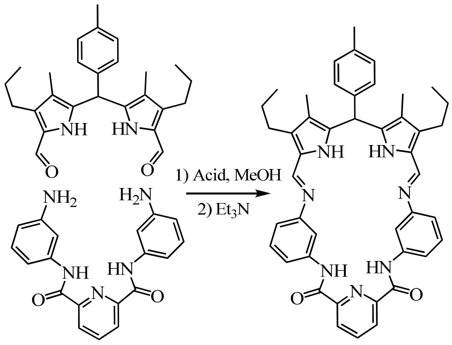

	Product	
Acid-template	**[1+1]**	**[2+2]**
H_3PO_4	+	+
H_2SO_4	+	+
HCl	+	−
$HReO_4$	+	−

	$H_2PO_4^-$	HSO_4^-	Cl^-	NO_3^-	I^-	ReO_4^-	TcO_4^-
K_a, UV in DMSO	3.7	3.8	3.9	3.0	**5.3**	**4.8**	**5.1**

Kolesnikov G.V., German K.E, Kirakosyan G., Tananaev I.G., Ustynyuk Yu.A., Khrustalev V.N., Katayev E.A. // Org.Biomol.Chem. - 2011.

$HReO_4$ as a good template for macrocycle synthesis

- **Two positive charges due to protonated imine fragments**
- **Pyrrolic and amide H-bonds bind each ReO_4^-**

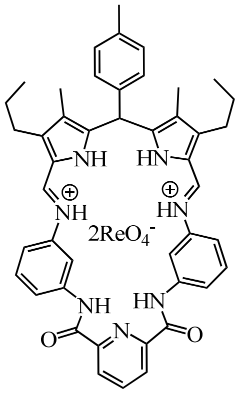

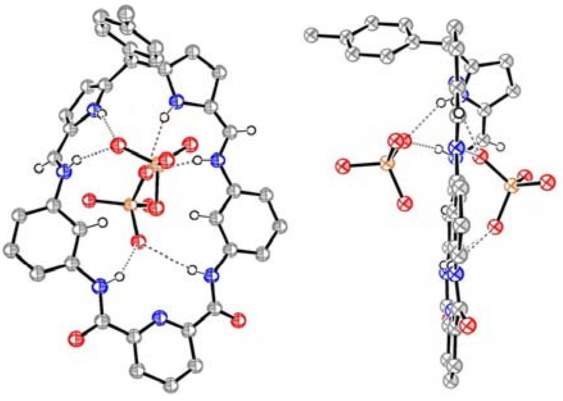

Kolesnikov G.V., German K.E, Kirakosyan G., Tananaev I.G., Ustynyuk Yu.A., Khrustalev V.N., Katayev E.A. // Org.Biomol.Chem. - 2011.

^{99}Tc-NMR titration, Bu_4N^+ $^{99}TcO_4^-$ in $CDCl_3$

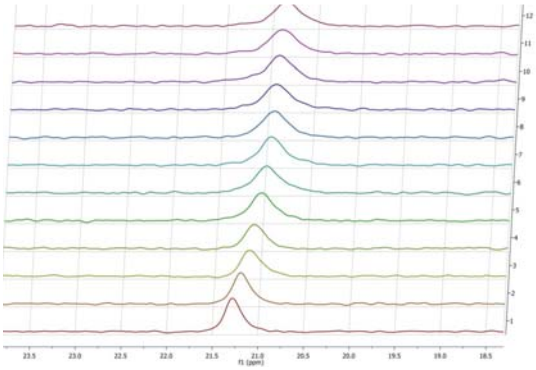

^{99}Tc-NMR strengths

- Clear signal
- Good correlation with UV

	^{99}Tc ЯМР, $CDCl_3$	**UV, dichloroethane**
Imine-amide macrocycle	log(β_{11}) = 3.2	log(β_{11}) = 5.1
Cyclo[8]pyrrole·2(HCl)	log(β_{12}) = 3.8	log(β_{12}) = 6.0

Kolesnikov G.V., German K.E, Kirakosyan G., Tananaev I.G., Ustynyuk Yu.A., Khrustalev V.N., Katayev E.A. // Org.Biomol.Chem. - 2011.

Dendrimers are efficient but not selective

- **Larger dendrimer and lower pH, lead to better extraction**

pH	Anion	2ndGEN-C_6H_{13}	2ndGEN-$C_{12}H_{25}$		3ndGEN-C_6H_{13}	2ndGEN-$C_{12}H_{25}$
7.4	ReO_4^-	38%	36%	➡	84%	74%
	TcO_4^-	48%	46%		90%	83%
5.4	ReO_4^-	92%	91%		98%	97%
	TcO_4^-	96%	95%		99%	99%

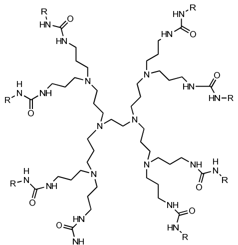

2ndGEN, R = C_6H_{13}
2ndGEN, R = $C_{12}H_{25}$

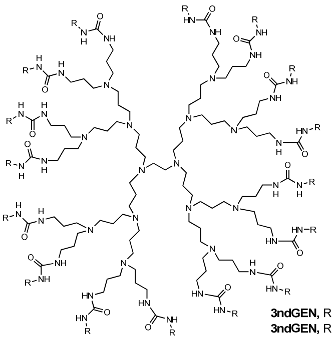

3ndGEN, R=C_6H_{13}
3ndGEN, R=$C_{12}H_{25}$

Stephan H., Spies H., Johannsen B., Klein L., Vögtle F. // Chem.Comm. – 1999.

The nature of the filler influences the extraction

- **More hydrophobic filler is more efficient**

Sorbent	Functional groups	Degree of extraction, %		
		0,1 M HNO_3	0,1 M $NaNO_3$	0,1 M NaOH
AV-17	NR_4	**92**	**91**	**91**
AN-31	NHR_2 + NR_3	88	61	23
POLYORGS-17	1,(3)5-dimethylpyrazole	**96**	**98**	**96**
POLYORGS-33	Hydrazidine+Amidoxime	67	20	6
POLYORGS-35	Hydrazidine	79	9	0

N.N. Popova, I.G. Tananaev, G.V. Myasoedova, B.F. Myasoedov
7-th International Symposium on Technetium and Rhenium – 2011.

ISIDA property prediction WEB server
infochim.u-strasbg.fr/webserv/VSEngine.html

Name	Log P
$NOct_3$	9.50
$NOct_4$	8.44
NBu_3	4.16
NH_2Oct_2	2.77
$NHBu_2$	2.45
NBu_4	1.32
$NHBu_3$	0.66
1,5 pyrazole	0.60
1,3 pyrazole	0.53
NH_2Bu_2	-0.79
Me-amidoxyme	-0.96
H-amidoxyme	-1.01
Hydrazine	-1.03
NEt4	-2.54

Some important rules for hunting the TcO_4^- and ReO_4^-

Receptor property		*Binding*	*Selectivity*
Bigger size	=>	better	better
More (+) charge	=>	better	worse
More hydrophobic cavity	=>	better	better
Excess of H-bond groups	=>	no clear answer	
Harder to synthesize	=>	usually better	

Thank you for your kind attention!

Weak Interactions - Actinides

D. Meyer, J.F. Dufrêche, T. Zemb

ICSM CEA CNRS

Introduction

Chemistry of Systems
- Examples (Liquid-Liquid system, mulstiscale matter)

The Weak forces

Actinides

Chemistry: Art of Changing, Tuning the Matter

High Temperature Chemistry
Metallurgy
Glass
Ceramics

Controlling more and more
weaker interactions

Low Temperature Chemistry
Minerals, elements, Metal complexes, extraction chemistry

19th Century
Inorganic, Organic Chemitry

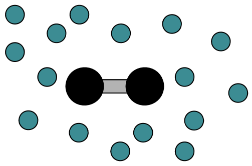

20th Century
Modern Biochemistry
Polymers

20th-21th Century
Supramolecular Chemistry

Physical Description of soft Matter and weak interactions

Thermodynamics:
Decreasing of the internal Energy cutoff

Main Considerations – Approaches CHEMISTRY OF SYSTEMS

Properties <->
Energy Grid
of the interactions

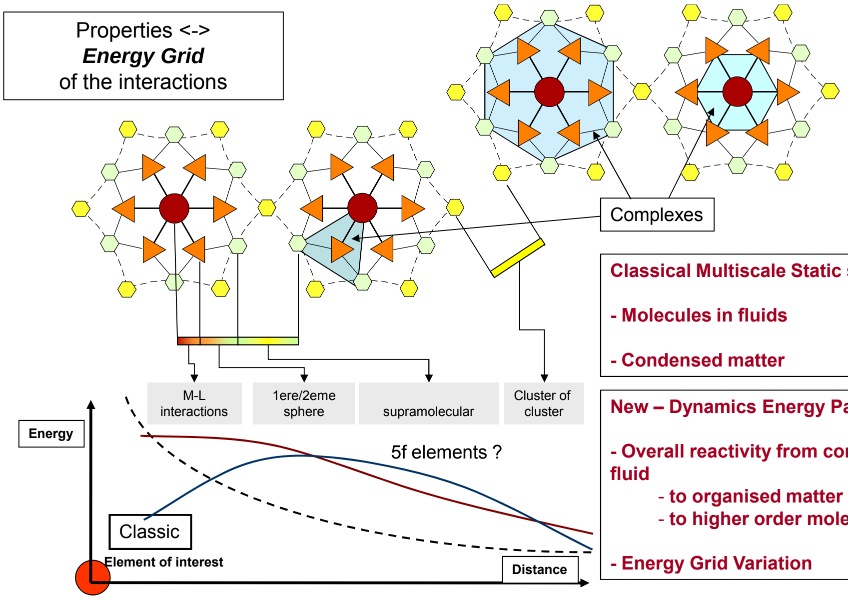

Classical Multiscale Static structure

- Molecules in fluids

- Condensed matter

New – Dynamics Energy Pattern

- Overall reactivity from complex fluid
  - **to organised matter**
  - **to higher order molecules**

- Energy Grid Variation

Reactivity of SYSTEMS: Mesoporous systems

Organisation in solution

Add-ons in solution

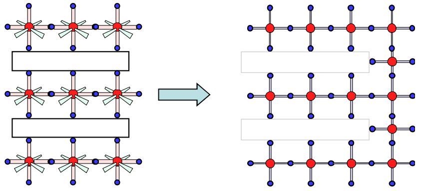

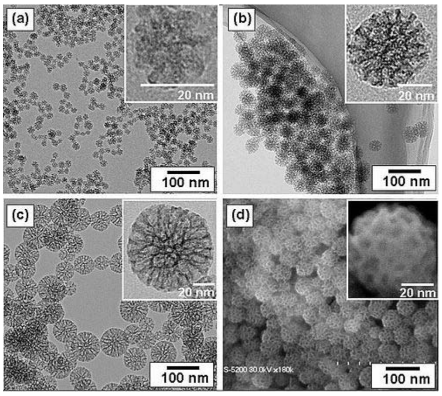

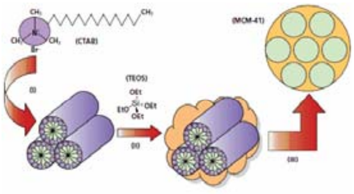

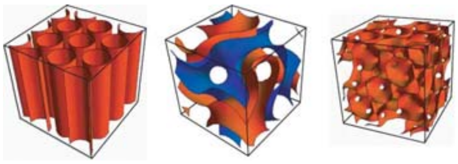

Synthesis of Mesoporous Materials
Material Matters 2008, 3.1, 17.

Reactivity of SYSTEMS : From Biology

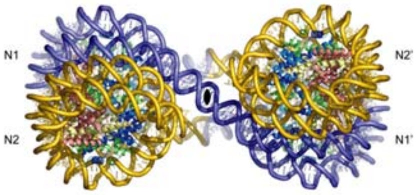

chromatin remodeling
Prof. Dr. Timothy J. Richmond,
Institute of Molecular Biology and Biophysics,
ETH Zurich

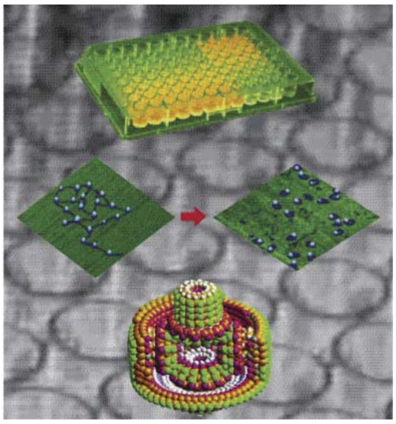

The formation of supramolecular DNA circles (scanning force microscopy image, center right) from oligomeric DNA-protein conjugates (center left). Applications of the nanostructured DNA-protein conjugates in the life sciences are represented by the microtiter plate at the top and the potential nanotechnology uses are symbolized by the model at the bottom.
Functional devices from DNA and proteins
Christof M. Niemeyer , Nano Today Volume 2, Issue 2, April 2007, Pages 42–52

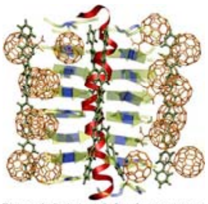

This supramolecular structure in the form of a porous sensor was designed to model a class of bio-organic macromolecules. In 2005, a publication based on work performed in this field at the Section of Chemistry and Biochemistry received the Oscar of the Chemical Abstracts Service as the article most consulted by the international scientific community.

Colloids and biomolecule assembly
University of Geneve

Liquid-Liquid Separation Problematics

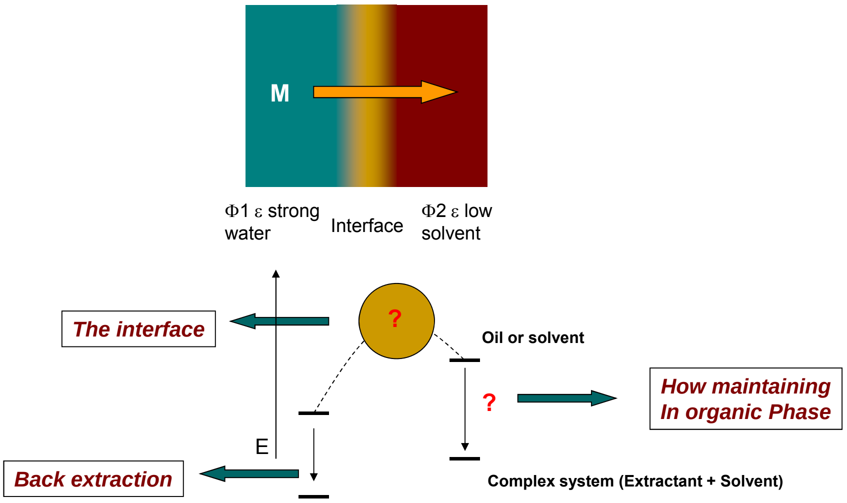
M

Φ1 ε strong
water

Interface

Φ2 ε low
solvent

The interface

?

Oil or solvent

?

***How maintaining
In organic Phase***

E

Back extraction

Complex system (Extractant + Solvent)

The interface: A dynamical problem, kinetic consideration

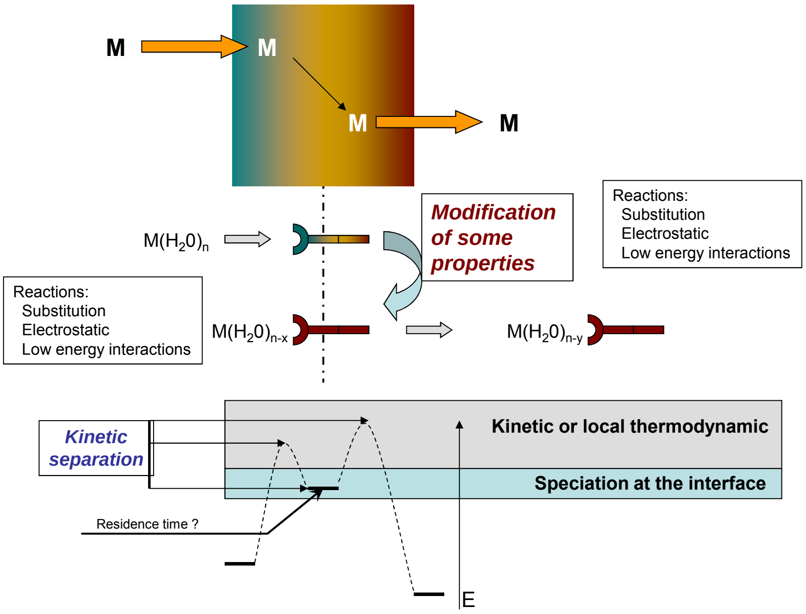
M

M

M

M

$M(H_{2}0)_{n}$

***Modification
of some
properties***

Reactions:
Substitution
Electrostatic
Low energy interactions

Reactions:
Substitution
Electrostatic
Low energy interactions

$M(H_{2}0)_{n-x}$

$M(H_{2}0)_{n-y}$

***Kinetic
separation***

Kinetic or local thermodynamic

Speciation at the interface

Residence time ?

E

The organic phase: a complex fluid

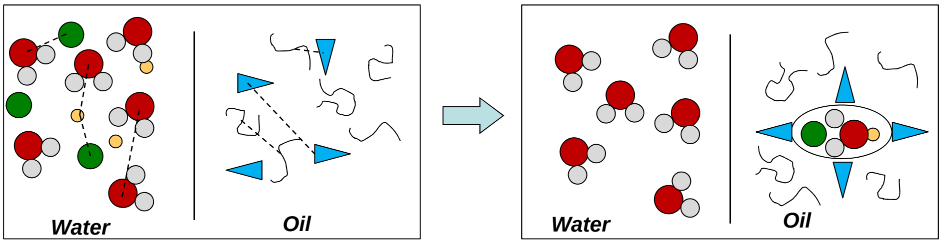

Maintaining in organic phase

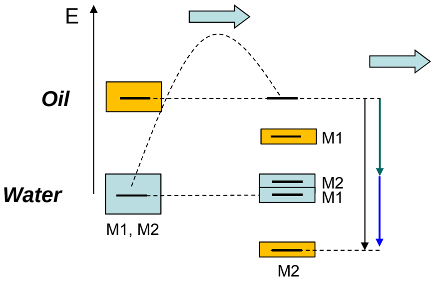

- Complexation
- ionic bonding
- Weak Interactions

Thermodynamic separation

Clear the
internal (enthalpy)
vs
external (enthropy)
Energies

=> DEFINING the ELEMENTAL PARTICLE

The Weak Interactions : 4 forces (T .Zemb)

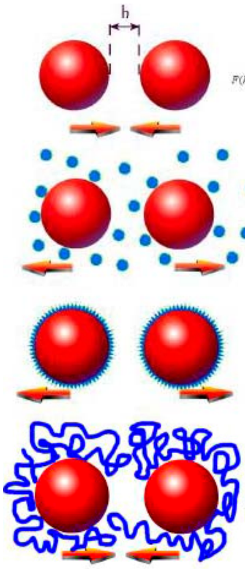

DISPERSION

$$F(h) \approx \frac{1}{12}\left(\frac{3kT}{4}\left(\frac{\varepsilon_1-\varepsilon_2}{\varepsilon_1+\varepsilon_2}\right)^2+\frac{3\hbar}{4\pi}\int_{\omega_k}^{\infty}\left(\frac{\varepsilon_1-\varepsilon_2}{\varepsilon_1+\varepsilon_2}\right)^2 d\omega\right)\frac{1}{(h+R_1+R_2)^2}$$

ELECTROSTATIC

$$F(h) = 64\pi\left(kT/_{\kappa}\right)Rc*\gamma^2.\exp(-\kappa h)$$

"HYDRATION"

$$F(h) = F_{cont}.\exp\left(-\,h/_{\langle H_2O\rangle}\right)$$

DEPLETION

$$F(h) \approx S.(\rho.kT);\quad 0 < \mathrm{h} < \mathrm{gyr.\ rad.}$$

« Complexation » is considered in the supra-molecular part

R G French and V A Parsegian, Rev Mod. Phys. 2010 2010, 82, 1887.

Electrostatic interaction

Forces between 2 particles with the same charge

- Globally repulsive
- Depending on the small ions

Mean force over all small ions configurations

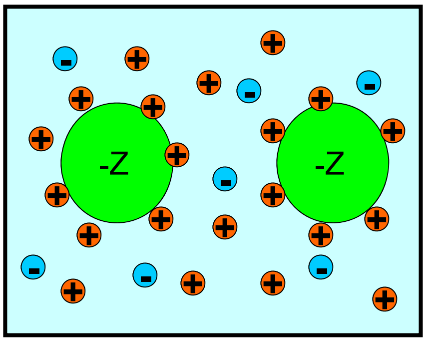

Electrostatic interaction

Calculation

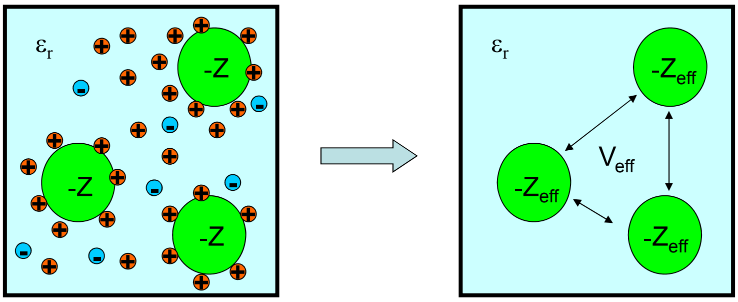

Theory of the Double Diffusion Layer around each particle

Debye Lenght $L_D=\kappa^{-1}$ size of the layer, dépending on the concentration of small ions

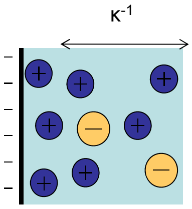

Electrostatic interaction: Description

Force électrostatique : bilan

$$V_{\text{élec}}(r) = V_{\text{DLVO}}(r) = \frac{Z_{\text{DLVO}}^2 e^2}{4\pi\varepsilon_0\varepsilon_r}\frac{e^{-\kappa r}}{r} \quad \text{avec} \quad Z_{\text{DLVO}} = Z_{eff}\frac{\exp(\kappa R)}{1+\kappa R}$$

☞ exp(-κr)/r au lieu de 1/r

☞electrostatic Shielding

☞ Repulsive force

☞ Zeff Effective charge (different from Z)

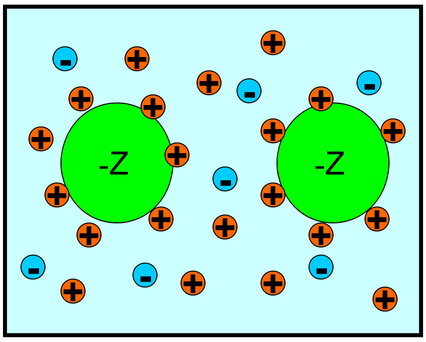

Approximation:
Direct Addition ionic atmosphere $r >> \kappa^{-1}$

Van der Waals forces

Forces between two (macro)-particules identical charges

☞Van der Waals forces

$$\begin{aligned} V^{VdW}(r) &= -\frac{A}{6}\left[\frac{2R^2}{r^2-4R^2}+\frac{2R^2}{r^2}-\ln\frac{r^2}{r^2-4R^2}\right] \\ &= -\frac{16}{9}A\left(\frac{R}{r}\right)^6 \quad \text{si} \quad r >> r \end{aligned}$$

A > 0
Attractive Interaction

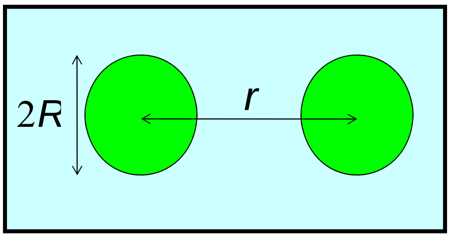

Van der Waals

Johannes Diderik van der Waals
(1837-1923)

1873
Attractive forces exist
between atomes and molecules

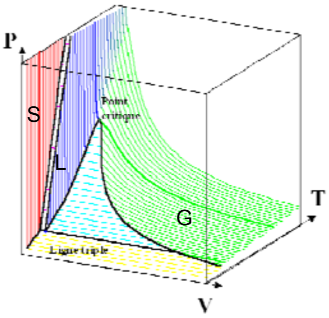

Liquid – Gaz separation

$$\left(P+\frac{A}{V^2}\right)(V-b)=kT$$

Van der Waals interactions

Keesom
Mobil dipole/
Mobil dipole

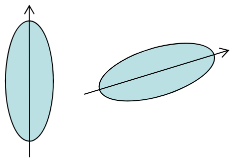

$$V(r)=-\frac{p_1^{\,2}p_2^{\,2}}{3(4\pi\varepsilon_0)^2kTr^6}$$

< kT (weak)

Debye
Mobil dipole /
Induced dipole

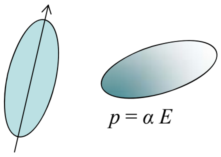

$$V(r)=-\frac{p_1^{\,2}\alpha_2}{(4\pi\varepsilon_0)^2r^6}$$

< kT (weak)

London
Induced dipole/
Induced dipole

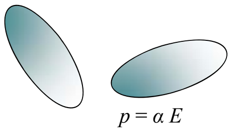

$$V(r)=-\frac{3h\nu\alpha^2}{(4\pi\varepsilon_0)^2r^6}$$

$I=h\nu$

≈ kT

In the presence of ion

Ion /
Mobile dipole

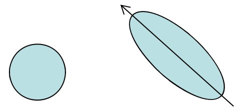

$$V(r) = -\frac{Q_1^2 p_2^2}{6(4\pi\varepsilon_0)^2 kTr^4}$$

≈ kT

Ion /
Induced dipole

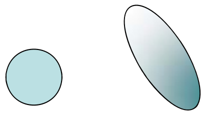

$p = \alpha E$

$$V(r) = -\frac{Q_1^2 \alpha_2}{2(4\pi\varepsilon_0)^2 r^4}$$

≈ kT

Ion/
Ion

$p = \alpha E$

$$V(r) = \frac{Q_1 Q_2}{4\pi\varepsilon_0 r} + \frac{Q_1^2 \alpha_2 + Q_2^2 \alpha_1}{2(4\pi\varepsilon_0)^2 r^4}$$

≈ kT

London Forces : Steric Hindrance

Classical Molecular modelling and dynamics

London Forces (Induces dipoles) => Steric Hindrance

$$V_{ij} = 4\varepsilon_{ij}\left[\left(\frac{\sigma_{ij}}{r_{ij}}\right)^{12} - \left(\frac{\sigma_{ij}}{r_{ij}}\right)^{6}\right]$$

Lorentz-Berthelot rules

$$\begin{cases} \sigma_{ij} = (\sigma_i + \sigma_j)/2 \\ \varepsilon_{ij} = \sqrt{\varepsilon_i \varepsilon_j} \end{cases}$$

Interaction atome/atome

(means site/site)

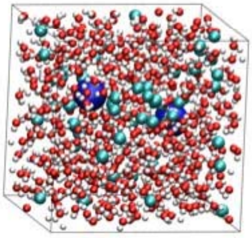

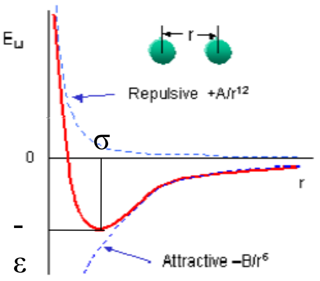

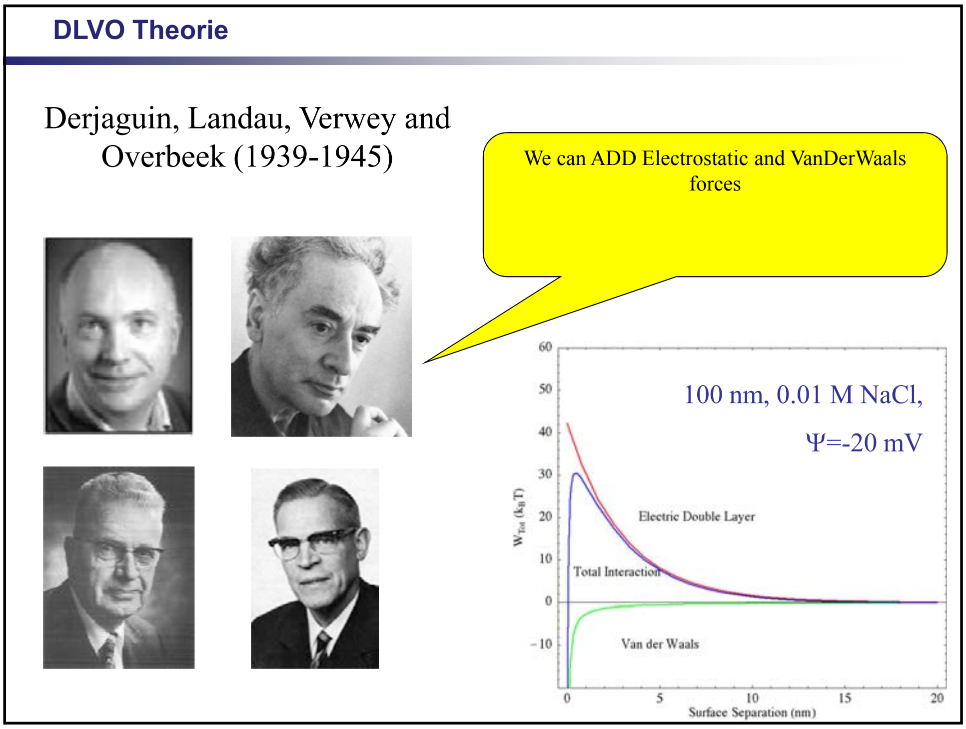

DLVO Theorie

Derjaguin, Landau, Verwey and Overbeek (1939-1945)

We can ADD Electrostatic and VanDerWaals forces

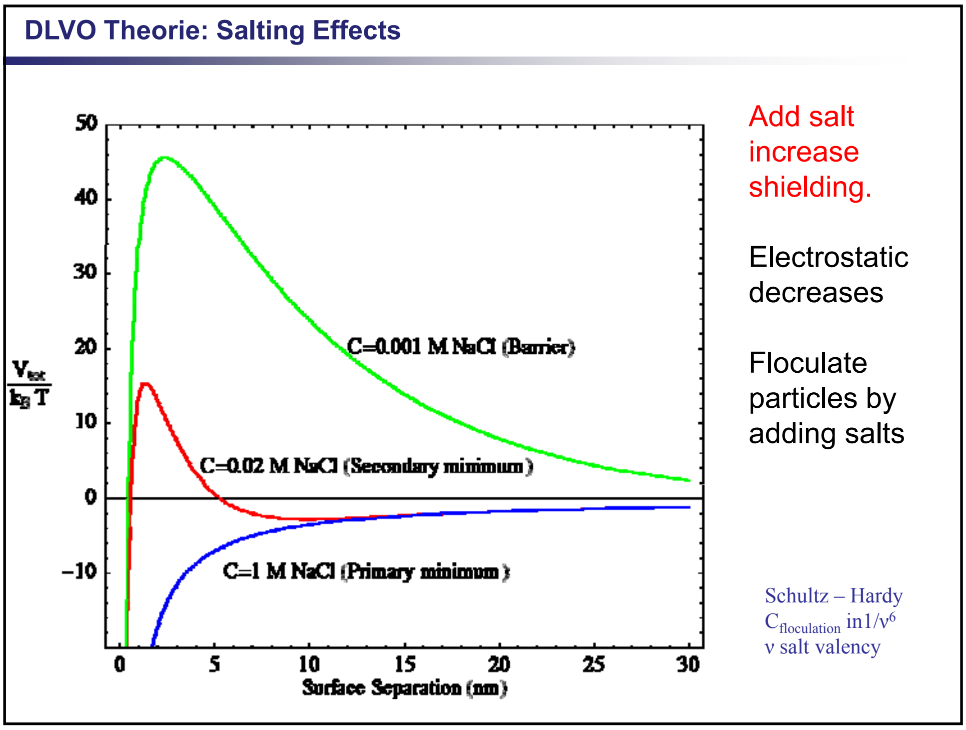

DLVO Theorie: Salting Effects

Add salt increase shielding.

Electrostatic decreases

Floculate particles by adding salts

Schultz – Hardy
$C_{floculation}$ in $1/\nu^6$
ν salt valency

Solvent and Depletion : Micelles considerations

Amphiphilic Molecule

Hydrophobic Tail/ Hydrophilic Head

Who looks like the same goes togeteher…

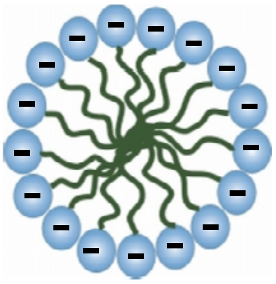

Be careful Strong Electrostatic Repulsion !

Something is missing…

Role of the Solvent

Cannot be neglected in some cases

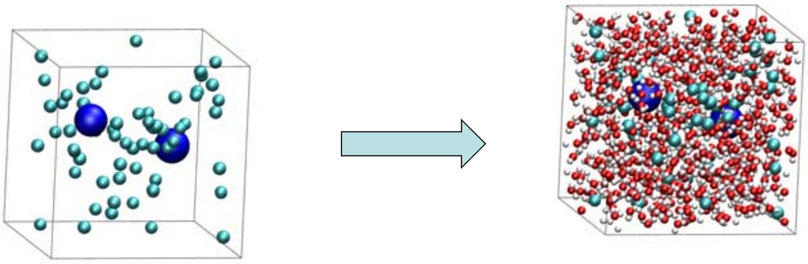

Solvent interaction cannot be described by a continuum in some cases

Take into account the **Entropy of the solvent**

Depletion Phenomena

Mixing small and big spheres

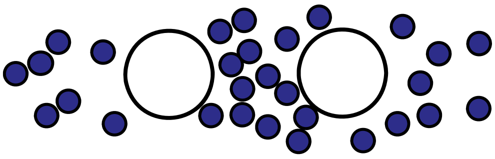

- Hard Big Sphere (colloides)
- Hard Small Sphere (polymer)

Usually this system is repulsive but …. It's attractive

Possible Interpretation is:

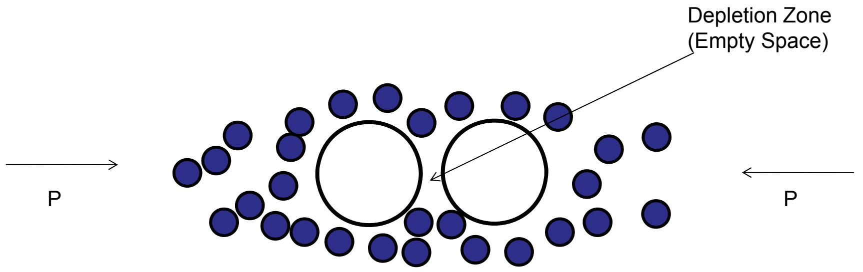

Depletion Phenomena

Statistical thermodynamics

Potentiel of Asakura et Oosawa

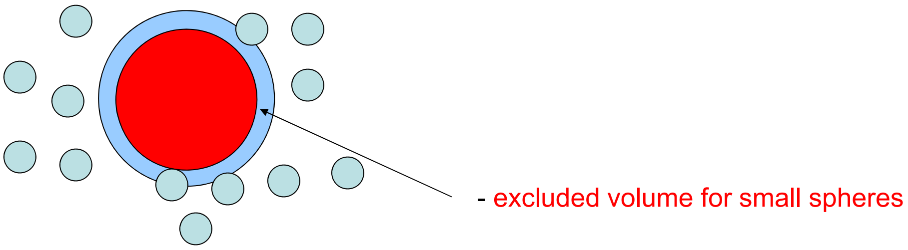

2 Close colloids

- Overlapping of excluded volumes
- no space for small spheres
- entropy increses

⇨attraction

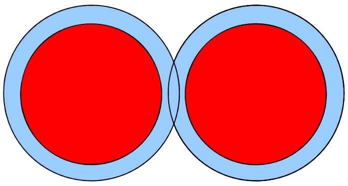

Depletion Phenomena

Statistical thermodynamics

Potentiel of Asakura et Oosawa

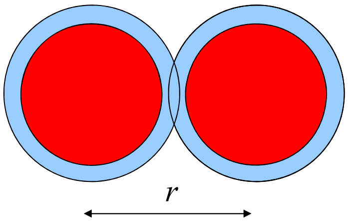

$$Z = \int dr \int dr^N e^{-\beta V}$$

$$= \int dr \int dr^N (V - V_{exclu})^N$$

$$F(x) = -kT \ln Z = F^{id} + V_{eff}(r)$$

D' où :

$$V_{eff}(r)/kT = \rho \frac{\pi D^3}{6}\left(1 - \frac{3r}{2D} + \frac{r^3}{2D^3}\right)$$

$$2R \quad < \quad r \quad < \quad 2R + \sigma = D$$

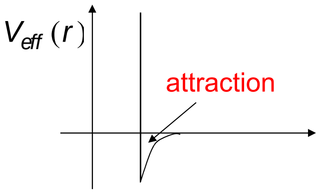

Effective Potential

Mean potential over Solvent configurations

Practical Aspects of Depletion

Phase séparation

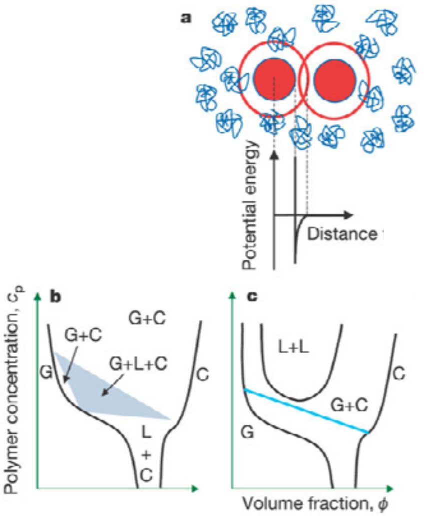

Nature, **416**, 801 (2002)

Direct measure

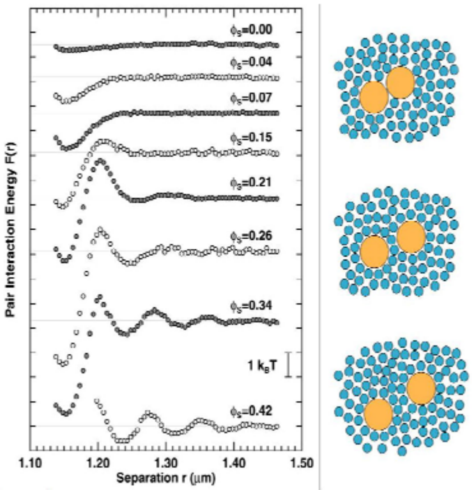

Phys. Rev. Lett., **81**, 4004 (1998)

Oscillation comes from non continu solvent : Entropy Driven

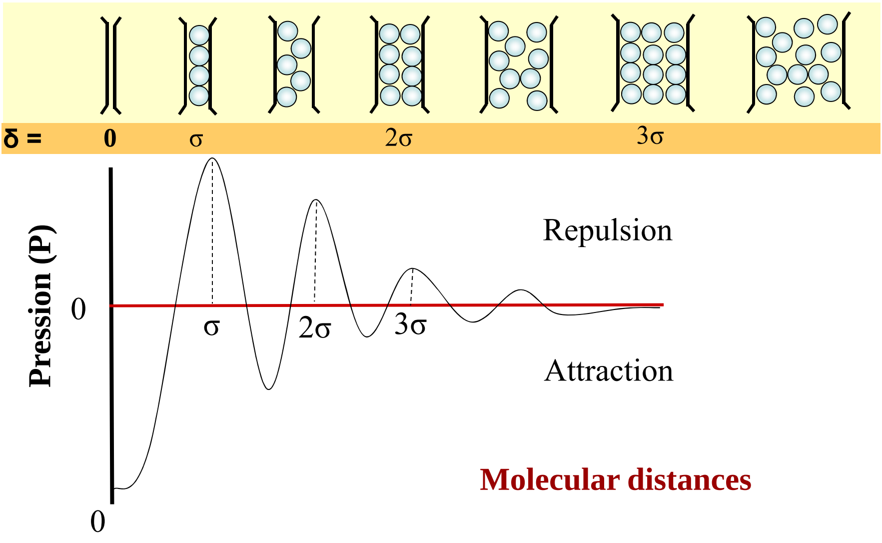

δ = distance

Actinides

Electronic Specificity

Chemistry
Physics

- orbitals 5f
- électrons 5f

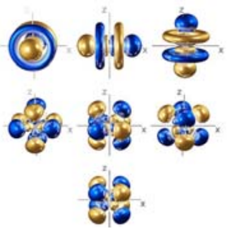

5f orbitals

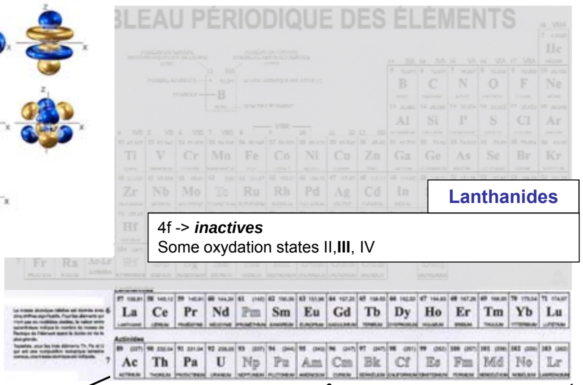

Lanthanides

4f -> ***inactives***
Some oxydation states II,**III**, IV

Light Actinides

Orbitales 5f ***actives***
Electrons 5f ***delocalised***
High number of oxidation states **III, IV, V, VI, VII**

Heavy Actinides

Orbitales 5f ***inactives***
Electrons 5f ***localised***
Quelques degrés d'oxydation **III**, IV

Actinides specificity

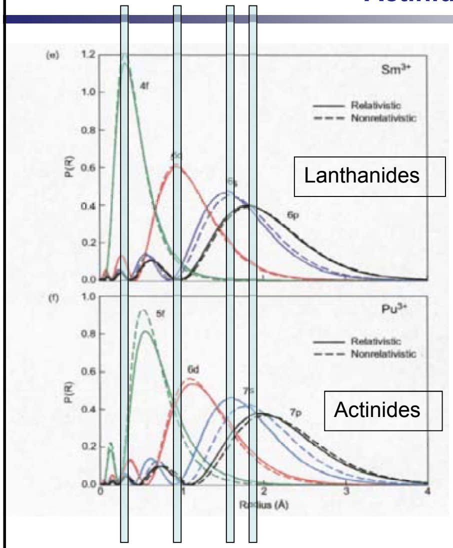

Lanthanides

Actinides

- Orbitals expension f **et d**
- Relativistic effects f et p

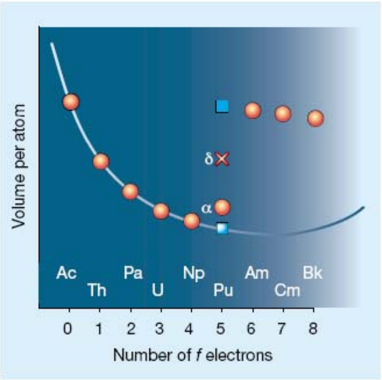

Metallic state

Actinides and condensed metallic matter

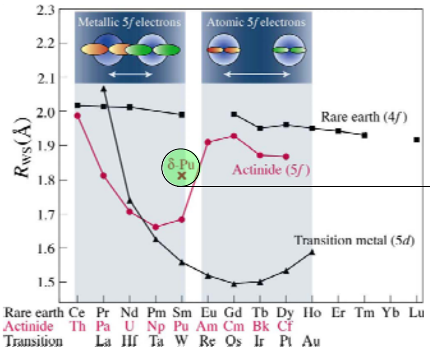

5f electrons are « semi-délocalised »
Freezed Phase transition
Conductor > semi-conductor
Puzzle du Plutonium

Plutonium: Condensed-Matter Physics
A survey of theory and experiment
Michael Boring and James L. Smith
***Los Alamos Science* Number 26 2000**

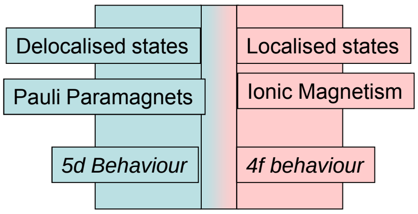

Delocalised states
Pauli Paramagnets
5d Behaviour

Localised states
Ionic Magnetism
4f behaviour

- Review of Modern Physics, vol 81, jan-march 2009
-Nature, vol 410,,759, 2001

-J. Alloys and Compounds,,444-445 (2007), 142-144

-Quantum Criticality, Physics Today, feb 2011,29.

General Coordination Chemistry (Most Common)

High Oxidation states (V et VI)

5-coordinate (2 + 3)	**6-coordinate (2 + 4)**	**7-coordinate (2 + 5)**	**8-coordinate (2 + 6)**
$[UO_2\{N(SiMe_3)_2\}_3]^-$	$Cs_2[UO_2Cl_4]$	UO_2Cl_2	UO_2F_2
	$(Me_4N)_2[UO_2Br_4]$	UO_2(superphthalo)	UO_2CO_3
	$MgUO_4$	$[UO_2(NO_3)_2(Ph_3PO)]$	$[UO_2(NO_3)_2(H_2O)_2]$
	$BaUO_4$	$[UO_2(L)_5]^{2+}$	$CaUO_4$
		(L,H2O, DMSO, urea)	$SrUO_4$
			$Rb[UO_2(NO_3)_3]$

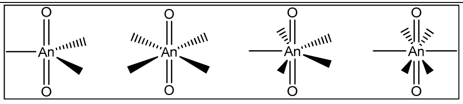

Low Oxidation states (III et IV)

Formula	**Thorium species present**	**Coord. No.**
$MTh(NO_3)_6$ (M = Mg, Ca)	$[Th(NO_3)_6]2^-$	12
$Ph_4P+ [Th(NO_3)_5(OPMe_3)_2]^-$	$[Th(NO_3)_5(OPMe_3)_2]^-$	12
$Th(NO_3)4.5H_2O$	$\mathbf{[Th(NO_3)_4(H_2O)_3]}$	**11**
$Th(NO_3)_4.2.67Me_3PO$	$\{[Th(NO_3)_3(Me_3PO)_4]^+\}_2\ [Th(NO_3)_6]^{2-}$	10, 12
$Th(NO_3)_4.2Ph_3PO$	$\mathbf{[Th(NO_3)_4(OPPh_3)_2]}$	**10**
$Th(NO_3)_4.5Me_3PO$	$[Th(NO_3)_2(OPMe_3)_5]^{2+}$	9

Structure of $Th(NO_3)_4(H_2O)_3$.

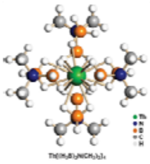

$Th[(H_3B)_2N(CH_3)_2]_4$

Lanthanide and Actinide Chemistry, Simon Cotton, Wiley 2006.

Actinyl Moity

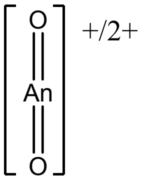

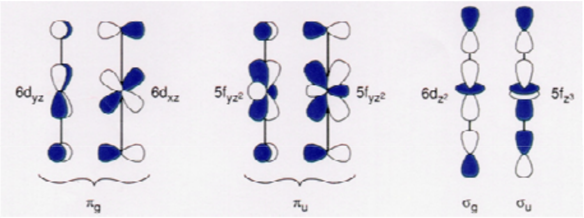

Complex ion
Multipolar

Molecular Orbitals => Boning An-O is covalent
An(5f, 6d) + O(2p)

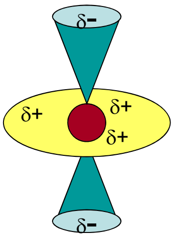

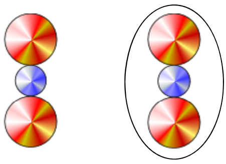

UO_2^{2+}
U CN 7
O CN 3

UO_2^{+}
U CN 7
O CN 3

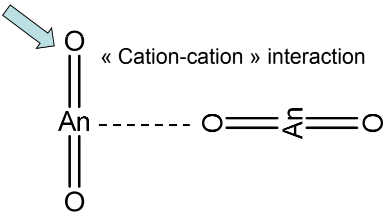

« Cation-cation » interaction

R_{SP1976}(UVI)=81 pm
R_{SP1976}(UV)=84 pm

Redox Potentials

	Th	U	Np	Pu	Am	Cm
M^{3+}/M		*-1.8*	*-1.79*	*-2.03*	*-2.32*	
M^{4+}/M	*-1.83*	*-1.38*	*-1.3*	*-1.25*	*-0.9*	
M^{4+}/M^{3+}	**-3.7**	**-0.63**	0.15	0.98	**2.3**	**3.1**
MO_2^{2+}/M^{4+}		0.32	0.94	1.04		
MO_2^{2+}/M^{3+}			0.68	1.03	**1.69**	
MO_2^{+}/M^{4+}		0.58	0.74	1.17	1.04	
MO_2^{+}/M^{3+}			0.45		**1.74**	
MO_2^{2+}/MO_2^{+}		0.06	1.14	0.91	1.6	

Formal redox Potentials (V) 25° C, 1M $HClO_4$

Advanced inorganic Chemistry, Cotton et Wilkinson, 5^{ed}.

Differences U(III) Ce(III) Electron 5f vs 4f

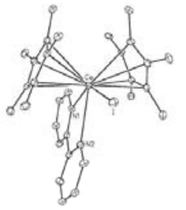

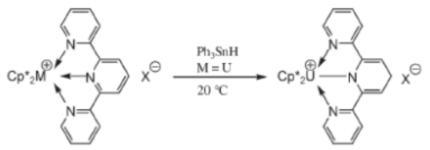

[(Cp)$_2$M(III)Terpy]+
M=Ce et U
Diff of M-N distance 0.2A

Reaction with Ph$_3$SnH
(Goves H radicals)

Only with U

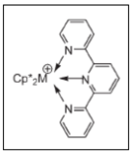

[(Cp)$_2$M(III)Terpy]$^+$

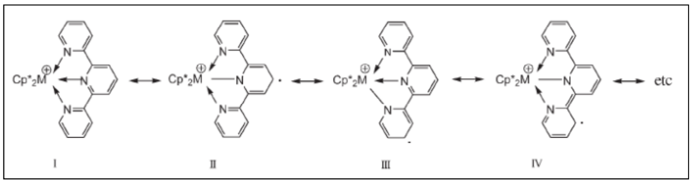

Better Described as [(Cp)$_2$U(IV)Terpy $^{\cdot -}$]$^+$

T. Mehdoui, J. C. Berthet, P. Thuery, L. Salmon, E. Riviere and M. Ephritikhine, *Chem.–Eur. J.*, 2005, **11**, 6994

Th(III) Electronic configuration

X-ray structure

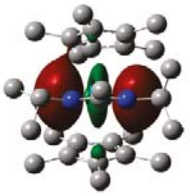

6d Orbirtal

TD-DFT

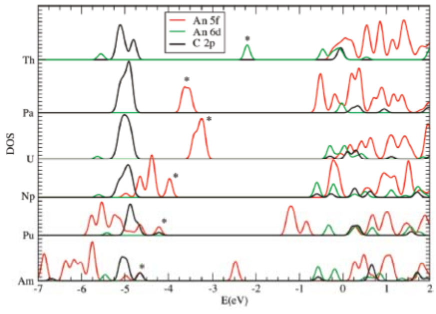

6d1
Rather then
5f1

Inorg. Chem. 2010, 49, 10007–10012

4f 5f - Micro and Nano

4f Coordination Polymer

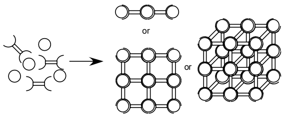

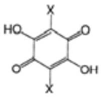

+ Zr(IV) / THF, anhydre
or
+ Ln(III) / An(III) aqueux
or
+ Nd/Gd / aqueux

(Ln=Eu, Nd, Gd,
An = U, Th, Pu, Am)

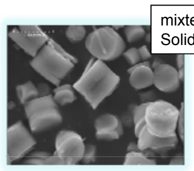

mixte M1/M2
Solid Solution

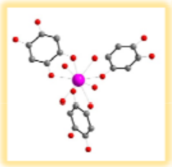

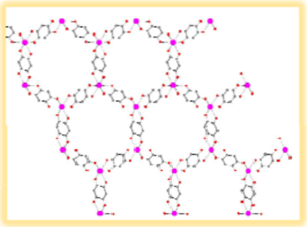

2D network coming from strong interactions

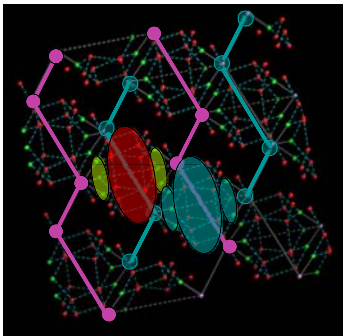

3eme dimension, weaker interactions

Micrometric scale: Weak interactions and the crystal over-structure

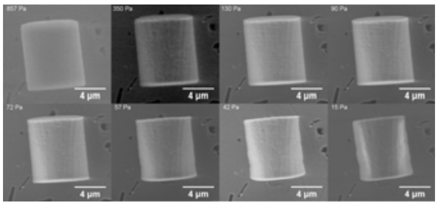

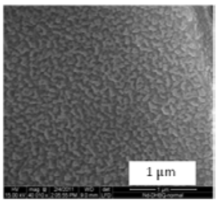

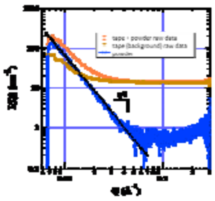

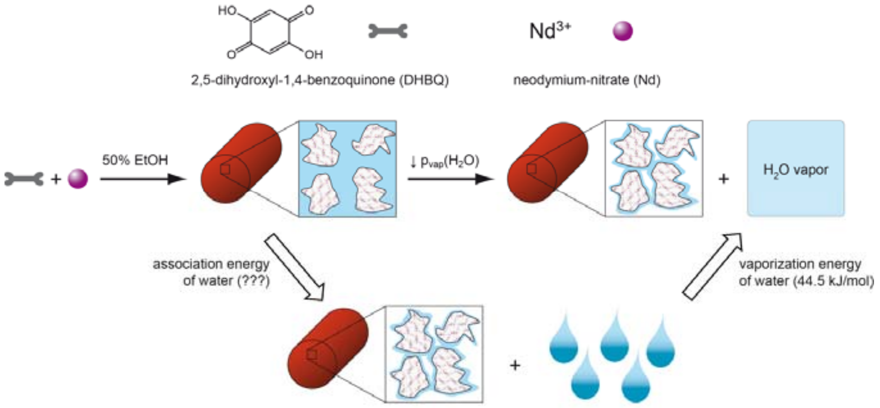

2,5-dihydroxyl-1,4-benzoquinone (DHBQ)

Nd^{3+}

neodymium-nitrate (Nd)

50% EtOH

↓ $p_{vap}(H_2O)$

+

H_2O vapor

association energy of water (???)

vaporization energy of water (44.5 kJ/mol)

+

Micrometric : Morphology controlled by Kinetics of weak interactions

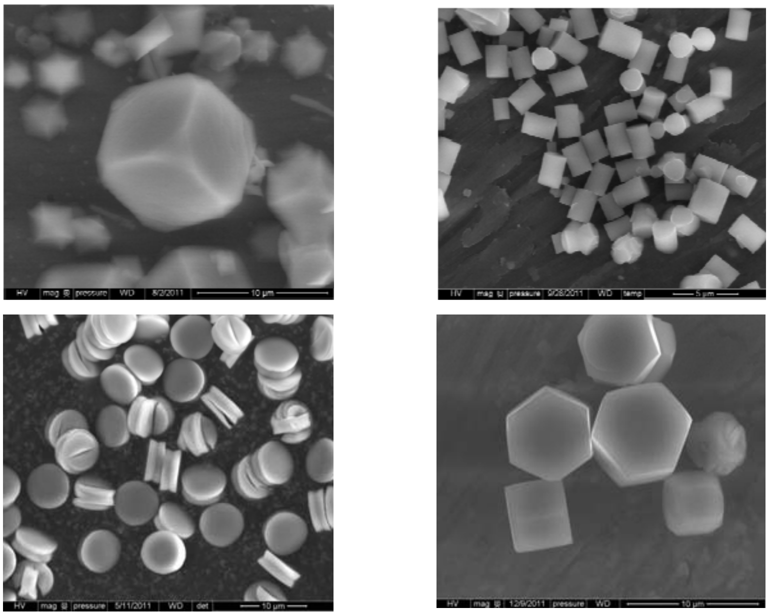

Supramolecular Chemistry and Nanoparticles

ICSM/LCPA - ITU

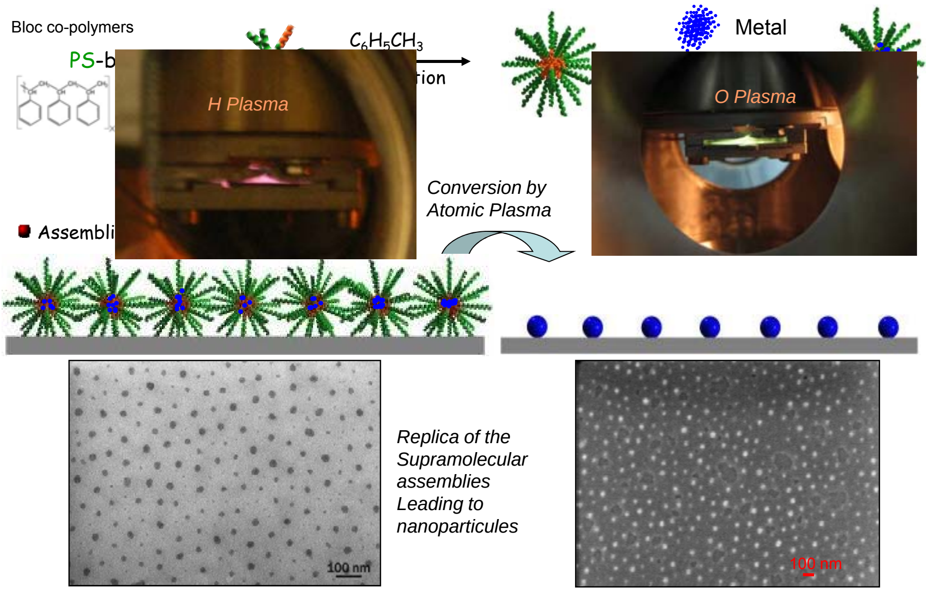

Conversion by Atomic Plasma

Replica of the Supramolecular assemblies Leading to nanoparticules

---

NP: Size, Morphology and Repartition

$PS_{1654}P2VP_{400}$ ≈ 15 nm

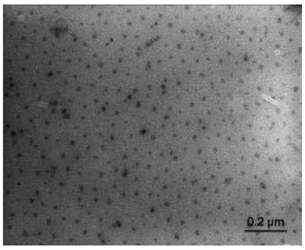

R=4,1

$PS_{529}P2VP_{476}$ ≈ 25 nm

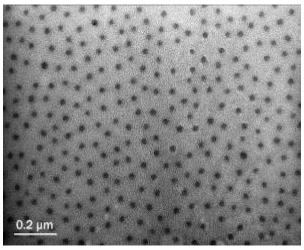

R=1,1

$PS_{115}P2VP_{405}$ ≈ 42 nm

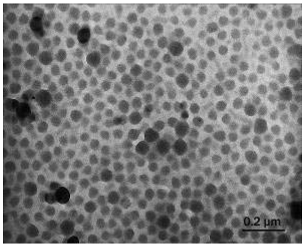

R=0,28

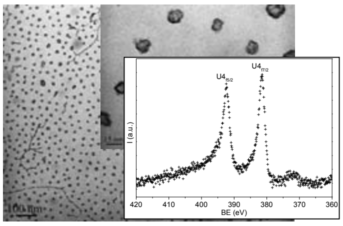

Plasma H -> UO_2
Plasma O -> UO_3

XPS

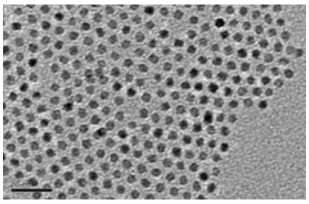

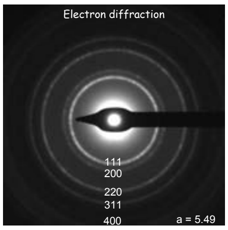

Actinides Nanoparticles

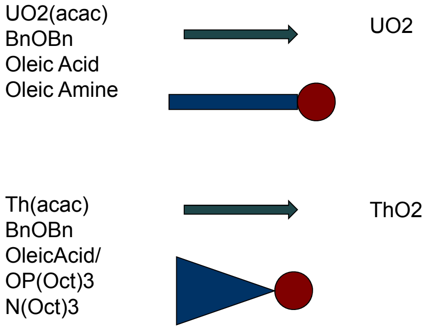

UO2(acac)
BnOBn
Oleic Acid
Oleic Amine

UO2

Th(acac)
BnOBn
OleicAcid/
OP(Oct)3
N(Oct)3

ThO2

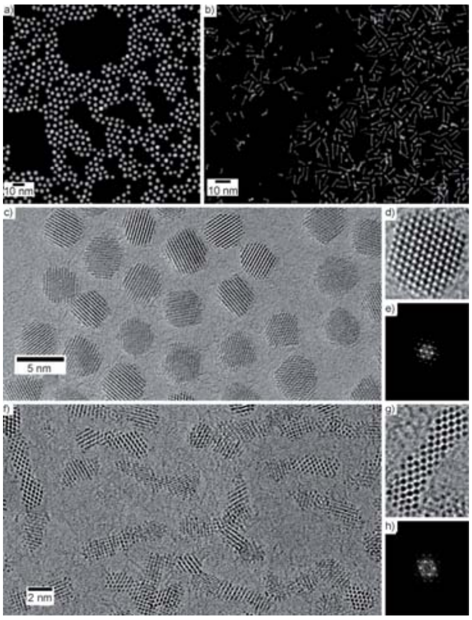

CHEMISTRY-A EUROPEAN JOURNAL Volume: 18 Issue: 27 Pages: 8283-8287

Aknowledgements:

Th. Demars (ICSM)
C. Genre (ICSM)
J. Maynadié (ICSM)
R. Podor and J. Raveau (SEM ICSM)

T. Sievers (MPI Potsdam)
D. Hudry (ICSM, ITU)

J.F. Dufrêche, T. Zemb

Thank you for your attention

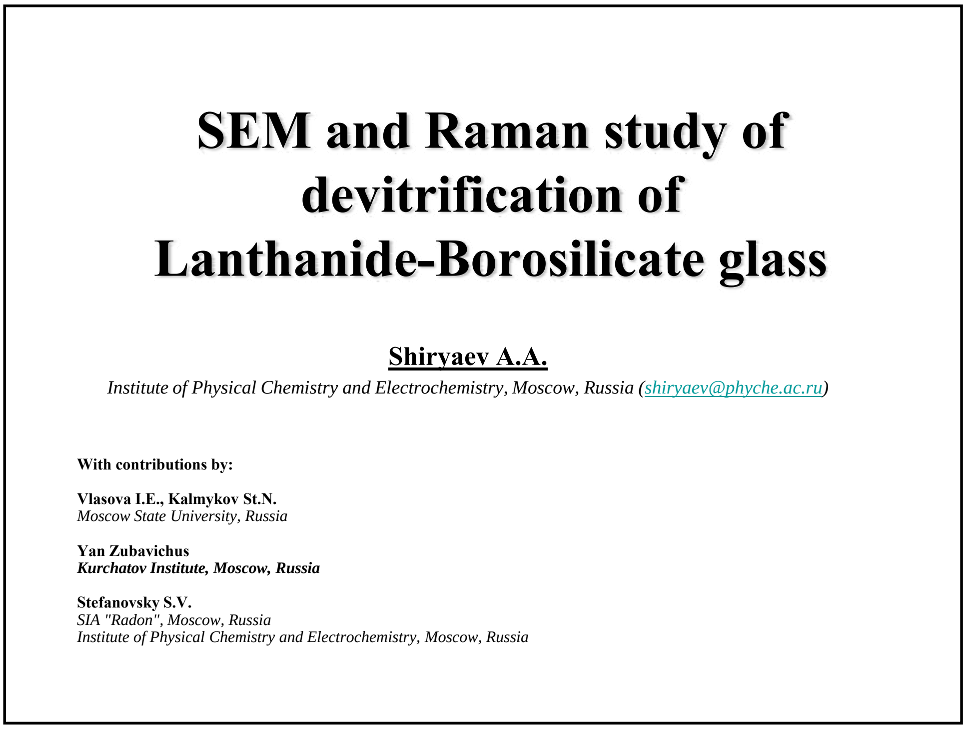

SEM and Raman study of devitrification of Lanthanide-Borosilicate glass

Shiryaev A.A.
Institute of Physical Chemistry and Electrochemistry, Moscow, Russia (shiryaev@phyche.ac.ru)

With contributions by:

Vlasova I.E., Kalmykov St.N.
Moscow State University, Russia

Yan Zubavichus
Kurchatov Institute, Moscow, Russia

Stefanovsky S.V.
SIA "Radon", Moscow, Russia
Institute of Physical Chemistry and Electrochemistry, Moscow, Russia

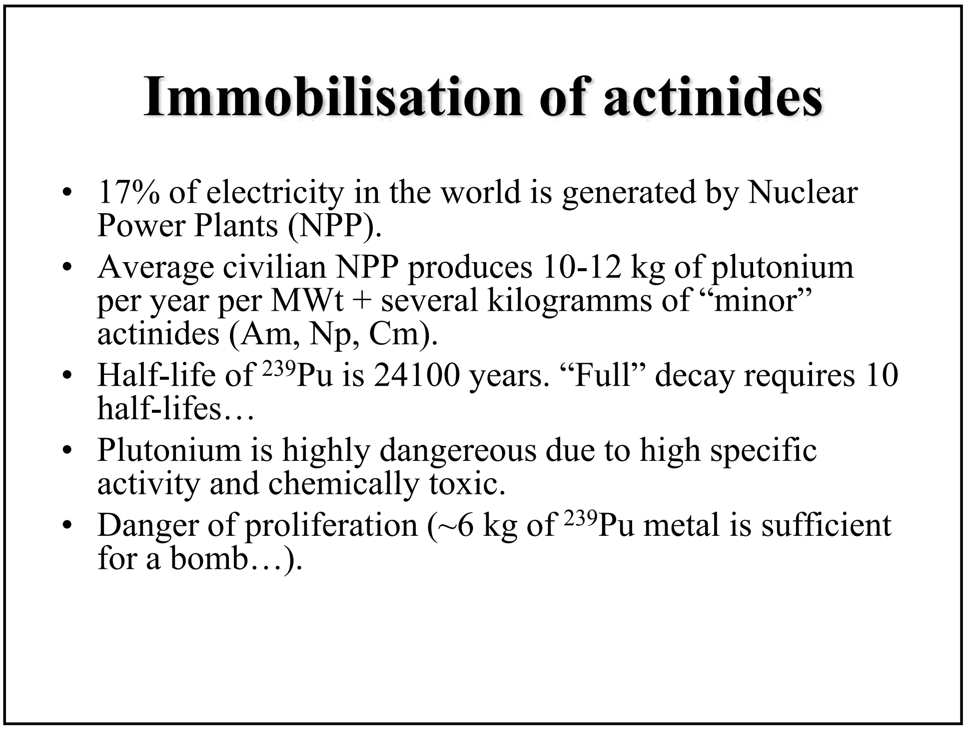

Immobilisation of actinides

- 17% of electricity in the world is generated by Nuclear Power Plants (NPP).
- Average civilian NPP produces 10-12 kg of plutonium per year per MWt + several kilogramms of "minor" actinides (Am, Np, Cm).
- Half-life of ^{239}Pu is 24100 years. "Full" decay requires 10 half-lifes…
- Plutonium is highly dangereous due to high specific activity and chemically toxic.
- Danger of proliferation (~6 kg of ^{239}Pu metal is sufficient for a bomb…).

Immobilisation of actinides

- High-purity Pu (weapons-grade) can be used in new generation of power plants in MOX (mixed oxide) fuel.
- However, lower quality Pu, “scrap” etc. is <u>not</u> suitable for MOX => must be safely immobilised (in US ~20 metric tons…+ Russia, UK, France, China…).

Forms for immobilisation

- Ceramics
- Glass-ceramics
- Glasses (e.g., borosilicate, phosphate)

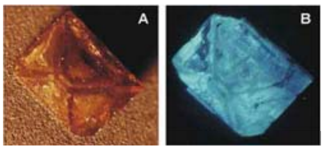

Courtesy by B.Burakov

VITRIFICATION **Pouring glass to immobilize radioactive waste.**

Lanthanide-Borosilicate glass

- Maximum PuO_2 concentration in conventional borosilicate glasses is ~2-3 wt.%. Lanthanide-Borosilicate (LaBS) glasses were designed to incorporate up to ~10 wt.% PuO_2 (*Strachan et al.*, 1998).
- ***Behaviour of Pu and of some other constituents in LaBS glasses and its long-term stability is still poorly constrained.***

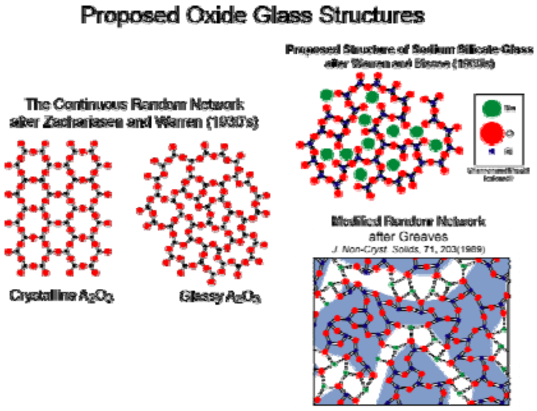

http://www.grandinetti.org/Research/Applications/GlassStudies/

Glass preparation

- PuO_2 powder mixed with chemicals, heated to 1500 °C at a rate of 10 °C/min, kept for 30 min and quenched.
- In contrast to Pu-free glasses of the same composition (Pu→Hf) it is very difficult to obtain homogeneous glass if high PuO_2 loads are used. In some runs the sample is clearly segregated into crystal-like and glassy parts.

Range of target chemical compositions (wt%)

Al_2O_3	B_2O_3	Gd_2O_3	HfO_2	La_2O_3	Nd_2O_3	PuO_2	SiO_2	SrO
8-20	10-22	8-12	4-14	11-18	11-14	0-9.5	18-28	2.5

Characterisation methods

- XAFS spectra of Pu, Hf, REE (La, Gd, Nd) in fluorescence and transmission geometries from powdered sample. Data treatment with FEFFIT8 package and wavelet analysis with program HAMA (www.esrf.fr/exp_facilities/BM20/Software/Wavelets.html)
- XRD using 2D Imaging Plate detector; energy 17 keV (λ = 0.688 Å; Zr edge).
- TEM
- Raman spectroscopy (λ = 488 nm)
- Rutherford Backscattering (RBS)
- Leaching in natural water at 75 °C for 45 days
- SEM/EDS before and after leaching
- ICP-MS of solution

Pu-free glass

Hf in Pu-free glass

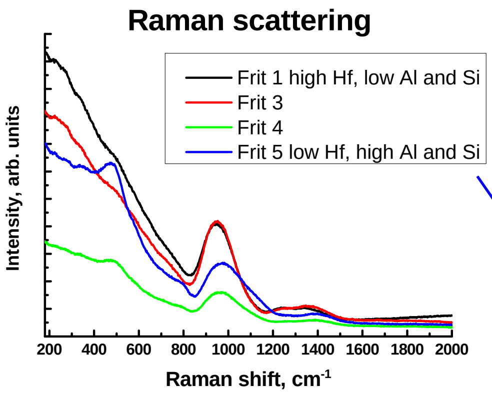
Raman scattering

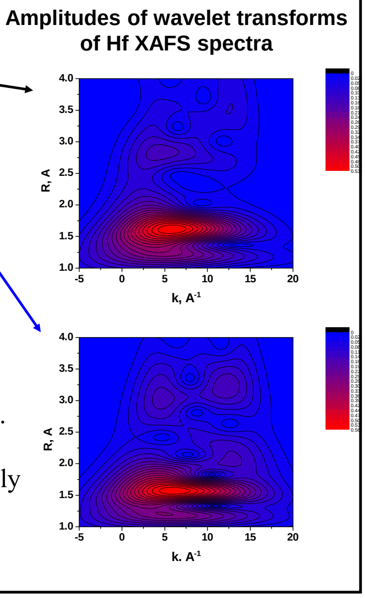
Amplitudes of wavelet transforms of Hf XAFS spectra

No spectral manifestations of HfO_2 as a separate phase.
Hf is mostly in vitreous environment with CN≈6
Weak second coordination sphere is present and strongly depends on glass composition.

No evolution of Hf environment with storage time.

Pu-loaded glass

The glass seems to be homogeneous on mm-scale (RBS data), but is **markedly** heterogeneous on sub-mm scale if high PuO_2 loads are used!

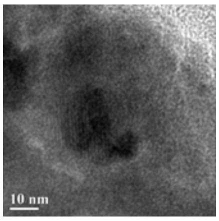

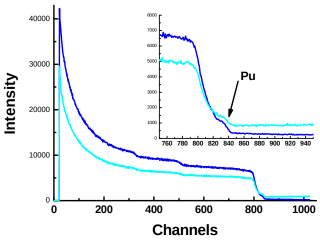

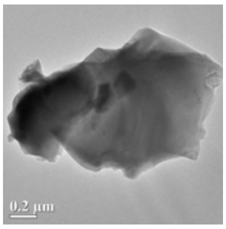

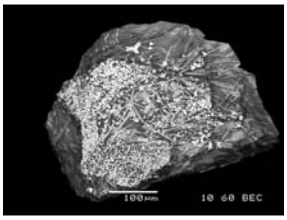

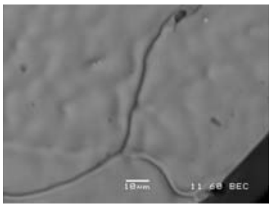

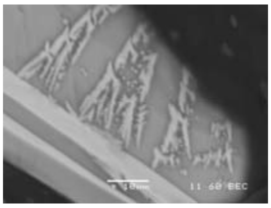

Phase composition of the LaBS glass

(9.5 wt% PuO_2)

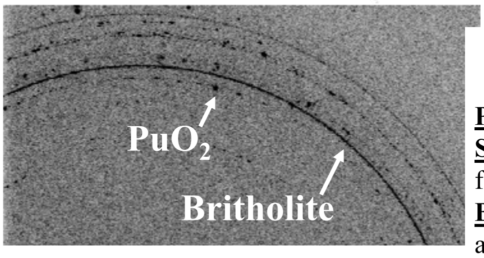

Identified phases (XRD+SEM/EDX)

PuO_2: crystallites with sizes of >50 nm.
Solid solution of (Pu, Hf)O_2 with a fluorite structure (SEM/EDX/XRD)
Britholite: (approx. $REE_{10}Si_6O_{24}(OH)_2$) is a “real” powder.

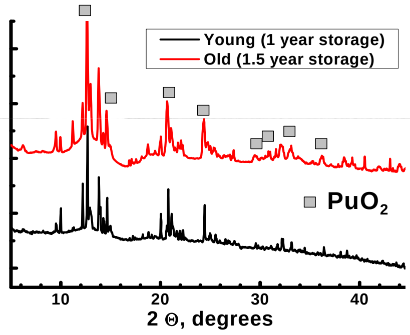

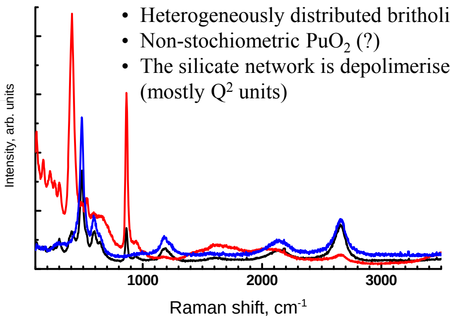

- Heterogeneously distributed britholite
- Non-stochiometric PuO_2 (?)
- The silicate network is depolimerised (mostly Q^2 units)

Evolution of Pu environment with glass aging: XAFS data

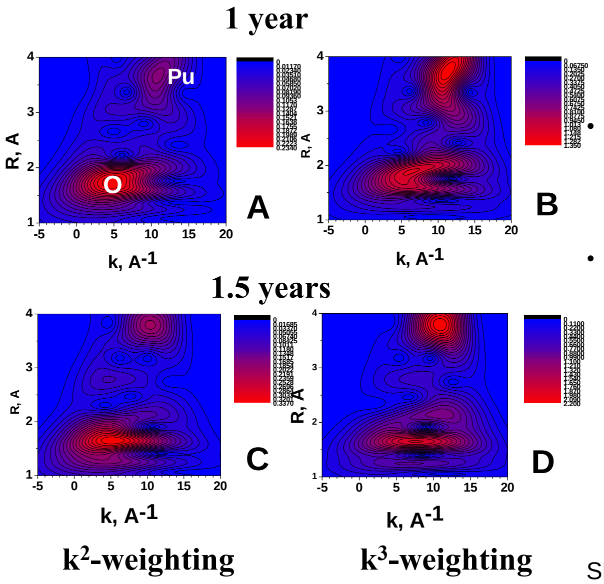

- Precipitation of (Pu, Hf)O_2 and britholite; the grain size and crystallographic perfection increases.
- Sharpening of the maxima in R-space indicates better separation of contributions from glassy and crystallines phases.

Shiryaev et al., MRS Proc. 2010

LaBS glass with 9.5 wt% PuO_2: SEM of partly crystallized sample

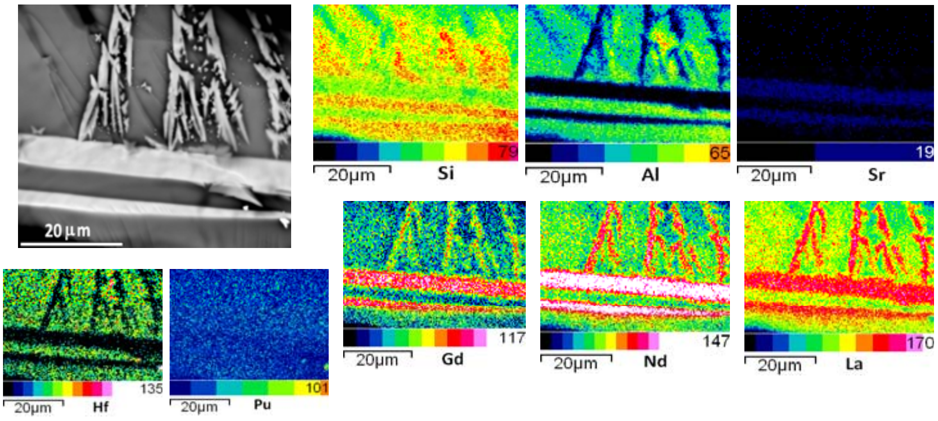

•Precipitation of britholite (?) $REE_{10}Si_6O_{24}(OH)_2$. The glass retains Al, Hf (supports XAS).
•REE, Sr and Si partition to the precipitate.
•Pu concentrations are roughly similar for the glass and the precipitate.

The Pu-rich sample is glass-crystalline ceramics. Britholite is resistant to radiation. May we use this material for safe long-term immobilisation of Pu?

Scanning Electron Microscopy of Uranium-loaded glass

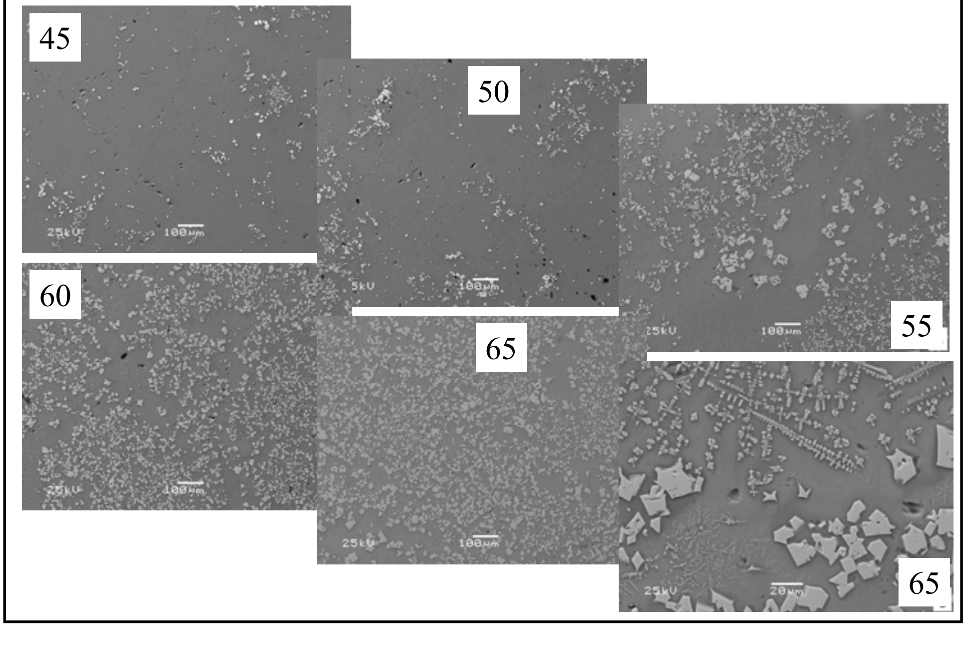

X-ray Absorption Spectroscopy

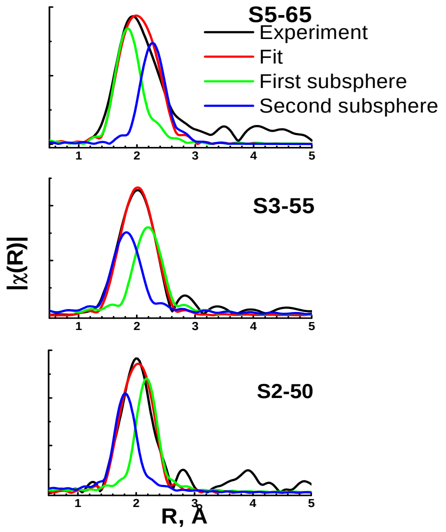

Despite obvious presence of crystalline precipitates uranium remains in the vitreous fraction

---

What happens if the LaBS glass contacts with hot water?

Leaching experiments

- Small pieces of glass in water
- Water composition similar to some relevant natural locations: $CaHCO_3$ – 187.5 mg/l, $NaHCO_3$ – 62.5 mg/l, pH = 6.7
- 42 days at 75 °C
- (Quasi)-Static conditions (minor shaking of the vials on extraction of the solution aliquot for ICP-MS)

Main goal:

investigation of surface alteration

No saturation of Pu release in 42 days experiment

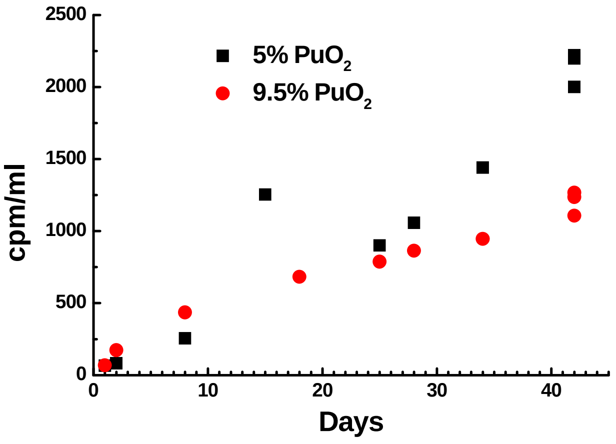

Surface alteration:
Pu-free glass

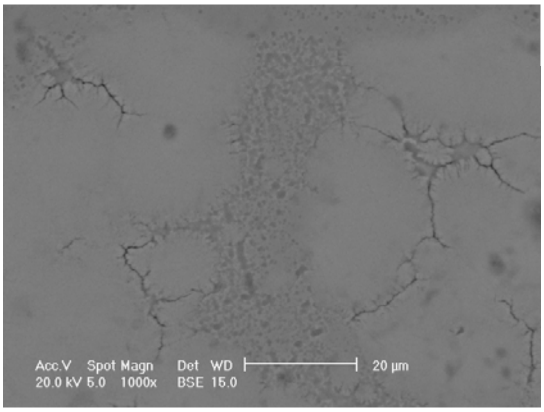

Formation of altered layer, which may crack and detach from underlying bulk
Rather uniform process on the whole glass surface

Surface alteration:
Pu-loaded glass

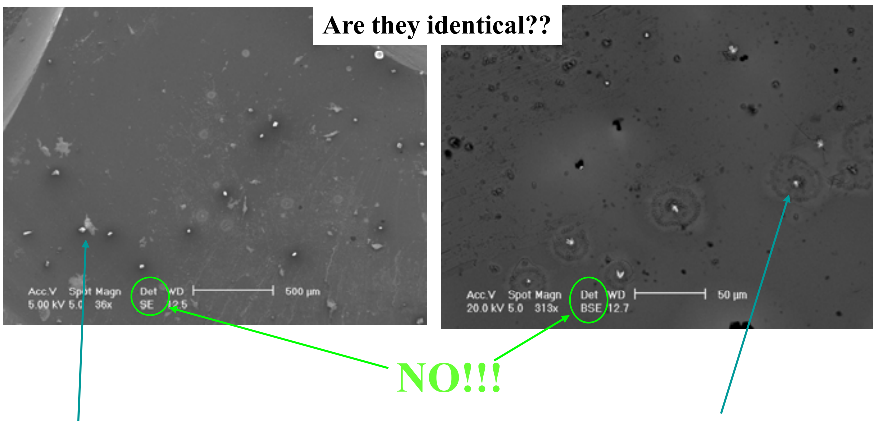

5 wt% PuO_2

9.5 wt% PuO_2

Are they identical??

NO!!!

Carbonate precipitates from water
Rather uniform glass alteration

“Heavy” spots
Alteration…

The “heavy spots”: a closer look

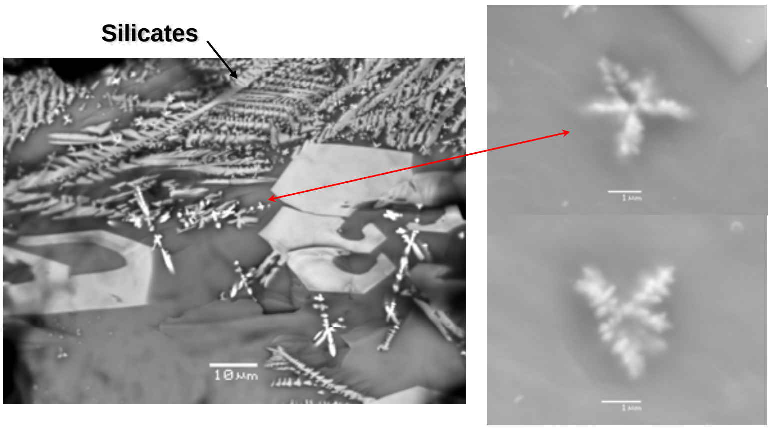

Precipitates of (Pu, Hf)O_2 solid solution and of REE-Al phase!!
Dendritic morphology consistent with CaF_2-structural type dendrites
Exsolution (rapid?) of excess PuO_2?

Alteration of Pu-rich glass

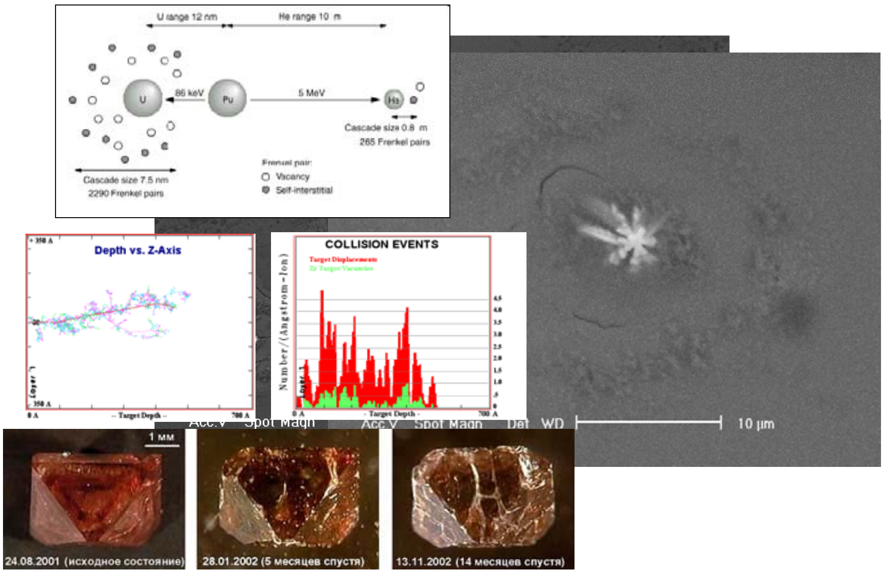

Conclusions

- The solubility of PuO_2 in LaBS glass may reach 5-6 wt%.
- In the vitreous phase oxygen environment of Pu resembles axially squeezed tetragonal pyramid.
- Hf enters predominantly the vitreous phase and is stable in time.
- At higher loads exsolution of fluorite-type $(Pu, Hf)O_2$, britholite and REE-Al-phase occurs.
- Highly Pu-loaded glass dissolves in water with pronounced pitting and cracking around PuO_2 precipitates.

XAFS at the Pu L3 edge

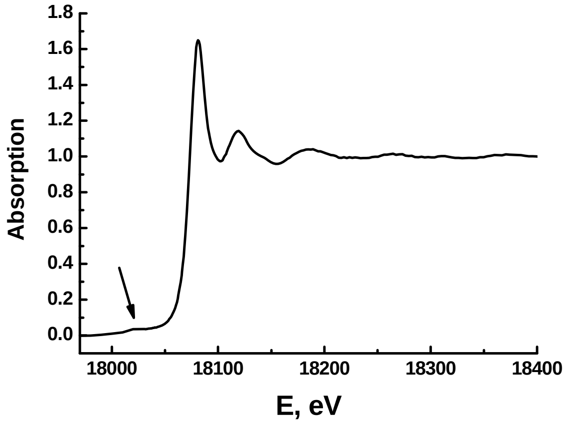

XAFS results I: Pu L_{III}-edge

- Pu is mainly tetravalent (XANES and XPS)
- First shell shows similarity to PuO_{2+x} ($PuO_{2.2}$?)
- Weakness of the Pu-Pu peak at 3.7 Å suggests that the main fraction of Pu is in the vitreous phase.
- With increasing storage time the splitting of the first sphere becomes more pronounced. In the fresh glass it can be fitted by two subspheres, whereas for the 2 years old glass the first sphere is best fitted by 3 components (similar to *Conradson et al., JACS, 126, 13443, 2004*).

Sample	Atom	Distance, A	Occupation
2 y.o. glass	O	1.87-1.92	0.15-0.47
	O	2.09-2.12	~1.2
	O	2.20-2.27	4±1
	Pu	3.74	2±0.5
Fresh glass	O	2.13	1.3
	O	2.25-2.28	5
	Pu	3.66-3.69	2.5±0.5

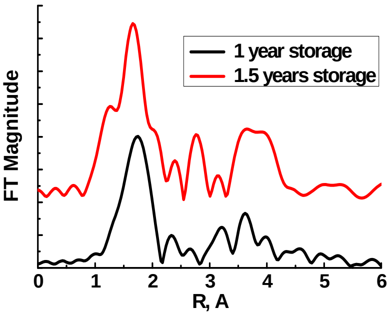

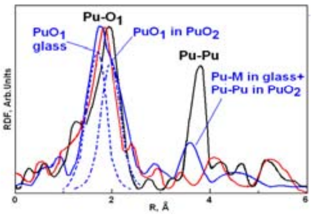

FT peak of the first coordination shell is asymmetric – superposition of contributions from various phases.

Structure of the glass: Raman scattering

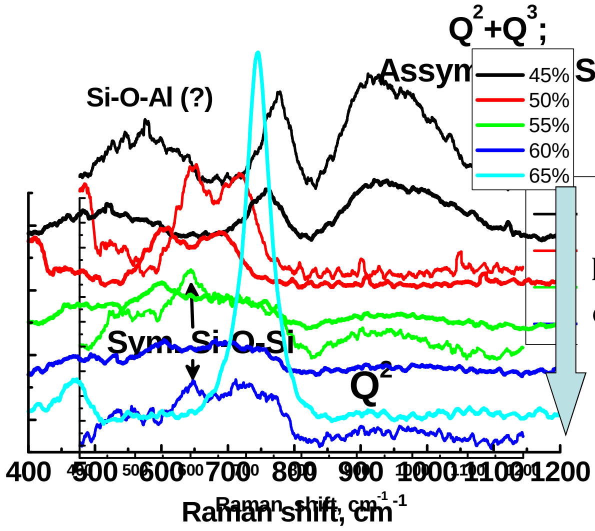

Glass polymerisation correlates with waste loading

Summary of Raman results

The glass with the smallest amount of waste:

the silicate network mostly consists of Q^2 silicate units with minor Q^1.

Increase of the waste loading leads to decrease of Si/Al ratio => development of alumosilicate network. At high waste loadings the glass consists of rather depolymerised silicate network (mostly Q^2 units) and increasing fraction of polymerised alumosilicates (Q^4(*m*Al)). Such process lead to precipitation of nepheline and of other minerals.

This scenario is consistent with XRD and SEM data, showing higher degree of crystallinity and precipitation of separate phases with increase of the waste loading.

Summary of structural and compositional data

- Samples are glass-crystalline: a U-bearing matrix glass depleted with iron and a Fe-rich spinel structure phase.
- Vitreous phase is enriched with Na, Al, Si, Zr, U.
- U enters vitreous phase only. No U was found in spinel phase within measurement error.
- Magnetite-type spinel is strongly enriched with Fe, Cr, Mn, Ni, Zn. Minor Cu and Mg.
- Two spinels of first and second generations with somewhat different compositions crystallized at early and later stages of melt solidification were found in the samples with 50 and 55 wt.% waste loading.
- Nepheline is present in glass at high waste loadings (60 and 65 wt.%).

EXAFS

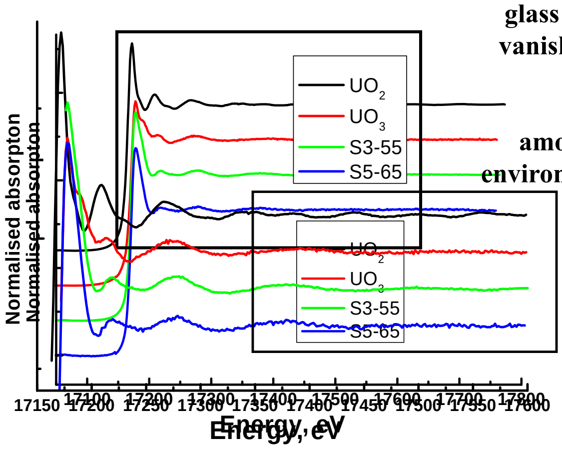

Oscillations in the glass samples vanish rapidly

⇓

amorphous environment of U

XANES

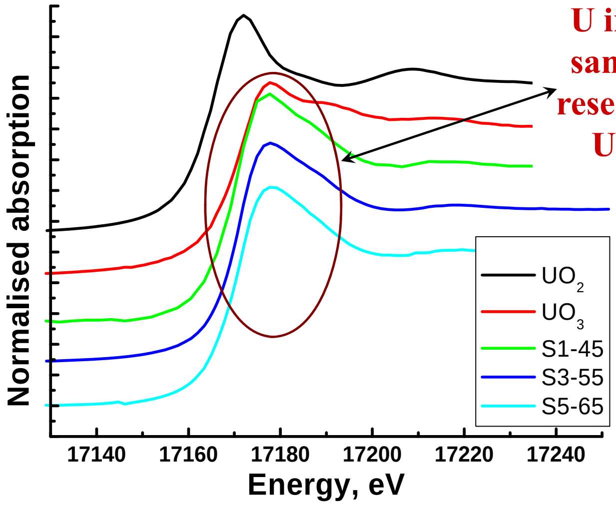

U in the samples resembles UO_3!

PERTECHNETATE-ION BINDING BY ORGANIC LIGANDS IN AQUEOUS SOLUTIONS

B.V. Egorova[1], G.V. Kolesnikov[1], S.N. Kalmykov[1], Yu.A. Ustynyuk[1],

K.E. German[2], B.F. Myasoedov[2]

[1] *Lomonosov Moscow state university*

[2] *A.N. Frumkin Institute of Physical Chemistry and Electrochemistry RAS*

^{99}Tc is produced in nuclear power stations as a fission product of ^{235}U and ^{239}Pu in relatively large quantities. Pertechnetate, TcO_4^-, is the most stable under oxidizing conditions of the first step of PUREX reprocessing and the main form of ^{99}Tc in liquid nuclear wastes. Co-extraction of TcO_4^- with U and Pu is followed by important Tc catalytic interference at the actinide separation stage and leads to formation of highly insoluble precipitates if reductive separation of plutonium is stabilized by chelate addition at some variants of PUREX process [1-2]. Precipitates formed make serious difficulties for effective fuel reprocessing. Thereby it is very important to remove technetium before plutonium separation. In addition macro concentrations of nitrate-ion make selective and effective separation of $TcO_4^-$from nuclear waste solutions even more difficult.

On the other hand isotope ^{99m}Tc is considered as ideal imaging agent in nuclear medicine. Typically $^{99m}TcO_4^-$ is reduced to Tc (III-V) to form stable covalent complexes with organic substances. These complexes are used directly for imaging purposes. Development of selective anionic receptors for pertechnetate could lead to the new generation radiopharmaceuticals, where $^{99m}TcO_4^-$ is strongly and non covalently bounded in aqueous solutions. Elimination of reduction step is highly desirable.

This work presents experiments of pertechnetate extraction by acyclic ligands **1-3** from organic into aqueous media. Ligands under consideration possess positively charged moieties:

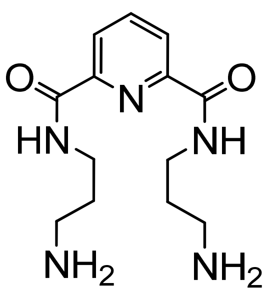

1

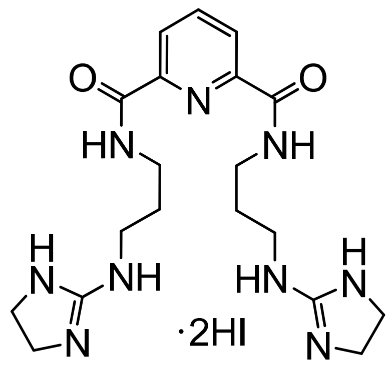

2

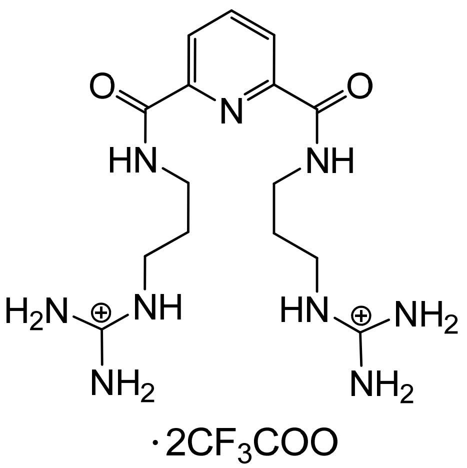

3

Extraction experiments were carried out to study pertechnetates anion complex at ion inaqueous solutions.

A 10^{-6}M stock solution of tetrabutylammonium pertechnetates in dichloroethane and 10^{-4} M aqueous solution of ligands **1-3** were used to investigate extractability of TcO_4^- from organic phase into aqueous. pH level was maintained by addition of HCl or NaOH, with pH-meter control.

The highest efficiency 80-90% was found for ligand **2** in pH range from 2 to 6 while others were not efficient when compared with blank test (distilled water without any ligand).

Ligand **2** efficiency was confirmed by competitive extraction experiments of TcO_4^- with Aliquat-336 in organic phase.

We have found that presence of ligand with NH_4TcO_4 (10^{-6} M) in aqueous phase leads to decrease of TcO_4^- transfer into dichloroethane promoted by Aliquat-336. Increase of ligand 2 concentration from 0 to 10-3 M led to decrease of pertechnetate transfer from 100 to 34 %.

1. A.B. Melent’ev, A.N. Mashkin, O.V. Tugarina, D.N. Kolupaev, K.E. German, I.G. Tananaev, Effect of Complexing Agents (DTPA and Oxalic Acid) on the Extraction Behavior of Technetium in the TBP–N2H5NO3–HNO3 System // Radiochemistry, 2011, Vol. 53, No. 2, pp. 172–177.
2. K.E. German, A.B. Melent’ev, Ya.V. Zubavichyus, S.N. Kalmykov, A.A. Shiryaev, I.G. Tananaev, Synthesis, Structure, and Properties of New Difficultly Soluble Complex Compounds of Technetium with Diethylenetriaminepentaacetic Acid // Radiochemistry, 2011, Vol. 53, No. 2, pp. 178–185.

MOSCOW STATE UNIVERSITY
CHEMISTRY DEPARTMENT, DIVISION OF RADIOCHEMISTRY
LABORATORY OF DOSIMETRY AND ENVIRONMENTAL RADIOACTIVITY

Pertechnetate-ion binding by organic ligands in aqueous solutions

B.V. Egorova, G.V. Kolesnikov, S.N. Kalmykov,
Yu.A. Ustynyuk, K.E. German, B.F. Myasoedov

Nuclear fuels: U, Pu compounds

Tc in spent nuclear fuel

↓ *PUREX process*

TcO_4^- Oxic conditions:
High solubility,
High mobility

1. Environmental contamination
2. Problems in Pu, U extraction

Tc in nuclear medicine

^{99m}Tc E=140 keV, $T_{1/2}$= 6 h

Diagnostic agent SPECT

$TcO_4^- \xrightarrow[SnCl_2]{reduction}$ Tc(II, III, IV, V)

Chelation by N-, S-, P-

Effective extraction of TcO_4^- on first steps of spent fuel treatment
Water soluble receptors for detection and medical application

Properties of pertechnetate

anion	*ΔH$_{hydr,}$kJ/mol*	*Q/S·10^2, Å^{-2}*	*Q/V·10^2, Å^{-3}*
TcO_4^-	*-247*	*1.27*	*2.04*
NO_3^-	*-312*	*2.48*	*5.55*
Cl^-	*-367*	*2.43*	*5.37*

Extraction of TcO_4^-

Cationic agents	Neutral extractants
NR_4^+, PR_4^+, AsR_4^+	*TBP*

Positively charged ligands

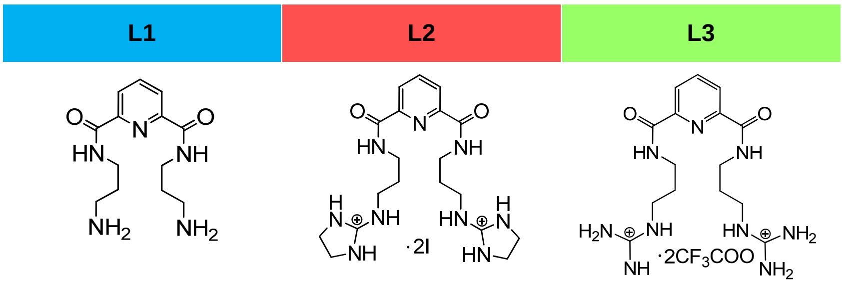

To investigate binding of pertechnetate:

1) Extraction of TcO_4^- from organic phase to water
2) Transfer of TcO_4^- from aqueous solution with L to organic phase by Aliquat-336

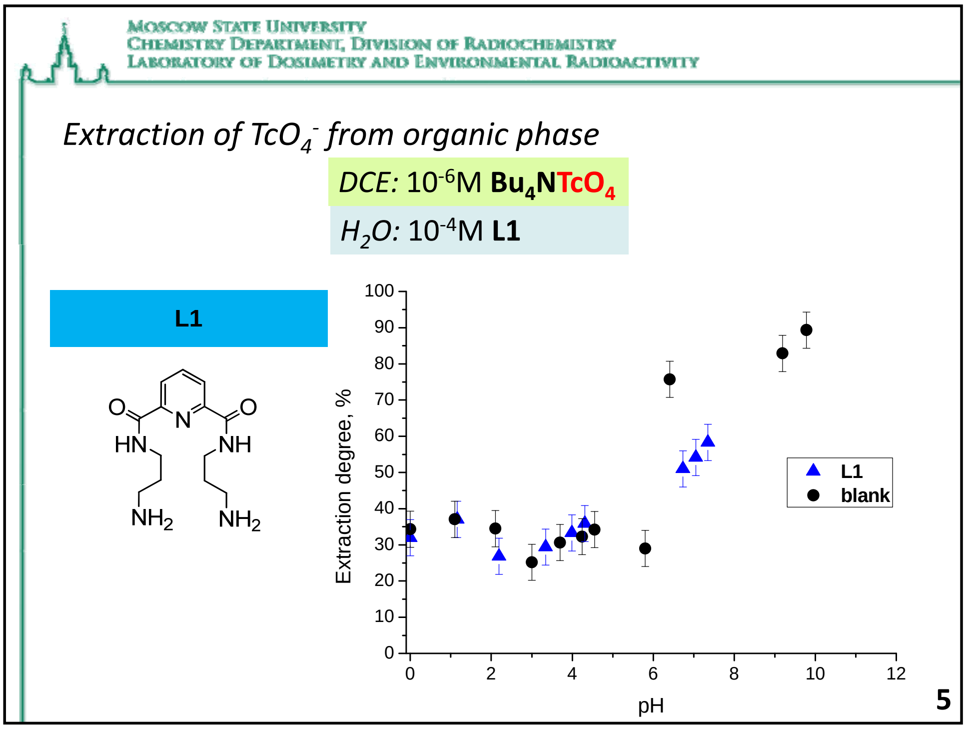

Moscow State University
Chemistry Department, Division of Radiochemistry
Laboratory of Dosimetry and Environmental Radioactivity

Extraction of TcO_4^- from organic phase

DCE: 10^{-6}M **Bu_4NTcO_4**

H_2O: 10^{-4}M **L1**

L1

5

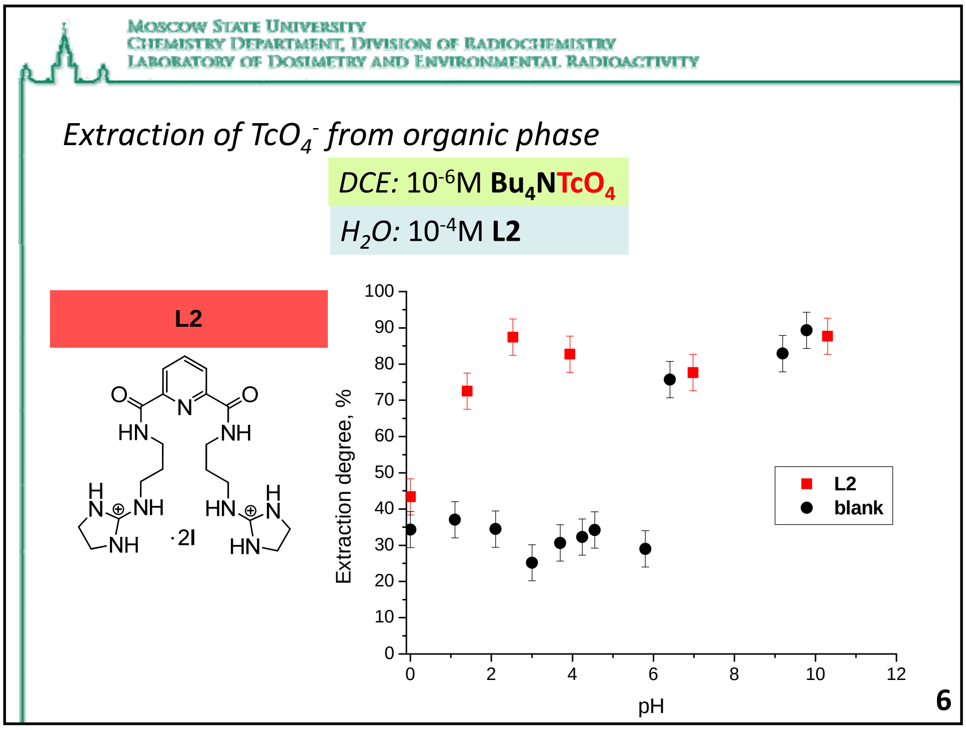

Moscow State University
Chemistry Department, Division of Radiochemistry
Laboratory of Dosimetry and Environmental Radioactivity

Extraction of TcO_4^- from organic phase

DCE: 10^{-6}M **Bu_4NTcO_4**

H_2O: 10^{-4}M **L2**

L2

6

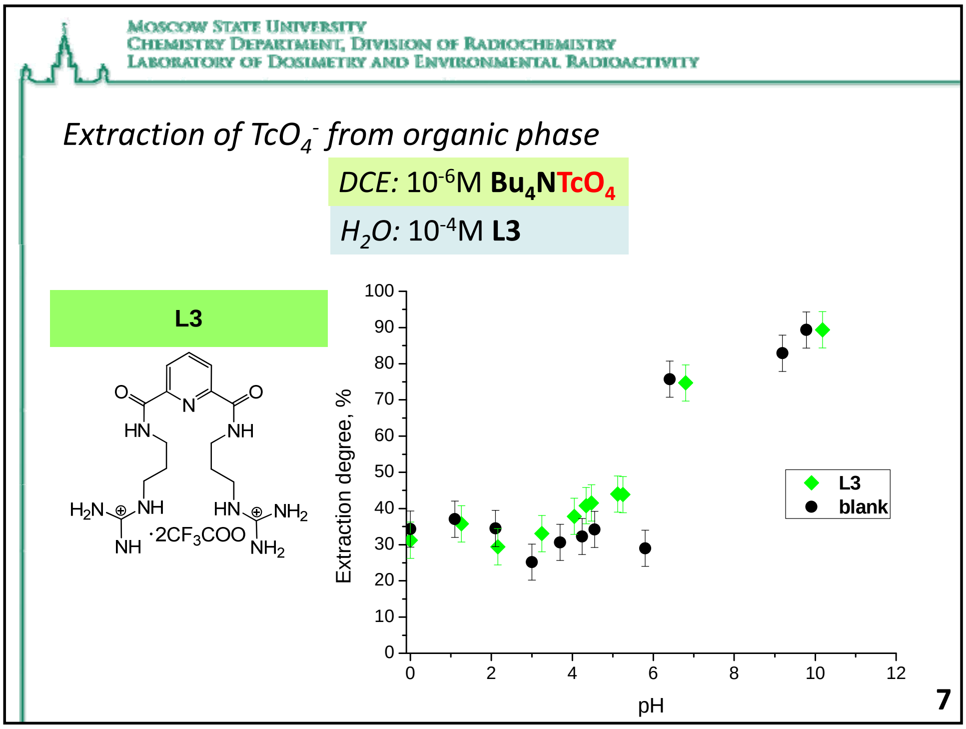

MOSCOW STATE UNIVERSITY
CHEMISTRY DEPARTMENT, DIVISION OF RADIOCHEMISTRY
LABORATORY OF DOSIMETRY AND ENVIRONMENTAL RADIOACTIVITY

Extraction of TcO_4^- from organic phase

DCE: 10^{-6}M **Bu_4NTcO_4**

H_2O: 10^{-4}M **L3**

L3

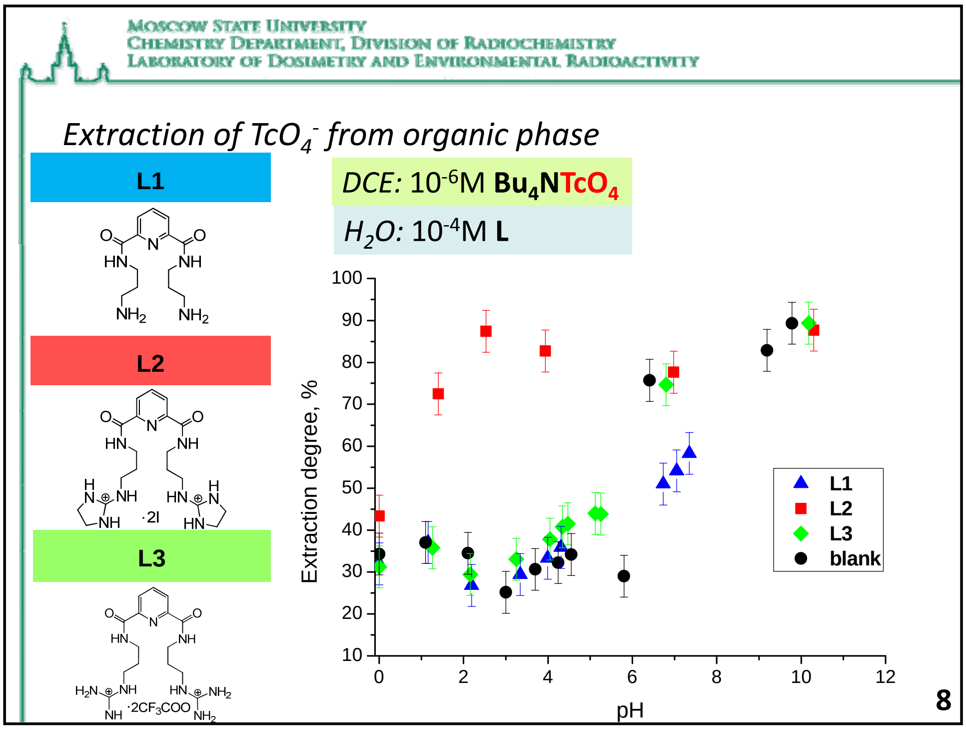

MOSCOW STATE UNIVERSITY
CHEMISTRY DEPARTMENT, DIVISION OF RADIOCHEMISTRY
LABORATORY OF DOSIMETRY AND ENVIRONMENTAL RADIOACTIVITY

Extraction of TcO_4^- from organic phase

DCE: 10^{-6}M **Bu_4NTcO_4**

H_2O: 10^{-4}M **L**

L1

L2

L3

Extraction of TcO_4^- from aqueous solution with L

DCE: 10^{-5}M **Aliquat-336**

H_2O: 10^{-6}M **NH_4TcO_4**
10^{-6}→10^{-2}M **L1; L2; L3**

Extraction of TcO_4^- from aqueous solution with L

DCE: 10^{-5}M **Aliquat-336**

H_2O: 10^{-6}M **NH_4TcO_4**
10^{-6}→10^{-2}M **L1; L2; L3**

L1

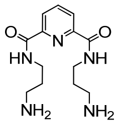

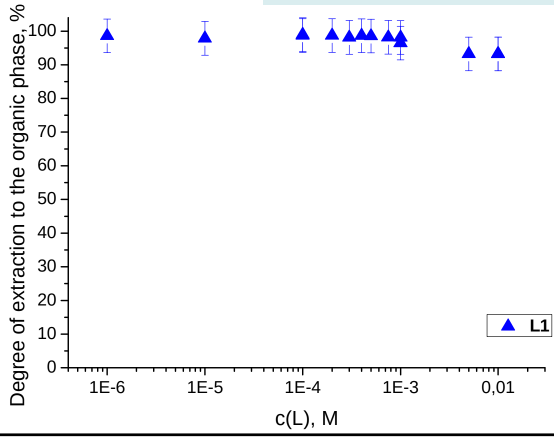

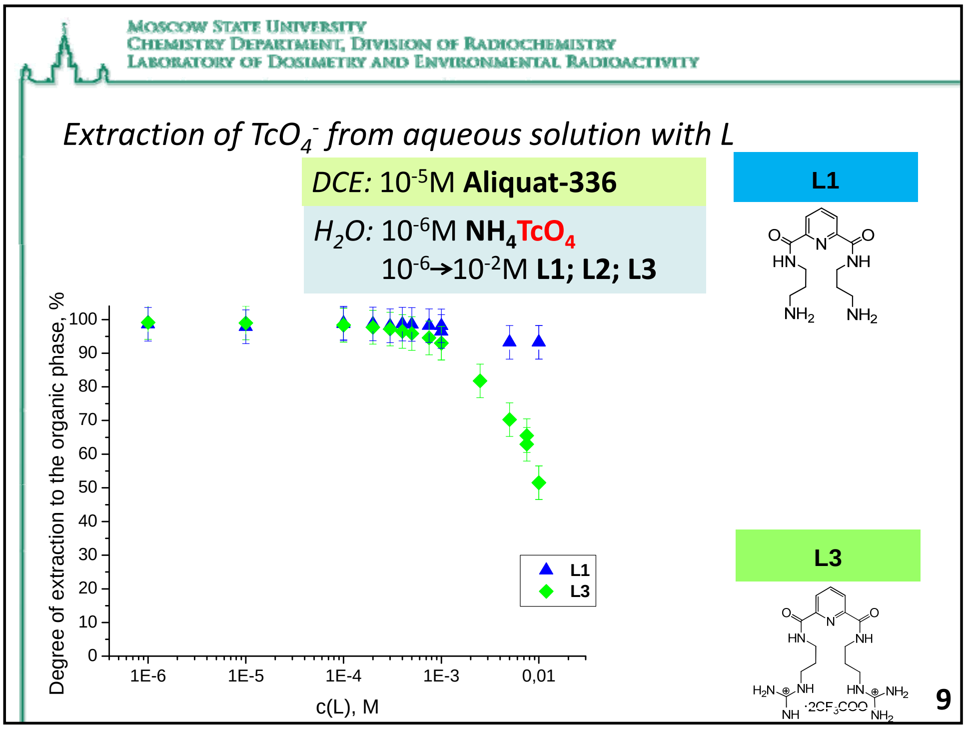

Moscow State University
Chemistry Department, Division of Radiochemistry
Laboratory of Dosimetry and Environmental Radioactivity

Extraction of TcO_4^- from aqueous solution with L

DCE: 10^{-5}M **Aliquat-336**

H_2O: 10^{-6}M **NH_4TcO_4**
$10^{-6}\rightarrow10^{-2}$M **L1; L2; L3**

9

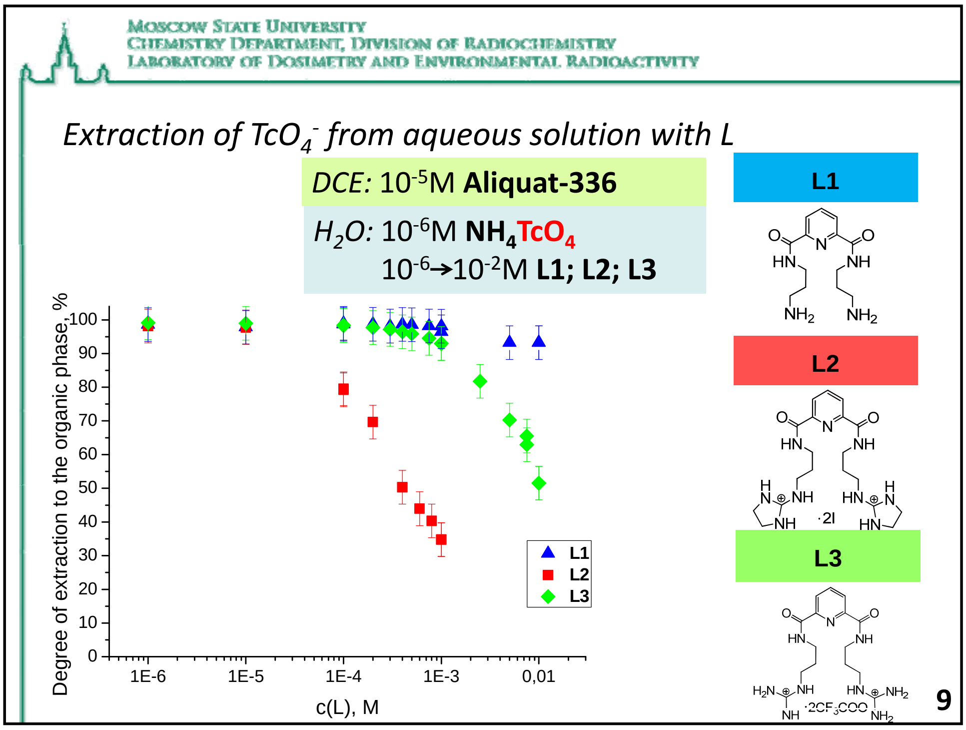

Moscow State University
Chemistry Department, Division of Radiochemistry
Laboratory of Dosimetry and Environmental Radioactivity

Extraction of TcO_4^- from aqueous solution with L

DCE: 10^{-5}M **Aliquat-336**

H_2O: 10^{-6}M **NH_4TcO_4**
$10^{-6}\rightarrow10^{-2}$M **L1; L2; L3**

9

Our preliminary studies of water soluble positively charged organic receptors showed:

✓ They can transfer pertechnetate-ion from organic phase into water

✓ They can retain pertechnetate-ion in water in the presence of Aliquat-336

Thank you for your attention!

UV-vis spectrophotometry

L2

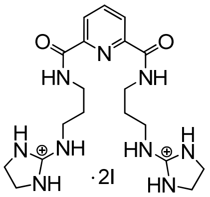

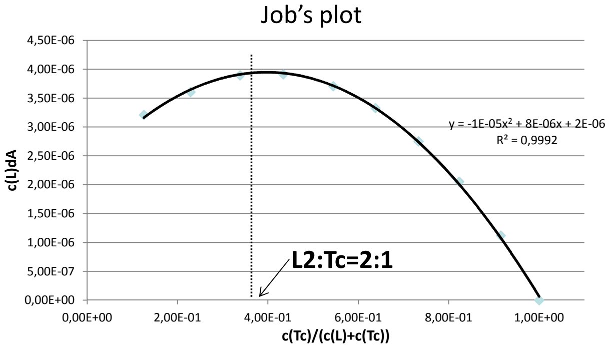

A1

Extraction of TcO_4^- from aqueous solution with L

DCE: 10^{-5}M **Aliquat-336**

H_2O: 10^{-6}M **NH_4TcO_4**

$10^{-4} \rightarrow 10^{-3}$M **L2**

L2

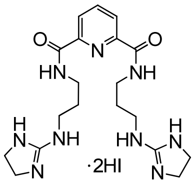

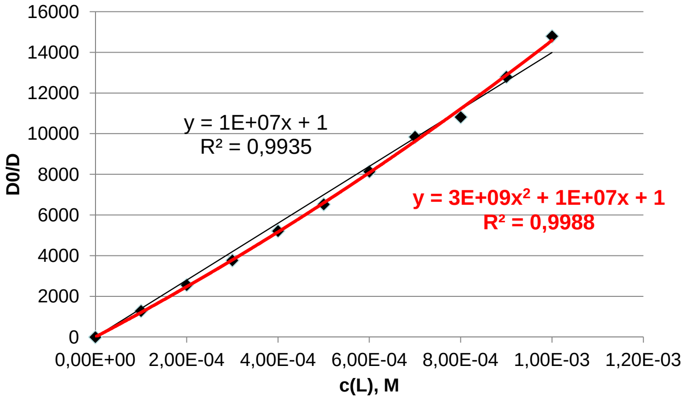

$\lg\beta_{11}=7$
$\lg\beta_{21}=9{,}5$

A2

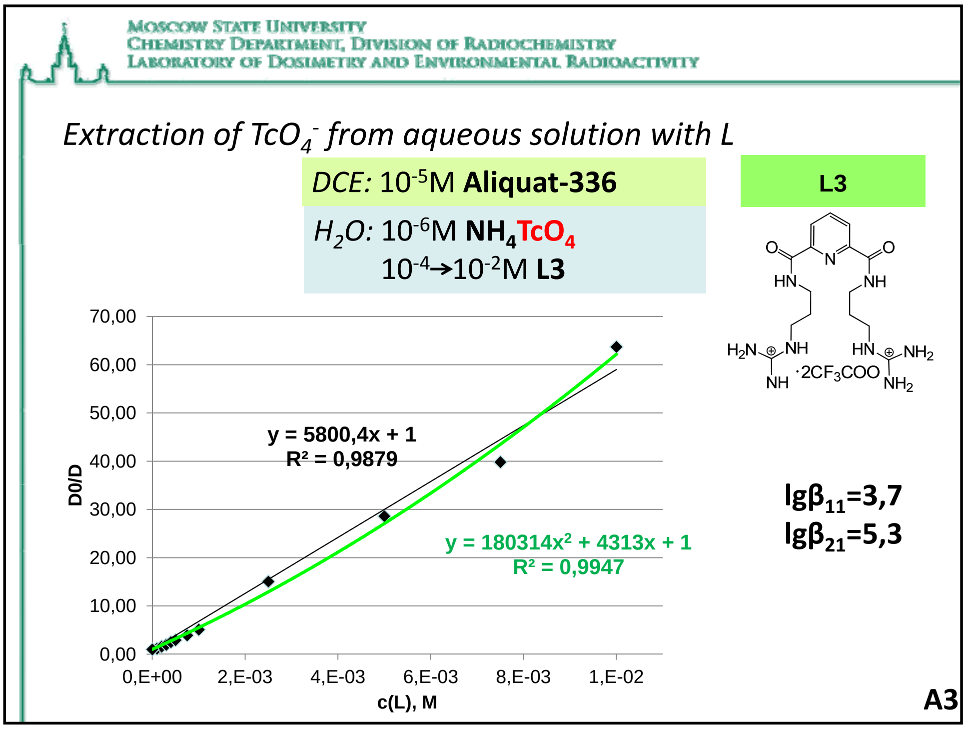

Moscow State University
Chemistry Department, Division of Radiochemistry
Laboratory of Dosimetry and Environmental Radioactivity

Extraction of TcO_4^- from aqueous solution with L

DCE: 10^{-5}M **Aliquat-336**

H_2O: 10^{-6}M **NH_4TcO_4**
$10^{-4} \rightarrow 10^{-2}$M **L3**

L3

$\lg\beta_{11}=3{,}7$
$\lg\beta_{21}=5{,}3$

A3

New radiopharmaceuticals based on technetium-99m with bifunctional chelating agents

A.Ya. Maruk, A.B. Bruskin, G.E. Kodina

Burnasyan Federal Medical Biophysical Center of FMBA Russia

^{99m}Tc

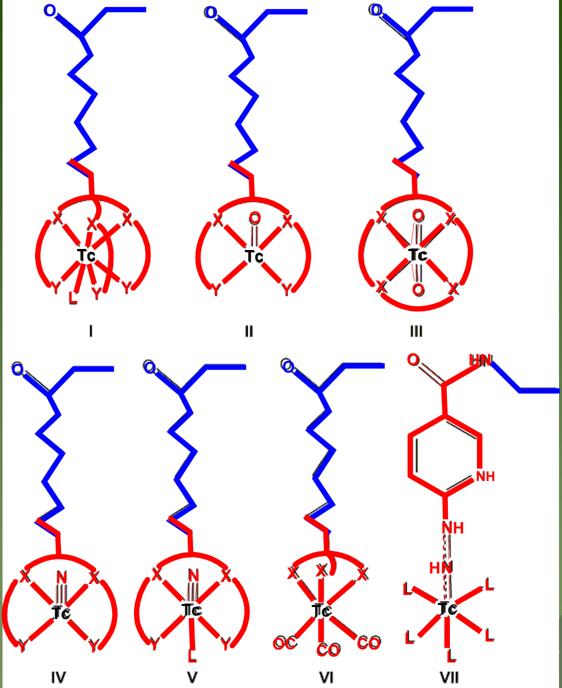

BCA - bifunctional chelating agents

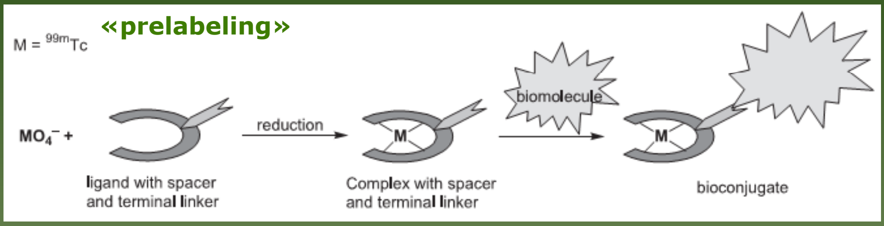

or

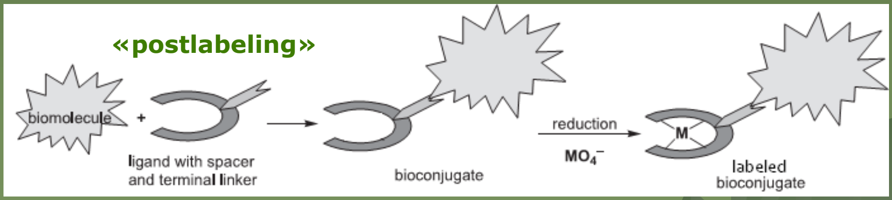

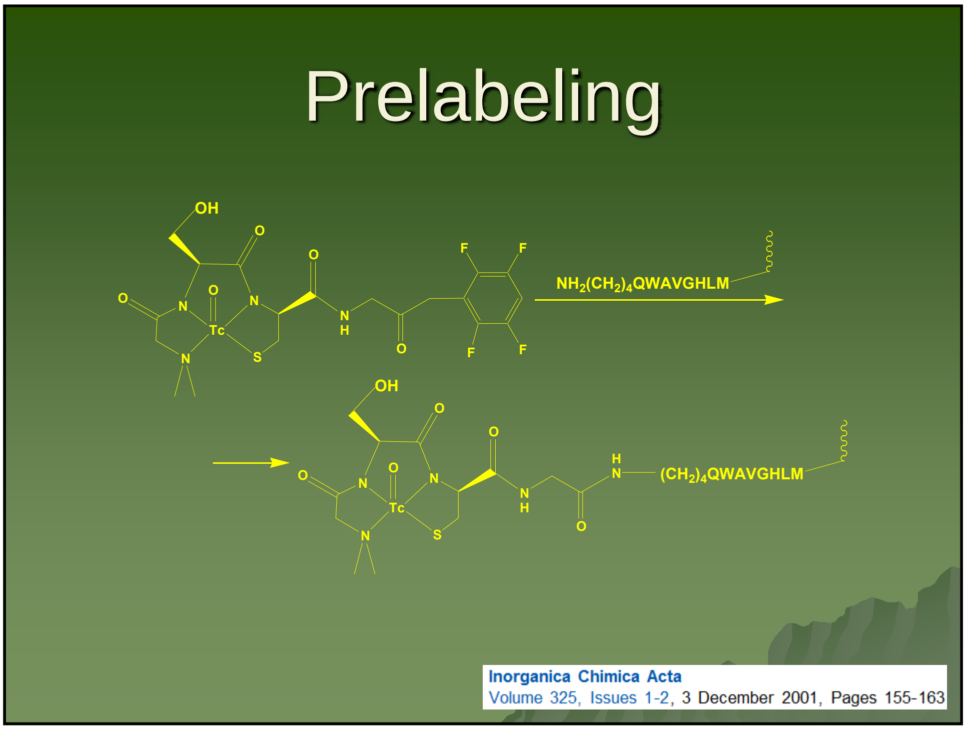

Prelabeling

Inorganica Chimica Acta
Volume 325, Issues 1-2, 3 December 2001, Pages 155-163

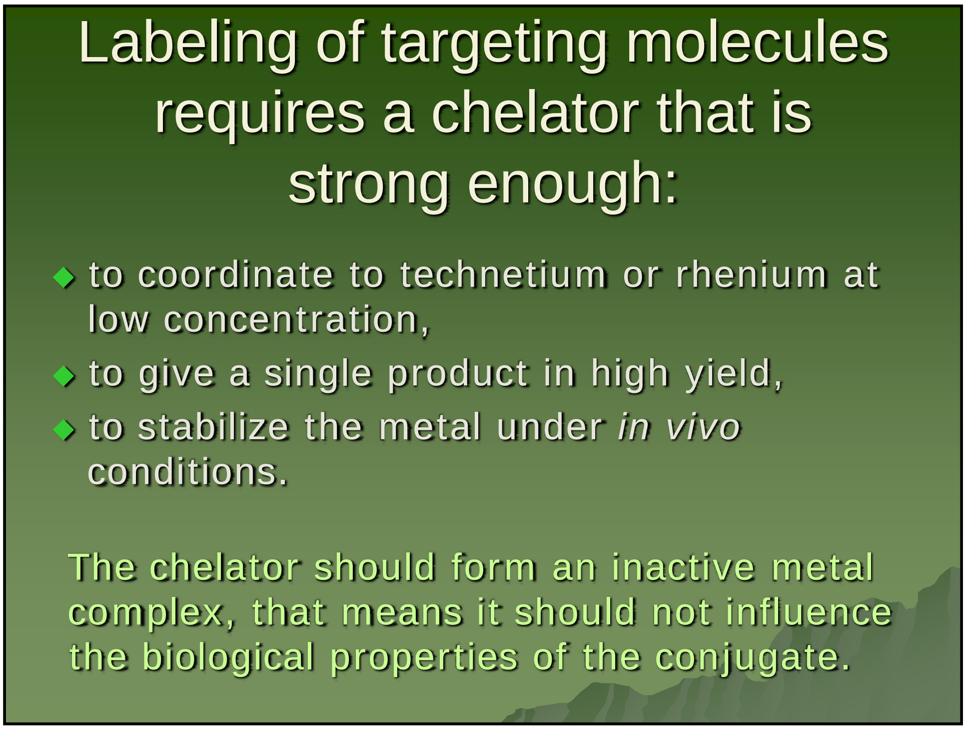

Labeling of targeting molecules requires a chelator that is strong enough:

- to coordinate to technetium or rhenium at low concentration,
- to give a single product in high yield,
- to stabilize the metal under *in vivo* conditions.

The chelator should form an inactive metal complex, that means it should not influence the biological properties of the conjugate.

BCA - bifunctional chelating agents

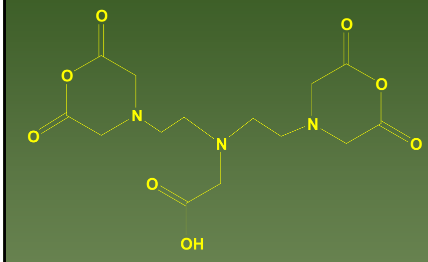

DADTPA

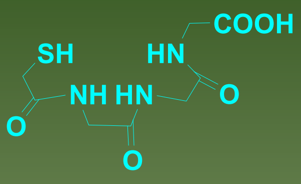

MAG_3

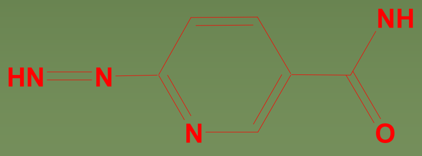

HYNIC

DTPA analogues

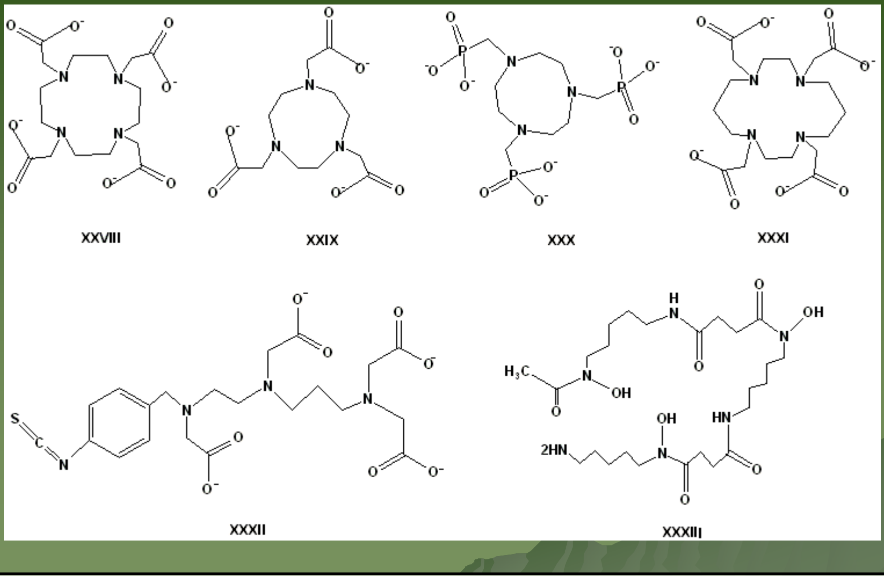

DTPA analogue - DOTA

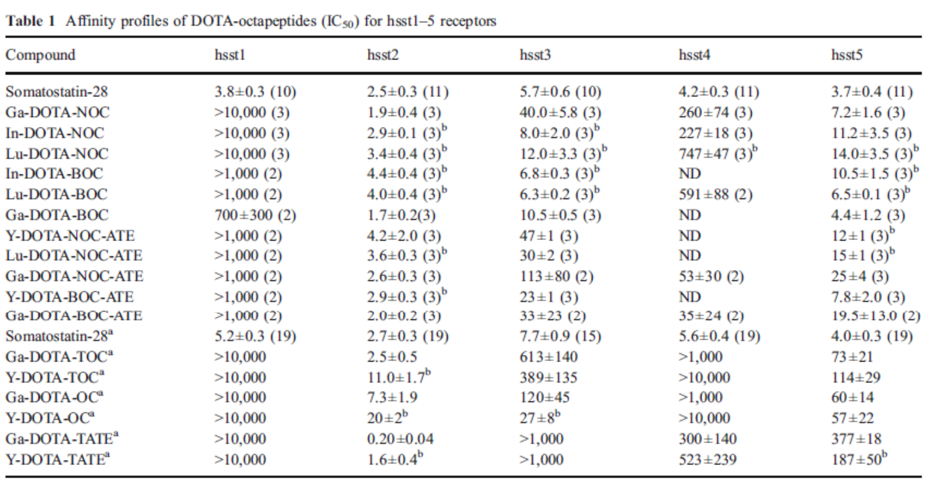

Table 1 Affinity profiles of DOTA-octapeptides (IC_{50}) for hsst1–5 receptors

Compound	hsst1	hsst2	hsst3	hsst4	hsst5
Somatostatin-28	3.8±0.3 (10)	2.5±0.3 (11)	5.7±0.6 (10)	4.2±0.3 (11)	3.7±0.4 (11)
Ga-DOTA-NOC	>10,000 (3)	1.9±0.4 (3)	40.0±5.8 (3)	260±74 (3)	7.2±1.6 (3)
In-DOTA-NOC	>10,000 (3)	2.9±0.1 (3)^b	8.0±2.0 (3)^b	227±18 (3)	11.2±3.5 (3)
Lu-DOTA-NOC	>10,000 (3)	3.4±0.4 (3)^b	12.0±3.3 (3)^b	747±47 (3)^b	14.0±3.5 (3)^b
In-DOTA-BOC	>1,000 (2)	4.4±0.4 (3)^b	6.8±0.3 (3)^b	ND	10.5±1.5 (3)^b
Lu-DOTA-BOC	>1,000 (2)	4.0±0.4 (3)^b	6.3±0.2 (3)^b	591±88 (2)	6.5±0.1 (3)^b
Ga-DOTA-BOC	700±300 (2)	1.7±0.2(3)	10.5±0.5 (3)	ND	4.4±1.2 (3)
Y-DOTA-NOC-ATE	>1,000 (2)	4.2±2.0 (3)	47±1 (3)	ND	12±1 (3)^b
Lu-DOTA-NOC-ATE	>1,000 (2)	3.6±0.3 (3)^b	30±2 (3)	ND	15±1 (3)^b
Ga-DOTA-NOC-ATE	>1,000 (2)	2.6±0.3 (3)	113±80 (2)	53±30 (2)	25±4 (3)
Y-DOTA-BOC-ATE	>1,000 (2)	2.9±0.3 (3)^b	23±1 (3)	ND	7.8±2.0 (3)
Ga-DOTA-BOC-ATE	>1,000 (2)	2.0±0.2 (3)	33±23 (2)	35±24 (2)	19.5±13.0 (2)
Somatostatin-28^a	5.2±0.3 (19)	2.7±0.3 (19)	7.7±0.9 (15)	5.6±0.4 (19)	4.0±0.3 (19)
Ga-DOTA-TOC^a	>10,000	2.5±0.5	613±140	>1,000	73±21
Y-DOTA-TOC^a	>10,000	11.0±1.7^b	389±135	>10,000	114±29
Ga-DOTA-OC^a	>10,000	7.3±1.9	120±45	>1,000	60±14
Y-DOTA-OC^a	>10,000	20±2^b	27±8^b	>10,000	57±22
Ga-DOTA-TATE^a	>10,000	0.20±0.04	>1,000	300±140	377±18
Y-DOTA-TATE^a	>10,000	1.6±0.4^b	>1,000	523±239	187±50^b

MAG_3 and its analogues

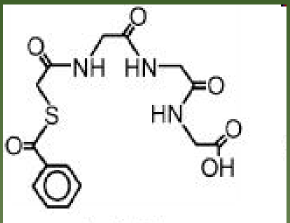

betiatide

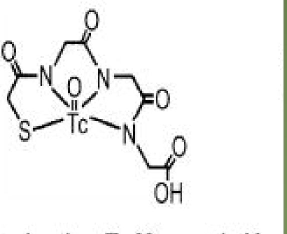

technetium Tc 99m mertiatide

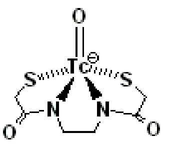

XXXIV

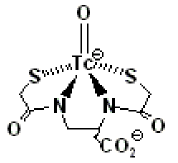

XXXV

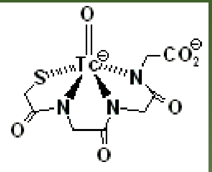

XXXVI

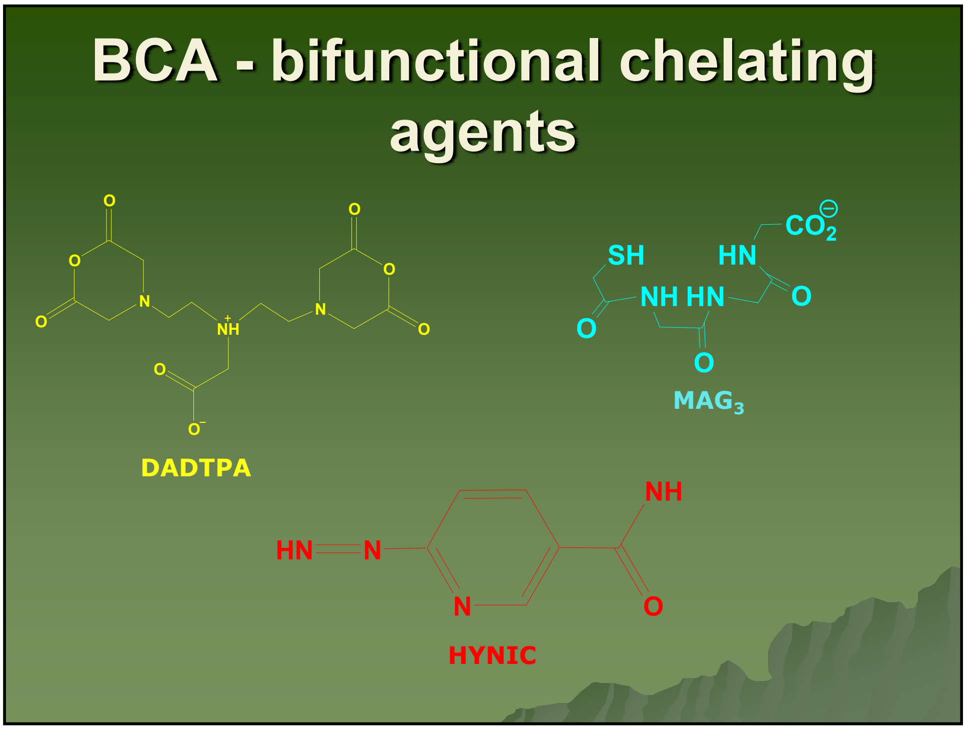

BCA - bifunctional chelating agents

DADTPA

MAG_3

HYNIC

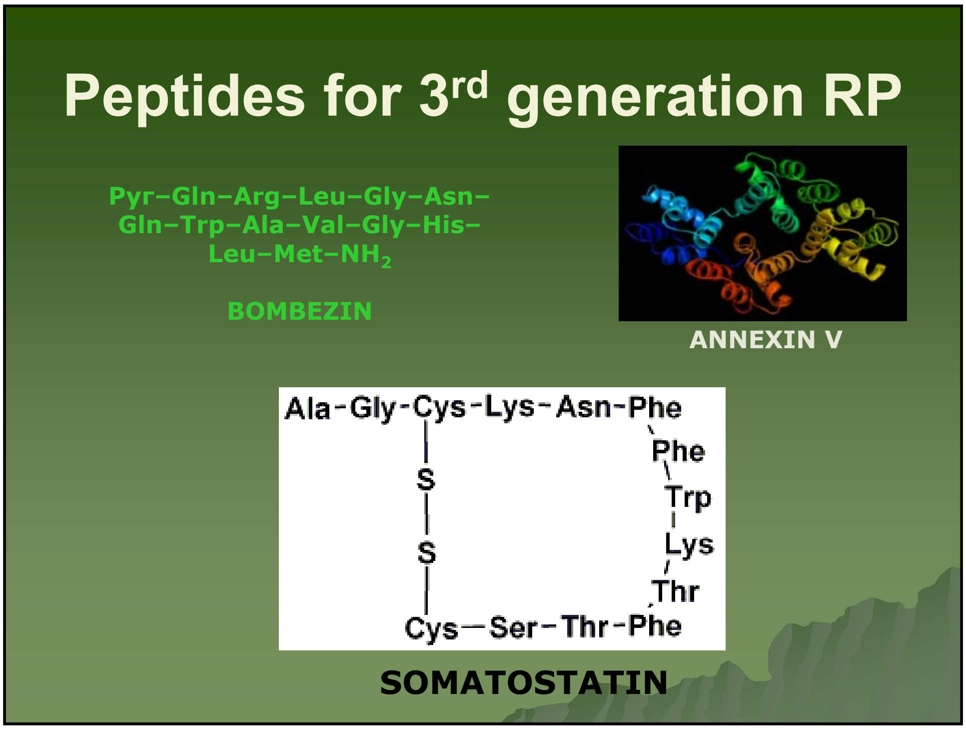

Peptides for 3rd generation RP

Pyr–Gln–Arg–Leu–Gly–Asn–
Gln–Trp–Ala–Val–Gly–His–
Leu–Met–NH_2

BOMBEZIN

ANNEXIN V

SOMATOSTATIN

Somatostatin synthetic analogues

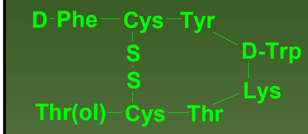

TOC

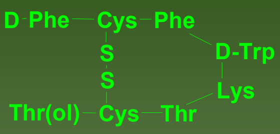

OCT

Vaptreotide

^{111}In

Labeling biomolecules with ^{99m}Tc using BCA

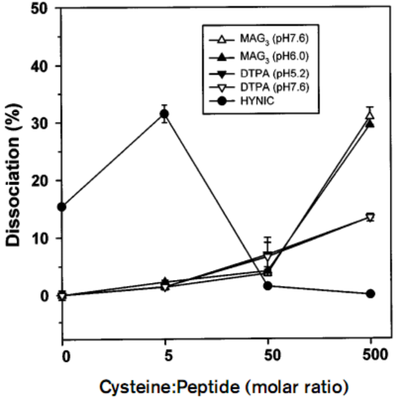

Fig. 3. The results of a cysteine challenge assay of labelled HNE2 showing the percent transchelation of ^{99}Tc^{m} from peptide to cysteine after a 1 h incubation in saline at 37°C, and in solutions of cysteine at three different concentrations at 37°C. Abbreviations as in the legend to Fig. 1.

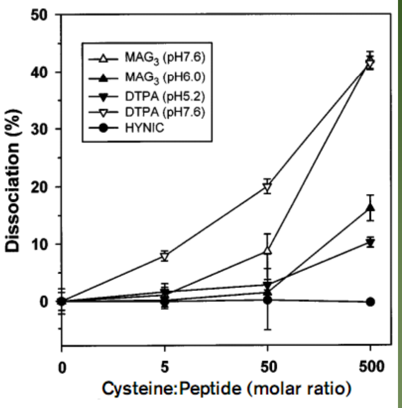

Fig. 4. The results of a cysteine challenge assay of labelled HNE4 showing the percent transchelation of ^{99}Tc^{m} from peptide to cysteine after a 1 h incubation in 37°C saline and in solutions of cysteine at three different concentrations at 37°C. Abbreviations as in the legend to Fig. 1.

Nuclear Medicine Communications, 2001, **22**, 203–215

Labeling of targeting molecules requires a chelator that is strong enough:

- to coordinate to technetium or rhenium at low concentration,
- to give a single product in high yield,
- to stabilize the metal under *in vivo* conditions.

The chelator should form an inactive metal complex, that means it should not influence the biological properties of the conjugate.

Cell accumulation of ^{99m}Tc versus time in tissue culture

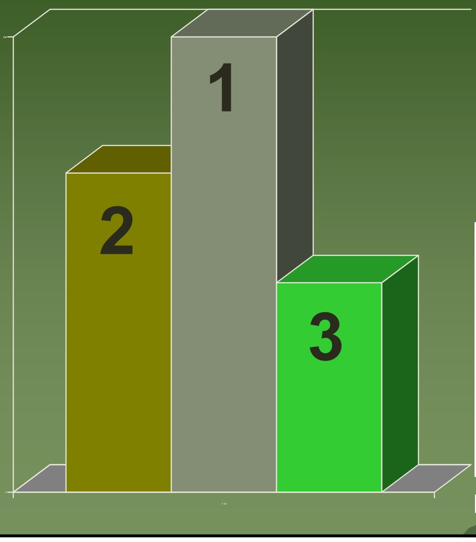

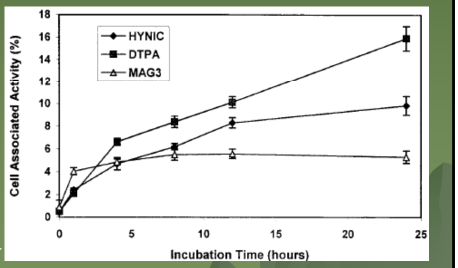

European Journal of Nuclear Medicine Vol. 27, No. 11, November 2000

Efflux of ^{99m}Tc versus time from cells in tissue culture after preincubation

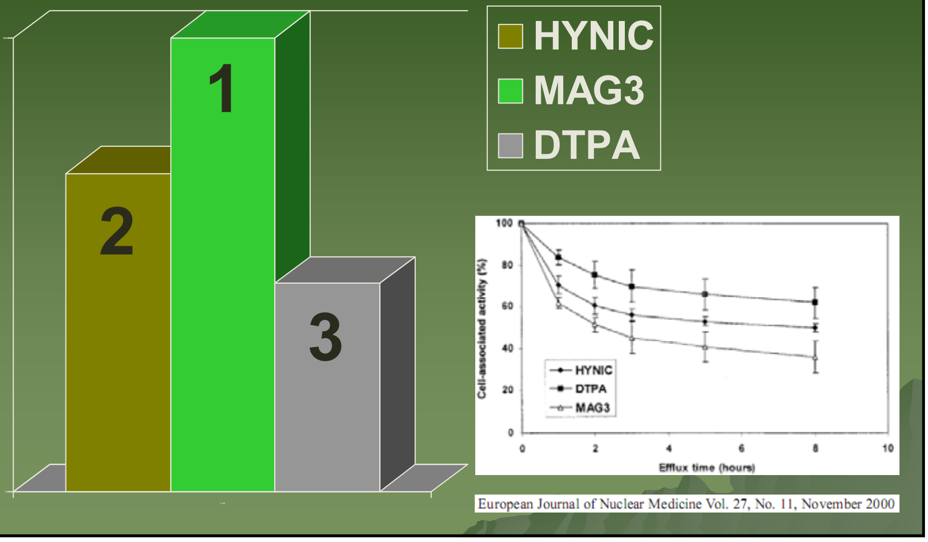

European Journal of Nuclear Medicine Vol. 27, No. 11, November 2000

HYNIC - 6-Hydrazinopyridine-3-carboxylic acid

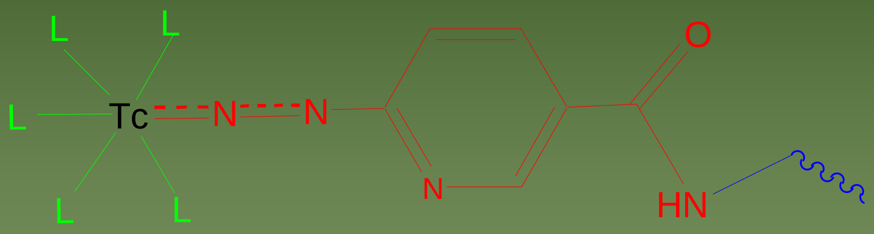

HYNIC co-ligands

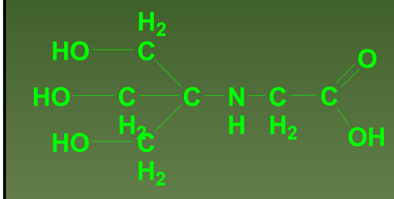

tricine

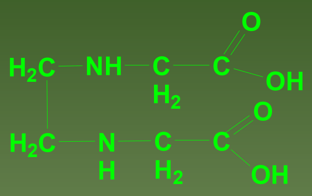

EDDA

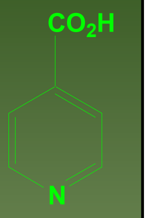

ISONIC

Biodistribution: peptides and coligands

Organ /tissue	^{99m}*Tc-HYNIC-*Vaptreotide-tricine	^{99m}*Tc-HYNIC-*Vaptreotide-EDDA	^{99m}*Tc-HYNIC-*TOC- tricine	^{99m}*Tc-HYNIC-*TOC- EDDA	^{99m}*Tc-HYNIC-*OCT-tricine	^{99m}*Tc-HYNIC-*OCT-EDDA
Tumor	3,5±0,5*[30]	2±1* [30]	~1* [27] 10±1* [30] ~3,5* [40]	10±2* [30] ~3* [40]	~2,5* [40]	2±1* [40]
Kidneys	~6** [20] 8±1** [28] 13±2*[29]	11±5* [30]	~1*** [21] ~9* [27] ~14** [27] 15±3* [30] 11±1* [40] ~2,5**** [41]	5±1* [30] 9±1* [40]	13±2** [28] 11,5±1* [40]	9±1* [40]
Liver	~26** [20] 10±2** [28] 16±5* [30]	8±1* [30]	~0,2*** [21] ~2* [22] ~2** [27] ~2* [30] ~1* [40]	~1* [30] ~1* [40]	~3** [28] ~2,5* [40]	~1* [40]

*** - mice with tumor, ** - normal mice, *** - normal rats**

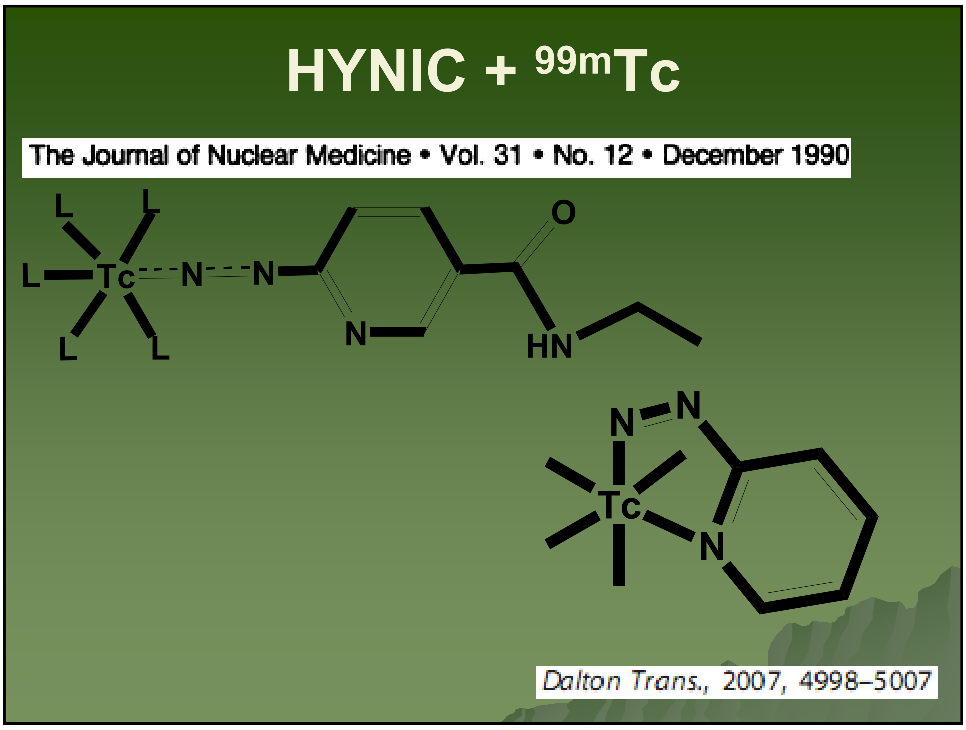

HYNIC + ^{99m}Tc

The Journal of Nuclear Medicine • Vol. 31 • No. 12 • December 1990

Dalton Trans., 2007, 4998–5007

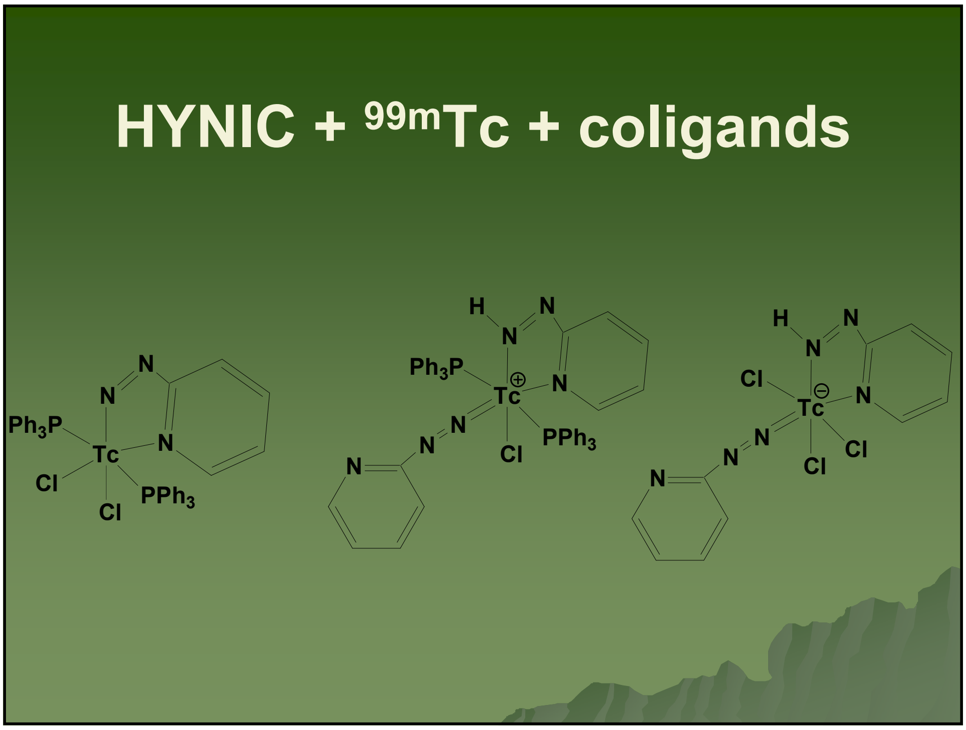

HYNIC + ^{99m}Tc + coligands

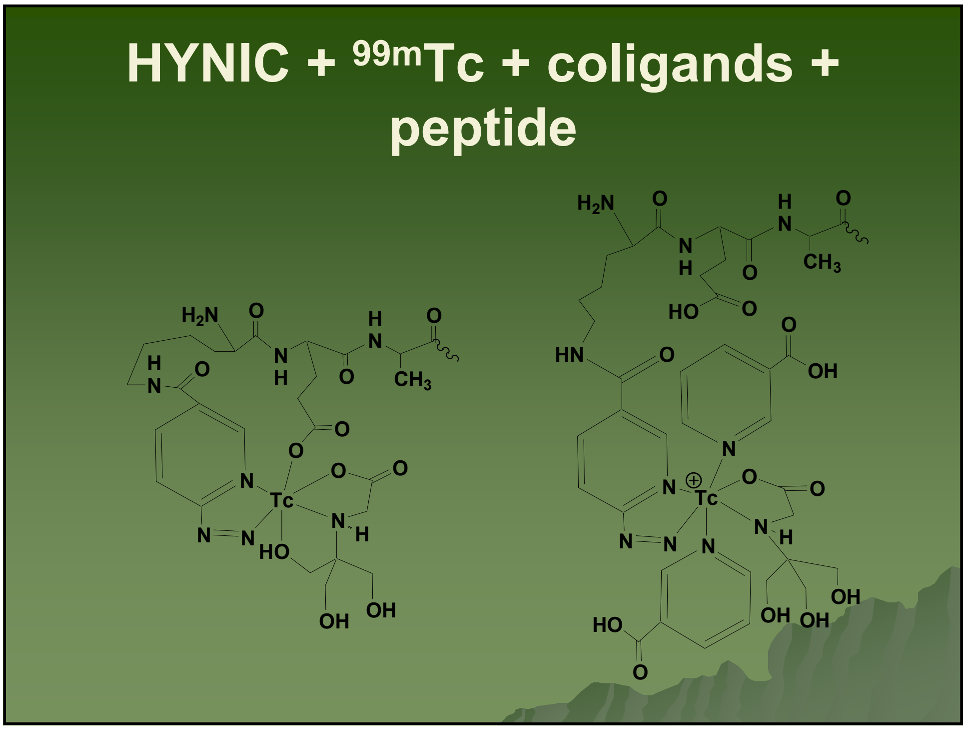

HYNIC + ^{99m}Tc + coligands + peptide

2011, Poland

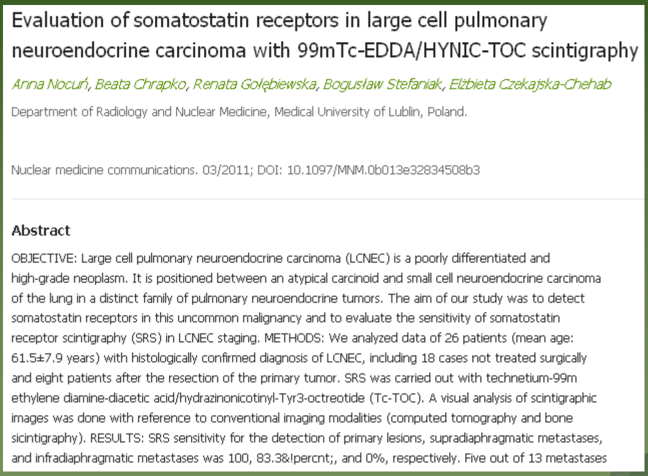

Evaluation of somatostatin receptors in large cell pulmonary neuroendocrine carcinoma with 99mTc-EDDA/HYNIC-TOC scintigraphy

Anna Nocuń, Beata Chrapko, Renata Gołębiewska, Bogusław Stefaniak, Elżbieta Czekajska-Chehab

Department of Radiology and Nuclear Medicine, Medical University of Lublin, Poland.

Nuclear medicine communications. 03/2011; DOI: 10.1097/MNM.0b013e32834508b3

Abstract

OBJECTIVE: Large cell pulmonary neuroendocrine carcinoma (LCNEC) is a poorly differentiated and high-grade neoplasm. It is positioned between an atypical carcinoid and small cell neuroendocrine carcinoma of the lung in a distinct family of pulmonary neuroendocrine tumors. The aim of our study was to detect somatostatin receptors in this uncommon malignancy and to evaluate the sensitivity of somatostatin receptor scintigraphy (SRS) in LCNEC staging. METHODS: We analyzed data of 26 patients (mean age: 61.5±7.9 years) with histologically confirmed diagnosis of LCNEC, including 18 cases not treated surgically and eight patients after the resection of the primary tumor. SRS was carried out with technetium-99m ethylene diamine-diacetic acid/hydrazinonicotinyl-Tyr3-octreotide (Tc-TOC). A visual analysis of scintigraphic images was done with reference to conventional imaging modalities (computed tomography and bone sicintigraphy). RESULTS: SRS sensitivity for the detection of primary lesions, supradiaphragmatic metastases, and infradiaphragmatic metastases was 100, 83.3&!percnt;, and 0%, respectively. Five out of 13 metastases

Conclusions

- BCA are the future of modern nuclear medicine
- BCA radiopharmaceuticals with 99mTc must take part to routine medical studies
- The most promising BCA for today are DTPA, MAG_3 and HYNIC
- Giving a little preference between these agents to HYNIC
- Choice of coligand(s) – the way to improve biocinetic properties radiopharmaceuticals with HYNIC
- Best coligands for today are tricine and EDDA
- way to choose coligand(s) - studying the structure of complexes

Thank you!

SORPTION PRECONCENTRATION OF RADIONUCLIDES USING DETONATION NANODIAMONDS

Yulia P. Buchatskaya,[1] **Anna Yu. Romanchuk**[1], **Andrei A. Shiryaev**[2], **Inna I. Kulakova**[1], **Stepan N. Kalmykov**

1) *Lomonosov Moscow State University, Chemistry Department*
julia.buchatskaya@gmail.com
2) *Frumkin Institute of Physical Chemistry and Electrochemistry of RAS*

Nanodiamonds (ND) obtained by detonation of explosives (eg, TNT and RDX) with a negative oxygen balance, are potentially promising carbon nanomaterial with a highly developed surface (250-300 m^2 / g or more), a large number of oxygen-containing functional groups on it, chemical and radiation resistance, economically viable and relatively easy production [1].

These unique properties of ND can be used to isolate alpha-emitting radionuclides from liquid radioactive waste for further vitrification and actinides subsequent separation for analytical purposes.

The aim of this work was to establish the sorption behavior of radionuclides (Tc(VII), U(VI), Np(V), Th(IV), Pu(IV), Am(III), Eu(III) and Sr(II)) on detonation ND and to determine the effect of functionalization of the surface on the sorption.

Kinetics of sorption shows that steady state condition is achieved within first 30 minutes of interaction.

. Figure 1 shows dependence of actinide sorption on pH suspension. The sorption is very high for U(VI), Th(IV), Am(III) and Pu(IV) even in the range of pH 1-3. The high sorption of Tc(VII) on ND in solutions of hydrochloric and nitric acids was obtained. The sorption capacity of ND was defined. It is comparable with respect to U(VI) to the values typical for other carbon materials.

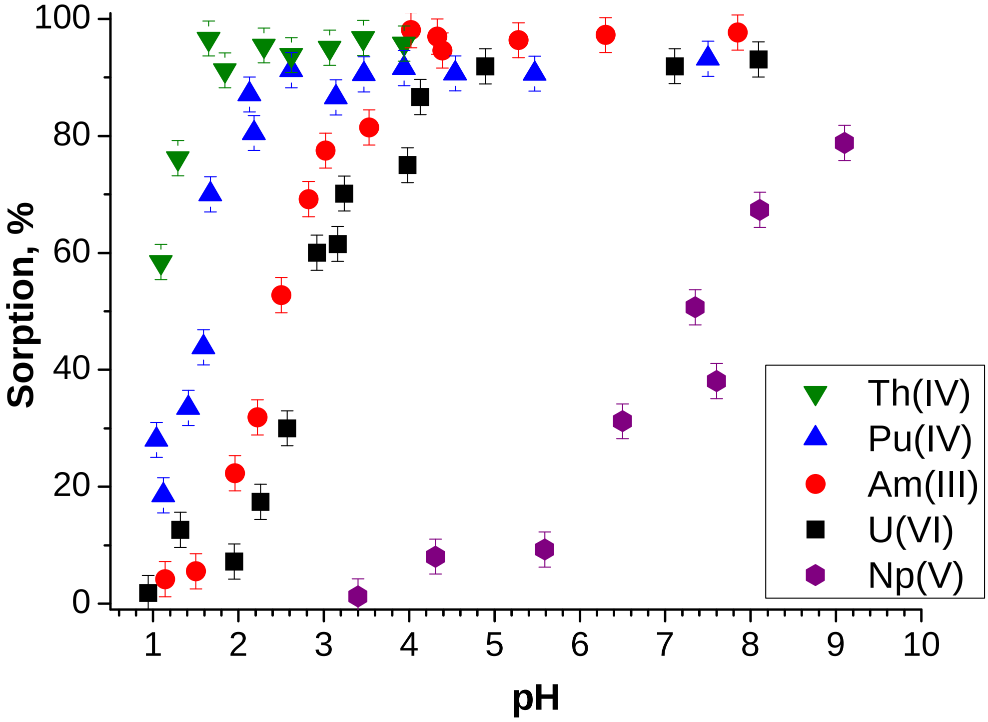

Fig. 1. pH-dependence of actinide sorption on non-modified ND.

In our experiments different types of ND were used: treated with hydrogen (800 °C, 5 h) ozone, air (400°C, 5 h) and ND functionalized with different groups by covalent grafting (glycine and CN-group).

The different types of ND were characterized by IR spectroscopy, X-ray photoelectron spectrometry and measurements of ζ-potential at different pH of the suspensions and the particle size using Dynamic Light Scattering.

It was observed that sorption of U(VI) on non-modified ND is higher than on modified ND at the same pH. This effect can be explained by presence of more carboxylic acid groups on the non-modified ND surface.

Efficiency of Tc(VII) sorption onto ND functionalized by different groups is very similar. This effect can be explained by resistance of effective sorption sites to modification. Such similarity contrasts the results reported in [2], where type of the surface treatment was shown to be important.

[1] V.Yu. Dolmatov, *Russian Chemical Reviews*, **70** 607 (2001)
[2] Obruchnikova Ya.A. et al., *Proc. of 7th Int. Symp. On Technetium and Rhenium – Science and Utilization*, Moscow, 439 (2011)

MOSCOW STATE UNIVERSITY
CHEMISTRY DEPARTMENT, DIVISION OF RADIOCHEMISTRY
LABORATORY OF DOSIMETRY AND ENVIRONMENTAL RADIOACTIVITY

Sorption preconcentration of radionuclides using detonation nanodiamonds

Yulia P. Buchatskaya –

Lomonosov Moscow State University, Chemistry Department

Detonation nanodiamonds – Production methods and properties

Detonation of O-poor explosives (TNT/hexogen…) in a closed volume

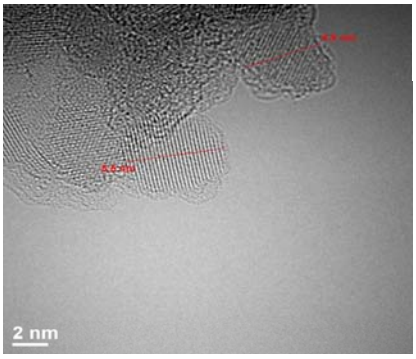

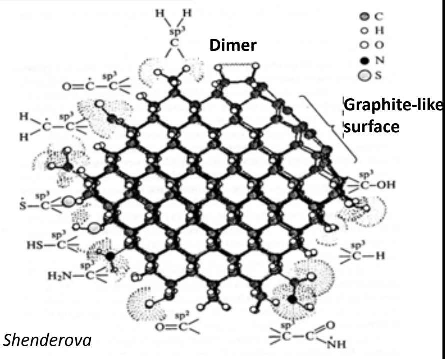

O. Shenderova

- **Narrow size distribution 4-5 nm**
- **Aggregation into larger very stable clusters (100-200 nm)**

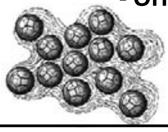

- **High surface area: 150-400 m^2/g**
- **Functional surface groups:**
  - **OH, >C=O, -COOH, -NH$_2$**

Detonation nanodiamonds

Advantages:

- ✓ Small size (4-5 nm)
- ✓ Mass production and relatively low price
- ✓ Chemical and radiation resistance
- ✓
- ✓
- ✓
- ✓ Biological compatibility (virtually nontoxic)

To establish the sorption behavior of radionuclides on detonation ND

Problems:

Very strong aggregation of nanograins: difficult (but possible!) to separate individual particles

Characterization of nanodiamonds

IR-spectroscopy

X-ray photoelectron spectroscopy

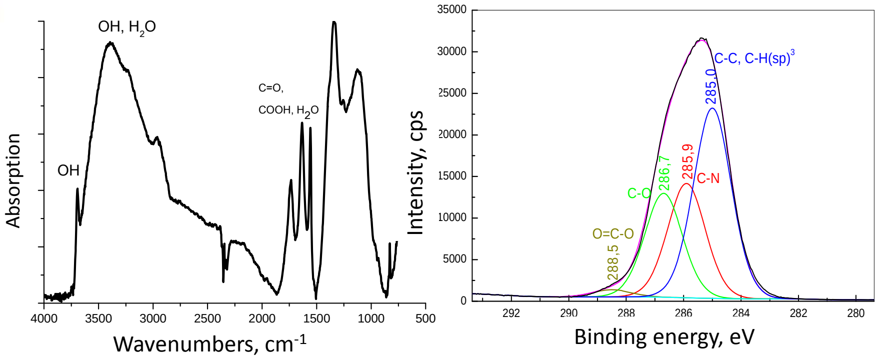

U(VI) sorption on ND

Radionuclides concentration:
$C = 10^{-10} – 10^{-7}$ M
Nanodiamonds content:
$C_{ND} = 6\cdot10^{-2}$ g/l

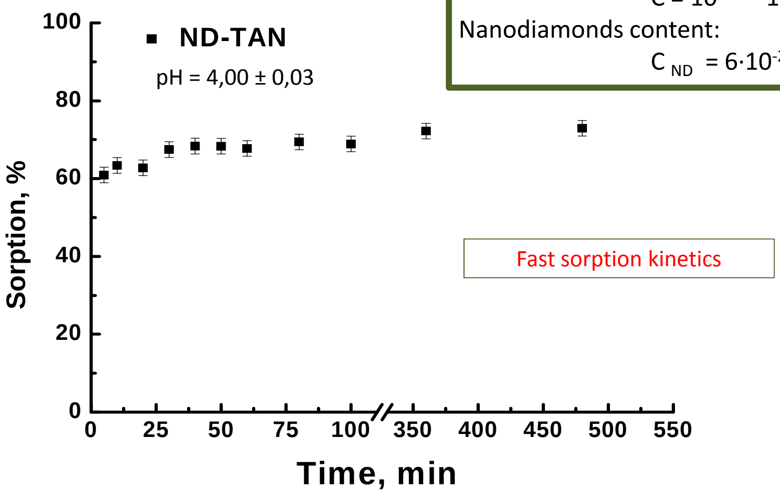

---

pH – dependence of nuclides sorption on ND-TAN

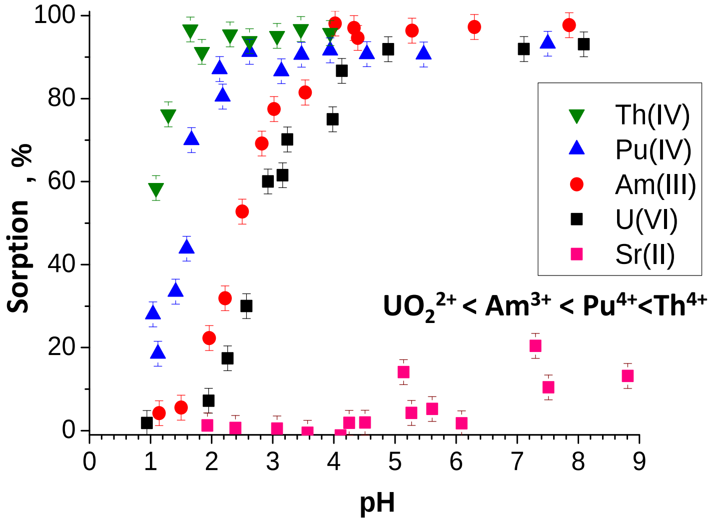

$UO_2^{2+} < Am^{3+} < Pu^{4+} < Th^{4+}$

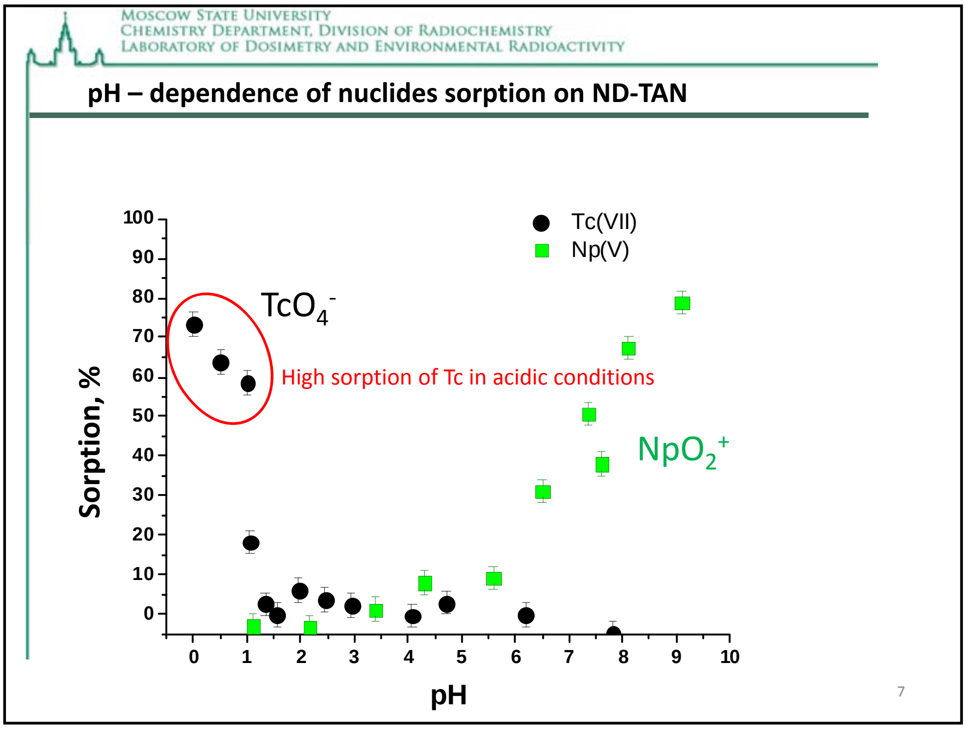

pH – dependence of nuclides sorption on ND-TAN

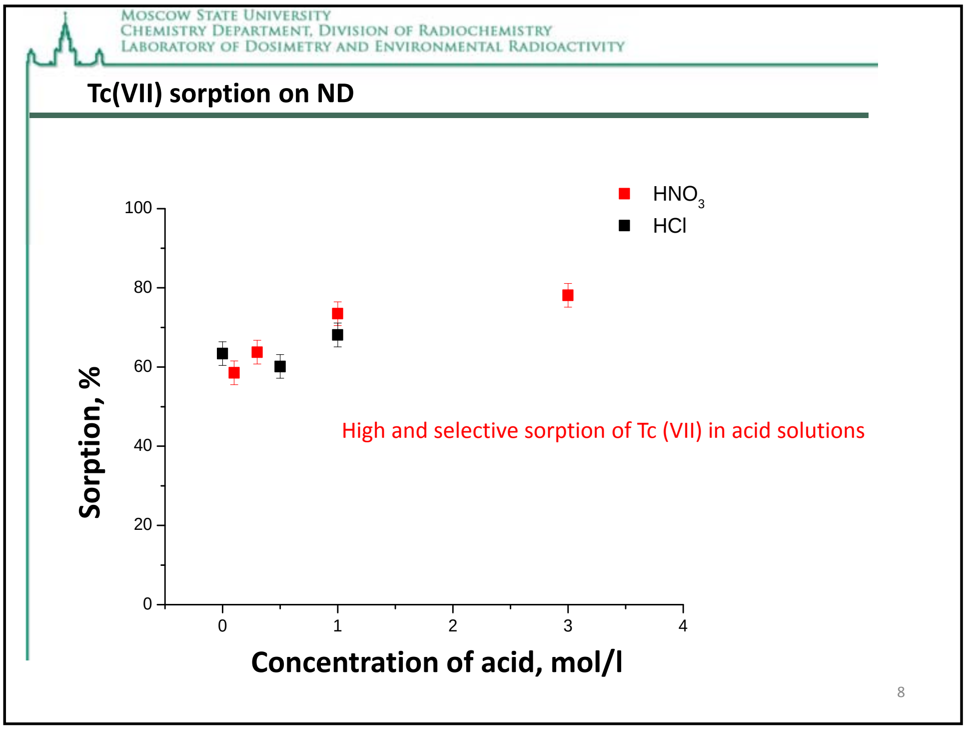

Tc(VII) sorption on ND

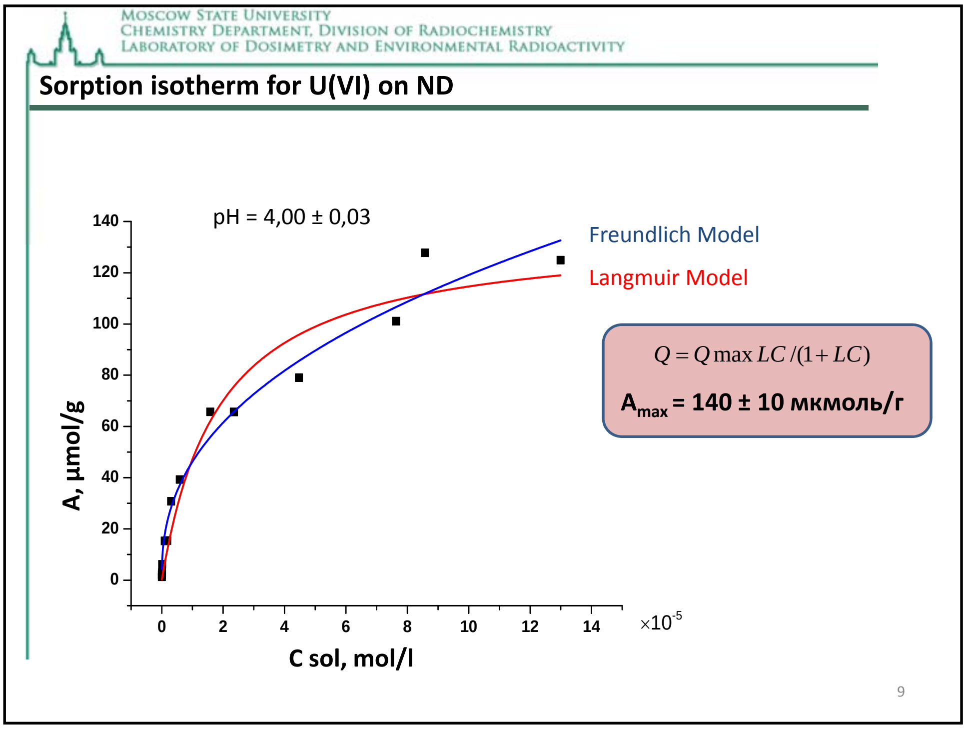

Sorption isotherm for U(VI) on ND

pH = 4,00 ± 0,03

$$Q = Q\max LC/(1+LC)$$

A_{max} = 140 ± 10 мкмоль/г

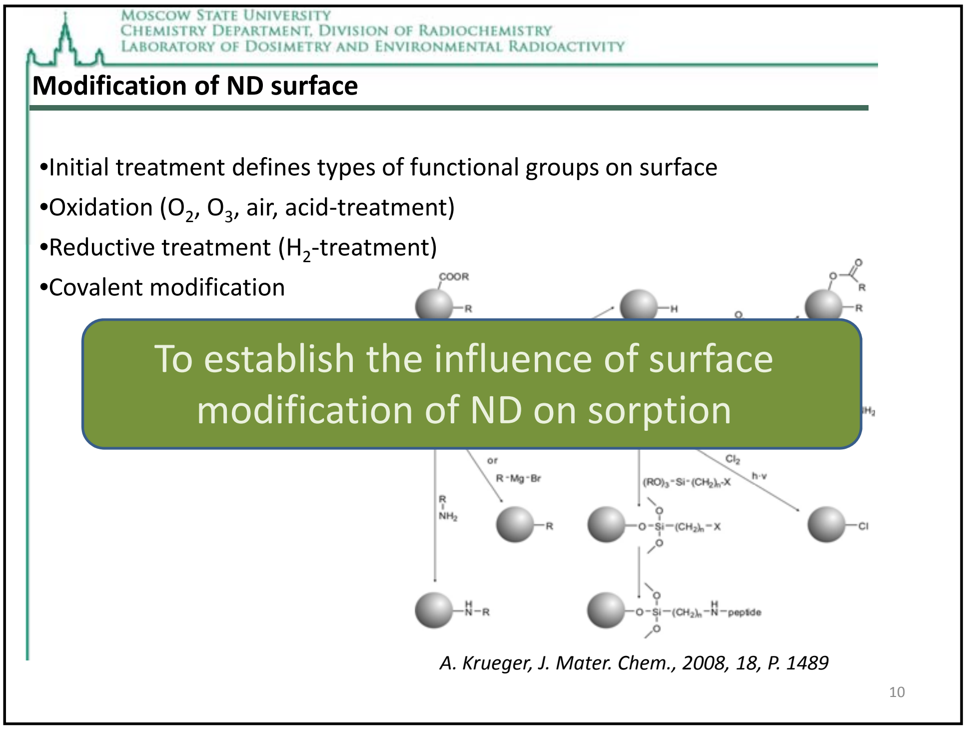

Modification of ND surface

- Initial treatment defines types of functional groups on surface
- Oxidation (O_2, O_3, air, acid-treatment)
- Reductive treatment (H_2-treatment)
- Covalent modification

To establish the influence of surface modification of ND on sorption

A. Krueger, J. Mater. Chem., 2008, 18, P. 1489

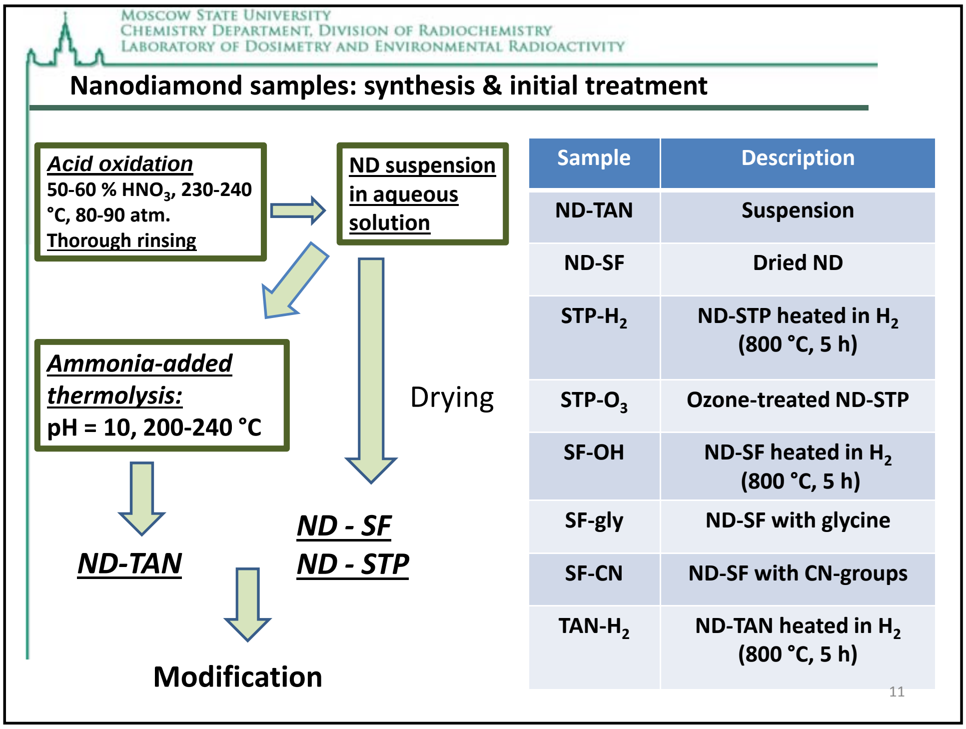

Moscow State University
Chemistry Department, Division of Radiochemistry
Laboratory of Dosimetry and Environmental Radioactivity

Nanodiamond samples: synthesis & initial treatment

Acid oxidation
50-60 % HNO_3, 230-240 °C, 80-90 atm.
Thorough rinsing

ND suspension in aqueous solution

Ammonia-added thermolysis:
pH = 10, 200-240 °C

Drying

ND-TAN

ND - SF
ND - STP

Modification

Sample	Description
ND-TAN	Suspension
ND-SF	Dried ND
STP-H_2	ND-STP heated in H_2 (800 °C, 5 h)
STP-O_3	Ozone-treated ND-STP
SF-OH	ND-SF heated in H_2 (800 °C, 5 h)
SF-gly	ND-SF with glycine
SF-CN	ND-SF with CN-groups
TAN-H_2	ND-TAN heated in H_2 (800 °C, 5 h)

11

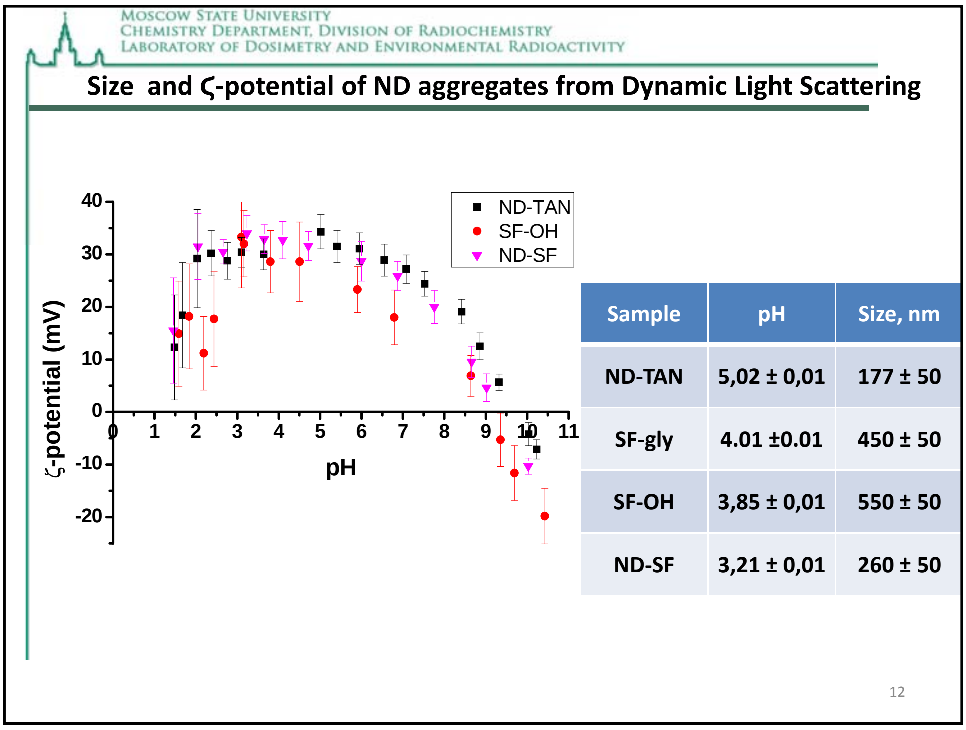

Moscow State University
Chemistry Department, Division of Radiochemistry
Laboratory of Dosimetry and Environmental Radioactivity

Size and ς-potential of ND aggregates from Dynamic Light Scattering

Sample	pH	Size, nm
ND-TAN	5,02 ± 0,01	177 ± 50
SF-gly	4.01 ±0.01	450 ± 50
SF-OH	3,85 ± 0,01	550 ± 50
ND-SF	3,21 ± 0,01	260 ± 50

12

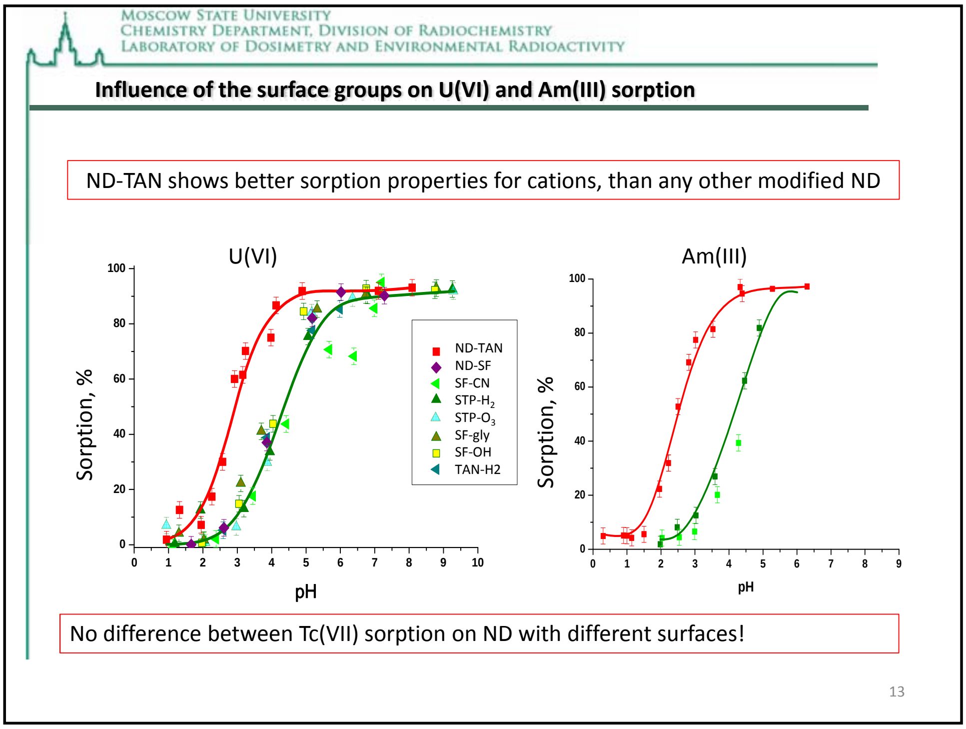

Moscow State University
Chemistry Department, Division of Radiochemistry
Laboratory of Dosimetry and Environmental Radioactivity

Influence of the surface groups on U(VI) and Am(III) sorption

ND-TAN shows better sorption properties for cations, than any other modified ND

No difference between Tc(VII) sorption on ND with different surfaces!

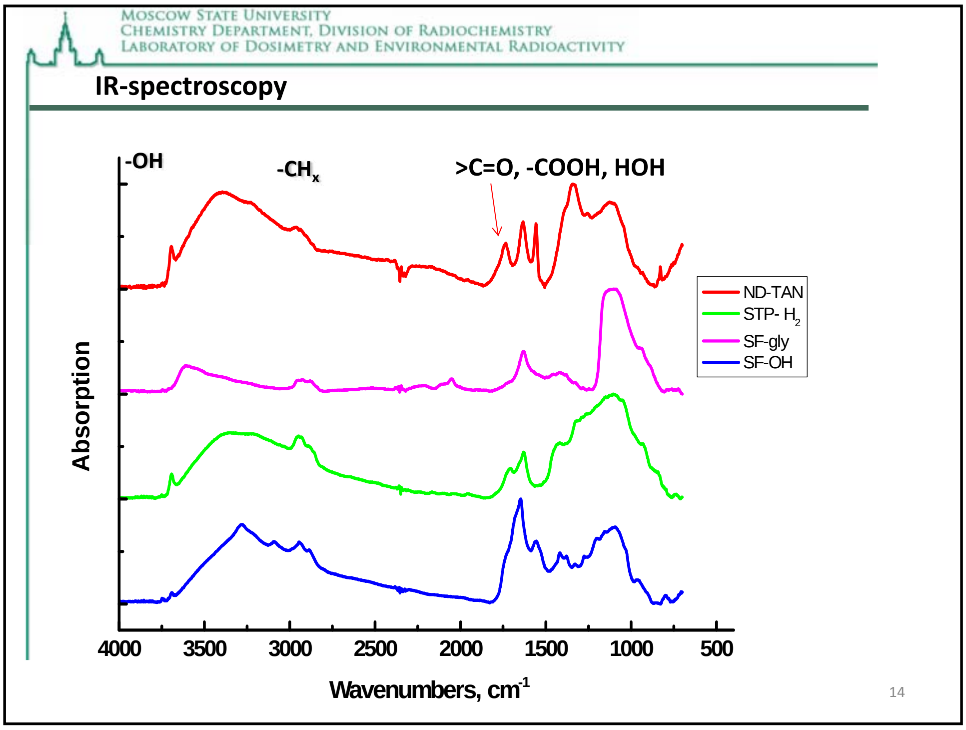

Moscow State University
Chemistry Department, Division of Radiochemistry
Laboratory of Dosimetry and Environmental Radioactivity

IR-spectroscopy

Conclusions

1. **Nanodiamonds are useful sorbents for radionuclides.**
2. Steady state condition is achieved within first 30 minutes of interaction.
3. The sorption is very high for U(VI), Th(IV), Am(III) and Pu(IV) even in the range of pH 1-3.
4. The high sorption of Tc(VII) on ND in solutions of hydrochloric and nitric acids was obtained.
5. The sorption capacity of ND was defined. It is comparable with respect to U(VI) to the values typical for other carbon materials.
6. Sorption of U(VI) on ND-TAN is higher than on any other modified ND at the same pH. This effect can be explained by presence of more carboxylic acid groups on the ND-TAN surface.
7. Efficiency of Tc(VII) sorption onto ND functionalized by different groups is very similar. This effect can be explained by resistance of effective sorption sites to modification.

Thanks to…

- Ann Yu. Romanchuk – PhD of Lomonosov MSU, Faculty of Material Sciencies,
- Dr. Inna I. Kulakova - Division of Petroleum Chemistry and Organic catalysis of Lomonosov MSU,
- Prof. Stepan N. Kalmykov - Head of Radiochemistry division of Lomonosov MSU,
- Dr. Andrei A. Shiryaev - Frumkin Institute of Physical Chemistry and Electrochemistry of RAS

SUPRAMOLECULAR POLYMER SYSTEMS BASED ON IONIC LIQUIDS - TETRADECYL PHOSPHONIUM SALTS AS ION SELECTIVE ELECTRODE MEMBRANES FOR THE DETERMINATION OF *CLOSO*-BORATE ANIONS

* A.V.Kopytin, * K.Y.Zhizhin, * Y.A.Politov, +A.F.Zhukov, × K.E.German, *N.T. Kuznetsov

* N S Kurnakov Institute of General and Inorganic Chemistry of the Russian Academy of Sciences (IGIC RAS)
+ Mendeleyev University of Chemical Technology of Russia
× A N Frumkin Institute of Physical Chemistry and Electrochemistry.

Potentiometric methods based on ion selective electrodes (potentiometric sensors) refer to the methods of non-destructive testing of solutions and due to comparative simplicity, rapidity and high selectivity these methods are widely used in the practice of chemical analysis [1-2]. At present there are many different types of potentiometric sensors for the determination of various ions in water solutions [3].

For determination of the lipophilic anions, ion selective potentiometric sensors which are based on ion associates are widely used [4-5]. The ion selectivity for this class of sensors depends on the energy of ionic hydration. Therefore, the selectivity to anions can be arranged in the Hofmeister series [4]. Typical polymer membrane of such sensor minimum has three components of the polymer - plasticizer - carrier ions (ionophore) and it is common supramolecular system, where the electroanalytical properties are highly dependent on the ratio of the components.

The research has shown that some ionic associates, based on onium salts (ammonium and phosphonium), form the ionic liquid compositions with $T_m < 0$ ° C and thus are good plasticizers of polyvinyl chloride (PVC), mixable with it in a wide range of concentrations. So it is possible to obtain a polymer membrane with ion permeability, which contain only two components: polymer (PVC) and the ionic liquid, which served two functions simultaneously: ionophore and PVC plasticizer [6-7]. Originally, the first such ionic liquids were suggested in 1982 by the team of scientists headed by academician E. Pungor (Budapest Technical University). They tested the liquid salts of tetradecylphosphonium trichloromercurate [8, 9] and tetradecyl phosphonium tetrachlorotallate [10-11] successfully for the development of $[HgCl_3]^-$ - and $[TlCl_4]^-$ - selective electrodes. It was shown that ionic liquids were well compatible with PVC in various weight ratios at room temperature. Using this property of tetradecylphosphonium salts (such as PVC plasticizers), it was managed to get the polymer compositions, which help to made the first electrodes with ionic liquids, that are also served as a plasticizer and elektrodoaktive component. This developed electrodes have several advantages over traditional (PVC plasticizer-exchanger), in particular for the limit detection [8-11]. The identified advantages of membrane electrodes based on ionic liquids were confirmed for $[Au(CN)]_2^-$-selective electrodes, which are based on ionic liquid dicyanoaurate tetradecyl phosphonium [12].

Nowadays the salts with cluster boron anions - *closo*-borates, are widely used in various fields of science and technology. In particular, it is due to the high boron ability of isotope ^{10}B to capture of neutrons. One of the most important practical applications of these compounds is the ^{10}B-neutron capture therapy (^{10}B-NCT) of tumors [13-14]. For the successful actualization of ^{10}B-NCT it is necessary to have express-monitoring boron content of the drug in the tissue (tumor) and fluids (blood), which can be done with using of ion selective sensor with high selectivity towards anions *closo*-borates. Our research has shown that many quaternary onium bases with such anions are ionic liquids that are compatible with the entire range of PVC-weight ratios.

Below we consider some properties of the self-organiged supramolecular systems, which contain polyvinylchloride and liquid ion exchanger based on different ionic liquids with *closo*-borates anions, in terms of their using as an ion selective membrane of potentiometric sensors.

EXPERIMENTAL PART

Preparation of elektrodoaktive membranes components (ionophores)

Ionophores – are the salts of tetradecyl phosphonium with the *closo* - borate anions obtained by the extraction method (ion exchange extraction). For this purpose, a water solution of 0.01 M $[(C_{10}H_{21})_4P]Br$ in chloroform (liquid ion exchanger) contacts with 0.01 M water solutions of cesium salts of the corresponding *closo* - borates: $Cs_2[B_{10}H_{10}]$, $Cs_2[B_{12}H_{12}]$ in the phase ratio of the Waters: Organic component = 1: 1. As a result of ion exchange the *closo* – borate anions will transfer in the organic phase. As the research work has shown that one contact is sufficient for a complete substitution (> 99%) of bromide - ions in liquid ion exchanger for *closo* – borate anions. The completeness replacement controlled by content Br^- - ions in the water phase after extraction by ionometric method (using bromide - selective electrode). The organic phase was separated and washed by distilled water and then chloroform was removed by evaporation at room temperature. As a result, it was produced a ductile oils - ionic liquids with freezing point <0 ° C.

The resulting ionic liquids were identified by elemental analysis, infrared spectroscopy (IR) and nuclear magnetic resonance (NMR) ^{11}B:

$((C_{10}H_{21})_4P)_2[B_{10}H_{10}]$ (98% yield) – IR: 2444 cm^{-1}(ν_{B-H}), NMR ^{11}B: -0,6 (d, 2B), -28,7 (d, 8B);
$((C_{10}H_{21})_4P)_2[B_{12}H_{12}]$ (98% yield) - IR: 2462 cm^{-1} (ν_{B-H}), NMR ^{11}B: -15,9 (d, 12B).

Elemental analysis for carbon and hydrogen was carried out on automatic gas analyzer CHNS-3 FA 1108 Elemental Analyser (Carlo Erba). The containing of boron and phosphorus in the samples was determined by atomic absorption spectrometry with electrothermic atomization on spectrometers Perkin Elmer, model 2100 (with HGA-700) and 403 (with HGA-72). IR-spectrums of compounds were recorded on IR Fourier – spectrometer **Infralum FT-02** in the field 400-4000 cm^{-1}. The samples were prepared by suspending of the substance in nujol or in «Fluorolube». ^{11}B, ^{11}B-{^1H} NMR spectra of compounds (in CH_3CN) were recorded on the spectrometer Bruker AVANCE II-300 (frequency 96.32 Hz). The external standard was a boron trifluoride etherate.

Membrane preparation and their research

For the membrane preparation it was added to 1 ml of the corresponding solution of *closo*-borate salts tetradecyl phosphonium in o - nitrophenyloctyl ester the PVC and cyclohexanone (CH). The mixture was stirred until complete dissolution of the PVC. The resulting solution was placed in a glass ring, located on the glass slide with a 3 cm diameter. After the evaporation of CH polymer film by the thickness about 0.5 mm was made, which was cut out the indicator membrane, which was mounted in a standard package IS561 by Philips.

In the study of electrode function for membranes it was used the cell circuit with transfer:

Ag │ AgCl │ KCl 1.0m ‖test solution│membrane│reference solution│AgCl │ Ag

Reference solution contained 1.10^{-3}M cesium salt defined ion and 1.10^{-2}M KCl. Before measurements, the electrodes were conditioned in 10^{-3}M solutions of the corresponding *closo*-borate salts of cesium during the day. For the preparation of membranes were used reagents for ionometry (Selectofore ®) «Fluka» company: 81392 PVC 73732- o - nitrophenyloctyl ester , 87580 ($C_{40}H_{84}BrN$)and 29,132 CH. Cesium salts with *closo*-borate anions prepared as methods [15,16]. As a reference electrode used silver chloride electrode OP - 0821R (Radelkis, Hungary). The potential measurements were carried out on potential microprocessor ionometer OR-300 (Radelkis, Hungary). It was used the combination electrode OP - 0808P (Radelkis, Hungary) for the determination of the solutions. Standard 1.10^{-2}M and

1.10^{-3}M solutions cesium *closo*-borate salts were prepared by accurately weighed, and the other - by successive dilution.

The determination of electro analytical parameters of ion selective potentiometric sensors

The limit detection and determination of selectivity coefficients were performed in accordance with the recommendations of the IUPAC. In this work, it was used the direct method of determining the coefficient of selectivity by mixed solutions [17]. For this purpose, the solutions with different ratios of $[B_nH_n]^{2-}$ anions and j (interfering ion) were prepared, in which case the concentration C_j was constant /C_j= const/. Concentration of $[B_nH_n]^{2-}$ was varied in the range of 10^{-2}M - 10^{-7}M [8]. Salt concentrations of interfering anions selected in each type of test electrode in accordance with its interferences. The selectivity of the electrodes was determined by mixing solutions at a constant concentration of interfering ions. Selectivity coefficient was assumed to be $<10^{-6}$, if the potential of the electrode in the 0.1 M solution of foreign ion concentration corresponded to $\leq 10^{-7}$ M of i-ion.

Results and Discussion

In developing anionoselektive electrodes often use quaternary ammonium or phosphonium salts with different radicals. If the number of carbon atoms increase, it will be the decrease of lower limit detection [18].

The limit detection depends on the distribution constant ionophore between the water and organic phases, which depends on the lipophilicity of the compound. Search quantitative correlation between lipophilicity and molecular structure led to the additivity Hunch [19-20]: the distribution of matter in normalize two-phase system, for example, water - octanol formed separately of all structural groups of compounds. Moreover, if the parameter is in the range of 4 - 8, the organic compound has the properties of poorly soluble in water, which is well kept in the phase of the membrane. If the Hunch parameter is less than 4, the substance will be washed out of the membrane, and if more than 8, it will be increase of the fixing of standing potential time , due to reduced the mobility of the gegenion in the membrane phase. Calculation of Hunch parameters for quaternary phosphonium salts bases showed that the optimum parameter (log P_{oct}) is reached when using symmetric salts of the phosphonium bases a tetradecyl phosphonium (5,11) and a tetraundecyl phosphonium (7,11). In the real work used salts of tetradecyl phosphonium with of *closo* – borane anions.

Figure 1 shows the electrode characteristics of the developed electrode for determination of different anions *closo* – borates anions, on the basis of which set the limits detection of anion $[B_{10}H_{10}]^{2-}$(pH = 6,8 or 1,6 × 10^{-7} M) and $[B_{12}H_{12}]^{2-}$ (pH = 7,2; or 2,0 × 10^{-8} M).

With the increasing number of boron atoms in the cluster compounds of boron $[B_nH_n]^{2-}$ the lower limit detection is improved. The change of pH in the range of 2 to 10 has no influence on the potentials of the studied electrodes.

Selectivity coefficients developed electrodes are shown in Table 1, 2. The values of selectivity coefficients permit to locate ions analyzed in the following series $ClO_4^- > [B_{12}H_{12}]^{2-} > [B_{10}H_{10}]^{2-} > NO_3^-$. The selectivity of the *closo*-dodecaborate anion is about 10^2 times higher than the *closo*-decaborate anion. Using electrodes on the basis of liquid ionophore in a phase of a membrane it is not observed selective interaction of a defined ion with a lipophilic anion. Therefore changes of selectivity of definition cluster anions can be connected with change of energy of hydration of ions in water solutions.

Table 1

Anion	$[B_{10}H_{10}]^{2-}$	ClO_4^-	CNS^-	BF_4^-	J^-	NO_3^-	Br^-	$[B_{12}H_{12}]^{2-}$
Lg K	1	-1,7	-3,3	-3,2	-3,3	-4,5	--5,1	1,8

Table 2

Anion	$[B_{12}H_{12}]^{2-}$	ClO_4^-	CNS^-	BF_4^-	J^-	NO_3^-	$[B_{10}H_{10}]^{2-}$
Lg K	1	-1,1	-2,7	-2,4	-3,2	-5,0	-2,0

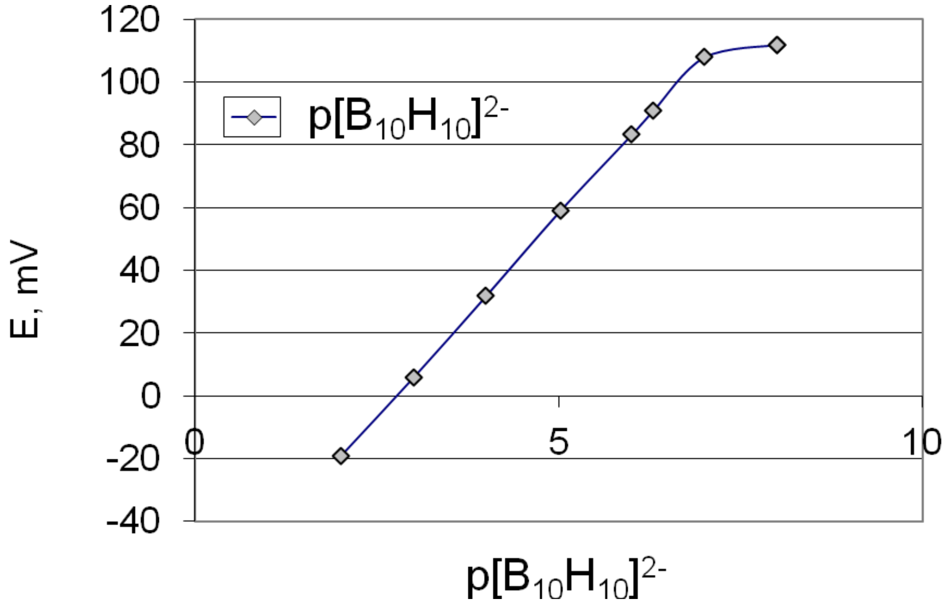

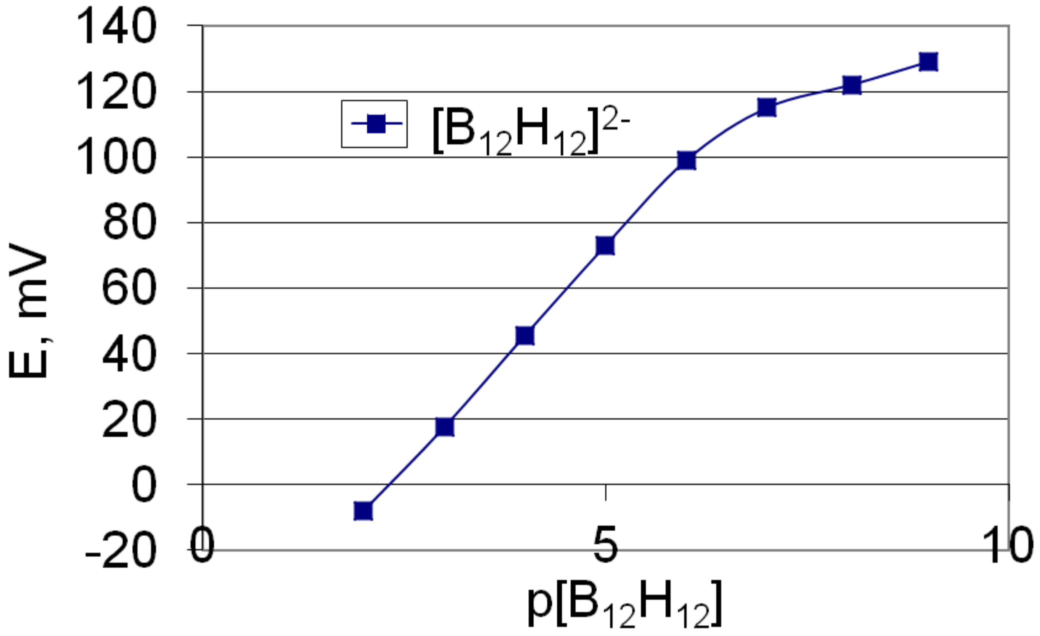

Developed are the ion selective potentiometric sensors (ion selective electrodes) for determination *closo* – borates ions $[B_{12}H_{12}]^{2-}$and $[B_{10}H_{10}]^{2-}$. The sensors are based on the membranes prepared with use of ionic liquids (IL) as the ionophore. At the same time these IL play the role of PVC plasticizers. The main electroanalytical characteristics of the developed sensors are defined (fig. 1 and 2).

ЛИТЕРАТУРА

1. Камман К. Работа с ионселективными электродами. М.: Мир, 1980. 283с.
2. Никольский Б.П., Матерова Е.А. Ионоселективные электроды - Л.: Химия, 1980. 240с.
3. Корыта И., Штулик К. Ионоселективные электроды: Пер. с чешск. М.:Мир, 1989. 272с.
4. Морф В. Принципы работы ионоселективных электродов и мембранный транспорт. М.: Мир, 1985. 280с.
5. В.В.Егоров //Ж. Рос. хим. об-ва им.Д.И.Менделеева.2008, т.52, №2, с.37.
6. Н. В. Шведене, Д. В. Чернышёв, И. В. Плетнёв// Ж. Рос. хим. об-ва им. Д.И. Менделеева. 2008, т.52, № 2.с.80.
7. В.В.Свиридов, О.А.Авраменко, А.А.Раева, И.В.Плетнев, В.Е.Баулин, Н.В.Шведене //Вест. Моск. ун-та, сер.2. Химия. 2007. т.48, №4, с.245.
8. A.V.Kopityin, Gáborné Klatsmányi Piroska, V.P.Izvekov, Pungor Ernȍ //Magyar Kemiai Folyoirat. 1982, 88, p.122
9. A.V.Kopityin, P.Gabor-Klatsmanyi, V.P.Izvekov, E.Pungor, G.A.Yagodin //Anal. Chim. Acta. 1983. V148. p.35.
10. A.V.Kopityin, Gáborné Klatsmányi Piroska, Pungor Ernȍ, G.A.Jagodin //Magyar Kemiai Folyoirat. 1983, 89, p.42
11. A.V.Kopityin, P.Gabor-Klatsmanyi, V.P.Izvekov, E.Pungor, G.A.Yagodin //Anal. Chim. Acta. 1984. V162. p.123

12. А.В.Копытин, Е.Н.Пятова, А.Ф.Жуков и др.//Журн. Аналит. Химии. 2008, т.63, №9, с.976.
13. Hawthorne M.F. The Role of Chemistry in the Development of Boron Neutron Capture Therapy of Cancer. — Angew. Chem. Int. Ed. Engl. 1993. V.32. P.950.
14. Спрышкова Р. А. Биологические основы нейтронно-захватной терапии на боре-10. Дисс. доктора биол. наук. - М.: ОНЦ им. Н.Н.Блохина РАМН, 1999.
15. Miller H.C., Miller N.E., Muetterties E.L.// J. Am. Chem. Soc. 1963. V.85. N.23. P.3885.
16. Greenwood N.N., Morris J.H. // Proc. Chem. Soc. 1963. N.11. P.338.
17. Buck R.P., Linder E. //Pure and Appl. Chem., 1994, V.66, N.12, P.2527.
18. Malon A., Radu A., Qin W., Ceresa A., Maj – Zurawska M., Bakker E., Pretsch E. // Anal.Chem., 2003,v.75, p.3865.
19. Hansch, C .: in “Phisicochemical aspects of dray action” Oxford: Pergamon Press, 1968
20. C. Hansch, A.Y.Leo , “Substituent Constants for Correlation Analisis in Chemistry and Biology” , N.Y. ,1979

MICROBIOLOGICAL DECOMPOSITION OF RADIONUCLIDE CONTAINING TRANSFORMATOR OIL

Safonov A.V. , Tregubova V.E.

Russian academy of sciences A.N. Frumkin Institute of Physical chemistry and Electrochemistry RAS **(IPCE RAS)**
31 Leninsky prospect, Moscow GSP-1, 119071 Russia

Large amount of radioactive waste oil is accumulated from processing nuclear fuel cycle, nuclear power plants and fleet. Oil’s radionuclide contamination is a result of contacting with both radioactive aerosols and gas-or vapor volatile radioactive compounds, such as iodine and cesium, during the operation of nuclear power plant 134Cs, 137Cs and 60Co were shown to be the main radionuclides, defining activity of oil waste.

This research purpose is to develop an effective and inexpensive way of degradation oil waste products by microorganisms. Depending on the type of oil and the degree of physical destruction there is a significant variation of chemical composition: in average, oil contains at least three dozen different organic and inorganic compounds. Biological approach of disposal is determined primarily by component composition of oils.

Biological process is carried out a number of enzymes catalyzing the transformation of various petroleum hydrocarbons, n-alkanes, aromatic compounds and heteroatomic compounds. In addition, biosurfactants play an important role in the degradation of hydrocarbons.

During the work, different microorganisms were selected of genera Pseudomonas, Flavobacterium, Acinetobacter Aeromonas, Arthrobacter, Rhodococcus, living in oil reservoirs and reservoir fluid of different underground ecosystems. Based on strains there were made five physiologically different consortia (microbial communities) working in both aerobic and anaerobic conditions, OD 1-5.

All microorganisms were able to destruct n-alkanes in the temperature ranges from 15 to 35 0C, many of them form biosurfactants. Most bacteria have a high resistance to ionizing radiation.

The bacteria were cultivated for a month on an organic medium with the addition of transformer oil 1:10. Over month of incubation at 20 0 C and pH values of 7.5 there was an abrupt change in the solubility of the organic phase compared to the original model (Figure 1). Mass-spectrometric analysis of the oil after microbiological treatment showed a decrease in the n-alkane fraction from 18 to 50%, izoalkene by 20 - 25%, which has greatly reduced the volume of the organic phase. A comparison of the weight of the oil sample without adding microorganisms with a weight of control sample were shown 10-67% degradation, which suggests the possibility of using enzymatic processes for the degradation of radionuclide containing petroleum oils.

Fig.1. appearance of oil samples with (1-5) and without bacteria (K) after 30 days of cultivation

Table 1. The mass of 1 cm^3 oil after cultivation

Culture	The mass of 1 cm^3 oil (g)	% of destruction
OD1	0,81	10,98
OD2	0,3	67,03
OD3	0,52	42,85
OD4	0,54	40,65
OD5	0,66	27,47
K without	0,90	0,98

bacteria		

This work was supported by the financial assistance of the President of the Russian Federation (grant MK-2330.2012.3) and Ministry of Education and Science (grant 1.2.1-12-000-2007-032)

THE STUDY OF BIO-SORPTIONAL PROCESSES FOR BIOREMEDIATION OF CONTAMINATED AREA

Safonov A.V. Tregubova V.E.

Russian academy of sciences A.N. Frumkin Institute of Physical chemistry and Electrochemistry RAS **(IPCE RAS)**
31 Leninsky prospect, Moscow GSP-1, 119071 Russia

The main sources of contamination are nuclear explosions for military or civilian purposes, technological and accidental releases at facilities of the nuclear fuel cycle (NFC), nuclear facilities naval and civilian fleets, radiation accidents, mining and processing of uranium, production and processing of waste from nuclear reactors, materials nuclear power plants (NPPs), disposal of solid and liquid radioactive waste. A wide range of man-made radionuclides, including long-lived, into the environment remains an environmental hazard for hundreds and thousands of years.

Microbial populations can affect the geochemical parameters of radionuclides with biosorption, bioaccumulation and dissimilyation recovery of metals and metalloids such as U^{VI}, Tc^{VII} and others. Microorganisms can accelerate radionuclide’s migration during transport or slow migration by the concentration in the biofilm formation of dominant types of radionuclides and mineral phases, including new mineral formations, production of complexing agents, the change of pH and Eh.

In this paper we study the processes of radionuclide biosorption by biomass of microorganisms isolated from the deep repository of liquid radioactive waste. For the experiment, were obtained pure culture of Pseudomonas Putida (put), Native culture, containing a wide range of microorganisms (nat) and a mixture of the above two cultures.

Activity of radionuclides (except for 137Cs), remaining in the liquid phase was measured by liquid-scintillation spectrometer SCS-07P-B11 (Russia) using a scintillator «Opti Phase HiSafe-3." Most solutions containing 137Cs, were measured using a semiconductor gamma spectrometer with a coaxial detector of purity germanium (Ge-2520, Canberra).The microorganisms were cultivated in a mineral Adkins medium following composition: NH4Cl - 1 g / l, NaCl - 0,8 g / l, CH3COOH - 2 g / L, NaNO3 - 1 g / l, KCl, MgSO4, Na2SO4 - 0,1 g / l, in anaerobic conditions, at neutral pH, 20 ° C for 10 days with the addition of the following concentrations of radionuclides: Cs (195Bk/ml) -, Sr (38 Bq / ml) -, U (as UO2-1 mg / ml) -, Th (1 mg / ml),-Tc (253,9 Bq / ml). The final biomass concentration was 1.5 -2 g / l.

The experiment found that 1 g of biomass to sorb

0.177 g UO2,;

0.217 g of Th;

10.16 Bq Sr;

10.42 Bq Cs;

31.47 Bq-Tc.

The results of the percentage of sorption are shown in Fig. 1.

According to the study, the sorption of Th was almost 100%, U - 85%, the sorption of Cs, on average - 10%, Sr - 50%, and Tc - 25%.

Thus, studied microorganisms living in natural ecosystems, were found to be able to reduce the migration of artificial radionuclides in the environment, sorbing them on their surface, which can be used to develop the technology for bioremediation of contaminated sites by theory.

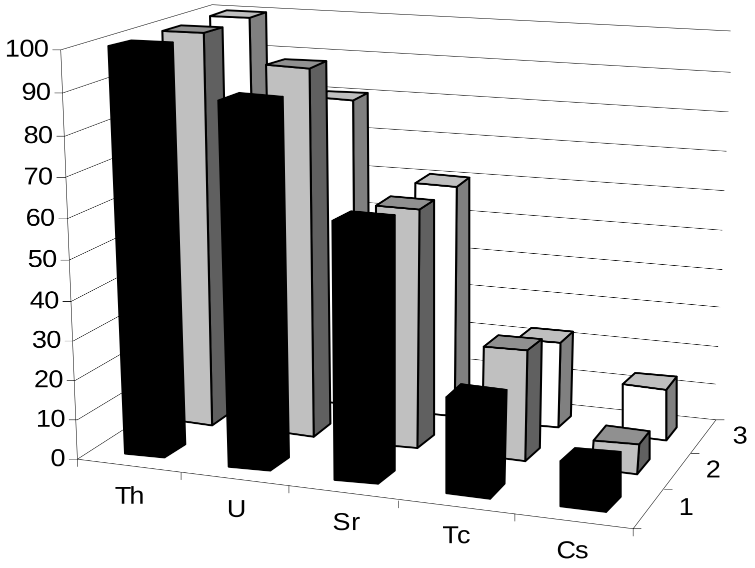

Fig 1. Percentage of sorption of radionuclides by microorganisms ☐ - Put, ■ - Nat, ▨- Mix1.

This work was supported by the financial assistance of the President of the Russian Federation (grant MK-2330.2012.3) and Ministry of Education and Science (grant 1.2.1-12-000-2007-032)

FORMATION OF NANOCLUSTERS IN NITRIC ACID SOLUTIONS CONTAINING MOLYBDENUM AND ZIRCONIUM (IV)

N. Kravchenko, A. Maslennikov, A. Shirjaev

A.N. Frumkin Institute of Physical Chemistry and Electrochemistry
Russian Academy of Sciences (IPCE RAS), 31, Leninsky pr, Moscow,
119991, Russia

During the process of dissolution of spent nuclear fuel, and a first cycle of extraction of uranium and plutonium, Mo is capable of forming Mo residues of variable composition, which, in turn, are determined by the chemical state of molybdenum in solutions of nitric acid. This work was intended to determine the possible chemical state of molybdenum in solutions 0.5-6.0 M HNO3 using the small-angle X-ray scattering technique (SAXS).

The state of solutions which were obtained by the dissolution of metallic molybdenum, Na_2MoO_4, nitrate, and zirconium (IV) in 0.5-6.0 M HNO_3.of different composition was investigated. It was shown that solutions contain nanosized aggregates (3 -25 nm) and monodisperse small particles (0.2-0.4 nm), which is believed may be the nucleation centers of precipitation $ZrMo_2O_7(OH)_2{\cdot}2H_2O$ [1]. Boundary Mo and Zr concentrations of nanoparticles formation were defined. Dependance of the nanoparticles sizes on conditions was investigated. At concentrations of Mo and Zr, less than 0.01 M, all solutions are true. In weak acid (0.5-1.5 M) at concentrations of Mo and Zr, equal to 0.02 M, the solutions are characterized by strong scattering, there is formation of small monodisperse particles and large aggregates. At concentrations of Mo and Zr is higher than 0.02 M, there is a sufficiently strong scattering in all solutions, aggregates and monodisperse particles are formed regardless of acid concentration. Analysis of solutions containing dissolved metallic molybdenum with a concentration of 0.01 M Mo, did not show the presence of aggregates and small particles. The dissolution of metallic molybdenum in solutions 0.5-6.0 M HNO3 with concentrations of 0.03-0.04 M Mo resulted to the formation of colored solutions (from yellow to brownish-red color). Also, the precipitation of brown residues occurred in 0.5-3.0 M HNO_3 solutions. This experimental fact indicates the formation of Mo in the oxidation state lower than (+6) during the dissolution, as evidenced by the results of previous work in the Table. 1 [2]. Analysis of these solutions revealed the presence only the small monodisperse particles. Probably, the produced molybdenum aggregates precipitate instantly in the form of insoluble polymeric chains of Mo (VI)-Mo (V). Therefore, in these solutions aggregates are not observed by SAXS.

Table 1. Material balance of the dissolution of metallic Mo in solutions of 0.5 - 3.0 M HNO_3

[HNO3], mol/l	Dissolution rate Mo^* mg /cm^2/hour	Accumulation rate $Mo(VI)^{**}$ mg /cm^2/hour	Yield, Mo(VI), %
0,5	0,03788	$(72,2\pm1,4)*10^{-5}$	2,0
3,0	4,4924	1,58±0,03	35,2

Mixed solutions containing dissolved metallic molybdenum and zirconium (IV) in 1.5-3.0 M HNO_3 also show the presence of only a monodisperse particle of 0.3-0.5 nm size . When Na_2MoO_4 was used for preparing of mixed nitric acid solutions with zirconium (IV) in 1.5-3.0 M HNO_3 the formation of solutions containing aggregates (17-19 nm) and monodisperse particles (0.3-0.6 nm) was observed. The size of the resulting monodisperse particles and aggregates in nitric acid solutions containing both Mo, and Zr, exceeded the size of the particles obtained in nitric acid solutions of individual elements.

References.

1. Doucet F.J., Goddard D.T., Taylor C.M., Denniss I.S., Hutchinson S.M., Bryan N.D. The formation of hydrated zirconium molybdate in simulated spent nuclear fuel reprocessing. // Phys. Chem. Chem. Phys. 2002, v. 4, No. 14, p. 3491-3499.

2. И.В. Хонина, А.А.Лумпов,А.Ю. Шадрин, Б.Я. Зильберман, Н.Г. Кравченко. Образование осадков гидратированного молибдата циркония в концентрированных растворах уранилнитрата. Радиохимия, 2010, т.52, вып. 2, с. 151-154.

Olga Kryzhovets
Alex Kopytin

SEPARATION OF RADIONUCLIDES FORMED IN THORIUM TARGET
IRRADIATED WITH PROTONS

Aleksandr Vasiliev$^{1)}$, Valentina Ostapenko $^{1)}$, Stepan Kalmykov $^{1)}$,
Ramiz Aliev $^{1)}$, Elena Lapshina $^{2)}$, Stanislav Ermolaev $^{2)}$
$^{1)}$ Lomonosov Moscow State University, Stavrogin.aleksandr@yandex.ru
$^{2)}$ Institute for Nuclear Research of Russian Academy of Sciences

As a result of irradiation of natural thorium with high-energy protons various fission and activation products of ^{232}Th are formed. Among them ^{225}Ac is formed, which has characteristics that enable to use it in radiotherapy of cancer. There is a growing demand for this radionuclide, while current methods for producing actinium have significant limitations and cannot satisfy it completely. Production of actinium from ^{233}U is limited by its inaccessibility. In addition the formation of ^{223}Ra should be noted, which is also a promising α-emitter for medicine.

For fast effective isolation of actinium and radium from the thorium target the separation of macroscopic quantities of thorium is conducted. For this purpose method of solvent extraction is proposed.

Irradiated thorium is dissolved in a mixture of concentrated hydrochloric and nitric acids, or in concentrated nitric acid with the addition of catalytic amounts of hydrofluoric acid.

Tributylphosphate and trioktylphosphinoxide (TOPO) were used in extraction experiments. The behavior of radionuclides, depending on the composition of the aqueous phase is studied. By both extractants the principal amount (80%) of thorium was transferred in the organic phase. Disadvantage of TOPO is its low extraction capacity. ^{95}Zr (70%), ^{223}Ra (40%), ^{230}Pa, and ^{233}Pa (75%), ^{99}Mo (22%), etc was transferred along with thorium in the organic phase. ^{103}Ru, ^{126}Sb, ^{132}Te, ^{136}Cs, ^{140}Ba, ^{140}La, ^{144}Ce, ^{147}Nd remain in the aqueous phase. Loss of actinium is 4%. The conditions of ^{223}Ra back extraction from an organic solution after extraction of thorium macroamounts are obtained.

Sorbents AG-1 (BioRad), Ln Resin (Eichrom), TRU Resin (Eichrom), TDi-2 (Karpov Institute) were taken for further chromatographic separations. The sorption capacity of AG-1 forwards thorium is investigated. The sorption behavior of radionuclides, depending on the parameters of the column is given. It is shown that ^{225}Ac quantitatively adsorbed on Ln Resin and TDi-2 from dilute nitric acid (0.05 M HNO_3). Desorption was carried out with acid of higher concentration (3 M). Significant difference in the sorption behavior of ^{225}Ac for Ln Resin and TDi-2 was not observed. Actinium is eluted together with cerium and lanthanum. Therefore, for further separation the 3 M nitric acid was passed through the sorbent TRU Resin.

The possibility of separation of the radionuclide ^{103}Ru, which makes some difficulties for the production of final preparation ^{225}Ac, by extraction with carbon tetrachloride in comparison with other methods of its isolation is observed.

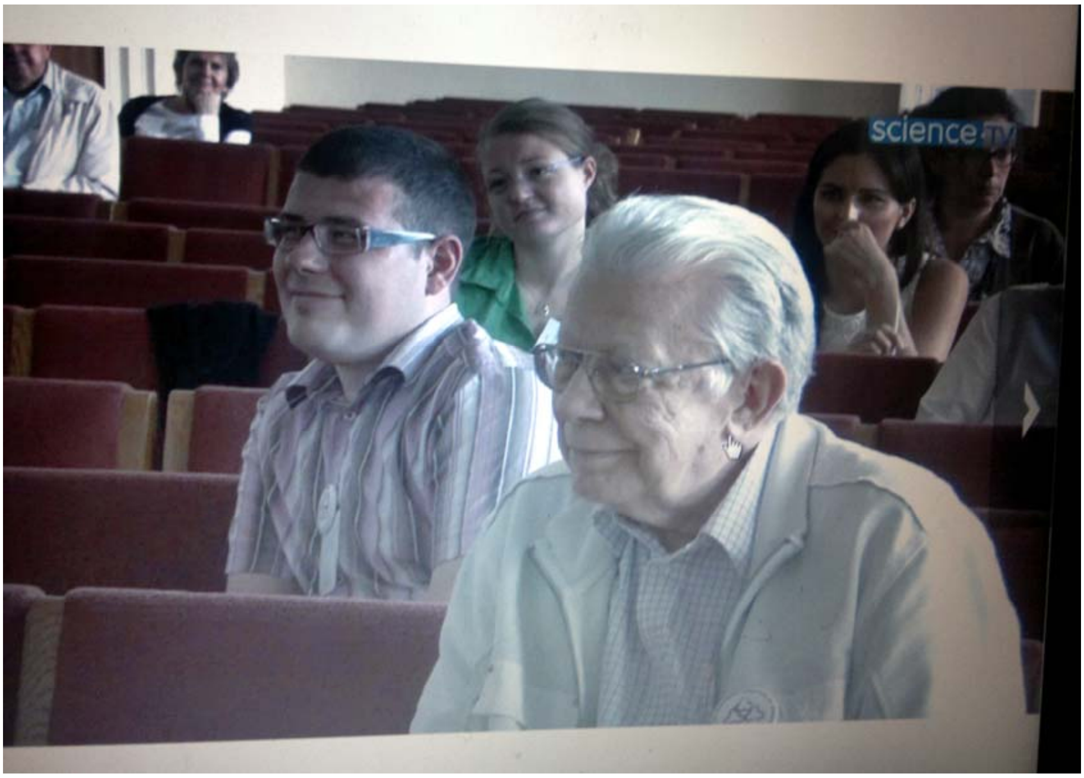

Pawel Jewula (awarded with Lomonossov Medal) and academician Myasoedov
at the award ceremony, 23 July 2012

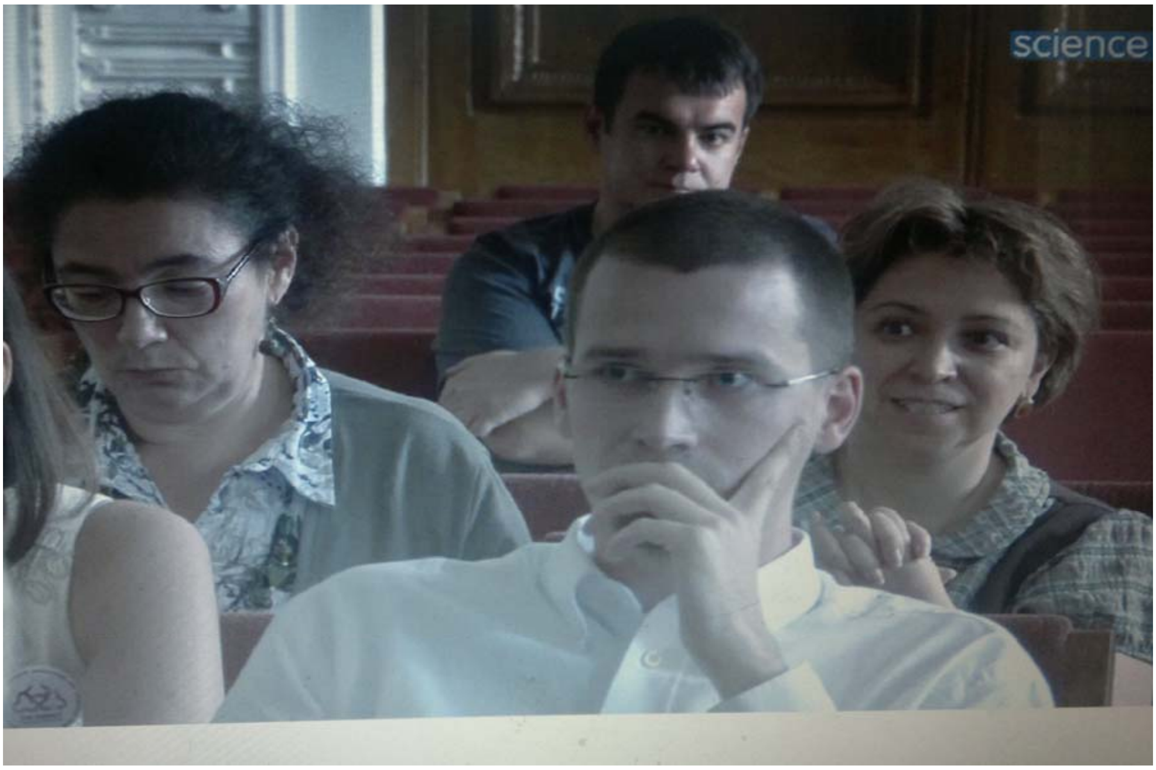

Dr. B. Beele (awarded with “For Achievements in Sciences” Medal) and Prof. Yu. Gorbunova
at the award ceremony 23 July 2012

6 наиболее активных молодых ученых на школе-конференции
наградили медалями Менделеева и Ломоносова.
Доклады участников и учеников школы-конференции
опубликуют в ведущих западных журналах.

Ms. O. Pecheur (awarded with Mendeleev Medal – For achievements in chemistry), Dr. Shiryaev, Dr. A.Safonov and Dr. I. Vlasova at the award ceremony
23 July 2012.

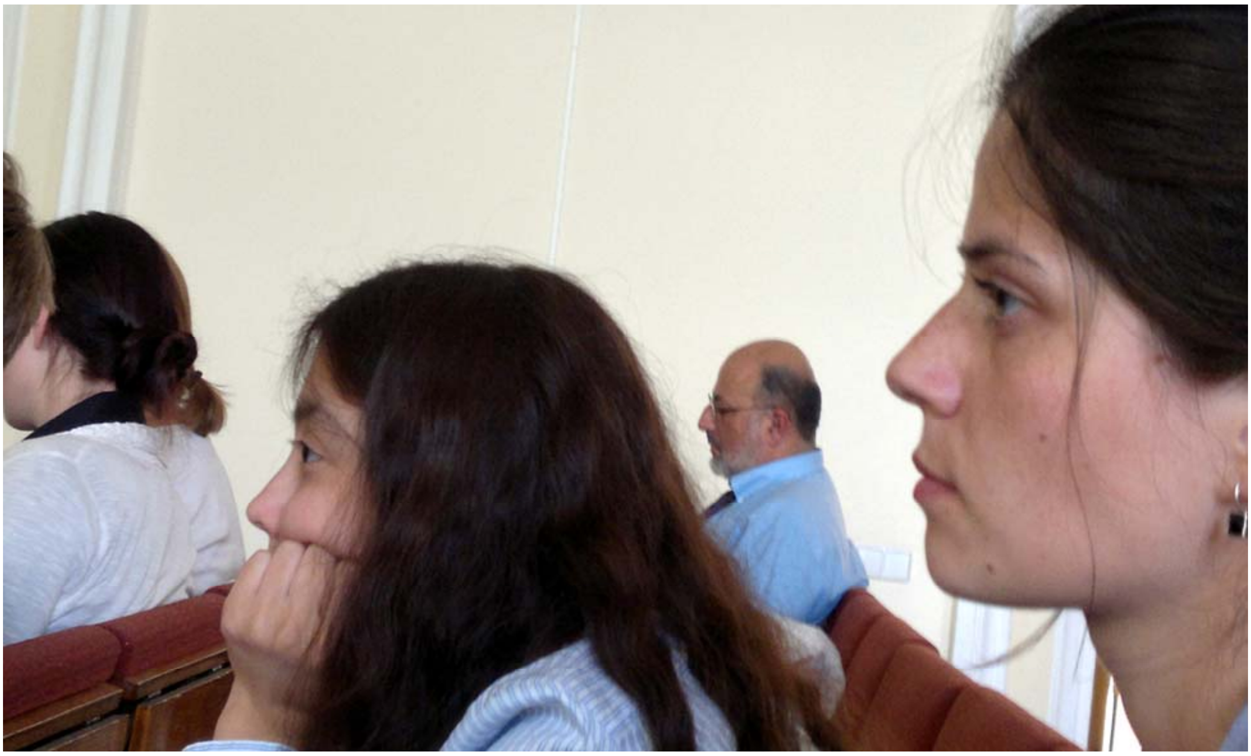

Ms. Ya. Obruchnikova (awarded with Mendeleev Medal – For achievements in chemistry), Prof. W. Hosseini and Ms. N. Kravchenko at the award ceremony 23 July 2013

Prof.Tobias .Reich, acad. A.Yu. Tsivadze, acad. B.F. Myasoedov and Prof. Horst Geckeis

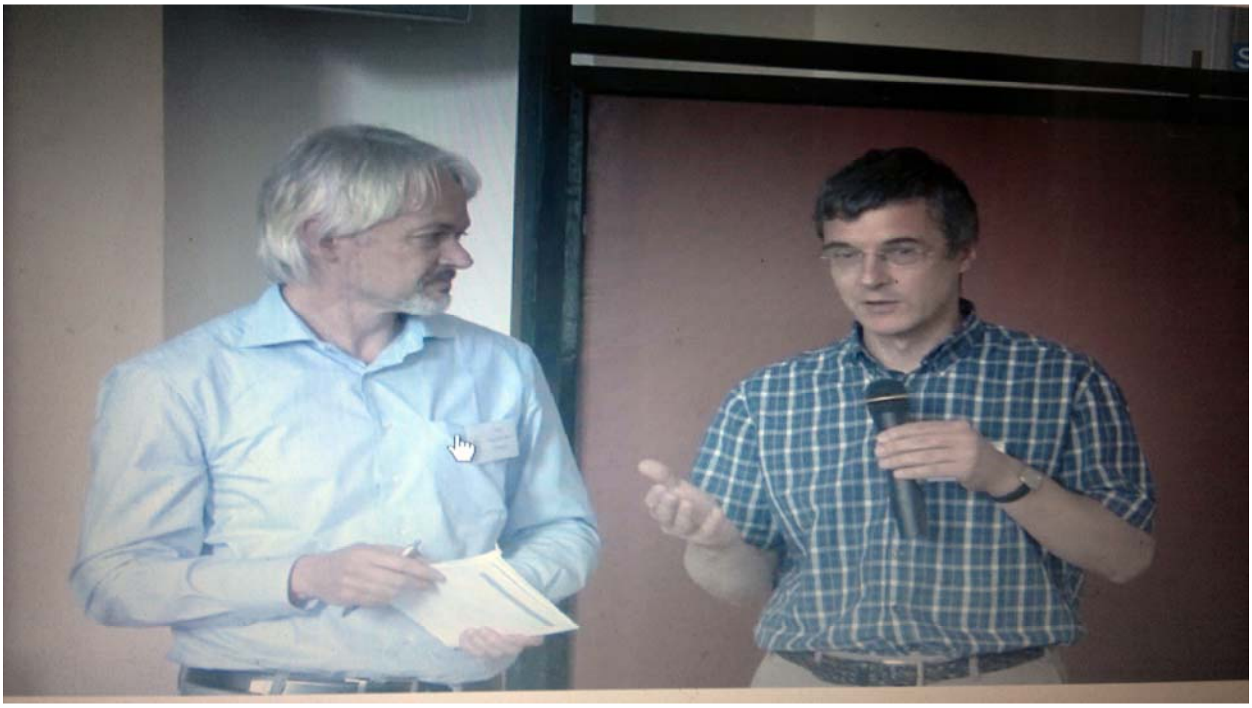

Prof. T. Reich announcing the decision that the 8th European Summer School will be hold in Mainz, Germany in 2013

Author index

Contents

Preface

PROGRAM

Nils Stöbener, P. Schönberg, G. Passler, T. Reich, N. Trautmann. Resonance ionization mass spectrometry (RIMS) - a powerful tool for ultratrace analysis of long-lived radionuclides. Ugras Kaplan, S. Amayri, J. Drebert, D.R. Fröhlich, D. Grolimund, T. Reich. Interaction of Plutonium with Natural Clay. Alexandre Varnek. Chemoinformatics: time to predict. Horst Geckeis. Actinide environmental behavior – role of nanoparticle formation. Werner Kunz. Specific ion effects in solutions, at interfaces, and in colloidal systems. Yana Obruchnikova. Speciation and separation chemistry of Tc for SNF reprocessing. Veronika Fisher. Deep Eutectic Solvents Michael Klossek. Nanostructured Liquids, Colloids and Environmentally Acceptable Liquid Media Alexander Martynov. Synthesis and conformational behaviour of phthalocyanines, bearing lateral coordinating macrocyclic substituents. Stepan Kalmykov – “Environmental Chemistry of actinides in microparticles from different nuclear sites”. Björn B. Beele, Udo Müllich, Andreas Geist, Petra J. Panak. Partitioning and Transmutation – BTP-type N-Donor ligands in the SANEX Process. Grigory Kolesnikov Konstantin German. “Macro-receptors for Tc and Re: Structural predictions, supramolecular-based template synthesis and new properties”. Daniel Meyer - "Colloidal and supra-molecular aspects of 5f elements in solution". Andrei Shirjaev - “Speciation in radioactive Pu-waste-glassforms.” Bayrita Egorova. Pertechnetate-ion binding by organic ligands in aqueous solutions. A.Ya. Maruk, A.B. Bruskin, G.E. Kodina. New radiopharmaceuticals based on technetium-99m with bifunctional chelating agents.	

Yulia Buchatskaya. “Sorption preconcentration of radionuclides using detonation nanodiamonds”. Kopytin Kryzhovets Safonov Safonov	

Signed to print on 21.12.2012.
Format 60x90/16. Edition # 402. Print run 500 issues.

Publishing group “Granica”
123007 Moscow, highway Horoshevskoe, building 38
Telephone (495) 941-26-66, fax: (495 941-36-46
E-mail: granica_publish@mail.ru